Development and Application of Inductively Coupled Plasma-Mass Spectrometric Techniques for the Precise Measurement of Trace Elements and Lead Isotopic Compositions in Geological Materials

By

Zongshou Yu (M.Sc.)

UNIVERSITY OF TASMANIA

CODES

Submitted in fulfilment of the requirements
for the degree of Doctor of Philosophy
University of Tasmania

September 2000

DECLARATION OF ORIGINALITY

This thesis contains no material which has been accepted for a degree or diploma by this university or other institution, except by way of background information and duly acknowledged in this thesis, and to the best of my knowledge and belief no material previously published or written by another person except where due acknowledgment in the text of this thesis.

Date: 19/2/2001

Signature: 

STATEMENT OF AUTHORITY OF ACCESS

This thesis may be made available for loan and limited copying in accordance with the Copyright Act 1968

Date: 19/2/2001

Signature: 

ABSTRACT

Inductively coupled plasma-mass spectrometry (ICP-MS) is a powerful analytical technique, regarded as one of the most successful in atomic spectrometry, and widely used for measurement of a wide range of trace elements in geological materials. In general, this established technique has the merits of high sensitivity, fast analysis capacities, true multi-element abilities, and a very large dynamic linear concentration range. Sample preparation is also relatively simple.

This study has systematically investigated analytical performance characteristics of a high resolution (HR)-ICP-MS instrument (Finnigan Mat Element, Germany). This instrument has been found to be more sensitive, with less spectral interferences (due to the pre-defined setting of different resolutions) than quadrupole instruments. It has been found that only a single internal standard is sufficient to compensate for the instrumental drift during an analytical sequence. The detection limits for some trace elements studied were found to be as low as pg g^{-1} levels in solution.

To obtain accurate analytical results using ICP-MS, complete sample dissolution is required. Decomposition techniques for the dissolution of different types of geological materials have been studied. Savillex Teflon beaker HF/HNO_3 digestion has been found to be sufficient for the complete dissolution of basaltic samples. High pressure $HF/HClO_4$ digestion (PicoTrace® TC-805 digestion system, Bovenden, Germany) can be used for the dissolution of ultramafic rocks such as dunite and peridotite, in which many geologically useful trace elements are at very low abundance, and also granites (which may contain difficult to dissolve zircon) and magnetite-rich samples. It has been found that a lithium tetraborate fusion method allows complete dissolution of different types of geological materials, but this method precludes analysis of volatile elements due to the high fusion temperature (approximately 1000 °C). The sodium peroxide sinter method may enable fast determination of Y, Sc and REE in different types of geological materials. However, neither the lithium tetraborate fusion nor sodium peroxide sinter method can be used

for the measurement of low abundance geological samples, due to the lack of ultra-pure reagents. In general, the microwave digestion method has been found to be unsuitable for the total decomposition of geological materials.

Systematic investigation of chelates between several complexing reagents (citrate, tartrate, EDTA and DTPA) and Zr, Nb, Ta, Hf, Th and U ("high field strength elements" - HFSE) has shown that DTPA can form stable HFSE complexes in solution. These prevent the hydrolysis of HFSE and hence allow the accurate determination of HFSE in geological materials. A complexing method has been developed, which coupled with an appropriate digestion method and ICP-MS, can lead to the accurate determination of HFSE at different levels (particularly higher than 1 $\mu g\ g^{-1}$ of Nb and Ta) in geological reference materials.

As a comparison study and a geological application of the ICP-MS techniques developed in this study, trace element concentrations of seventeen oceanic basalt glasses from Macquarie Island have been measured by both solution-based HP-ICP-MS & quadrupole ICP-MS and solid sampling-based laser ablation ICP-MS. The majority of elements measured by the three analytical protocols showed discrepancies of <10% and most showed discrepancies of less than 5% with the exception of Tl and Cd (showing unacceptably large variations of more than 20%). The new high-precision data for a wide range of elements in a suite of primitive mid-ocean ridge basalts (MORB)-like suite allow evaluation of the relative incompatibility levels of these elements, and comparison of the order evident from the Macquarie Island suite with the widely accepted incompatibility 'order' proposed for mantle melting by Sun and McDonough (1989). Significant discrepancies have been observed. For the most incompatible elements, those primitive glasses representing the lowest-degree partial melts show significantly higher Ba, K, Th and P contents relative to Nb (and thus slightly different orders of incompatibility than that proposed by Sun and McDonough 1989) than glasses representing higher degree partial melts. This is taken to reflect involvement of one or more K- and P-bearing phases in the earliest stages of partial melting, which are eliminated early in the melting history. Subsequent partial melts do not reflect these anomalous enrichments. Sulfur is shown to have a bulk $K_D \approx 1$ during partial melting that generated the Macquarie Island basalt magmas, suggesting that a sulfide buffers melt

S contents across the melting range represented. Lead is highly incompatible (close to La) compared to Zn and Cu, and Cu is close to Ni in being among the most compatible elements in this mantle-melt system. This may indicate that the mantle sulfide is Cu-bearing pentlandite on a Cu-(Ni-)-bearing monosulfide solid solution. Zinc shows a moderate compatibility level, close to that of V, whereas Mo behaves similarly to La, and Sb is similar to Ce, both metals being significantly more incompatible than suggested by Sun and McDonough (1989)

Analytical methods for the precise measurement of lead isotopic compositions using HR-ICP-MS and the latest quadrupole ICP-MS (HP 4500 *plus*) have been successfully developed in this study. Based on a series of measurements of geological reference materials and lead-bearing samples, the precision (%RSD) values for $^{208}Pb/^{204}Pb$, $^{207}Pb/^{204}Pb$, $^{206}Pb/^{204}Pb$, $^{208}Pb/^{206}Pb$ and $^{207}Pb/^{206}Pb$ ranged from 0.05 to 0.12 for HR-ICP-MS and from 0.06 to 0.15 for quadrupole ICP-MS. By comparison with lead isotope data obtained by thermal ionisation mass spectrometry (TIMS), the accuracy of both methods was found to be generally better than 0.20%. The ICP-MS methods tested here are simple and cost-effective compared to TIMS, suggesting greater potential for application to geological problems in the future.

Finally, lead isotope ratios in base metal sulfide samples collected from the Lady Loretta deposit in northern Australia have been successfully measured by the quadrupole ICP-MS technique. The results are in excellent agreement with the lead isotope data previously measured by TIMS. The wide variation in the lead isotopic compositions from the Lady Loretta deposit suggests multiple sources for lead in the ores.

ACKNOWLEDGEMENTS

This study would not be possible if there were not the financial support provided by the Center of Ore Deposit Research of the University of Tasmania. The author would like to thank the following:

Dr Peter McGoldrick of the Center for Ore Deposit Research, University of Tasmania, for his general supervision, advice and assistance throughout my PhD project.

Associate Professor Anthony J. Crawford of the Center for Ore Deposit research, University of Tasmania, for his guidance, advice and support throughout my study. His support, encouragement and assistance were particularly appreciated at the beginning of this project.

Dr Ashley T. Townsend at the Central Science Laboratory of the University of Tasmania for his technical advice, assistance in using HR-ICP-MS facilities and valuable discussion during this project.

Philip Robinson at the School of Earth Sciences, University of Tasmania, for his assistance in the experimental work and valuable discussion. His support, assistance and encouragement in the quadrupole ICP-MS work are also appreciated.

Professor Ross Large, Drs Marc Norman and Vadim S. Kamenetsky for support and useful discussion.

Finally, my acknowledgements should extend to all my colleagues who have made my study very enjoyable during my stay at this university.

CONTENTS

LIST OF FIGURES

LIST OF TABLES

Chapter 1
INTRODUCTION

Understanding the behaviour of trace elements over a wide range of temperatures, pressures and environments applicable to the Earth has played an important role in formulating models of a variety of geological processes. These processes include magmatic and metamorphic differentiation, mantle and crustal anatexis as well as ore-formation. Evaluating models for these processes requires accurate and precise measurements of trace element abundances in rocks and minerals, a major focus of analytical geochemistry for many decades.

Gray (1989) conducted a survey of available and emerging spectrometric techniques suitable for multi-element analysis and concluded that atomic mass spectrometry (MS) was the only potential technique which could offer the combination of simple spectra, adequate resolution and low detection limits that was desirable for multi trace element determination in complex matrices. In order to improve the precision, sensitivity, detection limit and increase dynamic range of the conventional MS technique, inductively coupled plasma-mass spectrometry (ICP-MS) was initially developed from the work of Gray (1975), who demonstrated that good detection limits can be obtained and isotope ratios can be determined when a solution is introduced into a d. c. plasma (DCP) at atmospheric pressure and the ions formed are extracted into a mass spectrometer.

At present, although ICP-MS has become a standard and routine analytical technique for the analysis of trace elements in geological samples (e.g. Jenner et al. 1990; Eggins et al. 1997), quality analysis of geological materials presents a particularly challenge for ICP-MS due to:

(a) Limitations of conventional sample decomposition techniques; these have not kept pace with the development of ICP-MS instrumentation;

(b) limitation in low abundance analysis due to the low sensitivity of the older generations of quadrupole instruments and other problems such as memory effects (particularly for low abundance Nb and Ta analyses);

(c) the hydrolysing tendency of high field strength elements (HFSE: Nb, Ta, Zr, Hf, Th and U) in aqueous solutions (e.g. Perrin 1964; Heslop and Jones 1976; Münker 1998).

Furthermore, attempts were made to analyse lead isotope ratios using old generations of quadrupole instruments to reduce the high cost of lead isotope ratio measurement in geological materials using the conventional thermal ionisation mass spectrometry (TIMS) (Smith et al. 1984; Date and Cheung 1987; Longerich et al. 1992). However, those instruments were specifically designed for the rapid scanning of relatively large mass ranges and sensitivities were relatively low. Therefore, the precision and accuracy of lead isotope ratio data were limited by counting statistics.

In order to overcome and better understand these limitations, this thesis presents a systematic investigation of dissolution techniques for different types of geological materials, analytical methods for the reliable measurement of trace elements at low abundance, and a new technique for measuring lead isotopè ratios using a high resolution (HR)-ICP-MS and current generation quadrupole ICP-MS.

1.1 Inductively Coupled Plasma-Mass Spectrometry

The original concept of ICP-MS arose in the 1970s from a requirement for a new generation of a powerful multi-element analytical instrument systems needed to follow the then rapidly developing technique of ICP-AES (Gray 1975; Date and Gray 1983a & 1983b). Gray (1975) initially explored the use of an atmospheric pressure d. c. plasma as an ion source for the direct analysis of solutions introduced into the plasma from a nebuliser. In Gray's early work, ions were extracted from the plasma into a vacuum system and were focused into a quadrupole mass analyser. At the initial stage of the ICP-MS technique, the pioneering work was conducted primarily in three laboratories: the Ames Laboratory at Iowa State University, headed by Fassel; the laboratories at Sciex; and the University of Surrey (headed by Gray), the

British Geological Survey (headed by Date) and VG Instruments (Horlick et al. 1987).

The first ICP-MS system certainly showed promise of very high sensitivity, giving essentially zero background levels between mass peaks and signals of between 10^4 and 10^5 counts per second (cps) for fully ionised mono-isotopic elements such as Co at a concentration in solution of 1 $\mu g\ ml^{-1}$ (Gray 1989). Houlk et al. (1980) studied inductively coupled argon plasma (ICAP) as an ion source for mass spectrometric determination of trace elements and found that the positive ion mass spectrum obtained during nebulization of a typical solvent (1% HNO_3 in H_2O) consisted mainly of ArH^+, Ar^+, H_3O^+, NO^+, O_2^+, HO^+, Ar_2^+, Ar_2H^+ and Ar^{2+}, and the mass spectra of the trace elements investigated consisted mainly of singly charged monatomic (M^+) or oxide (MO^+) ions in the correct relative isotopic abundances. Based on the elements studied, Houlk et al. (1980) found that working range generally covered nearly 4 orders of magnitude with detection limits of 0.002-0.06 $\mu g\ ml^{-1}$. As summarised by Jarvis and Jarvis (1992), the main advantages of ICP-MS for the analysis of geological materials include:

1. rapid simultaneous multi-element measurement;
2. superior sensitivity and detection limits, particularly for heavy elements;
3. wide linear dynamic range of at least 6 orders of magnitude;
4. simple spectra and low background even for complex matrices;
5. adequate precision, reproducibility and good accuracy;
6. rapid isotope ratio capacity, enabling stable-isotope tracer studies and the use of isotope-dilution techniques for optimum precision and accuracy;
7. excellent performance for "difficult" elements (such as rare earth and high field strength elements).

In the early 1983s, the development of ICP-MS was extremely rapid. Work reported by Date and Gray (1983a and 1983b) introduced the use of continuum sampling mode, and boundary layer and continuum sampling modes were identified and compared. The advantage of low background, good detection limits, and low extracted ion energy characteristic of the boundary layer sampling mode were offset by a number of shortcomings. These included the inability of the system to accept

solution concentrations in excess of 10 μg ml^{-1}, and the use of large apertures in the continuum mode, which should greatly increase the upper concentration limit of the system, was initially prevented by the formation of the "pinch" discharge in the aperture mouth caused by compression of the electron population of the plasma gas. Date and Gray (1983a and 1983b) found that, by regulating the pressure immediately behind the sampling aperture, it was possible to suppress the discharge and achieve controlled expansion of the plasma gas into the vacuum system. By sampling in this way with ICP-MS, the sampled gas was no longer cooled immediately in front of the aperture, and there was little salt condensation around the aperture rim for salt concentrations up to 1000 μg ml^{-1}. Furthermore, because the ionisation equilibrium in the sampled plasma corresponded more closely to plasma rather the boundary layer temperatures, ionisation suppression was greatly reduced.

In the meantime, Gray and Date (1983) studied inductively coupled plasma source mass spectrometry using continuum flow ion extraction. Detailed operating characteristics and performance of the continuum flow ion extraction system were investigated in the work. Houk et al. (1983) investigated mass spectra and ionisation temperatures in an argon-nitrogen inductively coupled plasma. Positive ions were extracted from the axial channel of an inductively coupled plasma (ICP) in which the out gas flow was Ar, N_2 or a mixture of Ar and N_2 in their work. They found that Ar^{2+}, O_2^+ and ArH^+ reacted with N-containing species in the plasma and/or during the ion extraction process and ionisation temperatures measured from the ratio Cd^+/I^+ were 5750-6700 K for a N_2 outer flow ICP at a forward power of 1.2 kW.

In 1983, two commercial instruments were launched (Gray 1989), the PlasmaQuad, based on the Surrey system, by VG Isotopes Ltd in the UK, and the Elan in Canada by SciexInc., based on the work of the Toronto group, and which is now marketed by the Perkin Elmer Corporation. Since then, many workers (e.g. Olivares and Houk 1985; Tan and Horlick 1986; Vaughan and Horlick 1986; Lichte et al. 1987; Jarvis 1988; Jackson et al. 1990; Longerich et al. 1992; Garbe-Schönberg 1993; Xie et al. 1994; Yoshida et al. 1996; Rautiainen et al. 1996; Eggins et al. 1997) have applied the quadrupole ICP-MS technique to geo-analysis

ICP mass spectrometers equipped with a double-focusing magnetic sector mass spectrometer, instead of a quadrupole filter, have also been commercially available since 1989. These instruments are also referred to as HR-ICP mass spectrometers due to their ability to resolve isotopes from molecular ions, which cannot be done using quadrupole instruments. The heart of a double-focusing instrument is a magnetic sector field. If ions that have uniform energy but different mass are injected perpendicular to a magnetic sector field, they pass the field on a circular trajectory because of Lorentz force. The radius of the trajectory depends on the mass of the ion, leading to a mass dispersion.

However, it was not until 1996 that precise measurement of isotope ratios with a double-focusing magnetic sector ICP mass spectrometer was reported by Vanhaecke et al. (1996). It was also found that double-focusing magnetic sector ICP-MS, operated under low resolution conditions, yielded a remarkable improvement in isotope ratio precision relative to quadrupole-based ICP-MS. Vanhaecke et al. (1997) also studied the applicability of HR-ICP-MS for the accurate and precise measurements of isotope ratios of which at least one of the isotopes involved was spectrally interfered when measured at low resolution (using copper as a typical example). Their study showed that HR-ICP-MS, operated at a resolution setting of 3000, could be successfully used to determine the natural $^{63}Cu/^{65}Cu$ ratio in both an Antarctic sediment sample and a human serum reference material, even though the isotopes involved severely isobarically interfered with each other at low resolution.

In comparison with quadrupole instruments, HR-ICP-MS is still a relatively new technique, and although it has been applied to many fields such as food, semiconductor, soil, and environmental sample analysis (see review by Jakubowsski et al. 1998), little has been reported concerning the measurement of trace elements at various levels (at very low levels in particular) and lead isotopic compositions of geological materials. Therefore, for this study, the HR-ICP-MS performance characteristics (such as sensitivity, stability, memory effects, interferences, internal standards, etc.) associated with geo-analysis have been systematically investigated.

1.2 Decomposition of Geological Samples

Sample decomposition is a fundamental and critical stage in the process of geochemical sample analysis. It is often the limiting factor to sample throughput, which is particularly true with the recent application of the fast and modern multi-element measurement instrumentation, such as ICP-AES and more recently ICP-MS.

Many digestion methods have been used for the decomposition of geological samples. These include open and closed vessel acid digestion methods (Moselhy et al. 1978; McQuaker et al. 1979; Lechler et al. 1980; Church 1981; Uchida et al. 1980; Lechler et al. 1980; McLaren et al. 1981; Hee and Boyle 1988; Karstensen and Lund 1989; Dulski 1994; Münker 1998; Liang et al. 2000), microwave dissolution (Lamothe et al. 1986; Borman 1988; Kingston and Jassie 1988; Mathes 1988; Matusiewicz and Sturgeon 1989; Kemp and Brown 1990; Nölter et al. 1990; Totland et al. 1995; Yoshida et al. 1996), Na_2O_2 sintering (Robinson et al. 1986; Potts 1987; Chao and Sanzolone 1992), and fusions with alkali fluxes such as $LiBO_2$, $Li2B_4O_7$, Na_2O_2 etc. (Burman et al. 1978; Bankston et al. 1979; Walsh and Howie 1980; Brenner et al. 1980; Norman et al. 1989).

Despite this multitude of techniques, in practical ICP-MS analysis, caution must be taken when adapting them for multi-element determination since some of the digestion procedures were only developed for measurement of one or several elements. In fact, the solution chemistry involved in many dissolution procedures is poorly understood and refinements and understanding of these techniques have not kept pace with the rapid development in modern analytical instrumentation (Totland et al. 1992).

Hence, one of the main aims of this thesis is a systematic investigation on the decomposition technique for a wide range of geological reference materials with a view to achieving complete dissolution.

1.3 Low Abundance Analysis

Lithophile trace elements can be present at very low levels (~ng g^{-1}) in some rocks, particularly ultramafic rocks (such as peridotite and dunite), and the limited instrumental sensitivity generally associated with older generations of quadrupole ICP-MS means that their quantitative measurement often becomes problematic and complicated. For instance, Makishima and Nakamura (1997) used flow injection ICP-MS to measure Rb, Sr, Y, Cs, Ba, REE, Pb, Th and U at ng g^{-1} levels in silicate samples.

The determination of high field strength elements (HFSE) in solution is particularly difficult because:

1. HFSE are often contained in refractory minerals that are resistant to acid attack, and they also have a tendency to polymerise or hydrolyse in aqueous solution.
2. Memory effect is one of the most important problems associated with the accurate measurement of HFSE. As reported by McGinnis et al. (1997), the HFSE generally exhibit a "sticky" nature in which they may adhere to the surfaces of the sample introduction system, allowing for the possibility of remobilisation by trace amounts of hydrofluoric acid (HF) present in the rock solution.
3. Sample dissolution often needs to be carried out in strict "clean-room" laboratory conditions when analysing low levels (Ionov et al. 1992).

For the purpose of low level analysis, this thesis presents an application of HR-ICP-MS techniques in conjunction with high pressure $HClO_4$/HF digestion by developing a reliable analytical method for low abundance analysis. The technique is tested on six selected low abundance reference materials (including BIR-1, DTS-1, PCC-1 etc.).

1.4 Measurement of Lead Isotope Ratios

The study of the lead isotopic composition of rocks and minerals began in the early years of the twentieth century and was initially used as a geochronological tool (Holmes 1913). After World War II, with the advent of better analytical

instrumentation, notably TIMS, lead isotopic analysis became widely applied. The widespread use of lead isotopes in geological studies began in the 1950s & 60s (Cannon et al. 1961 and Rankama 1963) and it has received increasing attention since then (Doe and Stacey 1974; Gulson and Mizon 1979; Smith et al. 1984; Gulson 1986; Marcoux and Möelo 1991; Le Guen et al. 1992; Arribas and Tosdal 1994; Foley and Ayuso 1994; Arias et al. 1996; Childe 1996).

Currently, TIMS is the technique of choice for all types of geological lead isotope measurements in order to achieve satisfactory accuracy and precision. However, the relative high cost of the instrumentation and complicated chemical pre-treatment of geological samples, usually involving ion exchange separation due to serious isobaric interferences (Potts 1987), have imposed serious limitations on the widespread application of Pb isotope techniques to routine geological exploration programs.

The ability of quadrupole ICP-MS to measure lead isotopic ratios was initially demonstrated by Smith et al. (1984), followed by Date and Cheung (1987) and Longerich et al. (1992). However, quadrupole ICP-MS instruments are specifically designed for the scanning of relatively large mass ranges, and such are inherently less stable than magnetic sector ICP-MS and cannot achieve the accuracy and precision needed for isotope ratio analysis.

After carefully considering all possible causes of instrumental bias, Begley and Sharp (1997) recently undertook a rigorous investigation of lead isotopic ratios using a quadrupole ICP-MS instrument. The precision obtained from the analysis of NIST Standard Reference Material (SRM) 981 Natural Lead ranged from 0.04 to 0.12% (depending on the ratio studied). This accuracy and precision has been until now the best presented from a quadrupole ICP-MS instrument. However, despite the use of high Pb concentration (1000 ng g^{-1}) in testing solutions, Begley and Sharp (1997) were still unable to report the ratio data of $^{207}Pb/^{204}Pb$ and $^{208}Pb/^{204}Pb$ using an early model quadrupole ICP-MS instrument (VG Micromass Model 12-12S).

Sector field ICP-MS overcomes many of the inherent problems exhibited by quadrupole instruments, and is becoming more used for the precise measurement of lead isotopic ratios (Vanhaecke et al. 1996, 1997; Shuttleworth et al. 1997). To date

it has been applied in a variety of fields such as environmental and biological analysis, and the monitoring of radionuclides (Becker and Dietze 1997). However, to date little has been made of the sector field ICP-MS for measuring lead isotopic ratios in geological samples (Shuttleworth et al. 1997).

In this thesis, the feasibility of precisely measuring lead isotope ratios in geological materials (mainly sulfides) using sector field ICP-MS (Finnigan MAT Element) and a recent quadrupole ICP-MS (HP 4500 *plus*) is systematically investigated. In addition, as a case study, a group of selected sulfides from the Lady Loretta deposit is measured for lead isotopic compositions using the HP 4500 ICP-MS.

1.5 Measurement of HFSE

HFSE play an important role in understanding and interpreting petrogenetic processes (Sun and McDonough 1889; Rollinson 1993). However, due to their tendency to hydrolyse in aqueous solutions, reliable measurement of HFSE has been a challenge (e.g. Perrin 1964; Heslop and Jones 1976; Münker 1998).

Using lithium metaborate fusion and cupferron separation, Hall and Pelchat (1990) analysed geological reference materials for Zr, Nb, Hf and Ta using a quadrupole ICP-MS. Although a final acidity of approximately 1 M HNO_3 was recommended in the study to prevent the hydrolysis of HFSE in solution, most Ta results in reference basalts (BHVO-1, BIR-1), granites (G-2, GA, GH and GS-N), syenites (STM-1, SY-2 and SY-3), marine sediments (MESS-1 and BCSS-1) and lake sediments (SL-1 and Sl-3) were lower than recommended values. Similarly, using HF-HNO_3-HCl Savillex beaker digestion and keeping 1 M HNO_3 in final solution, low results for both Nb and Ta in the reference basalt, gabbro, diabase, pyroxenite, dunite and syenite were reported by Poitrasson et al. (1993). Although Hall et al. (1990) tried using HF in final solution to form ZrF_7^{3-}, HfF_7^{3-}, NbF_7^{2-} and TaF_7^{2-} and hence prevent the hydrolysis of HFSE, low results for Ta in geological reference materials were also found. This indicates that the HFSE-fluoride simple complexes are not stable enough to prevent the HFSE cations from hydrolysing in aqueous solutions. In another investigation, ICP-MS determination of HFSE in peridotites and their minerals was performed by Ionov et al. (1992) using HF-$HClO_4$ mixture (1:1) digestion, the

measured concentrations of Zr, Nb, Hf and Ta were found to be lower than those provided by isotope dilution-spark source mass spectrometry (ID-SSMS) and instrument neutron activation analysis (INAA). Low results for Zr, Nb, U Th were also noted with the analysis of Japanese rock reference samples (including basalt, granodiorite, rhyolite, gabbro and andesite) by ICP-MS (Yoshida et al. 1996). Preliminary work for this thesis, despite the use of H_2SO_4/HF high pressure digestion method and fresh solution determinations, yielded low HFSE recoveries for high HFSE abundance rock standards, due to the hydrolysis of HFSE in aqueous solutions. For instance, recoveries for Nb, Hf and Ta were found to less than 50% of published values (Govindaraju 1994). Low Ta recovery was also found for samples containing more than 1 $\mu g\ g^{-1}$ in solid, such as AC-E, GSR-1, YG-1, TASBAS and TASGRAN.

This study reports the investigation of a range of chelating reagents to prevent or minimise hydrolysis of HFSE in aqueous solutions in order to obtain reliable analytical data for HFSE in geological materials.

1.6 Scope of this Study

In summary, the major objectives of this project have been to evaluate and optimise a variety of geoanalytical techniques based on ICP-MS analysis of multi trace elements and lead isotope ratios in geological samples. Specifically, I report herein:

- an investigation of the performance characteristics of HR-ICP-MS associated with the measurement of multi trace elements in geological samples.

- optimized decomposition techniques for the analysis of geological samples (mainly silicates such as basalt, granite, dunite, peridotite, dolerite, serpentine etc.) by ICP-MS.

- application of a high pressure acid digestion technique to low abundance (at $ng\ g^{-1}$ levels in solid samples) analysis.

- an investigation of the use of complexing reagents to improve the accuracy of HFSE measurements in geological materials using ICP-MS.

- development of a method for the accurate and precise measurement of lead isotope ratios in geological samples using HR-ICP-MS, and study the interference and correction of Hg and W on the measurement of Pb isotope ratios.

- development of a method for the accurate and precise determination of lead isotopic compositions in geological samples using a modern quadrupole ICP-MS.

Application of these techniques is demonstrated via two case studies:

- an evaluation of the relative compatibility/incompatibility of a range of trace elements, especially the rarely analyzed (in basaltic rocks) Mo, Sn and Sb in a suite of basaltic glasses from Macquarie Island in the Southern Ocean.

- a Pb isotope investigation of a representative suite of sulfides from the Lady Loretta sediment hosted Pb-Zn deposit in northern Australia.

Chapter 2

PERFORMANCE CHARACTERISTICS OF SECCTOR FIELD ICP-MS FOR THE DETERMINATION OF TRACE ELEMENTS IN GEOLOGICAL MATERIALS

2.1 Introduction

Although ICP-MS has its origin in the 1970s, in comparison with some other analytical techniques (such as INAA, XRF and ICP-AES etc.), it is still a relatively new technique for high precision trace element analysis in geological samples. In the past, the analytical performance of the quadrupole ICP-mass spectrometer has been studied and the quadrupole ICP-MS has been successfully applied to the analysis of trace elements in geological samples by several workers (e.g. Riddle et al. 1988; Garbe-Schönberg 1993; Hollocher and Ruiz 1995; Eggins et al. 1997). By contrast, little has been reported on the analytical performance, and applications to the analysis of trace elements in geological samples by sector field ICP-MS. In this chapter, comprehensive performance characteristics of a sector field ICP-MS (Finnigan MAT Element ICP-mass spectrometer with a double-focusing magnetic sector mass analyser of reversed Nier-Johnson geometry) for determination of trace elements in geological materials will be discussed.

2.2 Experimental

2.2.1 Reagents and Standards

HF (50% w/w Analar, AR grade), HCl (33% w/w BDH, AR grade) and HNO_3 (70% w/w BDH, AR grade) were all used in this study for sample decomposition. HCl and HNO_3 were further doubly distilled in a sub-boiling quartz distillation system before use. HF was doubly distilled in a sub-boiling Teflon distillation system and ultra-

pure $HClO_4$ (70% w/w ARISTAR®, BDH Chemicals) was also used. Ultra-pure water (≥ 16.7MΩ) used in the study was first distilled with a glass distillation system and then further purified with a MODULAB Water Purification System (Continental Water System Corporation, Melbourne, Australia).

External calibration standards were prepared by gravimetric serial dilution from 100 $\mu g\ ml^{-1}$ multi-element standards (QCD Analyst, USA). The standard solutions were prepared at the beginning of each analytical sequence with doubly distilled water and 2% HNO_3.

Indium and lutetium standard solutions ($1000 \pm 3\ \mu g\ ml^{-1}$ in 2% HNO_3, High-Purity Standards (South Carolina, USA)) were diluted to working concentration in 2% HNO_3 before use as internal standards for ICP-MS analysis. An ^{84}Sr isotope solution (83.2% ^{84}Sr, provided by the University of Adelaide), Re and Bi (high purity standard from Spex Chemical & Sample Preparation, USA) were additionally used as internal standards for comparison purposes.

2.2.2 Instrumentation

A Finnigan MAT Element ICP-mass spectrometer (Bremen, Germany) was used in this study (**Figure 2.1**). The instrument is in operation at the Central Science Laboratory of the University of Tasmania, and is equipped with a compact double-focusing magnetic sector mass spectrometer of reversed Nier-Johnson geometry. The mass range of the double-focusing magnetic sector field analyser extends from 5 to 260 atomic mass units. Pre-defined resolution settings ($m/\Delta m$ at 10% valley definition) of 300 (low), 3000 (medium) and 7500 (high) allow the operating resolution to be adjusted, depending mainly on the analytical matrices met. As a result, this type of instrumentation is often referred to as sector field or high-resolution (HR) ICP-MS. Both "sector field ICP-MS" and "HR-ICP-MS" are used throughout this thesis. In this investigation, isotopes of interest were measured using electric scanning, with the magnet held at fixed mass. Instrument tuning and optimisation were performed daily using a 10 $ng\ g^{-1}$ multi-element solution containing the elements of interest. In general, instrument parameters were adjusted to obtain optimum intensity and stability. The typical instrumental settings for the

study are summarised in **Table 2.1**. Further details regarding this instrument have been reported elsewhere (Moens et al. 1994; Townsend et al. 1998; Robinson et al. 1999; Yu et al. 2000).

Table 2.1. Typical instrumental settings for the Finnigan MAT Element

Instrument	Finnigan MAT Element
Resolution (m/Δm)	Low = 300, Medium = 3000
Rf power	~1250 W
Nebuliser	Meinhard
Coolant argon flow rate	12-13 l/min
Auxiliary argon flow rate	0.8-1 l/min
Nebuliser argon flow rate	0.8-1.2 l/min (adjusted daily to obtain optimum signal intensity and stability)
Sample uptake rate	~0.75ml/min
Spray chamber	Scott (double pass) type cooled at 3.5-5 °C
Sampler cone	Nickel, 1.1 mm aperture i.d.
Skimmer cone	Nickel, 0.8 mm aperture i.d.
Instrument tuning	Performed using a 10 ng g^{-1} multi-element solution
Ion transmission	~1,000,000 cps per 10 ng g^{-1} indium at low resolution
Rinse time between standards or samples	200 sec (with 5% HNO_3)
Takeup and equilibrium time	240 sec
Scan type	Magnetic jump with electric scan over small mass range
Ion sampling depth	Adjusted daily in order to obtain maximum signal intensity
Ion lens settings	Adjusted daily in order to obtain maximum signal intensity and optimum resolution

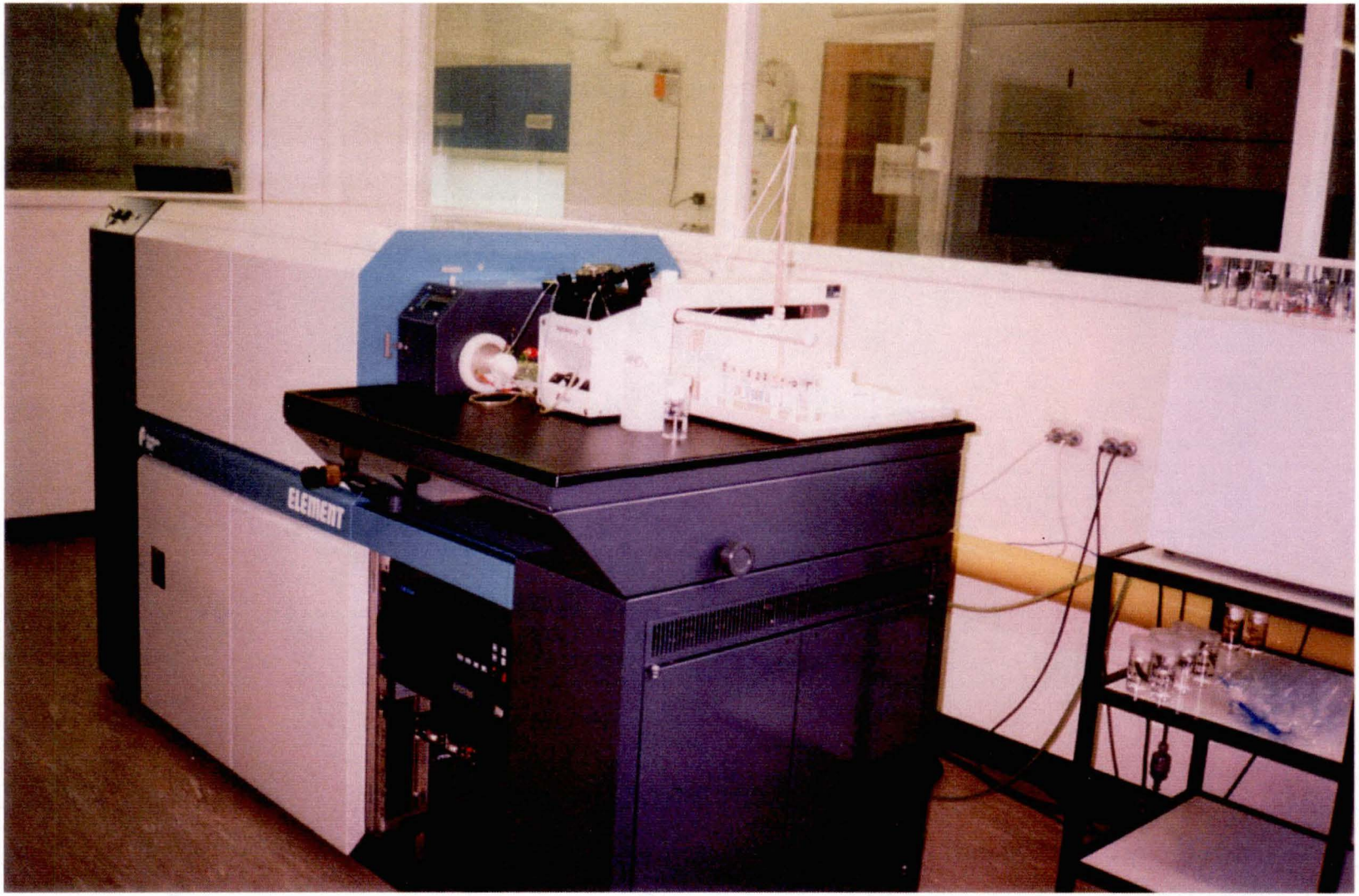
ELEMENT

2.3 Instrumental Sensitivity

Instrumental sensitivity (counts s^{-1} per ng g^{-1}) depends on the efficiency of sample introduction, ion transmission through the plasma - vacuum interface and lens stack, instrumental tuning, and the performance of the detector in ICP-MS analysis.

The mean sensitivities (counts s^{-1} per ng g^{-1}) for REE at low resolution (R = 300) and medium resolution (R = 3000) are given in **Figure 2.2.** The mean instrumental sensitivities at low resolution are the average intensity values of 7 separate measurements during a 12-hour analytical run. **Figure 2.2** (top) shows that HR-ICP-MS is a very sensitive analytical technique. The intensity range for REE is between 103925 and 52989 counts s^{-1} per ng g^{-1} from the intensity normalised to 100% isotopic abundance. The measured instrumental intensities for REE are in the range of 16018 to 103925 counts s^{-1} per ng g^{-1}. Gadolinium shows the lowest instrumental intensity (16018 counts s^{-1} per ng g^{-1}) simply due to the lowest isotope abundance of 15.68% for the isotope ^{157}Gd. On the other hand, the normalised intensities for REE are in the range of 52989 to 103925 counts s^{-1} per ng g^{-1}. Terbium has the maximum normalised intensity, whereas Y has the minimum normalised intensity. The saw-toothed shape for the measured intensity curve is largely produced by the difference in isotopic abundance. For instance, the intensities for ^{139}La, ^{141}Pr, ^{159}Tb, ^{165}Ho, ^{169}Tm and ^{175}Lu with 100% or close to 100% isotopic abundance are clearly higher than those (ie. ^{140}Ce 88.50%, ^{146}Nd 17.22%, ^{147}Sm 14.97%, ^{151}Eu 47.80%, ^{157}Gd 15.68, ^{163}Dy 24.97%, ^{167}Er 22.94% and ^{172}Yb 21.82%) with lower isotopic abundance. In addition, the difference in the ionisation energy may also be responsible in part for the saw-toothed shape for the measured intensity curve (Jarvis et al. 1992).

Due to strong interferences by silicon oxides (such as $^{29}Si^{16}O$ and $^{28}Si^{16}O^{1}H$, also see Finnigan MAT Element ICP-MS Interference Table for more information), Sc is generally determined at medium resolution (R = 3000). In practical HR-ICP-MS analysis, in order to avoid severe interferences from a complicated matrix, Y and REE are also determined at medium resolution. Hence, the instrument intensities for Sc, Y and REE are also described herein. Normally, the instrumental intensities of REE at medium resolution are much lower than those measured at low resolution.

The mean instrumental sensitivities at medium resolution were the average intensity values of 6 separate measurements during a 10-hour analytical sequence. **Figure 2.2** (bottom) shows that HR-ICP-MS is still a very sensitive analytical technique, even at medium resolution. The measure intensity is between 176 and 2384 counts s^{-1} per ng g^{-1}. Again Gd gave the lowest measured intensity value mainly due its low isotope abundance. The intensity range for REE is between 2535 and 1122 counts s^{-1} per ng g^{-1} from the intensity normalised to 100% isotopic abundance. It also can be found that Dy has the maximum intensity, and Tb has the lowest intensity from the intensity normalised to 100% isotopic abundance. Similarly, the saw-toothed shape for the measured intensity curve is mainly caused by the difference in isotopic abundance and ionisation energy of individual isotopes.

The mean sensitivities (counts s^{-1} per ng g^{-1}) for trace elements at low resolution (R = 300) during a 10-hour analytical run are given in **Figure 2.3.** The intensity range for trace elements is from 98748 to 12318 counts s^{-1} per ng g^{-1} from the intensity normalised to 100% isotopic abundance, which is much higher than the normal quadrupole ICP-MS (Begley and Sharp 1997). Uranium has the maximum intensity, and Te has the minimum intensity from the intensity normalised to 100% isotopic abundance. The saw-toothed shape for the measured intensity curve is also caused by the difference in isotopic abundance and ionisation energy of individual isotopes. The isotopic abundances of trace elements used in this work are 72.15% for ^{85}Rb, 82.56% for ^{88}Sr, 51.46% for ^{90}Zr, 100% for ^{93}Nb, 15.72% for ^{95}Mo, 24.03% for ^{118}Sn, 57.25% for ^{121}Sb, 6.99% for ^{125}Te, 100% for ^{133}Cs, 11.32% for ^{137}Ba, 27.14% for ^{178}Hf, 99.99% for ^{18}Ta, 70.5% for ^{205}Tl, 52.3% for ^{208}Pb, 100% for ^{209}Bi, 100% for ^{232}Th and 99.27% for ^{238}U. As clearly seen **in Figure 2.3**, Mo, Te and Ba gave very low values of the measured instrumental intensities mainly due to their low isotope abundances.

Comparison between sector field and quadrupole ICP-MS methods: Sector field ICP-MS is more sensitive than quadrupole ICP-MS in terms of signal intensity (counts per second - cps). For instance, the sensitivity for the HR-ICP-MS used in this study (Finnigan MAT Element ICP-mass spectrometer with a double-focusing magnetic sector) can normally reach as high as (1.2-1.8) x 10^5 counts s^{-1} per ng g^{-1}

^{115}In, whereas the attainable sensitivity for a quadrupole instrument has been reported as (2-5) x 10^4 counts s^{-1} per ng g^{-1} ^{115}In (Eggins et al. 1997).

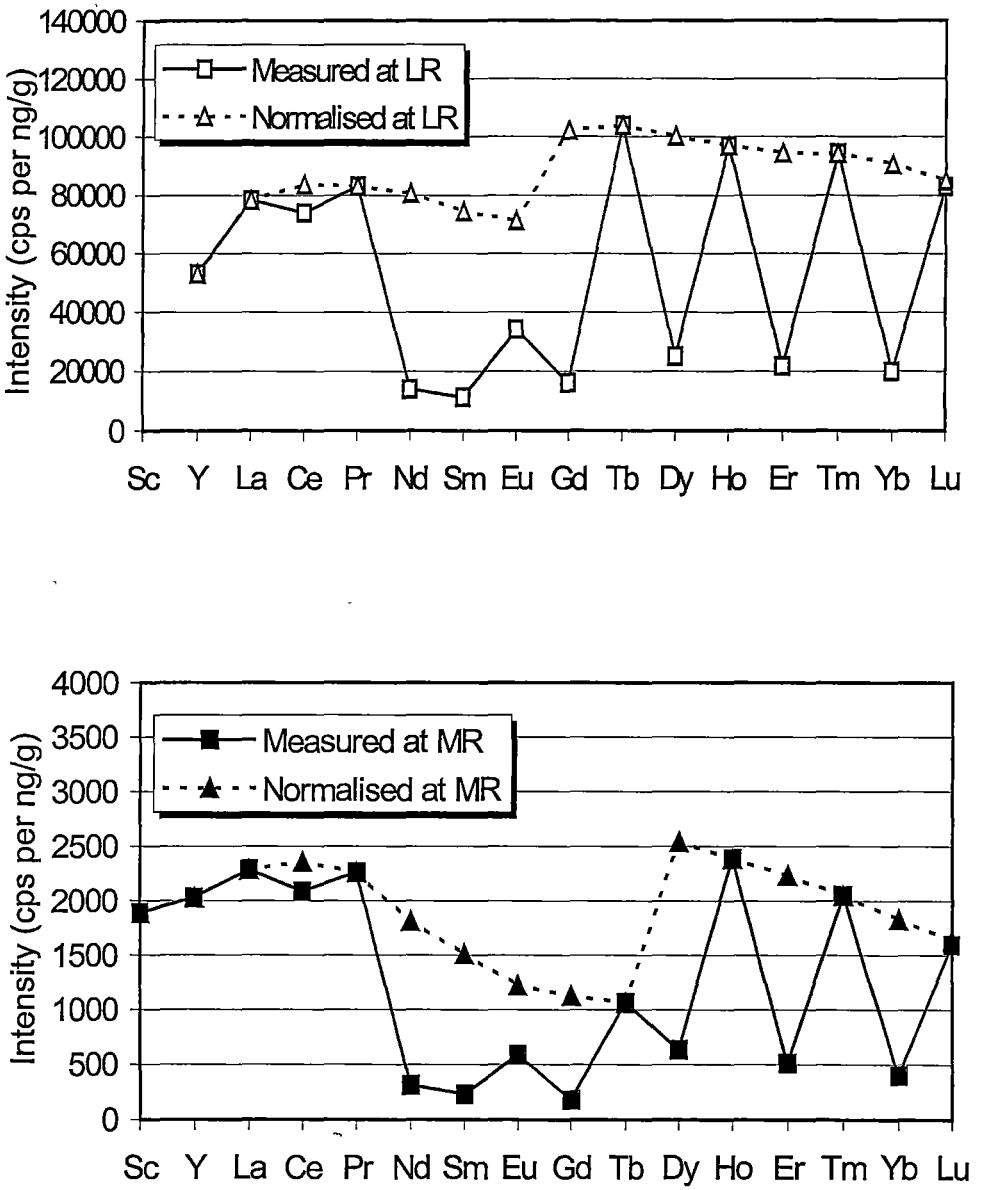

Figure 2.2. Mean instrumental sensitivity for REE at both LR (low resolution) (top, R = 300) and MR (medium resolution) (bottom, R =3000). The testing solutions were in 2% HNO_3. The measured shows the instrumental intensity at the analytical masses (^{45}Sc, ^{89}Y, ^{139}La, ^{140}Ce, ^{141}Pr, ^{146}Nd, ^{147}Sm, ^{151}Eu, ^{157}Gd, ^{159}Tb, ^{163}Dy, ^{165}Ho, ^{167}Er, ^{169}Tm, ^{172}Yb and ^{175}Lu). The normalised plots show the intensity normalised to 100% isotopic abundance.

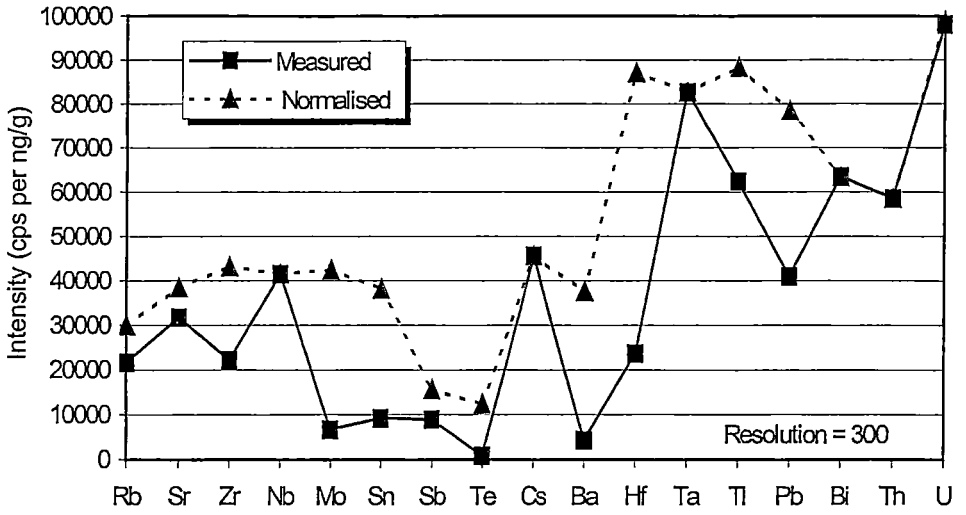

Figure 2.3. Mean instrumental sensitivity for trace elements showing the average instrumental intensity of seven analytical runs. The testing solutions were in 2% HNO_3. Masses used in this investigation are ^{85}Rb, ^{88}Sr, ^{91}Zr, ^{93}Nb, ^{95}Mo, ^{118}Sn, ^{121}Sb, ^{125}Te, ^{133}Cs, ^{137}Ba, ^{178}Hf, ^{181}Ta, ^{205}Tl, ^{208}Pb, ^{209}Bi, ^{232}Th and ^{238}U.

2.4 Instrumental Drift

One of the principal limitations on the accuracy of the ICP-MS technique is the drift of the instrumental response relative to the calibration standard during the course of an analytical sequence. Instrumental drift is often a complicated function of mass and can be the single most important factor in determining the accuracy of an ICP-MS analysis (Norman 1997). The instrumental drift expressed as the maximum deviation of a single measurement on the calibration standard from the average is usually less than 20% within one shift (8-12 hour) run (Jackson et al. 1990). With a quadrupole ICP-MS method, several internal standards are generally spiked into sample solutions to correct the instrumental drift (Jackson et al. 1990; Jenner et al. 1990; Eggins et al. 1997). For instance, Jenner et al. (1990) used three mass-dependent drift correction factors to correct the instrumental drift. A light mass correction factor, based on either Rb or Y, was applied to Li through Mo; a middle mass correction factor, based on Ce, was applied to Cs to W; and a heavy mass correction factor, based on Pb, was applied to Tl through U.

In this work, however, only indium was spiked into the sample solutions as the internal standard to correct the instrumental drift. Normalised intensity drift curves for both uncorrected and corrected instrumental intensity drift in a 10-hour analytical run have been studied using a 10 ng g^{-1} calibration standard solution (multi-element atomic spectroscopy standards from Perkin-Elmer Corporation, USA) (**Figures 2.4 and 2.5**). Mass range covered in this investigation was from 45 to 238 amu. Isotopes used for the study are ^{45}Sc, ^{89}Y, ^{118}Sn, ^{139}La, ^{175}Lu, ^{208}Pb and ^{238}U. **Figure 2.4** shows that the normalised intensity drift of uncorrected intensity was generally between 0.93 and 1.08 within a 10-hour analytical run. In other words, the uncorrected instrumental drift for the HR-ICP-MS studied is normally less than ±8% with the 10 ng g^{-1} calibration standard solution over a 10-hour analytical run, which demonstrates that the HR-ICP-MS is generally more stable than the quadrupole ICP-MS (e.g. Jackson et al. 1990; Jenner et al. 1990). **Figure 2.5** shows the normalised intensity drift of ^{115}In corrected intensity (intensity/internal standard intensity). After the correction, a considerable improvement on the normalised intensity drift is observed, and the range of the drift over a 10-hour run was generally from 0.95 to 1.04. Although it has been reported that the stability of the signal measured at low resolution by HR-ICP-MS was found to be similar to the values achieved by a quadrupole instrument (Moens et al. 1995), the results obtained in the present study are comparable or better than previous studies using the quadrupole ICP-MS (e.g. Jackson et al. 1990; Jenner et al. 1990).

In addition, relative standard deviations (%RSD) of instrumental drift for individual elements over a 10 and 12-hour analytical sequence have also been studied. **Figure 2.6** shows the %RSD of the instrumental drift for REE over a 10-hour analytical run at medium resolution (R = 3000). The %RSD value of the uncorrected intensity on a 10 ng g^{-1} calibration standard solution was from 9.67 (^{147}Sm) to 5.71 (^{139}La), and the %RSD value of the instrumental drift for the corrected intensity (intensity/internal standard intensity) was from 6.88 ($^{45}Sc/^{115}In$) to 1.19 ($^{141}Pr/^{115}In$). Similarly, the %RSD of instrumental drift for trace elements with a 12-hour analytical run at low resolution (R = 300) is shown in **Figure 2.7**. The RSD value of the uncorrected intensity (cps) on the 10 ng g^{-1} calibration standard was in the range of 7.14% (^{88}Sr) to 4.35% (^{209}Bi), and the %RSD value of the HR-ICP-MS drift for the corrected intensity was from 4.23 ($^{232}Th/^{115}In$) to 0.24 ($^{125}Te/^{115}In$). In general, the %RSD

value of instrumental drift at low resolution is lower than that at medium resolution, which can be easily explained by the stability of the instrument itself.

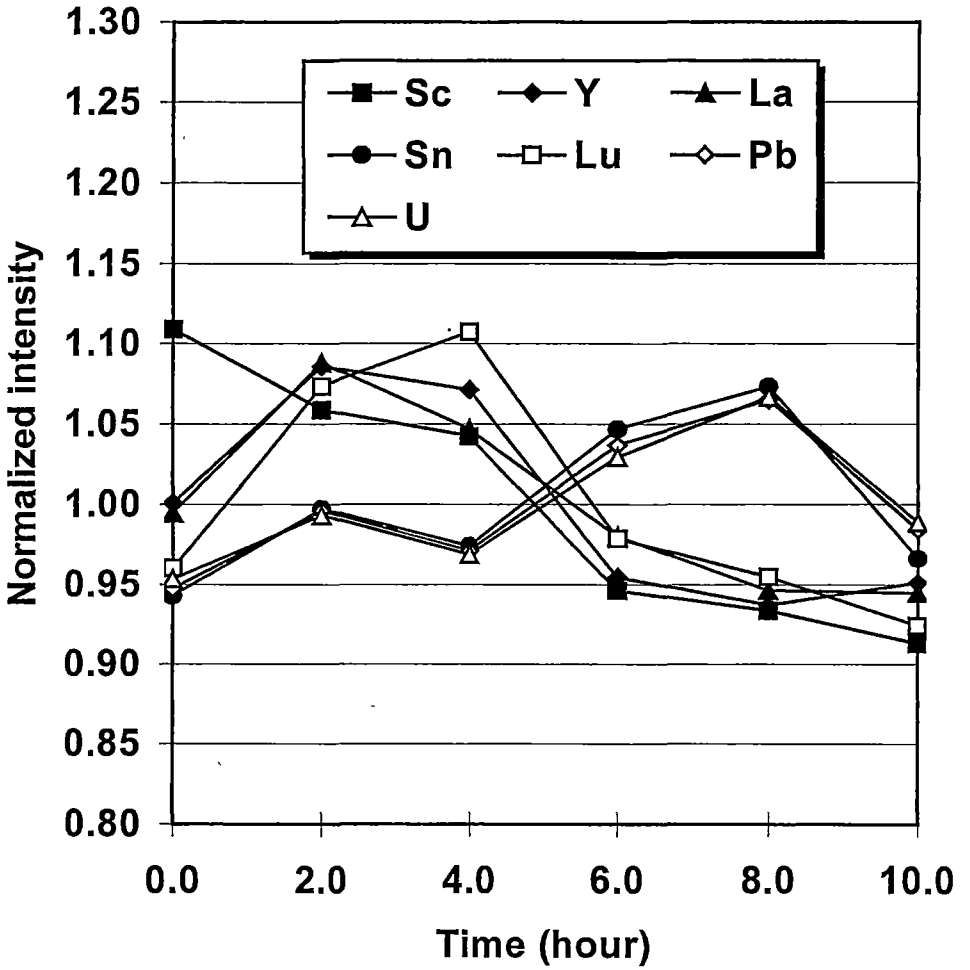

Figure 2.4. Normalised intensity drift curves for uncorrected intensity (counts s^{-1} per ng g^{-1}) drift in a 10-hour analytical run with a 10 ng g^{-1} calibration standard solution (multi-element atomic spectroscopy standards from Perkin-Elmer Corporation, USA). Mass range covered in this investigation was from ^{45}Sc to ^{238}U. HR-ICP-mass spectrometer was operated at low resolution (R= 300) for Sn, Pb and U, and at medium resolution (R = 3000) for Y, Sc, La and Lu. The intensity of each isotope was normalised to the mean value of the 10-hour analytical sequence.

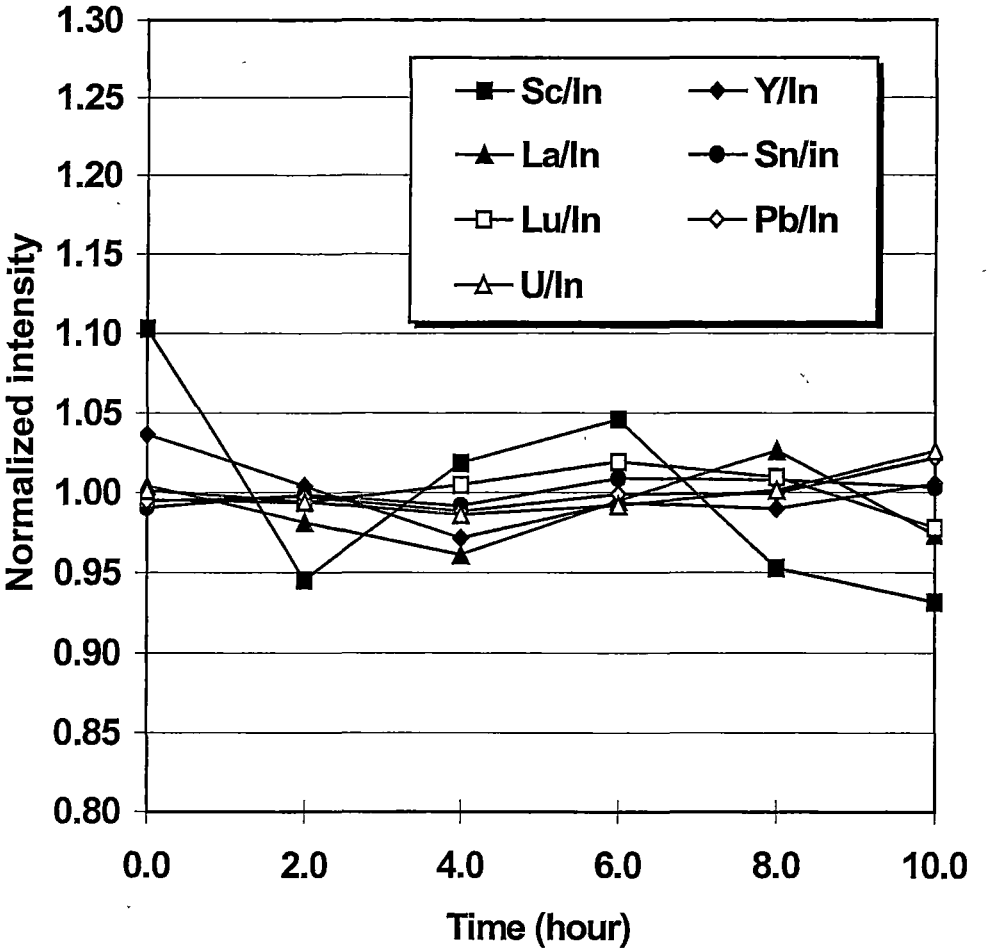

Figure 2.5. Normalised intensity drift curves for the ^{115}In corrected instrumental intensity (counts s^{-1} per ng g^{-1}/counts s^{-1} per ng g^{-1} ^{115}In) drift in a 10-hour analytical run with a 10 ng g^{-1} calibration standard solution (multi-element atomic spectroscopy standards from Perkin-Elmer Corporation, USA). Mass range covered in this investigation was from ^{45}Sc to ^{238}U. HR-ICP-mass spectrometer was operated at low resolution (R= 300) for Sn, Pb and U, and at medium resolution (R = 3000) for Y, Sc, La and Lu. The intensity of each isotope was normalised to the mean value of the 10-hour analytical sequence.

From the above discussion, it can be concluded that the instrumental drift problems can be largely addressed using only ^{115}In corrected intensity (intensity/internal standard intensity) over a large mass range (from 45 to 238 amu in this study), which is obviously one of the advantages of the high resolution ICP-MS over the quadrupole ICP-MS (e.g. Jackson et al. 1990; Jenner et al. 1990; Yu et al 2000).

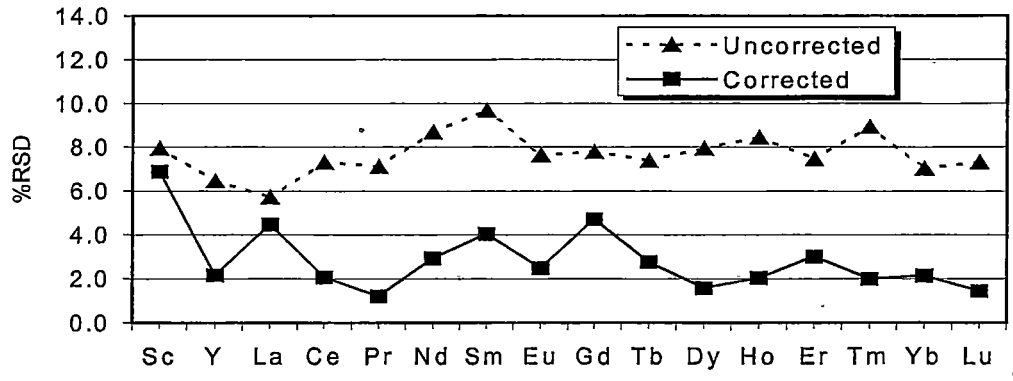

Figure 2.6. The precision (%RSD) of the instrumental drift for REE in a 10-hour analytical sequence. Sector field ICP-mass spectrometer was operated at medium resolution (R = 3000).

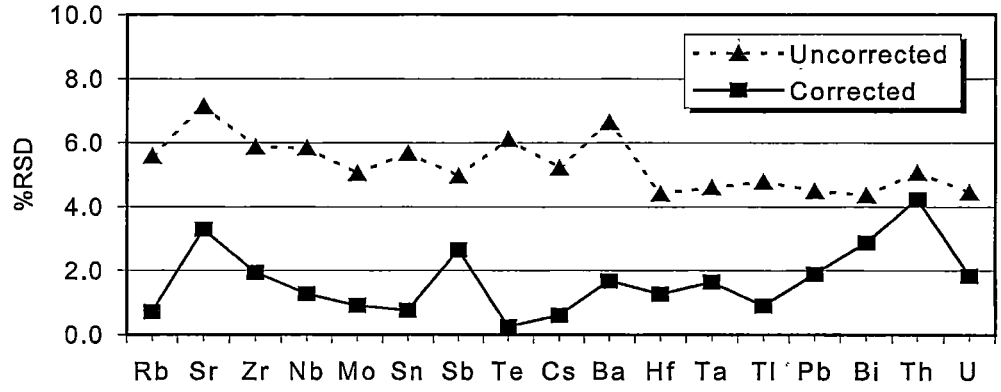

Figure 2.7. The precision (%RSD) of instrumental drift for trace elements in a 12-hour analytical sequence. Sector field ICP-mass spectrometer was operated at low resolution (R = 300).

2.5 Memory Effects

Memory effects are defined as signal enhancements in a sample resulting from erosion of elements deposited along the sample path during nebulisation of a previous sample. In previous studies, the memory effects of a few elements on ICP-

MS measurement were investigated by Jackson et al. (1990), Williams (1992) and Xie et al. (1994). In general, it was found that the magnitude of memory effects is a function of washing time, concentration of the elements in the sample solution, and specific behaviour of certain elements.

In practical sample analysis, it has been found that memory effects can be induced by (1) contaminated Teflon vessels at the decomposition stage, and (2) by the sample introduction system during ICP-MS analysis. These effects can be minimised by thorough cleaning of the Teflon decomposition vessels (using HF) and monitored by measurement of procedure blanks. However, it should also be noted that the reagents used in sample digestion can strongly affect the final result, particularly if there are trace amounts of F^- left in solution.

As a result of its high sensitivity and low instrumental background, the HR-ICP-MS instrument is particularly susceptible to memory effects. In order to test any memory effects, experiments were conducted with the use of external standard solutions. 5% HNO_3 was used to flush for 180 seconds between samples under investigation. To test the memory effect for trace elements at low resolution, testing solutions were analysed in the following sequence: reagent blank, std-1 (1 ng g^{-1}), std-2 (5 ng g^{-1}), std-3 (10 ng g^{-1}), std-4 (25 ng g^{-1}), std-5 (50 ng g^{-1}), reagent blank, followed by 6 repeated analyses in the sequence of 1-ng g^{-1} external standard, 50-ng g^{-1} external standard, and 1-ng g^{-1} external standard. In this work, memory effects were effectively tested by the two 1 ng g^{-1} external standard solutions. The measured concentrations of the two 1 ng g^{-1} external standards (before and after 50 ng g^{-1} external standard flush) are given in **Table 2.2**. It can be seen that the maximum concentration variation due to memory effects was 0.050 ng g^{-1} for Te even after a 50 times higher external standard flush. There were little memory effects observed for Zr, Sb, Ba, Ta, Tl, Bi and U in the present investigation.

Similarly, the memory effects on REE at medium resolution were also investigated and results are given in **Table 2.3**. It can be seen that there were no significant memory effects for Sm, Er, Tm, Yb and Lu. The increase (or elevation) of concentration due to the memory effects was between 0.003 ng g^{-1} for Ce and 0.036 ng g^{-1} for Y.

However, as reported by McGinnis et al. (1997), the high field strength elements (HFSE: Zr, Nb, Hf, Ta, Th and U) generally exhibit a "sticky" nature. In practical ICP-MS work, these "sticky" HFSE can adhere to the surfaces of the sample introduction system, which are subsequently remobilised by trace amounts of hydrofluoric acid (HF) present in the rock solution. Although the memory effects of HFSE are not significant at high concentrations, it has been found that, in order to minimise memory effects, care must be taken when the concentrations of HFSE are below 1 ng g^{-1} in testing solutions (such as the analysis of ultramafic rocks).

In order to investigate the memory effects of HFSE, four replicates (100 mg) of the international basaltic reference material BIR-1 were digested with 3 ml HF + 0.5 ml HNO_3 in Savillex Teflon beakers. The digestion method was similar to that used by Robinson et al. (1999). However, at the evaporation stage, two of the samples were evaporated to dryness twice with the addition of 1 ml $HClO_4$, whereas the other two samples were evaporated to dryness twice with the addition of 1 ml HNO_3. Finally, all of the residues were taken up with 2 ml HNO_3 and 1 ml HCl, and diluted to 100 g. Indium (10 ng g^{-1}) was spiked into each solution as an internal standard before HR-ICP-MS analysis.

For measurement of these samples, a comprehensive wash protocol similar to that reported by McGinnis et al. (1997) was used to minimise memory effects associated with HFSE. Before and after sample solutions, the sample introduction system was flushed with 10% w/w HNO_3 + 0.05% w/w HF solution for 120 seconds, followed by a 120-second flush of 10% w/w HNO_3 only, and a final 120-second flush of 5% w/w HNO_3.

At first, the four BIR-1 solutions were analysed by HR-ICP-MS with an uncleaned sample introduction system (i.e. nebuliser, spray chamber, sampler and skimmer cones were not cleaned and Teflon tubes were not replaced with a new set). Then, the sample introduction system was cleaned by soaking the nebuliser and spray chamber in concentrated HNO_3 overnight, polishing the sampler and skimmer cones with special grinding paste and replacing the Teflon tubes with a new set. The four BIR-1 solutions were re-analysed again with the clean sample introduction system.

Table 2.4 shows HFSE memory effects associated with the determination of basalt BIR-1. It can be seen that, even using this complicated wash protocol, results for the BIR-1 solutions with HNO_3 evaporation showed clear memory effects for Nb, Hf, Ta, Th and U using the unclean sample introduction system, and for Nb and Ta using the clean sample introduction system. No obvious memory effect for Zr was observed due to the high concentration for Zr in BIR-1. Low and consistent Ta results were obtained with $HClO_4$ evaporation and a clean sample introduction system, whereas high and erratic Ta occurred with HNO_3 evaporation. Tantalum from standards and samples hydrolyses easily and is therefore likely to precipitate in the tubing. Subsequent change in F^- concentration might complex the tantalum oxide again and cause the observed overabundance. The different memory effects between $HClO_4$ and HNO_3 evaporation are clearly due to the different boiling points of these acids. That is, $HClO_4$ with a relatively high boiling point of 203 °C can virtually drive off all of the HF (boiling point 112 °C) in solution during the repeat evaporations, whereas the boiling point of HNO_3 (120 °C) is only slightly higher than that of HF, and cannot completely drive off all HF in solution. The trace amounts of F^- left in sample solutions can subsequently remobilise any "sticky" HFSE in the sample introduction area, and memory effects are observed (McGinnis et al. 1997). Although the memory effects of the "sticky" HFSE after HNO_3 evaporation, as shown in **Table 2.4**, can be largely minimised for Hf, Th and U using a clean sample introduction system, the memory effects of Nb and Ta cannot be neglected due to the presence of trace amounts of F^- in sample solutions.

In summary, it was found that a clean sample introduction system and $HClO_4$ evaporation are essential for low Nb and Ta analyses with our instrument. Digestion involving HF/HNO_3 resulted in trace F^- remaining in solution that leached residual Nb and Ta from the instrument. This residual Nb and Ta could neither be removed by extensive cleaning nor by using the McGinnis et al. (1997) wash protocol. It is believed that the latter may be an option on a new instrument when few rock samples have been analysed or if the instrument is dedicated to very low level Nb and Ta samples for long periods (e.g. Ionov et al. 1992; Eggins et al. 1997). However, the risk of remobilising residual Nb and Ta in the sample injection system is great.

Another option (Jenner et al. 1990) is to keep Nb and Ta standard solutions out of the ICP-MS entirely and use a surrogate calibration.

A disadvantage, however, of not having a trace of F^- in the final solution is the danger that Nb and Ta will drop out of solution as a result of hydrolysis. A final sample solution of 2% HNO_3 + 1% HCl (Münker 1998) instead of the more commonly used HNO_3 solution, along with analysing all samples in duplicate or triplicate, helps with this problem for typical Nb-Ta abundances in rocks.

Table 2.2. Memory effects for trace elements at low resolution (R = 300)

Element	Measured concentration of 1 ng g^{-1} external standard (ng g^{-1})		Concentration variations (ng g^{-1})
	Before 50 ng g^{-1} standard flush (n=6)	After 50 ng g^{-1} standard flush (n=6)	
Rb	0.881	0.904	+0.023
Sr	0.990	1.010	+0.020
Zr	0.789	0.781	-0.008
Nb	1.064	1.079	+0.015
Mo	1.004	1.041	+0.037
Sn	0.952	0.953	+0.001
Sb	1.028	1.008	-0.020
Te	1.020	1.070	+0.050
Cs	1.053	1.065	+0.012
Ba	1.305	1.293	-0.012
Hf	0.861	0.872	+0.011
Ta	1.110	1.100	-0.010
Tl	1.081	1.081	0.000
Pb	0.876	0.902	+0.026
Bi	1.011	1.010	-0.001
Th	1.007	1.016	+0.009
U	1.055	1.054	-0.001

n = number of measurements.

Table 2.3. Memory effects for REE at medium resolution (R = 3000)

Element	Measured concentration of 1 ng g^{-1} external standard (ng g^{-1})		Concentration variations (ng g^{-1})
	Before 50 ng g^{-1} standard flush (n=6)	After 50 ng g^{-1} standard flush (n=6)	
Sc	1.008	1.038	0.030
Y	1.030	1.066	0.036
La	1.036	1.058	0.022
Ce	1.044	1.047	0.003
Pr	1.023	1.035	0.012
Nd	0.996	1.031	0.035
Sm	1.052	1.032	-0.020
Eu	1.042	1.076	0.035
Gd	1.028	1.050	0.022
Tb	1.054	1.060	0.006
Dy	1.035	1.048	0.013
Ho	1.016	1.031	0.015
Er	1.032	1.007	-0.025
Tm	1.044	1.039	-0.005
Yb	1.060	1.010	-0.050
Lu	1.052	1.052	0.000

n = number of measurements.

Table 2.4. Example HFSE memory effects associated with the determination of BIR-1

Element	Unclean SIS		Clean SIS		Jochum et al., 1994	Eggins et al. 1997
	$HClO_4$ evap n=2	HNO_3 evap n=2	$HClO_4$ evap n=2	HNO_3 evap n=2		
Zr	15.41	15.15	14.93	15.01	15.4	14.47
Nb	0.398	0.676	0.508	0.659	0.50	0.558
Hf	0.724	0.822	0.623	0.626	0.51	0.562
Ta	0.026	0.490	0.021	0.254	0.030	0.041
Th	0.030	0.045	0.032	0.036	0.031	0.0302
U	0.0094	0.0129	0.0104	0.0104	0.0097	0.0100

SIS = sample introduction system; n = number of measurements; evap = evaporation.

2.6 Interferences

With the introduction of ICP-MS in the early 1980s there was great hope that the technique would finally be free from interferences. However, even in the early publications of the ICP-MS technique (Gray, 1975; Houk et al., 1980) various interference species such as O^+, HO^+, NH_3^+, Ar^{2+}, $^{40}ArH^+$, and $(ArH^+)Ar$ were observed in mass spectra of reference solutions. Some extensive investigations have been carried out to identify, quantify, understand and even eliminate the main problem areas.

The interferences associated with ICP-MS analysis can be divided into two groups, 'spectroscopic' and 'non-spectroscopic'. The former group can be further subdivided into four areas. Those due to:

(1) isobaric overlap, which occurs where two elements have isotopes of essentially the same mass, such as ^{48}Ti and ^{48}Ca;

(2) polyatomic or adduct ions which results from the short lived combination of two or more atomic species present in the plasma, e.g. ArO^+. Argon, hydrogen and oxygen are the dominant species and these may combine with each other or with elements from the analyte matrix;

(3) refractory oxide ions, such as $^{130}Ba^{16}O$, $^{141}Pr^{16}O$, $^{140}Ce^{16}O$, $^{165}Ho^{16}O$ and so on, which occur either as a result of incomplete dissociation of the sample matrix or from recombination in the plasma tail and,

(4) doubly charged ions, controlled by the second ionisation energy of the element and the condition of plasma equilibrium (Jarvis et al. 1992); elements concerned are typically alkaline earths, some transition metals and REE.

The second type of interferences is more complicated and possibly less well understood, but may be broadly divided into suppression/enhancement effects and physical effects caused by total dissolved solids concentration in solutions. It is

normal practice to minimise the non-spectroscopic interferences by avoiding high dissolved solids in solutions and matching the matrixes of samples and standards.

In practical ICP-MS analysis, isobaric overlaps are avoided by using isotopes without isobaric overlap interferences. Or in some cases, the isobaric overlap interferences may be minor due to the low abundance of the interference isotope itself. For instance, Ba, La and Ce all have an isotope at 138 amu, with ^{138}Ba abundance = 71.7%. If Ba at low abundance is measured in a sample, then this would be the preferred isotope, since it provides the most sensitive analysis. In most sample types, however, the concentration of Ba is many times higher than that of La or Ce, and ^{138}La and ^{138}Ce are of low abundance. Thus, in practical analysis, ^{138}Ba can be measured without the need of any correction to the data. Generally speaking, spectroscopic interferences due to the presence of polyatomic ions are not serious and in most cases the polyatomic ions peaks occur only up to 82 amu.

The possible interferences reported by Jenner et al. (1990), Vandecasteele and Block (1995) and Eggins et al. (1997) are doubly charged REE and their oxides are summarised in **Table 2.5**. It can be seen that $^{169}Tm^{2+}$, $^{170}Er^{2+}$, $^{170}Yb^{2+}$ and $^{170}Yb^{2+}$ interfere on ^{85}Rb, and $^{175}Lu^{2+}$, $^{176}Lu^{2+}$ and $^{176}Yb^{2+}$ interfere on ^{88}Sr. However, as reported by Vandecasteele and Block (1995), the ratio of M^{2+} to M^{+} is below 0.01% for the doubly charged ions under investigation. Hence, the interferences of doubly charged ions were not considered in this study. Although the overall oxide interferences with ICP-MS have been investigated by Vaughan and Horlick (1986) and Vandecasteele and Block (1995), the most significant interferences are barium and REE oxides on the REE, Hf and Ta, as reported elsewhere (Jenner et al. 1990). However, operating conditions affect oxide formation significantly (e.g. Vaughan and Horlick 1986; Lichte et al. 1987).

In order to observe the oxide interferences on REE, pure 100 ng g^{-1} Ba, Ce, Pr, Nd, Gd, Sm, Eu, Tb and Dy solutions prepared from Spex® pure reagents were used to study the signal enhancement (contribution) individually on REE at low resolution. In this study, the oxide interferences shown in **Table 2.5** were investigated. Among them, significant interferences include $^{141}Pr^{16}O$ on ^{157}Gd, followed in order of severity by $^{159}Tb^{16}O$ on ^{175}Lu, $^{156}Gd^{16}O$ on ^{172}Yb, $^{151}Eu^{16}O$ on ^{167}Er, $^{147}Sm^{16}O$ on

^{163}Dy, $^{143}Nb^{16}O$ on ^{159}Tb, and $^{135}Ba^{16}O$ on ^{151}Eu. Under the given experimental condition (the concentration of all of the standards used for the oxide investigation was 100 ng g^{-1}), it has been observed that:

1. for the barium oxide interferences, $^{130}Ba^{16}O$ contributes 0.002 ng g^{-1} of the signal at mass 146 (used to measure Nd), and $^{135}Ba^{16}O$ contribute 0.0148 ng g^{-1} of the signal at mass 151 (used to measure Eu).

2. for the cerium oxide interferences, $^{140}Ce^{17}O$ contributes 0.1714 ng g^{-1} of the signal at mass 157 (used for measuring Gd).

3. for praseodymium oxide interferences, $^{141}Pr^{16}O$ contributes 3.338 ng g^{-1} of the signal at mass 157 (also used for measuring Gd), which is the most severe oxide interferences among those studied in the present work.

4. for neodymium oxide interferences, $^{143}Nd^{16}O$ contributes 0.081 ng g^{-1} of signal at mass 159 (used to measure Tb), $^{145}Nd^{18}O$ and $^{146}Nd^{17}O$ contribute 0.06 ng g^{-1} of the signal at mass 163 (used to measure Dy).

5. for gadolinium oxide interferences, $^{156}Gd^{16}O$ contributes 0.2815 ng g^{-1} of signal at mass 172 (used to measure Yb).

6. for samarium oxide interferences, $^{147}Sm^{16}O$ contributes 0.114 ng g^{-1} of signal at mass 163 (used to measure Dy), and $^{149}Sm^{16}O$ contributes 0.03 ng g^{-1} of signal at mass 165 (used to measure Ho).

7. for europium oxide interferences, $^{151}Eu^{16}O$ contributes 0.124 ng g^{-1} of signal at mass 167 (used to measure Er), and $^{153}Eu^{16}O$ contributes 0.034 ng g^{-1} of signal at mass 169 (used to measure Tm).

8. for terbium oxide interferences, $^{159}Tb^{16}O$ contributes 0.336 ng g^{-1} of signal at mass 175 (used to measure Lu).

9. finally, for dysprosium oxide interferences, $^{156}Dy^{16}O$ contributes 0.065 ng g^{-1} of signal at mass 172 used to measure Yb).

The severity of these interferences are usually compositionally dependent, with the more light rare earth element (LREE) enriched rocks more affected than rock types with LREE depletion or flat REE patterns. The praseodymium oxide interferences on Gd must be corrected for most geological samples according to Pr and Gd concentrations in individual samples. The rest of the REE oxide interferences might be corrected according to their concentration levels in testing solutions. In addition, it should also be noted that although the $^{135}Ba^{16}O$ interference is not severe on Eu at the Ba concentration of 100 ng g^{-1} under this investigation, the interference can become significant when Ba concentration in testing sample is higher than 1000 ng g^{-1}. Therefore, it is advisable that the Ba oxide interferences should be monitored for the analysis of most geological samples using HR-ICP-MS, and corrected when necessary.

In addition, as another advantage of the HR-ICP-MS technique, some of spectral interferences can be eliminated or minimised by operating the instrument at higher resolutions. To obtain a higher resolution, the width of the entrance and exit slits of the HR-ICP mass spectrometer are reduced. Consequently the ion transmission and the sensitivity of the spectrometer will also be decreased. It has been found that the sensitivity drops to about 8% of its original value when changing the resolution from 300 to 3000. At a resolution of 7000 the sensitivity is about 10% of the value observed at the resolution of 3000. In this study, the spectral interference of $^{29}Si^{16}O$ on ^{45}Sc is resolved at medium resolution (R = 3000). In practical ICP-MS analytical work, few spectral interferences by poly-atomic ions require a resolution of higher than 3000. Moens et al. (1995) reported that the interferences of $^{35}Cl^{16}O$ on ^{51}V, $^{40}Ar^{12}C$ on ^{52}Cr and $^{40}Ar^{16}O$ on ^{56}Fe can be resolved at the resolutions of 2572, 2375 and 2505. A resolution of about 7500 is required to eliminate the interference of $^{40}Ar^{35}Cl$ on ^{75}As and of a number of interferences on Ge isotopes (^{72}Ge, ^{73}Ge and ^{76}Ge). However, it should be pointed out that the interferences of isobaric nuclides cannot be resolved by the proposed HR-ICP-MS technique.

Table 2.5. Oxide, doubly charged ion interferences and relative abundances of trace elements

Mass (m/z)	Element	Relative abundance	Oxide and doubly charged ion interferences
45	Sc	100	
85	Rb	72.15	$^{169}Tm^{2+}$, $^{170}Er^{2+}$, $^{170}Yb^{2+}$, $^{169}Tm^{2+}$
88	Sr	82.56	$^{175}Lu^{2+}$, $^{176}Lu^{2+}$, $^{176}Yb^{2+}$
89	Y	100	
90	Zr	51.46	
93	Nb	100	
95	Mo	15.72	
118	Sn	24.03	$^{235}U^{2+}$
121	Sb	57.25	
125	Te	6.99	
133	Cs	100	
137	Ba	11.32	
139	La	99.91	
140	Ce	88.48	
141	Pr	100	
146	Nd	17.22	$^{130}Ba^{16}O$
147	Sm	14.97	
151	Eu	47.82	$^{135}Ba^{16}O$
157	Gd	15.68	$^{141}Pr^{16}O$, $^{140}Ce^{17}O$*
159	Tb	100	$^{143}Nd^{16}O$
163	Dy	24.97	$^{147}Sm^{16}O$, $^{145}Nd^{18}O$*, $^{146}Nd^{17}O$*
165	Ho	100	$^{149}Sm^{16}O$
167	Er	22.94	$^{151}Eu^{16}O$
169	Tm	100	$^{153}Eu^{16}O$
172	Yb	21.82	$^{156}Dy^{16}O$, $^{156}Gd^{16}O$
175	Lu	97.41	$^{159}Tb^{16}O$
178	Hf	27.14	$^{162}Dy^{16}O$, $^{162}Er^{16}O$
181	Ta	99.99	$^{165}Ho^{16}O$
205	Tl	70.50	
208	Pb	52.30	
209	Bi	100	
232	Th	100	
238	U	99.27	

* Presented in Finnigan MAT ICP-MS Interference Table.

2.7 Internal Standards

The calibration or correction of one element using a second as a reference point is used in many forms of analytical atomic spectrometry, e.g. ICP-AES. An internal standard can be used to monitor and correct short and long-term instrumental signal fluctuation and to correct unspecified matrix effects (Jarvis et al. 1992). The effectiveness of an internal standard requires that its behaviour accurately reflects that of other elements. For instance, if an internal standard is used to calibrate for a second element, either their sensitivities should be the same or the sensitivity relationship between the two should be known and remain constant. Therefore, to some extent, the use of an internal standard in ICP-MS is a historical inheritance from ICP-AES.

In order to monitor and correct the fluctuation in instrumental signal and matrix effects, many users of quadrupole ICP-MS (e.g. Garbe-Schönberg 1993; Hollocher and Ruiz 1995; Eggins et al. 1997; Norman et al. 1998) found the implementation of several internal standards for data correction very attractive. Schönberg (1993) used ^{9}Be, ^{115}In and ^{187}Re as internal standards to determine 37 elements in 28 international rock standards. NIST glass reference materials 611, 612, 614 and 1834 were analysed using 5 internal standards (e.g. ^{9}Be, ^{71}Ga, ^{115}In, ^{187}Re and ^{209}Bi) (Hollocher and Ruiz 1995). In another investigation, Eggins et al. (1997) used 9 internal standards (e.g. ^{6}Li, ^{84}Sr, ^{103}Rh, ^{115}In, ^{147}Sm, ^{169}Tm, ^{187}Re, ^{209}Bi and ^{235}U) to measure more than 40 trace elements in geological samples. In routine ICP-MS analysis, however, it can be troublesome to select a group of internal standards. The choice of elements is actually limited by those which are naturally present, since a known or constant amount of an internal standard is added to each blank, standard and sample. The internal standard should not suffer from any isobaric overlap or polyatomic ion interference, or indeed generate them on isotopes of interests. As an alternative, an element which occurs naturally in the sample, and which has been determined prior to ICP-MS analysis, can be chosen. In this case, the concentration will probably vary from sample to sample and this must be accounted for during the final data manipulation stage.

In order to simplify the analytical procedure, the possibility of using a single internal standard (^{115}In) instead of several internal standards for the measurement of trace and rare earth elements by HR-ICP-MS is investigated in this section. Preliminary HR-ICP-MS results indicated only one internal standard (^{115}In) may suffice for the analysis of rock solutions of 1000x dilution. In order to confirm this, three rock standard materials (BHVO-1, TAFAHI and TASBAS) were selected for the investigation. Among them, BHVO-1 is an international basalt standard, TAFAHI is an in-house basalt standard at Research School of Earth Sciences, Australian National University (Eggins et al. 1997), and TASBAS is an in-house basalt standard at the Geology Department, University of Tasmania (Robinson et al. 1986). The later has been analysed by several laboratories using different techniques, such as X-ray fluorescence (XRF), spark-source mass spectrometry (SSMS), neutron activation analysis (NAA) and quadrupole ICP-MS. The three samples were digested in screw-top Savillex beakers using HF-HNO_3 acid digestion. The measured concentrations for trace and rare earth elements with either a single (^{115}In) or 4 (^{84}Sr, ^{115}In, ^{175}Lu and ^{209}Bi) internal standards are summarised in **Tables 2.6 to 2.8**.

With the four internal standard investigation, each selected isotope standard was used for a particular mass range (e.g. using ^{84}Sr to correct ^{45}Sc to ^{95}Mo, ^{115}In to correct ^{118}Sn to ^{146}Nd, ^{175}Lu to correct ^{147}Sm to ^{181}Ta, and ^{209}Bi to correct ^{205}Tl to ^{238}U). In addition, the concentration values for Sc, Rb, Y, Zr, Nb and Mo were corrected for ^{84}Sr according to the Sr concentrations in references.

Tables 2.6 to 2.8 indicate that, as a rule, for HR-ICP-MS the measured trace and rare earth element concentrations were almost identical for BHVO-1, TAFAHI and TASBAS using both the single and four internal standards. An excellent correlation of the trace elemental concentrations for the three selected basaltic reference materials-BHVO-1, TAFAHI and TASBAS between single and four internal standards can be clearly seen in **Figures 2.8 to 2.10,** which further demonstrates that a single internal standard (^{115}In) can provide excellent analytical results by HR-ICP-MS.

In this study, it has also been investigated whether there is any difference using different elements as single internal standard. Rhenium was used as one of the

internal standards in ICP-MS analysis by several workers (Dulski 1992; Garbe-Chönberg 1993; Hollocher and Ruiz 1995; Eggins et al. 1997; Pin and Joannon 1997). Although ^{187}Re (62.6% abundance) was used as internal standard in most cases, ^{185}Re (37.4% abundance) has been chosen as internal standard in the present investigation considering the ^{187}Os interference on ^{187}Re. **Figures 2.11 and 2.12** give the comparison of the HR-ICP-MS results for BHVO-1 and TASBAS using ^{115}In and ^{185}Re as internal standards respectively. Generally speaking, both indium and rhenium can be used as internal standards for HR-ICP-MS analysis. The differences between the measured results and reference values for BHVO-1 and TASBAS are generally less than ±5% using ^{115}In as internal standard and ±10% using ^{185}Re as internal standard. On the other hand, it also can be seen that systematically lower results were generated when ^{185}Re was used as the internal standard. This might be due to (1) the presence of trace rhenium in both BHVO-1 and TASBAS and (2) the difference of the ionisation energies for indium and rhenium (Jarvis et al. 1992). Most of the elements considered in the present study have ionisation energies of less than 7 eV, which are similar to that of indium (Gray 1989). However, it should be pointed out that in routine analytical work, the systematic discrepancy between the two internal standards can be corrected by modifying analytical results against a well-characterised international standard rock, such as BHVO-1, BIR-1, AGV-1 etc. (Govindaraju 1994).

From the above discussion, it is concluded that a single internal standard (^{115}In) is adequate for the accurate measurements of trace and rare earth element in geological materials using sector field ICP-MS.

Table 2.6. A comparison of measured trace element concentrations (μg g^{-1}) for international rock standard BHVO-1 using single and four internal standards

Element	Single internal standard			4 internal standards			Reference
	Conc μg g^{-1}	STD (n=5)	Internal standard	Conc μg g^{-1}	STD (n=5)	Internal standard	value*
Sc	30.0	0.42	^{115}In	30.5	0.46	^{84}Sr	31.8
Rb	9.10	0.07	^{115}In	9.27	0.06	^{84}Sr	11
Y	22.8	0.21	^{115}In	23.9	0.11	^{84}Sr	27.6
Zr	163	2.08	^{115}In	166	1.89	^{84}Sr	179.
Nb	18.2	0.21	^{115}In	18.6	0.18	^{84}Sr	19
Mo	1.06	0.02	^{115}In	1.08	0.02	^{84}Sr	1.02
Sn	1.14	0.35	^{115}In	1.14	0.35	^{115}In	2.1
Sb	0.15	0.01	^{115}In	0.15	0.01	^{115}In	0.16
Te	0.011	0.01	^{115}In	0.011	0.01	^{115}In	0.0064
Cs	0.099	0.002	^{115}In	0.099	0.002	^{115}In	0.13
Ba	128	1.98	^{115}In	128	1.98	^{115}In	139
La	14.6	0.09	^{115}In	14.6	0.09	^{115}In	15.8
Ce	35.7	0.29	^{115}In	35.7	0.29	^{115}In	39
Pr	5.03	0.01	^{115}In	5.03	0.01	^{115}In	5.7
Nd	23.1	0.18	^{115}In	23.1	0.18	^{115}In	25.2
Sm	5.63	0.09	^{115}In	6.24	0.13	^{175}Lu	6.2
Eu	1.91	0.03	^{115}In	2 12	0 04	^{175}Lu	2.06
Gd	5.75	0.05	^{115}In	6.38	0.07	^{175}Lu	6.4
Tb	0.84	0.01	^{115}In	0.93	0.01	^{175}Lu	0.96
Dy	4.81	0.04	^{115}In	5 34	0.06	^{175}Lu	5.2
Ho	0.89	0.01	^{115}In	0.99	0.01	^{175}Lu	0.99
Er	2.32	0.02	^{115}In	2.58	0.05	^{175}Lu	2.4
Tm	0.30	0.002	^{115}In	0.33	0.003	^{175}Lu	0.33
Yb	1.86	0.02	^{115}In	2.06	0.03	^{175}Lu	2.02
Hf	4.25	0.06	^{115}In	4.53	0.08	^{175}Lu	4.38
Ta	1.21	0.12	^{115}In	1.29	0.13	^{175}Lu	1.23
Tl	0.047	0.004	^{115}In	0.048	0.004	^{209}Bi	0.058
Pb	1.96	0.05	^{115}In	1.95	0.03	^{209}Bi	2.6
Th	1.12	0.02	^{115}In	1.11	0.03	^{209}Bi	1.08
U	0.42	0.005	^{115}In	0.41	0.008	^{209}Bi	0.42

Conc = Concentration; STD = Standard deviation.

* Reference values are from Govindaraju (1994).

Table 2.7. A comparison of measured trace element concentrations (μg g^{-1}) for rock standard TAFAHI using single and four internal standards

Element	Single internal standard			4 internal standards			Reference
	Conc μg g^{-1}	STD (n=10)	Internal standard	Conc μg g^{-1}	STD (n=10)	Internal standard	value*
Sc	45.2	1.15	^{115}In	45.8	1.98	^{84}Sr	45.50
Rb	1.72	0.03	^{115}In	1.75	0.07	^{84}Sr	1.75
Y	7.64	0.13	^{115}In	7.81	0.28	^{84}Sr	9 11
Zr	11.3	0.28	^{115}In	11.5	0.46	^{84}Sr	12.07
Nb	0.55	0.07	^{115}In	0.56	0.07	^{84}Sr	0.456
Mo	0.52	0.013	^{115}In	0.52	0.02	^{84}Sr	0.44
Sn	0.22	0.11	^{115}In	0.22	0.11	^{115}In	0.24
Sb	0.024	0.005	^{115}In	0.024	0.005	^{115}In	0.024
Te	0.001	0.002	^{115}In	0.001	0 002	^{115}In	-
Cs	0.067	0.002	^{115}In	0.067	0.002	^{115}In	0.066
Ba	39.7	0.79	^{115}In	39.7	0.79	^{115}In	40.3
La	0.88	0.02	^{115}In	0.88	0.02	^{115}In	0.938
Ce	2.11	0.05	^{115}In	2.11	0.05	^{115}In	2.22
Pr	0.35	0.007	^{115}In	0.35	0.007	^{115}In	0.361
Nd	1.83	0.05	^{115}In	1.83	0.05	^{115}In	1.93
Sm	0.68	0.02	^{115}In	0.68	0.02	^{175}Lu	0.722
Eu	0.30	0.008	^{115}In	0 33	0.008	^{175}Lu	0.305
Gd	1.00	0.02	^{115}In	1.09	0.027	^{175}Lu	1.069
Tb	0.18	0.004	^{115}In	0.20	0.004	^{175}Lu	0.207
Dy	1.33	0.031	^{115}In	1.46	0.032	^{175}Lu	1.384
Ho	0 32	0.006	^{115}In	0.34	0.006	^{175}Lu	0.322
Er	0.93	0.014	^{115}In	1.02	0.017	^{175}Lu	0.98
Tm	0.15	0.004	^{115}In	0.16	0.004	^{175}Lu	-
Yb	0.97	0.014	^{115}In	1.06	0.015	^{175}Lu	0.992
Hf	0.39	0.08	^{115}In	0.42	0.08	^{175}Lu	0.395
Ta	0.025	0.016	^{115}In	0.027	0.017	^{175}Lu	0.0219
Tl	0.018	0.007	^{115}In	0.024	0.008	^{209}Bi	0.0142
Pb	0.93	0.036	^{115}In	1.01	0.04	^{209}Bi	0.95
Th	0.11	0.13	^{115}In	0.12	0.014	^{209}Bi	0.12
U	0.074	0.002	^{115}In	0.079	0.002	^{209}Bi	0.0728

Conc = Concentration; STD = Standard deviation; - = no value available.

* Reference values are from Eggins (1997).

Table 2.8. A comparison of measured trace element concentrations (μg g^{-1}) for in-house rock standard TASBAS using single and four internal standards

Element	Single internal standard			4 internal standards			Reference value*
	Conc μg g^{-1}	STD (n=4)	Internal standard	Conc μg g^{-1}	STD (n=4)	Internal standard	
Sc	14.0	0.41	^{115}In	14.0	0.21	^{84}Sr	14.1
Rb	15.5	0.11	^{115}In	15.7	0.12	^{84}Sr	16.21
Y	17.8	0.16	^{115}In	18.4	0.23	^{84}Sr	19 5
Zr	243	2.78	^{115}In	246	2.36	^{84}Sr	262.2
Nb	58 4	0.59	^{115}In	59.0	0.52	^{84}Sr	58.37
Mo	7.39	0.09	^{115}In	7.47	0.08	^{84}Sr	7.41
Sn	2.51	0.12	^{115}In	2.51	0.12	^{115}In	3.2
Sb	0.097	0.012	^{115}In	0.097	0.012	^{115}In	0.101
Te	0.019	0.008	^{115}In	0.019	0.008	^{115}In	-
Cs	1.01	0.01	^{115}In	1.01	0.01	^{115}In	1.14
Ba	177	1.01	^{115}In	177	1.01	^{115}In	187
La	40.9	0.43	^{115}In	40.9	0.43	^{115}In	43.2
Ce	81.0	1.15	^{115}In	81.0	1.15	^{115}In	85.24
Pr	9.37	0.12	^{115}In	9.36	0.12	^{115}In	10 12
Nd	36.4	0 89	^{115}In	36.4	0.89	^{115}In	41.68
Sm	7.27	0.19	^{115}In	7.79	0.19	^{175}Lu	8.24
Eu	2.27	0.06	^{115}In	2.46	0.07	^{175}Lu	2.63
Gd	6.46	0.10	^{115}In	7.01	0.16	^{175}Lu	6 79
Tb	0.83	0.007	^{115}In	0.90	0.015	^{175}Lu	1.01
Dy	4.11	0.08	^{115}In	4.53	0.05	^{175}Lu	4.76
Ho	0.70	0.01	^{115}In	0.76	0.008	^{175}Lu	0.80
Er	1.64	0.03	^{115}In	1.81	0.02	^{175}Lu	1.79
Tm	0.20	0 005	^{115}In	0.22	0.002	^{175}Lu	0 22
Yb	1.20	0.015	^{115}In	1.31	0.016	^{175}Lu	1.27
Hf	5.30	0 03	^{115}In	5.68	0.03	^{175}Lu	5.43
Ta	3.27	0.02	^{115}In	3.51	0.02	^{175}Lu	3.74
Tl	0.083	0.003	^{115}In	0.084	0.003	^{209}Bi	<0.1
Pb	4.76	0.44	^{115}In	4.75	0 43	^{209}Bi	4.57
Th	4.14	0.03	^{115}In	4.12	0 03	^{209}Bi	4.69
U	1.78	0.01	^{115}In	1.78	0.02	^{209}Bi	1.87

Conc = Concentration; STD = Standard deviation; - = no value available.

* Reference values are from a compilation of Robinson et al. (1986) and other sources.

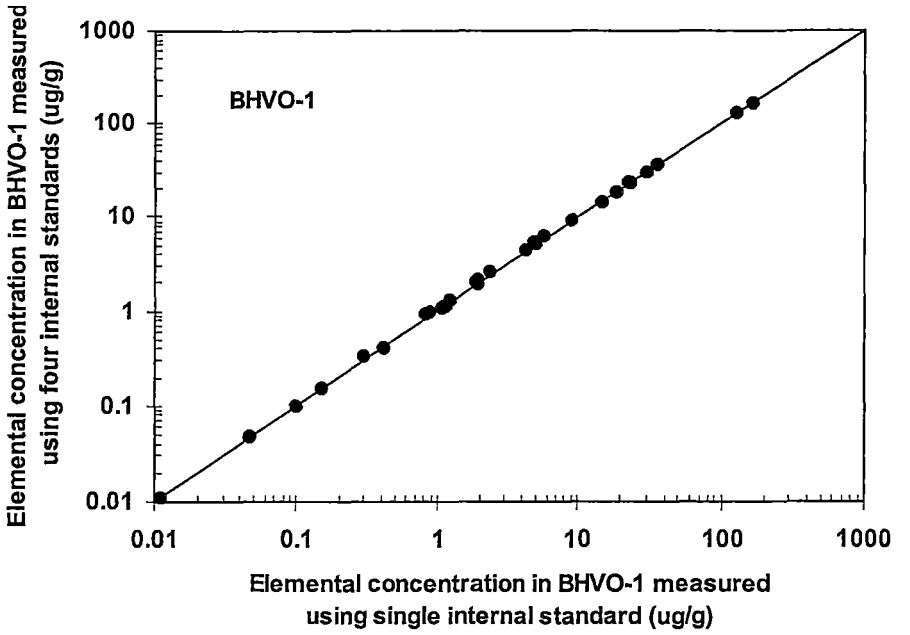

Figure 2.8. Correlation of trace element concentrations for the basaltic rock reference material-BHVO-1 between single and four internal standards

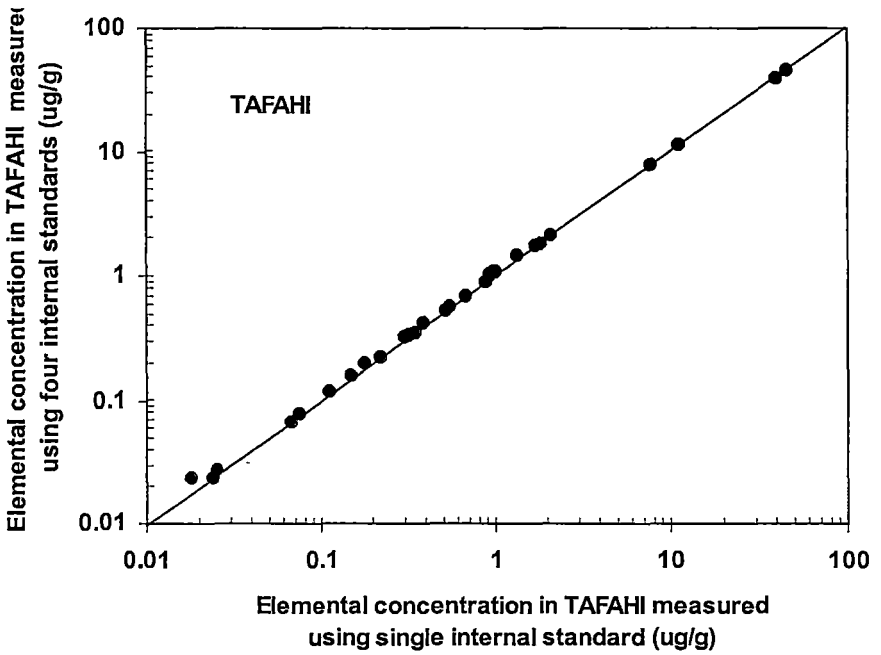

Figure 2.9. Correlation of trace elements concentrations for the basaltic rock reference material-TAFAHI between single and four internal standards

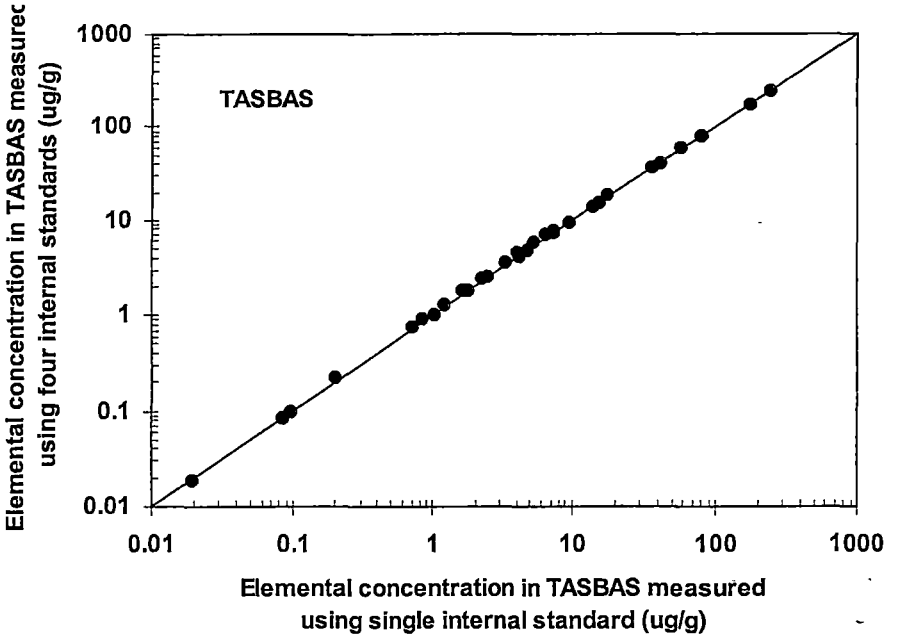

Figure 2.10. Correlation of trace elements concentrations for the basaltic rock reference material-TASBAS between single and four internal standards

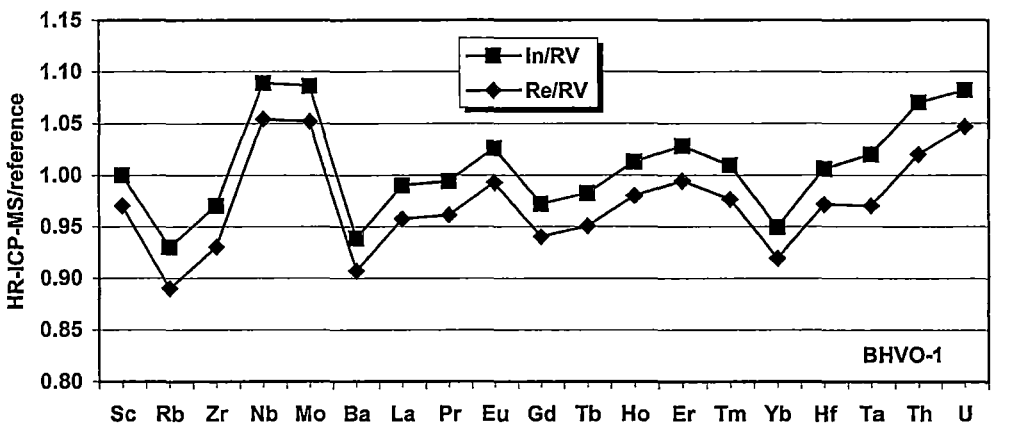

Figure 2.11. Comparison of analytical results for international rock standard BHVO-1 using ^{115}In and ^{185}Re as internal standards respectively. In/RV = HR-ICP-MS results using ^{115}In as internal standard/reference value, and Re/RV = HR-ICP-MS results using ^{185}Re as internal standard/reference value (Govindaraju 1994). The concentration of indium and rhenium in testing solutions is 10 ng g^{-1}.

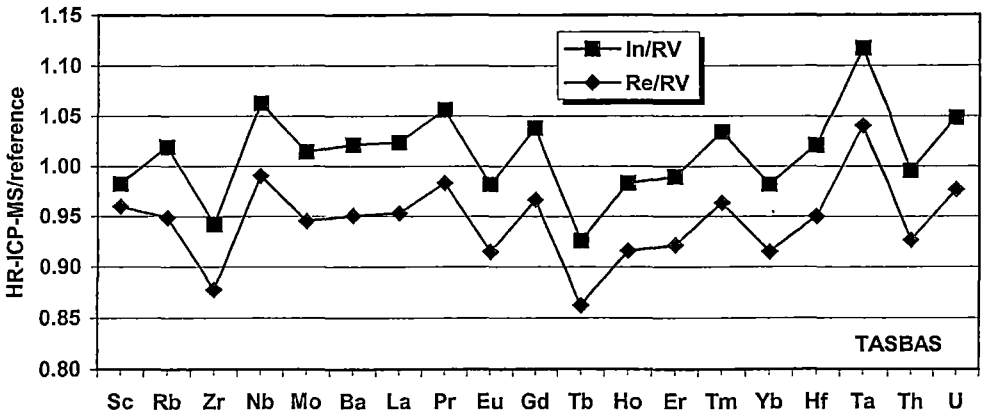

Figure 2.12. Comparison of analytical results for the in-house rock standard TASBAS using ^{115}In and ^{185}Re as internal standards respectively. In/RV = HR-ICP-MS results using ^{115}In as internal standard/reference value, and Re/RV = HR-ICP-MS results using ^{185}Re as internal standard/reference value (Robinson et al. 1986 and other sources). The concentration of indium and rhenium in testing solutions is 10 ng g^{-1}.

2.8 Detection Limits

ICP-MS is characterised by greater sensitivity and lower instrumental detection limits than any other rapid multi-element measuring technique (Gray 1989). Although *detection limits* (defined as 3 times standard deviation of the background for quadrupole ICP-MS methods) have been described by several authors (e.g. Lichte et al. 1987; Jarvis 1988; Jarvis and Williams 1989; Eggins et al. 1997), even lower detection limits can be achieved by powerful HR-ICP-MS in the low resolution mode. In the present work, the detection limits, based on 3 times standard deviations (Potts 1987), for HR-ICP-MS at low and medium resolutions were calculated by 10 and 11 independent procedure blank (2% HNO_3) intensities respectively. A comparison of analytical performance of HR-ICP-MS and some other techniques commonly used for determination of the REE are given in **Table 2.9**. It can be seen that the detection limits obtained in the present work are even lower that those achieved by quadrupole ICP-MS (Jarvis 1988), and typically two to four orders of magnitude lower than those achieved by ICP-AES (Cantagrel and Pin 1994), INAA (Potts 1987) and XRF (Robinson et al. 1986) techniques. It has to be pointed out,

however, that the detection limits for INAA and XRF were measured on solid samples, whereas the detection limits for ICP-AES, ICP-MS and HR-ICP-MS were measured in solutions. In general, detection limits of sub-pg g^{-1} for rare earth elements in solution are achievable if the HR-ICP mass spectrometer is run at low resolution. In routine work, 100 mg powdered solid sample is diluted to 100 ml solution for the HR-ICP-MS analysis (e.g. solid samples are diluted 1000 times). Therefore, the detection limits of sub-ng g^{-1} for rare earth elements in solid samples are achievable using HR-ICP-MS technique.

The detection and quantitation limits for 33 trace and rare earth elements were obtained by running a procedure blank 12 times through an analytical run (about 10 to 12 hours). Results are summarised in **Table 2.10**. The concept of *quantitation limit* was recommended by the American Chemical Society Committee on Environmental Improvement (1980) to ensure additional confidence in a unit designed to estimate the limit of quantitative analysis (Potts 1987). Quantitation limits are defined as 10 times the standard deviation (STD) above the mean of the background distribution. A few workers (Jarvis 1988; Jarvis et al. 1992) have used the concept of quantitation limits to compare the ICP-MS detection limits with other analytical technique. Medium resolution was used to measure the detection limit of Sc, Y and REE and low resolution was used to measure the detection limit for other trace elements in **Table 2.10.** The detection limits of all 33 elements are in the low ng g^{-1} levels. The detection limits for many of the trace elements (such as Sb, Cs, Pr, Tb, Er, Tm, Yb, Lu, Hf, Ta, Tl, Bi, Th and U) are at pg g^{-1} level. It also can be seen that the quantitation limits for all of the elements investigated are below sub-ng g^{-1} level. The quantitation limits for some elements, such as Sb, Lu and U even reach pg g^{-1} level.

In addition, the *instrumental detection limits* for the HR-ICP-MS used in this work are also given in **Table 2.10** for the purpose of comparing the performance of different instruments (Jarvis 1992). The instrumental detection limits were obtained by recording ten consecutive determinations of signal (intensity) produced by a blank solution (consisting of ultra pure water, 10 ng g^{-1} indium and 1 M HNO_3). Three sigma standard deviations calculated from the obtained data were expressed as instrumental detection limits.

Table 2.9. A comparison of REE detection limits between HR-ICP-MS and some other instrumental techniques

Element	Mass	Detection Limits (in solid)					
	(m/z)	HR-ICP-MS[1]	HR-ICP-MS[2]	ICP-MS[3]	ICP-AES[4]	INAA[5]	XRF[6]
		(ng g^{-1})	(μg g^{-1})	(μg g^{-1})	(μg g^{-1})	(μg g^{-1})	(μg g^{-1})
Sc	45	n.d.	0.022	n.d.	50	0.02	0.17
Y	89	0.80	0.010	0.10	10	n.d.	0.49
La	139	0.35	0.021	0.075	80	0.25	0.35
Ce	140	0.88	0.040	0.1	140	0.75	0.33
Pr	141	0.16	0.008	0.09	300	n.d.	0.31
Nd	146	1.21	0.027	0.2	100	2.31	0.26
Sm	147	1.48	0.021	0.2	80	0.05	0.23
Eu	151	0.42	0.011	0.06	4	0.02	0.22
Gd	157	3.02	0.054	0.1	70	1.95	0.20
Tb	159	0.57	0.003	0.03	n.d.	0.05	0.20
Dy	163	0.86	0.025	0.1	70	n.d.	0.19
Ho	165	0.61	0.047	0.04	n.d.	0.85	0.18
Er	167	1.39	0.007	0.06	50	n.d.	0.17
Tm	169	1.05	0.004	0.01	n.d.	0.17	0.17
Yb	172	0.51	0.005	0.06	4	0.07	0.17
Lu	175	1.08	0.002	0.05	6	0.05	0.15

Detection limits are 3 times standard deviations of background intensities. n.d. = not determined. Solid detection limits are calculated using a dilution factor of 1000.

[1] Detection limits for HR-ICP-MS from this work was obtained by a Finnigan MAT Element ICP-mass spectrometer (with a double-focusing magnetic sector) at the Central Science Laboratory of the University of Tasmania. Medium resolution (R = 300) was employed.

[2] Detection limits for HR-ICP-MS from this work was obtained by a Finnigan MAT Element ICP-mass spectrometer (with a double-focusing magnetic sector) at the Central Science Laboratory of the University of Tasmania. Medium resolution (R = 3000) was employed.

[3] Data from Jarvis (1988) using a quadrupole VG Isotopes® PlasmaQuad ICP-mass spectrometer.

[4] Data from Cantagrel and Pin (1994).

[5] Data from Potts (1987).

[6] The detection limits were obtained by an ion exchange–X-ray fluorescence technique (Robinson et al. 1986).

Table 2.10. Detection and quantitation limits for trace elements*

Element	Mass (m/z)	Detection limit ng g^{-1}	Quantitation limit ng g^{-1}	Instrumental detection limit pg g^{-1}
Sc	45	0.022	0.072	3.23
Rb	85	0.010	0.347	3.24
Sr	88	0.068	0.226	1.81
Y	89	0.010	0.032	2.41
Zr	90	0.010	0.033	0.38
Nb	93	0.015	0.049	0.32
Mo	95	0.012	0.040	0.67
Sn	118	0.031	0.103	7.90
Sb	121	0.003	0.009	0.97
Te	125	0.028	0.092	6.11
Cs	133	0.009	0.031	1.88
Ba	137	0.044	0.146	11.34
La	139	0.021	0.071	1.89
Ce	140	0.040	0.136	4.87
Pr	141	0.008	0.026	0.66
Nd	146	0.027	0.090	5.21
Sm	147	0.021	0.069	7.07
Eu	151	0.011	0.035	5.14
Gd	157	0.054	0.181	4.91
Tb	159	0.003	0.010	3.20
Dy	163	0.025	0.081	6.00
Ho	165	0.047	0.016	1.16
Er	167	0.007	0.024	4.02
Tm	169	0.004	0.013	0.75
Yb	172	0.005	0.017	2.66
Lu	175	0.002	0.008	0.37
Hf	178	0.004	0.013	0.56
Ta	181	0.005	0.016	0.09
Tl	205	0.007	0.024	0.37
Pb	208	0.155	0.517	3.43
Bi	209	0.009	0.029	0.90
Th	232	0.003	0.011	0.14
U	238	0.002	0.005	0.18

* Sc, Y and REE were measured at medium resolution (R = 3000), the rest of trace elements were measured at low resolution (R = 300).

Detection limits were 3 times standard deviations of procedure bank values, and quantitation limits were equal to 10 times standard deviation.

In summary, the detection limits for rare earth and other trace elements by HR-ICP-MS are better than those by ICP-AES, INAA, ion exchange-XRF and quadrupole ICP-MS. The detection limits for all trace elements studied are well under ng g^{-1} level and the detection limits for some trace elements can reach pg g^{-1} level in solution. However, it should be pointed out that the detection limits and instrumental detection limits for HR-ICP-MS, as for other instrumental techniques, vary from day to day, and many factors can affect the detection limits and instrumental detection limits for HR-ICP-MS. For instance, apart from the resolution settings, cleanness of the sample introduction system (e.g. nebuliser, spray chamber and solution tubing) and sample and skimmer cones can also affect the detection limits and instrumental detection limits dramatically in some circumstances, causing either an increase of background or decrease of signal intensities.

2.9 Precision

The overall precision of the method has been evaluated by 20 independent sample preparations of the TAFAHI standard basalt. The sample decomposition technique used is similar to the proposed digestion technique by Eggins et al. (1997). At first, samples were digested in 10-ml Savillex Teflon beakers using 2 ml HF and 0.5 ml HNO_3 on a 130-150 °C hotplate for 48 hours. After evaporating to incipient dryness twice with addition of 1 ml HNO_3, the final residues were taken up with 2 ml HNO_3 and diluted to 100 ml in 2% HNO_3. Then, 50 ng g^{-1} indium was spiked in to each testing solution and used as internal standard for the HR-ICP-MS analysis. The obtained 20 testing solutions were divided in to Groups A and B. With Group A, Sc, Y and REE were measured at medium resolution (R = 3000) and other elements were measured at low resolution (R = 300). With Group B, trace elements and REE were measured at low resolution (R = 300), except Sc was measured at medium resolution (R = 3000).

Measured results and precisions from two groups of 20 independent determinations are shown in **Table 2.11**. The relative standard deviation (%RSD) values for the analysis of Group A solutions are generally better than 5% for concentrations higher than 1 μg g^{-1} with exceptions of Dy (6.68%) and Yb (5.57%). Even in the case of

Table 2.11. Trace element concentrations (μg g^{-1}), precision and reference values for TAFAHI

Element	This work				Reference values
	Result A (n = 10)	%RSD	Result B (n = 10)	%RSD	
Sc	45 ± 1.2	2.55	45 ± 2	4.36	45.5
Rb	1.76 ± 0.04	2.32	1.72 ± 0.03	1.45	1.75
Sr	135 ± 1.9	1.43	n.d.		138.9
Y	8.2 ± 0.2	2.72	7.6 ± 0.1	1.74	9.11
Zr	11.7 ± 0.2	2.01	11.3 ± 0.3	2.45	12.07
Nb	0.50 ± 0.01	2.84	0.55 ± 0.03	4.71	0.456
Mo	0.46 ± 0.01	3.14	0.52 ± 0.01	2.52	0.44
Sn	0.22 ± 0.02	7.25	0.22 ± 0.02	9.55	0.24
Sb	0.023 ± 0.002	7.02	0.024 ± 0.002	8.33	0.024
Cs	0.063 ± 0.003	5.16	0.067 ± 0.002	2.99	0.066
Ba	38.3 ± 1.2	3.25	39.7 ± 0.8	1.99	40.3
La	0.95 ± 0.05	5.43	0.88 ± 0.02	2.27	0.938
Ce	2.2 ± 0.1	4.91	2.11 ± 0.05	2.42	2.22
Pr	0.33 ± 0.02	5.21	0.35 ± 0.007	2.00	0.361
Nd	1.89 ± 0.08	4.24	1.83 ± 0.05	2.51	1.93
Sm	0.71 ± 0.05	7.46	0.68 ± 0.02	3.37	0.722
Eu	0.29 ± 0.02	8.03	0.300 ± 0.008	2.67	0.305
Gd	1.04 ± 0.08	7.22	1.00 ± 0.02	2.00	1.069
Tb	0.19 ± 0.02	7.99	0.182 ± 0.004	2.20	0.207
Dy	1.39 ± 0.09	6.68	1.33 ± 0.03	2.32	1.384
Ho	0.31 ± 0.02	7.89	0.315 ± 0.006	1.90	0.322
Er	0.97 ± 0.07	7.35	0.93 ± 0.01	1.50	0.98
Tm	0.141 ± 0.009	6.14	0.146 ± 0.004	2.74	n.d.
Yb	1.03 ± 0.06	5.57	0.97 ± 0.01	1.44	0.992
Lu	0.147 ± 0.009	6.26	n.d.		0.153
Hf	0.40 ± 0.01	2.68	0.39 ± 0.02	5.70	0.395
Ta	0.024 ± 0.003	13.12	0.025 ± 0.003	12.00	0.0219
Tl	0.009 ± 0.001	13.64	0.018 ± 0.004	22.22	0.0142
Pb	0.94 ± 0.05	4.97	0.93 ± 0.04	3.88	0.95
Th	0.117 ± 0.004	3.17	0.111 ± 0.007	6.31	0.12
U	0.076 ± 0.003	3.56	0.074 ± 0.002	2.70	0.0728

Reference values are from Eggins et al. 1997; n.d. = not determined; Result A = Sc, Y and REE were measured at medium resolution (R = 3000) and the rest were measured at low resolution (R = 300); Result B = Sc was measured at medium resolution and the rest were measured at low resolution.

very low concentration (0.0088 μg g^{-1}) with Tl, a %RSD value of 13.97% is quite acceptable. As predicted, in general, the relative standard deviation (%RSD) values of REE for the analysis of Group B solutions are better than those for the testing solutions of Group A. The range of precision values is from 1.44% for Yb and 3.37% for Sm. The slightly higher value of precision for Sm is mainly due to the low isotope abundance (14.97%) of ^{147}Sm used for HR-ICP-MS analysis. As with Group A, Tl has the worst precision (22.22%) due to its very low concentration. The average precision of all elements considered for Group A and B are 5.52% and 4.22%, and the average precision of REE considered for Group A and B are 6.46% and 2.26%.

From the above discussion, it is clear that sector field ICP-MS under low resolution (R = 300) can produce better precision than under medium resolution (R = 3000). Therefore, it is recommended that, in general, low resolution should be used for the measurement of trace elements when matrix interferences are negligible.

2.10 Summary

From the above discussion the advantages of sector field ICP-MS technique can be summarised as follows:

1. Sector field ICP-MS is a very sensitive analytical technique when operating at low resolution mode. The signal intensity can reach as high as (1.2-1.8) x 10^5 counts s^{-1} per ng g^{-1} ^{115}In, whereas the attainable sensitivity of a quadrupole instrument has been reported as (2-5) x 10^4 counts s^{-1} per ng g^{-1} ^{115}In (Eggins et al. 1997). Similar intensity (2-4) x 10^4 counts s^{-1} per ng g^{-1} ^{115}In) has also been observed using a new generation of quadrupole ICP-MS (HP 4500 (*plus*) ICP-MS) by this author. Sector field ICP-MS generally offers higher sensitivity compared to quadrupole instrument due to two reasons. First, the ion transmissions of quadrupoles is mass dependent, leading to losses at the higher end of the mass range, whereas this is not the case for magnetic sector devices. Second, the lens systems of double focusing instruments do not need a central beam stop for noise reduction, where additional losses can accur (Jakubowski et al. 1998). Furthermore, on the basis of systematic comparison

between the sector field ICP-MS (Finnigan MAT) and various quadrupole instruments, sector field ICP-MS has been considered to be more sensitive than quadrupole-base ICP-MS (Montaser 1998).

2. Some of the spectral interferences can be eliminated by using higher resolution ICP-MS technique. For instance, the spectral interference of $^{29}Si^{16}O$ on ^{45}Sc can be resolved at the medium resolution (R = 3000) and the interference of $^{40}Ar^{36}Cl$ on ^{75}As and of a number of interferences on Ge isotopes (^{72}Ge, ^{73}Ge and ^{76}Ge) can be eliminated using a resolution of 7500.

3. In comparison with the quadrupole ICP-MS method, the sector field ICP-MS is a straightforward technique. Instead of using several internal standards to monitor instrumental drift through an analytical run, a single internal standard such as ^{115}In has been proved sufficient enough to compensate the instrumental drift for the sector field ICP-MS method.

4. Sector field ICP-MS provides better detection limits for the trace elements analysis than quadrupole ICP-MS, ICP-AES, INAA and ion exchange-XRF techniques. The detection limits for most trace elements studied are well under ng g^{-1} level and the detection limits for some of the trace elements (such as Sb, Cs, Tb, Er, Tm, Yb, Lu, Hf, Ta, Th, U etc.) can reach pg g^{-1} level in solutions.

Chapter 3

IMPROVED DECOMPOSITION TECHNIQUES FOR THE ANALYSIS OF GEOLOGICAL SAMPLES

This chapter reviews sample decomposition techniques and describe refinements and optimisation of digestion methods for the analysis of geological materials using ICP-MS. The decomposition methods investigated in the present study include Savillex Teflon beaker acid digestion, high pressure digestion, microwave digestion, lithium tetraborate fusion and sodium peroxide sinter decomposition techniques for the digestion of a wide range of geological reference materials (including basalts, iron formations, dolerites, dunites, peridotites, serpentines, granites etc.) in combination with the determination of more than 30 elements by HR-ICP-MS. On the basis of this investigation, optimal decomposition techniques for dissolution of different types of geological samples are proposed.

3.1 Introduction

Acid digestion was carried out in both open vessels (Moselhy et al. 1978; McQuaker et al. 1979; Lechler et al. 1980; Church 1981) or in closed pressure decomposition vessels (Uchida et al. 1980; Lechler et al. 1980; McLaren et al. 1981; Hee and Boyle 1988; Karstensen and Lund 1989) to obtain multi-element concentrations in geological materials using an ICP-AES method. Fusion digestion has also been conducted by a few authors (Burman et al. 1978; Bankston et al. 1979; Walsh and Howie 1980; Brenner et al. 1980; Norman et al. 1989). As ICP-AES and ICP-MS techniques share a common source (an inductively coupled plasma is employed to excite either atomic emission (ICP-AES) or ions (ICP-MS)), many of the sample decomposition techniques can be used for both techniques (Totland et al. 1992; Jarvis et al. 1992).

In an open vessel acid digestion, hydrofluoric acid (HF), in combination with a range of other mineral acids, is normally used to digest geological samples. Hydrofluoric acid is the most effective mineral acid for breaking up the strong Si-O bond. During digestion, there are two reactions. Firstly, H_2SiF_6 formed in solution by the attack of HF on silicate materials is efficiently decomposed, leading to the volatilisation of silicon tetrafluoride:

$$6HF + SiO_2 = H_2SiF_6 + 2H_2O$$
$$H_2SiF_6 = SiF_4\uparrow + 2HF$$

The disintegration of the silicate lattice leads to the release of metals bound within the silicate structure. The sample solutions produced in open vessel acid digestion have the following advantages (Potts 1987):

(1) The resultant solutions are much more stable since Si in solution trends to hydrolyse and precipitate on standing.
(2) The corrosion action of HF on normal glassware is negated because fluorides can be removed by heating with a higher-boiling mineral acid such as HNO_3, $HClO_4$ and H_2SO_4.
(3) Salt content in the obtained solution is reduced to an acceptable level for multi-element determination by ICP-AES and ICP-MS.

Although the open vessel acid digestion is routinely used to digest geological samples for the analysis of ICP-AES and ICP-MS (Moselhy et al. 1978; McQuaker et al. 1979; Lechler et al. 1980; Church 1981; Lichte et al. 1987; Jarvis 1988; Jenner et al. 1990; Rautiainen et al. 1996; Eggins et al. 1997; Norman et al. 1998), there are some limitations with this approach (e.g. Bock 1979; Chao and Sanzolone 1992; Jarvis et al. 1992):

(a) Refractory minerals such as chromite, garnet, magnetite and zircon may be only partially attacked.
(b) Some elements (Cr, Hf, Mo, Sc, and Zr) yield inconsistent analytical data and display incomplete recovery in certain sample types, such as granites.

(c) The heavy REE (Gd to Lu) may also be partly insoluble, particularly in zircon-bearing rocks.

(d) Volatile elements or those that form volatile fluorides such as As, B, Ge, Hg, Nb, Os, Re, Se, Sb, Ta, Te, and Ti may be partially lost during evaporation.

In order to increase the effectiveness of the acid decomposition, an acid digestion bomb (closed vessel acid digestion) was initially introduced for analysis via atomic absorption spectrometry (AAS) by Bernas (1968), and Langmyhr and Paus (1968). Buckley and Cranston (1971) also used the acid digestion bomb to decompose aluminosilicate minerals and marine sediments prior to the determination of 18 elements by AAS. Compared with other decomposition techniques, closed vessel acid digestion generally has the following advantages as addressed by Chao and Sanzolone (1992) and Jarvis et al. (1992):

(1) Pressure decomposition with mixed acids may attack certain minerals (such as kyanite, staurolite, pyrite, chalcopyrite, and pyrrhotite) which are not decomposed or are only partly decomposed by an open vessel acid decomposition.

(2) Volatile elements, such as As, B, Cr, Hg, Sb, Se, and Sn will remain in solution.

(3) Less reagent is required, since there is almost no evaporation through the sample digestion.

(4) Contamination is reduced by lowering reagent amount and because the sealed system excludes the possible introduction of airborne particles during decomposition.

Closed vessel acid digestion techniques are routinely used in the decomposition of geological samples for elemental analysis by ICP-AES and ICP-MS (Uchida et al. 1980; Lechler et al. 1980; McLaren et al. 1981; McLaren et al. 1987; Hee and Boyle 1988; Karstensen and Lund 1989; Jenner et al. 1990; Jarvis et al. 1992; Hollocher and Ruiz 1995; Grégoire et al. 1995; Xie and Kerrich 1995; Liang et al. 2000).

A high pressure acid digestion technique (similar to acid digestion bomb method) has also been used in the decomposition of geological samples (Dulski 1994;

Münker 1998). Dulski (1994) reported REE measurement in andesite, granite and granodiorite following a high pressure acid digestion method. In his work, in order to obtain good recovery for REE, geological samples were first digested with an $HF+HClO_4$ mixture and then the obtained residue was evaporated a few times with addition of 5 mol l^{-1} HCl. Although this procedure provided an accurate analysis for REE, the multi-stage HCl evaporations obviously introduce a large amount of chloride in solution which interferes with determination of light mass elements (less than 80 amu) by ICP-MS (Tan and Horlick 1986). The other disadvantages of this method are that it is time-consuming, and may involve introduction of impurities through the addition of HCl solutions. Recently, Münker (1998) conducted the decomposition of geological samples using a high pressure acid digestion technique to measure concentrations of Nb and Ta. He found low recovery for some geological materials (such as granite) using this $HF/HClO_4$ pressure digestion method, suggesting that the $HF/HClO_4$ mixture is not efficient enough for the complete decomposition of some types of geological materials.

Recently, techniques using a microwave energy source have been developed for the decomposition of various samples (Lamothe et al. 1986; Mathes 1988; Matusiewicz and Sturgeon 1989). Specially designed PTFE or Teflon PFA (tetrafluoroethylene-tetrafluoroalkoxyethylene) vessels are generally used for such microwave digestion systems. In general, microwave energy not only affects the digestion medium, it is also absorbed by sample molecules. This certainly increases the kinetic energy of the matrix and causes internal heating and differential polarisation, and thus aids acid attack on refractory materials. Microwave digestion has been demonstrated to successfully dissolve a range of materials, and dramatically shorten decomposition times (Lamothe et al. 1986; Borman 1988; Kingston and Jassie 1988; Mathes 1988; Matusiewicz and Sturgeon 1989).

Applications using a microwave decomposition technique to dissolove geological samples are reported in Lamothe et al. (1986), Mathes (1988), Rantala and Loring (1989), Kemp and Brown (1990), Nölter et al. (1990), Totland et al. (1995), and Yoshida et al. (1996). However, with the exception of Nölter et al. (1990), these workers did not use this digestion technique with ICP-MS. Nölter et al. (1990) used closed-vessel acid digestion, followed by open vessel evaporation for a range of

geological samples, prior to analysis by ICP-MS. Microwave digestion does not always allow determination of Cr, Hf and Zr, and assessing the effectiveness of microwave procedures for the retention of volatile elements (such as As, Ga, Ge, Hg, Sb, and Se) needs further work (Jarvis et al. 1992). Yoshida et al. (1996) decomposed basalt, granodiorite, rhyolite, gabbro, and andesite by microwave decomposition with a mixture of HF, HNO_3 and $HClO_4$, prior to analysis using ICP-MS. The results obtained for some elements were in good agreement with published values, the results for Zr, Nb, U and Th were somewhat low and the results for Co, Cu, Ge, Rb, Cd, Sn, Sb, W and Tl were very low.

Wang (1961) first proposed the $Li_2B_4O_7$ fusion dissolution procedure to solve the problem of crystal and particle-size differences of soils, silicates, refractories, and slags by transforming them to homogeneous materials before analysing them by optical emission spectrography or X-ray fluorescence. Later, $LiBO_2$ was used for the decomposition of silicate rocks, prior to chemical analysis (Ingamells 1964). Lithium tetraborate ($Li_2B_4O_7$) and lithium metaborate ($LiBO_2$) are now commonly used to digest geological samples for analysis by ICP-AES and ICP-MS (Potts 1987; Chao and Sanzolone 1992; Jarvis et al. 1992). All major rock-forming silicates and some refractory accessory minerals (such as chromite, ilmenite, etc.) can be readily decomposed (Cremer and Schlocker 1976; Feldman 1983). The difference between $Li_2B_4O_7$ and $LiBO_2$ lies in the higher acidity (higher content of B_2O_3) of the former. Therefore, in general, lithium tetraborate is better for basic rocks (low silica), and lithium metaborate is better for acidic rocks (high silica) (Bennett and Oliver 1976).

Cremer and Schlocker (1976) carried out a detailed study on the digestion of a wide range of minerals and ores by either $LiBO_2$ fusion or a 2:1 mixture of $Li_2B_4O_7$ to $LiBO_2$. Zircon, some metal oxides, some rare-earth phosphates, and many sulfides (galena, pyrite, and sphalerite, etc.) were found in the insoluble residues after fusion decomposition. Another major disadvantage of this method is that the levels of total dissolved solids (TDS) are high, therefore reducing the number of trace elements that can be measured by ICP techniques. Generally, it is required that the TDS level in final solution should be less than 1% for ICP-AES and 0.1% for ICP-MS (Totland et al. 1992). Large dilutions prior to analysis restrict the number of trace elements that are quantifiable with fusion decomposition.

Rafter (1950) investigated sodium peroxide decomposition of a range of minerals and found that many refractory minerals (chromite, zircon, rutile, ilmenite, beryl, titanite, and cassiterite/tantalite, etc.) can be effectively decomposed by heating with Na_2O_2 at a temperature of 480-500 °C for a few minutes to 20 minutes. For the decomposition of sulfides, arsenides and rare-earth phosphates, vanadates, zirconium oxides, and W, Nb and Ta minerals, a Na_2O_2 fusion decomposition at 650-700 °C is also effective (Johnson and Maxwell, 1981). As a powerful decomposition technique, Na_2O_2 sintering (at 480-500 °C) and fusion (at 650-700 °C) have been used for the digestion of different types of geological samples for analysis by photometry, X-ray fluorescence, and ICP-AES (Gregory and Jeffrey 1967; Rodgers 1972; Koeva et al. 1975; Hou et al. 1985; Buchman and Dale 1986). Although Na_2O_2 sintering or fusion can provide an efficient decomposition for many types of geological samples, the TDS levels in final solutions are high and blank levels might be high due to the lack of ultra pure Na_2O_2, which can restrict the use of this decomposition technique for the determination of trace elements by ICP-MS method. To date, this decomposition technique has found little application to trace element determination in geological samples by ICP-MS.

3.2 Experimental

3.2.1 Reference Materials

Eleven geological reference materials used in this study are mainly international geological standard samples. Two in-house rock standards prepared in early 1970s at the School of Earth Sciences of the University of Tasmania have also been used **(Table 3.1)**.

3.2.2 Reagents and Cleaning of Labware

As mentioned in the previous chapter, HF (Analar, AR grade), HCl (BDH, AR grade), HNO_3 (BDH, AR grade), $Li_2B_4O_7$ (AR grade, Sigma Chemicals, WA, Australia), and Na_2O_2 (AR grade, Merk) were used in this study. HCl and HNO_3 were double distilled with a quartz distillation system before use. HF was double

distilled using a Teflon distillation system. Ultra pure $HClO_4$ was provided by BDH Chemicals and ultra pure H_2SO_4 (double sub-boiling in quartz) was from Seastar Chemicals INC in Canada. Ultra pure water used in the study was distilled with a normal glass distillation system and then further purified with a MODULAB Water Purification System (Continental Water System Corporation, Melbourne, Australia).

General physical properties of the mineral acids used for sample digestion and preparation in this project are listed in **Table 3.2.** In addition to the acid strength, determined by the concentration and degree of dissociation, these acids can be oxidising (HNO_3, $HClO_4$ and hot concentrated H_2SO_4) or non-oxidising (HF, HCl, dilute $HClO_4$ and dilute H_2SO_4) (Johnson and Maxwell 1981).

Lithium tetraborate (AR grade, Sigma Chemicals, WA, Australia) and sodium peroxide (AR grade, Merck, Germany) were used for the fusion and sinter decompositions respectively. The melting points of lithium tetraborate ($Li_2B_4O_7$) and sodium peroxide (Na_2O_2) are 930 and 480 °C (Potts 1987).

External calibration standard solutions were prepared by gravimetric serial dilution from 100 $\mu g\ g^{-1}$ multi-element atomic spectroscopy standards (Perkin-Elmer Corporation, USA). The standard solutions were diluted with double distilled water and HNO_3 to 2% HNO_3 solutions when needed. Indium standard solution (1000 ± 3 µg/ml in 2% HNO_3) was from High-Purity Standards (South Carolina, USA) and also diluted to a working solution in 2% HNO_3 before using as an internal standard for ICP-MS analysis.

Table 3.1. Geological reference materials studied

Sample name	Description	Reference
BHVO-1	Basaltic lava from Kilauea caldera, Kilauea volcano, Hawaii, USA	Govindaraju 1994
TAFAHI	Basalt collected from north Tonga, used as an in-house reference material by the Research School of Earth Sciences, Australian National University	Eggins et al. 1997
AC-E	Granite from a quarry in Ailsa Craig island in the firth of Clyde, southwest Scotland. The Ailsa Craig microgranite comprises alkali feldspar (low albite with small proportions of orthoclase) and quartz with less than 10% of amphibole, pyroxene, aenigmatite and accessory minerals. It contains significant amounts of both light and heavy REE giving a flat chondrite normalised abundance distribution at about the 100 times chondrite level	Teall (1892), Howie and Walsh (1981), Harding (1983), Potts and Holbrook (1987)
GSR-1	A grey medium-grained biotite granite from Binzhou, Hunan province, PRC. Mineralisation of tungsten, tin and molybdenum occurs in the contact zone between the granite and carbonate rocks	Xie et al. 1985
G-2	Westerly granite from Sullivan quarry, Bradford, Rhode Island, USA, collected by Felix Chayes, Geophysical Laboratory, Carnegie Institution of Washington. G-2 is rich in plagioclase and biotite	Flanagan (1967)
MA-N	Albite-lepidolite granite ("quartz albitite"), de Beauvoir (Clemont-Ferrand, Massif Central), France. MA-N is a special granite in the sense that transition elements and REE are at very low concentrations whereas elements such as Ag, Be, Cd, Cs, Ga, Li, Nb, Rb, Sn, Ta and W are at "unusually high concentrations	Govindaraju (1994)
YG-1	Medium-grained felsic granite with occasional feldspar megacrysts up to 20 mm from the Yewangara pluton, Wyangala batholith, Lachlan granite province, New South Wales, Australia	Thompson et al. (1999)
FeR-2	Iron formation sample (magnetite rich) from Griffith Mine, Bruce Lake, Ontario, Canada	Govindaraju (1994)
FeR-4	Iron formation sample (magnetite rich) from Sherman Mine, Temagami, Ontario, Canada	Govindaraju (1994)
TASBAS	Basalt from Tasmania, Australia (an in-house reference material at School of Earth Sciences, University of Tasmania	Robinson et al. (1986)
TASGRAN	Granite from Tasmania, Australia (an in-house reference material at School of Earth Sciences, University of Tasmania	Robinson et al. (1986)

Table 3.2. General physical properties of mineral acids used for sample digestion and preparation

Acid	Chemical formula	Conc. % acid (w/w)	M	sg	b. pt. (°C)	% acid of constant boiling mixture
Hydrofluoric acid	HF	48	29	1.15	112	38.3
Nitric acid	HNO_3	70	16	1.42	120	68
Hydrochloric acid	HCl	36	6.8	1.18	110	20.24
Perchloric acid	$HClO_4$	70	12	1.67	203	72.4
Sulfuric acid	H_2SO_4	98	18	1.84	338	98.3

Conc. = concentrated; M = molarity; sg = specific gravity; b. pt. = boiling point.

All of the labware used in this study was carefully cleaned prior to sample digestion and analysis, in order to minimise any possible contamination during sample digestion and ICP-MS analysis, Savillex beakers and PTFE (polytetrofluorethylene) digestion vessels were washed with laboratory detergent, rinsed and soaked in 20% HCl and 10% HNO_3 solutions at ~80 °C for at least 24 hours, respectively. The vessels were then rinsed with ultra-pure water before adding 2 ml HF and heating at 180 °C under pressure for ~20 hours. This additional cleaning step using HF was found to be particularly necessary to remove memory of HFSE. Finally, the digestion vessels were rinsed with ultra-pure water prior to sample digestion. Plastic containers, pipette tips and test tubes used in the experimental work were soaked in 20% HCl and 10% HNO_3 solutions at room temperature for at least 24 hours, respectively, and finally rinsed with ultra-pure water before use.

3.2.3 Equipment

3.2.3.1 Acid Pressure Digestion System

The acid pressure digestion system used in the study is a PicoTrace® TC-805 Pressure Digestion System (Bovenden, Germany, **Figure 3.1**). Digestion time and temperature can be controlled automatically by a time-temperature controller and were varied according to the types of sample being tested. PTFE digestion containers can be used for geological materials as long as temperatures and pressures do not exceed 180 °C and 20 bar (~290 psi). During pressure digestion the PTFE containers are inserted into the digestion block and tightly sealed with PTFE lids which are reinforced by pressure disks and plates. The digestion block is coated with PFA (perfluoroalkoxy) and its working temperature is up to 180 °C. During evaporation the PTFE containers remain in the pressure digestion unit and are covered with a special PTFE evaporation plate. Evaporated acid fumes are removed by a water vacuum pump and adsorbed by a strong alkaline solution.

3.2.3.2 Microwave Digestion System

Microwave decomposition was carried out with the MLS-1200 MEGA Microwave Digestion System (Milestone, Italy, **Figure 3.2**) in combination with an MDR (microwave digestion rotor) 1000/6/100/110 system. The power emission of the microwave system can be controlled from 10 to 1000 W (in 10 W increments). Different digestion programs can be chosen for different samples. There are several steps with each digestion program, and a different time can be set up for each step of digestion. TFM (tetrafluormethaxil) vessels (100 ml) are used with the MDR 1000/6/100/110 system. The maximum pressure in the vessel can reach as high as 110 bar (~1595 psi). TFR features include high density, very compact surface, high insulating power, and high working temperature (approximate 330-350 °C).

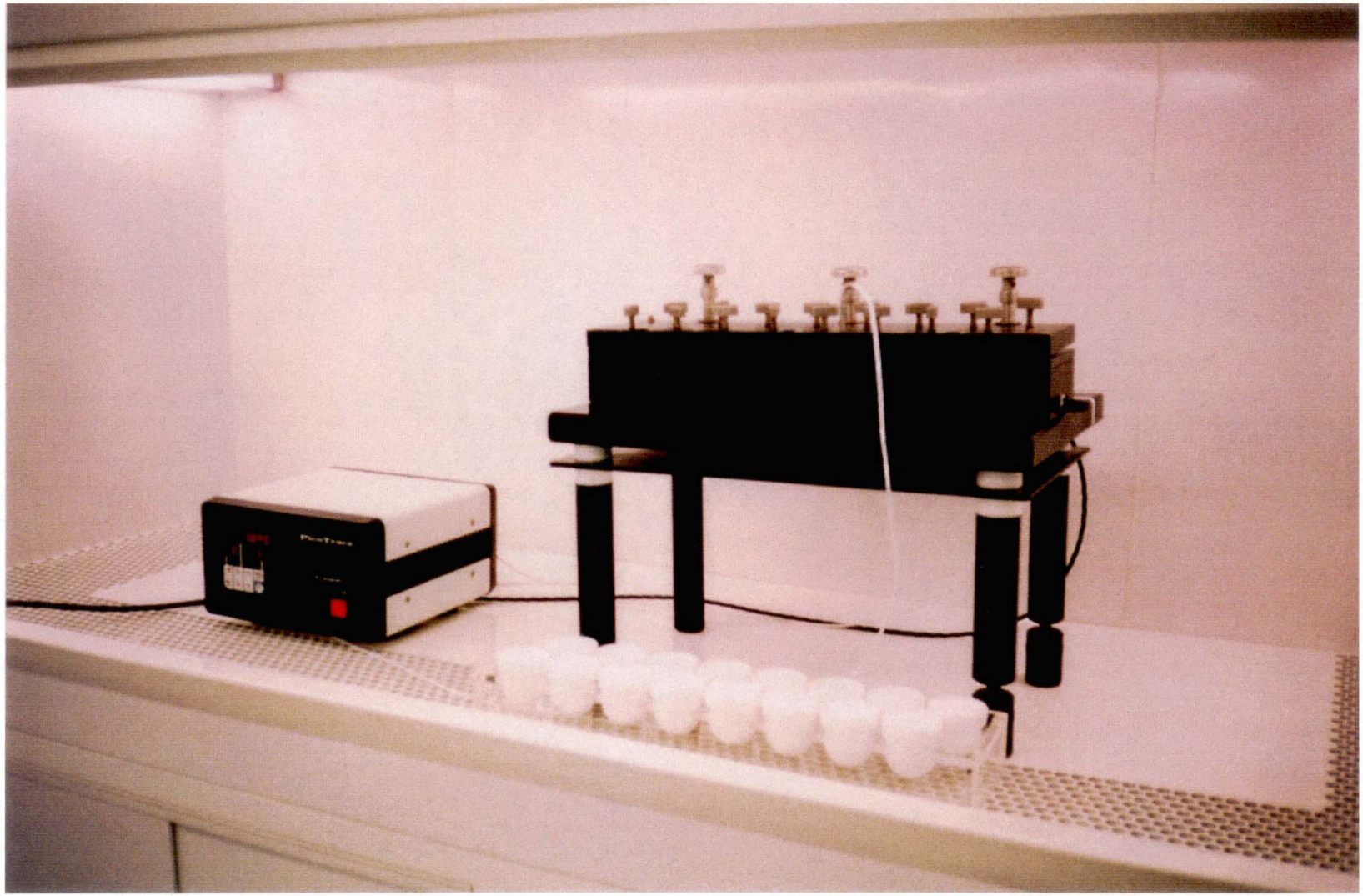

3.2.4 Instrumentation

The experimental work in the study was performed using a Finnigan MAT Element ICP-mass spectrometer (Bremen, Germany). Further details regarding the operational conditions of this instrument can be found in **Chapter 2** of this thesis.

3.3 Digestion Procedures

The following different dissolution procedures have been used in this study. In most cases two or three procedure blanks were included with each batch of samples.

3.3.1 Savillex Teflon Beaker

100 mg aliquots of rock powder were weighed into 7 ml screw-top Savillex® Teflon beakers. After wetting with a few drops of ultra pure water, the sample was spiked with 0.1 ml 10 μg g^{-1} In solution and 2 ml HF and 0.5 ml HNO_3 were slowly added. After screwing the lid on, the beaker was placed on the hotplate at 130-150 °C for 48 hours during the digestion the beaker was shaken occasionally. During digestion, the sample beaker was removed from the hotplate twice (at the beginning and in the middle of the digestion) and placed in an ultrasonic bath for a couple of minutes to agitate the (HF + HNO_3 + sample) mixture. The mixture was evaporated on a hotplate at 130-150 °C to incipient dryness. The evaporation was repeated twice after adding1 ml HNO_3 each time. The digestion residue was taken up using 2 ml HNO_3 and 3-5 ml ultra pure water on a hotplate. Finally, the solution was transferred into a polypropylene bottle and diluted to 100 ml with ultra pure water before ICP-MS analysis.

3.3.2 High Pressure Digestion System

A. $HF/HClO_4$ (basalts, ultramafics and ironstones)

100 mg powdered sample was weighed into 30-ml PTFE digestion containers. After wetting the sample with a few drops of ultra pure water and adding 0.1 ml of 10 μg g^{-1} In solution into each digestion container, 3 ml HF and 3 ml $HClO_4$ were slowly

added. After thorough mixing by shaking the PTFE containers a few times, they were left in the digestion block at 180 °C for 16 hours for ultramafics or 48 hours for basalts and ironstones. The PTFE vessels are designed to withstand pressures up to 20 bar (~290 psi) before degassing at the lid/vessel interface. The digestion mixture was evaporated to dryness at 180 °C for about 12 hours in the evaporation block. Finally, 2 ml HNO_3, 1 ml HCl and 10 ml ultra pure water were added to the PTFE containers. The residue was dissolved by warming the solution in the digestion block at 60 – 70 °C for an hour or so. After the solution became clear, it was transferred into a polypropylene bottle and diluted to 100 ml with ultra pure water for ICP-MS analysis.

B. HF/H_2SO_4 (granites and other samples with resistant minerals)

As above using H_2SO_4 instead of $HClO_4$. Evaporation time was approximately four days. 1 ml $HClO_4$ was added to the residue and dried down before adding the final HNO_3 and HCl.

3.3.3 Microwave Digestion

Each powdered sample (100 mg) was weighed into a TFM (tetrafluormethaxil) vessel. After wetting with a few drops of ultra pure water and spiking with In solution as internal standard, 2ml HF and 0.5 ml HNO_3 were added to each vessel. The beaker was shaken a few times to disaggregate and mix up the (HF + HNO_3 + sample) mixture thoroughly. The TFM vessel was introduced into the HS-08 HTC protection shield and digested at 250W, 400W, 650W and 250W for 10 minutes respectively (maximum pressure can be up to about 1595 psi in the TFM vessel), followed by venting the TFM vessel and the rotor for 5 min. The TFM digestion vessel was then carefully removed and transferred onto a hotplate at about 150 °C and evaporated to crystalline paste. To ensure the complete removal of HF, two further 1 ml aliquots of HNO_3 were added and evaporated again to near dryness. Finally, 2 ml HNO_3 and 5 - 10 ml ultra pure water were added to the digestion beaker. The digestion beaker was replaced in the microwave and the residue was redissolved at 250W, 400W, 650W and 250W for one minute. This final solution

was transferred into a polypropylene bottle and diluted to 100 ml with ultra pure water for ICP-MS analysis.

3.3.4 Lithium Tetraborate Fusion

A 100 mg sample was weighed into a platinum crucible, and thoroughly mixed with 200 mg lithium tetraborate ($Li_2B_4O_7$) using a plastic spatula. The mixture was fused at 1000 °C for 30 min in a muffle furnace. Then the platinum crucible was taken out of the muffle furnace and allowed to cool before slowly adding 5 ml HF and 2 ml HNO_3 into the crucible. The crucible was left on a 130-150 °C hotplate and the resulting solution was evaporated at 130-150 °C to incipient dryness. The residue was evaporated to incipient dryness twice after adding 1 ml HNO_3. Finally, each digestion residue was taken up in 2 ml HNO_3 and 10 ml ultra pure water, transferred into a polypropylene bottle, spiked with 0.1 ml 10 $\mu g\ g^{-1}$ In solution and diluted to 100 ml with ultra pure water before ICP-MS analysis.

3.3.5 Sodium Peroxide Sinter (for REE)

0.4 gram of freshly powdered Merck Na_2O_2 was weighed into a clean platinum crucible, followed by adding 100 mg finely ground sample (Note: 0.6 grams of Na_2O_2 is required for the decomposition of magnetite, chromite and sulfides) and mixed thoroughly with a plastic spatula. The mixture was sintered for one hour at 480 °C in a muffle furnace. A small amount of ultra pure water was added drop-wise to the crucible until the vigorous reaction ceased. The sinter residue was transferred quantitatively to centrifuge tubes, followed by adding ultra pure water, mixing, centrifuging and decanting clear liquid from the centrifuge tubes. In the same way, the residue was washed again. This removed the sodium and silica salts, while REE and some HFSE (high field strength elements) are retained in the sinter residue. 2 ml nitric acid and 10 ml ultra pure water were added to the centrifuge tube, after which the tube was placed in a water-steam bath to dissolve the residue. One drop of HF was added to stabilise the HFSE. The solution obtained was transferred into a polypropylene bottle, spiked with 0.1 ml 10 $\mu g\ g^{-1}$ In solution and diluted to 100 ml with ultra pure water before ICP-MS analysis.

3.4 Results and Discussion

3.4.1 Savillex Teflon Beaker Digestion

Three basalts (BHVO-1, TAFAHI and TASBAS) and three granites (GSR-1, AC-E and TASGRAN) have been used in the present study to investigate the decomposition of geological materials using the Savillex Teflon beaker digestion method by HR-ICP-MS. 100 mg of the basaltic samples was digested using 2 ml HF/0.5 ml HNO_3 on a hotplate at about 130 to 150 °C for 48 hours. The final solution was prepared in 2% HNO_3 and 1% HCl. All of the solutions were freshly analysed (within 24 hours after dissolution) by HR-ICP-MS. The results obtained demonstrate that basalts can be quatitatively dissolved by the Savillex Teflon beaker digestion technique. **Table 3.3** shows the measured trace element concentrations ($\mu g\ g^{-1}$), precisions and reference values for the three basaltic rock standards. In general, there was good agreement between the results measured in this work by HR-ICP-MS and reference values. In comparison with the reference values of BHVO-1 (Govindaraju, 1994), the analytical accuracy was generally within ±4%, except for Y (-17%) and Cs (+15%). The average precision (%RSD) of 27 trace elements for BHVO-1 on the basis of five independent digestions was 1.89%. The precision was in the range of 0.20% for Pr to 9.92% for Ta. The average analytical accuracy of 27 trace elements for TAFAHI was excellent and generally better than ± 1% comparing the mean measured results with the reference values reported by Eggins et al. (1997). The analytical accuracy for Sn was -10% and for Ta was 11%. Despite low abundances for most trace elements, the average precision for TAFAHI, on the basis of ten independent digestions, was about 5%. It has been found that the precision was in the range of 2.01% for Zr to nearly 8.00% for Tb. Comparing with the reference values of TASBAS (Robinson et al. 1986), measured results showed that the analytical accuracy was generally better than ±3%. The accuracy was found to be from -12% to 4%. On the basis of four separate digestions, the precision was excellent and the average precision was 0.33% for the 27 elements measured. The precision for TASBAS was in the range of 0.1% to 2.78%. As an additional assessment, the average analytical accuracy can be easily seen by plotting the ratio of the measured results to the reference values versus elements of interest. As shown in

Figure 3.3, the variations between measured results and reference values were normally less than ±10% for the three basaltic standard materials.

In order to investigate the effects of different acid mixtures and ratios on the digestion efficiency of granitic samples, three granitic rock standards (AC-E, GSR-1 and TASGRAN) were also digested with two different acid mixtures of HF/HNO_3 and $HF/HCl/HNO_3$. The detailed different mixtures and ratios used in this study are as follows:

A 1 ml HF + 2 ml HNO_3

B 1 ml HF + 1 ml HNO_3

C 2 ml HF + 1 ml HNO_3

D 2 ml HF + 0.5 ml HNO_3

E 1 ml HF + 3 ml HCl + 1 ml HNO_3

F 1 ml HF + 1 ml HCl + 3 ml HNO_3

For each acid mixture, 100 mg powdered sample was digested at 130 –150 °C for 48 hours. Duplicate digestions were applied to each sample and digestion condition. **Figures 3.4 to 3.6** show the comparison between the average measured results and reference values. In comparison with the reference values for ACE compiled by Govindaraju (1994), the average recoveries of 30 trace elements were 92%, 82%, 98%, 99%, 97% and 90% for digestion conditions A, B, C, D, E and F respectively. As shown in **Figure 3.4**, low recoveries for REE can be clearly seen with acid mixtures B and F. The good recoveries with acid mixtures C, D and E might indicate that there are only very small proportions of refractory accessory minerals (such as zircon, rutile etc.) in granite AC-E. In contrast, GSR-1 showed low recoveries under all digestion conditions. The average recoveries were 79%, 67%, 87%, 88%, 88% and 58% for digestion conditions A, B, C, D, E and F respectively. Similarly, very low recoveries for REE were also seen for acid mixtures B and F (**Figure 3.5**). The recoveries for REE were in the range of 45% for La to 69% for Lu using 1 ml HF/1 ml HNO_3 digestion and in the range of 26% for La to 56% for Lu using 1 ml HF/1 ml HCl/3 ml HNO_3 digestion. This might indicate that there is not sufficient HF under those digestion conditions (B and F) to break up the Si-O bond (Choa and Sanzolone, 1992). The recovery for TASGRAN was similar to those for GSR-1. The

Table 3.3. Measured trace element concentrations (μg g^{-1}), precision and reference values for the three basaltic rock standards: international standard material BHVO-1, laboratory standard TAFAHI and an in-house standard TASBAS by Savillex Teflon beaker digestion*

Ele-	BHVO-1			TAFAHI			TASBAS		
ment	Result n=5	%RSD	Ref. value	Result n=10	%RSD	Ref. value	Result n=4	%RSD	Ref. value
Sc	30	1.40	31.8	45.2	2.55	45.5	13.97	0.41	14.1
Rb	9.1	0.77	9.5	1.76	2.32	1.75	15.52	0.11	16.16
Y	22.8	0.92	27.6	8.24	2.72	9.11	19.58	0.16	19.5
Zr	163	1.28	179	12.1	2.01	12.07	243	2.78	245.9
Nb	18.2	1.15	19	0.501	2.84	0.456	58.4	0.59	58.37
Mo	1.06	1.89	1.02	0.458	3.14	0.44	7.55	0.09	7.41
Sn	1.98	4.04	2.1	0.217	7.25	0.24	2.94	0.12	3.2
Cs	0.15	6.67	0.13	0.063	5.16	0.066	1.01	0.01	1.05
Ba	128	1.55	133	38.3	3.25	40.3	186	1.01	185.2
La	14.6	0.62	15.5	0.950	5.43	0.938	44.1	0.43	43.2
Ce	35.7	0.81	38	2.17	4.91	2.22	85.2	1.15	85.24
Pr	5.03	0.20	5.45	0.331	5.21	0.361	9.37	0.12	10.12
Nd	23.1	0.78	24.7	1.89	4.24	1.93	41.9	0.89	40.23
Sm	5.63	1.60	6.2	0.711	7.46	0.722	7.97	0.19	8.14
Eu	1.91	1.57	2.06	0.288	8.03	0.305	2.27	0.06	2.58
Gd	5.75	0.87	6.22	1.04	7.22	1.069	6.46	0.10	6.89
Tb	0.84	1.19	0.96	0.212	7.99	0.207	0.94	0.01	0.93
Dy	4.81	0.83	5.2	1.39	6.68	1.384	4.11	0.08	4.67
Ho	0.89	1.12	0.95	0.311	7.89	0.322	0.7	0.01	0.79
Er	2.32	0.86	2.4	0.965	7.35	0.98	1.89	0.03	1.84
Yb	1.86	1.08	2.02	1.03	5.57	0.992	1.2	0.015	1.27
Lu	0.288	3.47	0.291	0.147	6.26	0.153	0.179	0.08	0.18
Hf	4.25	1.41	4.3	0.402	2.68	0.395	5.3	0.03	5.52
Ta	1.21	9.92	1.2	0.024	7.77	0.0219	3.88	0.02	3.76
Pb	2.56	1.95	2.6	0.941	4.97	0.95	4.76	0.44	4.67
Th	1.12	1.79	1.08	0.117	3.17	0.12	4.14	0.03	4.69
U	0.42	1.19	0.42	0.076	3.56	0.0728	1.99	0.01	1.91

*Digestion conditions: 2 ml HF and 0.5 ml HNO_3 for 100 mg powdered rock sample.

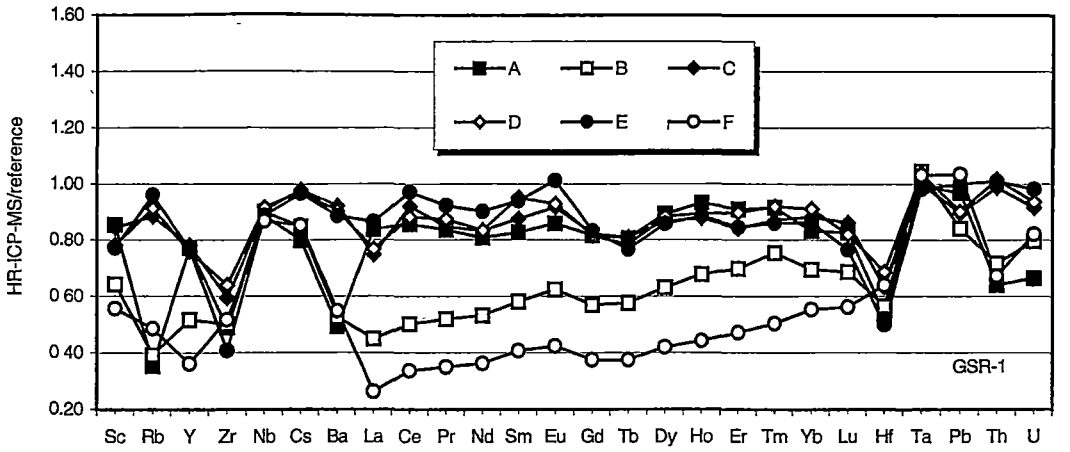

Figure 3.3. Comparison between the measured results and reference values for three basaltic rock standard materials (BHVO-1, TAFAHI and TASBAS) by Savillex Teflon beaker digestion. 2 ml HF and 0.5 ml HNO_3 were used to digest 100 mg samples.

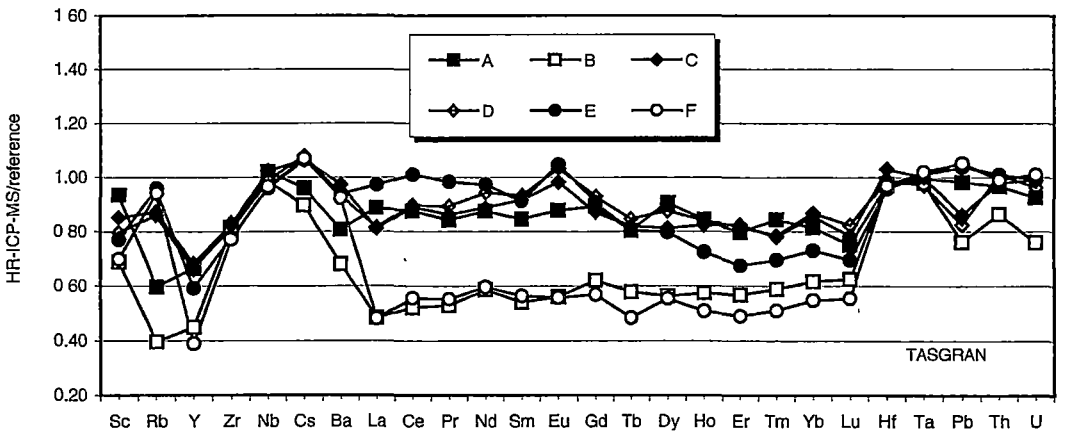

Figure 3.4. Comparison between the measured results and reference values for AC-E. Digestion conditions: A = 1 ml HF + 2 ml HNO_3; B = 1 ml HF + 1 ml HNO_3; C = 2 ml HF + 1 ml HNO_3; D = 2 ml HF + 0.5 ml HNO_3; E = 1 ml HF + 3 ml HCl + 1 ml HNO_3; F = 1 ml HF + 1 ml HCl + 3 ml HNO_3. Sample weight = 100 mg.

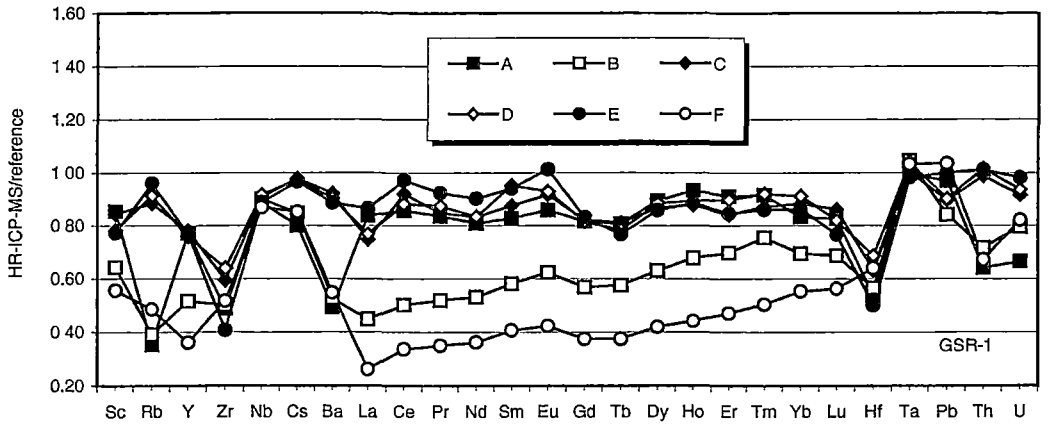

Figure 3.5. Comparison between the measured results and reference values for GSR-1. Digestion conditions: A = 1 ml HF + 2 ml HNO_3; B = 1 ml HF + 1 ml HNO_3; C = 2 ml HF + 1 ml HNO_3; D = 2 ml HF + 0.5 ml HNO_3; E = 1 ml HF + 3 ml HCl + 1 ml HNO_3; F = 1 ml HF + 1 ml HCl + 3 ml HNO_3. Sample weight = 100 mg.

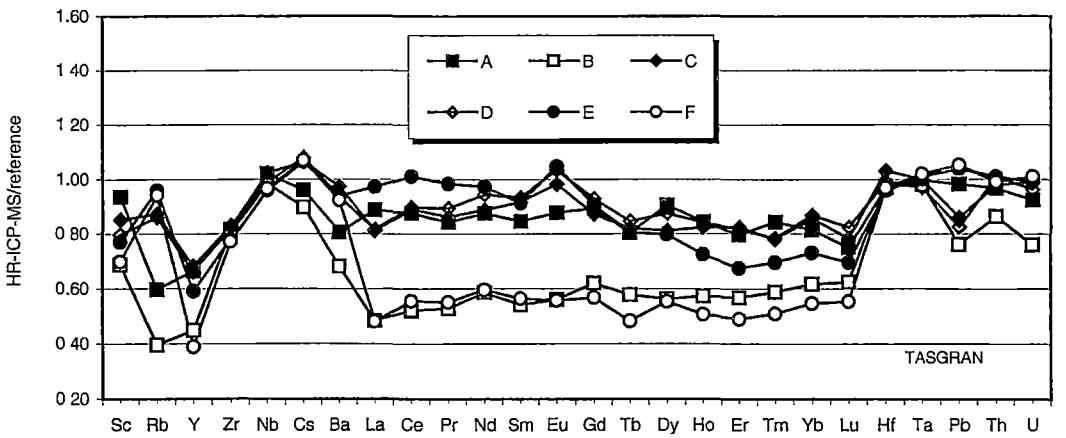

Figure 3.6. Comparison between the measured results and reference values for TASGRAN. Digestion conditions: A = 1 ml HF + 2 ml HNO_3; B = 1 ml HF + 1 ml HNO_3; C = 2 ml HF + 1 ml HNO_3; D = 2 ml HF + 0.5 ml HNO_3; E = 1 ml HF + 3 ml HCl + 1 ml HNO_3; F = 1 ml HF + 1 ml HCl + 3 ml HNO_3. Sample weight = 100 mg.

Table 3.4. Comparison between HR-ICP-MS results and reference values for the granitic rock standards (AC-E, GSR-1 and TASGRAN) using Savillex Teflon beaker digestion*

Element	HR-ICP-MS/reference value (recovery)		
	AC-E (n=2)	GSR-1 (n=2)	TASGRAN (n=2)
Sc	1.01	0.78	0.80
Rb	0.94	0.91	0.86
Sr	1.11	0.92	0.91
Y	0.80	0.76	0.66
Zr	0.97	0.64	0.83
Nb	1.00	0.92	0.99
Mo	0.90	0.99	0.65
Sn	0.98	0.90	0.92
Sb	1.10	0.96	0.84
Cs	1.02	0.97	1.08
Ba	0.98	0.90	0.93
La	0.97	0.77	0.82
Ce	1.02	0.88	0.90
Pr	0.99	0.87	0.89
Nd	1.02	0.83	0.94
Sm	1.04	0.95	0.93
Eu	1.02	0.93	1.03
Gd	0.99	0.82	0.93
Tb	0.90	0.78	0.85
Dy	1.02	0.88	0.88
Ho	0.92	0.89	0.84
Er	0.96	0.90	0.82
Tm	1.02	0.92	0.78
Yb	0.99	0.91	0.87
Lu	0.97	0.82	0.82
Hf	1.02	0.69	0.99
Ta	1.05	1.04	0.97
Pb	0.96	0.90	0.82
Th	1.10	1.02	1.01
U	1.05	0.94	0.96

*Digestion conditions: 2 ml HF and 0.5 ml HNO_3 for 100 mg rock powdered sample.

average recoveries under different acid mixtures A, B, C, D, E and F were 86%, 67%, 89%, 90% and 74%. Again, the very low recoveries have been found for the acid mixtures B and F. Under all different digestion conditions, best recoveries are always found using 1 ml HF + 0.5 ml HNO_3 for 100 mg rock samples and very low recoveries are found using 1 ml HF + 1 ml HNO_3 for AC-E, and 1 ml HF + 1 ml HCl + 3 ml HNO_3 for GSR-1 and TASGRAN. Under the optimum digestion condition (2 ml HF + 0.5 ml HNO_3 for 100 mg powdered sample), HR-ICP-MS/reference value for 30 trace elements was from 0.80 to 1.11 for AC-E, 0.64 to 1.04 for GSR-1 and 0.65 to 1.20 for TASGRAN. **Table 3.4** gives the comparison between measured results and reference values for the three granitic standards (AC-E, GSR-1 and TASGRAN).

In summary, basalts are completely dissolved by HF/HNO_3 Savillex Teflon beaker digestion. By contrast, granitic rocks cannot be completely decomposed by this digestion technique.

3.4.2 Acid High Pressure Digestion

3.4.2.1 HF/$HClO_4$ Digestion

This section presents the results of the HF/$HClO_4$ high pressure digestion technique for to basalt, granite and iron formation samples.

3.4.2.1.1 Basalt and Iron-rich Materials

One basalt (BHVO-1) and two iron formation (magnetite rich) materials (FeR-2 and FeR-4) were digested using the 3 ml HF/3 ml $HClO_4$ high pressure digestion method. After 48 hours digestion at 180 °C, the measured results were in good agreement with the reference values compiled by Govindaraju (1994). **Table 3.5** lists the measured results and compares them to reference values. Each result obtained represents the mean value of two separate digestions.

In comparison with the reference values, it has been found that the results of the three geological reference materials studied show good recoveries. The recovery for

32 elements in BHVO-1 generally ranged from 90% to 110%. The recovery for REE was excellent. Results show that the recoveries were 100%, 99%, 98%, 104%, 108%, 112%, 113%, 103%, 109%, 108%, 118%, 110%, 108% and 106% for La, Ce, Pr, Nd, Sm, Eu, Gd, Tb, Dy, Ho, Er, Tm, Yb and Lu respectively. The recoveries for HFSE are 94%, 99%, 106%, 105%, 122% and 108% for Zr, Nb, Hf, Ta, Th and U respectively. The lowest recovery is 71% for Tl. On the other hand, in comparison with the reference values the average recoveries of 32 elements for FeR-2 and FeR-4 are 108% and 104% respectively. The recovery of 32 trace elements is in the range of 82% to 144% for FeR-2 and 73% to 152% for FeR-4. The recovery of REE for FeR-2 is from 91% for Ho to 144% for Gd and the recovery of REE for FeR-4 is from 86% for Pr to 152% for Er. Although there are some differences between the measured and reference values, they are reasonable considering that some of the reference values provided by Govindaraju (1994) are only information values.

It is well known that the REE have very similar chemical and physical properties. Understanding of subtle variations in REE abundances can help unravel petrological processes, and many more implications for the genesis of ore deposits. REE concentrations in geological materials are commonly normalised to chondrite values for interpretation in geochemistry (Sun and McDonough 1989; Rollinson 1993). In order to eliminate the abundance variation between odd and even atomic number elements and allow easier the observation of any fractionation of the REE group relative to chondritic meteorites, REE chondrite normalised patterns are usually smooth and so 'smoothness' has also been widely used as an additional assessment of the quality of the REE analytical data (e.g. Jarvis 1988; Ionov et al. 1992; Dulski 1994; Makishima and Nakamura 1997; Robinson et al. 1999). The REE distribution patterns obtained for FeR-2 and FeR-4 using high pressure acid digestion method are clearly flatter and smoother than those based on the reference values (Govindaraju 1994). Therefore, the analytical accuracy of REE for FeR-2 and FeR-4 has also been further demonstrated by the chondrite distribution patterns in this work. **Figure 3.7** shows the chondrite normalised distribution patterns of REE for FeR-2 and FeR-4 by 3 ml HF/3 ml $HClO_4$ 48-hour high pressure digestion.

In addition, in order to test a shorter digestion time BHVO-1 was also digested for 16 hours. Results (**Table 3.5**) show an average recovery of 92% for 32 elements

Table 3.5. Measured results (μg g^{-1}) for basalt and iron formation reference materials

Element	BHVO-1			FeR-2		FeR-4	
	Measured DT=48hr n=2	Measured DT=16hr n=2	Reference value*	Measured DT=48hr n=2	Reference value*	Measured DT=48hr n=2	Reference value*
Sc	29.6	29.7	31.8	5.31	6	1.09	1.5
Rb	9.26	9.24	11	61.8	67	14.9	16
Sr	383	378	403	60.9	58	60.4	62
Y	23.3	22.1	27.6	13.2	16	7.87	9
Zr	168	153	179	45.8	39	18.4	18
Nb	18.8	17.9	19	3.95	-	0.776	-
Mo	1.13	1.21	1.02	6.05	3	0.142	-
Sn	1.97	1.62	2.1	0.99	1	1.11	1
Sb	0.161	0.168	0.16	0.692	0.7	1.12	1
Cs	0.097	0.100	0.13	4.95	4.5	0.667	0.7
Ba	138	129	139	243	230	38.3	39
La	15.8	15.1	15.8	13.6	12	8.47	8
Ce	38.8	37.3	39	27.8	25	13.7	11
Pr	5.61	5.37	5.7	3.35	3	1.72	2
Nd	26.2	23.7	25.2	13. 6	12	8.22	8
Sm	6.69	5.83	6.2	3.02	2.5	2.39	2.1
Eu	2.32	2.06	2.06	1.48	1.25	0.79	0.74
Gd	7.23	5.94	6.4	2.88	2	1.44	1.1
Tb	0.987	0.878	0.96	0.398	0.32	0.185	0.15
Dy	5.65	4.82	5.2	2.51	2	1.16	1
Ho	1.07	0.945	0.99	0.545	0.6	0.251	0.2
Er	2.83	2.34	2.4	1.64	1.5	0.761	0.5
Tm	0.363	0.313	0.33	0.237	0.2	0.108	-
Yb	2.18	1.83	2.02	1.59	1.25	0.717	0.7
Lu	0.308	0.252	0.291	0.239	0.2	0.112	0.1
Hf	4.64	4.01	4.38	1.35	1	0.572	0.5
Ta	1.29	1.09	1.23	0.194	0.2	0.051	-
Tl	0.041	0.042	0.058	0.228	-	0.060	-
Pb	2.17	2.04	2.6	8.48	11	7.14	8
Bi	0.017	0.015	0.018	0.189	-	0.044	-
Th	1.32	1.16	1.08	3.22	2.4	0.976	0.8
U	0.455	0.446	0.42	1.29	1.2	0.641	0.5

DT is digestion time; * Reference values are form Govindaraju, 1994; - = no value available.

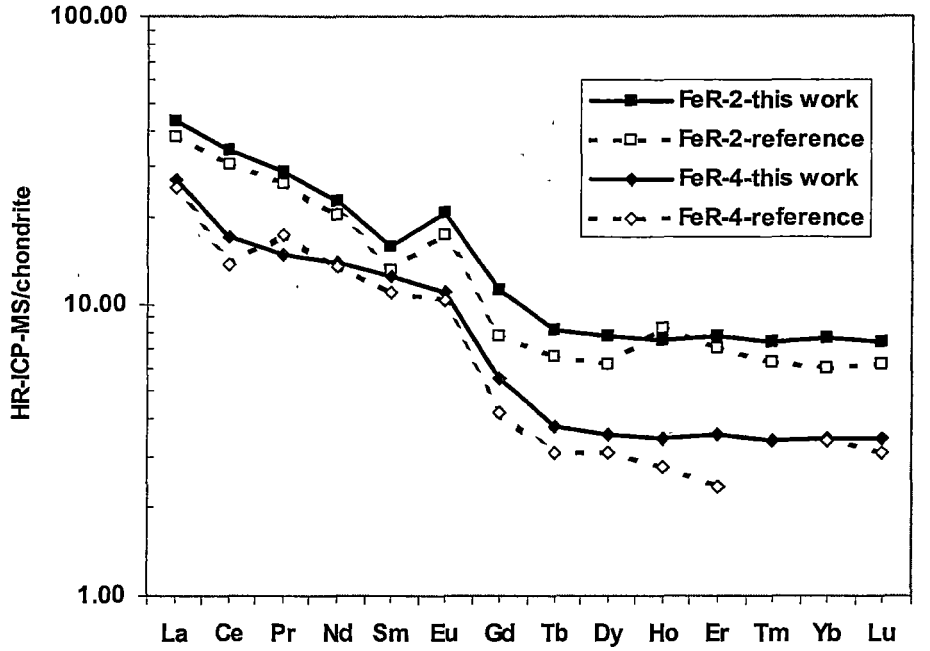

Figure 3.7. Chondrite normalised distribution patterns of REE for FeR-2 and FeR-4 by 3 ml HF/3 ml $HClO_4$ high pressure digestion. Digestion time = 48 hours. FeR-2-reference and FeR-4-reference are from Govindaraju (1994).

comparing with the reference values. This is substantially lower than for 48-hour digestion time. Recoveries for Zr, Nb, Hf and Ta are 86%, 94%, 91% and 89% respectively. Recovery for heavy REE is higher than 91% except 87% for Lu and higher than 94% for light REE. Thus, it is recommended that a minimum of 48-hours digestion time should be applied for a complete decomposition of basaltic and iron formation samples.

In summary, basalts and iron formation materials can be completely decomposed using the acid mixture of 3 ml HF and 3 ml $HClO_4$ with a high pressure digestion technique. It is also suggested that a digestion time of 48 hours and a digestion temperature of 180 °C are needed in order to achieve a complete decomposition.

3.4.2.1.2 Granites

In order to study granite digestion by $HF/HClO_4/HNO_3$ and $HF/HClO_4$ high pressure technique, GSR-1, G-2 and AC-E were digested under different conditions. These are:

Group A: 3 ml HF, 2 ml $HClO_4$ and 2 ml HNO_3 were used for 100 mg powdered samples. After 16 hours digestion at 180 °C, sample solutions were evaporated at 180 °C to dryness. Finally, the residues were taken up by 2 ml HNO_3 and diluted to 100 ml before the instrumental analysis.

Group B: 3 ml HF, 2 ml $HClO_4$ and 2 ml HNO_3 were used for 100 mg powdered samples. After 16 hours digestion at 180 °C, sample solutions were evaporated at 180 °C to dryness. Finally, the residues were taken up by 2 ml HNO_3 and 1 ml HCl and diluted to 100 ml before the instrumental run.

Group C: 3 ml HF and 3 ml $HClO_4$ were used for 100 mg powdered samples. After 16 hours digestion at 180 °C, sample solutions were evaporated at 180 °C to dryness. Then 5 ml HCl was added to the digestion vessel and evaporated to dryness again. Another aliquot of 5 ml HCl was then added and the digestion vessel was sealed with a lid, put back to the digestion block and reinforced with the pressure disk and plate. The residue was taken up by keeping the digestion vessel at 150 °C for 16 hours, followed by adding 10 ml ultra pure water to the vessel and warming for about an hour. The final solution was diluted to 100 ml of 5% HCl in a plastic container.

Group D: 3 ml HF and 3 ml $HClO_4$ were used for 100 mg powdered samples. After 16 hours digestion at 180 °C, sample solutions were evaporated at 180 °C to dryness. Then 5 ml HCl was added to the digestion vessel and evaporated to dryness again. 2 ml HNO_3 and 1 ml HCl were added to each digestion vessel. Then digestion vessel was sealed with a lid, put back to the digestion block and reinforced with the pressure disk and plate. The residue was taken up by keeping the digestion vessel at 150 °C for 16 hours, followed by adding 10 ml ultra pure

water to the vessel and warming for about an hour. Finally, the sample solution was diluted to 100 ml in a plastic container and made up to 2% HNO_3 and 1% HCl.

Group E: 3 ml HF and 3 ml $HClO_4$ were used for 100 mg powdered samples. After 16 hours digestion at 180 °C, sample solutions were evaporated at 180 °C to dryness. Then 5 ml HCl was added to the digestion vessel and evaporated to dryness again. A further 5 ml HCl was added to each digestion vessel, which was then sealed with a lid, put back to the digestion block and reinforced with the pressure disk and plate. The residue was taken up by keeping the digestion vessel at 150 °C for 16 hours, followed by evaporating to dryness again. Finally, the residues were taken up in 2 ml HNO_3 and 1 ml HCl and diluted to 100 ml before the instrumental run.

Note that 0.1 ml 10 ng g^{-1} In solution was spiked into each sample vessel for Groups A to E before digestion. Groups A and B are referred to as one-stage digestion and Groups C, D and E are called two-stage digestion. In digestion Groups C, D and E, sample residues were digested again for another 16 hours with the addition of either 5 ml HCl or 2 ml HNO_3 and 1 ml HCl.

Tables 3.6 to 3.8 show the average measured results of two separate digestions for GSR-1, G-2 and AC-E by $HF/HClO_4/HNO_3$ and $HF/HClO_4$ high pressure digestion techniques. As a rule, the measured results from the present work are lower than the reference values for digestion Groups A to D. In comparison with the reference values (Xie et al., 1989), the average recoveries of 32 trace elements for GSR-1 are only 78%, 77%, 88% and 82% with Groups A, B, C and D respectively. Comparing the measured results for the four digestion groups, similar recoveries can be observed for Zr, Nb, Hf and Ta. However, the highest recoveries for Th and U have been found with digestion Group C, and the recoveries of Th and U are normally 20 to 30% higher than those with the digestion Groups A, B, and D. Similarly, the highest recoveries for REE have also been found with digestion Group C, and recoveries for both light and heavy REE are normally 20% higher than those with the digestion Groups A, B, and D. In comparison with the compiled values (Govindaraju 1994) the

average recoveries of 32 trace elements for G-2 are 83%, 80%, 90% and 81% by digestion Groups A, B, C and D respectively. Comparing the measured results within the four digestion groups, similar recoveries can be observed for Zr, Nb, Hf and Ta. The highest recoveries, again for Th and U, are found with digestion Group C, and recoveries are normally 5 to 10% higher than those with the other digestion groups. Similarly, the highest recoveries for REE have also been found with digestion Group C, and recoveries for both light and heavy REE are normally 5 to 15% higher than those with the digestion Groups A, B, and D. In comparison with the reference values compiled by Govindaraju (1994), the average recoveries of 32 trace elements for AC-E are 65%, 69%, 85% and 83% by digestion Groups A, B, C and D respectively. Comparing the measured results for the four digestion groups, similar recoveries can also be observed for Nb and Ta. The recoveries of Zr and Hf are almost identical between digestion Groups C and D. On the other hand, the recoveries of Zr and Hf with Group C and Group D digestions are about 40 and 50% higher than those with Group A and Group B respectively. The highest recoveries for Th and U are found with digestion Group C, and are normally 5 to 50% higher than those with the digestion Groups A, B and D. Similarly, the highest recoveries for REE are also found with digestion Group C, and the recoveries for both light and heavy REE are normally 20% higher than those with the other digestion groups.

In this study, GSR-1 and G-2 were also digested with another two-stage $HF/HClO_4$ high pressure digestion method (Group E). In an earlier investigation, a similar digestion method was used by Dulski (1994) to measure the concentrations of Ba and REE in granitic samples. **Tables 3.6** and **3.7** show that among all of the digestion groups, the highest recoveries of the 32 elements are obtained by digestion E, for which the average recoveries of 32 trace elements for GSR-1 and G-2 are 97% and 94% respectively, and analytical errors are generally less than ±10%. **Figure 3.8** further shows the detailed recoveries of HFSE and REE for GSR-1 and G-2 under Group E digestion conditions. It can be clearly seen that the recovery is generally better than 90% in comparison with the reference values. The average recoveries of HFSE and REE for GSR-1 and G-2 are 97% and 95% respectively. In other words, the analytical accuracy for HFSE and REE is in the range of ±3 - 5%. This indicates that granitic samples can be digested completely with the Group E digestion conditions. A representative comparison of recoveries for Zr, La, Ce, Lu, Ta and U in

Table 3.6. Measured concentrations (μg g^{-1}) for GSR-1 by $HF/HClO_4/HNO_3$ and $HF/HClO_4$ high pressure digestion (digestion time = 16 hours)

Element	Measured concentration					Reference
	Group A	Group B	Group C	Group D	Group E	value
Sc	4.43	4.20	6.41	3.82	5.86	6.1
Rb	411	405	454	427	453	466
Sr	86.6	79.9	100	97.4	96.5	106
Y	40.2	41.4	55.9	47.2	64.2	62
Zr	158	166	145	158	153	167
Nb	41.6	43.3	42.4	43.6	41.0	40
Mo	3.78	3.62	3.34	3.71	3.71	3.5
Sn	10.9	11.0	11.3	12.1	12.6	12.5
Sb	0.242	0.242	0.168	0.252	0.20	0.21
Cs	33.9	35.7	35.3	37.6	38.7	38.4
Ba	263	275	289	299	312	343
La	33.0	31.7	45.4	33.7	50.3	54
Ce	84.2	86.3	97. 7	91.5	107	108
Pr	8.15	7.88	11.1	8.26	11.9	12.7
Nd	28.4	27.5	38.3	28.7	42.5	47
Sm	6.13	5.82	8.18	6.20	9.63	9.7
Eu	0.536	0.475	0.736	0.582	0.83	0.85
Gd	5.89	5.50	7.77	6.33	8.70	9.3
Tb	1.01	0.943	1.31	1.06	1.51	1.65
Dy	6.35	5.97	8.19	6.90	9.76	10.2
Ho	1.39	1.32	1.78	1.54	2.11	2.05
Er	4.31	4.13	5.44	4.82	6.51	6.5
Tm	0.734	0.717	0.907	0.834	1.09	1.06
Yb	5.13	4.97	6.27	5.89	6.99	7.4
Lu	0.780	0.783	0.972	0.901	1.11	1.15
Hf	5.61	5.87	5.02	5.54	5.60	6.3
Ta	6.47	6.91	6.51	6.90	7.38	7.2
Tl	1.96	1.98	1.66	2.02	1.99	1.93
Pb	26.5	28.1	27.7	31.8	30.6	31
Bi	0.527	0.507	0.441	0.575	0.52	0.53
Th	31.2	30.9	45.7	35.1	51.7	54
U	12.1	11.2	16.5	8.73	19.0	18.8

Reference value is from Xie et al. (1989).

Table 3.7. Measured concentrations (μg g^{-1}) for G-2 by $HF/HClO_4/HNO_3$ and $HF/HClO_4$ high pressure digestion (digestion time = 16 hours)

Element	Measured concentration					Reference
	Group A	Group B	Group C	Group D	Group E	value
Sc	3.55	3.41	4.11	3.34	3.54	3.5
Rb	163	146	163	147	159	170
Sr	449	417	470	454	438	478
Y	8.29	7.82	8.79	8.45	9.31	11
Zr	258	262	267	264	267	309
Nb	12.4	12.1	12.7	12.2	12.1	12
Mo	0.303	0.349	0.293	0.257	0.33	1.1
Sn	1.26	1.51	1.61	1.63	0.06	1.8
Sb	0.056	0.029	0.084	0.036	0.03	0.07
Cs	1.38	1.31	1.32	1.33	1.38	1.34
Ba	1776	1714	1749	1685	1784	1882
La	73.6	69.4	76.9	68.6	82.5	89
Ce	141	140	149	141	159	160
Pr	13.4	12.9	14.7	13.0	16.2	18
Nd	43.0	40.6	46.4	41.5	51.1	55
Sm	5.73	5.59	6.50	5.74	7.23	7.2
Eu	1.27	1.23	1.37	1.28	1.52	1.4
Gd	4.28	4.02	4.35	4.18	4.63	4.3
Tb	0.390	0.380	0.419	0.396	0.48	0.48
Dy	1.73	1.69	1.85	1.80	2.14	2.4
Ho	0.300	0.294	0.318	0.313	0.37	0.4
Er	0.727	0.716	0.776	0.762	0.87	0.92
Tm	0.100	0.098	0.146	0.105	0.17	0.18
Yb	0.584	0.587	0.641	0.624	0.67	0.8
Lu	0.084	0.082	0.108	0.089	0.10	0.11
Hf	6.50	6.28	6.29	6.23	6.45	7.9
Ta	0.895	0.802	0.897	0.755	0.85	0.88
Tl	0.832	0.787	0.837	0.695	0.84	0.91
Pb	25.6	26.0	27.2	27.0	29.0	30
Bi	0.040	0.039	0.041	0.031	0.04	0.037
Th	19.5	19.4	22.0	20.0	24.0	24.7
U	1.51	1.46	1.80	1.59	2.05	2.07

Reference value is from Govindaraju (1994).

Table 3.8. Measured concentrations (μg g^{-1}) for AC-E by $HF/HClO_4/HNO_3$ and $HF/HClO_4$ high pressure digestion (digestion time = 16 hours)

Element	Measured concentration				Reference
	Group A	Group B	Group C	Group D	value
Sc	0.489	0.416	1.23	1.02	0.11
Rb	227	170	137	139	152
Sr	2.36	2.07	2.15	2.00	3
Y	52.3	82.9	153	141	184
Zr	338	256	737	718	780
Nb	114	111	117	109	110
Mo	2.55	2.73	2.23	2.10	2.5
Sn	4.55	5.07	5.77	6.62	13
Sb	0.372	0.385	0.290	0.311	0.4
Cs	3.27	3.06	2.73	2.75	3
Ba	61.5	53.3	49.5	48.6	55
La	37.1	39.3	50.4	47.3	59
Ce	104	98	141	131	154
Pr	12.5	14.0	19.0	18	22.2
Nd	51.8	59.1	78.6	74.3	92
Sm	12.4	15.1	21.7	20.5	24.2
Eu	0.905	1.15	1.71	1.63	2
Gd	12.6	15.8	23.1	22.9	26
Tb	1.99	2.67	4.11	4.06	4.8
Dy	11.4	16.2	25.8	25.3	29
Ho	2.29	3.37	5.52	5.45	6.5
Er	5.87	9.35	15.8	15. 4	17.7
Tm	0.823	1.37	2.39	2.34	2.6
Yb	4.69	8.14	14.9	14.6	17.4
Lu	0.646	1.17	2.12	2.07	2.45
Hf	11.8	9.75	23.9	24.1	27.9
Ta	6.31	6.17	5.94	5.85	6.4
Tl	0.801	0.774	0.759	0.787	0.9
Pb	36.4	38.4	32.3	31.4	39
Bi	0.359	0.290	0.246	0.248	0.4
Th	5.90	9.55	16.0	14.8	18.5
U	3.91	3.94	4.02	3.87	4.6

Reference value is from Govindaraju (1994).

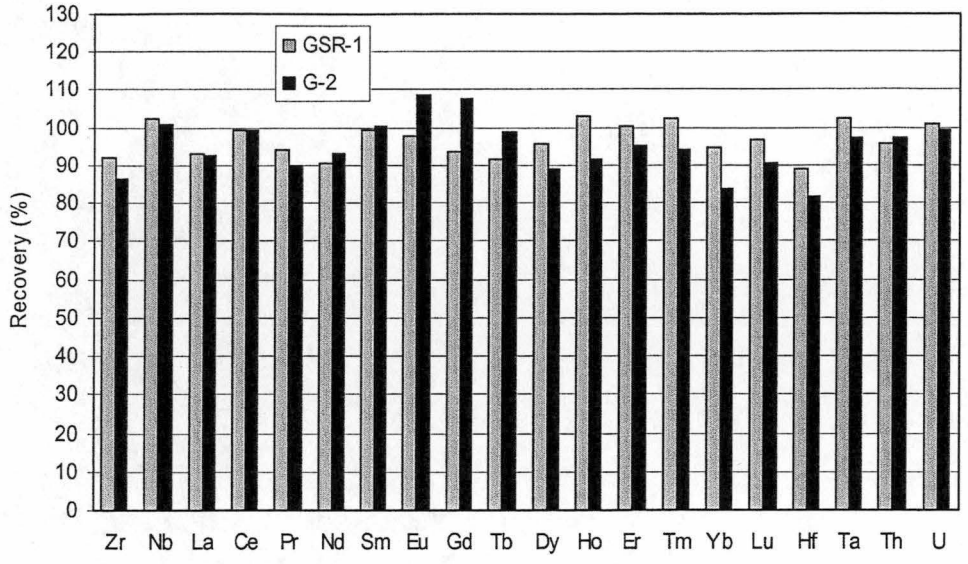

Figure 3.8. Recoveries of HFSE and REE for GSR-1 and G-2 by $HF/HClO_4$ high pressure digestion. Recovery (%) = (measured value/reference value) x 100. Digestion conditions were the same as Group E.

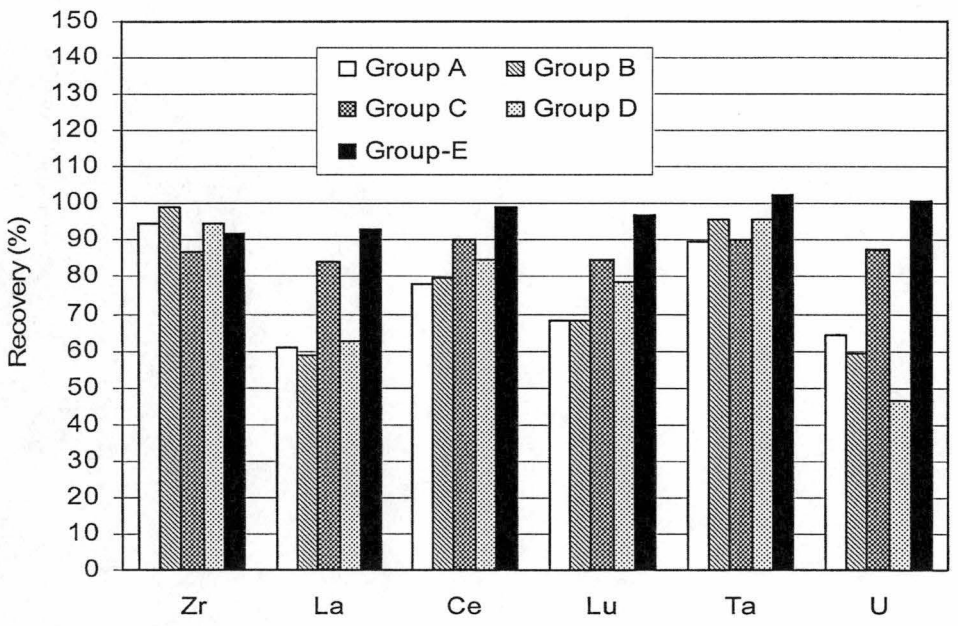

Figure 3.9. Representative elemental recoveries for GSR-1 using five different digestion methods.

GSR-1 under different digestion conditions is given in **Figure 3.9,** which shows that there were good recoveries for Zr and Ta under all digestion conditions, whereas the best recoveries for La, Ce, Lu and U appeared only under the Group E conditions. In this study, it has also been observed that there existed consistent good recoveries (generally in the range of 90% to 110%) for Rb, Zr, Nb, Cs, Ta, Tl, Pb and Bi under different digestion conditions. By contrast there was considerable variation in recoveries for La, Ce, Lu and U.

Münker (1998) reported that the addition of a small amount of HCl can stabilise the Nb and Ta in testing solutions for ICP-MS analysis even a few hours after sample solution preparation. In this experiment, all solutions were freshly prepared and HR-ICP-MS runs were always conducted within 24 hours. However, there was no obvious difference in the results of Nb and Ta for GSR-1, G-2 and AC-E between 2% HNO_3 and 2% HNO_3 + 1% HCl in final solutions under both Group A and Group B digestion conditions.

From the above discussion, it may be concluded that, in general, granites cannot be digested by the one-stage $HF/HClO_4/HNO_3$ and $HF/HClO_4$ high pressure digestion technique. However, the two-stage $HF/HClO_4$ high digestion pressure technique (Group E) can be used for granites.

3.4.2.2 HF/H_2SO_4 Digestion

In order to investigate the HF/H_2SO_4 high pressure digestion of different geological materials, six granites (GSR-1, AC-E, G-2, MA-N, YG-1 and TASGRAN), two iron formation (magnetite rich) samples (FeR-2 and FeR-4) and two basalts (TAFAHI and TASBAS) were selected for testing. All samples (100 mg powder) were dissolved in 3 ml HF/3 ml H_2SO_4 and digested at about 180 °C for 16 hours. Then, to drive off the 3 ml H_2SO_4, the solutions were evaporated to dryness, which took about 120 hours (cf. 100 hours reported by Münker (1998)). The residues were evaporated to dryness again with the addition of 1 ml $HClO_4$. This step is crucial in order to convert insoluble sulfates of the alkaline-earth metals and Pb in to their perchlorates (Bock 1979). Before the instrumental run, the residues were taken up with 2 ml HNO_3 and 1 ml HCl at 60 to 70 °C for an hour or so, followed by the addition of 10

ml ultra pure water. Finally, the solutions were warmed at 60 to 70 °C for another hour before diluting to 100 ml in plastic containers. All solutions were measured by HR-ICP-MS within 24 hours.

As shown in **Table 3.9**, GSR-1 and AC-E were analysed using four independent decompositions. The average measured results are in good agreement with the reference values for GSR-1 and AC-E, which were reported by Xie et al. (1989) and compiled by Govindaraju (1994). The lower results for Hf, Ta and Th are likely due to their hydrolysis in aqueous solutions (Makherij 1970; Heslop and Jones 1976; Münker 1998). For instance, Hf and Ta compounds readily undergo hydrolysis, even in acid solutions, to form insoluble hydrated oxides HfO_2 $(H_2O)_x$ and Ta_2O_5 $(H_2O)_x$ (Perrin 1964). AC-E used in this study might have been contaminated by Sc for some reason during its storage, since consistent higher Sc abundances in AC-E have been observed by HR-ICP-MS with different digestion methods. The analyte reproducibilities (%RSD) of trace elements are generally less than 10% and the reproducibilities of REE are less than 5% for GSR-1. The high RSD value (18.54%) for Ta can again be explained by its instability in aqueous solutions due to its hydrolysis. The reproducibilities for AC-E are similar to those for GSR-1 and the RSD values for HFSE are normally less than 5% except that for Ta. Furthermore, for AC-E, which contains significant amounts of both light and heavy rare earth elements, the RSD values are generally within 5%. In comparison with the reference values, the average analytical accuracies of 32 trace elements for GSR-1 and 31 trace elements for AC-E (excluding Sc) are generally better than ±3% and ±4% respectively.

Similarly, another four granitic rock standards (G-2, MA-N, YG-1 and TASGRAN), two iron formation reference materials (FeR-2 and FeR-4) and two basalts (TAFAHI and TASBAS) were also analysed using the proposed digestion method in order to investigate the applicability of this method for different types of rock samples. **Table 3.10** shows the results for the four granites with duplicate independent digestions. The reference values for G-2 are compiled from Gladney et al. (1992) and Govindaraju (1994), for MA-N are from Govindaraju (1994), for YG-1 are from Thompson et al. (1999) and for TASGRAN are compiled from Robinson et al. (1986) and analytical results from several laboratories. Generally speaking, the

results agree with the reference values. Lower values for Sr, Ba and Pb for G-2, MA-N and YG-1 are due to the insoluble sulfates in aqueous solutions, since perchloric acid cannot decompose all unsoluble sulfates under the experimental conditions and hence the insoluble sulfates are not completely converted into soluble perchlorates (Chao and Sanzolone 1992). The recoveries of Ba for G-2 and YG-1 are only 41% and 55% due to high concentration. Very strong hydrolysis of Nb and Ta in aqueous solutions has been recorded for experiments at high concentrations; for instance, the recoveries of Nb and Ta for MA-N were only 49% and 37% respectively. Among the four granitic standard materials, TASGRAN shows the best average recovery of 98.3%, whereas MA-N shows the worst of 74.2%. The low recovery value for MA-N is due to both the sulfate precipitations and the hydrolysis of HFSE (particularly Nb and Ta) under experimental conditions. On the other hand, good recoveries of REE, Zr and U for G-2, MA-N, YG-1 and TASGRAN indicate that complete dissolution was achieved. This further supports the above explanation about the lower results for Sr, Ba, Pb (due to the formation of insoluble sulfates) and Nb and Ta (due to the hydrolysis in aqueous solutions). As shown in **Table 3.11** the average results of duplicate measurements based on two separate digestions are generally in good agreement with the reference values of FeR-2, FeR-4 (compiled from Dulski 1992; Govindaraju 1994), TAFAHI (Eggins et al. 1997) and TASBAS (compiled from Robinson and other sources). Comparing with the reference values, the average recoveries for FeR-2, FeR-4 and TAFAHI were 96.6%, 102.2% and 105.4% respectively. Despite the low recovery of 76.3% for Ta due to its hydrolysis in aqueous solutions, TASBAS still showed an average recovery of 94.2% compared with the reference values.

In addition, in order to study the possibility of reducing digestion time (evaporation time) an effort was made to investigate whether the amount of both HF and H_2SO_4 can be reduced for the digestion of granites (GSR-1, G-2 and AC-E). Using 100 mg sample the ratios of HF and H_2SO_4 tested are 3 ml to 0.5 ml, 3 ml to 1 ml, 2 ml to 0.5 ml, 2 ml to 1 ml and 2 ml to 2 ml. Different digestion times (16 and 48 hours) were also investigated whether digestion efficiency can be increased by increasing the digestion time. **Tables 3.12 to 3.14** show the average concentrations of duplicate measurements on the basis of two independent digestions under each HF to H_2SO_4 ratio and digestion time. From the obtained results it can be seen that:

1. In general, the recoveries of trace elements increase with increasing of H_2SO_4 concentration. For instance, in comparison with the reference value the average recovery of GSR-1 increased from 69% to 93% with the increase of H_2SO_4 from 0.5 to 2 ml. Similarly, the average recovery of G-2 increased from 69% to 87%.

2. Similar recovery were found with 16 and 48-hour digestion time when the same H_2SO_4 concentration was employed. As can be seen in **Tables 3.12 to 3.14,** the recoveries of GSR-1, G-2 and AC-E are very similar with 16 and 48-hour digestion time when 2 ml HF/1 ml H_2SO_4 was used. It has been found that the recoveries for GSR-1 are 90% and 84%, for G-2 are 85% and 86% and for AC-E are the same (87%). This indicates that 16-hour digestion time is sufficient with the HF/ H_2SO_4 high pressure digestion.

3. The recovery of AC-E shows a different trend to those of GSR-1 and G-2 in this investigation. Unlike with GSR-1 and G-2, there is not a clear increase in the recovery of AC-E with increasing of H_2SO_4 concentration. This probably reflects mineralogical differences between AC-E and GSR-1 or G-2. As reported by Xie et al. (1989) and Flanagan (1967), GSR-1 and G-2 are both rich in biotite, whereas AC-E is alkali feldspar-rich and has very high zirconium abundance.

4. Granites cannot be digested completely when less than 3 ml HF and 3 ml H_2SO_4 are used under the proposed digestion conditions.

The recoveries of HFSE and REE for GSR-1 under various digestion conditions are shown schematically in **Figure 3.10.** It can be clearly seen that the recovery (measured/reference) can be improved by increasing the volumes of HF and H_2SO_4. The average recovery was about 97% when 3 ml HF and 3 ml H_2SO_4 were used. Although fresh solutions (within 24 hours after dissolution) are normally run by HR-ICP-MS, it has been observed about 15% Ta was actually lost. Again the low recovery for Ta was due to the strong hydrolysis of Ta in aqueous solutions.

Table 3.9. Measured concentrations (μg g^{-1}), precisions and reference values for GSR-1 and AC-E by 3 ml HF/3 ml H_2SO_4 high pressure digestion

Element	GSR-1			AC-E		
	Measured n=4	%RSD	Reference value	Measured n=4	%RSD	Reference value
Sc	6.20	6.02	6.1	0.916	4.31	0.11
Rb	473	1.23	466	148	5.00	152
Sr	101	2.85	106	2.74	8.14	3
Y	60.7	3.41	62	161	1.81	184
Zr	165	6.14	167	803	2.12	780
Nb	42.0	8.72	40	112	4.90	110
Mo	3.70	7.16	3.5	2.36	7.33	2.5
Sn	11.8	4.89	12.5	15.2	4.00	13
Sb	0.261	8.25	0.21	0.358	9.15	0.4
Cs	37.5	2.40	38.4	3.00	1.00	3
Ba	308	2.19	343	55.1	3.57	55
La	51.3	1.91	54	56.6	2.37	59
Ce	102	2.56	108	150	1.73	154
Pr	12.1	2.80	12.7	21.3	1.96	22.2
Nd	41.8	3.49	47	87.2	2.41	92
Sm	9.09	4.10	9.7	23.7	3.32	24.2
Eu	0.815	2.61	0.85	1.87	4.53	2
Gd	8.49	3.12	9.3	25.2	3.15	26
Tb	1.45	4.42	1.65	4.50	4.37	4.8
Dy	9.27	3.10	10.2	28.7	1.65	29
Ho	1.98	4.04	2.05	5.98	5.18	6.5
Er	6.17	3.14	6.5	17.4	3.21	17.7
Tm	1.01	3.10	1.06	2.58	6.60	2.6
Yb	7.13	2.96	7.4	16.5	2.69	17.4
Lu	1.11	1.94	1.15	2.34	5.51	2.45
Hf	5.88	5.72	6.3	27.1	3.15	27.9
Ta	6.18	18.54	7.2	5.90	19.94	6.4
Tl	2.09	6.23	1.93	0.929	4.74	0.9
Pb	31.1	8.08	31	35.0	0.33	39
Bi	0.587	13.17	0.53	0.358	12.99	0.4
Th	49.1	2.01	54	17.5	3.29	18.5
U	18.7	1.17	18.8	4.53	4.00	4.6

Table 3.10. Measured concentrations ($\mu g\ g^{-1}$), precisions and reference values for G-2, MA-N, YG-1 and TASGRAN by 3 ml HF/3 ml H_2SO_4 high pressure digestion

Element	G-2		MA-N		YG-1		TASGRAN	
	Measured n=2	Ref value	Measured n=2	Ref value	Measured n=2	Ref value	Measured n=2	Ref value
Sc	3.59	3.5	0.117	0.2	4.49	4.4816	6.89	6.85
Rb	169	170	3047	3600	149	153.99	259	251
Sr	438	478	73.5	84	83.3	88.53	146	145
Y	9.28	11	0.311	0.4	49.8	54.44	31.8	35.5
Zr	305	309	14.2	25	268	271.38	159	160
Nb	11.9	12	84.5	173	50.0	48.78	13.1	13.1
Mo	0.14	1.1	0.283	0.3	1.60	1.86	0.32	0.31
Sn	1.56	1.8	99.1	900	15.7	20.00	5.85	6.43
Sb	0.04	0.07	1.34	1.7	1.17	1.50	0.12	0.126
Cs	1.47	1.34	578	640	4.19	4.0789	12.8	12.1
Ba	775	1882	39.8	42	292	534.91	464	455
La	79.7	89	0.433	0.5	58.8	63.40	41.5	39.7
Ce	151	160	0.787	0.9	118	129.5	83.3	84.6
Pr	15.9	18	0.095	0.1	15.0	15.01	10.1	10.1
Nd	49.8	55	0.332	0.4	53.0	56.66	35.9	35.9
Sm	6.95	7.2	0.073	0.09	10.9	11.44	7.09	7.51
Eu	1.38	1.4	0.014	0.02	1.61	1.6346	0.83	0.82
Gd	4.37	4.3	0.052	0.08	10.5	10.85	6.10	6.27
Tb	0.47	0.48	0.010	0.01	1.69	1.7049	0.90	1.02
Dy	2.04	2.4	0.056	0.07	9.80	9.9257	5.51	5.83
Ho	0.35	0.4	0.011	0.017	2.01	1.9625	1.07	1.16
Er	0.85	0.92	0.027	0.04	5.47	5.303	3.19	3.4
Tm	0.12	0.18	0.004	0.007	0.79	0.7427	0.45	0.507
Yb	0.68	0.8	0.031	0.04	4.78	4.7345	3.06	3.19
Lu	0.10	0.11	0.003	0.005	0.72	0.6904	0.44	0.48
Hf	7.49	7.9	1.94	4.5	8.34	8.074	4.63	4.63
Ta	0.84	0.88	109	290	71.9	95.55	1.86	2.09
Tl	0.86	0.91	19.4	15	0.77	0.8094	1.53	1.2
Pb	26.4	30	24.8	29	19.7	22.50	25.2	26.07
Bi	0.03	0.037	1.67	-	0.33	0.30	0.24	-
Th	21.2	24.7	0.716	1.4	19.6	22.45	18.3	19.2
U	2.10	2.07	13.4	12.5	3.14	2.9388	3.30	3.02

- = no value available.

Table 3.11. Measured concentrations (μg g^{-1}), precisions and reference values for FeR-2, FeR-4, TAFAHI and TASBAS and by 3 ml HF/3 ml H_2SO_4 high pressure digestion

Element	FeR-2		FeR-4		TAFAHI		TASBAS	
	Measured n=2	Ref value	Measured n=2	Ref value	Measured n=2	Ref value	Measured n=2	Ref value
Sc	5.79	6	1.42	1.5	43.5	45.5	14.3	14.1
Rb	66.8	67	17.1	16	2.00	1.75	16.9	16.16
Sr	62.1	58	65.7	62	145	138.9	1014	1008
Y	12.7	16	8.42	9	9.94	9.11	17.9	19.5
Zr	37.5	39	20.6	18	10.7	12.07	243	245.9
Nb	2.67	-	1.50	-	0.0442	0.456	61.5	58.37
Mo	2.69	3	1.14	-	0.503	0.44	8.06	7.41
Sn	1.03	1	1.01	1	0.166	0.24	3.04	3.2
Sb	0.64	0.7	1.26	1	0.020	0.024	0.11	1.05
Cs	4.83	4.5	0.71	0.7	0.055	0.066	1.05	1.07
Ba	205	230	40.7	39	39.4	40.3	190	185.2
La	12.2	12	7.87	8	1.03	0.938	44.3	43.2
Ce	23.8	25	12.6	11	2.41	2.22	84.6	85.24
Pr	2.90	3	1.59	2	0.414	0.361	10.2	10.12
Nd	11.4	12	7.21	8	2.16	1.93	37.8	40.23
Sm	2.40	2.5	2.01	2.1	0.834	0.722	7.68	8.14
Eu	1.18	1.25	0.64	0.74	0.378	0.305	2.48	2.58
Gd	2.16	2	1.21	1.1	1.27	1.069	6.49	6.89
Tb	0.33	0.32	0.17	0.15	0.249	0.207	0.83	0.93
Dy	2.08	2	1.07	1	1.75	1.384	4.17	4.67
Ho	0.43	0.6	0.22	0.2	0.413	0.322	0.69	0.79
Er	1.29	1.5	0.67	0.5	1.22	0.98	1.65	1.84
Tm	0.18	0.2	0.09	-	0.185	-	0.20	0.232
Yb	1.22	1.25	0.60	0.7	1.18	0.992	1.21	1.27
Lu	0.18	0.2	0.09	0.1	0.184	0.153	0.16	0.18
Hf	1.09	1	0.53	0.5	0.294	0.395	4.99	5.52
Ta	0.27	0.2	0.11	-	0.0223	0.0219	2.87	3.76
Tl	0.21	-	0.09	-	0.010	0.0142	0.09	<0.1
Pb	9.40	11	7.06	8	0.985	0.95	6.24	4.56
Bi	0.25	-	0.19	-	0.003	-	0.19	<0.1
Th	2.37	2.4	0.78	0.8	0.136	0.12	4.36	4.69
U	0.89	1.2	0.56	0.5	0.078	0.0728	1.83	1.91

- = no value available.

Table 3.12. Measured concentrations (μg g^{-1}) for GSR-1 using different HF/H_2SO_4 ratio and digestion time

HF/H_2SO_4 (ml)	3/0.5	3/1	2/0.5	2/1	2/1	2/2	Reference value
D.T. (hr)	16	16	16	16	48	48	
Sc	2.56	2.59	2.94	4.99	4.02	5.20	6.1
Rb	322	318	337	408	370	435	466
Sr	63.2	73.0	67.1	91.8	94.6	97.5	106
Y	35.7	38.8	39.3	49.9	50.5	53.9	62
Zr	142	148	146	148	137	150	167
Nb	37.2	38.5	37.7	37.5	37.9	39.8	40
Mo	4.50	4.13	3.71	4.05	3.32	3.53	3.5
Sn	11.0	11.5	11.2	11.1	11.1	11.0	12.5
Sb	0.25	0.26	0.24	0.25	0.24	0.26	0.21
Cs	31.8	32.9	33.8	34.6	36.6	37.2	38.4
Ba	214	247	218	268	296	302	343
La	22.4	19.8	24.6	43.4	38.4	47.6	54
Ce	49.2	45.4	52.9	89.9	92.9	103	108
Pr	6.06	5.12	6.76	10.7	9.45	11.8	12.7
Nd	21.2	17.4	23.5	36.6	32.9	41.0	47
Sm	4.91	4.04	5.50	8.31	7.22	9.01	9.7
Eu	0.45	0.37	0.50	0.77	0.69	0.82	0.85
Gd	4.59	4.02	5.18	7.60	6.98	8.14	9.3
Tb	0.85	0.77	0.95	1.33	1.25	1.42	1.65
Dy	5.56	5.25	6.13	8.45	7.81	8.57	10.2
Ho	1.21	1.22	1.35	1.82	1.77	1.90	2.05
Er	3.84	3.94	4.22	5.61	5.35	5.70	6.5
Tm	0.68	0.72	0.74	0.95	0.93	0.98	1.06
Yb	4.70	5.15	5.14	6.55	6.50	6.75	7.4
Lu	0.74	0.82	0.81	1.02	0.99	1.03	1.15
Hf	5.15	5.37	5.33	5.39	4.97	5.35	6.3
Ta	5.88	6.08	5.86	6.19	4.18	5.13	7.2
Tl	2.11	2.08	2.18	2.21	2.00	2.12	1.93
Pb	27.0	28.4	27.8	31.6	31.4	32.3	31
Bi	0.52	0.54	0.52	0.57	0.52	0.54	0.53
Th	22.4	20.0	23.7	46.0	42.5	48.4	54
U	11.2	11.5	12.4	18.1	16.5	20.3	18.8

D.T. = Digestion time

Table 3.13. Measured concentrations (μg g^{-1}) for G-2 using different HF/H_2SO_4 ratio and digestion time

HF/H_2SO_4 (ml)	3/0.5	3/1	2/0.5	2/1	2/1	2/2	Reference value
D.T. (hr)	16	16	16	16	48	48	
Sc	2.12	1.93	1.95	3.21	2.94	3.19	3.5
Rb	95.8	97.7	93.1	144	139	152	170
Sr	284	341	288	400	445	441	478
Y	6.24	6.77	6.62	7.96	8.08	7.77	11
Zr	279	305	268	287	285	275	309
Nb	11.2	11.3	11.4	11.3	11.4	11.7	12
Mo	0.92	0.95	0.58	0.65	0.26	0.28	1.1
Sn	1.89	1.88	1.92	1.86	1.59	1.46	1.8
Sb	0.06	0.05	0.05	0.05	0.05	0.05	0.07
Cs	1.27	1.31	1.27	1.42	1.36	1.37	1.34
Ba	667	750	488	1165	1687	1668	1882
La	37.6	40.2	33.9	74.2	73.4	77.2	89
Ce	81.9	80.4	75.1	139	147	152	160
Pr	8.44	8.56	8.03	14.6	14.7	15.8	18
Nd	27.2	27.4	25.9	45.0	47.4	49.0	55
Sm	3.99	4.09	3.98	6.08	6.54	6.55	7.2
Eu	0.89	0.90	0.87	1.32	1.44	1.49	1.4
Gd	2.65	2.76	2.55	3.82	4.17	4.20	4.3
Tb	0.30	0.31	0.30	0.42	0.43	0.43	0.48
Dy	1.39	1.46	1.43	1.91	1.84	1.86	2.4
Ho	0.25	0.26	0.25	0.32	0.33	0.33	0.4
Er	0.60	0.64	0.62	0.76	0.78	0.78	0.92
Tm	0.09	0.09	0.09	0.11	0.11	0.11	0.18
Yb	0.51	0.54	0.54	0.63	0.66	0.67	0.8
Lu	0.08	0.08	0.08	0.09	0.10	0.10	0.11
Hf	6.72	7.26	6.50	7.12	7.23	7.17	7.9
Ta	0.84	0.77	0.77	0.79	0.77	0.77	0.88
Tl	0.82	0.83	0.88	0.92	0.90	0.88	0.91
Pb	20.0	21.6	19.4	24.6	30.5	30.2	30
Bi	0.05	0.05	0.05	0.05	0.04	0.04	0.037
Th	11.8	12.8	11.2	19.8	23.5	24.1	24.7
U	1.38	1.78	1.28	1.84	1.85	2.17	2.07

D.T. = Digestion time

Table 3.14. Measured concentrations ($\mu g\ g^{-1}$) for AC-E using different HF/H_2SO_4 ratio and digestion time

HF/H_2SO_4 (ml)	3/0.5	3/1	2/0.5	2/1	2/1	2/2	Reference value
D.T. (hr)	16	16	16	16	48	48	
Sc	0.78	0.82	0.81	0.84	0.87	0.77	0.11
Rb	139	134	134	139	132	127	152
Sr	1.78	1.82	1.73	1.83	1.93	1.81	3
Y	120	114	136	131	127	111	184
Zr	777	768	749	732	732	687	780
Nb	108	108	106	104	108	103	110
Mo	2.93	2.99	2.54	2.64	2.14	2.14	2.5
Sn	15.2	14.9	15.0	15.0	14.7	14.3	13
Sb	0.34	0.73	0.34	0.46	0.35	0.33	0.4
Cs	2.96	2.88	2.88	2.86	2.86	2.75	3
Ba	44.8	44.8	44.8	46.6	49.2	47.6	55
La	30.3	40.2	43.3	47.7	44.8	37.2	59
Ce	113	114	121	124	127	103	154
Pr	12.9	15.7	16.7	17.1	17.7	15.3	22.2
Nd	54.4	64.0	69.2	71.2	74.2	65.2	92
Sm	16.6	17.9	20.0	20.0	20.7	17.8	24.2
Eu	1.41	1.49	1.65	1.67	1.67	1.46	2
Gd	17.5	18.1	20.8	21.2	21.7	19.0	26
Tb	3.28	3.27	3.78	3.83	3.97	3.55	4.8
Dy	20.9	20.5	24.1	24.0	24.4	22.2	29
Ho	4.52	4.36	5.14	5.10	5.33	4.85	6.5
Er	13.0	12.5	14.8	14.5	15.1	13.8	17.7
Tm	2.04	1.92	2.30	2.26	2.37	2.18	2.6
Yb	12.9	12.1	14.4	13.9	14.6	13.6	17.4
Lu	1.82	1.73	2.11	2.03	2.09	1.93	2.45
Hf	26.8	26.5	26.4	26.3	25.2	23.8	27.9
Ta	5.25	5.58	4.84	5.74	5.86	5.79	6.4
Tl	1.01	0.98	0.97	0.95	0.93	0.91	0.9
Pb	31.9	32.1	31.3	35.0	38.0	35.6	39
Bi	0.29	0.29	0.28	0.29	0.28	0.27	0.4
Th	11.4	13.2	14.7	15.0	15.8	12.5	18.5
U	4.50	4.67	4.61	4.55	4.75	4.52	4.6

D.T. = Digestion time

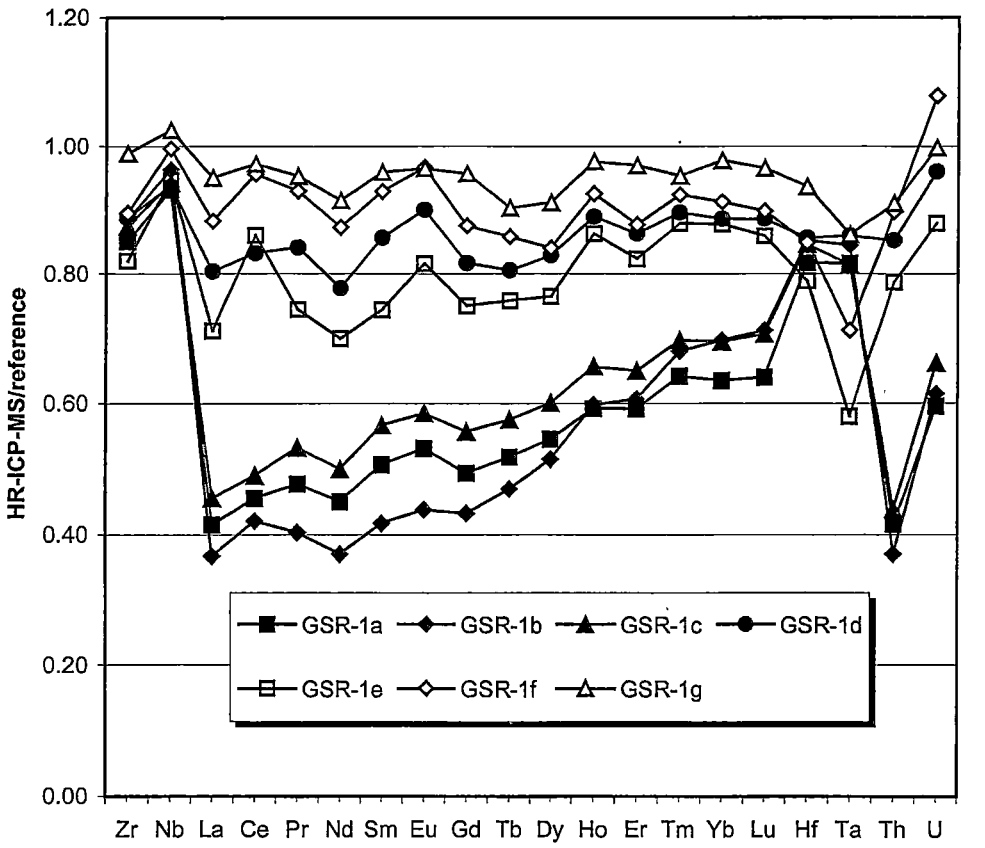

Figure 3.10. The recoveries of HFSE and REE for GSR-1 under various digestion conditions. Digestion conditions: GSR-1a = 16-hour digestion with 3 ml HF + 0.5 ml H_2SO_4, GSR-1b = 16-hour digestion with 3 ml HF + 1 ml H_2SO_4, GSR-1c = 16-hour digestion with 2 ml HF + 0.5 ml H_2SO_4, GSR-1d = 16-hour digestion with 2 ml HF + 1 ml H_2SO_4, GSR-1e = 48-hour digestion with 2 ml HF + 1 ml H_2SO_4, GSR-1f = 48-hour digestion with 2 ml HF + 2 ml H_2SO_4, GSR-1g = 16-hour digestion with 3 ml HF + 3 ml H_2SO_4. 100 mg rock sample was decomposed at 180°C for all of the digestions.

In summary, granites, basalts and iron formation rocks can be dissolved completely with 3 ml HF/3 ml H_2SO_4 high pressure digestion at 180 °C in 16 hours. Any reduction in the volumes of HF and H_2SO_4 will result in incomplete digestion for granites.

3.4.3 Microwave Acid Digestion

In recent years, microwave digestion techniques have been used to digest rock samples for ICP-MS (e.g. Jarvis et al. 1992; Totland et al. 1995; Yoshida et al. 1996). Ideally, in comparison with the high pressure digestion method, the microwave digestion technique should be less time-consuming, with rock samples being digested within one hour or so. However, Jarvis et al. (1992) also found that the microwave digestion did not always allow the measurement of refractory elements such as Zr and Hf especially when refractory mineral phases are present. In some cases, the measurement of the REE seemed to be a problem due to incomplete dissolution of rock samples (Yoshida et al. 1996). The work reported here uses a MLS-1200 MEGA Microwave Digestion System, which is more powerful microwave than those used by Jarvis et al. (1992), Totland et al. (1995) and Yoshida et al. (1996) (**Table 3.15**).

Table 3.15. Comparison of digestion power and pressure among different microwave digestion works

Parameter	This work	Jarvis et al. 1992	Totland et al. 1995	Yoshida et al. 1996
Maximum power (W)	650	not given	100	420
Maximum pressure (psi)	1595	120	200	70

A basalt (BHVO-1), two granites (GSR-1 and TASGRAN) and a magnetite-rich rock standard (FeR-2) were digested in two different acid mixtures. At first, 5 minutes for 250, 400, 650 and 250 W power stages respectively were used to decompose these rock reference materials using MILESTONE Application Notes as a guide, but this was changed to 10 minutes for each power stage, due to the incomplete dissolution using 5 minutes. The two acid mixtures used in the study were 2 ml HF + 0.5 ml HNO_3 and 2 ml HF + 0.5 ml HNO_3 + 2 ml $HClO_4$ + 0.2 ml H_2SO_4. After digestion in the microwave, sample solutions were evaporated to near dryness at about 180 °C on a hotplate. It has been observed that it took about 10 hours to drive off the 0.2 ml H_2SO_4 in the testing solution. After the first evaporation was completed, the test samples were evaporated to near dryness again with addition of 1 ml $HClO_4$ to

further drive off hydrofluoric acid and transfer the insoluble sulfate salts into perchlorate salts. The hot residue was taken up with 2 ml HNO_3 and ultra pure water, and finally diluted to 100 ml with ultra pure water in a clean polycarbonate container.

It was found that the BHVO-1 cannot be decomposed completely by the microwave digestion technique. **Figure 3.11** shows the comparison between measured results and reference values (Govindaraju 1994). The recoveries were found to be similar using 5 minutes for each power stage with 2 ml HF + 0.5 ml HNO_3 and 10 minutes for each power stage with 2 ml HF + 0.5 ml HNO_3 and 2 ml HF + 0.5 ml HNO_3 + 2 ml $HClO_4$ + 0.2 ml H_2SO_4. The average recoveries under the three different digestion conditions were about 91%. The recovery was better than 90% for light REE and most trace elements, and better than 85% for heavy REE. The recovery for Zr was about 83% using both 5 and 10 minutes for each power stage with two different acid mixtures. Yttrium showed the lowest recovery of less than 80%. The recoveries for U were 99.8%, 96.2% and 99.4% using 5 minutes for each power stage with 2 ml HF + 0.5 ml HNO_3 and 10 minutes for each power stage with 2 ml HF + 0.5 ml HNO_3 and 2 ml HF + 0.5 ml HNO_3 + 2 ml $HClO_4$ + 0.2 ml H_2SO_4. These recovery values agree with those for microwave digested basalts reported by Yoshida et al. (1996), who found, for example, that the average recoveries of Y, Zr and U for two Japanese basaltic samples (JB-1 and JB-2) were 84.5%, 90.5% and 96% respectively.

The recoveries for GSR-1 and TASGRAN were quite different. The reason for the different recoveries is not clear. It may be due to the difference in their mineral compositions (i.e. different refractory accessory minerals such as zircon etc. in the two rocks).

Recoveries of trace elements for GSR-1 generally increase with the increase of digestion time for each power stage and with the use of oxidising acids ($HClO_4$ and H_2SO_4). **Figure 3.12** shows the comparison between measured results and reference values for GSR-1 (Xie et al. 1989). From the results measured by HR-ICP-MS, the average recovery of 32 trace elements increases from 68.6% to 76% (for HF/HNO_3 acid mixture) by changing the digestion time from 5 to 10 minutes for each power

stage. Using 10 minutes for each power stage, the average recovery of 32 trace elements increases from 76% to 83.7% when $HF/HNO_3/HClO_4/H_2SO_4$ acid mixture is used. As shown in **Figure 3.12**, good recoveries (~100%) for Nb, Mo and Sb were found under the three different digestion conditions. The average recoveries of REE were about 61% and 72% respectively using 5 and 10 minutes for each power stage with HF/HNO_3 acid mixture, and about 77% using 10 minutes for each power stage with $HF/HNO_3/HClO_4/H_2SO_4$ acid mixture.

There were no obvious variations in the average recoveries of 30 trace elements for TASGRAN with either the increase of digestion time or the use of oxidising acids **(Figure 3.13)**. The average recoveries of 30 trace elements were about 69% and the average recoveries of REE are about 65% under the three different digestion conditions. Both Nb and Hf showed good recoveries (~100%). The recoveries of Mo, Sn and Ta were found to be higher than 90%.

The recovery variation for the magnetite-rich rock standard FeR-2 was similar to that of TASGRAN. In comparison with recommended reference values (Govindaraju 1994), there was no obvious change in the recovery with either the increase of digestion time or the use of oxidising acids **(Figure 3.14)**. The average recoveries of 29 trace elements for FeR-2 were 85.6% and 85.8% respectively using 5 and 10 minutes for each digestion stage with HF/HNO_3 acid mixture, and 87.8% using 10 minutes for each power stage with $HF/HNO_3/HClO_4/H_2SO_4$ acid mixture. The recoveries for most trace elements were higher than 80%. The recoveries of Sr, Gd, Tb and Yb were very good (~100%). Sn showed the lowest recovery from 36% to 48% under the three different digestion conditions. This may be mainly due to partial lost during the evaporation (Jarvis et al. 1992) rather than the incomplete dissolution.

Clearly rock samples cannot be completely decomposed by the proposed microwave digestion method. Even using 10 minutes for each power stage which has doubled the time recommended by the manufacturer (MILESTONE Application Notes), the best average recovery of 30 trace elements for basalt (BHVO-1) is only about 91% and the average recoveries for granites (GSR-1 and TASGRAN) and iron formation sample (FeR-2) investigated in this study are all less than 88%. This confirms previous observations of microwave digestion technique (Lamothe et al. 1986;

Totland et al. 1992; Yoshida et al. 1996) that demonstrated incomplete dissolution of some types of geological materials, especially when refractory minerals such as chromite, corundum, zircon etc. are present. Therefore, the microwave digestion techniques tested here are not generally suitable for the decomposition of rock samples for analysis by HR-ICP-MS.

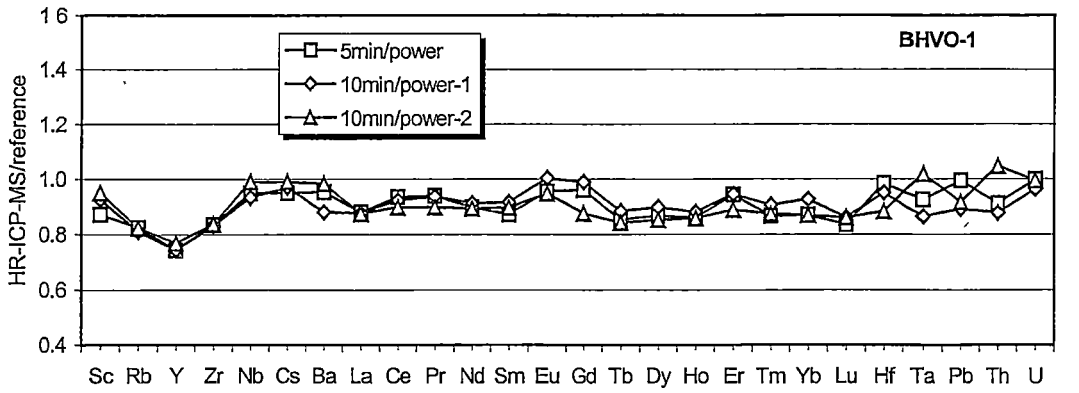

Figure 3.11. Comparison of HR-ICP-MS results with reference values for international basalt rock standard BHVO-1. 5 min/power = 5 minutes for each power stage with 2 ml HF + 0.5 ml HNO_3. 10 min/power-1 = 10 minutes for each power stage with 2 ml HF + 0.5 ml HNO_3. 10 min/power-2 = 10 minutes for each power stage with 2 ml HF + 0.5 ml HNO_3 + 2 ml $HClO_4$ + 0.2 ml H_2SO_4. Sample weight was 100 mg.

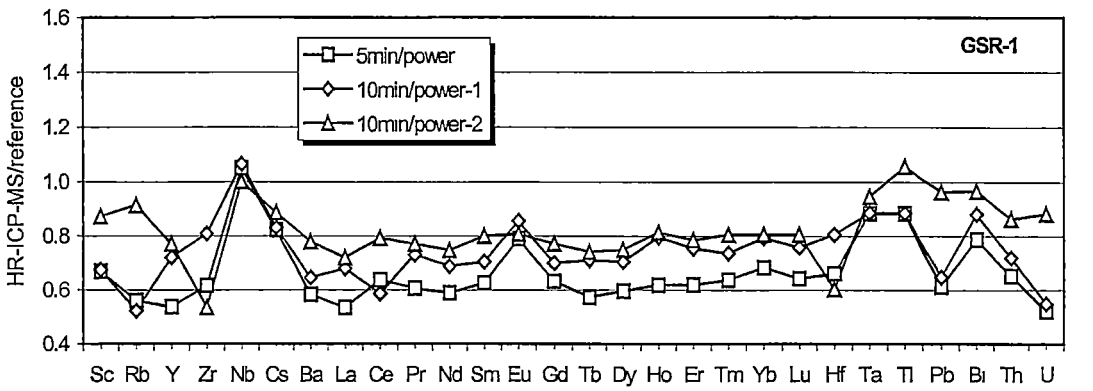

Figures 3.12. Comparison of HR-ICP-MS results with reference values for international granite rock standard GSR-1. 5 min/power = 5 minutes for each power stage with 2 ml HF + 0.5 ml HNO_3. 10 min/power-1 = 10 minutes for each power stage with 2 ml HF + 0.5 ml HNO_3. 10 min/power-2 = 10 minutes for each power

stage with 2 ml HF + 0.5 ml HNO_3 + 2 ml $HClO_4$ + 0.2 ml H_2SO_4. Sample weight

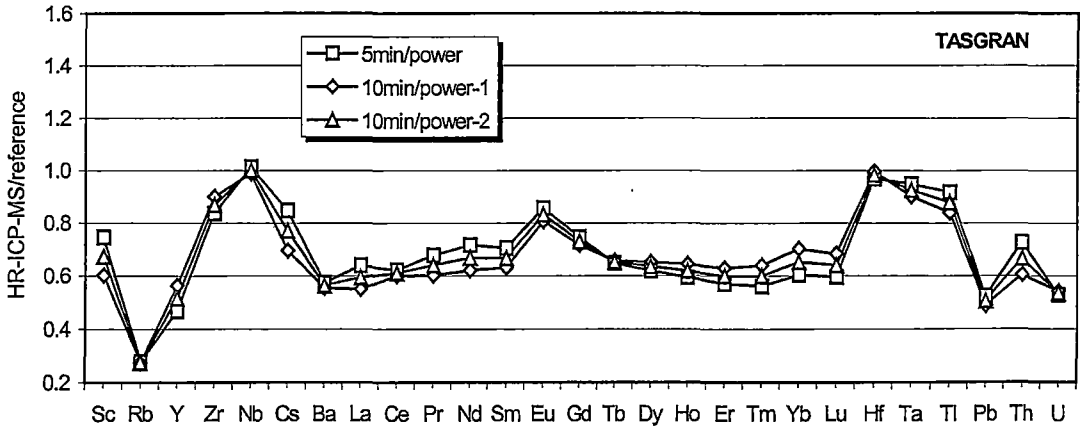

was 100 mg.

Figures 3.13. Comparison of HR-ICP-MS results with reference values for in-house granite rock standard TASGRAN. 5 min/power = 5 minutes for each power stage with 2 ml HF + 0.5 ml HNO_3. 10 min/power-1 = 10 minutes for each power stage with 2 ml HF + 0.5 ml HNO_3. 10 min/power-2 = 10 minutes for each power stage with 2 ml HF + 0.5 ml HNO_3 + 2 ml $HClO_4$ + 0.2 ml H_2SO_4. Sample weight was 100 mg.

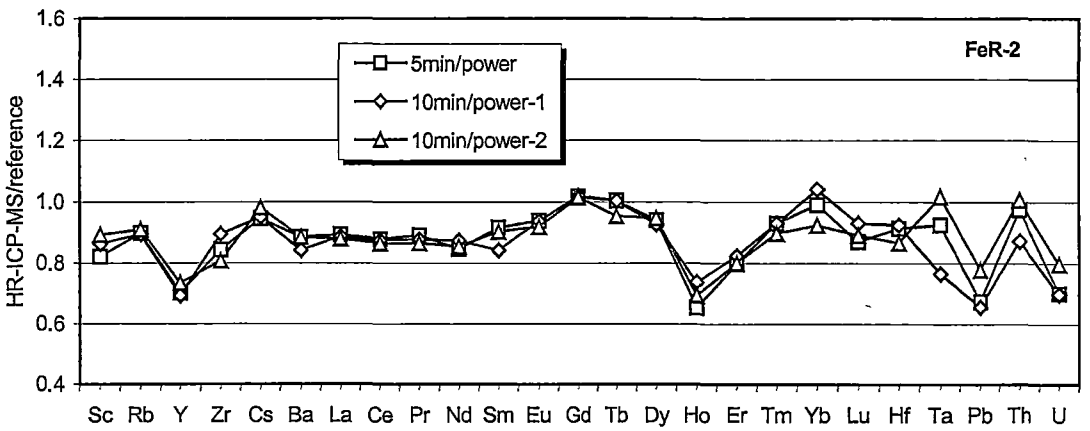

Figure 3.14. Comparison of HR-ICP-MS results with reference values for magnetite rich rock standard FeR-2. 5 min/power = 5 minutes for each power stage with 2 ml HF + 0.5 ml HNO_3. 10 min/power-1 = 10 minutes for each power stage with 2 ml HF + 0.5 ml HNO_3. 10 min/power-2 = 10 minutes for each power stage with 2 ml HF + 0.5 ml HNO_3 + 2 ml $HClO_4$ + 0.2 ml H_2SO_4. Sample weight was 100 mg.

3.4.4 Fusion Decomposition

Alkali fusion is an alternative decomposition techniques used to decompose refractory minerals (Potts 1987; Chao and Sanzolone 1992; Jarvis et al. 1992), despite the introduction of high levels of total dissolved solids during sample preparation which may restrict the quantification for some trace elements by ICP-MS (Totland et al. 1992). Alkali fusion was used by Jarvis (1990) and Totland et al. (1992) to decompose geological materials with lithium metaborate ($LiBO_2$) for trace element analysis. Quadrupole ICP-MS was used as the final analytical technique. However, it has been observed in the preliminary work of this study that, in most cases, the blank levels of trace elements are lower in lithium tetraborate ($Li_2B_4O_7$) (Sigma Chemicals) than in lithium metaborate (Sigma Chemicals). The blank levels for Sr, Zr, Mo, Ba, La and Ce were found to be 0.08, 0.15, 1.36, 3.45, 0.3 and 0.17 ng g^{-1} respectively, for Sc, Y, Nb, Cs, Nd, Hf, Ta, Th and U were found to be all below 0.01 ng g^{-1} and for Pr, Sm and heavy REE (from Eu to Lu) were found to be less than 0.002 ng g^{-1} in procedure blank solutions of the lithium tetraborate fusion decomposition method.

In this section of the present study, a lithium tetraborate has been used to decompose different types of geological reference materials for trace element analysis by HR-ICP-MS. In addition, the effect of total dissolved solids at the dilution factors of 1000, 2000 and 5000 on the analytical results has also been evaluated.

In order to study the effectiveness of lithium tetraborate ($Li_2B_4O_7$) fusion decomposition technique for geological materials, three basalts (BHVO-1, TAFAHI and TASBAS), three granites (GSR-1, AC-E and TASGRAN) and two iron formation (magnetite-rich) samples (FeR-2 and FeR-4) were decomposed by the proposed fusion technique. From the average results based on duplicate decompositions for each sample (**Table 3.16**), it can be seen that lithium tetraborate fusion is an effective decomposition technique for the geological materials. In the present study, 27 trace elements have been successfully determined by HR-ICP-MS using this lithium tetraborate fusion decomposition. In general, the measured results of the different types of rock samples show good agreement with the reference values. It has also been observed that, in some cases, this method gives slightly

higher concentrations for Zr, Nb, Hf, Ta, Th and U in the geological reference materials, especially in the three granite samples.

The analytical accuracy of 27 trace elements for BHVO-1 was generally within ±8% comparing with the reference value compiled from Govindaraju (1994) and Eggins et al. (1997). The accuracy for Sc, Rb, Sr, Zr, Mo, Cs, Ba, La, Ce, Pr, Nd, Tb, Ta, Th and U was found to be better than ±5%. Although the concentrations for some of the trace elements, such as Nb, Mo, Cs, La, Pr, Sm, Tb, Ho, Lu, Hf, Ta, Th and U, are very low (less than $\mu g\ g^{-1}$ in solid sample), the analytical accuracy of trace elements for TAFAHI compared with the reference values (Eggins et al. 1997) was always within ±10%, except for Rb. It also can be seen that the analytical accuracy for Sr, Ba, Ce, Eu, Tb, Er, Yb and U in TAFAHI was excellent and generally better than ±2%. In comparison with the reference values compiled from Robinson et al. (1986) and results measured using SSMS, XRF, solution ICP-MS, INAA by several external laboratories, the measured results by HR-ICP-MS showed good analytical accuracy. The difference for most trace elements in TASBAS was within ±4% using this fusion decomposition technique.

Good recoveries were also found for the granitic samples by the fusion decomposition technique. As shown in **Table 3.16,** the analytical accuracy of trace elements for GSR-1 are generally better than ±5% compared with reference values reported by Xie et al. (1989), whereas the accuracies for Tb, Lu and U are -9.7%, -7.0% and 5.3% respectively. In comparison with reference values (Govindaraju 1994), the analytical accuracies of Sr, Y, Nb, Ba, Tm and Hf for AC-E are found to be 10.3%, -8.7%, 6.4%, 6.4%, 6.2% and 8.2% respectively and for the other trace elements except Sc are found to be within ±6%. Again the high result for Sc may be due to contamination during sample storage. The analytical accuracy of trace elements for TASGRAN is normally better than ±5% compared with the reference values compiled from Robinson et al (1986) and results measured using SSMS, XRF, INAA and solution ICP-MS by several external laboratories. The accuracies for Mo, Tm, Hf, Ta, and U are -9.7%, -8.7%, 6.1%, 9.6%, and 13.9% respectively. However, it has to be pointed out that some of the trace element values for TASGRAN should be considered as average values only on the basis of a few measurements by different instrumental methods. For instance, the average

concentration of Ta for TASGRAN is 3.23 μg g^{-1} by two separate INAA analyses, compared with the value of 2.29 μg g^{-1} measured in this study by HR-ICP-MS.

The reference values of trace elements for two iron formation samples used in this study are compiled from two sets of data (i.e. Dulski 1992 and Govindaraju 1994). As seen in **Table 3.16** there is general agreement between measured results and reference values. But there are also some big variations. For instance, Ta and U for FeR-2 are -16% and –10.8% of the recommended values and the variations of Cs, Ce and most heavy REE for FeR-4 are higher than ±10%. This may reflect the fact that the two iron formation samples are not well characterised standard reference materials (Govindaraju 1994). Also, some of the big variations are for very low abundance elements (less than 1 μg g^{-1} in solid samples, equivalent to 1 ng g^{-1} in sample solutions considering a dilution factor of 1000 under the experimental conditions). Hence, the data reported here are probably of better quality than those compiled by Govindaraju (1994).

In addition, as shown in **Figure 3.15**, chondrite normalised REE plots show smooth patterns, also suggesting the measured results of REE for the eight geological reference materials used in this study are of good quality.

Although lithium tetraborate fusion is a powerful decomposition technique for geological materials by HR-ICP-MS, this method precludes the determination of volatile metals (such as Sn, Sb, Te, Tl, Pb and Bi) due to the high fusion temperature (1000 °C). It has also been observed in this study that the blank levels of some trace elements such as Sr, Zr, Mo, Ba and La using lithium tetraborate fusion decomposition method were higher than those using an acid digestion method. For instance, in a batch of analyses the blank levels for Zr, Mo, Ba and La were found to be 0.153, 1.36, 3.45 and 0.39 ng g^{-1} in solution (or equivalent to 0.153, 1.36, 3.45 and 0.39 μg g^{-1} in solid considering a dilution factor of 1000) respectively.

The Effect of TDS: Another major disadvantage of this method is that the levels of total dissolved solids (TDS) are higher than those using acid digestion methods, therefore reducing the number of trace elements that can be measured (Jarvis et al. 1992; Totland et al. 1992). Generally, it is required that the TDS level in final

solution should be less than 0.1-0.2% for ICP-MS (Totland et al. 1992). In this work, 100 mg powdered sample and 200 mg lithium tetraborate powder were used for the fusion and the final solution was diluted to 100 ml in a polycarbonate container. In order to investigate the effect of the TDS level on the present HR-ICP-MS method, a series of basalt (TASBAS) samples have been digested and diluted to 100, 200 and 500 ml in final solutions respectively, which gave the dilution factors of 1000, 2000 and 5000. The TDS levels were 0.1, 0.05 and 0 02% in terms of the total solid sample actually dissolved in final solutions. **Table 3.17** shows the comparisons of measured results of different TDS levels, and these results are also compared with the reference values (Robinson et al. 1986 and other sources). It has been found that there is good agreement among the three different TDS levels. The recoveries of trace elements for TASBAS are in the range of 93 to 109%. In other words, the analytical accuracy are within ±9% compared with the reference values. The average recoveries for the dilution factors of 1000, 2000 and 5000 were found to be 103%, 104% and 103% respectively. Therefore, it can be concluded that the proposed lithium tetraborate fusion decomposition procedure (using 100 mg solid sample and 200 mg lithium tetraborate powder in the fusion) can generally meet the requirement for HR-ICP-MS analysis of trace elements in rocks.

In summary, lithium tetraborate fusion can be used to decompose different types of geological samples (such as basalt, granite and magnetite rich sample) for the analysis of trace elements by HR-ICP-MS. However, this method precludes the determination of volatile elements such as Sn, Sb, Te, Tl, Pb and Bi due to the high fusion temperature (1000 °C) of this procedure. Moreover, this method may not be suitable for the measurement of some trace elements such as Sr, Zr, Mo, Ba and La at very low concentrations because of high levels of these elements in lithium tetraborate.

Table 3.16. Measured trace and rare earth element concentrations (μg g^{-1}) and comparison between HR-ICP-MS results and reference values for eight geological reference materials (BHVO-1, TAFAHI, TASBAS, GSR-1, AC-E, TASGRAN, FeR-2 and FeR-4) by lithium tetraborate fusion decomposition (number of analyses for each sample was 2)

Element	BHVO-1			TAFAHI		
	This work	Reference value	Variation (%)	This work	Reference value	Variation (%)
Sc	31.8	31.8	0.00	47.8	45.5	5.05
Rb	9.3	9.5	-2.11	1.98	1.75	13.1
Sr	414	403	2.73	138	138.9	-0.65
Y	25.1	27.6	-9.06	8.9	9.11	-2.31
Zr	172	179	-3.91	12.7	12.07	5.22
Nb	18.1	19.5	-7.18	0.492	0.456	7.89
Mo	1.04	1.02	1.96	0.468	0.44	6.36
Cs	0.098	0.1	-2.00	0.062	0.066	-6.06
Ba	142	139	2.16	41.0	40.3	1.74
La	15.9	15.8	0.63	0.96	0.938	2.35
Ce	38.0	39	-2.56	2.25	2.22	1.35
Pr	5.68	5.7	-0.35	0.384	0.361	6.37
Nd	26.3	25.2	4.37	1.98	1.93	2.59
Sm	6.67	6.2	7.58	0.773	0.722	7.06
Eu	2.22	2.06	7.77	0.305	0.305	0.00
Gd	6.83	6.4	6.72	1.12	1.069	4.77
Tb	0.97	0.96	1 04	0.209	0.207	0.97
Dy	5.76	5.25	9.71	1.45	1.384	4.77
Ho	1.06	1	6.00	0.348	0.322	8.07
Er	2.73	2.56	6.64	0.99	0.98	1.02
Tm	0.349	0.33	5.76	0.157		
Yb	2.13	2.02	5.45	1.00	0.992	0.81
Lu	0.31	0.291	6.53	0.161	0.153	5.23
Hf	4.69	4.38	7.08	0.408	0.395	3.29
Ta	1.23	1.23	0.00	0.024	0.0219	9.59
Th	1.21	1.26	-3.97	0.129	0.12	7.50
U	0.44	0.42	4.76	0.074	0.0728	1.65

Variation (%) is the relative deviation between the measured results in this work and the reference values; - = no value available.

Table 3.16. (Continued). Measured trace and rare earth element concentrations (μg g^{-1}) and comparisons between HR-ICP-MS results and reference values for eight geological reference materials (BHVO-1, TAFAHI, TASBAS, GSR-1, AC-E, TASGRAN, FeR-2 and FeR-4) by lithium tetraborate fusion decomposition (number of analyses for each sample was 2)

Element	TASBAS			GSR-1		
	This work	Reference value	Variation (%)	This work	Reference value	Variation (%)
Sc	15.8	14.7	7.48	6.17	6.1	1.15
Rb	16.7	16.4	1.83	450	466	-3.43
Sr	1053	1008	4.46	109	106	2.83
Y	22.0	21.4	2.80	64.6	62	4.19
Zr	263	259	1.54	173	167	3.59
Nb	63.8	62.2	2.57	40.9	40	2.25
Mo	7.63	7.41	2.97	3.50	3.5	0.00
Cs	1.07	1.07	0.00	39.3	38.4	2.34
Ba	184	186.5	-1.34	341	343	-0.58
La	47.5	44.46	6.84	52.3	54	-3.15
Ce	87.4	85.45	2.28	106	108	-1.85
Pr	10.5	10.25	2.44	12.1	12.7	-4.72
Nd	40.8	41.67	-2.09	45.2	47	-3.83
Sm	8.2	8.25	-0.61	9.50	9.7	-2.06
Eu	2.54	2.64	-3.79	0.83	0.85	-2.35
Gd	6.98	6.79	2.80	9.1	9.3	-2.15
Tb	0.91	0.96	-5.21	1.49	1.65	-9.70
Dy	4.76	4.77	-0.21	9.71	10.2	-4.80
Ho	0.827	0.8	3.37	2.05	2.05	0.00
Er	1.88	1.82	3.30	6.48	6.5	-0.31
Tm	0.228	0.232	-1.72	1.03	1.06	-2.83
Yb	1.30	1.27	2.36	7.4	7.4	0.00
Lu	0.174	0.17	2.35	1.07	1.15	-6.96
Hf	5.62	5.43	3.50	6.50	6.3	3.17
Ta	3.86	3.95	-2.28	7.2	7.2	0.00
Th	4.67	4.87	-4.11	56.5	54	4.63
U	1.90	1.89	0.53	19.8	18.8	5.32

Variation (%) is the relative deviation between the measured results in this work and the reference values.

Table 3.16. (Continued). Measured trace and rare earth element concentrations (μg g^{-1}) and comparisons between HR-ICP-MS results and reference values for eight geological reference materials (BHVO-1, TAFAHI, TASBAS, GSR-1, AC-E, TASGRAN, FeR-2 and FeR-4) by lithium tetraborate fusion decomposition (number of analyses for each sample was 2)

Element	AC-E			TASGRAN		
	This work	Reference value	Variation (%)	This work	Reference value	Variation (%)
Sc	0.7	0.11		6.73	6.85	-1.75
Rb	147	152	-3.29	244	251	-2.79
Sr	3.31	3	10.3	145	145	0.00
Y	168	184	-8.70	35.7	35.5	0.56
Zr	782	780	0.26	162	160	1.25
Nb	117	110	6.36	13.7	13.1	4.58
Mo	2.48	2.5	-0.80	0.280	0.31	-9.68
Cs	3.03	3	1.00	12.6	12.1	4.13
Ba	58.5	55	6.36	459	455	0.88
La	59.9	59	1.53	41.6	39.7	4.79
Ce	154	154	0.00	85.6	84.6	1.18
Pr	21.8	22.2	-1.80	10.3	10.1	1.98
Nd	89	92	-3.26	36.1	35.9	0.56
Sm	25.6	24.2	5.79	7.2	7.51	-4.13
Eu	2.03	2	1.50	0.79	0.82	-3.66
Gd	25.3	26	-2.69	6.43	6.27	2.55
Tb	4.75	4.8	-1.04	0.97	1.02	-4.90
Dy	30.0	29	3.45	5.85	5.83	0.34
Ho	6.17	6.5	-5.08	1.19	1.16	2.59
Er	18.3	17.7	3.39	3.30	3.4	-2.94
Tm	2.76	2.6	6.15	0.463	0.507	-8.68
Yb	18.1	17.4	4.02	3.07	3.19	-3.76
Lu	2.42	2.45	-1.22	0.459	0.48	-4.37
Hf	30.2	27.9	8.24	4.91	4.63	6.05
Ta	6.76	6.4	5.62	2.29	2.09	9.57
Th	18.9	18.5	2.16	19.0	19.2	-1.04
U	4.61	4.6	0.22	3.44	3.02	13.9

Variation (%) is the relative deviation between the measured results in this work and the reference values.

Table 3.16. (Continued). Measured trace and rare earth element concentrations (μg g^{-1}) and comparisons between HR-ICP-MS results and reference values for eight geological reference materials (BHVO-1, TAFAHI, TASBAS, GSR-1, AC-E, TASGRAN, FeR-2 and FeR-4) by lithium tetraborate fusion decomposition (number of analyses for each sample was 2)

Element	FeR-2			FeR-4		
	This work	Reference value	Variation (%)	This work	Reference value	Variation (%)
Sc	5.14	5.6	-8.21	1.20	1.2	0.00
Rb	62.6	67	-6.51	15.1	16	-5.63
Sr	62.6	62	0.97	62.0	63.5	-2.36
Y	14.1	14	0.71	8.7	9	-3.33
Zr	39.3	39	0.77	19.6	18	8.89
Nb	2.42			1.85		
Mo	2.94	3	-2.00	0.64		
Cs	4.47	4.5	-0.67	0.625	0.7	-10.7
Ba	233	230	1.30	37.3	39	-4.36
La	13.2	12	10.0	8.1	8	1.25
Ce	26.3	25	5.20	13.3	12	10.8
Pr	3.20	3	6.67	1.67	1.7	-1.76
Nd	12.6	12	5.00	7.96	8	-0.50
Sm	2.71	2.6	4.23	2.31	2.2	5.00
Eu	1.34	1.3	3.08	0.75	0.72	4.17
Gd	2.31	2.3	0.43	1.25	1.1	13.6
Tb	0.359	0.36	-0.28	0.178	0.15	18.7
Dy	2.37	2.3	3.04	1.20	1	20.0
Ho	0.519	0.5	3.80	0.236	0.2	18.0
Er	1.46	1.5	-2.67	0.70	0.5	40.0
Tm	0.216	0.22	-1.82	0.104	0.06	73.3
Yb	1.42	1.4	1.43	0.72	0.7	2.86
Lu	0.213	0.22	-3.18	0.111	0.1	11.0
Hf	1.09	1	9.00	0.526	0.5	5.20
Ta	0.168	0.2	-16.0	0.129		
Th	2.64	2.5	5.60	0.83	0.8	3.75
U	1.07	1.2	-10.8	0.525	0.5	5.00

Variation (%) is the relative deviation between the measured results in this work and the reference values; - = no value available.

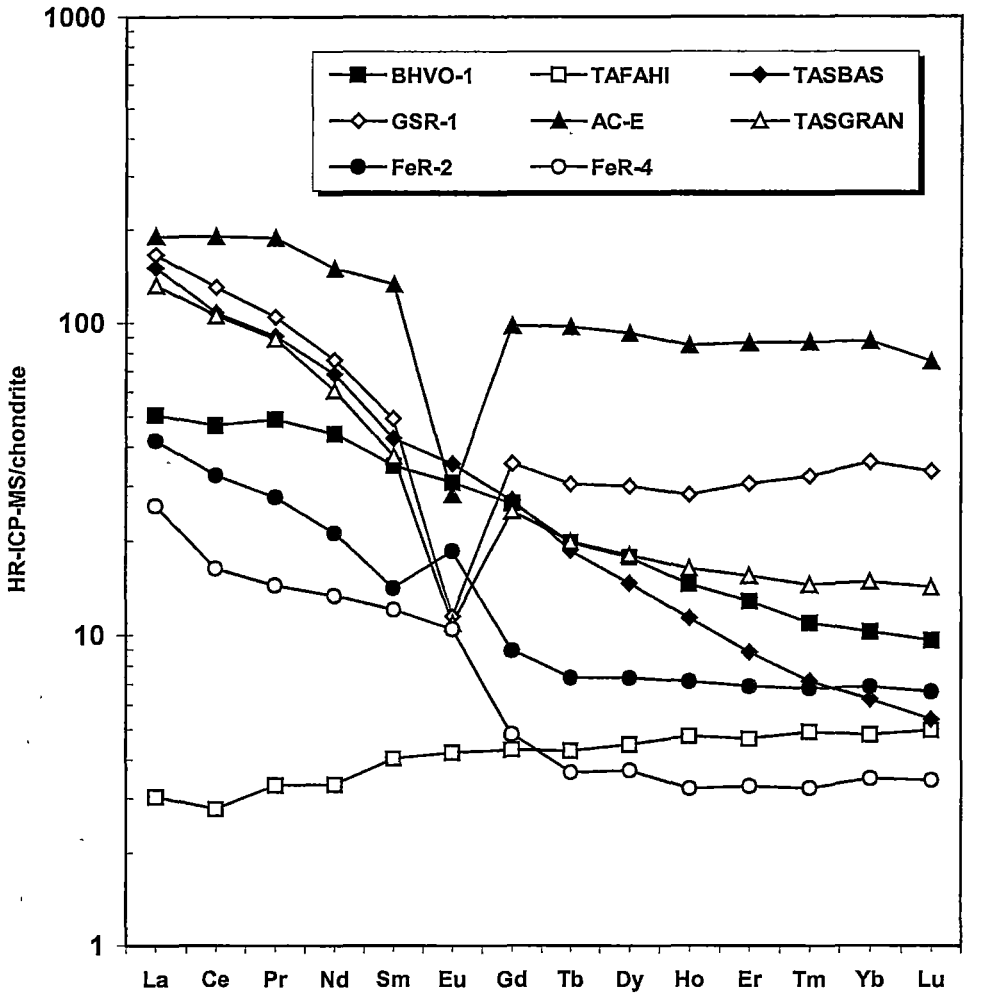

Figure 3.15. Chondrite normalised distribution patterns of rare earth elements for the eight selected geological reference materials (BHVO-1, TAFAHI, TASBAS, GSR-1, AC-E, TASGRAN, FeR-2 and FeR-4) using lithium tetraborate fusion digestion

Table 3.17. Effect of the levels of total dissolved solids (TDS) on the analytical results for rock reference material TASBAS using lithium tetraborate fusion decomposition by HR-ICP-MS

Element	Measured ($\mu g\ g^{-1}$)			Reference value* ($\mu g\ g^{-1}$)	Recovery (%)		
	0.1% Sample TDS	0.05% Sample TDS	0.02% Sample TDS		0.1% Sample TDS	0.05% Sample TDS	0.02% Sample TDS
Sc	13.2	13.4	13.7	14.1	94	95	97
Rb	16.6	17.0	16.7	16.21	102	105	103
Y	20.4	20.2	20.2	21.7	94	93	93
Zr	252	254	264	259	96	97	101
Nb	55.9	58.7	56.8	58.40	96	101	97
Cs	1.12	1.12	1.10	1.14	98	98	96
Ba	198	199	197	187	106	106	105
La	46.5	47.0	47.3	43.2	108	109	110
Ce	90	90	90	85.24	106	106	106
Pr	10.8	10.8	10.7	10.12	107	107	106
Nd	42.3	42.1	42.1	41.68	101	101	101
Sm	8.5	8.2	8.3	8.24	103	100	101
Eu	2.81	2.73	2.62	2.63	107	104	100
Gd	7.6	7.5	7.4	6.89	110	109	107
Tb	0.98	0.99	0.97	1.01	97	98	96
Dy	4.86	4.92	4.83	4.76	102	103	101
Ho	0.85	0.84	0.84	0.8	106	105	105
Er	1.94	1.94	1.88	1.79	108	108	105
Tm	0.252	0.250	0.247	0.23	110	109	107
Yb	1.38	1.37	1.34	1.27	109	108	106
Hf	6.04	6.04	5.88	5.52	109	109	107
Ta	3.92	4.02	4.04	3.76	105	107	108
Th	5.22	5.22	4.99	4.87	107	107	102
U	1.94	2.06	2.00	1.91	102	108	105

*Reference values are compiled from Robinson et al. (1986) and other sources.

3.4.5 Sodium Peroxide Sinter

As an alternative to the high temperature lithium tetraborate fusion, a lower temperature sodium peroxide sinter technique has also been investigated. Theoretically, the hydroxides of the REE, Y and Sc can be precipitated from aqueous or alkaline solutions as gelatinous precipitates (Cotton and Wilkinson 1980). Previous work demonstrated that the REE, Y and Sc can be quantitatively retained as precipitates in solution (Robinson et al. 1986). For ICP-MS work, soluble sodium and silica salts in Na_2O_2 sinter residues need to be washed out in order to reduce the TDS levels and stabilise the resultant solution (i.e. Si trends to hydrolyse in aqueous solution on standing). In this study, preliminary work also confirmed that the REE, Y and Sc can be kept as precipitates, whereas the other elements studied are either completely or partially lost through the pure water wash process. Therefore, only the REE, Y and Sc are determined for the proposed Na_2O_2 sinter method.

The geological reference materials used for this work include four granites (GSR-1, G-2, AC-E and TASGRAN), two iron formation (magnetite rich) rocks (FeR-2 and FeR-4) and three basalts (BHVO-1, TAFAHI and TASBAS). **Table 3.18** shows the measured results of Sc, Y, and rare earth elements, precisions (%RSD) and comparison between HR-ICP-MS results and reference values. There is general agreement between the measured results and reference values, variations being normally within ±10%.

As shown in **Table 3.18**, the precision for GRS-1 was generally less than ±5% and in the range of 0.75% for Tm to 8.2% for Tm. Although the average results measured in this work were generally lower than the reference values reported by Xie et al. (1989), the data lie within the uncertainty range of the recommended trace element concentrations for GSR-1. The precision for G-2 was from 0.57% for Pr to 8.53% for Ho. Comparing with the reference values compiled by Govindaraju (1994), the measured results were generally low, except the result for Eu was 8.57% higher than reference value. The precision for AC-E was generally within ±5% and in the range of 1.38% for Nd to 6.57% for Lu. In comparison with reference values compiled by Govindaraju (1994), variations for Y and REE were all within ±6%. The high result for Sc was most likely due to the Sc contamination during the storage of the standard

sample. The precision for TASGRAN based on four individual digestions was from 0.10% for La to 4.89% for Tb. In general, the results obtained in this work were slightly higher than those obtained by XRF (Robinson et al. 1986), except those for Sc and Y. Precisions for the two iron formation samples were generally within 6%. In comparison with the compiled values (Govindaraju 1994), the variations were within ±10% for FeR-2 and generally less than ±10% for FeR-4. Some relatively high variations such as 12.3% for Y, 13.3% for Tb and 41.7% for Tm were observed in comparison the measured results for FeR-4 with the published values. However, it should be pointed out that most of the reference values compiled by Govindaraju (1994) for FeR-2 and FeR-4 were based on information values. There is little information available regarding the concentrations of Sc, Y and REE for FeR-2 and FeR-4. The precision for BHVO-1 was from 0.43% for Sc to 6.78% for Sm. Based on six individual digestions, the relative variations of Sc and REE between measured results and reference values (Govindaraju 1994) were within ±8% and the relative variation of Y was -18.72%. The precisions of Sc, Y and REE for TAFAHI were in the range of 0.33% for La to 16.1% for Gd. The slightly high %RSD values were due to the low REE concentrations in TAFAHI. Concentrations for more than half of the REE were less than 1 ng g^{-1} in solutions considering a dilution factor of 1000. The relative variations of Sc, Nd, Sm, Eu, Gd, Tb, Dy, Er, Yb and Lu were within ±5%. The variations of Y, La, Ce, Pr and Ho were -14.4%, 15.1%, 15.3%, 11.1% and -7.14% respectively. Finally, the precisions of trace elements for TASBAS were from 0.85% for La to 7.83% for Lu. The relative variations were generally less than ±4%. The variations for Y and Yb were found to be -10.3% and 7.09% respectively.

In this study, consistent low Y results were observed for all of the selected samples compared with the published data. This has been reported in another investigation using ICP-MS and XRF (Robinson et al. 1999). The high Y results compiled from early reports may be a result of poor quality XRF data.

Again, the REE chondrite normalised distribution patterns have been used as an additional assessment of the quality of the data (e.g. Jarvis 1988; Ionov et al. 1992; Dulski 1994; Makishima and Nakamura 1997; Robinson et al. 1999); and smooth patterns suggest good quality data **(Figure 3.16)**.

Table 3.18. Measured rare earth element concentrations (μg g^{-1}), precision and comparison between HR-ICP-MS results and reference values for nine geological reference materials (GSR-1, G-2, AC-E, TASGRAN, FeR-2, FeR-4, BHVO-1, TAFAHI and TASBAS) by sodium peroxide sinter digestion

Sample ID	Element	Measured result	n	%RSD	Reference value	Variation (%)
GSR-1						
	Sc	5.5	3	3.83	6.1	-9.84
	Y	56	3	0.75	62	-9.68
	La	49	3	1.39	54	-9.26
	Ce	102	3	1.82	108	-5.56
	Pr	11.6	3	3.97	12.7	-8.66
	Nd	42.5	3	2.31	47	-9.57
	Sm	9.5	3	4.28	9.7	-2.06
	Eu	0.82	3	4.85	0.85	-3.53
	Gd	8.7	3	4.51	9.3	-6.45
	Tb	1.49	3	3.91	1.65	-9.70
	Dy	9.2	3	3.64	10.2	-9.80
	Ho	1.97	3	4.12	2.05	-3.90
	Er	6.23	3	4.10	6.5	-4.15
	Tm	1.06	3	8.20	1.06	0.00
	Yb	7.1	3	4.81	7.4	-4.05
	Lu	1.08	3	4.54	1.15	-6.09
G-2						
	Sc	3.13	3	6.88	3.5	-10.6
	Y	8.3	3	1.63	11	-24.5
	La	84	3	0.60	89	-5.62
	Ce	159	3	0.76	160	-0.63
	Pr	16.3	3	0.57	18	-9.44
	Nd	51	3	4.25	55	-7.27
	Sm	6.9	3	3.85	7.2	-4.17
	Eu	1.52	3	3.69	1.4	8.57
	Gd	4.29	3	4.49	4.3	-0.23
	Tb	0.44	3	5.20	0.48	-8.33
	Dy	2.24	3	3.77	2.4	-6.67
	Ho	0.37	3	8.53	0.4	-7.50

Table 3.18. (Continued). Measured rare earth element concentrations (μg g^{-1}), precision and comparison between HR-ICP-MS results and reference values for nine geological reference materials (GSR-1, G-2, AC-E, TASGRAN, FeR-2, FeR-4, BHVO-1, TAFAHI and TASBAS) by sodium peroxide sinter digestion

Sample ID	Element	Measured result	n	%RSD	Reference value	Variation (%)
G-2	Er	0.87	3	6.12	0.92	-5.43
	Tm	0.155	3	5.53	0.18	-13.9
	Yb	0.78	3	5.32	0.8	-2.50
	Lu	0.100	3	3.92	0.11	-9.09
AC-E						
	Sc	1.28	3		0.11	
	Y	156	3	2.80	165	-5.45
	La	57	3	2.36	59	-3.39
	Ce	152	3	4.01	154	-1.30
	Pr	21.0	3	1.87	22.2	-5.41
	Nd	87	3	1.38	92	-5.43
	Sm	23.9	3	2.79	24.2	-1.24
	Eu	1.97	3	3.11	2	-1.50
	Gd	26.0	3	4.48	26	0.00
	Tb	4.7	3	3.08	4.8	-2.08
	Dy	29.2	3	3.88	29	0.69
	Ho	6.3	3	5.33	6.5	-3.08
	Er	17.9	3	5.94	17.7	1.13
	Tm	2.69	3	5.39	2.6	3.46
	Yb	17.6	3	6.31	17.4	1.15
	Lu	2.43	3	6.57	2.45	-0.82
TASGRAN						
	Sc	6.74	4	0.32	6.85	-1.61
	Y	30.3	4	1.73	35.5	-14.6
	La	40.9	4	0.10	39.7	3.02
	Ce	88.7	4	0.69	84.6	4.85
	Pr	10.3	4	0.36	10.1	1.98
	Nd	39.4	4	0.75	35.9	9.75
	Sm	7.9	4	1.33	7.51	5.19
	Eu	0.85	4	3.04	0.82	3.66

Table 3.18. (Continued). Measured rare earth element concentrations (μg g^{-1}), precision and comparison between HR-ICP-MS results and reference values for nine geological reference materials (GSR-1, G-2, AC-E, TASGRAN, FeR-2, FeR-4, BHVO-1, TAFAHI and TASBAS) by sodium peroxide sinter digestion

Sample ID	Element	Measured result	n	%RSD	Reference value	Variation (%)
TASGRAN	Gd	6.5	4	1.83	6.27	3.67
	Tb	1.08	4	4.89	1.02	5.88
	Dy	5.9	4	1.84	5.83	1.20
	Ho	1.19	4	2.65	1.16	2.59
	Er	3.55	4	1.73	3.4	4.41
	Tm	0.51	4	3.11	0.51	0.00
	Yb	3.41	4	2.51	3.19	6.90
	Lu	0.49	4	1.35	0.48	2.08
FeR-2						
	Sc	5.3	6	5.63	5.6	-5.36
	Y	11.8	6	2.04	12	-1.67
	La	11.1	6	1.47	12	-7.50
	Ce	23.6	6	1.11	23	2.61
	Pr	2.76	6	1.18	3	-8.00
	Nd	11	6	1.12	12	-8.33
	Sm	2.37	6	2.24	2.5	-5.20
	Eu	1.19	6	1.37	1.25	-4.80
	Gd	2.08	6	3.14	2	4.00
	Tb	0.34	6	2.40	0.32	6.25
	Dy	2.02	6	5.85	2	1.00
	Ho	0.45	6	5.44	0.5	-10.0
	Er	1.37	6	2.69	1.5	-8.67
	Tm	0.195	6	2.09	0.2	-2.50
	Yb	1.32	6	2.47	1.25	5.60
	Lu	0.185	6	6.62	0.2	-7.50
FeR-4						
	Sc	1.31	6	3.08	1.35	-2.96
	Y	7.3	6	2.13	6.5	12.3
	La	7.8	6	0.92	8	-2.50
	Ce	12.6	6	3.87	12	5.00

Table 3.18. (Continued). Measured rare earth element concentrations (μg g^{-1}), precision and comparison between HR-ICP-MS results and reference values for nine geological reference materials (GSR-1, G-2, AC-E, TASGRAN, FeR-2, FeR-4, BHVO-1, TAFAHI and TASBAS) by sodium peroxide sinter digestion

Sample ID	Element	Measured result	n	%RSD	Reference value	Variation (%)
FeR-4	Pr	1.58	6	2.26	1.7	-7.06
	Nd	7.6	6	1.65	8	-5.00
	Sm	2.19	6	7.57	2.2	-0.45
	Eu	0.68	6	3.95	0.72	-5.56
	Gd	1.15	6	3.11	1.1	4.55
	Tb	0.17	6	2.56	0.15	13.3
	Dy	1.01	6	9.25	1	1.00
	Ho	0.22	6	4.07	0.2	10.0
	Er	0.56	6	4.79	0.5	12.0
	Tm	0.085	6	5.26	0.06	41.7
	Yb	0.66	6	5.42	0.6	10.0
	Lu	0.095	6	4.71	0.1	-5.00
BHVO-1						
	Sc	29.9	6	0.43	31.8	-5.97
	Y	22.4	6	0.73	27.6	-18.8
	La	14.7	6	0.48	15.8	-6.96
	Ce	37.7	6	0.97	39	-3.33
	Pr	5.3	6	2.16	5.7	-7.02
	Nd	23.9	6	6.04	25.2	-5.16
	Sm	6.1	6	6.78	6.2	-1.61
	Eu	2.08	6	1.35	2.06	0.97
	Gd	5.9	6	2.92	6.4	-7.81
	Tb	0.89	6	5.63	0.96	-7.29
	Dy	5.0	6	3.42	5.2	-3.85
	Ho	0.93	6	1.06	0.99	-6.06
	Er	2.32	6	1.34	2.4	-3.33
	Tm	0.31	6	6.54	0.33	-6.06
	Yb	1.90	6	3.82	2.02	-5.94
	Lu	0.279	6	2.41	0.291	-4.12

Table 3.18. (Continued). Measured rare earth element concentrations (μg g^{-1}), precision and comparison between HR-ICP-MS results and reference values for nine geological reference materials (GSR-1, G-2, AC-E, TASGRAN, FeR-2, FeR-4, BHVO-1, TAFAHI and TASBAS) by sodium peroxide sinter digestion

Sample ID	Element	Measured result	n	%RSD	Reference value	Variation (%)
TAFAHI						
	Sc	44	6	3.26	45.5	-3.30
	Y	7.8	6	3.77	9.11	-14.4
	La	1.08	6	0.33	0.938	15.1
	Ce	2.56	6	3.64	2.22	15.3
	Pr	0.401	6	0.78	0.361	11.1
	Nd	2.01	6	4.99	1.93	4.15
	Sm	0.73	6	8.81	0.722	1.11
	Eu	0.311	6	1.00	0.305	1.97
	Gd	1.05	6	16.1	1.069	-1.78
	Tb	0.216	6	9.30	0.207	4.35
	Dy	1.45	6	5.05	1.384	4.77
	Ho	0.299	6	11.5	0.322	-7.14
	Er	0.94	6	11.7	0.98	-4.08
	Tm	0.141	6	15.9		
	Yb	1.01	6	13.1	0.992	1.81
	Lu	0.149	6	15.6	0.153	-2.61
TASBAS						
	Sc	13.9	3	2.37	14	-0.71
	Y	19.2	3	1.04	21.4	-10.3
	La	43	3	0.85	44.45	-3.26
	Ce	86	3	3.97	85.45	0.64
	Pr	10.3	3	3.47	10.25	0.49
	Nd	40.6	3	1.92	41.67	-2.57
	Sm	8.33	3	2.16	8.25	0.97
	Eu	2.65	3	1.56	2.64	0.38
	Gd	7.03	3	5.61	6.79	3.53
	Tb	0.94	3	2.70	0.96	-2.08
	Dy	4.7	3	2.24	4.77	-1.47
	Ho	0.77	3	2.74	0.8	-3.75

Table 3.18. (Continued). Measured rare earth element concentrations (μg g^{-1}), precision and comparison between HR-ICP-MS results and reference values for nine geological reference materials (GSR-1, G-2, AC-E, TASGRAN, FeR-2, FeR-4, BHVO-1, TAFAHI and TASBAS) by sodium peroxide sinter digestion

Sample ID	Element	Measured result	n	%RSD	Reference value	Variation (%)
TASBAS	Er	1.82	3	4.02	1.82	0.00
	Tm	0.233	3	6.70	0.232	0.43
	Yb	1.36	3	2.94	1.27	7.09
	Lu	0.173	3	7.83	0.17	1.76

n is number of measurements.

Variation (%) is relative deviation between measured results and reference values.

- = no value available.

In comparison with other digestion techniques, the sodium peroxide sinter method can attack refractory minerals and is less time consuming for the determination of Sc, Y and REE in geological samples. Normally, a batch of samples can be digested within 4-5 hours. Therefore, it is possible to obtain 'same day' REE results by sodium peroxide digestion in conjunction with ICP-MS analysis. However, it should be pointed out that the sodium peroxide sinter method may not be suitable for analysis of low abundance rock samples, due to the lack of ultra-pure sodium peroxide.

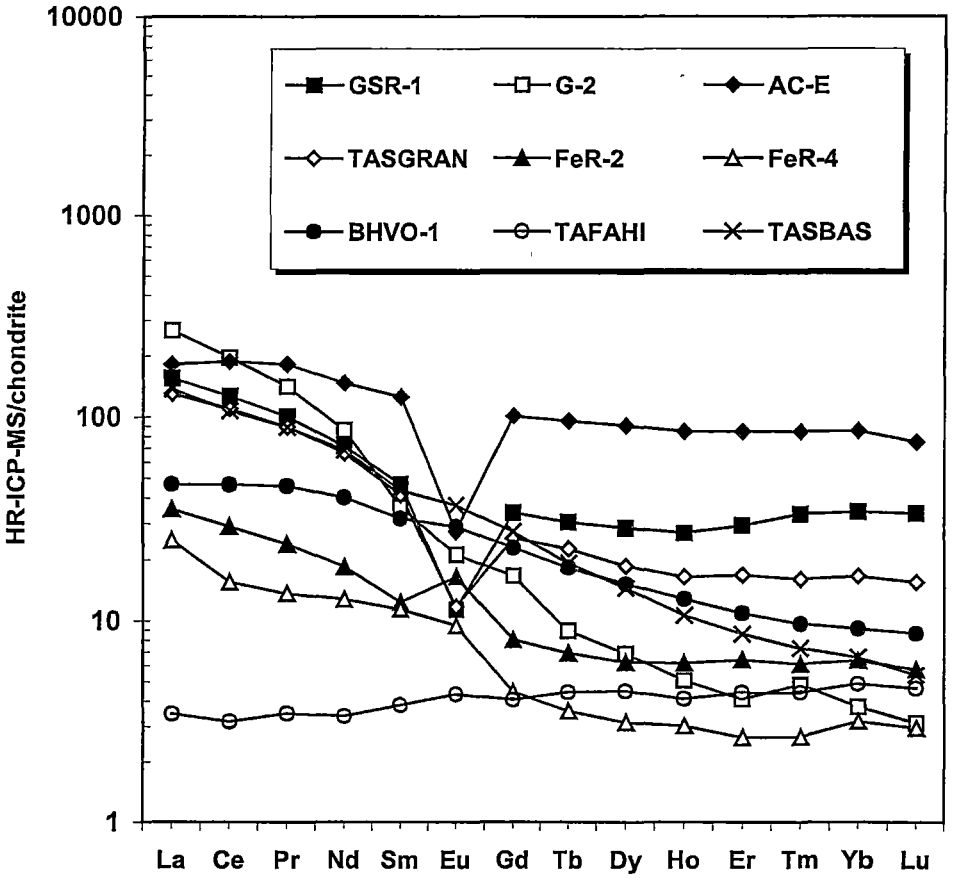

Figure 3.16. Chondrite normalised distribution patterns of rare earth elements for nine geological reference materials (GSR-1, G-2, AC-E, TASGRAN, FeR-2, FeR-4, BHVO-1, TAFAHI and TASBAS) using sodium peroxide sinter decomposition technique

3.5 Summary

Results of five different sample digestion procedures show that geological samples should be digested using different digestion techniques according to individual sample features. **Table 3.19** gives a brief summary of measurable elements by Savillex, PicoTrace, fusion and sinter digestion methods. The advantages and disadvantages of the five different digestion methods investigated in this study are summarised as follows:

Table 3.19. Summary of measurable elements by different digestion methods

	Savillex	PicoTrace		Fusion	Sinter
	HF/HNO_3	$HF/HClO_4$*	HF/H_2SO_4	$Li_2B_4O_7$	Na_2O_2
Basalt	REE, Sc, Rb, Sr, Y, Zr, Nb, Mo, Sn, Sb, Cs, Ba, Hf, Ta, Tl, Pb, Bi, Th and U	REE, Sc, Rb, Sr, Y, Zr, Nb, Mo, Sn, Sb, Cs, Ba, Hf, Ta, Tl, Pb, Bi, Th and U	REE, Sc, Rb, (Sr), Y, Zr, Nb, Mo, Sn, Sb, Cs, (Ba), Hf, Ta, Tl, (Pb), Bi, Th and U	REE, Sc, Rb, Sr, Y, Zr, Nb, Mo, Cs, Ba, Hf, Ta, Th and U	REE, Sc and Y
Granite			REE, Sc, Rb, (Sr), Y, Zr, Nb, Mo, Sn, Sb, Cs, (Ba), Hf, Ta, Tl, (Pb), Bi, Th and U	REE, Sc, Rb, Sr, Y, Zr, Nb, Mo, Cs, Ba, Hf, Ta, Th and U	REE, Sc and Y
Ironstone		REE, Sc, Rb, Sr, Y, Zr, Nb, Mo, Sn, Sb, Cs, Ba, Hf, Ta, Tl, Pb, Bi, Th and U	REE, Sc, Rb, (Sr), Y, Zr, Nb, Mo, Sn, Sb, Cs, (Ba), Hf, Ta, Tl, (Pb), Bi, Th and U	REE, Sc, Rb, Sr, Y, Zr, Nb, Mo, Cs, Ba, Hf, Ta, Th and U	REE, Sc and Y

Elements in brackets at high concentration cannot be measured due to the formation of insoluble sulfates in solution. Some low abundance ultramafic rocks such as dolerites, dunites, peridotites and serpentines can also be decomposed by the $HF/HClO_4$ method (see **Chapter 4**).

- Savillex Teflon beaker digestion can be used for the decomposition of basalts. The optimum ratio of HF to HNO_3 for 100 mg powdered rock sample is 2 ml to 0.5 ml. In order to achieve a complete dissolution, rock samples should be digested on a hotplate at about 130-150 °C for 48 hours. Granites and magnetite-rich samples cannot be completely decomposed by Savillex beaker digestion. It should also be pointed out that HNO_3 cannot drive off HF completely during evaporation due to its low boiling point (120 °C), and the trace amounts of HF left in solution will remobilise the "sticky" HFSE, which adhere to the surface of the sample introduction system when the solution is run by HR-ICP-MS. This results in memory effects and enhances the signal intensities of HFSE considerably at low abundance. Therefore, the Savillex Teflon beaker digestion may not be suitable for the digestion of low abundance samples such as ultramafic rocks.

- Basalts and iron formation samples can be completely digested by $HF/HClO_4$ high pressure digestion method at 180 °C for 48 hours. However, as reported in **Chapter 4,** some low abundance ultramafic rocks such as dunites, peridotites and serpentinites can be decomposed by $HF/HClO_4$ at about 180 °C for 16 hours. Generally, granites cannot be digested by the $HF/HClO_4$ high pressure digestion method unless a complicated two-stage digestion method similar to that recommended by Dulski (1994) for the measurement of Ba and REE is applied. The two stage technique can give an average recovery of more than 95% for more than 30 trace elements investigated in granites. Samples of basalts, granites and ironstones can be completely decomposed by 3 ml HF/3 ml H_2SO_4 high pressure digestion method at 180 °C for 16 hours. The main disadvantage of the HF/H_2SO_4 high pressure digestion method is that the evaporation time is very long, taking takes 5 days to evaporate the 3 ml HF + 3 ml H_2SO_4 + sample mixture to dryness. It has also been found that, in order to achieve complete decomposition, the volumes of either HF or H_2SO_4 for 100 mg powdered samples should be controlled at 3 ml and any reduction in the volumes of HF and H_2SO_4 may result in the incomplete dissolution of rock samples.

- Microwave digestion methods are not suitable for geological samples. The average recovery of the 32 trace elements for BHVO-1 (basalt) was only about 90% in comparison with reference values.

- The lithium tetraborate fusion decomposition method can generally be used to decompose different geological samples such as basalts, granites and magnetite rich ironstones. However, this method precludes the measurement of volatile elements such as Sn, Sb, Te, Tl, Pb and Bi due to the high decomposition temperature (1000 °C). It has also been found that the proposed method increases the levels of total dissolved solid in solution and hence strongly degrades the instrumental intensity after an analytical run. In addition, the lithium tetraborate fusion decomposition method may not be suitable for the decomposition of low abundance rock samples, due to the lack of ultra pure lithium tetraborate.

- Finally, different geological samples can be completely decomposed by the sodium peroxide sinter method. This decomposition method can provide fast analysis for Sc, Y and REE, and geological samples can normally be decomposed and analysed in the same day. HFSE cannot be measured due to the high levels of HFSE in procedure bank solution. Again, this method is not recommended for the measurement of low abundance samples because of the high blank levels.

This work also highlights the necessity of carefully charactering decomposition procedures with respect to specific geological materials of interest before any analysis of large batches of samples. Hence, it should be reiterated that no single decomposition protocol will allow the measurement of multi trace elements in all types of geological samples by ICP-MS.

Chapter 4

DETERMINATION OF TRACE ELEMENTS AT ng g^{-1} LEVELS IN GEOLOGICAL SAMPLES AFTER HF/$HClO_4$ PRESSURE DIGESTION

4.1 Introduction

In this section, as an application of the digestion methods (**Chapter 3**), the HF/$HClO_4$ high pressure digestion method has been used to digest a selection of geological reference materials with low trace element abundances.

The rock reference materials used were BIR-1 (basalt), DTS-1 (dunite), DNC-1 (dolerite), PCC-1 (peridotite), UB-N (serpentine) and TAFAHI (basalt as described in **Chapter 3**). They are listed and described in **Table 4.1**. They were digested using a 3 ml HF/3 ml $HClO_4$ high pressure digestion technique.

Table 4.1. A list of low abundance geological reference materials studied

Sample name	Description	Reference
DTS-1	Dunite collected by U.S. Geological Survey from Twin Sisters area, Hamiton, Washington, USA. DTS-1 is mainly composed of olivine (99%)	Flanagan (1967)
PCC-1	Peridotite collected by U.S. Geological Survey from the Cazadero ultramafic mass, East Austrin Creek, Sunoma County, California, USA. PCC-1 is composed of olivine (58%), serpentine (32%) and orthopyroxene (9%)	Flanagan (1967)
BIR-1	Basalt from an interglacial lava flow (Reykjavik dolerites). The site is about 12 km east of Reykjavik (Iceland)	Govindaraju (1994)
DNC-1	Dolerite collected by P.C. Ragland and J.R. Butler of Geology Department, University of North Carolina Chapel Hill. The sample is known as the Braggtown Dolerite	Govindaraju (1994)
UB-N	Serpentine from the col des Bagenelles (Vosges), France	Govindaraju (1994)

4.2 Detection Limits

It is known that detection limits are influenced by instrumental sensitivity, memory effects, spectral interferences and contamination from analytical reagents. The detection limits using HR-ICP-MS are given in **Table 4.2** and compared with the detection limits using a quadrupole ICP-MS by previous workers (Ionov et al. 1992; Makkishima and Nakamura 1997; Pin and Joannon 1997). Detection limits are given as the concentration equivalent to three times the standard deviation of procedural blank solution (3 ml HF and 3 ml $HClO_4$ digestion followed by diluting to 100 ml with ultra pure water in 2% HNO_3) intensities on the basis of an average for 15 data acquisition runs. In addition, **Table 4.2** also shows the detection limits based on the concentration equivalent to three times the standard deviation of standard blank solution (2% HNO_3 ultra pure water solution) intensities on the basis of an average for 10 data acquisition runs. In general, the detection limits measured in this study were better than those obtained under the 'clean-room' laboratory conditions (Ionov et al. 1992) or by either CEC (cation-exchange chromatography)-ICP-MS (Pin and Joannon 1997) or FI (flow injection)-ICP-MS (Makkishima and Nakamura 1997). As seen in **Table 4.2** the procedure detection limits for REE were between 0.07 and 0.90 pg g^{-1} and most of the procedure detection limits of REE are actually less than 0.50 pg g^{-1}. This indicates that REE at ng g^{-1} or even sub ng g^{-1} levels in solid samples can be measured by HR-ICP-MS after HF/$HClO_4$ high pressure digestion considering a dilution factor of 1000 under the experimental conditions. The procedure detection limits for Zr, Nb, Hf, Ta, Th and U were 1.84, 0.95, 0.36, 0.12, 0.17 and 0.08 pg g^{-1} in solution. The slightly high values of the procedure detection limits for Sn, Ba and Pb were mainly attributed to be the contamination from the impurities in the mineral acids ($HClO_4$, HF, HNO_3 and HCl). The high detection limit (16.2 pg g^{-1} in solution) for Rb was due to the interference of oxychlorine species (Longerich 1993). Under the digestion conditions, trace amounts of perchlorate remained in the final solution when perchloric acid ($HClO_4$) was used to drive off hydrofluoric acid (HF) in the sample residue. It has been observed that $^{37}Cl^{16}O_3^+$ increased the background intensity level at 85 amu and resulted in interference on ^{85}Rb used for the measurement of Rb concentration.

Table 4.2. Procedure detection limits of the low-level analysis of geological reference materials by HR-ICP-MS and comparisons with those from previous workers

Ele-ment	Mass	Detection limit* pg g^{-1}	Detection limit** pg g^{-1}	Ionov et al. 1992 pg g^{-1}	Makishima and Nakamura 1997 pg g^{-1}	Pin and Joannon 1997 pg g^{-1}
Sc	45	3.32	13.9	10	-	-
Rb	85	16.2	4.72	2	8	-
Sr	88	3.91	1.66	6	15	-
Y	89	0.30	0.80	-	34	-
Zr	90	1.84	0.56	7	-	-
Nb	93	0.95	0.23	1	-	-
Mo	95	2.50	0.94	-	-	-
Sn	118	10.4	6.47	-	-	-
Sb	121	6.55	1.48	-	-	-
Cs	133	0.88	3.79	-	0.7	-
Ba	137	7.12	11.40	8	61	-
La	139	0.41	0.35	1.5	7	1.6
Ce	140	0.49	0.88	1.5	8	6.8
Pr	141	0.18	0.16	1	4	1.4
Nd	146	0.90	1.21	2	20	0.6
Sm	147	0.53	1.48	1.5	15	0.7
Eu	151	0.36	0.42	0.4	4	0.4
Gd	157	0.59	3.02	1	26	0.5
Tb	159	0.13	0.57	0.2	4	0.6
Dy	163	0.39	0.86	1	21	0.4
Ho	165	0.06	0.61	0.25	3	0.4
Er	167	0.42	1.39	0.6	23	0.5
Tm	169	0.07	1.05	0.2	3	0.5
Yb	172	0.37	0.51	0.4	6	0.5
Lu	175	0.09	1.08	0.2	4	0.5
Hf	178	0.36	0.49	1	-	-
Ta	181	0.12	0.27	0.2	-	-
Tl	205	0.37	0.93	-	-	-
Pb	208	26.8	3.03	5	16	-
Bi	209	0.38	0.79	-	-	-
Th	232	0.17	0.13	0.3	5	-
U	238	0.08	0.15	0.3	1	-

* based on procedural blank;
** based on 2% HNO_3 ultra pure water solution;
- = no value available.

On the other hand, comparing the detection limits using the procedural blank with those using 2% HNO_3 ultra pure water solution shows clearly that they would be further improved if purer reagents were available. In particular, this could considerably improve the detection limits for Sc, Rb, Sr, Zr, Nb, Sn, Ba, and Pb by HR-ICP-MS.

4.3 Sample Preparation and Analysis

Sample preparation was conducted with extra diligence in this study. The labware cleaning procedures employed were as described in **Section 3.2.2** of this chapter. The impurity levels for most elements (including REE, Y, Sb, Cs, Hf, Ta, Tl, Bi, Th and U) were typically between 0.1 and 5 ng g^{-1} in blank solutions. However, workable detection limits for some of the elements investigated (such as Rb, Sr, Zr, Nb, Sn, Ba and Pb) were occasionally higher than those discussed in **Section 4.2** due to lack of "clean-room" standard laboratory facilities, higher chemical blank levels, and memory effects. For instance, it has been observed that the highest blank level for Sn was as high as 878 ng g^{-1}. All samples were digested at least in duplicate and sometimes in triplicate for these very low level analyses. Two procedural blanks were prepared in each 16-sample digestion run.

In order to minimise memory effects, the data acquisition was conducted with particular care. Sample solutions were run by HR-ICP-MS within 24 hours after dissolution. All solutions (including calibration standard, rinse and sample solutions) were prepared in 2% HNO_3 and 1% HCl with ultra pure water. Instrumental drift was carefully monitored by inserting a drift monitor solution (1.00 ng g^{-1} calibration standard) every 5 to 10 sample solutions. Procedural blanks 1 and 2 were analysed every two hours to monitor the variation of blank levels. A 10 ng g^{-1} standard solution was also analysed at the end of each analytical run to calculate the concentrations of trace elements at high levels. A typical sequence consists of standard blank (a blank solution prepared with calibration standards), calibration standards (0.25, 0.50 and 1.00 ng g^{-1}), drift monitor, rinse solution (using standard blank), 5 to 10 samples, drift monitor, rinse (using standard blank),..., drift monitor and 10 ng g^{-1} standard solution. Blanks were measured after rinse solution to minimise the memory effects. Each sample solution was analysed in duplicate or

triplicate to check memory effects of HFSE, particularly Ta. Results where the measured abundance drops between repetitions of the same solution could then be discarded, since a contribution of memory to the signal is obvious. Instrumental drift was corrected against the concentration variation between the different testing solutions.

4.4 Blank Subtraction

Blank subtraction is generally not crucial for analysis of medium and high abundance samples, and may even be negligible in some cases, since the blank contribution to these samples is often within the analytical error. However, when the low abundance samples are analysed, blank subtraction becomes so important that it can affect the analytical accuracy. For some elements in geological samples, their levels are close to those of the blank solution and precision on the blank measured will control the accuracy of analytical results.

In order to demonstrate the importance of the blank subtraction for the measurement of low abundance samples, two blanks were monitored through a 12-hour analytical sequence. Trace elements in the two blanks were measured at approximately 2-hour intervals. In comparison with the concentration levels of the six rock standards, it has been found that the concentrations of REE, Y, Cs, Tl and Bi in the two procedural blanks were quite stable through a 12-hour analytical run. For instance, as observed using the procedural blank 1, the measured concentration range for Y was from 0.0013 to 0.0026 ng g^{-1} and for Tl was 0.0005 to 0.0022 ng g^{-1} through a 12-hour analytical run. Using the same procedural blank, it has also been found that in a 12-hour analytical run, the concentration range observed for REE was generally less than 0.001 ng g^{-1}. The concentration range of REE through a 12-hour analytical run by HR-ICP-MS are:

La: 0.0095 to 0.0115 ng g^{-1}.
Ce: 0.0027 to 0.0040 ng g^{-1}.
Pr: 0.0002 to 0.0009 ng g^{-1}.
Nd: 0.0008 to 0.0021 ng g^{-1}.
Sm 0.0001 to 0.0017 ng g^{-1}.

Eu: 0.0007 to 0.0013 ng g^{-1}.

Gd: 0.0002 to 0.0029 ng g^{-1}.

Tb: 0.0003 to 0.0007 ng g^{-1}.

Dy: 0.0001 to 0.0006 ng g^{-1}.

Ho: 0.0001 to 0.0004 ng g^{-1}.

Er: 0.0001 to 0.0008 ng g^{-1}.

Tm: 0.0002 to 0.0005 ng g^{-1}.

Yb: 0.0002 to 0.0011 ng g^{-1}.

Lu: 0.0001 to 0.0006 ng g^{-1}.

However, there were clear concentration variations for HFSE (Zr, Nb, Hf, Ta, Th and U) through a 12-hour analytical, especially for standards DTS-1 and PCC-1. As shown in **Figure 4.1,** the concentration variations of HFSE show the following:

1. In general, there was a clear decrease of the blank levels for Zr, Hf, Ta and Th in the first four-hour HR-ICP-MS run and variations become smaller from eight to twelve hours. The concentration variations of Zr and Ta can be seen through the 12-hour analytical run for both procedural blanks. The concentration variation of Hf became minor after 4 hours from the start of the sequence.

2. The range of the blank level for Zr was from 0.0118 to 0.0310 ng g^{-1}. The variation in concentration values of Zr for both procedural blanks became quite stable between 0.0118 and 0.0199 ng g^{-1} after 4 hours from the beginning of the sequence.

3. The blank level for Nb was quite unstable over the first 4 hours of the HR-ICP-MS run and became stable for the rest of the 12-hour analytical run. The range of the concentration of Nb was from 0.0047 to 0.0129 ng g^{-1}.

4. The range of the blank level for Hf was from 0.0005 to 0.0157 ng g^{-1} for the first four hours and from 0.0004 to 0.0024 ng g^{-1} after the first four hours from the beginning of the sequence.

5. The variation in the concentration of Ta for blank 1 was between 0.0012 and 0.0033 ng g^{-1} and for blank 2 was between 0.0010 and 0.0028 ng g^{-1} through the analytical sequence.

6. The range of the concentration for Th was from 0.0004 to 0.0090 ng g^{-1} for the first four hours from the beginning of the analytical sequence and from 0.0004 to 0.0035 ng g^{-1} for the rest of the sequence.

7. In comparison with the blank levels for Zr, Nb, Hf, Ta and Th in procedural blanks 1 and 2, the blank level for U was the lowest through the 12-hour analytical run. The range of the concentration variation of U for blank 2 was between 0.0002 and 0.0004 ng g^{-1} and for blank 1 was only between 0.0002 and 0.0005 ng g^{-1}.

Since these early data were obtained, the absolute blank levels for these trace elements have been considerably improved in our analytical laboratories. Hence, considering the concentrations of trace elements in some of the selected low abundance rocks such as DTS-1 and PCC-1, special attention needs to be paid to the blank subtraction, particularly for Nb and Ta. In general, it is recommended that blank levels used for trace element analysis should be carefully monitored throughout any low-level analytical sequence and blank subtraction should be performed using the nearest measured blank to the sample. In case of possible contamination, two procedural blanks prepared per batch of samples are essential.

Despite low procedural blanks and an apparently clean instrument, spuriously high levels of the HFSE can still result from matrix effects caused by the rock solutions themselves. A typical whole rock matrix in the sample solutions often seems to be more effective than the rinse solution (approximately 5% HNO_3) at leaching the HFSE, particularly Ta from the instrument. Therefore it is advisable to check that the instrument is truly clean by aspirating extremely low level standard rock solutions such as PCC-1 and DTS-1 or an artificial rock matrix made from Specpure oxides in triplicate before a sample sequence to check if there is any memory or tailing effects.

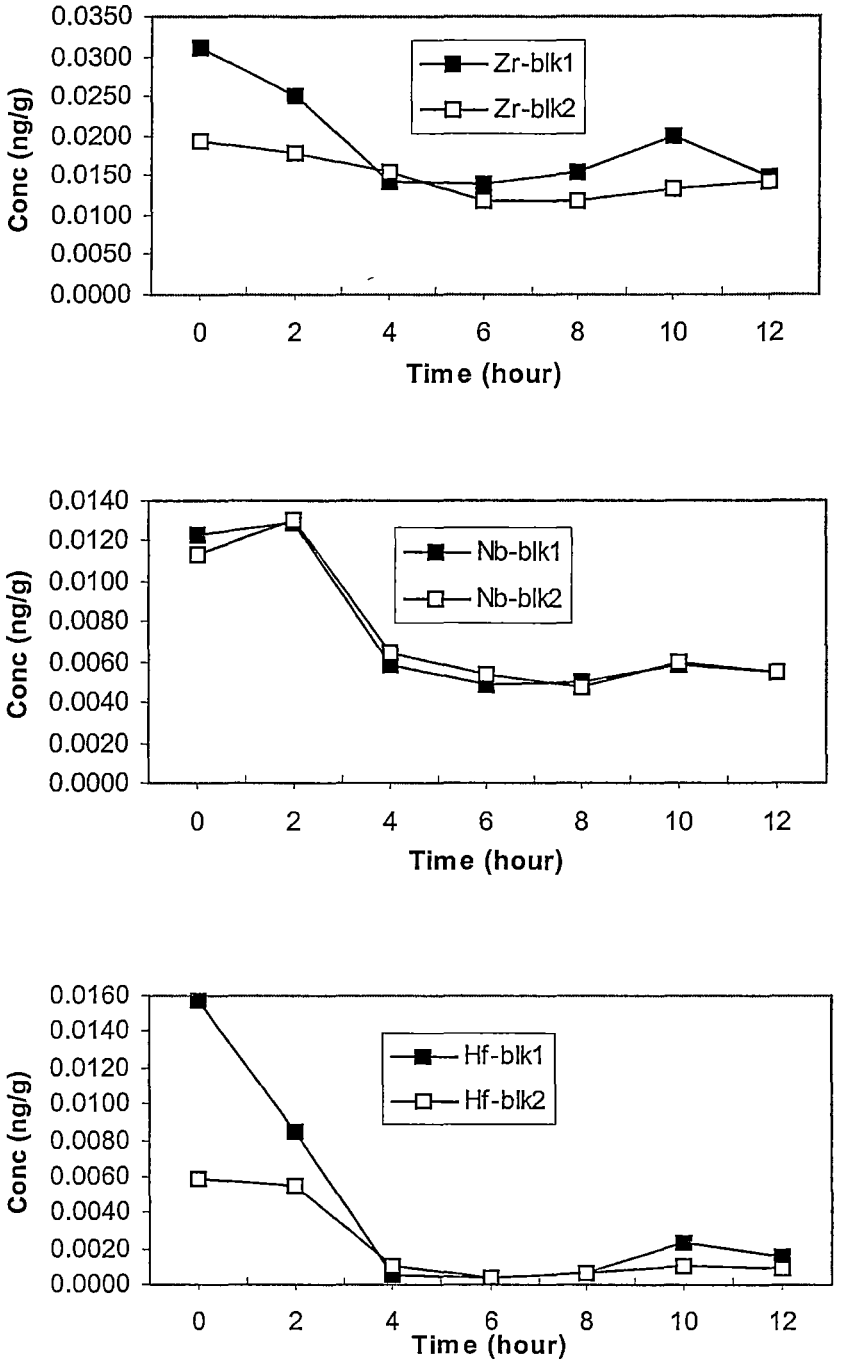

Figure 4.1. Concentration variations of HFSE through a 12-hour analytical run. The two procedural blanks (blk 1 and blk 2) were prepared individually in 2% HNO_3 and 1% HCl. Blank levels were measured at every 2-hour interval. Before the analytical run the sample and skimmer cones were cleaned, nebuliser was soaked in concentrated HNO_3 for 24 hours and all of the tubing for the sample introduction system of the HR-ICP-MS was changed in order to achieve high sensitivity and reduce memory effects.

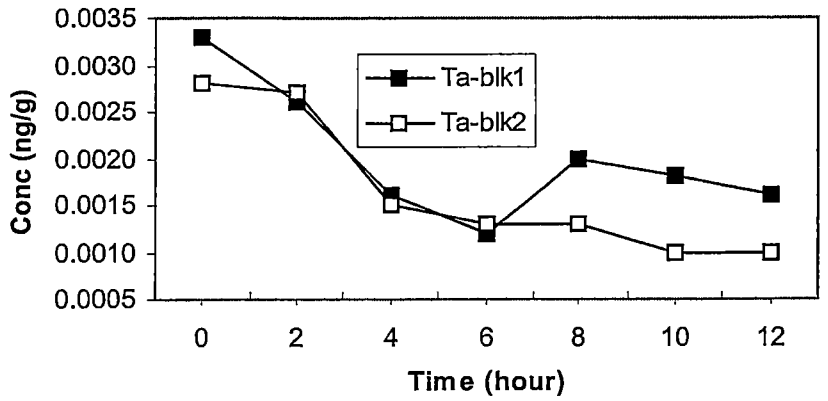

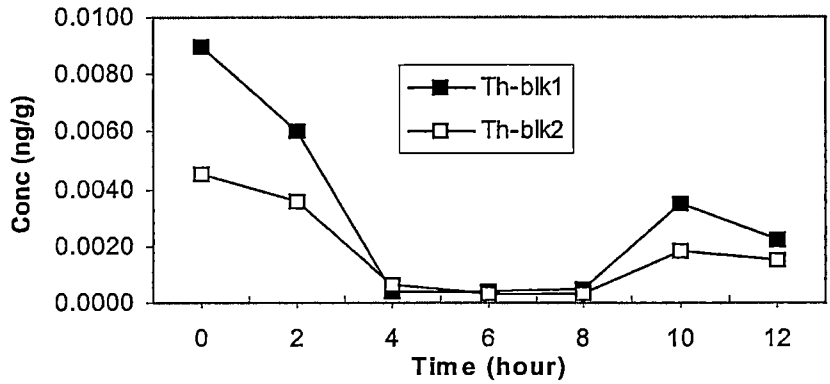

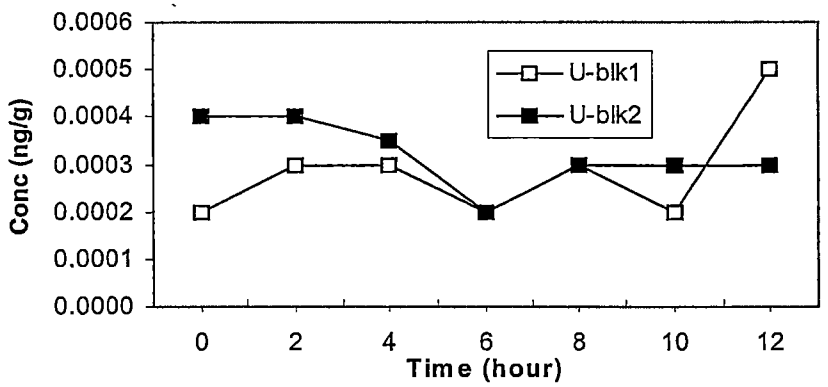

Figure 4.1. (Continued). Concentration variations of HFSE through a 12-hour analytical run. The two procedural blanks (blk 1 and blk 2) were prepared individually in 2% HNO_3 and 1% HCl. Blank levels were measured at every 2-hour interval. Before the analytical run the sample and skimmer cones were cleaned, nebuliser was soaked in concentrated HNO_3 for 24 hours and all of the tubing for the sample introduction system of the HR-ICP-MS was changed in order to achieve high sensitivity and reduce memory effects.

From the above discussion, it is clear that blank levels must be carefully monitored throughout an analytical run for the measurement of low abundance geological samples (such as ultramafic rocks) by HR-ICP-MS. Blank subtraction is crucial in order to obtain reliable analytical data.

4.5 Results

Tables 4.3 to 4.8 have listed the average measured results, precisions (%RSD, one standard deviation) and comparisons with published values for the six selected low abundance rock reference materials. The selected reference materials were separately digested and analysed 6 to 18 times over a period of six months.

In this section, the accuracy and precision of HR-ICP-MS for the trace elements measured in this study are discussed. HFSE are discussed separately as these elements show general memory effects, and both the decomposition and instrumental analysis should be performed with special care (See **Section 2.5**).

The results for BIR-1 were the average values measured by HR-ICP-MS on 18 separate dissolutions. As seen in **Table 4.3** the results for 32 trace and rare earth elements are in general agreement with the reference values reported by Garbe-Schönberg (1993), Jochum et al. (1994), Xie et al. (1994), Eggins et al. (1997), and Pin and Joannon (1997). The precision (%RSD) was in the range of 3.6% for Ho to 64.9% for Sb. The precisions for REE were normally less than 10%. In the 18 separate analyses, the precisions were 12.5%, 9.6%, 10.2%, 6.5% and 5.9% for La, Ce, Pr, Nd and Sm (light REE) respectively. The precisions for Eu, Gd, Tb, Dy, Ho, Er, Tm, Yb and Lu (heavy REE) were 6.2%, 7.6%, 5.8%, 4.6%, 4.0%, 4.9%, 4.2%, 4.6% and 4.9% respectively. The high %RSD values for Sb (64.9%) and Tl (53.9%) are attributed to their very low abundances in BIR-1. Comparing the measured results with the reference values for some of the trace elements such as Mo, Sn, Tl and Bi was difficult due to the paucity of quality data from the previous works. The data obtained by HR-ICP-MS in this study may make new more accurate contributions for these elements in BIR-1.

Table 4.3. Average measured results (μg g^{-1}), reproducibilities (%RSD) and comparisons with published values for BIR-1 (basalt)

Element	Measured n = 18	%RSD	Garbe-Schönberg 1993	Jochum et al. 1994	Xie et al. 1994	Govindaraju 1994	Eggins et al. 1997	Pin and Joannon 1997
Sc	44	8.12	41.0	-	46.1	44	43.8	-
Rb	0.27	30.2	0.32	0.24	0.172	0.25	0.195	-
Sr	97	19.1	94.2	110	112	108	106.4	-
Y	13.6	3.6	14.4	15.5	14.6	16	16.20	-
Zr	14.9	2.6	13.8	15.4	15.7	15.5	14.47	-
Nb	0.51	6.4	2 11	0.50	0.738	0.6	0.558	-
Mo	0.047	37.0	0.25	-	-	(0.5)	0.037	-
Sn	0.52	33.9	-	0.60	-	0.65	0.88	-
Sb	0.25	64.9	-	-	-	0.58	0.50	-
Cs	0.018	34.4	0.04	0.004	0.007	0.005	0.0053	-
Ba	4.9	40.1	9..7	7.1	6.47	7	6.52	-
La	0.68	12.5	0.61	0.61	0.614	0.62	0.604	0.624
Ce	1.70	9.6	1.85	1.95	1.93	1.95	1.897	1.89
Pr	0.34	10.2	0.36	0.38	0.382	0.38	0.378	0.368
Nd	2.22	6.5	2.21	2.34	2 47	2.5	2.38	2.39
Sm	1.04	5. 9	1.06	1.10	1.14	1.1	1.117	1.09
Eu	0.510	6.2	0.49	0.52	0.524	0.54	0.524	0.515
Gd	1.67	7.6	1.63	1.84	1.91	1.85	1.850	1.87
Tb	0.328	5.8	0 33	0.36	0.351	0.36	0.379	0.360
Dy	2.36	4.6	2.33	2.51	2.63	2.5	2.53	2.55
Ho	0.536	4.0	0.52	0.56	0.567	0.57	0.585	0.568
Er	1.60	4.9	1.54	1.66	1.72	1.7	1.734	1.65
Tm	0.236	4.2	0.22	0.25	0.26	0.26	-	0.262
Yb	1.60	4.6	1.52	1.63	1.71	1.65	1.1	1.67
Lu	0.239	4.9	0.23	0.25	0.259	0.26	0.247	0.269
Hf	0.53	1.9	0.61	0.51	0.639	0.6	0.562	-
Ta	0.031	12. 5	-	0.03	0.213	0.04	0.041	-
Tl	0.0024	53.9	<0.03	-	-	(0.01)	0.004	-
Pb	2.63	26.4	3.08	2 94	3.13	3	2.97	-
Bi	0.0047	37.7	<0.03	-	-	(0.02)	-	-
Th	0.0301	1 8	0.04	0.031	0.06	0.03	0.0302	-
U	0.0096	6.8	<0.03	0.0097	0.011	0.01	0.0100	-

n = number of digestions; - = no value available; () = information values; data underlined are recommended values; the number of digestions for the measurement of HFSE was 7.

Table 4.4. Average measured results (μg g^{-1}), reproducibilities (%RSD) and comparisons with published values for DTS-1 (dunite)

Element	Measured n = 18	%RSD	Ionov et al. 1992	Govindaraju 1994	Eggins et al. 1997	Makishima and Nakamura 1997
Sc	3.3	14.1	3.5	3.5	5.3	-
Rb	0.067	21.6	0.095	0.058	0.078	0.084
Sr	0.25	52.9	0.30	0.32	0.31	0.32
Y	0.034	14.0	-	0.04	0.038	0.042
Zr	0.17	11.3	0.11	(4)	0.253	-
Nb	0.032	6.9	0.042	(2.2)	0.012	-
Mo	0.045	74.4	-	(0.14)	-	-
Sn	0.45	57.6	-	0.55	0.99	-
Sb	0.33	20.6	-	0.5	-	-
Cs	0.0066	12.2	-	0.0058	0.0073	0.0069
Ba	0.24	58.1	-	(1.7)	0.33	0.33
La	0.0341	6.39	0.025	0.029	0.0246	0.023
Ce	0.0403	5.13	0.050	0.072	0.100	0.052
Pr	0.0049	11.0	0.0074	0.0063	0.0063	0.0066
Nd	0.021	11.4	0.027	0.029	0.0234	0.025
Sm	0.0041	11.6	0.007	0.0046	0.0031	0.0090
Eu	0.0010	49.1	0.0013	0.0012	0.0013	0.0019
Gd	0.0044	45.2	0.0063	(0.0038)	0.0044	0.0081
Tb	0.0006	46.0	0.001	0.0008	0.0007	0.0012
Dy	0.0043	13.8	0.0085	(0.003)	0.0038	0.0082
Ho	0.0014	45.8	0.0016	(0.0013)	0.0014	0.0024
Er	0.0053	41.1	0.0074	(0.004)	0.0050	0.0061
Tm	0.0011	29.4	0.0013	0.0014	-	0.0017
Yb	0.010	26.5	0.010	0.01	0.0090	0.011
Lu	0.0022	26.3	0.0022	0.0024	0.0019	0.0029
Hf	0.0056	17.7	0.0046	0.015	0.0069	-
Ta	0.0013	21.9	0.0021	0.039	0.002	-
Tl	<0.0004	-	-	(0.002)	-	-
Pb	6.0	26.2	7.5	12	13.06	7.5
Bi	0.0073	13.74	-	0.006	-	-
Th	0.011	13.0	0.0083	0.01	0.0098	0.011
U	0.0038	25.0	0.0038	0.0036	0.0018	0.0030

n = number of digestions; - = no value available; () = information values; data underlined are recommended values; the number of digestions for the measurement of HFSE was 5.

Table 4.5. Average measured results (μg g^{-1}), reproducibilities (%RSD) and comparisons with published values for DNC-1 (dolerite)

Element	Measured n = 10	%RSD	Govindaraju 1994	Eggins et al. 1997	Pin and Joannon 1997
Sc	30.5	5.8	31	31.1	-
Rb	3.7	16.5	4.5	3.6	-
Sr	130	5.4	145	141.4	-
Y	15.8	2.0	18	18.03	-
Zr	35.2	1.5	41	36.4	-
Nb	1.60	2.0	3	1.564	-
Mo	0.14	44.2	0.7	0.121	-
Sn	1.8	31.0	-	2.46	-
Sb	0.73	7.0	0.96	0.870	-
Cs	0.203	4.1	0.34	0.213	-
Ba	101	7.5	114	104.5	-
La	3.65	4.9	3.8	3.68	3.91
Ce	7.87	6.5	1.3	8.18	8.46
Pr	1.09	4.6	1.3	1.113	1.11
Nd	4.80	6.4	4.9	4.95	4.80
Sm	1.41	6.2	1.38	1.44	1.30
Eu	0.611	5.5	0.59	0.592	0.515
Gd	2.02	5.1	2	2.02	1.79
Tb	0.379	2.2	0.41	0.390	0.330
Dy	2.71	3.6	2.7	2.71	2.35
Ho	0.634	2.2	0.62	0.638	0.537
Er	1.94	4.0	2	1.945	1.63
Tm	0.292	2.0	0.33	-	0.271
Yb	1.96	4.7	2.01	1.915	1.80
Lu	0.303	2.8	0.32	0.292	0.300
Hf	0.98	2.1	1.01	0.955	-
Ta	0.091	4.9	0.098	0.089	-
Tl	0.0235	14.4	0.026	-	-
Pb	6.50	14.1	6.3	6.47	-
Bi	0.0095	22.4	0.02	-	-
Th	0.234	3.1	0.2	0.240	-
U	0.052	3.8	0.1	0.0549	-

n = number of digestions; - = no value available; the number of digestions for the measurement of HFSE was 5.

Table 4.6. Average measured results (μg g^{-1}), reproducibilities (%RSD) and comparisons with published values for PCC-1 (peridotite)

Element	Measured n = 18	%RSD	Ionov et al. 1992	Govindaraju 1994	Eggins et al. 1997	Makishima and Nakamura 1997
Sc	8.02	7.4	7	8.4	9.0	-
Rb	0.092	68.5	0.068	0.066	0.058	0.083
Sr	0.31	35.0	0.38	0.4	0.33	0.37
Y	0.0718	6.1	-	(0.1)	0.087	0.079
Zr	0.145	5.0	0.13	10	0.191	-
Nb	0.024	12.5	0.042	(1)	0.011	-
Mo	0.019	59.6	-	(2)	0.032	-
Sn	0.76	63.8	-	1.6	1.24	-
Sb	0.91	31.1	-	1.28	1.36	-
Cs	0.0049	15.2	-	0.0055	0.0045	0.0052
Ba	0.58	43.9	0.68	(1.2)	0.76	0.89
La	0.045	18.7	0.039	0.052	0.029	0.034
Ce	0.048	10.5	0.057	0.1	0.053	0.061
Pr	0.0062	9.9	0.0085	0.013	0.0068	0.0091
Nd	0.025	10.6	0.030	0.042	0.025	0.035
Sm	0.0053	21.8	0.008	0.0066	0.005	0.0095
Eu	0.0010	44.4	0.0018	0.0018	0.0011	0.0024
Gd	0.0057	23.7	0.008	(0.014)	0.0061	0.013
Tb	0.0009	23.9	0.0015	0.0015	0.0012	0.0014
Dy	0.0091	8.8	0.0013	0.01	0.0087	0.016
Ho	0.0027	13.7	0.0038	0.0025	0.0027	0.0034
Er	0.011	14.4	0.0123	(0.012)	0.0113	0.016
Tm	0.0026	19.8	0.0025	0.0027	-	0.0032
Yb	0.022	10.1	0.0215	0.024	0.0213	0.028
Lu	0.0046	7.6	0.0049	0.0057	0.0046	0.0054
Hf	0.0038	11.1	0.0055	(0.04)	0.0054	-
Ta	0.0005	59.0	0.003	(0.02)	0.002	-
Tl	0.0008	91.5	-	(0.002)	-	-
Pb	6.2	26.6	8.2	10	8.0	7.9
Bi	0.0037	18.1	-	0.008	-	-
Th	0.011	13.7	0.0095	0.013	0.0115	0.012
U	0.0042	9.6	0.0042	0.0045	0.0039	0.0051

n = number of digestions, - = no value available; () = information values; data underlined are recommended values; the number of digestions for the measurement of HFSE was 9.

Table 4.7. Average measured results (μg g^{-1}), reproducibilities (%RSD) and comparisons with published values for UB-N (serpentine)

Element	Measured n = 12	%RSD	Ionov et al. 1992	Garbe-Schönberg 1993	Govindaraju 1994	Pin and Joannon 1997
Sc	12	10.8	14	11.4	13	-
Rb	3.3	16.3	3.5	3.27	4	-
Sr	6.1	18.1	7.8	7.09	9	-
Y	2.33	4.2	-	2.39	2.5	-
Zr	4.24	3.6	3.3	3.6	4	-
Nb	0.068	4.7	0.080	<0.1	0.05	-
Mo	0.29	21.3	-	0.4	0.55	-
Sn	0.16	39.9	-	-	-	-
Sb	0.31	56.0	-	-	0.3	-
Cs	11	12.1	-	10.7	10	-
Ba	21	35.7	26	27.4	27	-
La	0.30	9.6	0.330	0.50	0.35	0.319
Ce	0.72	8.8	0.800	0.85	-	0.770
Pr	0.111	8.1	0.123	0.13	0.12	0.113
Nd	0.575	5.7	0.610	0.60	0.6	0.594
Sm	0.211	7.3	0.216	0.21	0.2	0.204
Eu	0.0816	4.71	0.081	0.08	0.08	0.0726
Gd	0.31	10.3	0.320	0.31	0.3	0.294
Tb	0.058	8.4	0.060	0.06	0.06	0.0540
Dy	0.414	7.0	0.420	0.41	0.38	0.377
Ho	0.0955	6.6	0.097	0.10	0.09	0.0843
Er	0.292	8.7	0.282	0.28	0.28	0.251
Tm	0.0438	6.9	0.434	0.05	0.045	0.0415
Yb	0.306	5.8	0.383	0.31	0.28	0.272
Lu	0.0477	6.2	0.046	0.05	0.045	0.0453
Hf	0.148	2.2	0.122	0.15	0.1	-
Ta	0.012	27.0	0.015	-	0.02	-
Tl	0.045	8.2	-	<0.03	0.06	-
Pb	12	22.4	-	12.2	13	-
Bi	0.14	33.9	-	0.11	0.1	-
Th	0.073	5.7	0.063	0.06	0.07	-
U	0.061	3.0	0.060	0.06	0.07	-

n = number of digestions; - = no value available; () = information values; data underlined are recommended values; the number of digestions for the measurement of HFSE was 5.

Table 4.8. Average measured results (μg g^{-1}), reproducibilities (%RSD) and comparisons with published values for TAFAHI (basalt)

Element	Measured n = 6	%RSD	Eggins et al., 1997	Deviation μg g^{-1}	Variation %
Sc	42.9	1.2	45.5	-2.5751	-5.7
Rb	1.85	4.9	1.750	0.0998	5.7
Sr	125	3.9	138.9	-14.1632	-10.2
Y	7.30	1.0	9.11	-1.8111	-19.9
Zr	11.7	2.2	12.07	-0.37	-3.1
Nb	0.50	6.2	0.456	0.044	9.6
Mo	0.39	15.6	0.44	-0.05	-11.4
Sn	0.33	10.1	0.24	0.09	37.5
Sb	0.0202	9.9	0.024	-0.0038	-15.8
Cs	0.074	8.0	0.066	0.008	12.1
Ba	39.8	3.6	40.3	-0.5207	-1.3
La	0.912	3.3	0.938	-0.0258	-2.8
Ce	2.18	3.4	2.22	-0.0409	-1.8
Pr	0.357	2.2	0.361	-0.0043	-1.2
Nd	1.89	1.6	1.93	-0.0406	-2.1
Sm	0.704	0.6	0.722	-0.0183	-2.5
Eu	0.312	1.5	0.305	0.0070	2.3
Gd	1.03	1.9	1.069	-0.0404	-3.8
Tb	0.187	1.7	0.207	-0.0198	-9.6
Dy	1.33	1.6	1.384	-0.0583	-4.2
Ho	0.303	1.5	0.322	-0.0186	-5.78
Er	0.938	2.2	0.980	-0.0423	-4.3
Tm	0.139	2.2	-	-	-
Yb	0.974	2.6	0.992	-0.0177	-1.8
Lu	0.148	3.0	0.153	-0.0048	-3.1
Hf	0.38	6.1	0.395	-0.015	-3.8
Ta	0.021	13.6	0.0219	-0.0009	-4.1
Tl	0.0151	3.9	0.0142	0.0109	6.3
Pb	1.08	1.1	0.95	0.2323	13.9
Bi	0.016	66.8	-	-	-
Th	0.114	3.3	0.120	-0.006	-5.0
U	0.070	3.4	0.0728	-0.0028	-3.9

n = number of digestions; - = no value available; Deviation = measured result form this work-reference value; the number of digestions for the measurement of HFSE was 7.

DTS-1 was also measured with 18 independent digestions. The mean results of 32 elements agree well with previous results reported by Ionov et al. (1992), Eggins et al. (1997), and Makishima and Nakamura (1997) (**Table 4.4**). It has been found that most of the results measured by HR-ICP-MS in this study are slightly lower than published results obtained by quadrupole ICP-MS. This might be due to the limitation of detection limits for trace elements by quadrupole ICP-MS. The precisions for DTS-1 are relatively high and in the range of 5.1% for Ce to 52.9% for Sr, because the concentrations of the trace elements for DTS-1 are generally at very low levels and some of them are actually close to the detection limits of the proposed HR-ICP-MS technique (**Table 4.2**). Due to the very low concentrations, the precisions for heavy REE are generally higher than those for light REE.

From **Table 4.5,** it can be seen that the average measured results for DNC-1 on the basis of 10 independent digestions are in agreement with published values reported by Govindaraju (1994), Eggins et al. (1997), and Pin and Joannon (1997). The precisions of 32 trace and REE are generally within 10%, except for 16% for Rb, 44.2% for Mo, 31.0% for Sb, 14.4% for Tl, 14.1 % for Pb, 22.4% for Bi, 14.2% for Th and 10.2% for U. The precisions were 4.9%, 6.5%, 4.6% 6.4%, 6.2% for La, Ce, Pr, Nd and Sm (light REE) respectively, and 5.5%, 5.1%, 2.2%, 3.6%. 2.2%, 4.0%, 2.0%, 4.7% and 2.8% for Eu, Gd, Tb, Dy, Ho, Er, Tm, Yb and Lu (heavy REE) respectively. High %RSD values for Mo (44.2%), Sn (31%) and Bi (22.4%) are due to very low concentrations of these elements in DNC-1.

As shown in **Table 4.6,** the average results of trace elements for PCC-1, measured from 18 independent dissolutions by HR-ICP-MS, are generally in good agreement with the results reported by Eggins et al. (1997) and slightly lower than the results measured by both Ionov et al. (1992) and Makishima and Nakamura (1997). The precisions of 32 trace elements are in the range of 6.1% for Y and 91.5% for Tl. The precisions for La, Ce, Pr, Nd and Sm (light REE) are 18.7%, 10.5%, 9.9%, 10.6% and 21.8% respectively. The precisions for Eu, Gd, Tb, Dy, Ho, Er, Tm, Yb and Lu (heavy REE) are 44.4%, 23.7%, 23.9%, 8.8%, 13.7%, 14.4%, 19.8%, 10.1% and 7.6% respectively. The high %RSD values for Rb (68.5%), Mo (59.6%), Sn (63.8%) and Tl (91.5%) are due to the very low abundances of these elements in PCC-1.

As shown in **Table 4.7**, in general, the average results for UB-N measured from 10 separate dissolutions are in good agreement with the reference values compiled by Govindaraju (1994), and those reported by Eggins et al. (1997) and Pin and Joannon (1997). Due to the relatively high concentrations of REE, the precisions for REE in UB-N are generally better than the precisions obtained for DTS-1 and PCC-1 in this study, being better than 10% except for Gd (10.3%).

Finally, there is an excellent agreement between the mean results of TAFAHI measured from 6 independent dissolutions and the reference values reported by Eggins et al. (1997). As shown in **Table 4.8**, the precisions for La, Ce, Pr, Nd and Sm (light REE) are 3.3%, 3.4%, 2.2%, 1.6% and 0.6 respectively, and the precisions for Eu, Gd, Tb, Dy, Ho, Er, Tm, Yb and Lu (heavy REE) are 1.5%, 1.9%, 1.66%, 1.6%, 1.5%, 2.2% 2.6% and 2.1% respectively. The best precision is only 1.0% for Y, and the worst is 66.8% for Bi. From the variation (%) values, it can be seen that the HR-ICP-MS results for REE are slightly lower than those obtained by the quadrupole ICP-MS, apart from that for Eu, where the HR-ICP-MS value is 2.3% higher than that measured by quadrupole ICP-MS (Eggins et al. 1997). High results for Sn and Pb by HR-ICP-MS could be due to contaminations from chemical reagents, distilled water or the digestion environment under the experimental conditions. To avoid the contamination of some common elements such as Sn, Ba, Pb etc., experimental work (including digestion and ICP-MS operation) should be conducted under a strict "clean-room" laboratory condition (Ionov et al. 1992).

As an additional assessment of the REE data, **Figures 4.2 to 4.7** show the chondrite normalised REE distribution patterns and comparisons with those obtained from the previous reference values for geological reference materials BIR-1 (basalt), DTS-1 (dunite), DNC-1 (dolerite), PCC-1 (peridotite), UB-N (serpentine) and TAFAHI (basalt) respectively. All profiles obtained in this study are smooth and internally consistent, suggesting high quality data, including those at ng g^{-1} levels for dunite (DTS-1) and peridotite (PCC-1). In addition, as shown in **Figures 4.2 to 4.7**, good general agreement exists between the chondrite normalised REE distribution patterns obtained in this study, and various those reported by the previous workers.

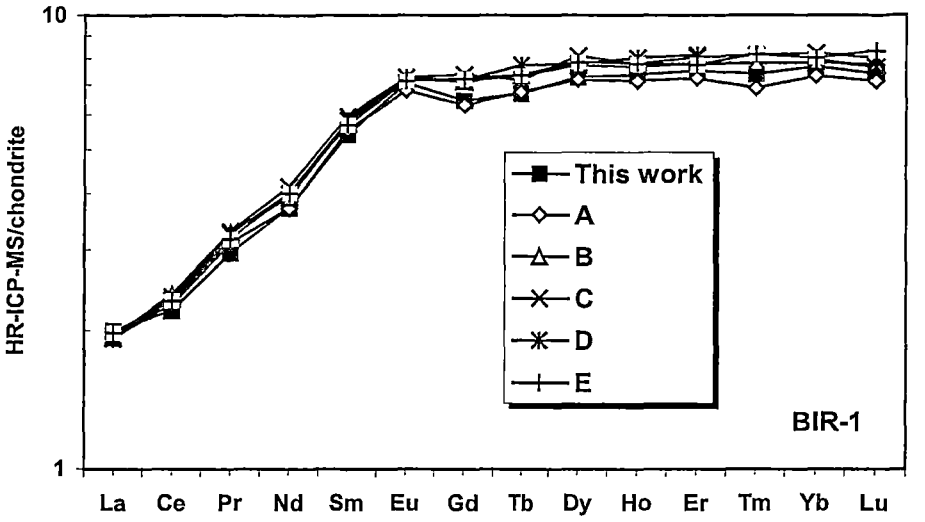

Figure 4.2. Chondrite normalised REE distribution pattern and comparison with those obtained from the previous reference values for geological reference material BIR-1 (basalt). A = Garbe-Schönberg 1993; B = Jochum et al. 1994; C = Xie et al. 1994; D = Eggins et al. 1997; E = Pin and Joannon 1997.

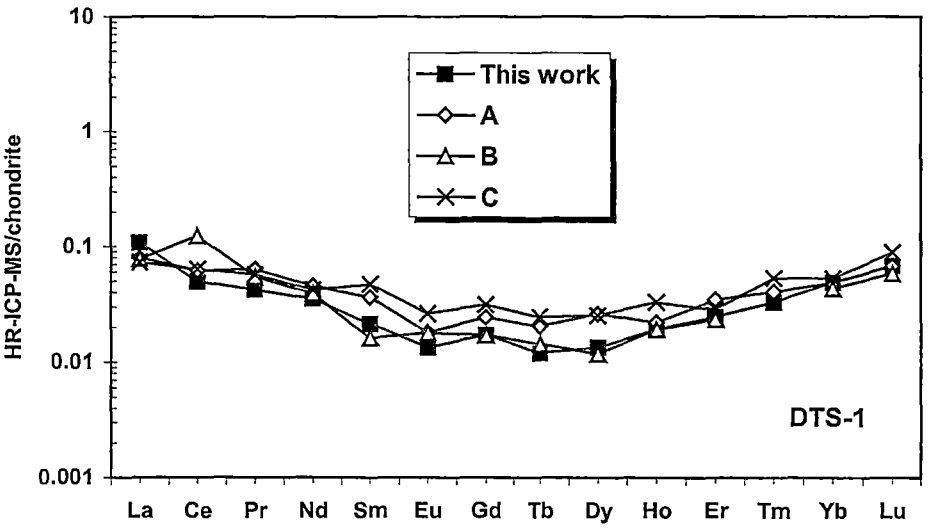

Figure 4.3. Chondrite normalised REE distribution pattern and comparison with those obtained from the previous reference values for geological reference material DTS-1 (dunite). A = Ionov et al. 1992; B = Eggins et al. 1997; C = Makishima and Nakamura 1997.

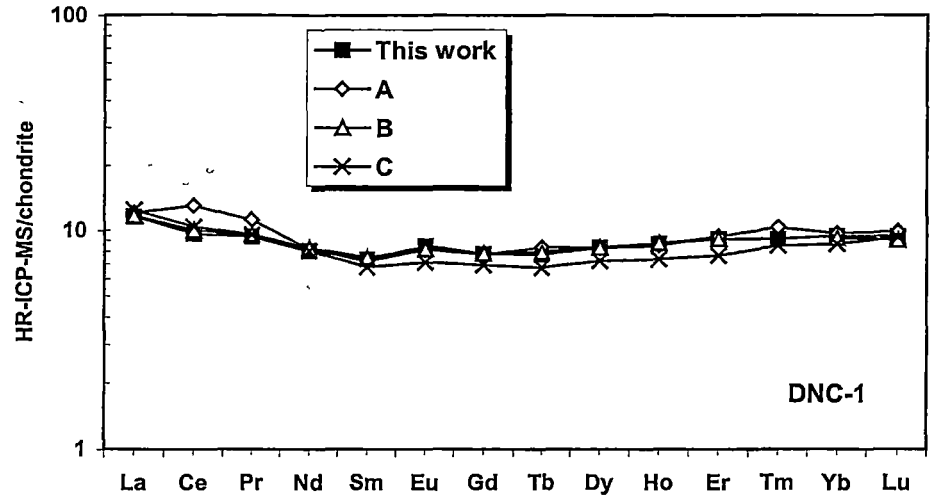

Figure 4.4. Chondrite normalised REE distribution pattern and comparison with those obtained from the previous reference values for geological reference material DNC-1 (dolerite). A = Govindaraju 1994; B = Eggins et al. 1997; C = Pin and Joannon 1997.

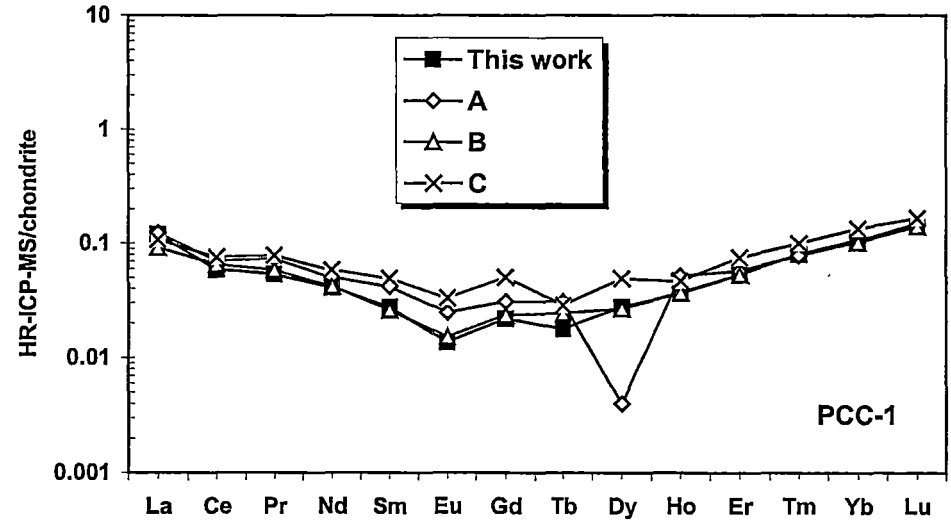

Figure 4.5. Chondrite normalised REE distribution pattern and comparison with those obtained from the previous reference values for geological reference material PCC-1 (peridotite). A = Ionov et al. 1992; B = Eggins et al. 1997; C = Makishima and Nakamura 1997.

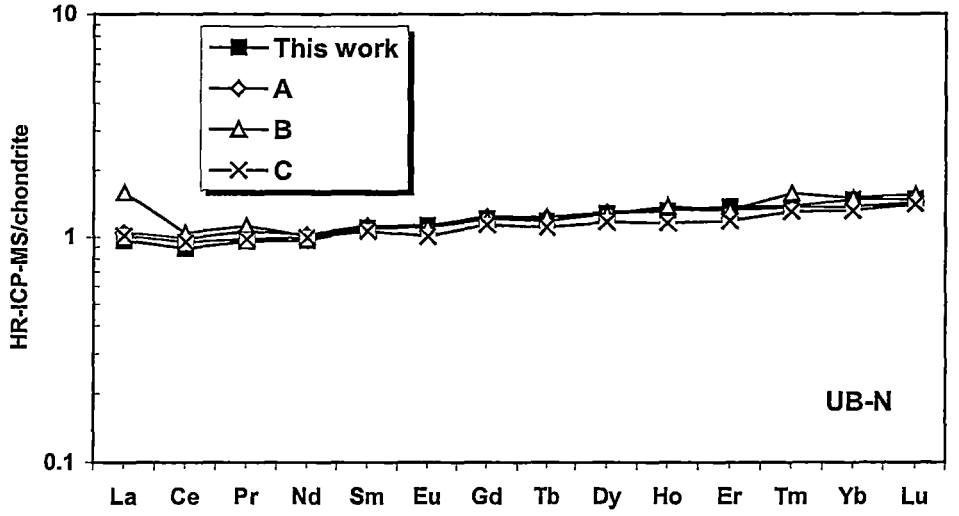

Figure 4.6. Chondrite normalised REE distribution pattern and comparison with those obtained from the previous reference values for geological reference material UB-N (serpentine). A = Ionov et al. 1992; B = Garbe-Schönberg 1993; C = Pin and Joannon 1997.

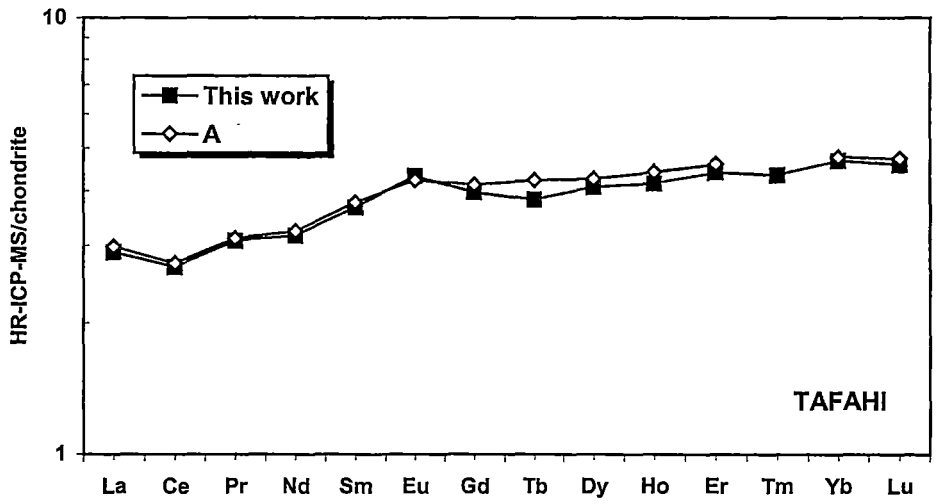

Figure 4.7. Chondrite normalised REE distribution pattern and comparison with those obtained from the previous reference values for geological reference material TAFAHI (basalt). A = Eggins et al. 1997.

Tables 4.3 to 4.8 also list the measured results, precisions and reference values of the six selected geological reference materials. The precisions (%RSD) were calculated on the basis of 9 independent digestions for PCC-1, 7 independent digestions for BIR-1 and TAFAHI, and 5 independent digestions for DNC-1, UB-N and DTS-1 (spread over a period of 3-6 months). In general, the precisions were found to vary considerably from element to element generally in accordance with elemental abundance. For instance, the RSD values of HFSE in BIR-1, DNC-1, UB-N and TAFAHI were generally less than 7%, whereas the RSD values for these elements in DTS-1 and PCC-1 were generally more than 10% due to the significant lower elemental concentrations. The precisions for Ta in the six selected samples varied from 4.9% to 59% as Ta concentrations changed from 91 to 0.5 ng g^{-1} in rock samples. The RSDs quoted in this study represent a good approximation to the true external reproducibility, compared to an internal (within an analytical sequence) repeatability which is generally much better. However, it should be pointed out that RSD values are also affected by other factors such as instrumental sensitivity and stability, heterogeneous distributions of trace elements in solid samples, blank levels and sample digestion efficiency.

The measured abundances of HFSE in the six selected geological reference materials by HR-ICP-MS are in general agreement with previous published values (Ionov et al. 1992; Garbe-Schönberg 1993; Govindaraju 1994; Jochum et al. 1994; Xie et al. 1994; Eggins et al. 1997; Makishima and Nakamura 1997; Münker 1998). The Ta data measured in this study were found to be 12, 1.3 and 0.5 ng g^{-1} for UB-N, DTS-1 and PCC-1 respectively, which are lower than previously published values.

Similarly, as an additional assessment of the quality of the analytical data measured in this study, **Figure 4.8** shows the representative comparison of primitive mantle normalised distribution of HFSE for BIR-1, DTS-1 and PCC-1. The new data for these three geological reference materials, when plotted normalised to the primitive mantle concentrations recommended by Sun and McDonough (1989) agree well with published results (Ionov et al. 1992; Jochum et al. 1994; Eggins et al. 1997). It can also be seen that there are smooth primitive mantle normalised distribution patterns from Nb to Hf for DTS-1 and PCC-1, suggesting that the proposed HR-ICP-MS

technique produces accurate low abundance analytical data for the petrogenetic use of these elements in geological materials.

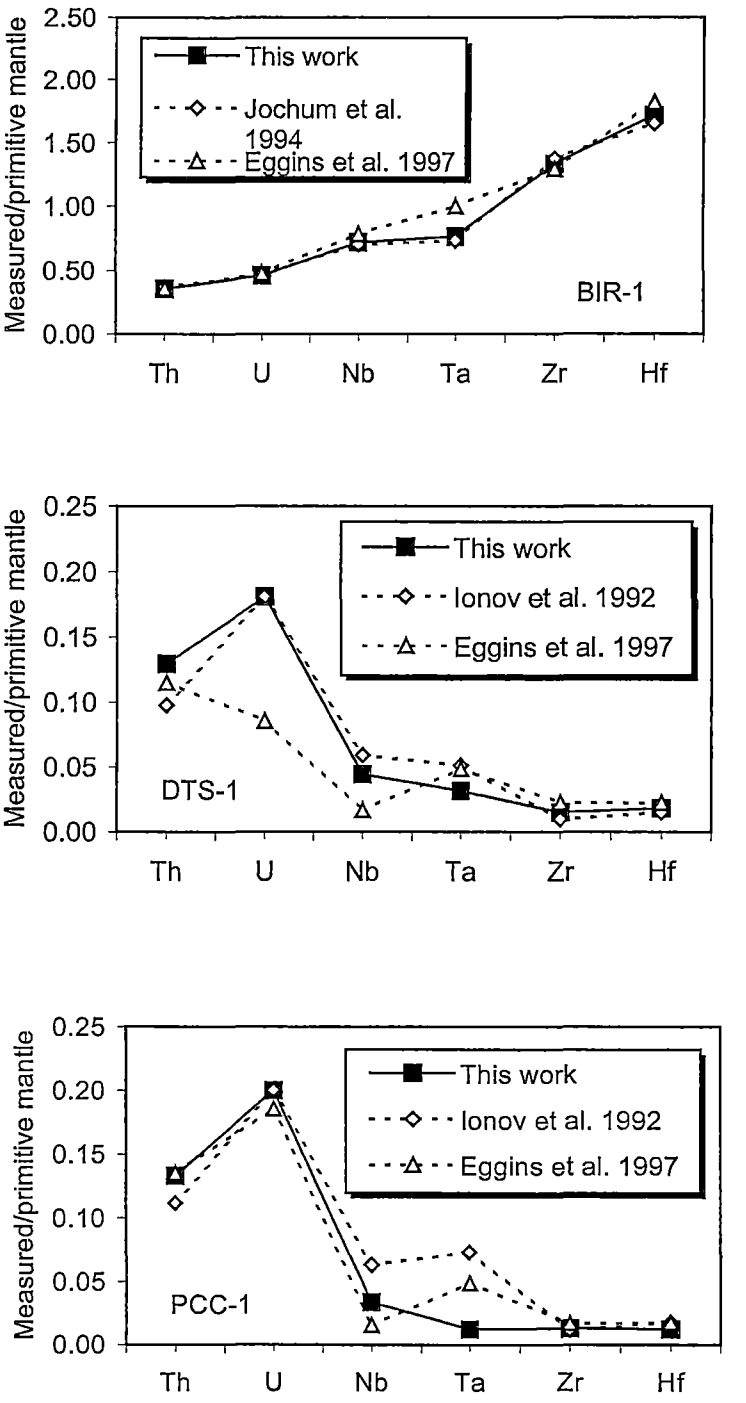

Figure 4.8. Comparison of primitive mantle normalised patterns for BIR-1, DTS-1 and PCC-1 (primitive mantle values from Sun and McDonough 1989)

From the above discussion, it can be summarised that low abundance geological materials (such as basalt, dunite, dolerite, peridotite, serpentine) can be effectively decomposed by the proposed $HF/HClO_4$ high pressure digestion technique. The results obtained in this work have also demonstrated the potential of the HR-ICP-MS method for the analysis of trace elements at very low concentrations in geological materials. Although low level HFSE can be accurately analysed by HR-ICP-MS, low HFSE recoveries for geological materials containing HFSE at moderate to high levels have been found due to their hydrolysis in aqueous solution. These problems will be addressed in the next chapter of this thesis.

Chapter 5

DETERMINATION OF HIGH FIELD STRENGTH ELEMENTS IN GEOLOGICAL REFERENCE MATERIALS USING CHELATING REAGENTS

5.1 Introduction

Although the HF/HCl_4 digestion described in Chapter 4 is suitable for measurement of HFSE at very low levels, accurate analysis of HFSE at higher levels is problematical because these elements readily hydrolyse in acid aqueous solutions (Perrin 1964; Heslop and Jones 1976; Münker 1998). The use of chelating reagents to stabilise some of the HFSE in aqueous solutions has been suggested by Perrin (1964), Cheng et al. (1982), and Sen Gupta and Bertrand (1995), but little has been reported about applying these complexing reagents to the HFSE determination in geological matrices.

In this section, the use of chelating reagents (citrate, tartrate, EDTA and DTPA), in conjunction with ICP-MS, is tested to see whether they can form stable complexes with HFSE and hence prevent the HFSE hydrolysis in aqueous solutions. The geological reference materials used in this study include some of those described in Chapter 3 (e.g. AC-E, GSR-1, MA-N, BHVO-1, YG-1, etc.) and five extra rock standards (**Table 5.1**).

The work conducted in this section can be divided into two parts. At first, the stability of various HFSE-chelating reagent complexes is systematically investigated. Following that, the accuracy of the chelating technique will be assessed using ten international geological reference materials.

Table 5.1. A list of extra geological reference materials studied

Sample name	Description	Reference
AGV-1	An andesite from the east wall of Guano Valley, Lake County, Oregon, USA	Govindaraju 1994
BE-N	Basalt collected from an old volcano near Essey-la-Côte, near Nancy, Meurthe et Moselle, France.	Govindaraju 1994
GSR-3	An olivine-basalt collected from Changjiakou, Hebei, China. The main minerals are plagioclase, olivine, magnetite and augite.	Xie et al. 1985
Mica-Fe	It is an iron-rich biotite containing many trace elements at high levels. Mica-Fe was obtained from the Massif de Saint-Sylvestre France, is probably the only biotite reference material available in the world.	Govindaraju 1994
WS-E	Dolerite collected from the Great Whin Sill, northern England. WS-E consists of plagioclase feldspar, clinopyroxene, orthopyroxene and opaque oxide. It has 'analysable' concentrations of many geologically important trace elements and shows a relatively flat chondrite normalised REE patterns.	Govindaraju et al. 1994

5.2 Background

Historically, complexing reagents have been widely used for different purposes, such as qualitative identification, quantitative titration, and for masking interference in solution inorganic chemistry (Perrin 1964; Cheng et al. 1982).

The early work of Perrin (1964) showed that citric acid, D-tartaric acid and EDTA can be used as masking reagents to prevent the interferences of coexisting cations in aqueous solution by forming stable complexes while a selected cation was titrated with another more sensitive complexing reagent. According to this report, citric acid, and tartaric acid can form stable complexes with all HFSE, and EDTA can form stable complexes with Hf and Zr in aqueous solution. It has also been reported that EDTA and DTPA, as powerful complexing reagents, can react with most cations and form very stable chelates in aqueous solution (Cheng et al. 1982). Previous work has shown that the chelate stability constants (log K_{ML}) for some HFSE are very high (**Table 5.2**). Chelate stability constants of HFSE with citric and tartaric acids and the

chelate stability constants of Nb and Ta with EDTA and DTPA are not available from the literatures. (e.g. Martell and Smith 1974, 1977, 1982 and 1989).

Moreover, it has been reported that O,O-donating chelating reagents (e.g. citric and tartaric acids) and O,N-donating chelating reagents (e.g. EDTA and DTPA) can react with most cations and form stable chelates in solutions (Cheng et al. 1982). Therefore, it should be possible to prevent the hydrolysis of HFSE in aqueous solutions by forming chelates.

Table 5.2. Chelate stability constants of high field strength elements

Element	Chelate stability constants (log K_{ML})			
	Citric acid	Tartaric acid	EDTA	DTPA
Zr	-	-	29.9[b], 29.4[c]	36.9[b], 35.8[c]
Nb	-	-	40.78[b]	-
Hf	-	-	25.9[b], 29.5[c]	35.4[b]
Ta	-	-	-	-
Th	-	-	23.2[b]	28.78[b,c], 26.4[d]
U	7.4[a]	2[a]	25.6[b], 17.87[c]	-

[a] = values are from Martell and Smith (1977).

[b] = values are from Cheng et al. (1982), log K_{ML} were measured in a medium of $\mu = 0.1$ (KCl. KNO_3 or $NaClO_4$) at 20 – 25 °C.

[c] = values are from Martell and Smith (1974).

[d] = values are from Martell and Smith (1989).

- = no value available.

5.3 Preparation of Chelate Reagent Solutions

The chelate reagents used in the present work are tri-sodium citrate (AJAX Chemicals, Sydney, Australia), sodium d-tartrate (BDH, England), di-sodium ethylenediaminetetracetate (May & Baker Ltd, England) and diethylene triamine pentaacetic acid (Sigma Chemicals, Germany). 20 mM stock solutions of the four chelate reagents were prepared with ultra pure water before diluting to 2 mM in testing solutions. **Table 5.3** gives some details about the preparation of the chelate reagent solutions.

In addition, in order to determine the impurities levels for the chelate reagent solutions under the experimental conditions (2 mM chelate reagents, 2% HNO_3 and 1% HCl in final solutions) the citrate, tartrate, EDTA and DTPA blanks were also measured for trace elements by HR-ICP-MS before using for any geological sample analysis. **Table 5.4** shows the measured results for HFSE for the four chelate reagent blank solutions and comparison with acid blank (2% HNO_3 and 1% HCl ultra pure water solution). The blank levels of the four chelate reagents for HFSE were generally similar to or slightly higher than that of the acid blank. The blank concentrations for Zr were from 0.0037 ng g^{-1} for DTPA to 0.0953 ng g^{-1} for EDTA. The blank concentrations for Nb were from 0.0031 ng g^{-1} for DTPA to 0.0717 ng g^{-1} for EDTA. The lowest blank level for Hf was 0.0007 ng g^{-1} for DTPA and the highest blank level for Hf was 0.0829 ng g^{-1} for EDTA. The blank levels of Ta were found to vary considerably among the four different chelate reagents. The blank levels for Ta were 0.0007, 0.0601, 0.1130 and 0.1274 ng g^{-1} for DTPA, EDTA, tartrate and citrate respectively. The blank level for Th was from 0.0017 ng g^{-1} for DTPA to 0.0225 ng g^{-1} for EDTA. Finally, the blank level for U was the lowest among HFSE for all of the chelate reagents, and from 0.0002 ng g^{-1} for citrate to 0.0033 ng g^{-1} for tartrate.

Table 5.3. Preparation of the 20 mM chelate reagent solutions

Chelate reagent	Formula	Formula weight	Amount (g) needed in 1000 ml solution
Citrate	$Na_3C_6H_5O_7 \cdot 2H_2O$	294.1	5.882
Tartrate	$Na_2C_4H_4O_6 \cdot 2H_2O$	230.09	4.602
EDTA	$Na_2C_{10}H_{14}N_2O_8 \cdot 2H_2O$	372.25	7.445
DTPA	$C_{14}H_{23}N_3O_{10}$	393.35	7.867

In addition, a comparison has also been made to observe the different levels for citrate, tartrate, EDTA, DTPA and acid blank. **Figure 5.1** shows that the blank level for U was the lowest for all of the chelate reagents and acid blanks. Although the blank levels of Ta for citrate and tartrate were slightly higher than 0.1 ng g^{-1}, these values were still well under the 1.0 ng g^{-1} at which there is obvious Ta hydrolysis in dilute HNO_3 solution (Münker 1998). Under the experimental conditions, EDTA

solution showed the highest average blank levels. The concentrations of HFSE measured in DTPA blank were similar to those measured in the acid blank, which indicates that DTPA might be a suitable chelate reagent for the low abundance geological sample analysis.

Table 5.4. Blank levels (ng g^{-1}) of citrate, tartrate, EDTA, DTPA and acid blank under the experimental conditions and comparison with acid blank

Element	Mass	Blank level (ng g^{-1})				
		Citrate	Tartrate	EDTA	DTPA	Acid blank
Zr	90	0.0196	0.0390	0.0953	0.0037	0.0031
Nb	93	0.0433	0.0390	0.0717	0.0031	0.0023
Hf	178	0.0228	0.0147	0.0829	0.0007	0.0006
Ta	181	0.1274	0.1130	0.0601	0.0007	0.0007
Th	232	0.0038	0.0028	0.0225	0.0017	0.0014
U	238	0.0002	0.0033	0.0008	0.0003	0.0003

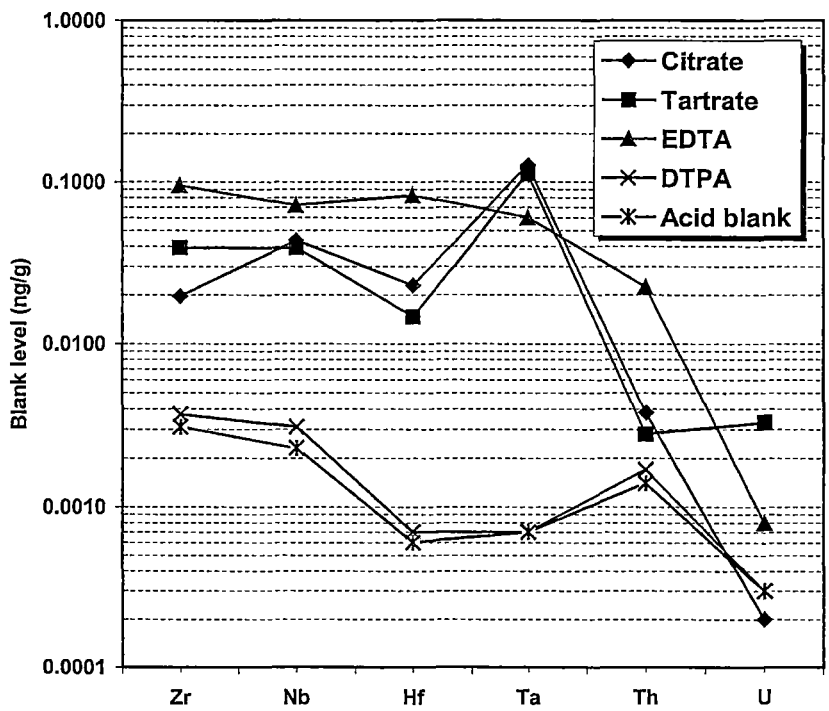

Figure 5.1. A comparison of blank levels (ng g^{-1}) for citrate, tartrate, EDTA, DTPA and acid blank. The concentration of complexing reagents was 2 mM, and all solutions were prepared in 2% HNO_3 and 1% HCl.

5.4 Stability of HFSE Complexes

In this section, the stability of HFSE - citrate, tartrate, EDTA and DTPA complexes is investigated. A geological reference material (Mica-Fe, a biotite) was used for the investigation. Powdered sample (100 mg) was digested at about 180 °C for 16 hours using HF/HSO_4 high pressure digestion. The digestion residue was taken up by 2 ml HNO_3 and 1 ml HCl at 60 °C. The final solution was diluted to 100 ml with 2 mM citrate, tartrate, EDTA and DTPA respectively. This corresponds to a 1000-fold dilution of the values in the solid samples. The reference values of Zr, Nb, Hf, Ta, Th and U for Mica-Fe are 800, 270, 26, 35, 150 and 80 $\mu g\ g^{-1}$ in solid sample respectively (Govindaraju 1994). These solutions were measured for HFSE using HR-ICP-MS at 1, 7, 21, 45 and 55 days respectively. In order to observe the variation of the HFSE concentrations with time, measured concentrations were normalised to the concentration obtained on the first of dissolution. Therefore the normalised concentration can be described in the following equation:

Normalised concentration = Measured concentration/Fresh concentration

Where: Measured concentration was measured by HR-ICP-MS at different days after sample dissolution.
Fresh concentration was measured by HR-ICP-MS within 24 hours after sample dissolution.

Figure 5.2 shows the relationship between the normalised concentration and time after sample dissolution. Although there is some reduction in the measured concentrations over time, it can be clearly seen that more than 80% of Zr, Nb, Hf, Th and U and 70% of Ta still remained in solution 55 days after dissolution, due to the complex formation of Zr-citrate, tartrate, EDTA and DTPA; Nb-citrate, tartrate, EDTA and DTPA; Hf-citrate, tartrate, EDTA and DTPA; Ta-citrate, tartrate, EDTA and DTPA; Th-citrate, tartrate, EDTA and DTPA and U-citrate, tartrate, EDTA and DTPA in aqueous solutions. From this experimental work, the stability of HFSE complexes can be described as follows:

Zirconium

In 2 mM citrate solution, due to the formation of Zr-citrate complex more than 96% of Zr still remained in aqueous solution 7 days after the sample dissolution. Then with the increase of time, the amount of Zr remaining in solution decreased slightly. Eventually, about 91% of Zr remained in solution 55 days after the sample dissolution. About 95% of Zr remained in solution 7 days after the sample dissolution for 2 mM tartrate solution. The amount of Zr remaining in solution decreased slightly with the increase of time. More than 93% of Zr was present in solution 55 days after sample dissolution. In 2 mM EDTA solution, more than 97% of Zr was still present 7 days after the sample dissolution. Then, with the increase of time, 95.5%, 94.8% and 89.5% of Zr remained at 21, 45 and 55 days after the sample dissolution. Finally, in the 2 mM DTPA solution, the amount of Zr remaining in solution was found to be 94.4%, 93.9%, 92.7% and 86.6% respectively 7, 21, 45 and 55 days after the sample dissolution.

Niobium

In 2 mM citrate solution, due to the formation of Nb-citrate complex more than 93% of Nb still remained in aqueous solution 7 days after the sample dissolution. Subsequently, the amount of Nb remaining in solution gradually decreased. After 55 days, about 82% of Nb remained in solution. For the 2 mM tartrate solution, about 89% of Nb remained in solution 7 days after the sample dissolution. The amount of Nb remaining in solution decreased slightly with the increase of time. Nearly 84% of Nb was present 55 days after sample dissolution. In the 2 mM EDTA solution, more than 92% of Nb still remained in solution 7 days after the sample dissolution. Then, with the increase of time, 91.3%, 89.2% and 85.8% of Nb was found 21, 45 and 55 days after the sample dissolution. Finally, in 2 mM DTPA solution, the amount of Nb remaining in solution was found to be 91.1%, 88.5%, 85.7% and 82.1% respectively 7, 21, 45 and 55 days after the sample dissolution.

Hafnium

In 2 mM citrate solution, due to the formation of Hf-citrate complex more than 94% of Hf still remained in aqueous solution 7 days after the sample dissolution, after which, the amount of Hf remaining in solution decreased gradually. Eventually, about 81% of Hf remained in solution 55 days after the sample dissolution. 93% of Hf remained in solution 7 days after the sample dissolution. The amount of Hf remaining in solution decreased gradually with the increase of time. More than 82% of Hf was found 55 days after sample dissolution. In the 2 mM EDTA solution, more than 97% of Hf was still found 7 days after the sample dissolution. Then, with the increase of time, 95.6%, 91.0% and 87.5% of Hf was found 21, 45 and 55 days after the sample dissolution. Finally, in 2 mM DTPA solution, the amount of Hf remaining in solution was found to be 95.9%, 92.8%, 89.2% and 87.8% respectively 7, 21, 45 and 55 days after the sample dissolution.

Tantalum

Unlike the stability for the Zr, Nb and Hf complexes, there was a clear decrease in the amount of Ta remaining in the citrate, tartrate, EDTA and DTPA solutions. On average, about 20% of Ta precipitated in the first 7 days of the sample dissolution. In the 2 mM citrate solution, only about 80% of Ta remained in solution 7 days after the sample dissolution. Then the amount of Ta remaining in solution gradually decreased to approximately 71% of the fresh concentration 55 days after the sample dissolution. About 78% of Ta remained in solution 7 days after the sample dissolution in the 2 mM tartrate solution. Fifty-five days after the sample dissolution, the amount of Ta remaining in solution reduced to 75.7%. With the 2 mM EDTA solution, 84% of Ta was found 7 days after the sample dissolution, and the amount of Ta remaining in solution was found to be 82.5%, 80.9% and 77.6% respectively 21, 45 and 55 days after the sample dissolution. Finally, in the 2 mM DTPA solution, 79% of Ta remained in solution 7 days after the sample dissolution. Subsequently, the amount of Ta remaining in solution decreased gradually. 71.9% of Ta remained in solution 55 days after the sample dissolution.

Thorium

Similar to the variation of Ta, there was a clear reduction in the amount of Th remaining in citrate, tartrate, EDTA and DTPA solutions. Approximately 11% of Th hydrolysed in the first 7 days of the sample dissolution. In the 2 mM citrate solution, about 89% of Th remained in solution 7 days after the sample dissolution. Then the amount of Th remaining in solution gradually decreased to about 82% of its fresh concentration 55 days after the sample dissolution. Nearly 87% of Th remained in solution 7 days after the sample dissolution in 2 mM tartrate solution. Fifty-five days after the sample dissolution, the amount of Th remaining in solution decreased to 84.5%. With 2 mM EDTA solution, 89% of Th was present 7 days after the sample dissolution, and the amount of Th remaining in solution was 87.2%, 85.8% and 84.7% respectively 21, 45 and 55 days after the sample dissolution. Finally, in the 2 mM DTPA solution, more than 87% of Th remained in solution 7 days after the sample dissolution, after which, the amount of Th remaining in solution decreased gradually, and 86.9% of Th remained in solution 55 days after the sample dissolution.

Uranium

The stability of U complexes was similar to that of Th complexes. Initially, there was a clear decrease in the amount of U remained in citrate, tartrate, EDTA and DTPA solutions. On average, about 12% of Th hydrolysed in the first 7 days of the sample dissolution. In the 2 mM citrate solution, about 88% of U remained in solution 7 days after the sample dissolution. Then the amount of U remaining in solution decreased slightly to about 87% of its fresh concentration 55 days after the sample dissolution. About 89% of U remained in solution 7 days after the sample dissolution in 2 mM tartrate solution. Fifty-five days after the sample dissolution, the amount of U remaining in solution decreased to 86.2%. With the 2 mM EDTA solution, nearly 83% of U was found to remain in solution 7 days after the sample dissolution, and the amount of U remaining in solution was 82.7%, 82.4% and 82.2% respectively 21, 45 and 55 days after the sample dissolution. Finally, in the 2 mM DTPA solution, more than 89% of U remained in solution 7 days after the sample dissolution. Subsequently, the amount of U remaining in solution reduced slightly. 84.3% of U remained in solution 55 days after the sample dissolution.

Results presented above shows that citrate, tartrate, EDTA and DTPA will stabilise the HFSE in aqueous solution. Although there is still a decrease in the HFSE concentrations a few days after sample dissolution, even 55 days after the sample dissolution, there was still generally more than 80% of HFSE remaining in aqueous solution relative to the concentrations measured in the fresh solutions (**Figure 5.2**).

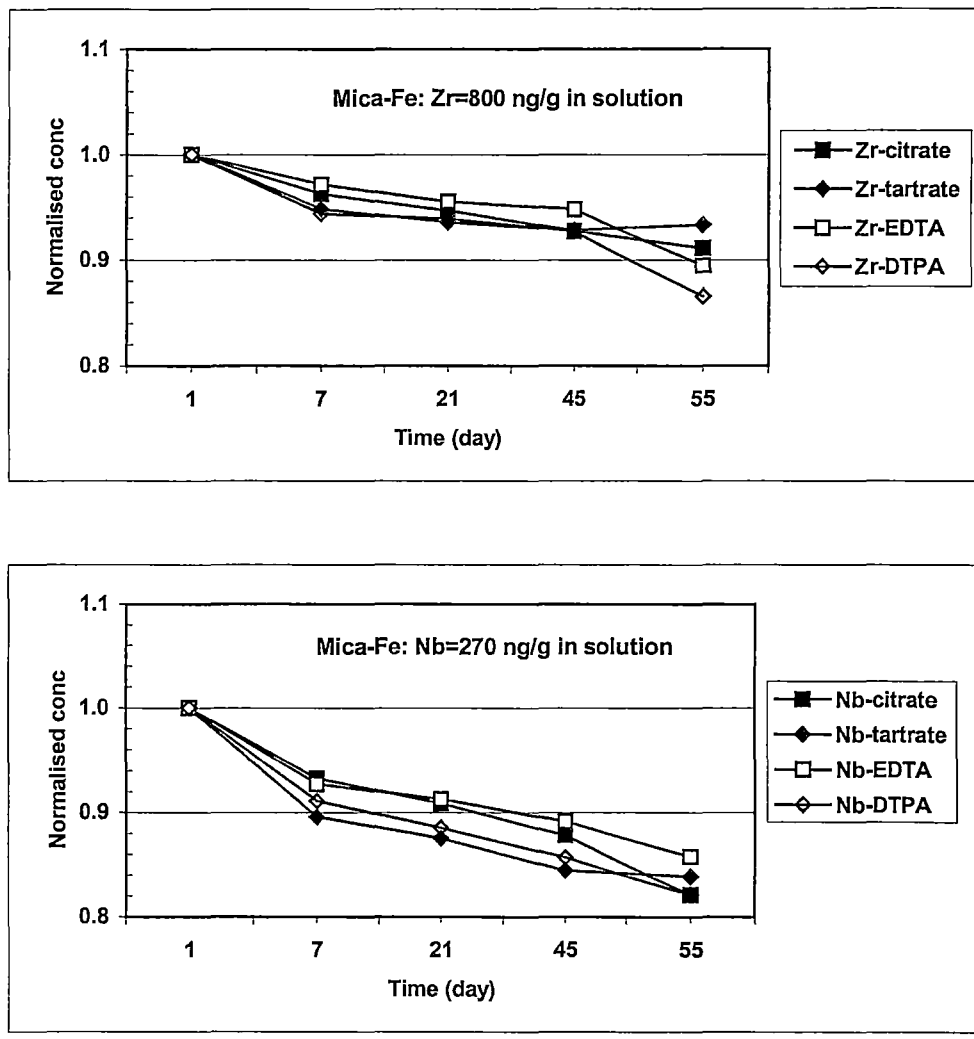

Figure 5.2. Complex stabilities of Zr-citrate, tartrate, EDTA and DTPA; Nb-citrate, tartrate, EDTA and DTPA; Hf-citrate, tartrate, EDTA and DTPA; Ta-citrate, tartrate, EDTA and DTPA; Th-citrate, tartrate, EDTA and DTPA and U-citrate, tartrate, EDTA and DTPA for rock reference material-Mica-Fe (biotite).

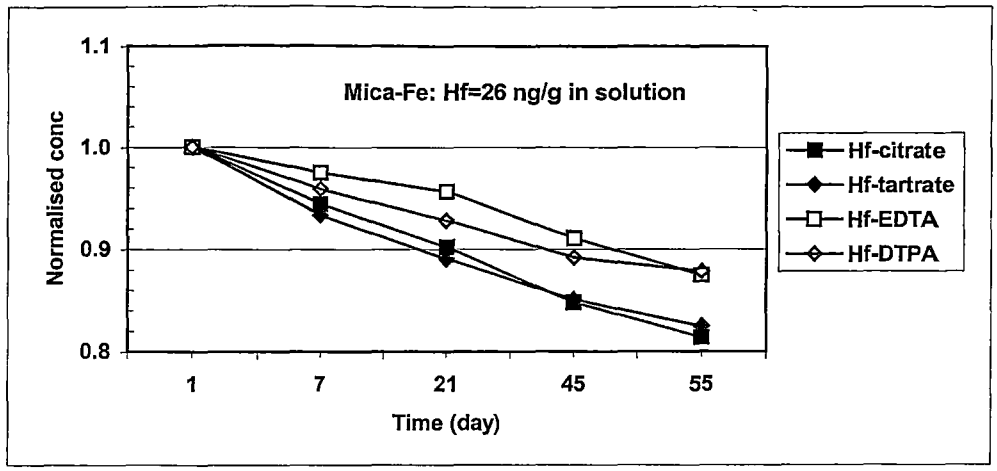

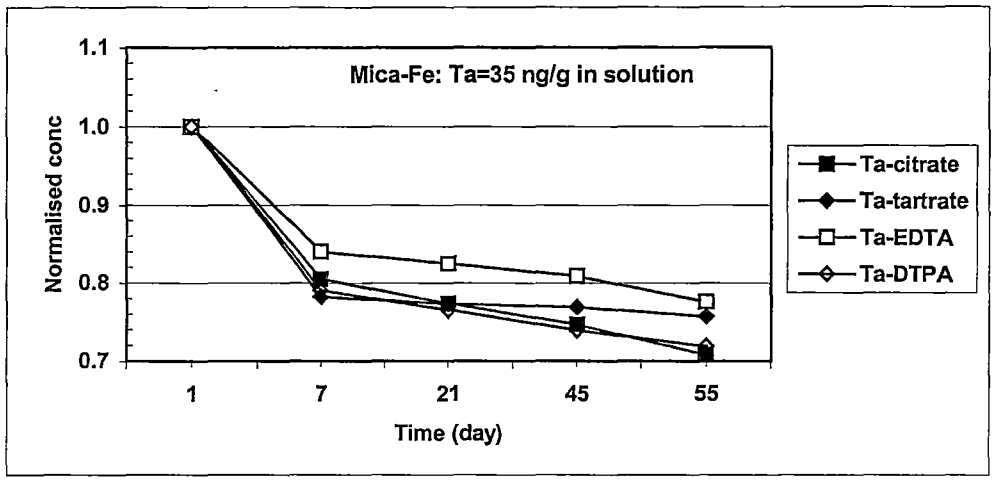

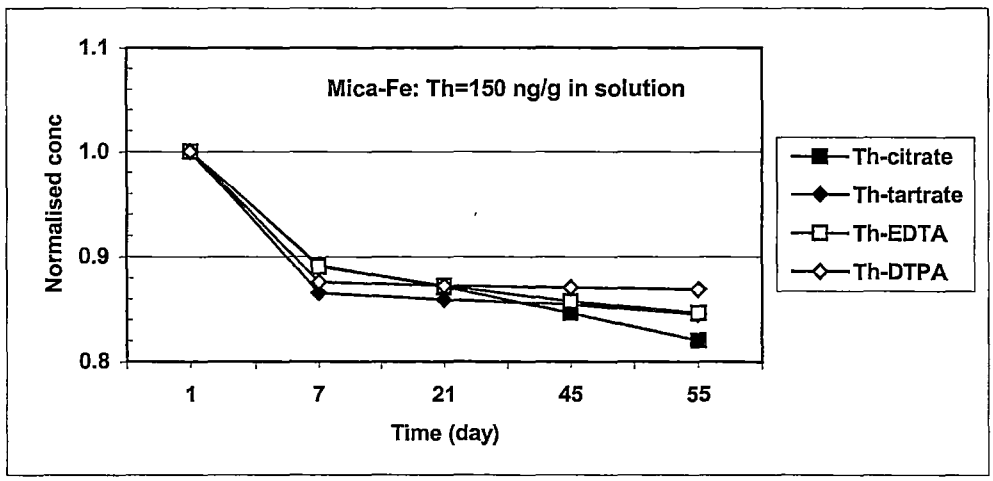

Figure 5.2. (Continued). Complex stabilities of Zr-citrate, tartrate, EDTA and DTPA; Nb-citrate, tartrate, EDTA and DTPA; Hf-citrate, tartrate, EDTA and DTPA; Ta-citrate, tartrate, EDTA and DTPA; Th-citrate, tartrate, EDTA and DTPA and U-citrate, tartrate, EDTA and DTPA for rock reference material-Mica-Fe (biotite).

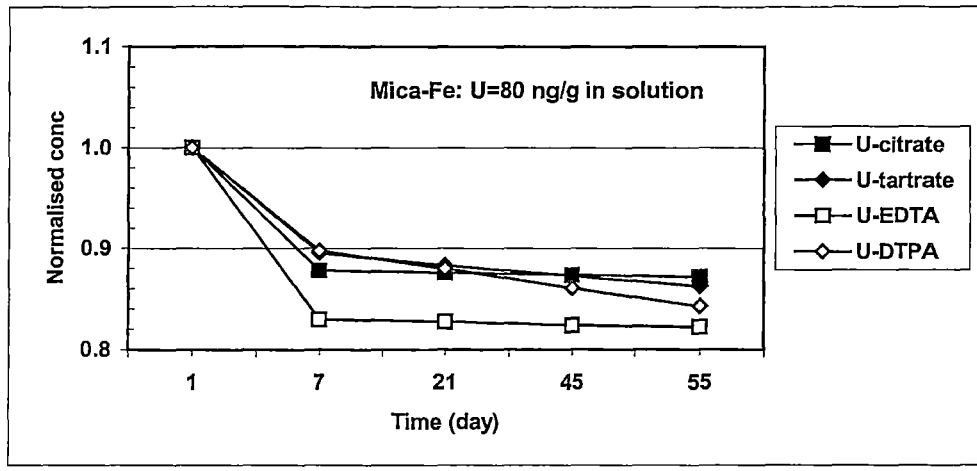

Figure 5.2. (Continued). Complex stabilities of Zr-citrate, tartrate, EDTA and DTPA; Nb-citrate, tartrate, EDTA and DTPA; Hf-citrate, tartrate, EDTA and DTPA; Ta-citrate, tartrate, EDTA and DTPA; Th-citrate, tartrate, EDTA and DTPA and U-citrate, tartrate, EDTA and DTPA for rock reference material-Mica-Fe (biotite).

5.5 Choice of Chelate Reagents

The previous discussion demonstrates that citrate, tartrate, EDTA and DTPA can be used as chelating reagents to prevent the hydrolysis of HFSE in aqueous solutions. However, it is not clear which of these is the best for stabilising the HFSE as a whole in solution. In this section, results of four individual digestions of geological reference material - YG-1 were used to assess which of the chelating reagents in optimal for the HFSE as a group. All solutions were analysed using HR-ICP-MS within 24 hours after sample dissolution and results are shown in **Figure 5.3**. Citrate produces the lowest results for Zr, Nb, Hf. Tartrate, EDTA and DTPA yielded similar results for Zr, Nb, Hf, Th and U. However, the concentration of Ta varies depending on the chelating reagent used. The measured concentration of Ta increases in order: citrate < tartrate < EDPA < DTPA. The concentrations of Ta using citrate, tartrate, and EDTA were 11.7%, 9.36% and 3.33% respectively lower than that using DTPA.

Hence, because DTPA yields the 'best' 'total' results, and because the available reagent has the lowest blank levels (see **Section 5.3**), it has been chosen as the best chelating reagent for stabilising HFSE in aqueous solutions.

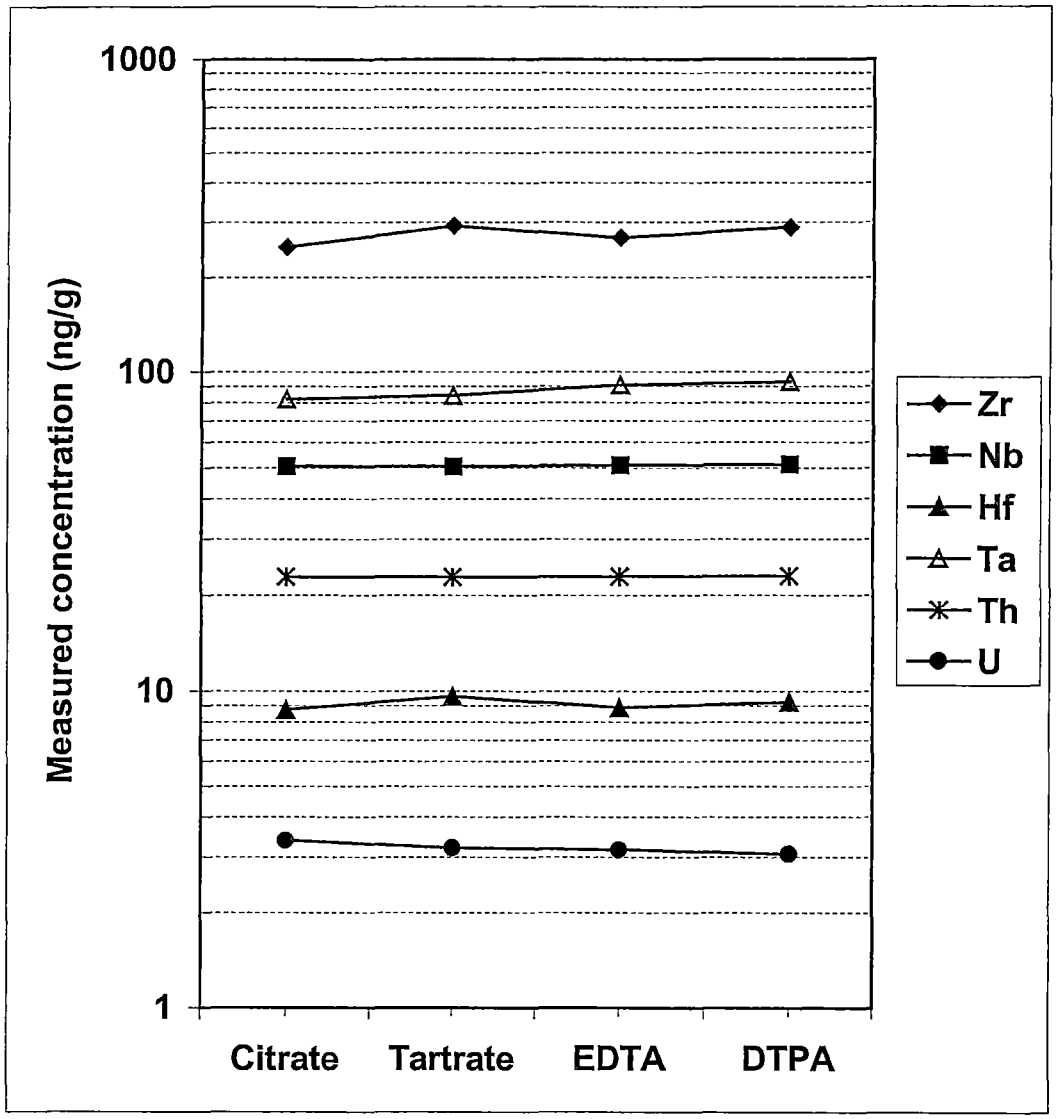

Figure 5.3. Measured concentrations of HFSE for the geological reference material - YG-1 by HR-ICP-MS using different chelate reagents. The concentrations of citrate, tartrate, EDTA and DTPA were 2 mM in final solution. The testing solutions were analysed within 24 hours after sample dissolution.

5.6 Stability of HFSE-DTPA Complexes

In this section of the thesis, both short-term (over a period of five days) and long-term (over a period of 28 days) stability experiments are carried out to further

investigate the stability of HFSE-DTPA complexes and to test whether it is necessary to conduct instrument analysis using fresh solutions.

5.6.1 Short-term Stability

In order to investigate the short-term stability of the HFSE-DTPA complexes, TASBAS, GSR-1, Mica-Fe, YG-1 and MA-N were digested using a HF/H_2SO_4 high pressure digestion method. Final solutions were all prepared in 2 mM DTPA – 2% HNO_3 – 1% HCl. Then, the testing solutions were analysed for HFSE at 1, 2, 3, 4 and 5 days respectively. **Figure 5.4** shows the stability of HFSE – DTPA chelates for the five selected geological reference materials over a period of 5 days after sample dissolution. From the measured results it has been found that:

(1) In general, little variations in Zr concentrations for TASBAS, GSR-1 and Mica-Fe were observed, and the decrease in Zr concentration was found to be less than 5% over a period of 5 days after dissolution. The decrease in Zr concentration for YG-1 was found to less than 1% two days after sample dissolution, decreasing to about 7% five days after dissolution. There was a clear decrease (about 21%) in Zr concentration for MA-N 2 days after sample dissolution.

(2) Nb-DTPA complex seemed quite stable 2 days after sample dissolution for all solutions, and the decrease in Nb concentration was found to be less than 5%. Subsequently, the concentration of Nb in all testing solutions decreased. In comparison with the fresh concentrations (concentrations measured one day after dissolution), the concentrations of Nb remaining in solution were 96% for Mica-Fe, 93% for TASBAS and YG-1, and about 90% for GSR-1 and MA-N.

(3) The variation for Hf in solution was found to be minor for both TASBAS and GSR-1, and the decrease of Hf concentration was less than 3% and 8% for TASBAS and GSR-1 respectively over a period of 5 days after sample dissolution. The variation for Hf in solution was similar for Mica-Fe, YG-1

and MA-N, and the decrease in Hf concentration was found to be less than 14% five days after sample dissolution compared to the initial concentration.

(4) Ta-DTPA was found to quite stable in TASBAS, GSR-1, Mica-Fe and YG-1, and the decrease in Ta concentration was generally less than 5% two days after sample dissolution. Subsequently, the concentration of Ta in solution decreased slightly. In comparison with the fresh concentration, the decrease of Ta concentration was about 10% five days after dissolution. It has been found that there was a clear decrease (about 20%) in Ta concentration for MA-N even two days after dissolution. Only 66% Ta remained in the DTPA solution five days after dissolution compared to the fresh concentration.

(5) The variation in Th concentration was minor for TASBAS, showing a decrease of less than 6% over a period of five days after dissolution. In comparison with the fresh concentration, Th remaining in solution was found to be 87%, 89%, 81% and 80% for GSR-1, Mica-Fe, YG-1 and MA-N respectively five days after sample dissolution.

(6) The concentrations of U for TASBAS and YG-1 were found to decrease slightly with time, 95% (TASBAS) and 97% (Mica-Fe) remaining five days after dissolution. Similar variation in the U concentration was observed for GSR-1 and YG-1. In comparison to the fresh concentration, the U concentration remaining in solution was 84% and 81% for GSR-1 and YG-1 5 days after sample dissolution. Finally, there was a clear decrease (about 16%) in U concentration for MA-N two days after dissolution. Five days after sample dissolution, only 77% of U concentration remained in solution.

Discussion: From these observations, it is concluded that HFSE in aqueous solution can be stabilised using DTAP due to the formation of HFSE-DTPA chelates. In comparison with the fresh concentrations, the decrease in measured HFSE concentrations for the five selected geological reference materials was generally less than 15% five days after sample dissolution; only the concentrations of Ta and U for MA-N were found to decrease about 34% and 23% respectively five days after sample dissolution.

It has also been found that the stabilities of HFSE-DTAP chelates also depend on Ta concentration in solution, even with the addition of DTPA in aqueous solutions. For instance, the highest Ta concentration is 290 μg g^{-1} in solid for MA-N (Govindaraju 1994) which is equivalent to 290 ng g^{-1} in solution under the experimental conditions. The concentrations of HFSE for MA-N were also found to be quite unstable in comparison with those for the other four geological reference materials a few days after sample dissolution. This is due to the tendency of Ta compounds easily undergo hydrolysis to give insoluble $Ta_2O_5(H_2O)_x$ even in acid solution (Perrin 1964). The instabilities of Zr, Nb, Hf, Th and U are due to their co-precipitation. Therefore, the higher the Ta concentration, the less stable Zr, Nb, Hf, Th and U are. A similar observation was also reported in an earlier work (Münker 1998).

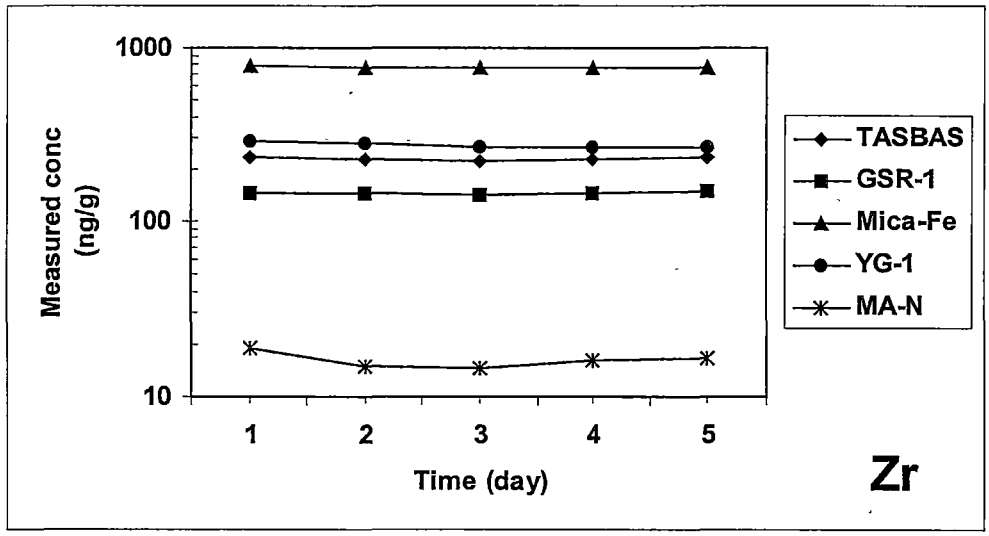

Figure 5.4. Stability of HFSE – DTPA chelates for the selected geological reference materials over a period of 5 days after sample dissolution

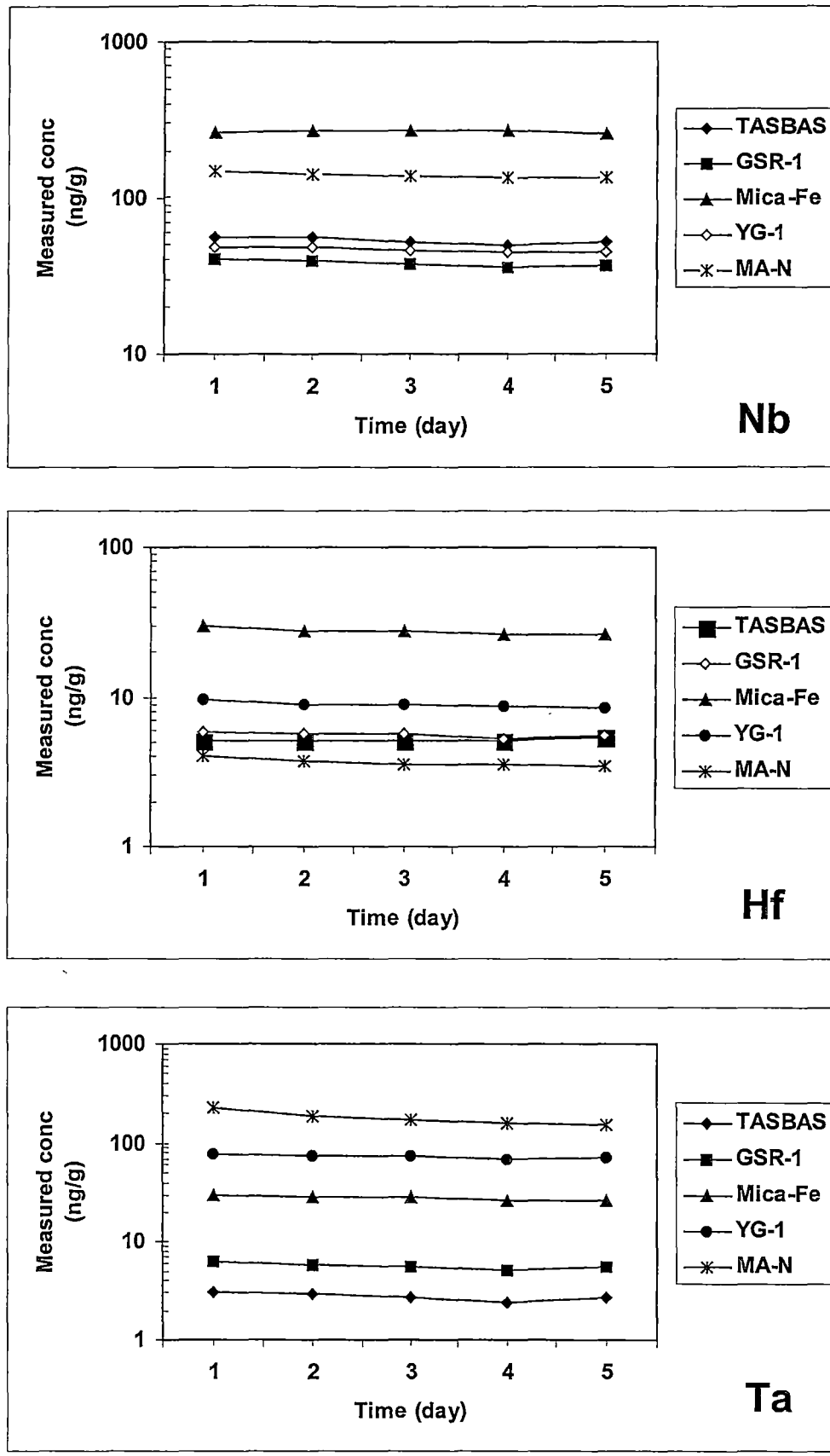

Figure 5.4. (Continued). Stability of HFSE – DTPA chelates for the selected geological reference materials over a period of 5 days after sample dissolution

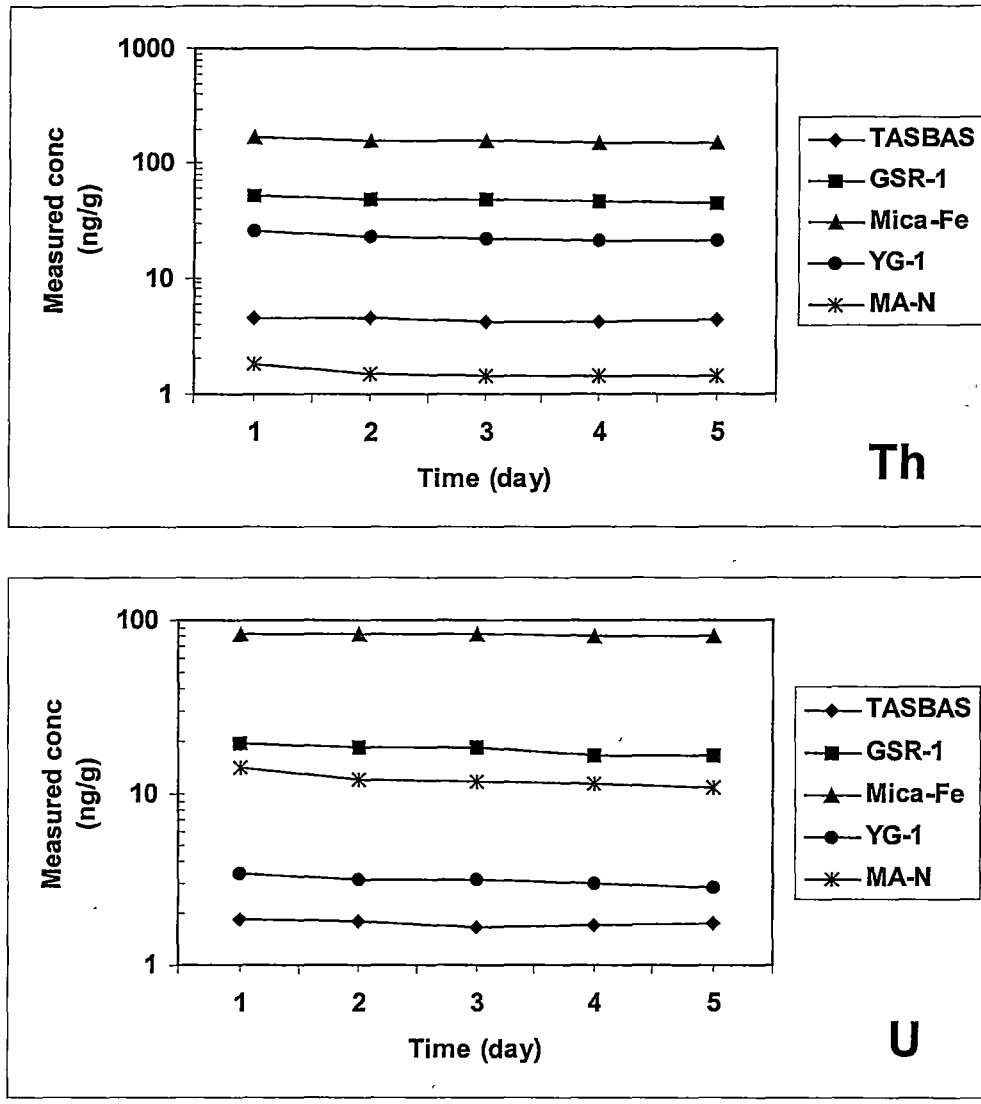

Figure 5.4. (Continued). Stability of HFSE – DTPA chelates for the selected geological reference materials over a period of 5 days after sample dissolution

5.6.2 Long-term Stability

Four geological reference materials have been used to assess the stability of HFSE – DTPA over a period of four weeks. Four geological reference materials (GSR-1, Mica-Fe, YG-1 and MA-N) were digested using HF/H_2SO_4 high pressure decomposition method. Digestion residues were taken up with 2 ml HNO_3 and 1 ml HCl and diluted to 100 ml with 2 mM DTPA solution. The concentrations of Zr, Nb, Hf, Ta, Th and U in the testing solutions were measured by HR-ICP-MS 1, 7, 14, 21 and 28 days after dissolution.

Generally speaking, the concentrations of Zr, Nb, Hf, Ta, Th and U in testing solutions decrease with time (**Figure 5.5**). In detail, different elements behave somewhat differently to each other. Furthermore, this behaviour is dependent on the reference material matrix. For instance:

- Zr concentrations remaining in solution 28 days after dissolution were 82%, 90%, 91% and 81% of the initial concentrations for GSR-1, Mica-Fe, YG-1 and MA-N respectively.

- Nb concentrations decreased with time. The decreases in Nb concentrations were 14%, 15%, 18% and 30% for GSR-1, Mica-Fe and YG-1 respectively 28 days after sample dissolution.

- The variations for Hf concentration were similar to those for Nb concentrations with increasing time. There was a clear decrease in Hf concentration for all four rock reference materials. However, the concentrations of Hf remained quite stable for Mica-Fe and YG-1 between 7 and 28 days after sample dissolution. The Hf remaining in solution changed from 86.2% to 84.6% for Mica-Fe and from 87.9% to 86.3% for YG-1 between 7 and 28 days after dissolution compared with the fresh concentrations. In contrast, there was a clear decrease in Hf concentration for MA-N between 7 and 28 days after sample dissolution and only 68% of Hf remained in solution 28 days after dissolution.

- The concentrations of Ta for all of the four geological materials were found to be the most unstable among the concentrations of HFSE, showing a clear decrease in Ta concentrations with time. In comparison with the fresh concentrations, Ta remaining in solution was found to be 56%, 74%, 64% and 31% for GSR-1, Mica-Fe, YG-1 and MA-N respectively, 28 days after sample dissolution.

- There was a clear decrease in Th concentrations for GSR-1, Mica-Fe, YG-1 and MA-N in the first week after sample dissolution. Subsequently, the

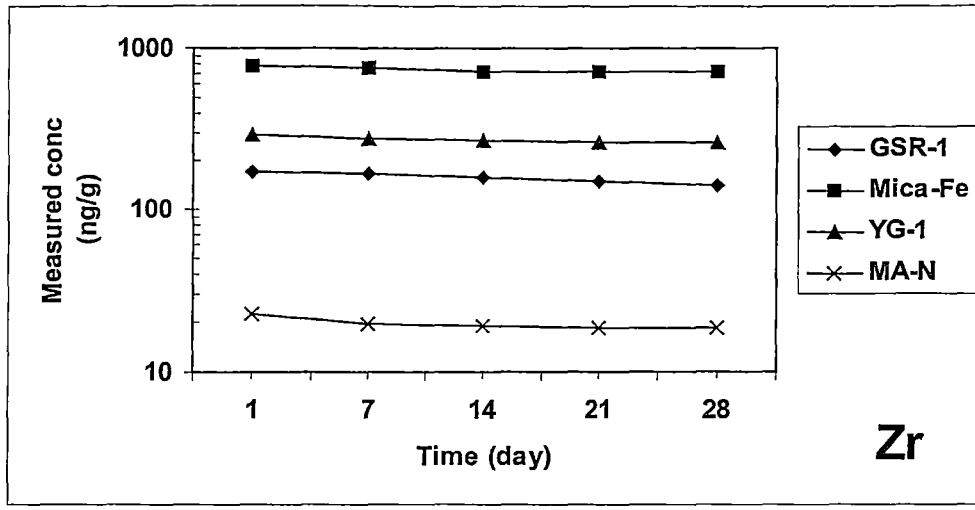

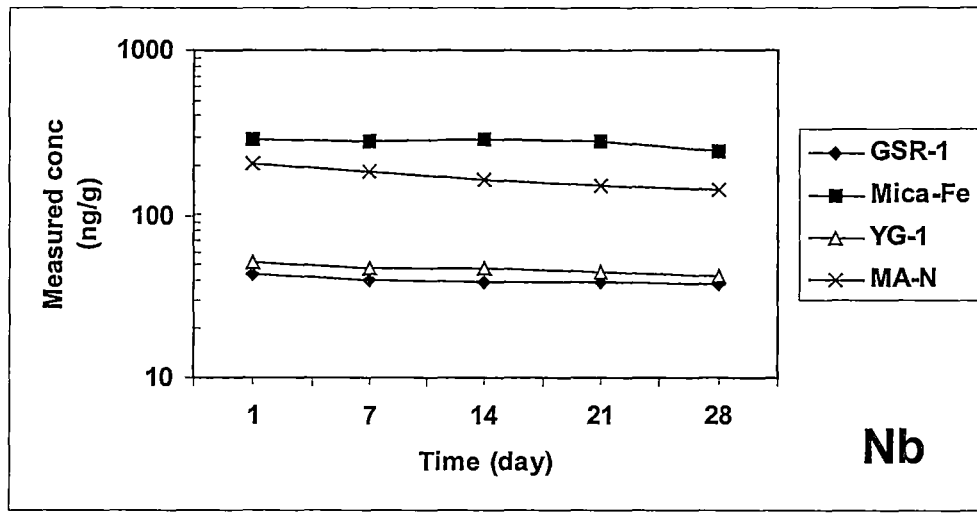

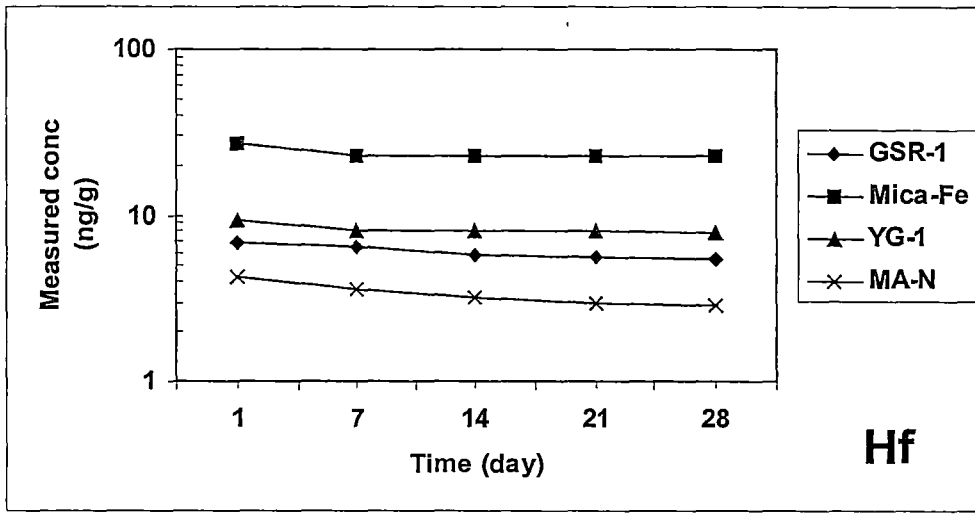

Figure 5.5. Stability of HFSE – DTPA chelates for the selected geological reference materials over a period of 28 days after sample dissolution

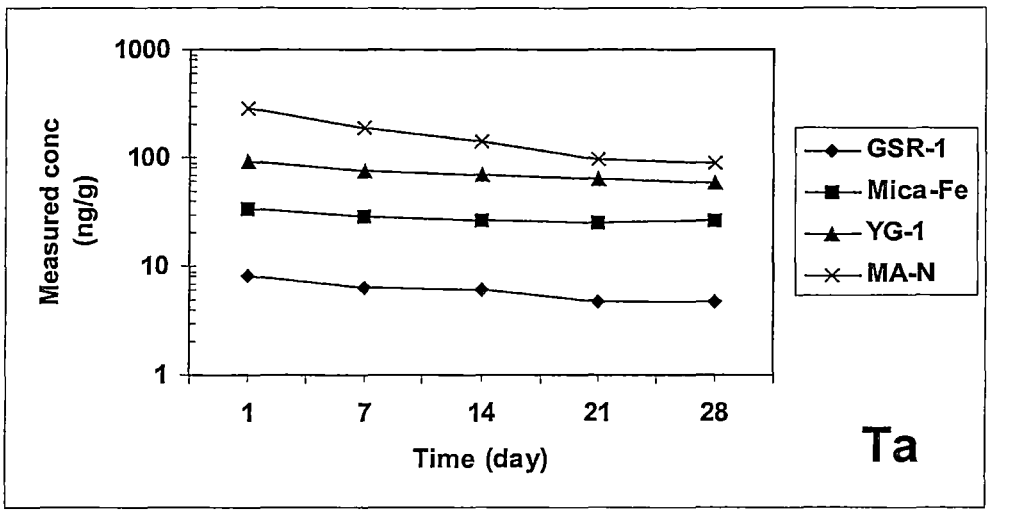

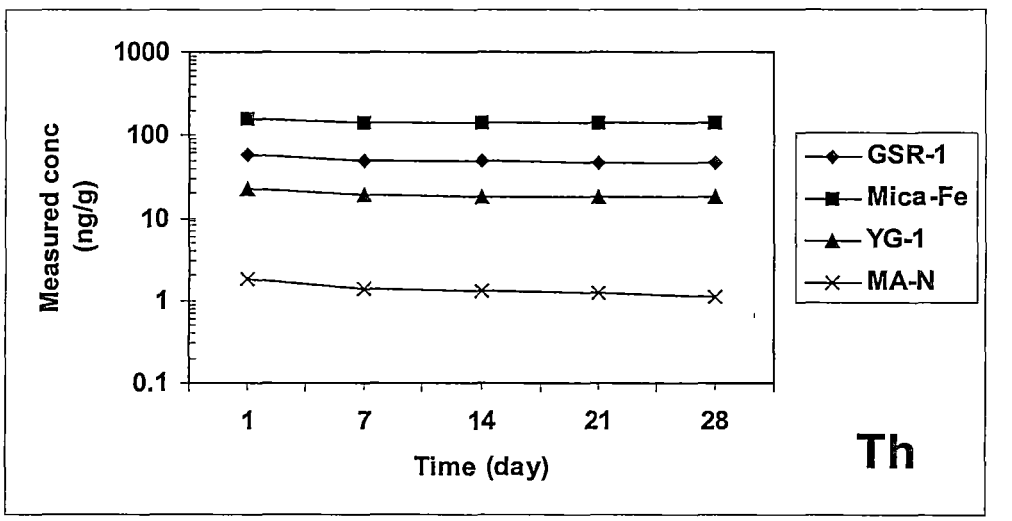

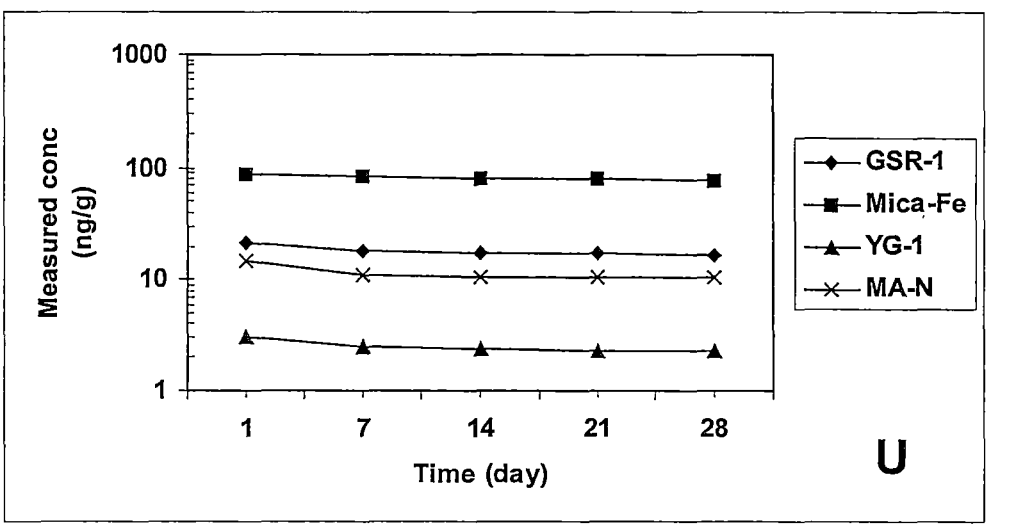

Figure 5.5. (Continued). Stability of HFSE – DTPA chelates for the selected geological reference materials over a period of 28 days after sample dissolution

concentrations of Th decreased gradually, with the exception of MA-N. The concentrations of Th remaining in solution were 79%, 87%, 78% and 63% for GSR-1, Mica-Fe and MA-N respectively, compared with the fresh concentrations.

- Finally, U concentrations also decreased with time. In comparison with fresh concentrations, the concentrations of U for GSR-1 were 83%, 82%, 80% and 79% respectively one, two, three and four weeks after sample dissolution. The U remaining in solution was 91%, 74% and 71% for Mica-Fe, YG-1 and MA-N four weeks after sample dissolution.

Based on the above observations, it can be seen that HFSE in aqueous solution can generally be stabilised using DTAP except for samples containing very high concentration of Ta (such as MA-N).

Figure 5.6 further highlights the variations of Ta concentrations in DTPA solutions for GSR-1, Mica-Fe, YG-1 and MA-N over a period of 28 days after sample dissolution. Clearly, normalised concentrations of Ta decreased with time. The normalised concentrations of Ta dropped to about 0.86 for Mica-Fe, to about 0.80 for both GSR-1 and YG-1, and to 0.65 for MA-N (containing the highest Ta among the four rock reference materials) seven days after sample dissolution. Therefore, it is strongly recommended that the measurement of Ta in geological samples should be conducted within 24 hours after dissolution, even with the addition of DTPA in aqueous solutions.

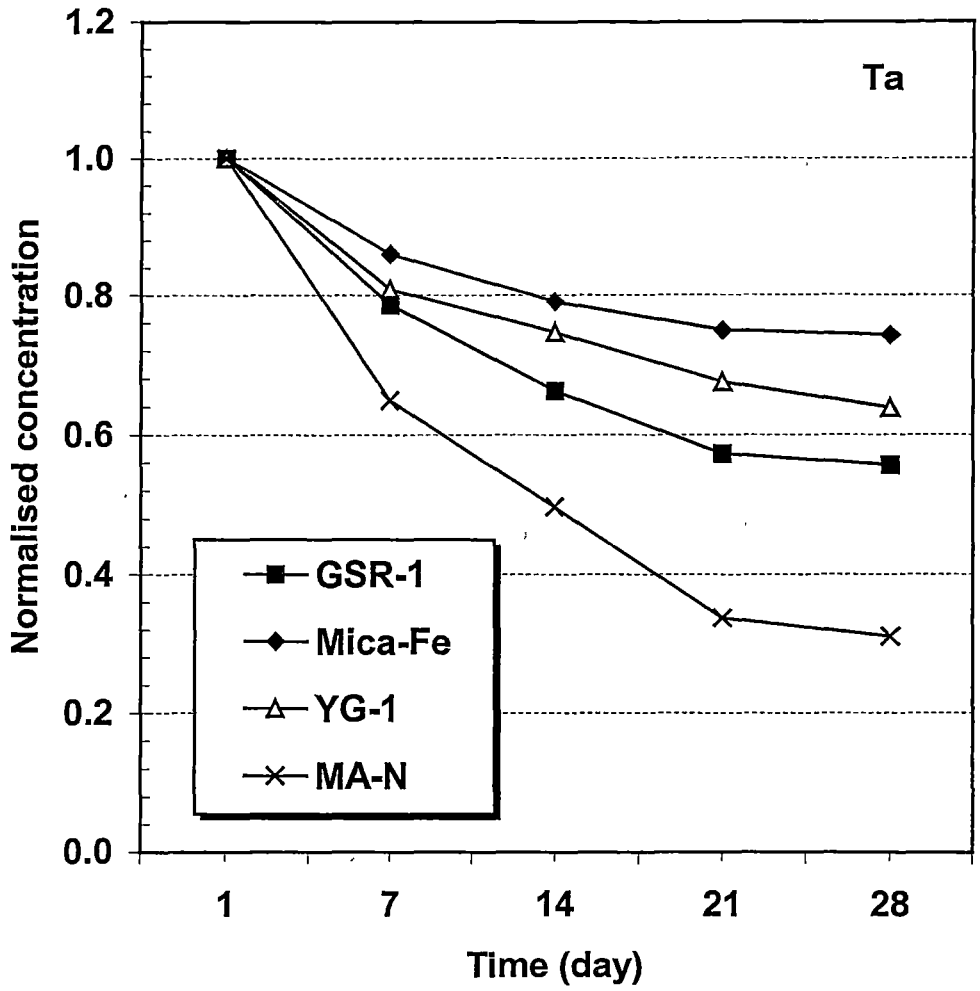

Figure 5.6. Variations of Ta concentrations for GSR-1, Mica-Fe, YG-1 and MA-N over a period of 28 days after sample dissolution. Normalised concentration = fresh concentration (analysed within 24 hours after dissolution)/measured concentration (analysed at different time after dissolution). All testing solutions were prepared in 2 mM DTPA, 2%HNO_3 and 1% HCl.

5.7 HFSE in Ten International Rock Standards

In order to assess the accuracy of the chelating technique, HFSE have been measured in a range of geological reference materials. These include basalts (BHVO-1, BE-N and GSR-3), granites (AC-E, GSR-1, MA-N and YG-1), iron-rich biotite (Mica-Fe),

andesite (AGV-1) and dolerite (WS-E). Most of the rock standards chosen for this study show relative high concentrations of HFSE, in particular Nb and Ta. For instance, as reported in previous studies (Govindaraju 1994; Thompson et al. 1999), Nb concentrations for MA-N, Mica-Fe and YG-1 are as high as 173, 270 and 48.78 $\mu g\ g^{-1}$ respectively, whereas Ta concentrations for MA-N, Mica-Fe and YG-1 are found to be 290, 35 and 95.55 $\mu g\ g^{-1}$. Considering a dilution factor of 1000 adopted through the sample preparation, these concentrations are generally above the levels at which Nb and Ta precipitate out of aqueous solutions reported by Münker (1998).

Using the techniques described and tested in **Chapter 3**, granites and iron-rich biotite were exclusively decomposed using 3 ml H_2SO_4 + 3 ml HF high pressure digestion method (PicoTrace), whereas basalts, andesite, and dolerite were prepared using either 3 ml H_2SO_4 + 3 ml HF or 3 ml $HClO_4$ + 3 ml HF high pressure digestion technique. For each individual rock standard between 2 and 8 separate digestions were carried out over a period of a few months. All of the final solutions were prepared in 2 mM DTPA + 2% HNO_3 + 1% HCl, spiked with 10 $\mu g\ g^{-1}$ ^{115}In and analysed (within 24 hours after the preparation of final solutions) by HR-ICP-MS.

Measured HFSE concentrations and precisions of the ten selected rock standards and comparisons with reference values are summarised in **Table 5.5**. In general, as highlighted in **Figure 5.7**, sixty individual analytical results of HFSE for the ten selected rock standards are plotted against their reference counterparts. A r^2 value of 0.9995 for a concentration range of sub $\mu g\ g^{-1}$ up to over 800 $\mu g\ g^{-1}$ (in rock) was observed, suggesting good linear relationship between the measured results and reference values.

In terms of precisions, it can be seen from **Table 5.5** that the majority (~67%) of RSD values are better than 5% except for the rock standard, WS-E and GSR-3, which do not have sufficient data for proper precision estimations. Only two RSD values of over 7% are 7.34% for Hf with AC-E and 7.01% for Th with MA-N.

The accuracy of the technique can also be assessed by the relative deviation between the measured and published values from various sources. As can be seen in **Table 5.5**, the relative deviations of HFSE for AC-E, BE-N and WS-E are all better than

±5%. Slightly high discrepancies, in terms of relative deviation, were found to be 9.38% and 6.64% for Nb and U with GSR-1, 6.94% for U with MA-N, 6.67% for Th with Mica-Fe, 5.78% for U with YG-1, -5.54% and –7.24% for Th and U with AGV-1, -6.20% for Zr with BHVO-1, and finally 6.08% for Th with GSR-3. The relative deviations for the rest are all within ±5%.

Some of the higher discrepancies might be related to the individual matrixes and slight HFSE heterogenous distributions of the rock standards studied. Insufficient random sample digestions and errors during the sample preparation could be another possible source of discrepancy despite the experience gained throughout the intensive investigation on decomposition of different types of geological materials in **Chapter 3** of this thesis. Also these high discrepancies might well reflect poor characterisation of rock standards which are newly released (such as WS-E in 1994 and YG-1 in 1999).

From the above discussion, it is clear that the proposed complexing technique, in conjunction with HR-ICP-MS, is capable of accurately measuring HFSE at different levels in geological samples. In other words, the high hydrolysis tendency of HFSE in aqueous solutions can be considerably improved by the proper addition of the chelate reagent, DTPA, which makes it possible for the accurate determination of HFSE in aqueous solutions.

Table 5.5. Measured results (μg g^{-1}) of HFSE for selected geological reference materials using DTPA. Reference values appeared in this table are quoted mainly from the compilation reported by Govindaraju (1994), together with those for YG-1, HBVO-1 and WS-E proposed by Thompson et al. (1999), Eggins et al. (1997) and Govindaraju et al. (1994) respectively.

Sample I.D.	Element	Measured result	Number of analyses	% RSD	Reference value	Deviation (%)
AC-E						
	Zr	791	6	2.92	780	1.46
	Nb	115	6	2.70	110	4.61
	Hf	28.1	6	7.34	27.9	0.86
	Ta	6.43	6	2.05	6.4	0.48
	Th	18.0	6	3.66	18.5	-2.72
	U	4.73	6	1.71	4.6	2.75
GSR-1						
	Zr	164	4	3.65	167	-1.80
	Nb	43.8	4	1.85	40	9.38
	Hf	6.23	4	1.40	6.3	-1.15
	Ta	7.51	4	1.57	7.2	4.31
	Th	56.1	4	2.13	54	3.85
	U	20.0	4	1.74	18.8	6.64
MA-N						
	Zr	24.4	4	5.24	25	-2.54
	Nb	174	4	6.63	173	0.86
	Hf	4.36	4	6.47	4.5	-3.11
	Ta	279	4	2.47	290	-3.68
	Th	1.47	4	7.01	1.4	4.68
	U	13.4	4	3.20	12.5	6.94
Mica-Fe						
	Zr	803	4	2.45	800	0.39
	Nb	280	4	5.05	270	3.61
	Hf	27.1	4	6.88	26	4.32
	Ta	33.5	4	6.62	35	-4.37
	Th	160	4	6.77	150	6.67
	U	83.1	4	3.26	80	3.90
YG-1						
(GeoPT3)	Zr	263	3	2.66	271.38	-3.21
	Nb	49.9	3	4.68	48.78	2.23
	Hf	8.17	3	4.45	8.074	1.17
	Ta	94.5	3	1.46	95.55	-1.09
	Th	23.5	3	4.11	22.45	4.63
	U	3.11	3	1.40	2.94	5.78

Table 5.5. Measured results (μg g^{-1}) of HFSE for selected geological reference materials using DTPA (continued). Reference values appeared in this table are quoted mainly from the compilation reported by Govindaraju (1994), together with those for YG-1, HBVO-1 and WS-E proposed by Thompson et al. (1999), Eggins et al. (1997) and Govindaraju et al. (1994) respectively.

Sample I.D.	Element	Measured result	Number of analyses	% RSD	Reference value	Deviation (%)
AGV-1						
	Zr	230	4	2.50	227	1.37
	Nb	14.8	4	4.47	15	-1.49
	Hf	5.02	4	5.24	5.1	-1.51
	Ta	0.91	4	4.68	0.9	1.16
	Th	6.14	4	2.94	6.5	-5.54
	U	1.78	4	3.34	1.92	-7.24
BHVO-1						
	Zr	169	6	3.53	180	-6.20
	Nb	18.9	6	4.37	19.5	-3.13
	Hf	4.34	6	3.60	4.30	0.85
	Ta	1.25	6	7.02	1.20	4.08
	Th	1.29	6	3.64	1.26	2.62
	U	0.426	6	5.78	0.42	1.37
BE-N						
	Zr	261	8	2.65	260	0.21
	Nb	107	8	2.62	105	1.83
	Hf	5.57	8	6.46	5.6	-0.52
	Ta	5.74	8	6.39	5.7	0.78
	Th	10 6	8	5.47	10.4	1.45
	U	2.49	8	6.96	2.4	3.60
WS-E						
	Zr	199	2		195	2.17
	Nb	18.3	2		18	1.41
	Hf	5.41	2		5.3	2.14
	Ta	1.15	2		1.16	-1.08
	Th	3.13	2		3	4.20
	U	0.450	2		0.45	0.00
GSR-3						
	Zr	289	2		277	4.38
	Nb	71.3	2		68	4.87
	Hf	6.21	2		6.5	-4.45
	Ta	4.33	2		4.3	0.70
	Th	6.36	2		6	6.08
	U	1.45	2		1.4	3.61

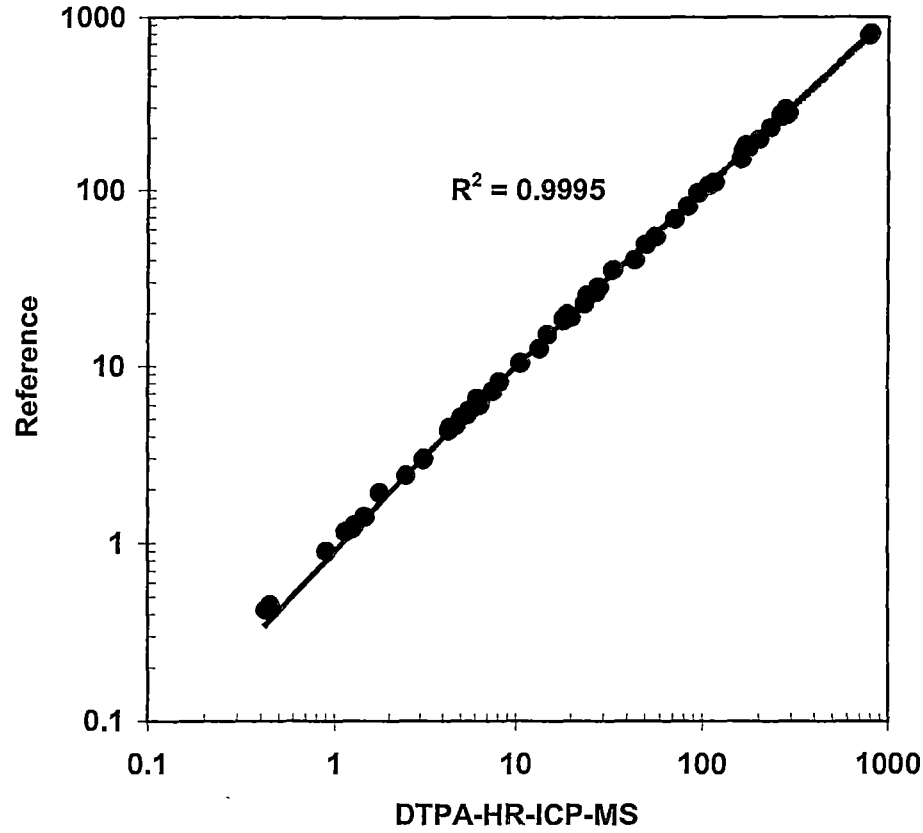

Figure 5.7. HFSE correlation plot between the measured results and reference values for the ten selected geological reference materials. Concentrations are given in $\mu g\ g^{-1}$. The reference values are quoted from Govindaraju (1994), Govindaraju et al. (1994), Eggins et al. (1997) and Thompson et al. (1999) respectively.

Chapter 6

COMPARASION OF THREE ICP-MS-BASED ANALYTICAL TECHNIQUES AND APPLICATION TO EVALUATING ELEMENT INCOMPATIBILITY DURING MANTLE MELTING

6.1 Introduction

So far, measurement of geological samples exclusively using solution-based ICP-MS has been described. However, as an alternative, trace element concentrations in geological materials can also be determined by laser ablation (LA) ICP-MS. Although the concept of LA-ICP-MS, based on the introduction of laser ablation sampling of geological samples, was initially mentioned in 1980s (Data and Gray 1983b; Gray 1985), it is still a relatively new analytical technique.

In comparison with solution ICP-MS, LA-ICP-MS allows in situ microanalysis of solid samples because of the small spatial resolution (10-100 um). The analysis time needed for each spot analysis is generally less than 5 minutes. In addition, matrix effects are often trivial for a wide range of target materials, allowing straightforward calibration of the analysis. These features make LA-ICP-MS another efficient analytical tool for the determination of trace element compositions in geological materials.

As powerful analytical tools, both solution and laser ablation ICP-MS techniques have been applied to diverse geochemical problems (e.g. Niu and Batiza 1997; Münker 1998; Eggins et al. 1998; Kamenetsky et al. 2000). In general, LA-ICP-MS allows accurate in situ microanalysis, and has the ability to avoid analysing small crystals in target glass, or altered parts of glasses or minerals (Norman et al. 1998), whereas solution ICP-MS can provide reliable bulk trace element data. However,

when glass samples are measured by the two different analytical techniques, discrepancy in trace element concentrations might occur due to the presence of (a) microphenocrysts of olivine, clinopyroxene, spinel, plagioclase and other liquidus minerals, (b) vesicles filled with fluid/gas and products of alteration, and (c) areas of glass recrystallisation.

For the purpose of comparison of these analytical techniques in this project, a set of pillow basalt glasses and hyaloclastites from Macquarie Island were analysed for trace elements using each of LA-ICP-MS, solution HR-ICP-MS and quadrupole ICP-MS techniques.

The reasons to choose the samples from Macquarie Island for this study are:

- there are extensive collections of well-studied Macquarie Island glasses at the University of Tasmania;

- detailed information about their geochemistry is available from a recent publication by Kamenetsky et al. (2000);

- they show a wide range of major and trace element abundances, allowing work at different concentration levels;

- the wide compositional range (e.g., in $(La/Yb)_n$ – chondrite normalised (Boynton 1994) La/Yb ratios) shown by primitive, relatively high-Mg# glasses, coupled with availability of a suite of lower-Mg# fractionated lavas with relatively constant (3-4) $(La/Yb)_n$ ratios, allows comparison of element behaviour due to source- or partial melting effects, with element behaviour due solely to fractionation.

In the first part of this chapter (6.1-6.4), an assessment of the analytical data obtained by the three different methods is presented. In the second part (6.5-6.8), an assessment is made of element compatibility during partial melting of upper mantle peridotite to produce broadly MORB-type magmas, and during fractionation of these magmas. Comparison is made with the frequently cited compatibility order proposed

by Sun and McDonough (1989). Attention is particularly focussed on the behaviour of the chalcophile elements (Cu, Pb and Zn), and of the economically important metals Sn, Mo and Sb.

For this study, seventeen basaltic glass samples from Macquarie Island have been measured for 41 trace element concentrations using the three different methods. The ICP-MS instruments used in this study were a Fisons PQ2 STE ICPMS (Britain) coupled with an ArF (193 nm) EXCIMER laser at the Australian National University, a magnetic sector Finnigan MAT Element HR-ICP-MS (Germany), and a quadrupole HP 4500 plus ICP-MS (Japan) at the University of Tasmania.

6.2 Description of Samples

All basaltic glasses used in this study are from Macquarie Island, an exposed slice of oceanic crust in the Antarctic southwest Pacific Ocean. Detailed localities and petrographic information for glass samples used in this study are as reported by Kamenetsky et al. (2000). All glasses analysed are perfectly fresh, and contain up to 5 modal% of olivine microphenocrysts which were easily avoided during hand-picking under a binocular microscope of pure glassy chips for solution ICP-MS analysis.

6.3 Analytical Techniques

6.3.1 Solution ICP-MS

Fresh chips were cleaned using acetone and dilute HCl, and then ground in an agate mortar with a pestle. The powdered samples (100 mg) were digested using 2 ml HF and 0.5 ml HNO_3 in Savillex Teflon beakers (further details of this sample preparation method can be found in Chapter 3 of this thesis). After digestion, each solution was spiked with Ge, In, Tm and Bi as internal standards for the following ICP-MS measurement.

Sample solutions were analysed for trace element concentrations by both quadrupole (HP 4500) and high resolution (Finnigan MAT ELEMENT) ICP-mass spectrometers.

The isotopes, internal standards and resolutions used in the trace element analysis are listed in **Table 6.1.** Further operational details concerning the two solution ICP-MS techniques can be found in Chapter 2 (high resolution instrument) and Chapter 6 (quadrupole instrument) respectively. Finally, trace element concentrations determined by both solution ICP-MS techniques were corrected against the compiled data of a well-characterised international rock reference material, BHVO-1 (Eggins et al. 1997) prior to any data assessment and geochemical applications.

6.3.2 Laser Ablation ICP-MS

For the purpose of comparison, concentrations of trace elements in these same glasses were also measured by LA-ICP-MS at the Research School of Earth Sciences, Australian National University, Canberra, using an ArF (193nm) EXCIMER laser, a Fisons PQ2 STE ICPMS, and custom-built sample introduction system (Eggins et al. 1998). These data are reported by Kamenetsky et al. (2000). The argon flow rates for plasma gas and coolant gas were 14 and 0.7 l min^{-1}, whereas the carrier gas was a mixture of helium and argon with flow rates of 0.3 and 0.9 l min^{-1} respectively. Analyses were performed using a spot size of 200 μm and a laser pulse rate of 5 repetitions per second. The total analysis time for each sample was 130 seconds, comprising a 60 seconds for background measurement and 60 seconds for analysis with laser beam on. 60 replicate measurements were made for each isotope. Data reduction was performed using background subtracted count rates and the methodology outlined in Longerich et al. (1996). Trace element concentrations were measured using the mean background intensities of each isotope and ratioing these corrected intensities to that of the internal standard isotope for each analytical sweep. An instrumental drift correction (external calibration) was also performed by applying a linear correction to analysed sample intensities between repeat measurements of the glass reference material NIST 612. ^{43}Ca was employed as the internal standard isotope to compensate for any instrumental drift through an analytical sequence, based on CaO results measured by electron microprobe prior to LA-ICP-MS analysis. In this study, analytical precision (RSD) of the measurements was found to be generally from 1 to 5% for most elements.

Table 6.1. Analysed elements, isotopes, abundances, internal standards and resolutions

Element	Isotope	Abundance (%)	Internal standard (element & mass)	Resolutions (m/Δm) for HR-ICP-MS
Li	7	92.5	Ge (73)	
Be	9	100	Ge (73)	
Sc	45	100	Ge (73)	3000
Ti	49	5.5	Ge (73)	3000
V	51	99.75	Ge (73)	3000
Cr	53	9.501	Ge (73)	3000
Co	59	100	Ge (73)	3000
Ni	60	26.22	Ge (73)	3000
Cu	65	30.83	Ge (73)	3000
Zn	66	27 9	Ge (73)	3000
Ga	71	39.89	Ge (73)	3000
Rb	85	72 17	Ge (73)	300
Sr	88	82.58	Ge (73)	300
Y	89	100	Ge (73)	300
Zr	90	51 45	Ge (73)	300
Nb	93	100	Ge (73)	300
Mo	95	15.92	Ge (73)	300
Cd	111	12.8	In (115)	300
Sn	118	24.23	In (115)	300
Sb	121	57.36	In (115)	300
Cs	133	100	In (115)	300
Ba	137	11.23	In (115)	300
La	139	99.91	In (115)	300
Ce	140	88 48	In (115)	300
Pr	141	100	In (115)	300
Nd	146	17 19	In (115)	300
Sm	147	15	Tm (169)	300
Eu	151	47.8	Tm (169)	300
Gd	157	15.65	Tm (169)	300
Tb	159	100	Tm (169)	300
Dy	163	24.9	Tm (169)	300
Ho	165	100	Tm (169)	300
Er	167	22.95	Tm (169)	300
Yb	172	21.9	Tm (169)	300
Lu	175	97.41	Tm (169)	300
Hf	178	27.30	Tm (169)	300
Ta	181	99.99	Tm (169)	300
Tl	205	70.48	Tm (169)	300
Pb	208	52.4	Bi (209)	300
Th	232	100	Bi (209)	300
U	238	99.27	Bi (209)	300

6.3.3 Electron Microprobe

A Cameca SX50 electron microprobe (Central Science Laboratory, University of Tasmania) was used to perform major element analysis of the basaltic glasses, which provide internal standard data (^{43}Ca) for the subsequent LA-ICP-MS analysis. Basaltic glass VG-2 was used as the calibration standard. Concentrations reported for each glass sample are the mean value of at least 15 analyses. Glasses were found to have very homogeneous compositions (low standard deviation values), and analytical precisions for determination of each of the major element oxides are as following:

SiO_2 and Al_2O_3:	0.7-0.9%
FeO, MgO and CaO:	1.5-2.2%
TiO_2, Na_2O and K_2O:	2.7-5%
P_2O_5:	12%

6.4 Assessment of Trace Element Compositions

Here, I compare data for the same glass suite obtained via the three different analytical methods described above.

Figures 6.1 and 6.2 show the representative comparison of trace element concentrations for six glass samples (namely: 60701, G855, G882b, 40428, G465 and G955b which have complete trace element results using all three ICP-MS-based analytical techniques). These average values are the mean results of laser ablation (LA), quadrupole (HP 4500) and high resolution (HR) ICP-MS methods. Clearly, there is good agreement among the three sets of analytical results for Li, Sc to V, Ba to Ta and Pb to U. Discrepancies are generally <5% relative to the average results. The variation for Cr, Co, Ni, Cu, Zn, Ga, Rb, Sr, Y, Zr, Nb and Mo was found to be moderate and generally within 10%.

In general, the discrepancy for Be, Sn, Sb and Cs was found to be mainly within ~10%; however a variation of ~20% can also be seen in some of the glass samples studied due to the very low abundance (<1 $\mu g\ g^{-1}$ in solid and <1 $ng\ g^{-1}$ in solution

considering a dilution factor of 1000 for the solution ICP-MS methods used in this study) of these elements in a number of glasses.

In comparison with the average results, considerable variation for Cd and Tl concentrations was found in almost all of analysed glasses. The highest variations for Cd and Tl were found to be 87% and 91% respectively for the concentration range measured (0.51 to 0.119 ppm for Cd and 0.026 to 0.200 ppm for Tl) in the samples studied. This large discrepancy is most likely due to either the lack of reliable Cd and Tl data in NIST 612 for laser sampling method, or the low concentration of Cd and Tl in these samples. Therefore, the analytical results for Cd and Tl in this study were not used for the following geochemical applications.

In order to further demonstrate the reliability of the analytical data obtained, correlation plots (**Figure 6.3**) between elements with similar incompatibility (Sun and McDonough 1989, i.e. Rb-Ba, Nb-Ta, Zr-Hf and Ho-Y) show excellent correlations between these pairs of elements. The r^2 values for seventeen individual analyses in this study were 0.98, 0.99, 0.97 and 0.97 for Rb-Ba, Nb-Ta, Zr-Hf and Ho-Y respectively, suggesting accurate analytical results.

Finally, as an additional assessment of the analytical results obtained in this study, the mean concentrations of Ti measured by LA-, HP-, & HR- ICP-MS and concentrations measured by electron microprobe was also investigated (**Figure 6.4**). The r^2 value for seventeen individual determinations was found to be 0.97, further indicating the reliable results for Ti in glass samples.

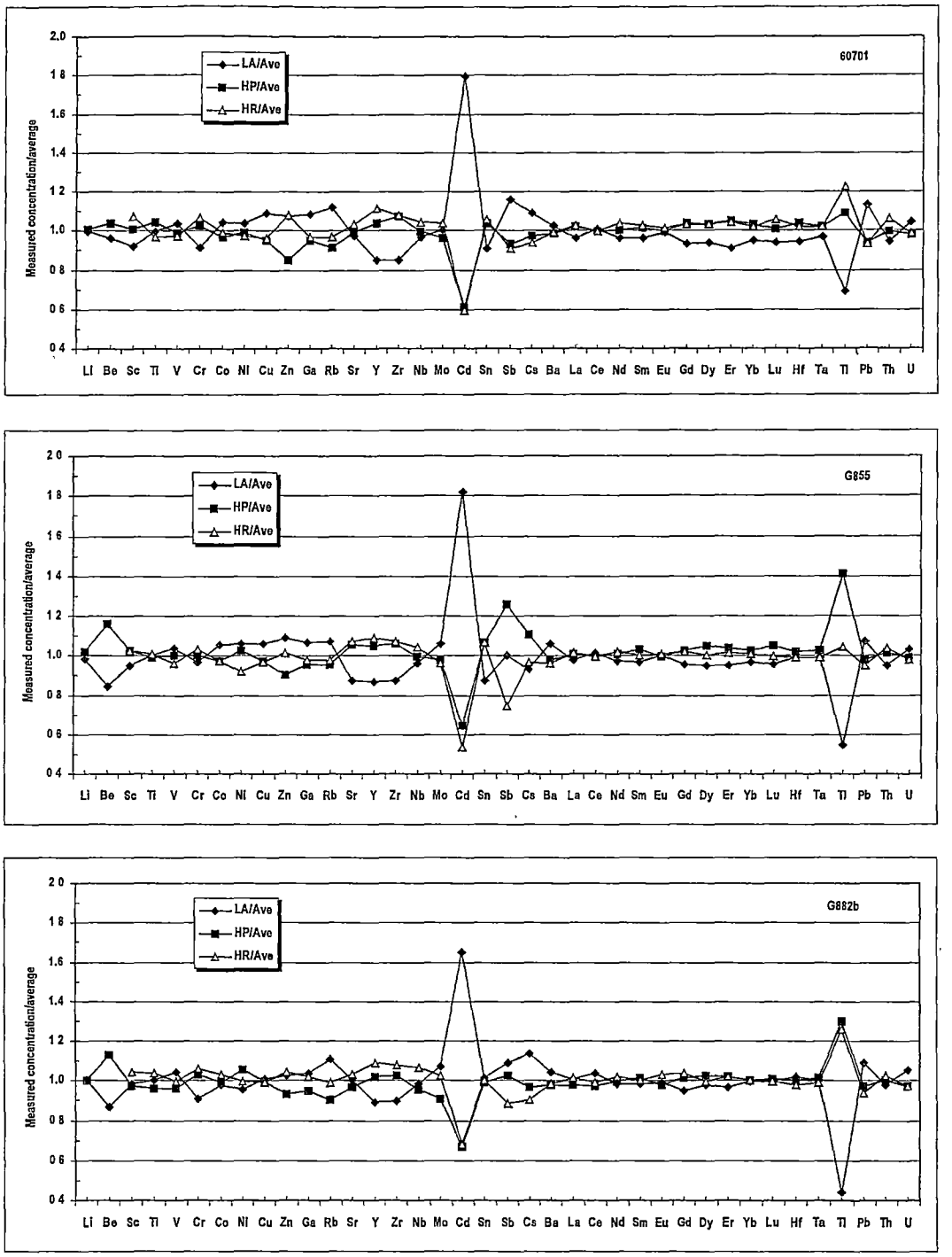

Figure 6.1. Comparison of trace element concentrations for glass samples, 60701, G855 and G882b using laser ablation (LA, solid sampling)-, quadrupole (HP 4500, solution sampling)- and high resolution (HR, solution sampling)- ICP-MS methods. Results obtained by different methods were normalised to average values.

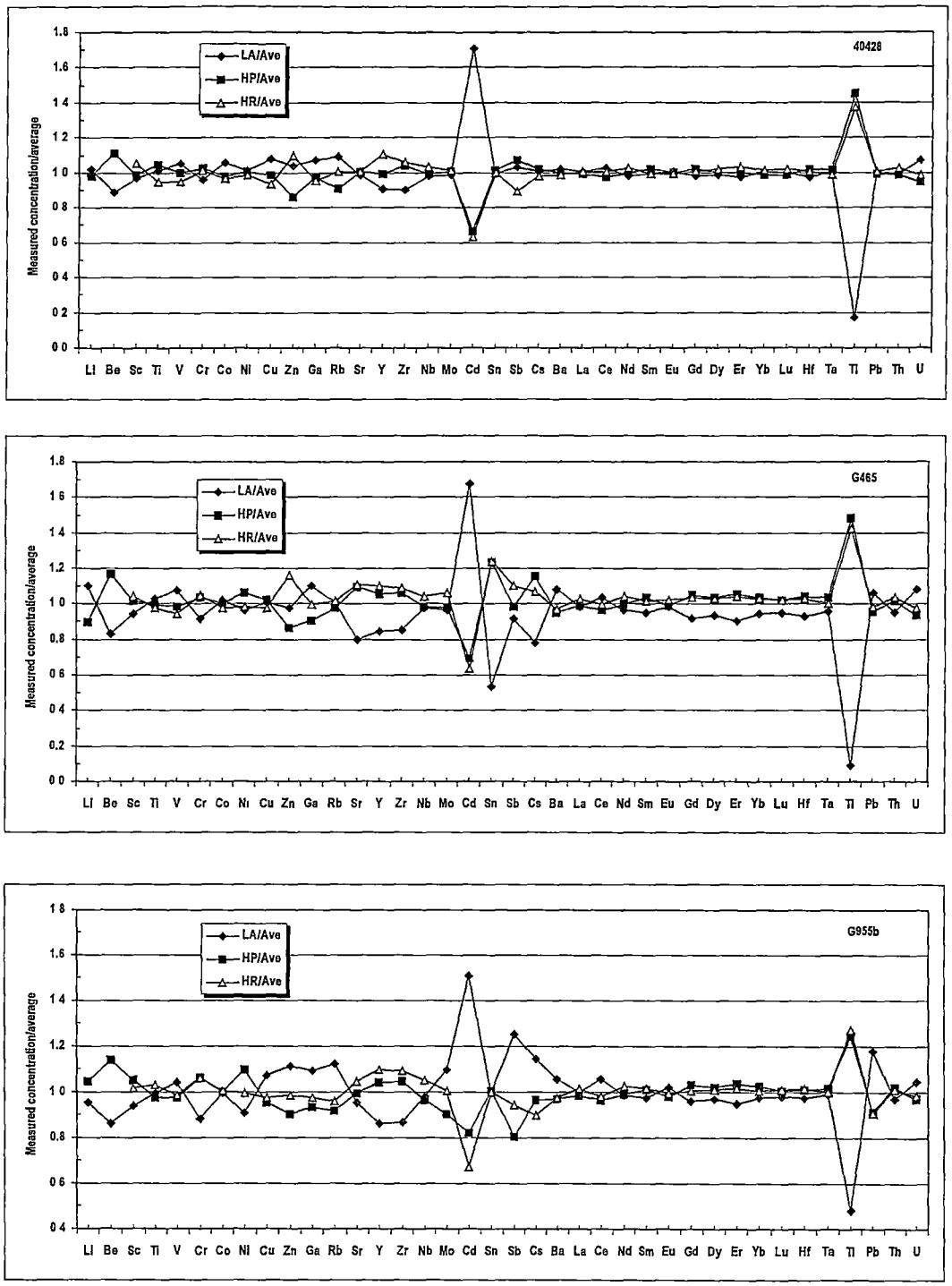

Figure 6.2. Comparison of trace element concentrations for glass samples, 40428, G465 and G955b using laser ablation (LA, solid sampling)-, quadrupole (HP 4500, solution sampling)- and high resolution (HR, solution sampling)- ICP-MS methods. Results obtained by different methods were normalised to average values.

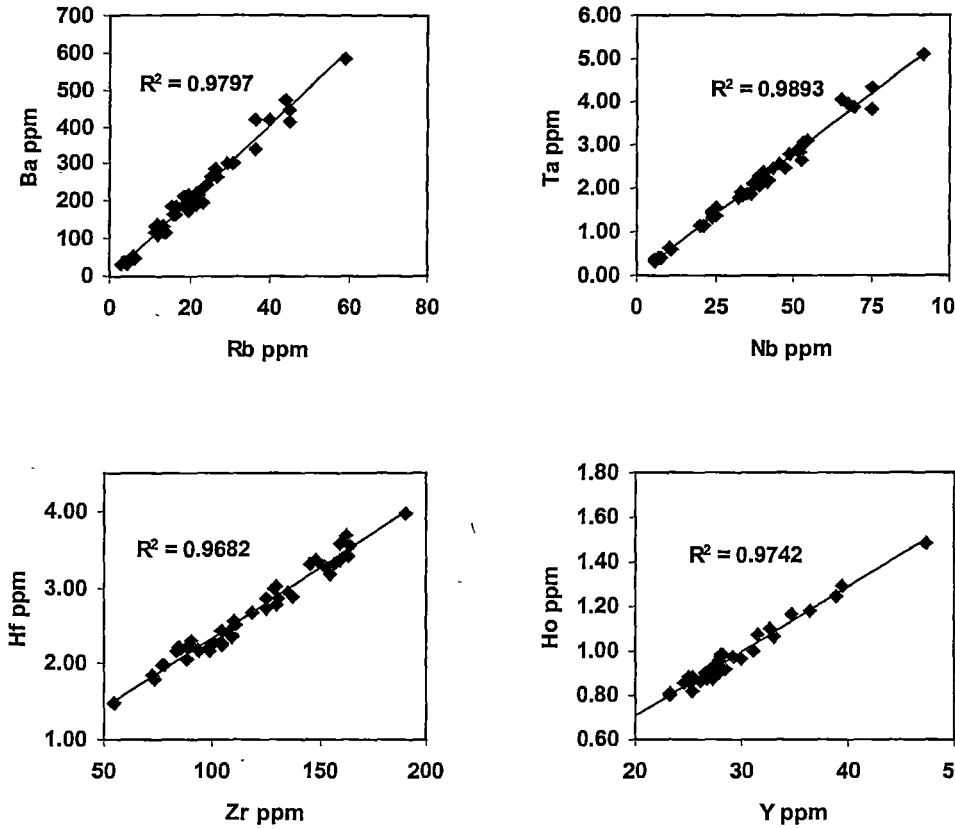

Figure 6.3. Correlation between measured concentrations for elements with same or very similar incompatibility (Sun and McDonough 1989). Data used for plots were the values of LA-, HP 4500 (quadrupole)- and HR-ICP-MS methods.

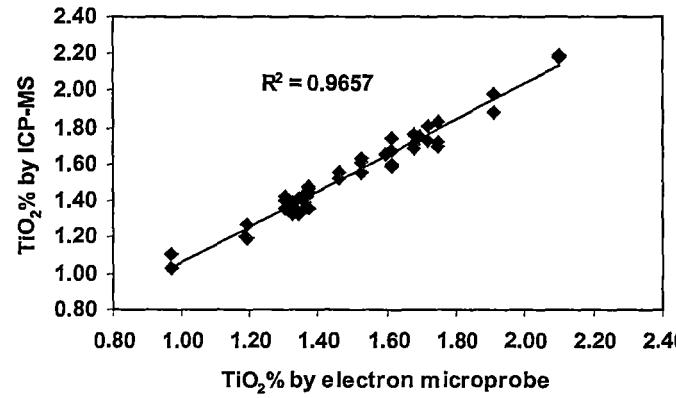

Figure 6.4. Correlation between TiO_2 concentrations (wt%) measured by both ICP-MS (including LA-, HP 4500 (quadrupole)- and HR-ICP-MS methods) and electron microprobe

6.5 Abundance Range of Minor and Trace Elements

The major and average trace element concentrations for the basaltic samples used in this study are summarised in two separate compositional groups (Tables 6.2 to 6.5), primitive glasses, and fractionated glasses. In general, trace element values are the mean results of LA-ICP-MS, solution HR-ICP-MS and quadrupole ICP-MS except that the concentrations for Li and Be are the mean results of LA-ICP-MS and solution quadrupole ICP-MS due to the lack of HR-ICP-MS data, the concentrations for Pr, Tb and Ho are the mean results of solution HR-ICP-MS and quadrupole ICP-MS due to no data from LA-ICP-MS, and the concentrations of Cr, Co, Ni, Cu, Mo, Cd, Sn and Sn in glass G565a are the mean results of solution HR-ICP-MS and quadrupole ICP-MS due to their LA-ICP-MS results are not available.

Analysed Macquarie Island basaltic glasses include a subset of relative unfractionated, primitive glasses with olivine phenocrysts having Fo $[Mg^{olivine}/(Mg^{olivine}+Fe^{olivine})]$ >85.8, and glass Mg# $[Mg/(Mg+Fe^{2+})$, $Fe^{2+}=0.9\ Fe^{total}]$ >0.63, and a more fractionated set with lower Fo ($Fo_{83.5-88.3}$, Kamenetsky et al. 2000) phenocrysts and Mg# values extending from 0.65-0.54 (**Figure 6.5**). The fractionated glasses show typically tholeiitic trends of increasing FeO*, TiO_2 and V with increasing fractionation (decreasing Mg#), and a concomitant decrease in MgO, Ni, and Cr. At the same time, they show (**Figure 6.6**) a range of $(La/Yb)_n$ values (1-8) that precludes them from being comagmatic, and demands derivation from diverse parental magmas.

The primitive glasses show a range of MgO values that extend to just <6% (**Figure 6.5**). However, this primitive subset shows a pronounced *decrease* of FeO* with decreasing MgO, so that even the lowest MgO glass still has a Mg# ~0.60. Since FeO* contents of these primitive glasses are very closely correlated with $(La/Yb)_n$ (correlation coefficient 0.85; **Figure 6.6**), and since $(La/Yb)_n$ is itself well correlated with Sr and Pb isotopic values (Kamenetsky et al. 2000), the trend of decreasing FeO* with increasing $(La/Yb)_n$ has been attributed to partial melting of a MORB source upper mantle modified by ingress of a small volume enriched component derived from or characteristic of a HIMU ocean island basalt (OIB)-type source. A geochemically suitable source for this enriched component exists nearby, in the

Balleny plume, the trace of which extends from just east of Tasmania to the current location in the Balleny Islands just off the Ross Sea coast of Antarctica.

Table 6.2. Major element concentrations (wt%) for "near-primitive" glass samples (Group I) from Macquarie Island

Sample I.D.	47979	25637	60701	GG53a	G855	GG256	G882b	47963
SiO_2	49.56	49.30	49.09	49.34	48.31	48.05	47.94	48.18
TiO_2	0.97	1.19	1.37	1.33	1.38	1.46	1.61	1.91
Al_2O_3	17.09	17.25	16.99	16.86	17.77	18.03	17.96	18.17
FeO	8.06	7.50	7.68	7.29	7.55	7.18	7.03	6.81
MnO	0.14	0.17	0.12	0.12	0.14	0.07	0.09	0.08
MgO	8.75	8.36	8.02	7.56	7.80	7.34	6.59	5.90
CaO	12.82	12.69	12.63	12.31	11.93	11.24	11.25	10.85
Na_2O	2.37	2.58	2.72	3.04	2.99	3 53	3.57	4.24
K_2O	0.14	0.42	0.59	0.70	0.75	0.88	1.29	1.76
P_2O_5	0.08	0 21	0.23	0.24	0.28	0.33	0.47	0.66
S	0.076	0.082	0.07	0.074	0.083	0.075	0.073	0.078

n.d. = not determined

Table 6.3. Major element concentrations (wt%) for "fractionated" glass samples (Group II) from Macquarie Island

Sample I.D.	G452a	HP135	38287	G465	40428	G955b	25601	G937	G565a
SiO_2	49.96	50.58	49.74	49.04	50.40	49.90	49.16	51.14	49.68
TiO_2	1.35	1.72	2.10	1.36	1.68	1.60	1.75	1.53	1.31
Al_2O_3	15.49	15.03	15.97	17.02	15.89	16.39	17.52	16.49	16.24
FeO	9.47	10.17	9.59	8.22	9.10	8.54	7.55	7.57	8.53
MnO	0.13	0.18	0.17	0.12	0.16	0.17	0.15	0.14	0.12
MgO	8.13	6.83	6.68	8.51	6.84	7.60	6.77	5.65	8.09
CaO	11.59	11.12	10.18	11.53	10.84	11.19	10.02	10.59	11.50
Na_2O	2.60	2.54	3.37	2 79	3.10	3.18	3.70	3.46	2.66
K_2O	0.12	0.20	0.66	0.42	0.58	0.58	1.10	1.11	0.42
P_2O_5	0.13	0.17	0.35	0.24	0.29	0.27	0.40	0.49	0.23
S	0.104	0.112	0.107	0.082	0.089	0.091	0.075	0.080	0.088

Table 6.4. Trace element concentrations (ppm) for "near-primitive" glass samples (Group I) from Macquarie Island

Sample I.D.	47979	25637	60701	GG53a	G855	GG256	G882b	47963
Li	5.51	4.71	5.06	5.12	5.30	5.29	4.80	5.01
Be	0.450	0.588	0.789	0.820	0.874	1.04	1 33	1.64
Sc	36.7	33.6	35.0	34.0	31.1	28.9	27.7	23.7
Ti	6401	7345	8216	8279	8794	9240	10417	10816
V	216	220	224	213	197	188	179	163
Cr	380	320	321	349	232	196	170	134
Co	48.0	40.4	40.5	36.3	38.2	35.5	31.4	27.9
Ni	176	148	123	107	117	100	82.1	65.4
Cu	107	82.2	80.4	76.4	73.3	70.2	64.3	53.5
Zn	64.9	58.5	64.7	59.7	60.9	59.4	56.2	53.0
Ga	16.0	15.0	15.3	14.3	15.4	15.5	15.6	15.9
Rb	3.89	12.3	17.4	20.6	22.8	28.6	40.5	51.9
Sr	164	250	298	316	385	392	554	642
Y	22.1	22.7	24.0	24.6	25.3	25.1	25.0	22.9
Zr	64.0	86.7	91.4	100	104	117	144	161
Nb	7.62	24.7	33.7	40.5	45.5	53.6	70.8	83.4
Mo	0.339	0.807	1.18	1.31	1.44	1.91	2.35	3.21
Cd	0.084	0.086	0.087	0.081	0.095	0.089	0.095	0.119
Sn	0.983	1.55	1.37	1.25	1.55	1.52	1.69	1.97
Sb	0.016	0.040	0.044	0.051	0.050	0.065	0.069	0.091
Cs	0.043	0.130	0.185	0.222	0.272	0.296	0.455	0.621
Ba	37.6	135	189	221	228	296	427	568
La	4.67	13.9	17.2	20.3	22.0	26.7	35.5	46.5
Ce	11.2	27.5	33.6	37.9	41.2	50.0	64.1	84.3
Pr	1.59	3.38	4.03	4.49	4.83	*5.57*	7.37	9.15
Nd	7.63	13.5	15.9	17.7	18.4	21.1	27.2	33.3
Sm	2.29	3.29	3.61	3.82	3.86	4.33	5.12	6.01
Eu	0.923	1.18	1.27	1.32	1.35	1.52	1.74	2.00
Gd	2.96	3.73	3.87	4.02	4.05	4.44	4.84	5.43
Tb	0.554	0.646	0.667	0.667	0.690	0.746	0.741	0.828
Dy	3.46	3.94	4.00	4.07	4.12	4.30	4.29	4.44
Ho	0.772	0.881	0.877	0.861	0.895	0.928	0.878	0.896
Er	2.14	2.41	2.39	2.45	2.45	2.53	2.37	2.40
Yb	2.03	2.27	2.23	2.29	2.31	2.39	2.17	2.13
Lu	0.303	0.335	0.329	0 345	0.354	0.362	0.321	0.316
Hf	1.52	2.07	2.11	2.31	2.33	2.73	3.05	3.67
Ta	0.417	1.46	1.84	2.27	2.48	3.02	3.89	4.99
Tl	0.043	0.027	0.030	0.073	0.057	0.106	0.082	0.082
Pb	0.316	0.932	0 995	1.23	1.29	1.58	2.04	2.66
Th	0.505	1.88	2.38	3.10	3.35	4.08	5.39	7.12
U	0.148	0.467	0.624	0.749	0.830	1.06	1.32	1.88

Table 6.5. Trace element concentrations (ppm) for "fractionated" glass samples (Group II) from Macquarie Island

Sample I.D.	G452a	HP135	38287	G465	40428	G955b	25601	G937	G565a
Li	2.90	2.61	6.90	4.95	6.70	6.19	6.35	6.32	5.13
Be	0.408	0.638	1.16	0.654	1.02	0.879	1.35	1.16	0.629
Sc	36.8	38.8	33.7	30.1	35.0	32.5	26.5	32.3	33.2
Ti	8144	10542	13096	8358	10136	10162	10197	9582	8367
V	264	310	303	217	270	249	195	226	227
Cr	330	246	230	332	279	314	264	221	280
Co	43.0	42.1	39.5	40.5	38.0	40.1	36.8	34.9	39.6
Ni	144	87.7	108	171	99.0	134	147	75.1	128
Cu	69.4	68.9	57 4	63.6	69.6	69.9	53.6	73.6	64.7
Zn	77.0	92.1	95 0	65.2	87.0	72.3	69.1	67.2	65.3
Ga	16.3	17.4	19.8	15.6	17.4	16.3	17.5	15.8	15.5
Rb	4.18	6.25	21.5	13.8	21.3	17.4	31.7	32.5	12.0
Sr	133	155	233	299	218	264	423	358	275
Y	30.2	37.0	43.1	26.5	35.1	30.1	27.0	28.8	26.3
Zr	82.1	118	175	98.7	143	125	155	143	96.9
Nb	5.98	10.7	40.3	24.4	38.1	34.3	52.4	55.6	20.5
Mo	0.258	0.476	1.52	0.828	1.14	1.22	2.22	2.02	0.773
Cd	0.085	0.101	0.130	0.089	0.115	0.080	0.106	0.108	0.051
Sn	1.28	1.50	2.02	2.19	1.76	1.56	1.86	1.94	1.53
Sb	0.018	0.034	0.058	0.027	0.054	0.043	0.066	0.067	0.027
Cs	0.057	0.251	0.229	0.162	0.239	0.190	0.357	0.363	0.130
Ba	32.2	50.9	189	123	196	168	315	314	116
La	4.33	7.40	20.9	12.8	19.6	17.0	27.9	28.9	11.6
Ce	11.7	18.3	43.8	26.8	39.7	34.7	52.5	53.8	24.5
Pr	1.87	2.77	5.50	3.44	5.01	4.29	5.97	5.41	3.22
Nd	9.60	13.4	23.1	14.2	20.7	17.7	23.3	23.3	13.7
Sm	3.14	4.02	5.66	3.53	4.86	4.20	4.89	4.78	3.39
Eu	1.16	1.43	1.85	1.29	1.60	1.45	1.69	1.62	1.21
Gd	4.05	5.07	6.34	4.01	5.38	4.62	4.94	4.93	3.90
Tb	0.760	0.926	1.11	0.726	0.919	0.806	0.777	0.746	0.690
Dy	4.92	6.04	6.86	4.37	5.71	4.92	4.66	4.87	4.25
Ho	1 10	1.31	1.48	0.977	1.26	1.07	0.965	0.971	0.919
Er	3.10	3.80	4.23	2.65	3.53	2.97	2.64	2.88	2.60
Yb	2.94	3.58	3.95	2.50	3.36	2.77	2.42	2.70	2.41
Lu	0.438	0.536	0.600	0.376	0.504	0.414	0.359	0.405	0.359
Hf	2.19	2.92	3.92	2.34	3.26	2.83	3.40	3.25	2.26
Ta	0.346	0.621	2.21	1.37	2.07	1.86	2.91	3.16	1.13
Tl	0.104	0.026	0.052	0.200	0.188	0.054	0.059	0.058	0.104
Pb	0.501	0.758	1.40	0.92	1.40	1.08	1.94	1.92	0.859
Th	0.446	0.830	2.95	1.72	2.96	2.48	4.07	4.88	1.48
U	0.118	0.216	0.758	0.468	0.694	0.667	1.09	1.20	0.385

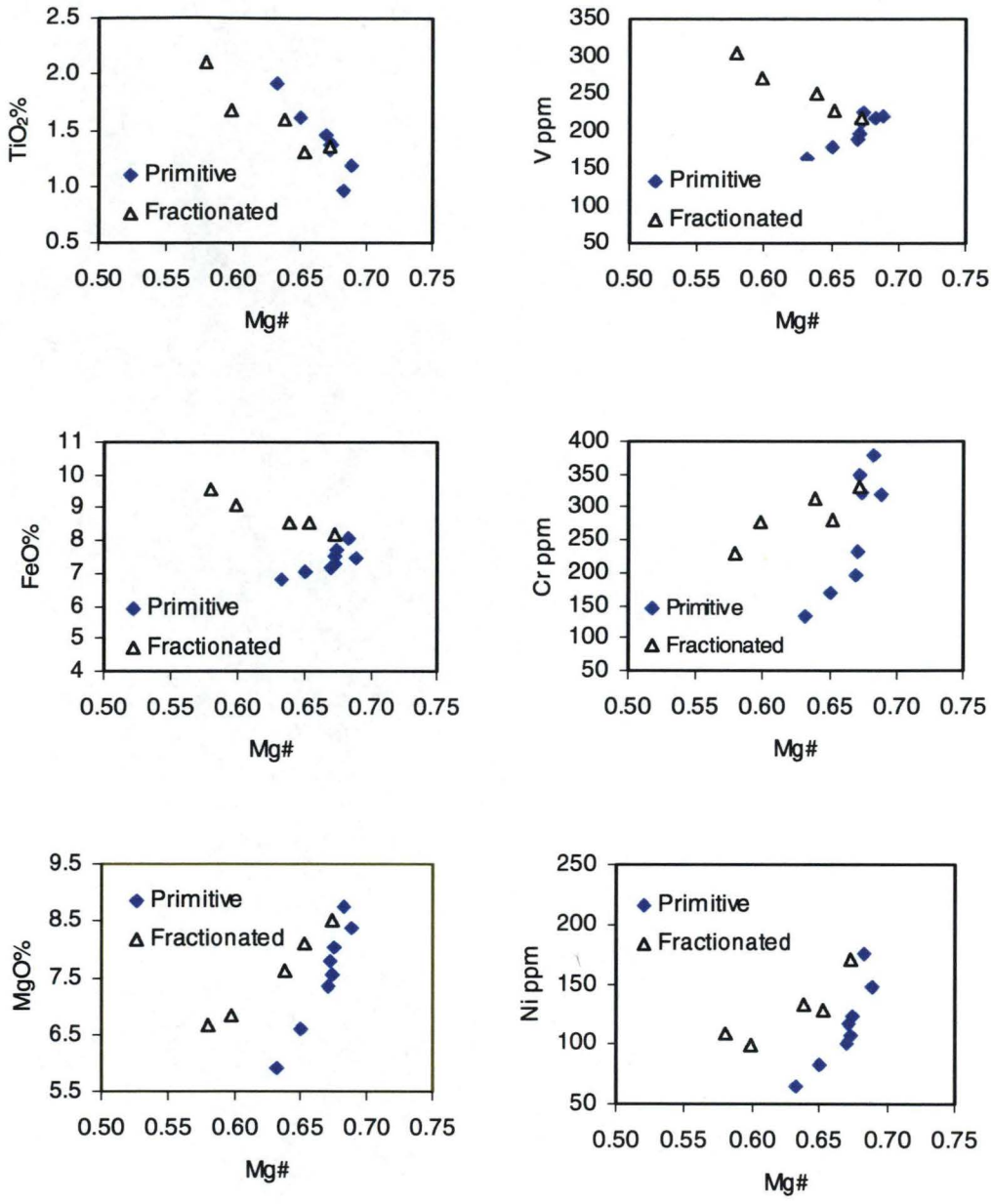

Figure 6.5. Relationship between Mg# and major & trace elements (TiO_2, FeO, MgO, V, Cr and Ni) in Macquarie Island primitive glasses (Group I) and fractionated glasses (Group II, $(La/Yb)_n$ = 3-4)

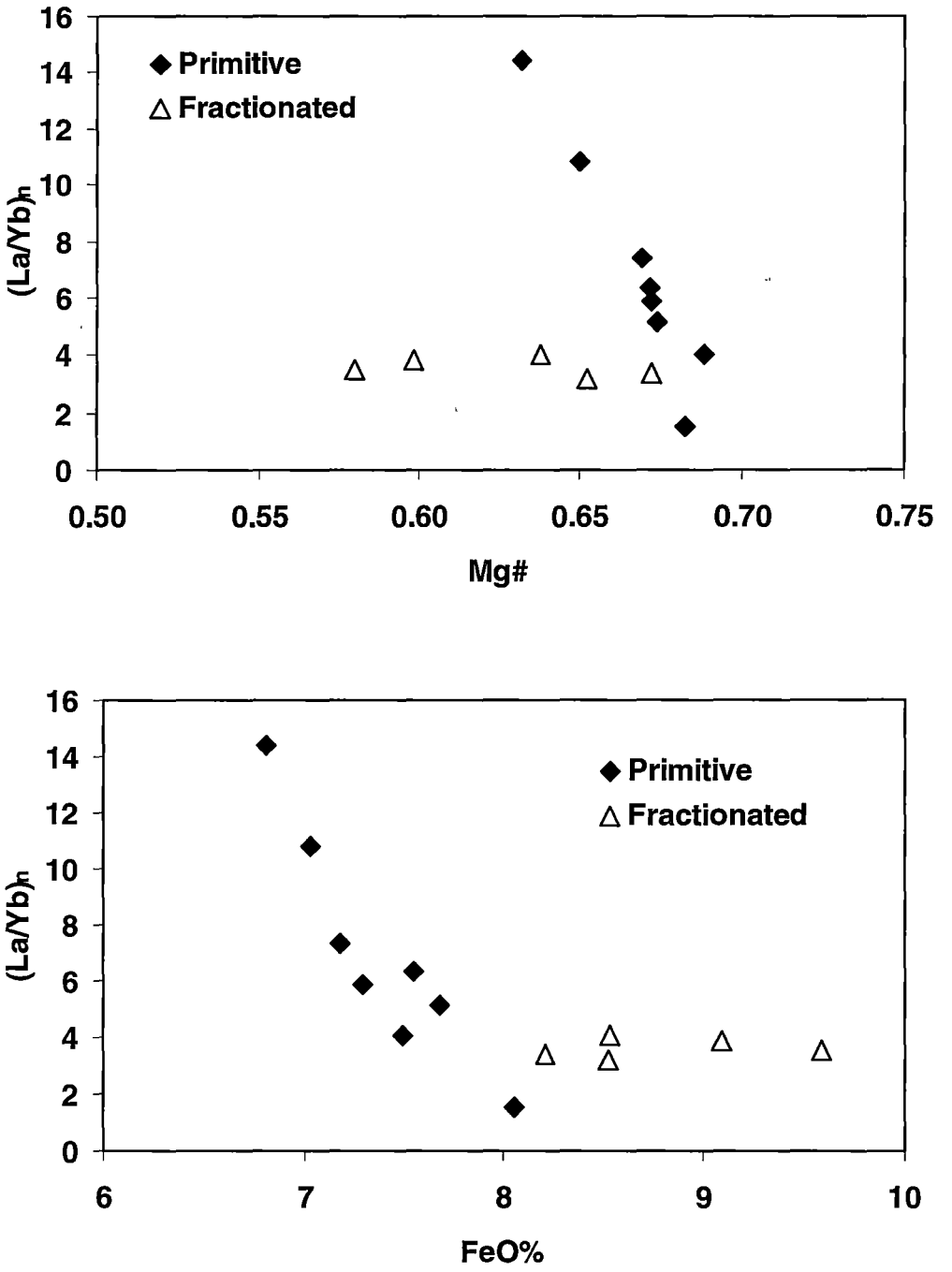

Figure 6.6. Relationship between $(La/Yb)_n$ and Mg# & FeO% in Macquarie Island primitive glasses (Group I) and fractionated glasses (Group II, $(La/Yb)_n$ = 3 - 4)

Despite the highest $(La/Yb)_n$ basaltic glasses from Macquarie Island having MORB-normalised extended element variation plots essentially identical (see later) to the Balleny Island OIB (Lanyon et al. 1993; Lanyon 1994), their major element compositions are strikingly different from typical OIB, with Al_2O_3 contents being ~5wt% higher than OIB, and FeO* contents about 5wt% lower. This clearly precludes magma mixing between MORB and a Balleny OIB as having produced the Macquarie Island glass suite. Low FeO* contents in near-primary partial melts of peridotitic sources are typically generated at low pressures, and by low degrees of melting (Kinzler and Grove 1992; Langmuir et al. 1992).

Assessment and discussion of the Kamenetsky et al. (2000) petrogenetic model for the Macquarie Island primitive glasses is beyond the scope of this thesis. Basically, it involves progressively increasing amounts of melting of a HIMU plume-modified MORB-source mantle, with the highest $(La/Yb)_n$ – lowest FeO* glasses representing the lowest degrees of partial melting (greatest enrichment in the 'enriched' HIMU component). Increasing degrees of partial melting led to gradual diminution of the HIMU signal both isotopically and in terms of diagnostic trace element ratios (eg. $(La/Yb)_n$, Zr/Nb), and an approach N-MORB compositions.

The availability of a suite of near-primary basaltic glasses derived by variable extents of partial melting of a HIMU OIB-modified MORB source peridotite allows an assessment of the behaviour, and relative compatibilities, of various important trace elements and element ratios during partial melting. I pay particular attention to the chalcophile and siderophile metals, and contrast their behaviour and incompatibility during increasing extents of partial melting, with their behaviour during fractionation at low pressures.

An effective way to demonstrate element enrichment or depletion for the Macquarie Island glasses is to plot abundances of each trace element versus $(La/Yb)_n$. **Figure 6.7** shows a series of such plots, differentiating only two glass groups, namely the primitive glasses, and the five fractionated glasses with $(La/Yb)_n$ values between 3.5 and 4. The latter are shown simply to illustrate the general course of fractionation for each element. Elements that are apparently unaffected by source composition and partial melting effects show near-zero slopes for the primitive suite of glasses on

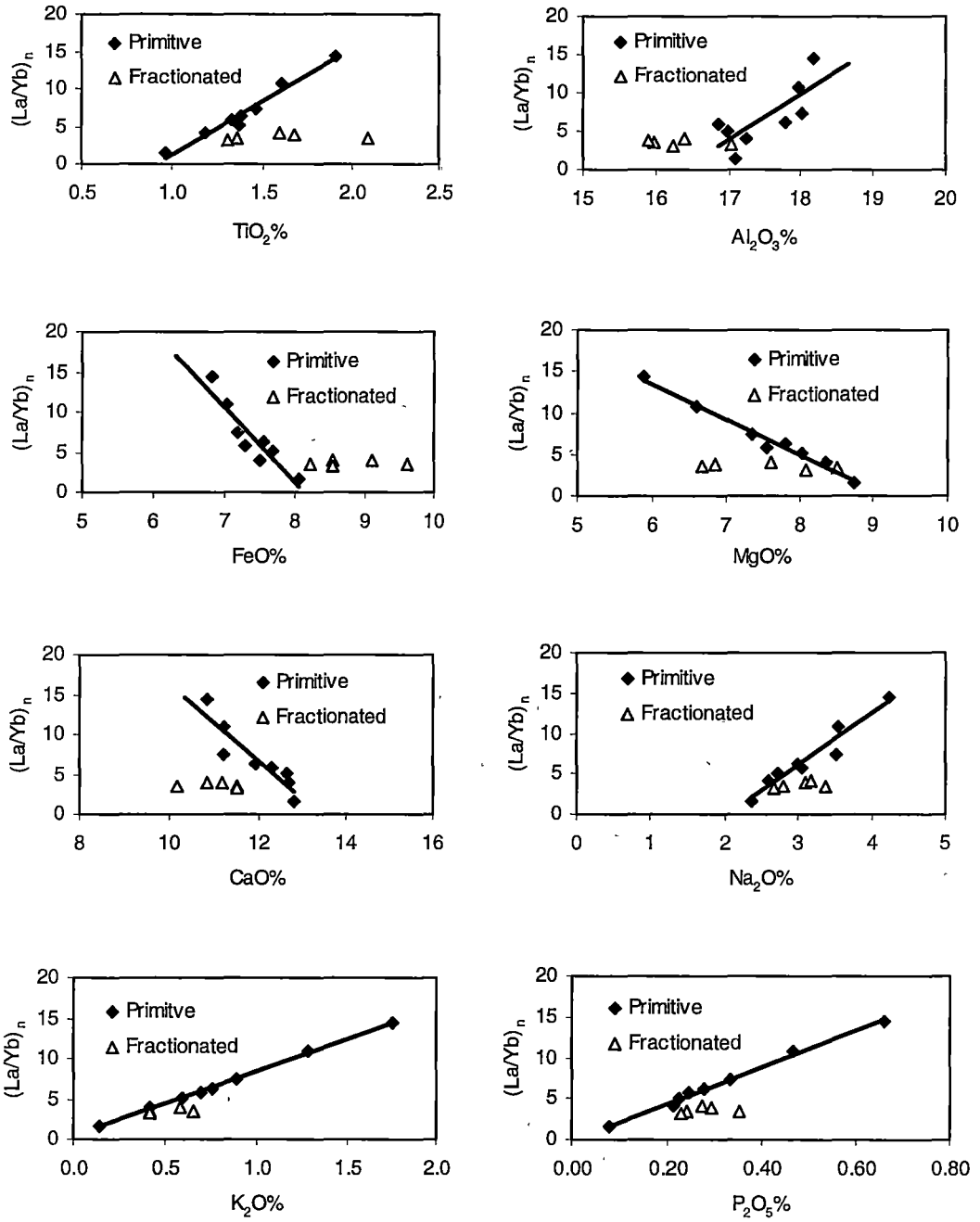

Figure 6.7. Abundance of major and trace elements vs $(La/Yb)_n$ in Macquarie Island primitive glasses and five fractionated glasses with $(La/Yb)_n$ between 3-4. Trace elements before Dy are in the incompatibility order proposed by Sun and McDonough (1989).

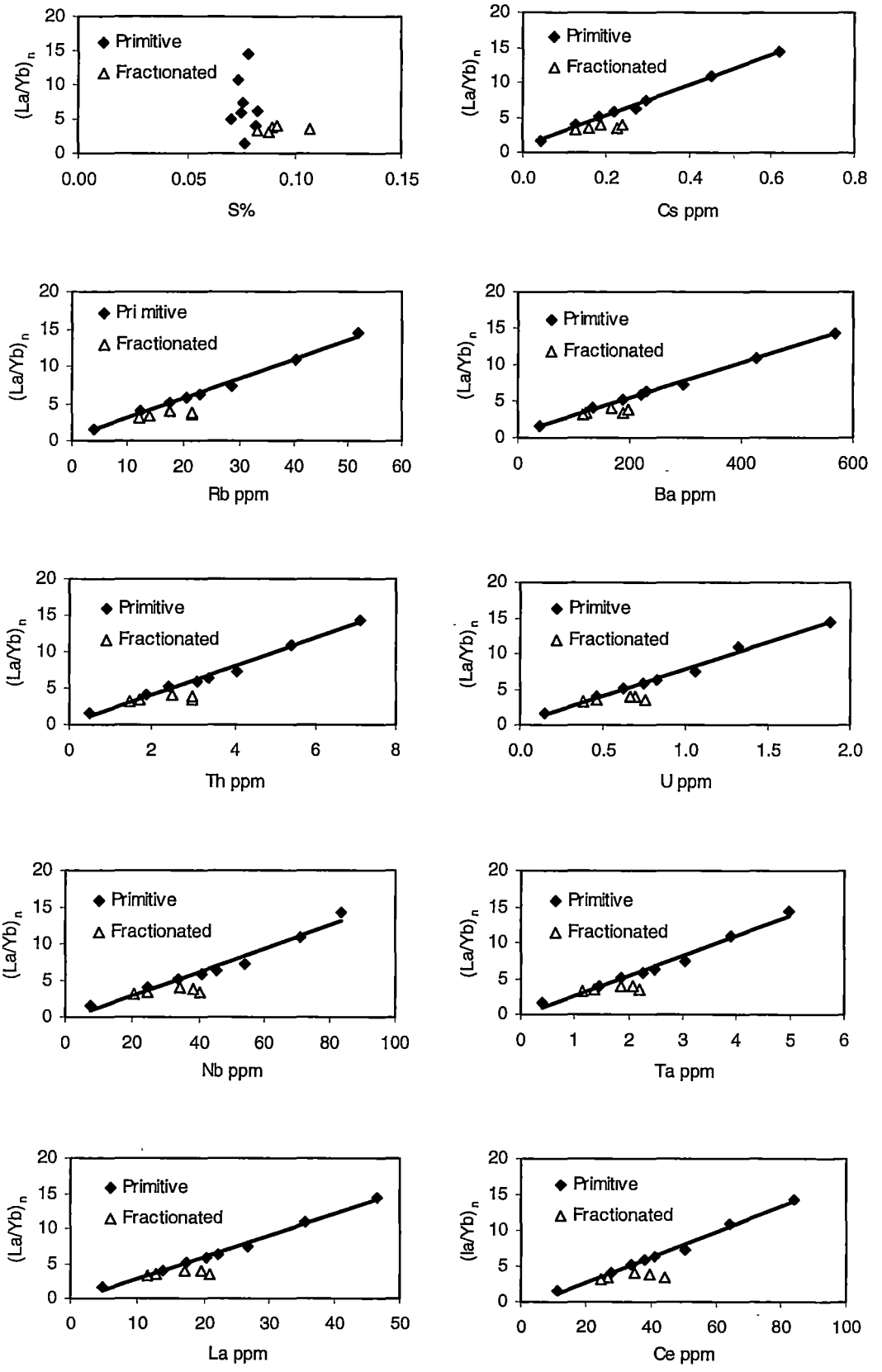

Figure 6.7. (Continued)

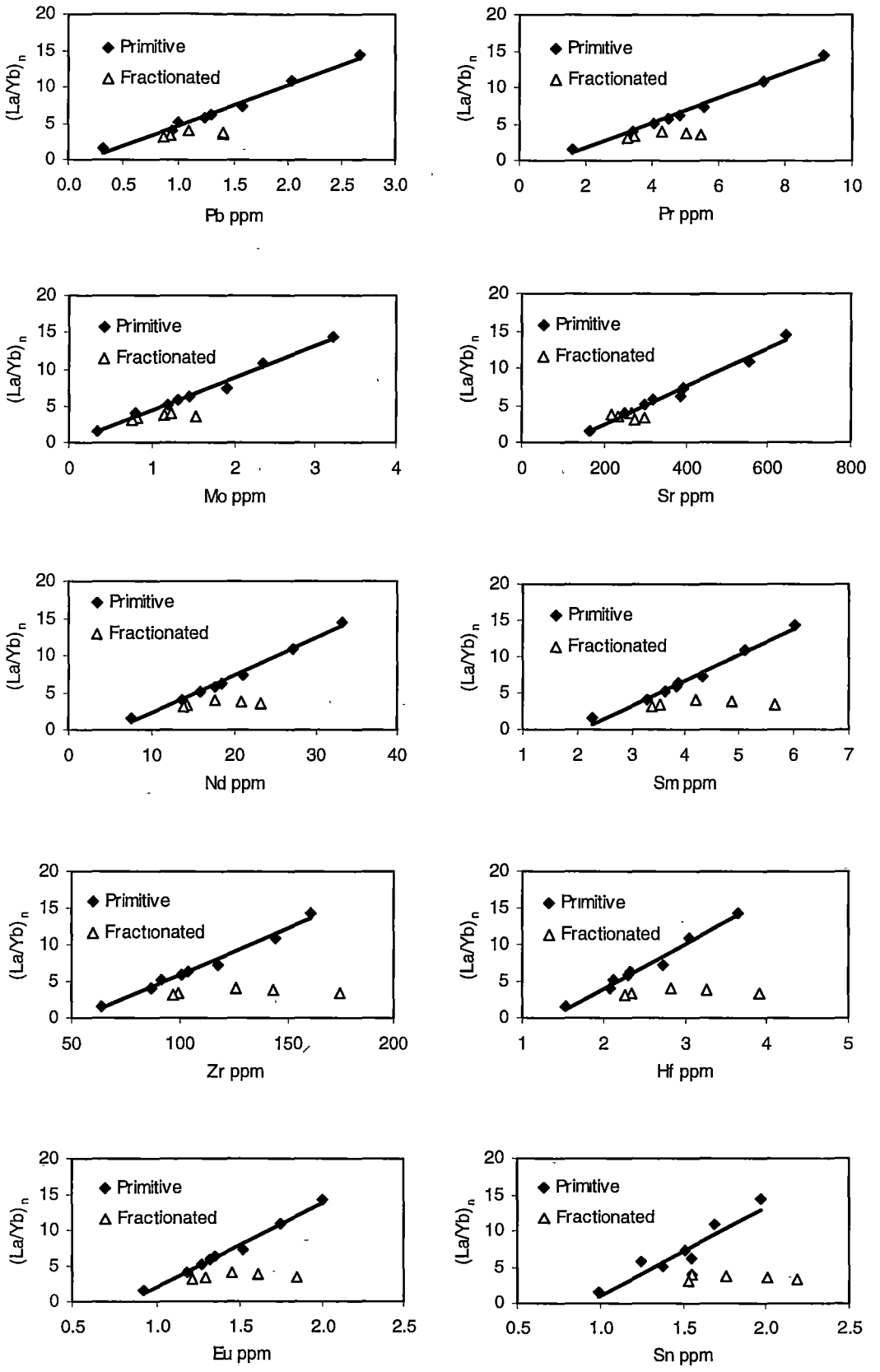

Figure 6.7. (Continued)

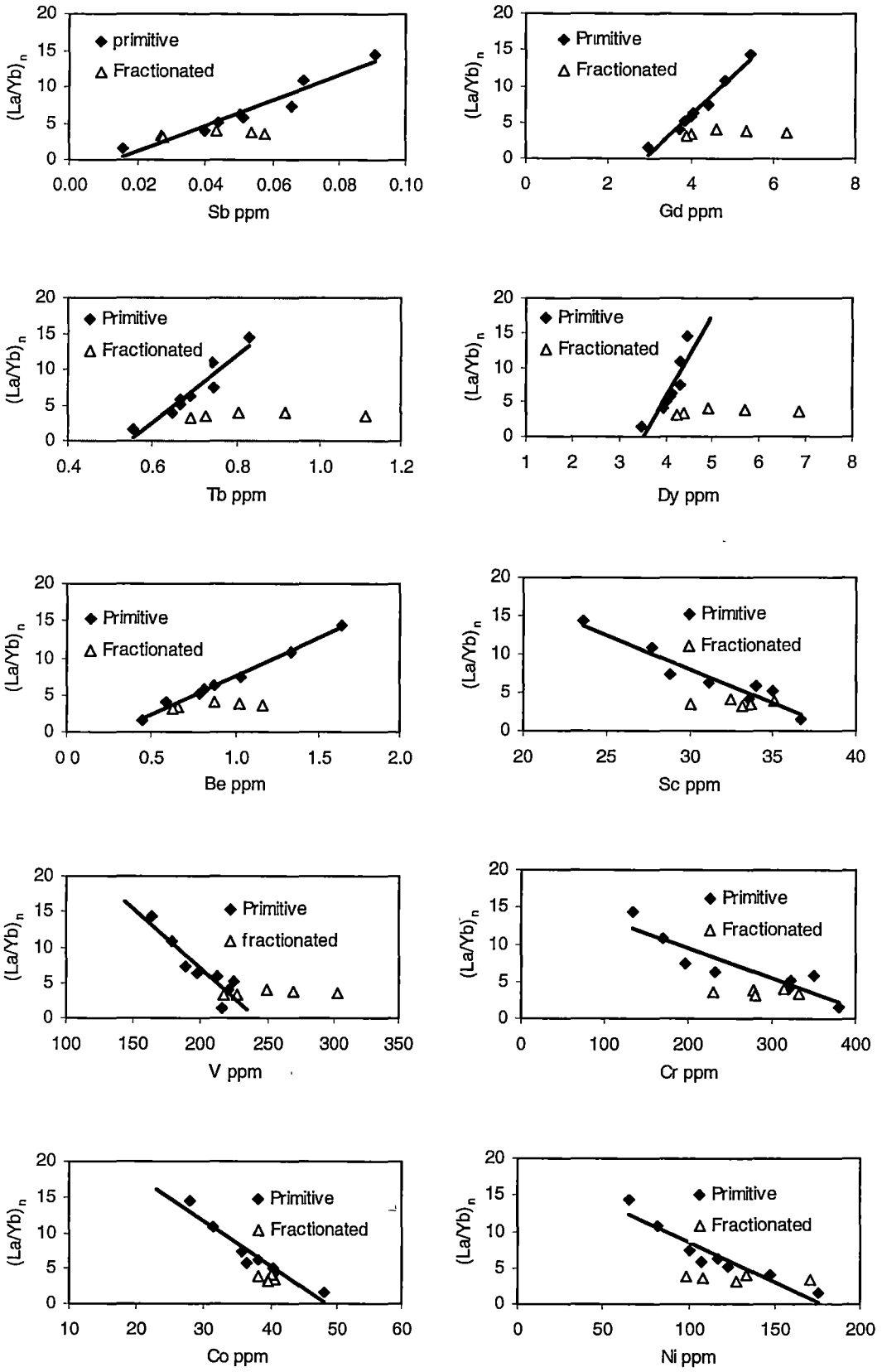

Figure 6.7. (Continued)

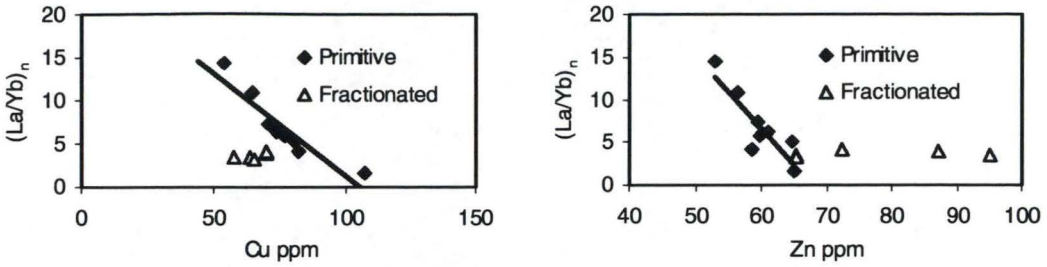

Figure 6.7. (Continued)

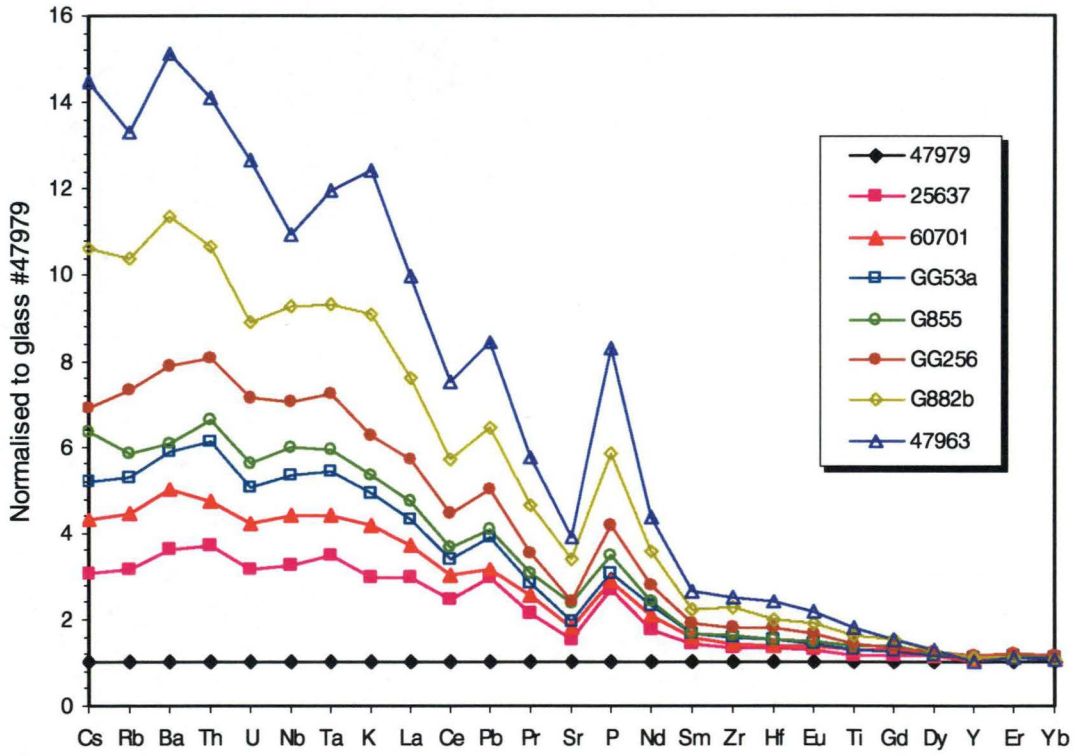

Figure 6.8. Plots of Macquarie Island primitive glasses normalised to most MORB-like sample #47979. Note: Elements are arranged in the element order of Sun and McDonough (1989).

these plots, implying bulk Kd's close to 1. Sulfur shows minimal variation over the entire $(La/Yb)_n$ range for the primitive glasses with abundances ranging from 0.07-0.083% (within the limits of precision of the electron microprobe). Fractionated glasses show a range of S abundance from 0.075-0.112%, and **Figure 6.10** shows these S contents to generally increase with increasing fractionation (decreasing Mg#).

The primitive glasses define linear, highly correlated variations (**Figure 6.7**) of all elements (except S) with $(La/Yb)_n$ Using the element order of Sun and McDonough (1989), **Figure 6.8** shows multi-element patterns for each sample, illustrating element enrichment factors in the primitive glasses normalised to most MORB-like sample #47979. The element incompatibility order proposed for Sun and McDonough (1989) for mantle melting and basalt generation predicts serially decreasing enrichment factors from Cs to Yb. In contrast, patterns for the Macquarie Island glasses (**Figure 6.8**) show significant departures from the predicted order of incompatibility, and these same differences are generally evident in all the primitive glasses. Specifically, Ba is apparently the most incompatible element, followed by (in order) Cs, Rb, Th, U, Ta, Nb, K, La, Ce, Pr, P, Nd, Sr, Sm, Zr, Hf, Eu, Ti, then the HREE in order of increasing atomic weight. Yttrium shows a level of incompatibility similar to Ho and Er. There is little change in Yb concentration over the enrichment range shown by $(La/Yb)_n$, suggesting that Yb has a bulk Kd close to 1.

6.6 Highly Incompatible Elements (Cs to Ce)

Several features of the highly incompatible section of the element enrichment patterns are worth noting. This is best illustrated using averaged group patterns (**Figure 6.9a**), with the three groups shown representing averages of slightly enriched, moderately enriched and strongly enriched glasses (see caption to **Figure 6.9a**). There is little change in the nature of patterns extending from the slightly to the moderately enriched patterns, suggesting that these represent decreasing amounts of partial melting of mineralogically similar sources. However, notable differences exist between the averaged moderately and strongly enriched patterns, especially for elements more incompatible than Ce. Key differences are that in moving from the averaged moderate to the enriched pattern, there is little change in Nb and Ta, or La

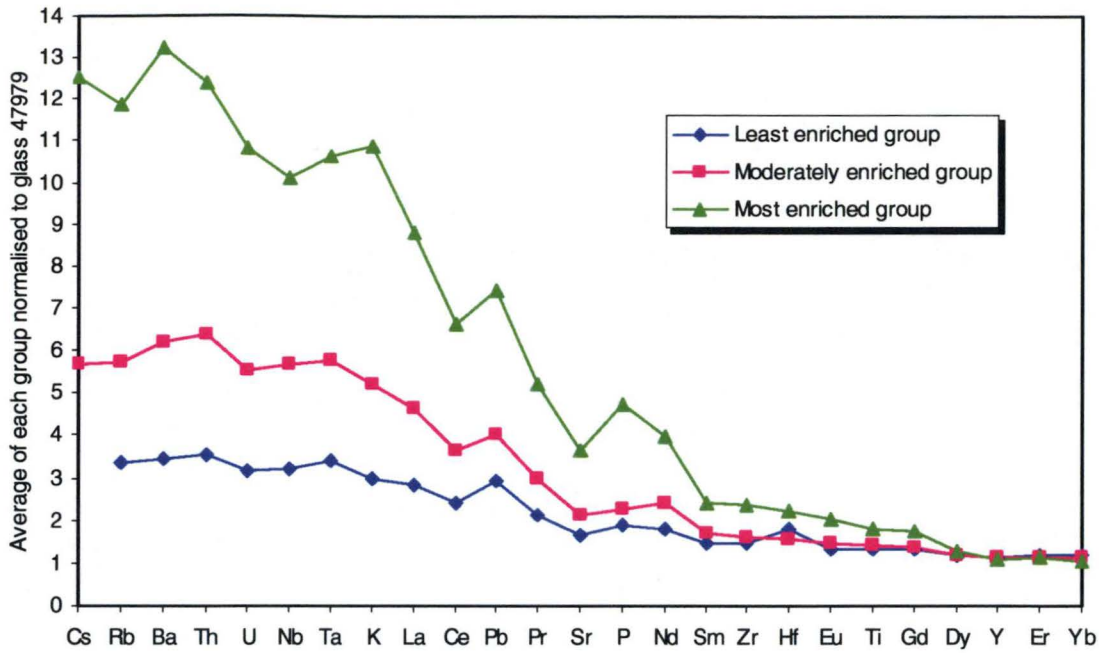

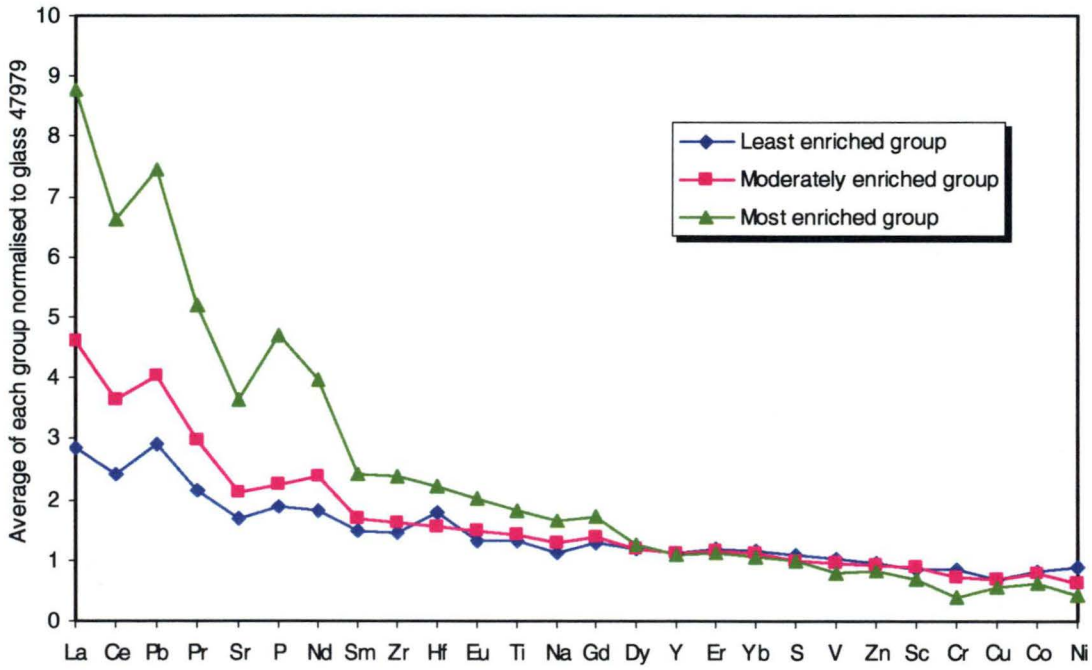

Figure 6.9. Plots of the average abundances of least, moderately and most enriched groups normalised to most MORB-like glass #47979. Least enriched group includes glasses G465 and 25637, moderately enriched group includes glasses 60701, GG55a, G855 and GG256, and most enriched group includes G88b and 47963. Plot ***a*** is from Cs to Yb in the element order of Sun and McDonough (1989) and plot ***b*** shows the elements less incompatible than La in the Sun and McDonough (1989) element order between La and Yb.

and Ce, but major increases in Cs, Rb, Ba, Th, U, K (and P). The increase in Rb is less pronounced than the other highly incompatible elements.

Mineralogically, these major increases in the abundances of highly incompatible K-group (Cs, Rb, Ba) elements and Th and U compared to Nb (and Ta) suggests that the lowest degree partial melts included a component of a K-bearing phase (phlogopite, pargasite or K-richterite), and probably apatite (note high P in the averaged most enriched pattern). These phases were melted out and exhausted during the early, low degree partial melting, and subsequent melt increments lack their 'signature'.

6.7 S and Chalcophile Elements

Figure 6.9b shows those elements less incompatible than La (in the Sun and McDonough (1989) element order) normalised to the least enriched Macquarie Island glass 47979. For the Macquarie Island primitive glass suite, S shows a bulk Kd during partial melting very close to 1 (**Figure 6.7**), and is thus behaving geochemically similarly to Yb and the heaviest REE. Presumably, this reflects buffering of melt S by a residual sulfide phase across the range of degrees of partial melting represented by the primitive glass suite from Macquarie Island. Several studies (see review in Wallace and Carmichael 1992) have suggested that MORB are S saturated at their source, implying that residual peridotite retains a minor sulfide component. This sulfide is usually a Ni+Cu-bearing monosulfide solid solution (Czamanske and Moore 1977; Peach et al. 1990), or a pyrrhotite-pentlandite-Cu-Fe sulfide intergrowth exsolved therefrom.

Of the three chalcophile metals Cu, Pb and Zn, Pb is clearly (**Figure 6.9b**) far more incompatible than Cu or Zn, showing across the enrichment range a systematic incompatibility level between that of La and Ce. Sun and McDonough (1989) and many other workers have assumed that Pb shows an incompatibility during mantle melting somewhat higher (of greater value) than Ce. The higher Pb contents, and the lower Kd for Pb in HIMU-sourced or HIMU-affected suites compared to 'normal' MORB suites may reflect an inherent character of the HIMU component in the source of these basalts. The slope of the Pb-Mg# correlation (**Figure 6.10**) for the

primitive glasses is far steeper than for the fractionation curve over the same Mg# range, suggesting involvement in the partial melting event of a phase in which Pb is significantly more compatible than either olivine or plagioclase, the two phases responsible for the 'fractionated' glasses trend on this plot.

Unlike Pb, the element Zn is significantly more compatible during partial melting, showing only a modest increase (53 to 65 ppm) across the $(La/Yb)_n$ range of enrichment of the primitive glasses (**Figure 6.7**). In contrast, Zn is moderately incompatible during fractionation, increasing from values around 65 ppm in the least fractionated glasses to 95 in the most fractionated (**Figure 6.10**). Comparing enrichments over the partial melting range with most MORB-like sample 47979 (**Figure 6.9b**), Zn shows a Kd between that of V and Sc, and just higher than S.

Even more compatible during mantle melting is Cu, which shows a significant decrease (**Figure 6.7**) with increasing $(La/Yb)_n$ (decreasing amounts of partial melting). This may reflect Cu compatibility in the monosulfide solid solution residual during the partial melting event. During fractionation, Cu shows very little change in abundance (**Figure 6.10**), possibly reflecting a balance between Cu abundance increasing (similarly to Zn) during fractionation of olivine and plagioclase, and Cu loss to a coexisting magmatic vapour phase. The latter has been demonstrated to occur during extended fractionation of a backarc basin basalt-andesite suite in the Manus Basin spreading centre (Kamenetsky et al. in press). Comparing enrichments over the partial melting range with most MORB-like glass 47979 (**Figure 6.9b**), Cu shows a Kd close to that of Ni.

6.8 Other Metals (Mo, Sn and Sb)

Figure 6.11a shows the abundances of elements more compatible than La in primitive glasses from Macquarie Island, normalised to most MORB-like glass 47979, and plotted using the order of incompatibility proposed for mantle melting by Sun and McDonough (1989) for elements more incompatible than Yb. Note the large positive anomalies of Mo and Sb relative to adjacent elements, suggesting that the Sun and McDonough (1989) element order is inappropriate for this suite. **Figure 6.11b** shows the same data organised into an element order of smoothly increasing

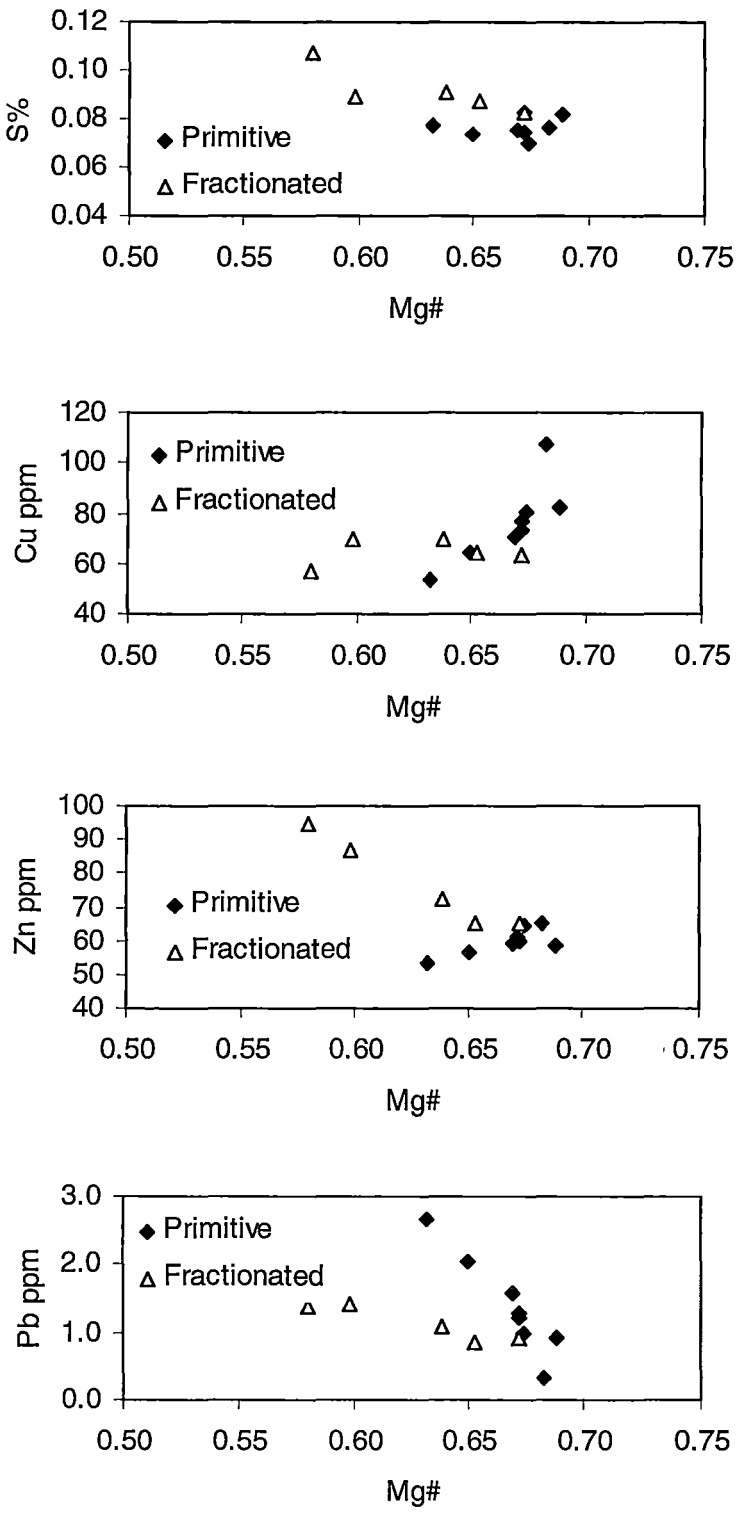

Figure 6.10. Mg# vs S, Cu, Zn and Pb in Macquarie Island primitive glasses and fractionated glasses with $(La/Yb)_n$ between 3 and 4

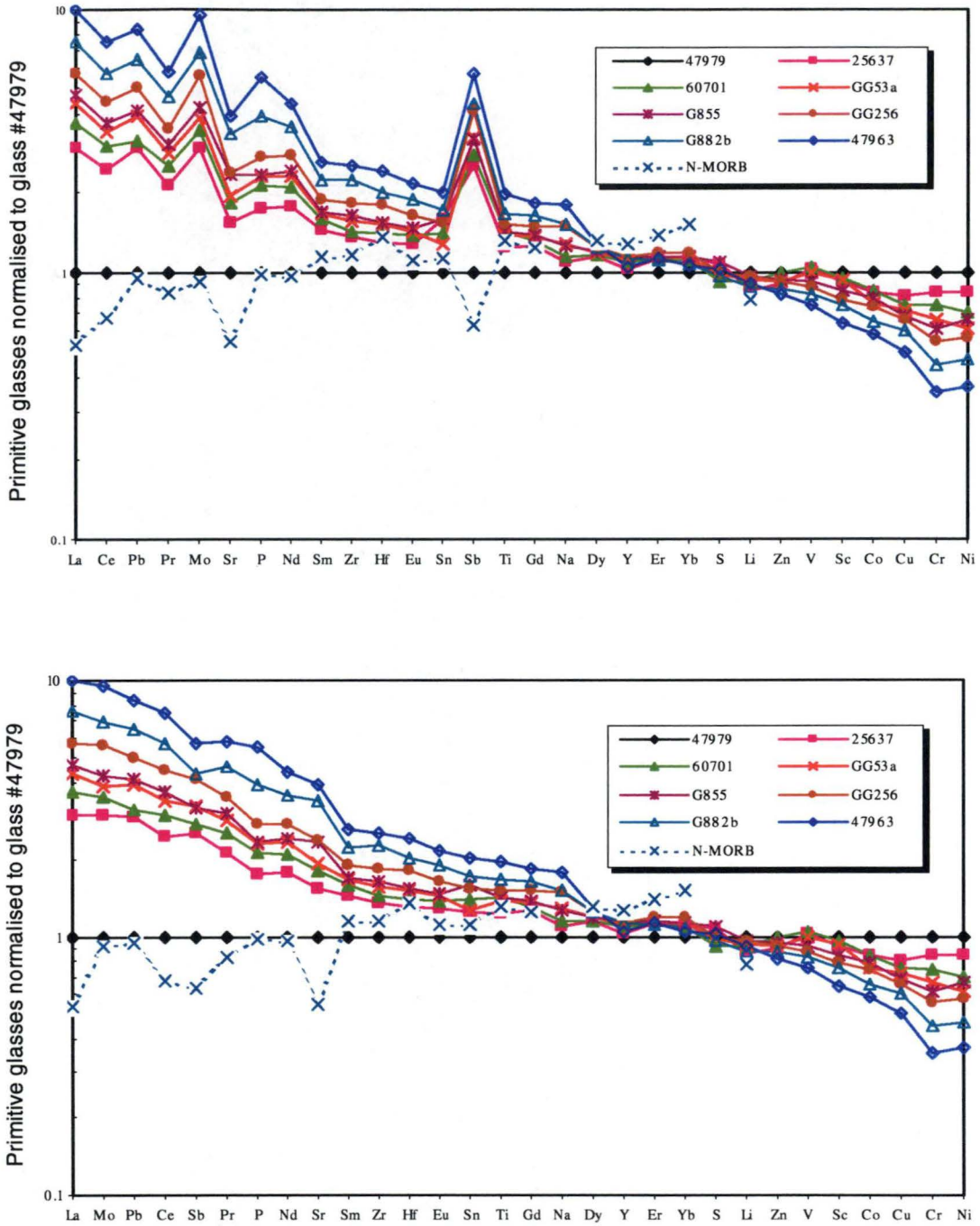

Figure 6.11. Most MORB-like glass #47979 normalised plots of Macquarie Island primitive glasses. ***a***: Plotted using the incompatibility order proposed by Sun and McDonough (1989) for elements more incompatible than Yb. ***b***: Organised according to systematically increasing incompatibility during mantle partial melting event responsible for the Macquarie Island primitive glass spectrum.

relative compatibility for the Macquarie Island primitive glass, removing the major 'anomalies'. This suggests that for HIMU-modified MORB suites, Mo is slightly more incompatible than Pb, and Pb than Ce. Antimony (Sb) is considerably more incompatible for this suite of primitive glasses than the level indicated by Sun and McDonough (1989), falling between Ce and Pr rather than Eu and Gd. In contrast, our data for Sn incompatibility agrees well with that proposed by Sun and McDonough (1989), falling between Eu and Ti. Not enough quality data is available for these elements in MORB suites to evaluate these data more fully, but the significantly increased incompatibility of Sb and Mo in the Macquarie Island HIMU-influenced MORB suite may reflect, as for Pb, an inherent feature of the HIMU component involved in the genesis of this suite.

6.9 Summary

A suite of primitive glasses from Macquarie Island at the eastern end of the Southern Ocean have been demonstrated by Kamenetsky et al. (2000) to represent a suite of mid-ocean ridge-type basalts, the mantle source of which had been influenced by a HIMU component linked to the nearby Balleny plume. These glasses, plus a second suite of more fractionated glasses from the same location, have been analysed for a comprehensive range of elements using three ICP-MS-based techniques, including high-resolution ICP-MS, quadrupole ICP-MS, and laser ablation ICP-MS. With the exception of Tl and Cd, which showed unacceptably large variations (discrepancies >20% between the three analytical protocols), the majority of elements measured showed a reproducibility of <10% for the three techniques, and most showed values lower than 5%.

The new high-precision data for a wide range of elements in a primitive MORB-like suite allow evaluation of the relative compatibility/incompatibility levels of these elements, and comparison of the order evident from the Macquarie Island suite with the widely accepted order proposed for mantle melting by Sun and McDonough (1989). Significant discrepancies emerge. For the most incompatible elements, those primitive glasses representing the lowest-degree partial melts show significantly higher Ba, K, Th and P contents relative to Nb (and thus slightly different orders of incompatibility than that proposed by Sun and McDonough) than glasses

representing higher degree partial melts. This is taken to reflect involvement of one or more K- and P-bearing phases in the earliest stages of partial melting, which are eliminated early in the melting history. Subsequent partial melts do not reflect these anomalous enrichments.

Sulphur, Cu, Pb and Zn show strongly contrasting levels of incompatibility in the Macquarie Island MORB-type mantle-melt system. There is little change of S abundance across the range of $(La/Yb)_n$ (representing range of extents of partial melting), indicating a bulk Kd for S during partial melting of very close to 1, presumably being buffered by a residual sulfide present during all stages of partial melting. Copper is the most compatible of the chalcophile elements, showing a compatibility level close to Ni. This probably reflects retention of Cu in the residual sulfide, which is normally considered to be a Cu-bearing pentlandite or Ni+Cu-bearing monosulfide solid solution. Zinc is moderately compatible through the partial melting process, showing a level of compatibility close to V. It is increasingly depleted in lower degree partial melts. Lead (Pb), by contrast, is highly incompatible, showing a level of incompatibility very close to La. According to Sun and McDonough (1989) and other studies, Pb is slightly less incompatible than Ce, so this change in the order of incompatibility of Pb may reflect an inherent feature of the HIMU component present in the Macquarie Island basalts' source mantle.

In similar fashion to Pb, the new data for Mo shows an increased incompatibility (between La and Ce, and very close to Pb) compared with that proposed for Mo by Sun and McDonough (1989), in which Mo was taken to be somewhat less incompatible than Pr. The Macquarie Island glass data reflect a strikingly higher incompatibility level for Sb (between those of Ce and Pr) than proposed by Sun and McDonough (1989), between Eu and Ti. This is again taken to reflect an inherent feature of the HIMU component in the source of these basalts. Macquarie Island Sn data indicate an incompatibly level close to Eu and Ti, as proposed by Sun and McDonough (1989).

Chapter 7

DEVELOPMENT OF A SECTOR FIELD ICP-MS METHOD FOR PRECISE ANALYSIS OF LEAD ISOTOPE RATIOS IN GEOLOGICAL SAMPLES

7.1 Introduction

This chapter describes the development of a fast, reliable and low-cost method for the accurate and precise analysis of lead isotope ratios in geological materials using a sector field ICP-MS. This technique is used to measure the lead isotope compositions of a NIST Pb SRM 982 lead standard, and galena and galena-bearing ores from Broken Hill and western Tasmania. Finally, these measurements are compared with lead isotope ratio data obtained using TIMS.

This work is based on a technique developed initially by Dr A. T. Townsend and the author and reported by Townsend et al. (1998). However, I have amplified and extended that work, and the following have been rigorously investigated:

- Instrumental detector dead time for the measurement of Pb isotope ratios and its correction.
- Effects of instrumental parameters (such as runs/passes, peak window width, number of scans, sample data points etc.) on Pb isotope ratio precision.
- Mass bias and correction.
- Effect of Pb concentration of the accuracy and precision of Pb isotope ratios.
- Hg interference (with and without the presence of W in solution) on Pb isotope ratios and its correction.
- Assessing the accuracy of Pb isotope ratios using both an equal-atom Pb standard (NIST Pb SRM 982) and sulfides previously analysed by TIMS.

7.2 Experimental

7.2.1 Reagents and Standards

Double distilled HNO_3, HCl, HF and ultra-pure deionised water (≥18 MΩ) were used exclusively in this work. The preparation of these reagents has been described in **Chapter 2**. The standard lead solution used in this work was diluted from a 100 μg ml^{-1} multi-element atomic spectroscopy standard (Perkin-Elmer Corporation, USA).

Two metallic lead standards, NIST Pb SRM 981 (common lead isotopic standard) and NIST Pb SRM 982 (equal-atom lead isotopic standard, $^{207}Pb/^{206}Pb = 1.00016$), were used in this study. Based on 95% confidence limits, the certified isotopic compositions for SRM 981 and 982 provided by National Institute of Standards and Technology (NIST), USA, are given as following:

SRM 981:
^{204}Pb, atom percent.....1.4255 ± 0.0012
^{206}Pb, atom percent.....24.1442 ± 0.0057
^{207}Pb, atom percent.....22.0833 ± 0.0027
^{208}Pb, atom percent.....52.3470 ± 0.0086
$^{206}Pb/^{204}Pb$.....16.9374
$^{207}Pb/^{204}Pb$.....15.4916
$^{208}Pb/^{204}Pb$.....36.7219
$^{207}Pb/^{206}Pb$.....0.91464
$^{208}Pb/^{207}Pb$.....2.1681

SRM 982:
^{204}Pb, atom percent.....1.0912 ± 0.0012
^{206}Pb, atom percent.....40.0890 ± 0.0072
^{207}Pb, atom percent.....18.7244 ± 0.0023
^{208}Pb, atom percent.....40.0954 ± 0.0077
$^{206}Pb/^{204}Pb$.....36.7385
$^{207}Pb/^{204}Pb$.....17.1595

$^{208}Pb/^{204}Pb$.....36.7443

$^{207}Pb/^{206}Pb$.....1.00016

$^{208}Pb/^{207}Pb$.....0.467071

7.2.2 Sample Preparation

The lead isotope standards (0.01 - 0.05 g) were dissolved in 25 ml 25% (v/v) HNO_3 (Potts 1987) in a Savillex® screw-top Teflon beaker on a hotplate at 130 °C for about one hour. After cooling, the resulting solution was further diluted to the working concentrations (generally between 10 and 50 ng g^{-1} to approximately match the lead concentration in test samples) before the sector field ICP-MS run.

Samples were dissolved in Savillex® screw-top Teflon beakers using HF-HNO_3-HCl (2:1:3) mixture on a hot plate at 130 °C overnight, then evaporated to dryness twice with the addition of 1 ml HNO_3 between evaporations. The concentration of the final solution was 0.1 g in 100 ml in 2% HNO_3, representing a total dissolved solids content of 0.1%.

7.2.3 Instrumentation

A Finnigan MAT Element ICP-mass spectrometer was used in the study. All measurements of lead isotopic ratios were conducted at low resolution (R = 300), providing flat-topped peaks and maximum instrument sensitivity (typically greater than 1,000,000 counts sec^{-1} for 10 ng g^{-1} ^{115}In, or 700,000 counts sec^{-1} for 10 ng g^{-1} ^{208}Pb). The mass range under this study was set from 201 to 208 amu. Counting mode was used as detector mode. The typical instrumental setting parameters used in this work were as described in **Chapter 2** of this thesis. Isotopes of interest were analysed using electric scanning, with the magnet held at fixed mass. The secondary electron multiplier detector (with discrete dynodes) was operated in counting mode. Instrument tuning and optimisation were performed daily using a 10 ng g^{-1} multi-element solution containing lead.

7.3 Results and Discussion

7.3.1 Dead Time Correction

The $^{208}Pb/^{204}Pb$, $^{207}Pb/^{204}Pb$ and $^{206}Pb/^{204}Pb$ isotopic ratios increase with the increase of lead concentration. The difference is caused by the ICP-MS instrumental detector dead time. Therefore, the measurement of lead isotopic ratios was corrected for dead time. This instrumental detector dead time was described by Price Russ (1989), and can be calculated by the following equation:

$$\tau = (1 - m/n)/n$$

where m and n are measured and true count rates, and τ is dead time in nanosecond. For this work, using the method described by Price Russ (1989), dead time was determined by the standard solutions of 10, 25 and 50 ng g^{-1} Pb and found to be, for the measurement of lead isotopic ratios, ~49 nsec. **Figures 7.1** to **7.3** show the relationship between the lead isotopic ratios for $^{208}Pb/^{204}Pb$, $^{207}Pb/^{204}Pb$ and $^{206}Pb/^{204}Pb$ and the instrumental detector dead time with different lead concentration in solutions. As can be clearly seen in these figures, lead isotopic ratios generally increase with the decrease of lead concentration in solutions before reaching the instrumental detector dead time, and the differences of lead isotope ratios with different concentrations become smaller and smaller when approaching the instrumental detector dead time. Lead isotopic ratios become almost identical with different lead concentrations at the instrumental detector dead time. Therefore, it is crucial to set up the instrumental detector dead time correctly for the measurement of lead isotopic ratios.

In addition, the instrumental detector dead time varies from instrument to instrument and element to element. For instance, detector dead time of 10 nsec was reported by Stürup et al. (1997) in their study of calcium isotopic ratios performed on a Plasma Trace-2 High Resolution Inductively Coupled Plasma Mass Spectrometer (Micromass Ltd, Manchester, England). Even with the same model of instrument as used here, Vanhaecke et al. (1997) reported an instrumental detector dead time of approximate 30 nsec for the measurements of lead and copper isotope ratios. Thus, the instrumental detector dead time should be determined for each individual instrument before measurement of lead isotopic ratios.

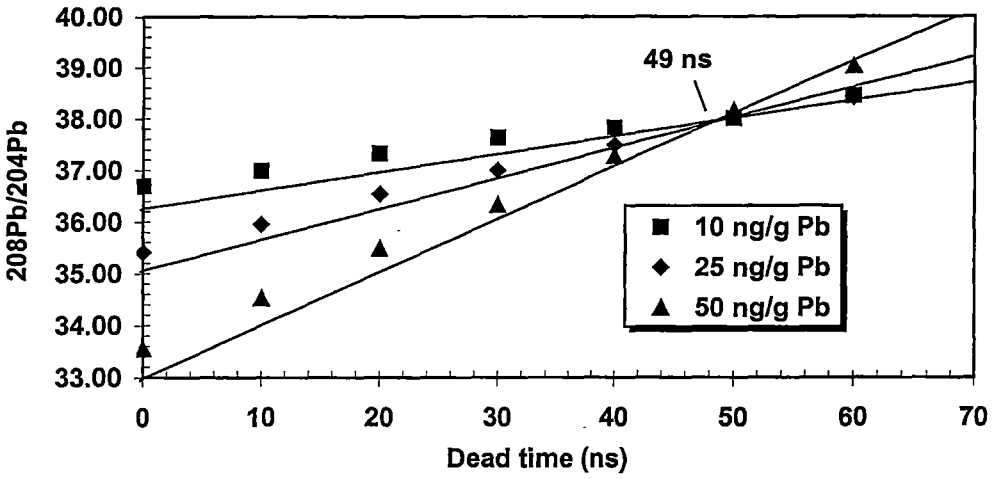

Figure 7.1. Observed relationship between $^{208}Pb/^{204}Pb$ ratio and instrumental dead time using 10, 25 and 50 ng g^{-1} lead solutions

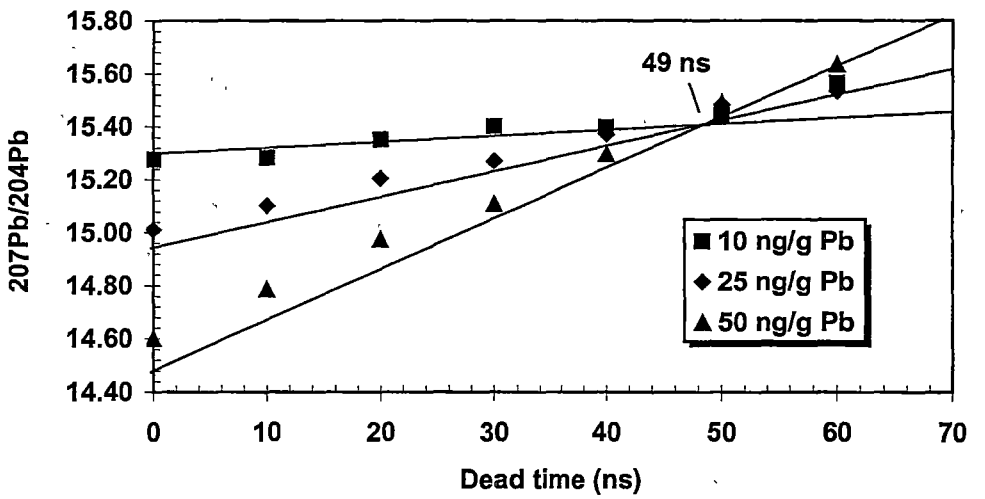

Figure 7.2. Observed relationship between $^{207}Pb/^{204}Pb$ ratio and instrumental dead time using 10, 25 and 50 ng g^{-1} lead solutions

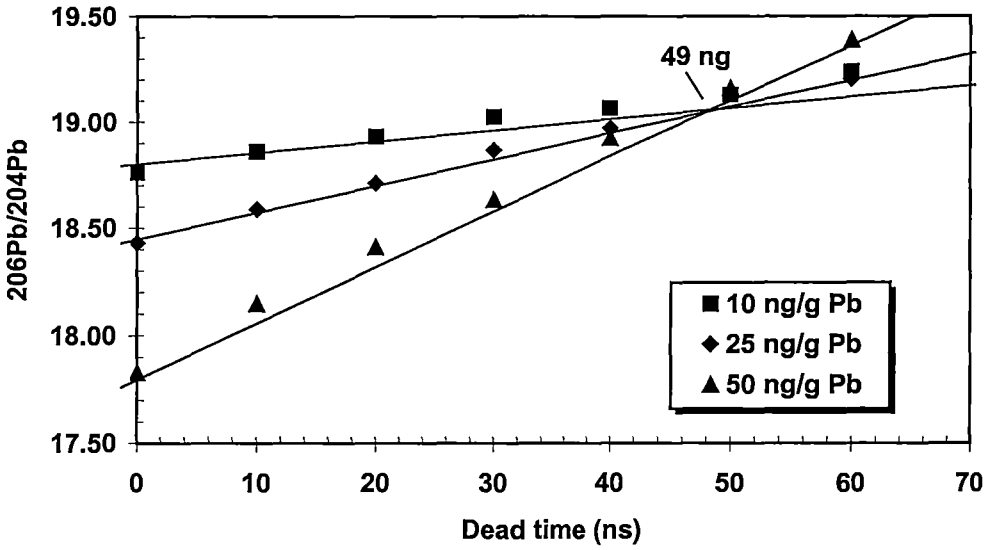

Figure 7.3. Observed relationship between $^{206}Pb/^{204}Pb$ ratio and instrumental dead time using 10, 25 and 50 ng g^{-1} lead solutions

7.3.2 Effects of Instrumental Parameters

7.3.2.1 Runs and Passes

In order to optimise instrumental conditions for measurement of lead isotopic ratios, the sector field ICP-mass spectrometer was run from 200 to 1000 passes at 3 runs and 5% peak window width. Lead concentrations used in the investigation were 25 and 50 ng g^{-1}. The instrumental statistic relative standard deviations (%RSD) of $^{208}Pb/^{204}Pb$, $^{207}Pb/^{204}Pb$, $^{206}Pb/^{204}Pb$, $^{208}Pb/^{206}Pb$ and $^{207}Pb/^{206}Pb$ isotope ratios are presented in **Table 7.1**, which shows that the best instrumental signal %RSD for the measurements of lead isotopic ratios can be obtained at 666 instrumental passes with both 25 and 50 ng g^{-1} Pb concentrations.

Table 7.1. Instrumental signal relative standard deviations (%RSD) of $^{208}Pb/^{204}Pb$, $^{207}Pb/^{204}Pb$, $^{206}Pb/^{204}Pb$, $^{208}Pb/^{206}Pb$ and $^{207}Pb/^{206}Pb$ isotope ratios at different passes

Passes	Instrumental signal relative standard deviations (%RSD)				
	$^{208}Pb/^{204}Pb$	$^{207}Pb/^{204}Pb$	$^{206}Pb/^{204}Pb$	$^{208}Pb/^{206}Pb$	$^{207}Pb/^{206}Pb$
25 ng g^{-1} Pb					
200	0.46	0.52	0.40	0.12	0.19
333	0.17	0.21	0.25	0.08	0.08
500	0.18	0.10	0.18	0.02	0.09
666	0.11	0.11	0.20	0.13	0.10
1000	0.15	0.18	0.30	0.21	0.18
50 ng g^{-1} Pb					
200	0.55	0.72	0.76	0.22	0.18
333	0.24	0.29	0.32	0.08	0.04
500	0.26	0.21	0.11	0.07	0.09
666	0.09	0.13	0.07	0.14	0.06
1000	0.24	0.24	0.16	0.07	0.08

7.3.2.2 Peak Window Width

It has been reported that the peak window width (PWW) can effect the data precision in the measurement of lead isotopic ratios (Shuttleworth et al. 1997). In order to ensure best instrumental signal precision, Shuttleworth et al. (1997) used a 10 % peak window width. In the present study, four different peak window widths (1%, 3%, 5% and 10%) were tested under either a constant 500 sample data points (SDP) or a total 1000 sample data points for each method. **Tables 7.2** and **7.3** show the instrumental signal %RSD for lead isotopic ratios under the two different conditions. The lead concentrations for the investigation were also 25 and 50 ng g^{-1}. From **Table 7.2**, using 500 sample data points for each method, a 3% peak window width is obviously the best parameter for an optimum instrumental signal relative standard deviations with both 25 and 50 ng g^{-1} Pb in solutions. On the other hand, under the condition of a total of a 1000 sample data points for each method, the best instrumental signal %RSD for lead isotopic ratios was found with 3% peak window width for 50 ng g^{-1} Pb in solution, whereas 5% peak window width gives a good %RSD for 25 ng g^{-1} Pb in solution (**Table 7.3**).

Table 7.2. Instrumental signal relative standard deviations (%RSD) of $^{208}Pb/^{204}Pb$, $^{207}Pb/^{204}Pb$, $^{206}Pb/^{204}Pb$, $^{208}Pb/^{206}Pb$ and $^{207}Pb/^{206}Pb$ isotope ratios under a consistent 500 sample data points for each method

PWW (%)	Instrumental signal relative standard deviations (%RSD)				
	$^{208}Pb/^{204}Pb$	$^{207}Pb/^{204}Pb$	$^{206}Pb/^{204}Pb$	$^{208}Pb/^{206}Pb$	$^{207}Pb/^{206}Pb$
25 ng g^{-1} Pb					
1	0.51	0.51	0.68	0.17	0.34
3	0.05	0.15	0.11	0.07	0.20
5	0.26	0.15	0.22	0.14	0.07
10	0.22	0.21	0.23	0.06	0.01
50 ng g^{-1} Pb					
1	0.42	0.43	0.34	0.15	0.22
3	0.07	0.13	0.09	0.03	0.10
5	0.11	0.16	0.17	0.08	0.07
10	0.12	0.13	0.15	0.05	0.05

Table 7.3. Instrumental signal relative standard deviations (%RSD) of $^{208}Pb/^{204}Pb$, $^{207}Pb/^{204}Pb$, $^{206}Pb/^{204}Pb$, $^{208}Pb/^{206}Pb$ and $^{207}Pb/^{206}Pb$ isotope ratios under a total 1000 sample data points for each method

PWW (%)	SDP per 1% PWW	Instrumental signal relative standard deviations (%RSD)				
		$^{208}Pb/^{204}Pb$	$^{207}Pb/^{204}Pb$	$^{206}Pb/^{204}Pb$	$^{208}Pb/^{206}Pb$	$^{207}Pb/^{206}Pb$
25 ng g^{-1} Pb						
1	1000	0.36	0.28	0.54	0.04	0.11
3	333	0.32	0.64	0.51	0.27	0.24
5	200	0.31	0.27	0.33	0.03	0.12
10	100	0.39	0.33	0.32	0.22	0.15
50 ng g^{-1} Pb						
1	1000	0.19	0.26	0.29	0.15	0.04
3	333	0.14	0.14	0.17	0.08	0.13
5	200	0.15	0.36	0.13	0.17	0.36
10	100	0.09	0.09	0.21	0.20	0.12

From these observations it is concluded that under the condition of a consistent sample data points for each method a 3% peak window width will ensure low instrumental signal relative standard deviations for the measurements of lead isotopic ratios.

7.3.2.3 Scans

During preliminary experimental work, it was noticed that scan number affects instrumental signal %RSD values. In order to ensure a best instrumental signal %RSD, different number of scans (1000, 2000 and 3000 scans) were tested using 30 ng g^{-1} Pb in solution. The scan numbers for the best instrumental signal %RSD were found to be 2000. **Table 7.4** gives details of the experimental results.

Table 7.4. Instrumental signal relative standard deviations (%RSD) of $^{208}Pb/^{204}Pb$, $^{207}Pb/^{204}Pb$, $^{206}Pb/^{204}Pb$, $^{208}Pb/^{206}Pb$ and $^{207}Pb/^{206}Pb$ isotope ratios at different scans (lead concentration = 30 ng g^{-1})

Scans	Instrumental signal relative standard deviations (%RSD)				
	$^{208}Pb/^{204}Pb$	$^{207}Pb/^{204}Pb$	$^{206}Pb/^{204}Pb$	$^{208}Pb/^{206}Pb$	$^{207}Pb/^{206}Pb$
1000	0.11	0.41	0.35	0.23	0.09
2000	0.14	0.10	0.10	0.04	0.07
3000	0.21	0.14	0.18	0.06	0.07

7.3.2.4 Sample Data Points

The effect of sample data points per peak on instrumental signal %RSD was also investigated in the study. Four different sample data points per peak were used to test the instrumental signal %RSD. The results (**Table 7.5**) show that the best average instrumental signal %RSD can be obtained with the use of 750 sample data points per peak.

Table 7.5. Instrumental signal relative standard deviations (%RSD) of $^{208}Pb/^{204}Pb$, $^{207}Pb/^{204}Pb$, $^{206}Pb/^{204}Pb$, $^{208}Pb/^{206}Pb$ and $^{207}Pb/^{206}Pb$ isotope ratios at different sample data points per peak

Sample data points per peak	Instrumental signal relative standard deviations (%RSD)				
	$^{208}Pb/^{204}Pb$	$^{207}Pb/^{204}Pb$	$^{206}Pb/^{204}Pb$	$^{208}Pb/^{206}Pb$	$^{207}Pb/^{206}Pb$
250	0.11	0.05	0.19	0.19	0.14
500	0.09	0.11	0.17	0.12	0.08
750	0.08	0.14	0.02	0.10	0.15
1000	0.23	0.29	0.33	0.12	0.09

From the above discussion, it is concluded that a set of optimised instrumental parameters (including runs/passes, peak window width, scan number, sample data points and so on) is essential to ensure a better instrumental signal relative standard deviation for the measurements of lead isotopic ratios. The optimised operating parameters for the sector field ICP-MS used in this study are summarised in **Table 7.6.**

7.3.3 Precision

Lead isotopic ratio precision data of three different standard solutions by sector field ICP-MS analysis was obtained at the lead concentration of ~40 ng g^{-1} in all testing solutions. The three standards used in the present work were:

(1) PE-Pb-STD - Lead standard solution from Perkin-Elmer Corporation, USA.
(2) SRM 981 - Common lead isotopic standard from NIST, USA.
(3) BH2 - A galena from Broken Hill, Australia.

In the investigation, each solution was analysed 10 consecutive times without any mass bias correction. As shown in **Table 7.7**, the precisions (%RSD) for the isotope ratios of $^{208}Pb/^{204}Pb$, $^{207}Pb/^{204}Pb$, $^{206}Pb/^{204}Pb$, $^{208}Pb/^{206}Pb$ and $^{207}Pb/^{206}Pb$ were found

Table 7.6. Optimised operating parameters for lead isotopic ratio measurements

Runs/Passes	3 runs/666 passes
Peak window width	3%
Sample data points per peak	750
Number of scans	2000
Mass ranges	^{201}Hg: 200.96 - 200.98
	^{202}Hg: 201.96 - 201.98
	^{204}Pb: 203.96 - 203.98
	^{206}Pb: 205.96 - 2.0598
	^{207}Pb: 206.97 - 206.99
	^{208}Pb: 207.97 - 207.99
Scan type	E-Scan
Segment duration	0.025 s
Settling time	0.1 s for first measured isotope, 0.001 s for subsequent peaks
Sample time	0.0011 s
Detector mode	Counting
Integration type	Average
Sample Uptake time	2 mins
Dead time	49 ns
Rinse time	3 mins (with 5% HNO_3)
Total time per sample	~ 15 mins

to be in a range of 0.041 to 0.13. From **Table 7.7**, similar measurement precision can be found for ^{208}Pb/^{204}Pb, ^{207}Pb/^{204}Pb, ^{206}Pb/^{204}Pb (%RSD in a narrow range of 0.10 to 0.13), while the measurement precision for ^{208}Pb/^{206}Pb and ^{207}Pb/^{206}Pb was between 0.041 and 0.047 %RSD. No significant difference in measurement precision was found between standard lead solutions and more "complex" galena digest samples. In addition, theoretical precisions based on Poisson counting statistics were also calculated and are given in **Table 7.7** (based on ^{208}Pb signals of the order of 1 - 3 x 10^6 counts s^{-1}).

External precisions, approximately 2 - 3 times worse than that predicted from Poisson counting statistics alone, were observed. This suggested noise contributions from other sources such as the sample introduction system, plasma flicker etc. The precisions obtained for ratios referenced to ^{206}Pb are similar to that found by Vanhaecke et al. (1996) using a similar sector field ICP-MS instrument to measure the $^{206}Pb/^{207}Pb$ ratio of a standard lead solution. The external precision values shown in **Table 7.7** are also similar to the best values obtained using a quadrupole ICP-MS by Begley and Sharp (1997).

In addition, a dramatic deterioration in lead isotopic ratio precision was observed when both counting and analog modes were used as the sector field ICP-MS detector mode. For instance, when 100 ng g^{-1} lead solution was analysed using both counting and analog modes and the precisions (%RSD) were found to be 0.52% for $^{206}Pb/^{204}Pb$, 0.51% for $^{208}Pb/^{204}Pb$ and $^{207}Pb/^{204}Pb$ with 10 consecutive measurements.

Table 7.7. Lead isotopic ratio precision data for a standard multi-element solution (PE-Pb-STD), NIST Pb SRM 981 and a Broken Hill galena (BH2). (Concentration of Pb was controlled at about 40 ng g^{-1} and number of analyses was 10 for each sample)

	$^{208}Pb/^{204}Pb$	$^{207}Pb/^{204}Pb$	$^{206}Pb/^{204}Pb$	$^{208}Pb/^{206}Pb$	$^{207}Pb/^{206}Pb$
PE-Pb-STD					
Ratio	36.969	15.260	18.820	1.9643	0.8108
STD	0.041	0.017	0.019	0.0008	0.0004
%RSD	0.11	0.11	0.10	0.041	0.047
Theo %RSD	0.054	0.055	0.055	0.015	0.016
SRM 981					
Ratio	36.533	15.358	16.845	2.1688	0.9117
STD	0.037	0.017	0.018	0.0010	0.0004
%RSD	0.10	0.11	0.11	0.046	0.048
Theo %RSD	0.049	0.050	0.050	0.014	0.015
BH2					
Ratio	35.338	15.225	15.897	2.2230	0.9578
STD	0.046	0.015	0.017	0.0009	0.0004
%RSD	0.13	0.10	0.11	0.043	0.044
Theo %RSD	0.052	0.053	0.053	0.015	0.016

Theo %RSD = theoretical relative standard deviation from Poisson counting statistics

7.3.4 Mass Bias

In ICP-MS analysis, isotope ratios observed or measured may deviate from the "true" value as a function of difference in mass between the two isotopes analysed. This effect is called mass bias and its value may be either positive or negative (Jarvis et al. 1992).

To the extent that all the bias effects vary smoothly with mass, it is normally adequate to lump them together in one correction and say that the measured ratio of isotopes A and B, $(A/B)_m$ is related to the true ratio, $(A/B)_t$, by a function of the mass difference, n, between A and B. The exact functional form of the effective bias can only be determined experimentally and will vary with the particulars of the individual ICP-MS system (Price Russ 1989). In practical terms it is only necessary to assume a functional form which fits the data to the limit of precision. The most common assumption is that bias is a constant amount per mass unit; therefore, the instrumental mass bias can be calculated from the following equation (Price Russ 1989):

$$(A/B)_m = (A/B)_t(1 + a)^n$$

where a is the bias per atomic mass unit (amu). In practical work, a linear approximation to this function described by the following equation:

$$(A/B)_m = (A/B)_t(1 + an)$$

is usually used.

In this work, the instrument mass bias was measured by comparing the measured lead isotopic ratios to the certified ratios for NIST common lead isotope standard SRM 981. **Table 7.8** shows instrument mass bias for lead isotope ratios. All of the values obtained for mass bias in this study were negative. Instrumental mass bias (a) was in the range of -0.0020 to -0.0058 amu^{-1}. The relative mass bias values are comparable to or less than the published values by either quadrupole or other model sector field ICP-MS for previous work (Begley and Sharp 1997; Stürup et al. 1997).

The relative mass bias can be expected to remain constant to a precision of ±0.1% amu^{-1} over a period of an eight-hour analytical run under a fixed instrumental parameters and lower mass bias values are often found for the heavier elements due to less mass discrimination (Price Russ 1989).

In the present work, instrument mass bias was corrected using NIST Pb 981 as an external standard. The other alternative, using a Tl internal standard for instrument mass bias correction, was not investigated in this study. The method involves measuring another isotope (Tl) which may behave in a different fashion to Pb whilst also increasing the analysis time for each scan (time which could be spent accumulating Pb data). The internal correction approach has an advantage, however, of continuously monitoring the mass discrimination for each individual sample. This method was outlined in detail by Begley and Sharp (1997).

Table 7.8. Instrument mass bias for lead isotope ratios*

Ratio	a amu^{-1}	%a amu^{-1}
$^{208}Pb/^{204}Pb$	-0.0028 to -0.0042	-0.28 to -0.42
$^{207}Pb/^{204}Pb$	-0.0020 to -0.0058	-0.20 to -0.58
$^{206}Pb/^{204}Pb$	-0.0041 to -0.0067	-0.41 to -0.67
$^{208}Pb/^{206}Pb$	-0.0013 to -0.0026	-0.13 to -0.26
$^{207}Pb/^{206}Pb$	-0.0038 to -0.0056	-0.38 to -0.56

* Lead concentrations used in this experiment were 4.35, 13.05, 21.7, 30, 39 and 47 ng g^{-1} respectively.

7.3.5 Effect of Concentration

From the experimental work, it is recommended that the lead concentration in the testing solution should be controlled in a range of 5 to 50 ng g^{-1}. At low lead concentrations, the accuracy of any isotopic ratio is limited by counting statistics. It has been noted that the signal intensity (counts s^{-1} per ng g^{-1}) for ^{204}Pb was very weak for any lead solutions below 5 ng g^{-1} Pb. In that case, ^{204}Pb concentration was less than 0.07ng g^{-1} in the testing solution and was actually below the detection limit (1.55 ng g^{-1} for Pb) by the sector field ICP-MS technique. It was also observed that

the signal intensity for ^{204}Pb was less than 1911 counts s^{-1} per ng g^{-1} ^{204}Pb. On the other hand, at high lead concentrations (> 50 ng g^{-1} Pb), signal intensity was so strong that the counting statistic was off scale for recording the intensities for ^{208}Pb, and the mass peak for ^{208}Pb was virtually truncated with the detector under the counting mode. ^{208}Pb concentration was higher than 26.2 ng g^{-1} in the testing solution. The signal intensity for ^{208}Pb in the mass spectrum was found to be higher than 60749 counts s^{-1} per ng g^{-1} ^{208}Pb.

In the present study, the effect of different lead concentrations (4.35, 13.05, 21.7, 30, 39 and 47 ng g^{-1} respectively) on measured lead isotopic ratios for the Broken Hill galena sample has been investigated. Triplicate analyses were performed for each lead concentration. The instrumental mass bias was corrected against NIST Pb SRM 981 standard. The relationship between lead isotopic ratios of $^{208}Pb/^{204}Pb$, $^{207}Pb/^{204}Pb$, $^{206}Pb/^{204}Pb$, $^{208}Pb/^{206}Pb$ and $^{207}Pb/^{206}Pb$ and lead concentrations are shown in **Figures 7.4 to 7.8.**

The observed lead isotopic ratios were also compared with conventional TIMS results. The results obtained show that:

(1) the difference for the $^{208}Pb/^{204}Pb$ ratio value between sector field ICP-MS and TIMS techniques was from -0.188 (Pb concentration = 4.35 ng g^{-1}) to 0.078 (Pb concentration = 47 ng g^{-1}), and the precision (%RSD) for the measurement was in the range of 0.012 to 0.07. As can be seen from **Figure 7.4**, the optimum lead concentration for the measurement of $^{208}Pb/^{204}Pb$ in testing solutions was between 30 and 40 ng g^{-1}.

(2) the difference for the $^{207}Pb/^{204}Pb$ ratio value between sector field ICP-MS and TIMS techniques was from -0.007 (Pb concentration = 39 ng g^{-1}) to 0.024 (Pb concentration = 47 ng g^{-1}), and the precision (%RSD) for the measurement was in the range of 0.011 to 0.039. **Figure 7.5** shows that the optimum lead concentration for the measurement of $^{207}Pb/^{204}Pb$ ratio in testing solutions was between 5 and 40 ng g^{-1}.

(3) the difference for the $^{206}Pb/^{204}Pb$ ratio value between sector field ICP-MS and TIMS techniques was from -0.008 (Pb concentration = 39 ng g^{-1}) to 0.039 (Pb concentration = 47 ng g^{-1}), and the precision (%RSD) for the measurement was in the range of 0.003 to 0.029. **Figure 7.6** shows that the optimum lead concentration for the measurement of $^{206}Pb/^{204}Pb$ ratio in testing solutions was similar to that for $^{207}Pb/^{204}Pb$ ratio (between 5 and 40 ng g^{-1} Pb).

(4) the difference for the $^{208}Pb/^{206}Pb$ ratio value between sector field ICP-MS and TIMS techniques was from -0.011 (Pb concentration = 4.35 ng g^{-1}) to -0.0006 (Pb concentration = 47 ng g^{-1}), and the precision (%RSD) for the measurement was in the range of 0.0004 to 0.0069. **Figure 7.7** shows that the optimum lead concentration for the measurement of $^{208}Pb/^{207}Pb$ ratio in testing solutions was between 30 and 50 ng g^{-1}.

(5) the difference for the $^{207}Pb/^{206}Pb$ ratio value between sector field ICP-MS and TIMS techniques was from -0.00095 (Pb concentration = 47 ng g^{-1}) to 0.0006 (Pb concentration = 21.7 ng g^{-1}), and the precision (%RSD) for the measurement was in the range of 0.00021 to 0.0015. **Figure 7.8** shows that the optimum lead concentration for the measurement of $^{207}Pb/^{204}Pb$ ratio in testing solutions was between 5 and 40 ng g^{-1}.

It is clear from the above summary that the lead concentration for any geological samples should be controlled in the range of 10 to 50 ng g^{-1} in order to obtain accurate values for lead isotopic ratios using the proposed sector field ICP-MS technique (the optimum concentration for the measurement of all lead isotopic ratios is between 30 and 40 ng g^{-1}).

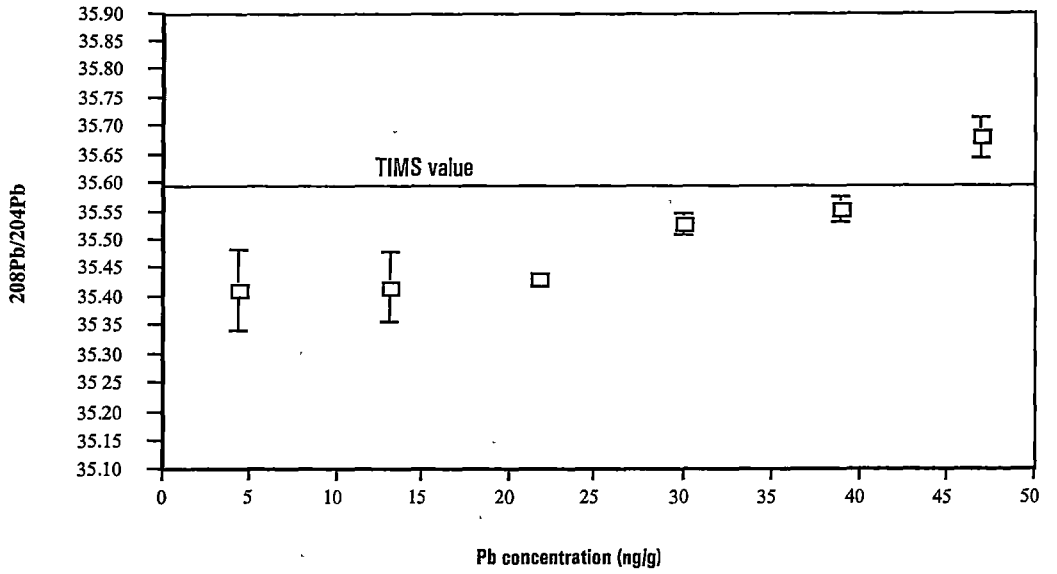

Figure 7.4. Relationship between $^{208}Pb/^{204}Pb$ ratio and lead concentrations. The error bars represent one standard deviation of the average result from triplicate analyses. Note that values shown were corrected for mass bias using SRM Pb 981.

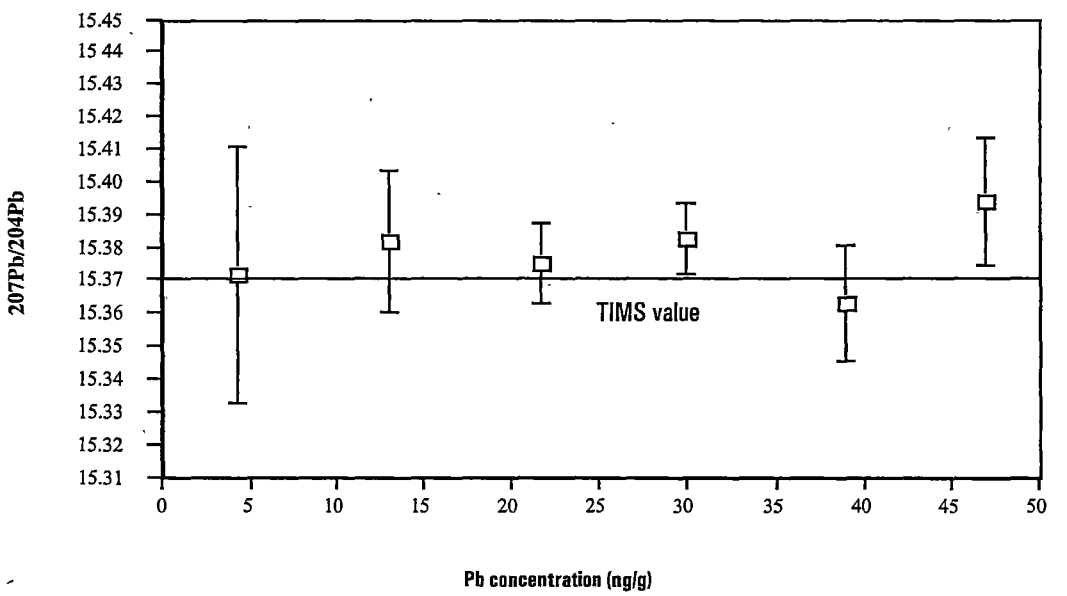

Figure 7.5. Relationship between $^{207}Pb/^{204}Pb$ ratio and lead concentrations. The error bars represent one standard deviation of the average result from triplicate analyses. Note that values shown were corrected for mass bias using SRM Pb 981.

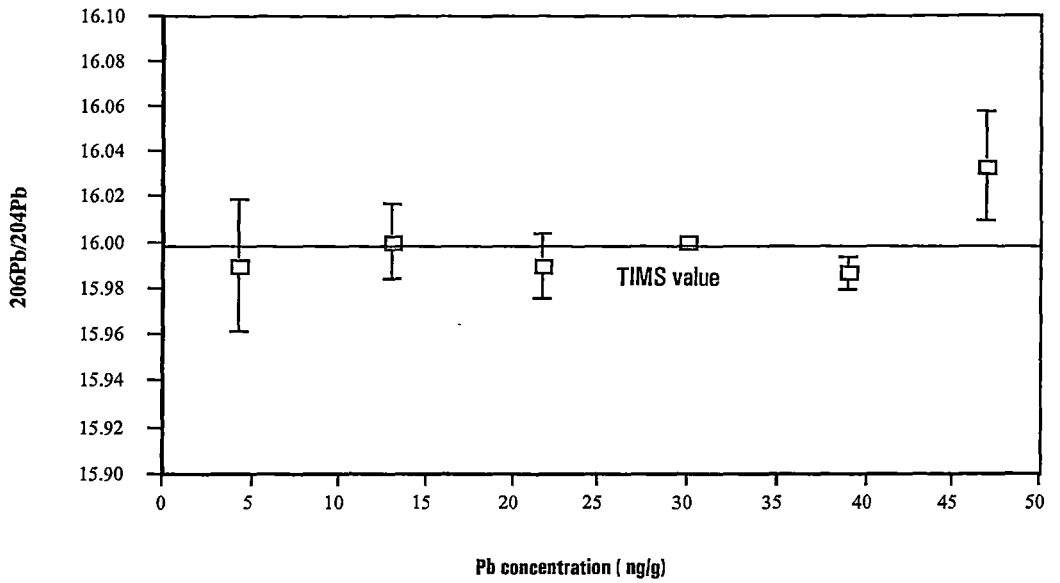

Figure 7.6. Relationship between $^{206}Pb/^{204}Pb$ ratio and lead concentrations. The error bars represent one standard deviation of the average result from triplicate analyses. Note that values shown were corrected for mass bias using SRM Pb 981.

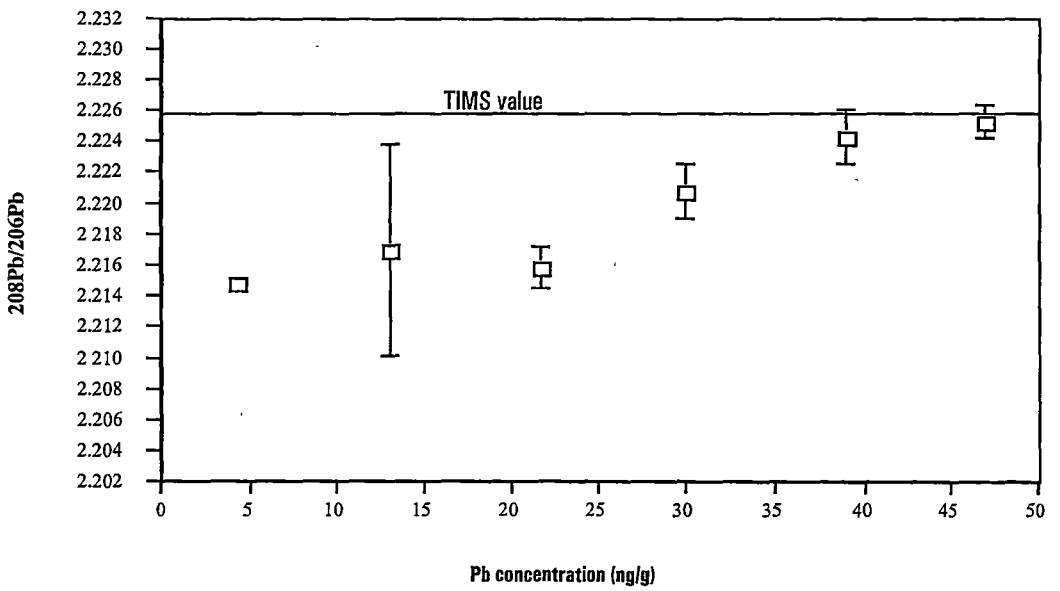

Figure 7.7. Relationship between $^{208}Pb/^{206}Pb$ ratio and lead concentrations. The error bars represent one standard deviation of the average result from triplicate analyses. Note that values shown were corrected for mass bias using SRM Pb 981.

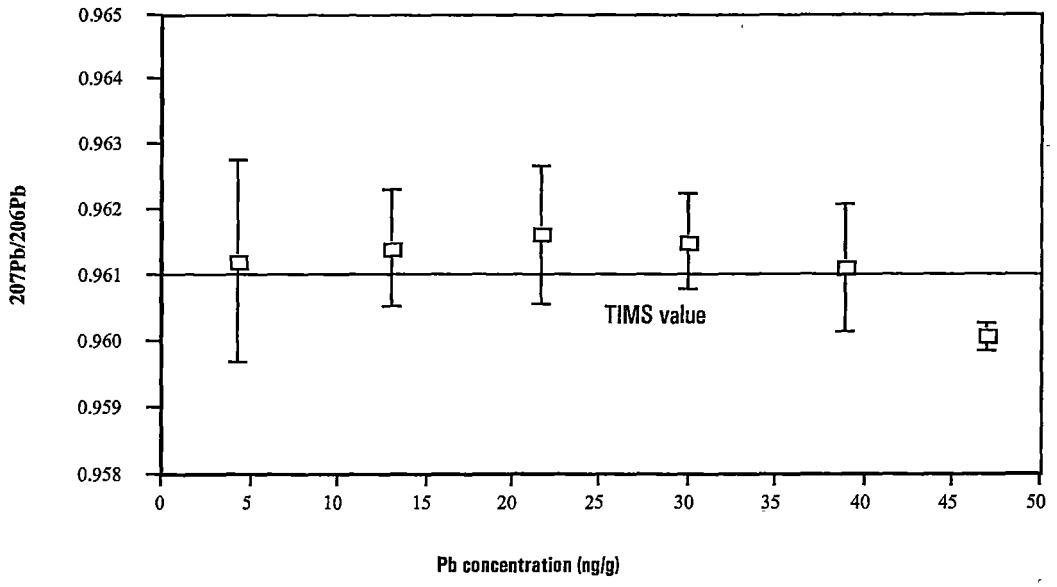

Figure 7.8. Relationship between $^{207}Pb/^{206}Pb$ ratio and lead concentrations. The error bars represent one standard deviation of the average result from triplicate analyses. Note that values shown were corrected for mass bias using SRM Pb 981.

7.3.6 Mercury Interference on Lead Isotopic Ratios

In this investigation, the sector field ICP-MS was operated at low resolution, in which mode, the instrument provides the most intense signals with flat topped peaks, which are desirable for increased measurement accuracy. However, a disadvantage for the Pb isotope ratio work is that ^{204}Pb (1.4% abundance) suffers from an interference from ^{204}Hg (6.85% abundance), which cannot be separated by the sector field ICP-MS at the low resolution setting (ie signals from both species overlap). Theoretically, all of Hg major isotopes (^{198}Hg, ^{199}Hg, ^{200}Hg, ^{201}Hg, and ^{202}Hg) can be used for the correction of any interference on ^{204}Hg. However, most of Hg major isotopes suffer from interferences of tungsten oxides ($^{182}W^{16}O$, $^{183}W^{16}O$, $^{184}W^{16}O$, and $^{186}W^{16}O$, respectively) (Longerich et al. 1992). Although ^{18}O (0.038% abundance) and ^{17}O (0.2% abundance) are low abundance isotopes of oxygen, it has also been reported that $^{183}W^{18}O$ and $^{184}W^{17}O$ give interference on ^{201}Hg (Finnigan MAT ICP-MS Interference Table). Tungsten contaminant can be around 40 $\mu g\ g^{-1}$ up to as high as more than 500 $\mu g\ g^{-1}$ if sample is prepared in tungsten crushing mills. In order to find the most appropriate way for the correction of ^{204}Hg on ^{204}Pb, the

^{201}Hg, and ^{202}Hg isotopes were chosen and investigated both with and without the presence of tungsten.

7.3.6.1 Mercury Interference

From previous work, it is known that BH2 (a Broken Hill galena) does not contain appreciable levels of mercury and tungsten (intensities at ^{201}Hg and ^{202}Hg are normally less than 115 and 230 cps in the mass spectrum). In this study, different concentrations (0, 2.5, 5.0, 7.5, and 10 ng g^{-1}) of Hg have been added into constant BH2 45 ng g^{-1} Pb solutions. Considering a dilution factor of 1000 (0.1 g sample powder in 100 ml finally solution), the Hg concentrations used in this study are equivalent to up to 10 μg g^{-1} Hg concentration in solid samples. Due to the strong memory effect of mercury, it took 15 to 30 minutes to wash the average peak intensity at ^{202}Hg down to under 300 cps with 5% HCl + 5% HNO_3 rinse solution. Therefore, the data acquisitions were carried out manually, one by one. NIST Pb 981 (about 45 ng g^{-1}) solution was used to correct any instrumental mass bias for the Pb isotope ratios for BH2. A comparison of lead isotopic ratios of uncorrected, ^{201}Hg corrected and ^{202}Hg corrected at different mercury concentrations by sector field ICP-MS with TIMS values is summarised in **Table 7.9**.

Table 7.9 shows that the presence of mercury in testing solutions interferes with lead isotopic ratios dramatically. Due to the overlap of the two isotopes in their mass spectra, ^{204}Hg enhances ^{204}Pb intensity in the mass spectrum of lead, so that values of lead isotopic ratios decrease with the increase of mercury concentration without mercury correction. Even in the presence of 2.5 ng g^{-1} Hg in testing solution, ^{204}Pb isotope suffers severely from ^{204}Hg isotope overlap, which produces differences of the lead isotopic ratios measured by sector field ICP-MS and TIMS at -1.0839, -1.0388, and -2.3666 for $^{206}Pb/^{204}Pb$, $^{207}Pb/^{204}Pb$, and $^{208}Pb/^{204}Pb$ respectively. At higher mercury concentration in testing solutions, the differences become even greater (-3.6893, -3.0553, and -8.1729 for $^{206}Pb/^{204}Pb$, $^{207}Pb/^{204}Pb$, and $^{208}Pb/^{204}Pb$ respectively for 10 ng g^{-1} mercury in testing solution).

Table 7.9. A comparison of lead isotopic ratios of uncorrected, ^{201}Hg corrected and ^{202}Hg corrected at different mercury concentrations by sector field ICP-MS with TIMS values

Hg conc	Sector field ICP-MS						TIMS
ng g^{-1}	206/204 uncor	%RSD n = 3	206/204 ^{201}Hg cor	%RSD n = 3	206/204 ^{202}Hg cor	%RSD n = 3	values
0.0	16.000	0.018	16.000	0.018	16.000	0.018	15.994
2.5	14.910	0.11	16.041	0.086	16.043	0.091	
5.0	13.895	0.56	16.033	0.055	16.032	0.055	
7.5	13.043	0.15	16.024	0.11	16.027	0.13	
10.0	12.315	0.54	16.053	0.11	16.057	0.005	
	207/204 uncor	%RSD n = 3	207/204 ^{201}Hg cor	%RSD n = 3	207/204 ^{202}Hg cor	%RSD n = 3	
0.0	15.377	0.007	15.377	0.007	15.377	0.007	15.37
2.5	14.331	0.13	15.418	0.073	15.420	0.087	
5.0	13.353	0.58	15.403	0.043	15.412	0.097	
7.5	13.043	0.15	15.403	0.11	15.406	0.13	
10.0	12.314	0.54	15.426	0.12	15.430	0.016	
	208/204 uncor	%RSD n = 3	208/204 ^{201}Hg cor	%RSD n = 3	208/204 ^{202}Hg cor	%RSD n = 3	
0.0	35.636	0.075	35.638	0.075	35.638	0.075	35.599
2.5	33.232	0.12	35.669	0.10	35.701	0.10	
5.0	31.023	0.75	35.697	0.030	35.696	0.030	
7.5	29.064	0.081	35.703	0.029	35.706	0.057	
10.0	27.426	0.521	35.732	0.034	35.744	0.063	

conc = concentration.

uncor = uncorrected.

cor = corrected.

%RSD = relative standard deviation.

n = number of measurements.

206/204 = $^{206}Pb/^{204}Pb$; 207/204 = $^{207}Pb/^{204}Pb$; 208/204 = $^{208}Pb/^{204}Pb$.

TIMS values were measured at the CSIRO laboratory in New South Wales and provided by Dr Peter McGoldrick (CODES, University of Tasmania).

However, this interference of mercury on Pb isotope ratios can be mathematically corrected using the intensity of either ^{201}Hg or ^{202}Hg if there is no tungsten in testing solutions. Generally speaking, the differences between the corrected lead isotopic ratios by sector field ICP-MS and ratios obtained by TIMS were found to be less the 0.05 for $^{206}Pb/^{204}Pb$ and $^{207}Pb/^{204}Pb$, and less than 0.1 for $^{208}Pb/^{204}Pb$. The slight increase in lead isotopic ratios at the high mercury concentration (higher than 7.5 ng g^{-1}) was attributed to the memory effect. In this investigation, a gradual increase (or accumulation) in mercury signals has been observed despite a wash time of more than 30 minutes.

In addition, good precisions were found in the triplicate analyses with both ^{201}Hg and ^{202}Hg corrections. In general, the precision (%RSD) for $^{206}Pb/^{204}Pb$ and $^{207}Pb/^{204}Pb$ was better than 0.10 and for $^{208}Pb/^{204}Pb$ better than 0.075.

7.3.6.2 Tungsten Interference

As discussed at the beginning of this section, most of mercury isotopes (^{198}Hg, ^{199}Hg, ^{200}Hg, ^{201}Hg, and ^{202}Hg) suffer from the interference of tungsten oxides ($^{182}W^{16}O$, $^{183}W^{16}O$, $^{184}W^{16}O$, $^{183}W^{18}O$, $^{184}W^{17}O$ and $^{186}W^{16}O$). Therefore, these tungsten oxides will interfere with lead isotopic ratios indirectly whenever mercury corrections are performed. In order to find out the appropriate Hg isotopes for the corrections of lead isotopic ratios, the overlaps of $^{183}W^{18}O$ and $^{184}W^{17}O$ on ^{201}Hg and $^{186}W^{16}O$ on ^{202}Hg have been investigated in the present work. The corrections of lead isotopic ratios were carried out at 201 amu (atomic mass unit) for $^{183}W^{18}O$ and $^{184}W^{17}O$ and at 202 amu for $^{186}W^{16}O$ to investigate any effect on lead isotopic ratios without appreciable levels of mercury in testing solutions. Similarly, BH2 and NIST Pb 981 were used as testing sample and standard, respectively. Lead concentration was controlled at 45 ng g^{-1} in all working solutions (including both testing solution and standard). The wash time used for the test was 3 minutes, and 5% HNO_3 was used as the wash solution. A comparison of lead isotopic ratios of uncorrected, ^{201}Hg corrected and ^{202}Hg corrected for different tungsten concentrations by sector field ICP-MS with TIMS values is presented in **Table 7.10**.

Table 7.10. A comparison of lead isotopic ratios of uncorrected, ^{201}Hg corrected and ^{202}Hg corrected at different tungsten concentrations by sector field ICP-MS with TIMS values

W conc	Sector field ICP-MS						TIMS
ng g^{-1}	206/204 uncor	%RSD n = 3	206/204 ^{201}Hg cor	%RSD n = 3	206/204 ^{202}Hg cor	%RSD n = 3	values
0	15.975	0.23	15.975	0.23	15.975	0.23	15.994
10	15.995	0.34	15.993	0.34	16.014	0.33	
20	16.014	0.16	16.014	0.17	16.056	0.18	
40	16.016	0.24	16.011	0.13	16.101	0.24	
80	16.022	0.13	16.021	0.025	16.196	0.14	
120	15.990	0.088	16.006	0.080	16.249	0.049	
160	16.023	0.071	16.033	0.048	16.347	0.20	
	207/204 uncor	%RSD n = 3	207/204 ^{201}Hg cor	%RSD n = 3	207/204 ^{202}Hg cor	%RSD n = 3	
0	15.360	0.14	15.360	0.14	15.360	0.14	15.37
10	15.387	0.26	15.392	0.19	15.381	0.30	
20	15.390	0.14	15.390	0.16	15.430	0.16	
40	15.392	0.23	15.387	0.12	15.474	0.24	
80	15.404	0.16	15.403	0.093	15.570	0.12	
120	15.382	0.11	15.398	0.11	15.632	0.068	
160	15.394	0.076	15.405	0.090	15.704	0.26	
	208/204 uncor	%RSD n = 3	208/204 ^{201}Hg cor	%RSD n = 3	208/204 ^{202}Hg cor	%RSD n = 3	
0	35.604	0.10	35.604	0.098	35.604	0.10	35.599
10	35.620	0.29	35.634	0.34	35.660	0.28	
20	35.623	0.10	35.648	0.11	35.765	0.20	
40	35.629	0.072	35.662	0.12	35.861	0.22	
80	35.671	0.042	35.694	0.041	36.051	0.085	
120	35.638	0.14	35.655	0.076	36.218	0.046	
160	35.632	0.067	35.683	0.025	36.409	0.25	

conc = concentration; uncor = uncorrected; cor = corrected; %RSD = relative standard deviation; n = number of measurements; 206/204 = $^{206}Pb/^{204}Pb$; 207/204 = $^{207}Pb/^{204}Pb$; 208/204 = $^{208}Pb/^{204}Pb$; TIMS values were measured at the CSIRO laboratory in New South Wales and provided by Dr Peter McGoldrick (CODES, University of Tasmania).

Comparing the uncorrected lead isotopic ratios by sector field ICP-MS with TIMS values, it is obvious that no corrections on the lead isotopic ratios are necessary over the range of tungsten concentrations from 0 to 160 ng g^{-1}. The differences between sector field ICP-MS and conventional TIMS Pb isotopic values were less than ±0.029, ± 0.035, and ±0.072 for $^{206}Pb/^{204}Pb$, $^{207}Pb/^{204}Pb$, and $^{208}Pb/^{204}Pb$, respectively, and precisions (%RSD) were from 0.067 to 0.34 on the basis of triplicate analyses for different tungsten concentrations.

Good agreement between sector field ICP-MS and conventional TIMS Pb isotopic ratio values has also been found when ^{201}Hg isotope corrections were performed. Very similar accuracy and precision between uncorrected and ^{201}Hg corrected can also be seen in **Table 7.11**. In other words, the enhancement (or contribution) of $^{183}W^{18}O$ and $^{184}W^{17}O$ on ^{201}Hg intensity in the mass spectrum is negligible under the experimental conditions.

Big differences between sector field ICP-MS and conventional TIMS Pb isotopic values were observed when isotope corrections at 202 amu on ^{204}Pb were applied. As a rule, $^{206}Pb/^{204}Pb$, $^{207}Pb/^{204}Pb$ and $^{208}Pb/^{204}Pb$ ratios increase with increasing tungsten concentration in testing solutions. The reason for the increase is that the tungsten oxide $^{186}W^{16}O$ from the two major isotopes (^{186}W abundance 28.6% and ^{16}O abundance 99.76%) enhances the mass spectrum intensity at 202 amu, and the enhancement increases with increasing tungsten concentration in testing solutions, although tungsten oxide does not actually make any contribution to the intensity of ^{204}Pb. When mathematical corrections are carried out according to the $^{186}W^{16}O$ intensity at 202 amu, the ^{204}Pb intensity is actually subtracted incorrectly, which raises the lead isotopic ratios of $^{206}Pb/^{204}Pb$, $^{207}Pb/^{204}Pb$ and $^{208}Pb/^{204}Pb$. It can, therefore, be concluded that mathematical corrections on ^{204}Pb cannot be performed at 202 amu when tungsten is present in testing solutions. This conclusion is also in general agreement with the early work using the quadrupole ICP-MS done by Longerich et al. (1992).

Table 7.11. A comparison of lead isotopic ratios of uncorrected, ^{201}Hg corrected and ^{202}Hg corrected under the co-presence of mercury and tungsten by sector field ICP-MS with TIMS values (Hg = 2.5 ng g^{-1} in all testing solutions)

W conc	Sector field ICP-MS						TIMS
ng g^{-1}	206/204 uncor	%RSD n = 3	206/204 ^{201}Hg cor	%RSD n = 3	206/204 ^{202}Hg cor	%RSD n = 3	values
0	14.960	0.26	16.017	0.16	16.019	0.15	15.994
50	14.902	0.15	15.997	0.11	16.055	0.12	
100	14.974	0.12	16.017	0.066	16.136	0.15	
150	14.933	0.25	16.017	0.16	16.184	0.19	
200	15.012	0.36	16.038	0.12	16.258	0.14	
	207/204 uncor	%RSD n = 3	207/204 ^{201}Hg cor	%RSD n = 3	207/204 ^{202}Hg cor	%RSD n = 3	
0	14.390	0.21	15.408	0.11	15.409	0.13	15.37
50	14.328	0.21	15.382	0.18	15.437	0.19	
100	14.384	0.11	15.391	0.075	15.501	0.12	
150	14.356	0.23	15.396	0.13	15.559	0.18	
200	14.422	0.26	15.411	0.092	15.614	0.032	
	208/204 uncor	%RSD n = 3	208/204 ^{201}Hg cor	%RSD n = 3	208/204 ^{202}Hg cor	%RSD n = 3	
0	33.353	0.19	35.652	0.059	35.649	0.065	35.599
50	33.202	0.15	35.644	0.11	35.772	0.12	
100	33.348	0.12	35.682	0.10	35.936	0.14	
150	33.291	0.27	35.682	0.066	36.075	0.20	
200	33.439	0.31	35.647	0.086	36.215	0.13	

conc = concentration.

uncor = uncorrected.

cor = corrected.

%RSD = relative standard deviation.

n = number of measurements.

206/204 = $^{206}Pb/^{204}Pb$; 207/204 = $^{207}Pb/^{204}Pb$; 208/204 = $^{208}Pb/^{204}Pb$.

TIMS values were measured at the CSIRO laboratory in New South Wales and provided by Dr Peter McGoldrick (CODES, University of Tasmania).

7.3.6.3 Mercury and Tungsten Interference

In this section, the combined interference of mercury and tungsten in solutions on lead isotopic ratios is investigated. BH2 and NIST Pb 981 were still used as the testing sample and instrumental calibration standard. Lead concentrations were controlled at about 45 ng g^{-1} in all working solutions. Mercury concentration in this investigation was kept at a consistent level of 2.5 ng g^{-1} in all testing solutions, whereas different concentrations of tungsten (from 0 to 200 ng g^{-1}) were added into a series of BH2 (Pb = 45 ng g^{-1}) + Hg (Hg = 2.5 ng g^{-1}) solutions. The rinse solution was 5% HCl + 5% HNO_3. A wash time of 15 minutes was applied based on previous experience with the mercury memory effect. A comparison of lead isotopic ratios of uncorrected, ^{201}Hg corrected and ^{202}Hg corrected under the co-presence of mercury and tungsten by sector field ICP-MS with conventional TIMS values is given **Table 7.11**. From this table it can be seen that:

(1) The uncorrected lead isotopic ratios by sector field ICP-MS are lower than conventional TIMS values due to the ^{204}Hg enhancement on ^{204}Pb intensity. For 2.5 ng g^{-1} Hg in testing solutions, the differences between sector field ICP-MS and TIMS techniques uncorrected lead isotopic ratios were more than -0.982, -0.948 and -2.160 for $^{206}Pb/^{204}Pb$, $^{207}Pb/^{204}Pb$ and $^{208}Pb/^{204}Pb$, respectively.

(2) The lead isotopic ratios measured by sector field ICP-MS were higher than conventional TIMS values when ^{202}Hg was used for the mathematical corrections of ^{204}Pb isotope intensity in the mass spectrum under the co-presence of mercury and tungsten in testing solutions. The reason for these higher results is that tungsten oxide ($^{186}W^{16}O$) enhances the ^{202}Hg isotope intensity and results in the over-correction of ^{204}Pb intensity and hence, an increase in all of the lead isotopic ratios. It also can been seen that with the increase of tungsten concentration in testing solutions, the ratio values for $^{206}Pb/^{204}Pb$, $^{207}Pb/^{204}Pb$ and $^{208}Pb/^{204}Pb$ increase. The biggest differences between sector field ICP-MS and TIMS values for $^{206}Pb/^{204}Pb$, $^{207}Pb/^{204}Pb$ and $^{208}Pb/^{204}Pb$ were found to be 0.264, 0.244 and 0.616, respectively.

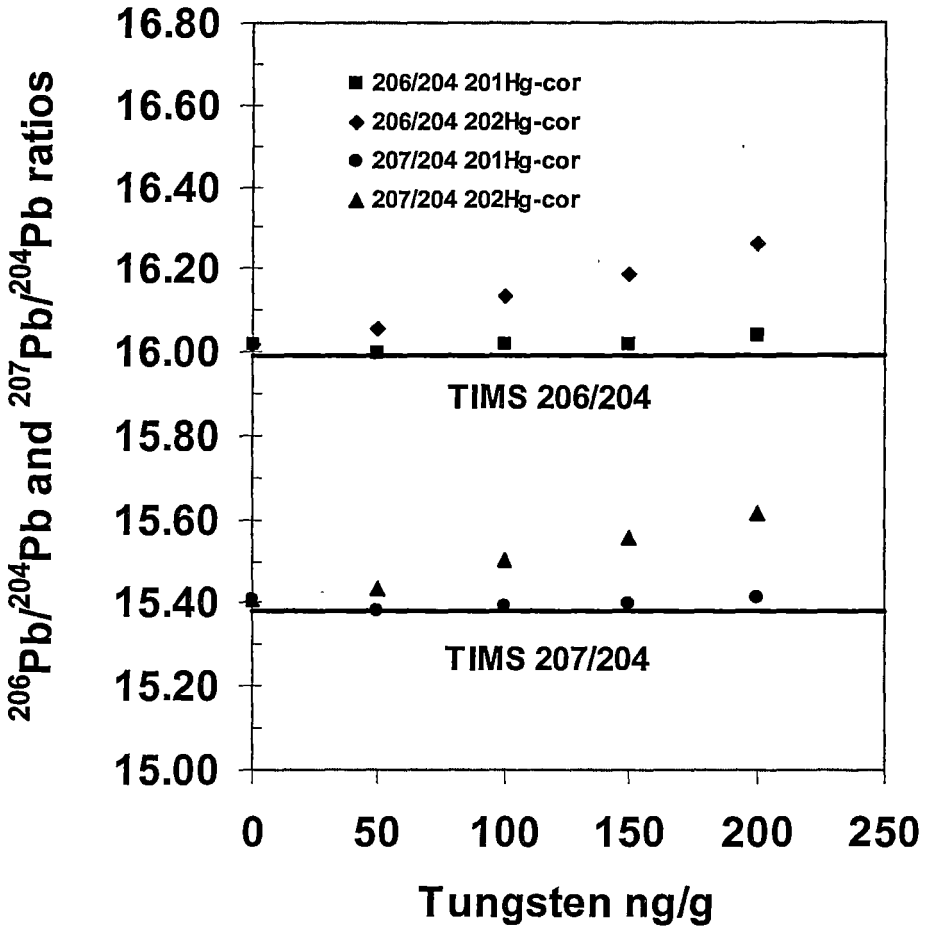

Figure 7.9. Corrections of the mercury and tungsten interferences on $^{206}Pb/^{204}Pb$ and $^{207}Pb/^{204}Pb$ using ^{201}Hg and ^{202}Hg isotopes respectively. Lead concentration was 45 ng g^{-1} and Hg concentration was 2.5 ng g^{-1} in all testing solutions. TIMS 206/204 represents $^{206}Pb/^{204}Pb$ ratio value and TIMS 207/204 represents $^{207}Pb/^{204}Pb$ ratio value obtained by the conventional TIMS technique for BH2 (a Broken Hill galena). 201Hg-cor = ^{201}Hg corrected and 202Hg cor = ^{202}Hg corrected.

(3) The interferences of mercury and tungsten on lead isotopic ratios can be mathematically corrected using ^{201}Hg isotope under the co-presence of mercury and tungsten in testing solutions. After the correction, the differences between sector field ICP-MS and TIMS values for $^{206}Pb/^{204}Pb$,

$^{207}Pb/^{204}Pb$ and $^{208}Pb/^{204}Pb$ were less than ±0.044, ±0.041 and ±0.085. Precisions (%RSD) were better than 0.16 for $^{206}Pb/^{204}Pb$, 0.18 for $^{207}Pb/^{204}Pb$, and 0.11 for $^{208}Pb/^{204}Pb$.

To summarise, the measurements of lead isotopic ratios by sector field ICP-MS suffer severely from the interference of co-present mercury in solution and thus, the lead isotopic ratios using sector field ICP-MS must be mathematically corrected for any samples with appreciable levels of mercury. In order to obtain good accuracy and precision, ^{201}Hg is the only isotope that can be used for accurate correction for ^{204}Hg interference on ^{204}Pb when both mercury and tungsten are present in sample solutions. **Figure 7.9** shows a summary of the corrections of the mercury and tungsten interferences on $^{206}Pb/^{204}Pb$ and $^{207}Pb/^{204}Pb$ using ^{201}Hg and ^{202}Hg isotopes respectively, which further highlights that the ^{201}Hg isotope can be used to correct the ^{204}Hg interference on ^{204}Pb in the present Hg and W.

7.3.7 Accuracy

In order to investigate the accuracy of the sector field ICP-MS method, equal-atom lead isotopic standard NIST Pb SRM 982 and 11 geological samples from several localities in Australia (mainly in western Tasmania) were analysed. In the present study, lead concentrations were controlled at the levels of 10 to 50 ng g^{-1}, and an effort was also made to match the lead concentration at about the same levels between lead standard and sample solutions in order to obtain good precision. NIST Pb SRM 981 was used to correct any instrumental mass bias in the investigation.

In an analytical run, each sample was alternated with NIST Pb 981 (as the correction standard). Each lead isotope ratio in the testing sample was corrected for mass bias using the average mass bias correction values measured from its two adjacent NIST Pb 981 standards.

In general, the lead isotopic ratios measured by sector field ICP-MS have been found to be in good agreement with those obtained with the CSIRO TIMS instrument. Samples were typically measured 2-3 times by sector field ICP-MS, with the Pb concentration of the NIST Pb SRM 981 external calibration standard and the

Table 7.12. A comparison of lead isotope ratios in NIST Pb RSM 982 and 11 geological samples from different localities in Australia by sector field ICP-MS and conventional TIMS

Ratio	Sample I.D.	n	This work	%RSD	TIMS	Dev	Rel Dev (%)
$^{208}Pb/^{204}Pb$							
	SRM 982	11	36.785	0.120	36.7443	0.041	0.11
	Z-5199	2	38.222		38.121	0.101	0.26
	Z-5221	3	38.402	0.128	38.417	-0.015	-0.04
	Z-5232	3	38.240	0.270	38.241	-0.001	-0.002
	Z-5237	3	38.474	0.097	38.472	0.002	0.004
	Z-5277	3	38.288	0.245	38.296	-0.008	-0.02
	BH2	15	35.530	0.289	35.599	-0.069	-0.19
	EB-1007	2	37.868		37.91	-0.042	-0.11
	EB-72086	2	37.887		37.91	-0.023	-0.06
	EB-72087	2	37.900		37.876	0.024	0.06
	EB-72096	2	38.083		38.041	0.042	0.11
	H-15	2	38.241		38.178	0.063	0.16
$^{207}Pb/^{204}Pb$							
	SRM 982	11	17.146	0.097	17.1595	-0.014	-0.08
	Z-5199	2	15.603		15.607	-0.004	-0.03
	Z-5221	3	15.651	0.100	15.622	0.029	0.19
	Z-5232	3	15.648	0.243	15.633	0.015	0.10
	Z-5237	3	15.644	0.186	15.625	0.019	0.12
	Z-5277	3	15.620	0.290	15.624	-0.004	-0.03
	BH2	15	15.383	0.162	15.37	0.013	0.09
	EB-1007	2	15.551		15.58	-0.029	-0.19
	EB-72086	2	15.583		15.58	0.003	0.02
	EB-72087	2	15.587		15.57	0.017	0.11
	EB-72096	2	15.628		15.605	0.023	0.15
	H-15	2	15.634		15.612	0.022	0.14
$^{206}Pb/^{204}Pb$							
	SRM 982	11	36.694	0.084	36.7385	-0.044	-0.12
	Z-5199	2	18.315		18.281	0.034	0.19
	Z-5221	3	18.492	0.076	18.531	-0.039	-0.21
	Z-5232	3	18.331	0.190	18.368	-0.037	-0.20
	Z-5237	3	18.550	0.291	18.561	-0.011	-0.06

Table 7.12. (Continued). A comparison of lead isotope ratios in NIST Pb RSM 982 and 11 geological samples from different localities in Australia by sector field ICP-MS and conventional TIMS

Ratio	Sample I.D.	n	This work	%RSD	TIMS	Dev	Rel Dev (%)
$^{206}Pb/^{204}Pb$							
	Z-5277	3	18.423	0.167	18.428	-0.005	-0.03
	BH2	15	16.003	0.169	15.994	0.009	0.06
	EB-1007	2	18.092		18.119	-0.027	-0.15
	EB-72086	2	18.063		18.075	-0.012	-0.06
	EB-72087	2	18.095		18.098	-0.003	-0.02
	EB-72096	2	18.198		18.191	0.007	0.04
	H-15	2	18.383		18.361	0.022	0.12
$^{208}Pb/^{206}Pb$							
	SRM 982	11	1.0048	0.0718	1.00016	0.0046	0.46
	Z-5199	2	2.0868		2.08528	0.0016	0.07
	Z-5221	3	2.0753	0.1078	2.073121	0.0022	0.11
	Z-5232	3	2.0894	0.2487	2.081936	0.0075	0.36
	Z-5237	3	2.0753	0.1052	2.072733	0.0026	0.13
	Z-5277	3	2.0841	0.0952	2.078142	0.0059	0.28
	BH2	15	2.2208	0.2339	2.2258	-0.0050	-0.23
	EB-1007	2	2.0877		2.092279	-0.0046	-0.22
	EB-72086	2	2.0929		2.097372	-0.0045	-0.21
	EB-72087	2	2.0946		2.092828	0.0018	0.08
	EB-72096	2	2.0953		2.091199	0.0041	0.20
	H-15	2	2.0780		2.079299	-0.0012	-0.06
$^{207}Pb/^{206}Pb$							
	SRM 982	11	0.4683	0.0641	0.467071	0.0012	0.26
	Z-5199	2	0.8519		0.853728	-0.0018	-0.21
	Z-5221	3	0.8459	0.1193	0.84302	0.0028	0.34
	Z-5232	3	0.8550	0.6349	0.8511	0.0039	0.46
	Z-5237	3	0.8439	0.1998	0.841819	0.0021	0.25
	Z-5277	3	0.8502	0.1011	0.84784	0.0024	0.28
	BH2	15	0.9613	0.1043	0.961	0.0003	0.03
	EB-1007	2	0.8609		0.859871	0.0010	0.12
	EB-72086	2	0.8627		0.861964	0.0007	0.08
	EB-72087	2	0.8613		0.860316	0.0010	0.12
	EB-72096	2	0.8588		0.857842	0.0010	0.11
	H-15	2	0.8502		0.85028	-0.00004	-0.005

n = number of analyses.

%RSD is the relative standard deviation of individual measurements expressed as percentage.

Dev is the deviation of the Pb isotopic ratio values obtained from this work and TIMS, negative values indicate the measured value from this work are lower than that from TIMS.

Rel Dev is the relative deviation.

TIMS's values were measured at the CSIRO laboratory in New South Wales and provided by Dr Peter McGoldrick (CODES, University of Tasmania). The isotopic compositions for SRM Pb 982 were provided by National Institute of Standards and Technology (NIST), USA.

Z-5199, 5221, 5232, 5237 and 5277 are galenas from Zeehan mineral field vein deposits and are located in Oceana, Argent#2, Swansea, Montana, and North Tasmania Mine ore deposits in Tasmania respectively. These samples were provided by Dr Paul Kitto (Centre for Ore Deposit Research, SRC, University of Tasmania).

BH2 is a galena from Broken Hill in New South Wales provided by Dr Peter McGoldrick (Centre for Ore Deposit Research, SRC, University of Tasmania).

EB-1007, 72086, 72087, and 72096 are massive sulfides (sphalerite galena) from Elliott Bay deposit in Tasmania provided by Dr J. Bruce Gemmell (Centre for Ore Deposit Research, SRC, University of Tasmania).

H-15 is a pyrite sphalerite galena from Hellyer deposit in Tasmania provided by Dr J. Bruce Gemmell (Centre for Ore Deposit Research, SRC, University of Tasmania).

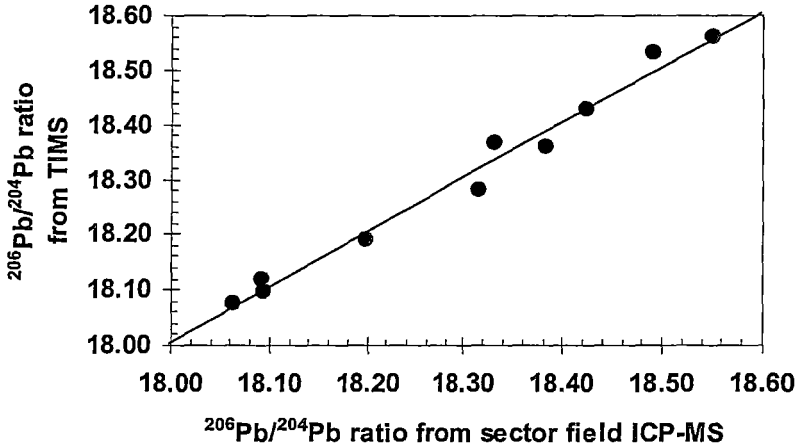

Figure 7.10. Correlation of lead isotopic ratio data between sector field ICP-MS and conventional TIMS techniques for $^{206}Pb/^{204}Pb$. Samples used for the figure were Z-5199, 5221, 5232, 5237 and 5277 galenas from Zeehan mineral field vein deposits (located in Oceana, Argent#2, Swansea, Montana, and North Tasmania Mine ore deposits in Tasmania respectively), EB-1007, 72086, 72087, and 72096 massive sulfides (sphalerite, galena) from Elliott Bay in Tasmania, and H-15 pyrite sphalerite galena from Hellyer deposit in Tasmania.

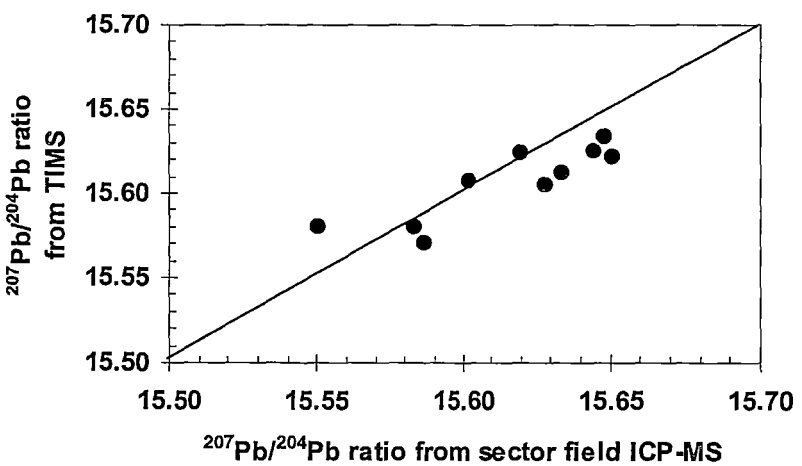

Figure 7.11. Correlation of lead isotopic ratio data between sector field ICP-MS and conventional TIMS techniques for $^{207}Pb/^{204}Pb$. Samples used for the figure were Z-5199, 5221, 5232, 5237 and 5277 galenas from Zeehan mineral field vein deposits (located in Oceana, Argent#2, Swansea, Montana, and North Tasmania Mine ore deposits in Tasmania respectively), EB-1007, 72086, 72087, and 72096 massive sulfides (sphalerite galena) from Elliott Bay deposit in Tasmania, and H-15 pyrite sphalerite galena from Hellyer deposit in Tasmania.

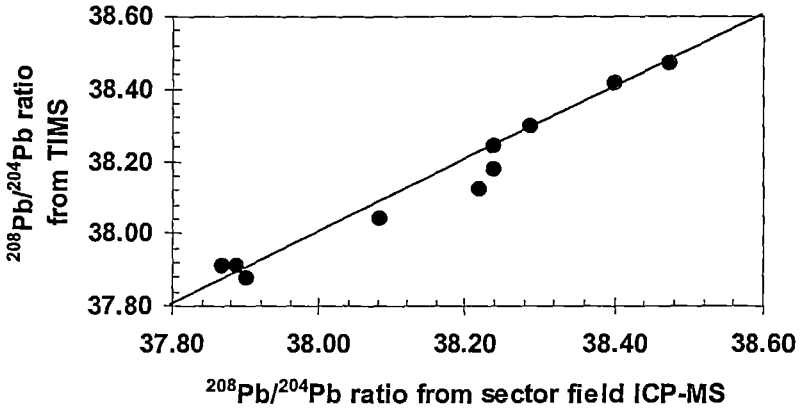

Figure 7.12. Correlation of lead isotopic ratio data between sector field ICP-MS and conventional TIMS techniques for $^{208}Pb/^{204}Pb$. Samples used for the figure were Z-5199, 5221, 5232, 5237 and 5277 galenas from Zeehan mineral field vein deposits (located in Oceana, Argent#2, Swansea, Montana, and North Tasmania Mine ore deposits in Tasmania respectively), EB-1007, 72086, 72087, and 72096 massive sulfides (sphalerite galena) from Elliott Bay deposit in Tasmania, and H-15 pyrite sphalerite galena from Hellyer deposit in Tasmania.

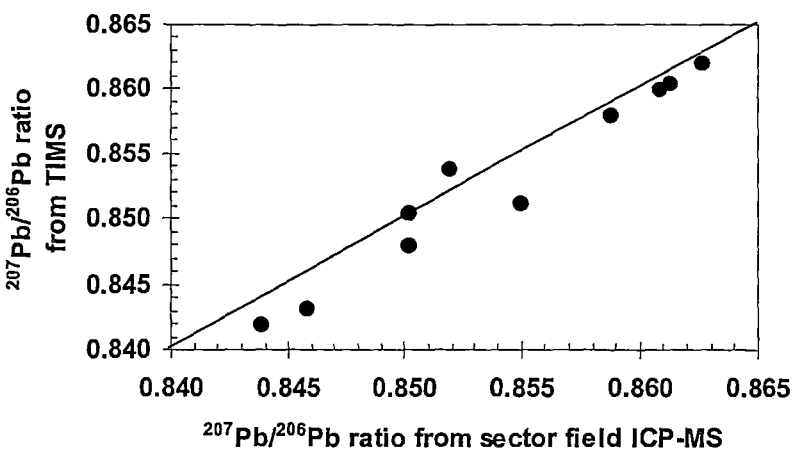

Figure 7.13. Correlation of lead isotopic ratio data between sector field ICP-MS and conventional TIMS techniques for $^{207}Pb/^{206}Pb$. Samples used for the figure were Z-5199, 5221, 5232, 5237 and 5277 galenas from Zeehan mineral field vein deposits (located in Oceana, Argent#2, Swansea, Montana, and North Tasmania Mine ore deposits in Tasmania respectively), EB-1007, 72086, 72087, and 72096 massive sulfides (sphalerite galena) from Elliott Bay deposit in Tasmania, and H-15 pyrite sphalerite galena from Hellyer deposit in Tasmania.

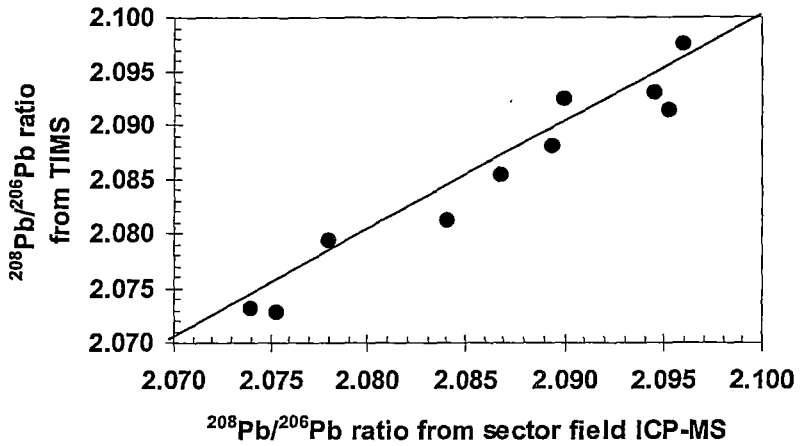

Figure 7.14. Correlation of lead isotopic ratio data between sector field ICP-MS and conventional TIMS techniques for $^{208}Pb/^{206}Pb$. Samples used for the figure were Z-5199, 5221, 5232, 5237 and 5277 galenas from Zeehan mineral field vein deposits (located in Oceana, Argent#2, Swansea, Montana, and North Tasmania Mine ore deposits in Tasmania respectively), EB-1007, 72086, 72087, and 72096 massive sulfides (sphalerite galena) from Elliott Bay deposit in Tasmania, and H-15 pyrite sphalerite galena from Hellyer deposit in Tasmania.

unknown Pb sample being closely matched. In comparison with the conventional TIMS technique, a summary of these measurements using sector field ICP-MS is reported in **Table 7.12.**

It can be seen from **Table 7.12** that the differences between sector field ICP-MS and the conventional TIMS values are generally better than ± 0.2% and fall in the range of 0.001-0.101 for $^{208}Pb/^{204}Pb$, 0.003-0.029 for $^{207}Pb/^{204}Pb$, 0.005-0.044 for $^{206}Pb/^{204}Pb$, 0.0012-0.0075 for $^{208}Pb/^{206}Pb$ and 0.00004-0.0039 for $^{207}Pb/^{206}Pb$, respectively.

In addition, from **Table 7.12**, it also can be seen that the precision (%RSD) of lead isotopic ratios measured by sector field ICP-MS was generally less than 0.3%, and was clearly better than that reported by previous works (Date and Cheung 1987; Ketterer 1992; Longerich et al. 1992) for quadrupole ICP-MS.

Finally, correlations of lead isotopic ratios for $^{206}Pb/^{204}Pb$, $^{207}Pb/^{204}Pb$, $^{208}Pb/^{204}Pb$, $^{207}Pb/^{206}Pb$ and $^{208}Pb/^{204}Pb$ between sector field ICP-MS and TIMS techniques are given in **Figures 7.10** to **7.14** by plotting sector field ICP-MS lead isotopic ratio data against the conventional TIMS values. These plots emphasise the good agreement between the two analytical techniques. In comparison with a similar figure reported by Date and Cheung (1987) for quadrupole ICP-MS, the present sector field ICP-MS technique clearly provides more accurate lead isotopic ratio data.

7.4 Geological Implications

Lead isotopes are powerful tools in exploration for mineral deposits and investigation of problems of ore genesis (Gulson 1986). However, unlike multi-element geochemical analysis, they are not commonly used when exploring for new deposits due to the expense of TIMS analysis. This work shows that lead isotope ratios can be measured relatively quickly by a sector field ICP-MS to the accuracy and precision approaching that obtained by TIMS on the same mixed acid digestion solutions normally used in commercial multi-element geochemical analysis.

With regard to accuracy and resolution needed for practical geological exploration, the tolerance limits are ±0.1 for $^{208}Pb/^{204}Pb$, ±0.05 for both $^{207}Pb/^{204}Pb$ and $^{206}Pb/^{204}Pb$ (pers. Communication, R Large, 1999). These tolerance limits are also supported by early work by Gulson (1986). In his report, the Cambrian volcanogenic massive sulfide (VMS) and post-Cambrian mineralisation in western Tasmania can be clearly distinguished when the difference of lead isotope ratios is less than 0.1 for $^{208}Pb/^{204}Pb$ and 0.05 for $^{207}Pb/^{204}Pb$ and $^{206}Pb/^{204}Pb$. Therefore, the lead isotopic ratios obtained in this study are reliable and well accepted.

In addition, the precision of the lead isotope ratios obtained by sector field ICP-MS is found to be comparable to that reported from the earlier lead isotope ratio measurements using TIMS (%RSD = 0.1% for $^{208}Pb/^{206}Pb$ and $^{206}Pb/^{204}Pb$ and 0.05% for $^{207}Pb/^{206}Pb$; Gulson et al. 1984).

Finally, the sector field ICP-MS method for lead isotope ratio analysis described here results in a considerable reduction in cost (approximately by a factor of 5) when

compared to commercial TIMS measurements. This means that the routine use of lead isotopes in geological exploration surveys for new mineral deposits is a realistic possibility.

7.5 Summary

The main conclusions that can be drawn form this chapter are:

- Lead isotope ratios in geological samples can be accurately measured by sector field ICP-MS.

- The precisions (%RSD) for $^{208}Pb/^{204}Pb$, $^{207}Pb/^{204}Pb$, $^{206}Pb/^{204}Pb$, $^{208}Pb/^{206}Pb$ and $^{207}Pb/^{206}Pb$, based on thirty analyses of three different samples (NIST SRM 981, BH2 and lead standard solution), were found to be better than 0.12, 0.11, 0.11, 0.046, and 0.048 respectively.

- There is good agreement between the lead isotope ratios determined by sector ICP-MS and TIMS. The absolute deviations for $^{208}Pb/^{204}Pb$, $^{207}Pb/^{204}Pb$, $^{206}Pb/^{204}Pb$, $^{208}Pb/^{206}Pb$ and $^{207}Pb/^{206}Pb$, based on a series of analyses of standard reference (NIST Pb SRM 982) solutions and 11 geological samples, were less than 0.101, 0.029, 0.039, 0.0075, and 0.0039 respectively.

- Lead isotope ratios with ^{204}Pb as the basis, can be corrected for the presence of Hg using ^{201}Hg. However, a loss of accuracy may result if the Hg concentration is high and any Hg memory remains from previous samples.

- The precision and accuracy achieved for the sector field ICP-MS technique can meet the general requirements for practical geological applications.

- Finally, in comparison to TIMS, the sector field ICP-MS is a relatively straightforward and cost-effective technique. For instance, lead isotope ratios can be measured using the same solutions as ordinary ICP-MS digests for trace elements analysis, which will result in significant cost reduction.

Chapter 8

DEVELOPMENT OF A QUADRUPOLE ICP-MS METHOD FOR PRECISE ANALYSIS OF LEAD ISOTOPE RATIOS IN GEOLOGICAL SAMPLES

8.1 Introduction

In the previous chapter of this project, a sector field ICP-MS method was described for the precise and accurate determination of lead isotope ratios in geological samples. In this chapter, an investigation of the possibility of measuring lead isotope ratios precisely in geological samples using a new generation of quadrupole ICP-MS (Hewlett Packard HP 4500 *plus*) is carried out in attempt to further reduce the cost of measuring lead isotope ratios. The effects of instrumental parameters (including dead time, data point, integration time, repetition etc.) on the precision of quadrupole ICP-MS Pb isotope ratio measurement are systematically investigated, and both short and long-term precision of the method are checked. The dynamic Pb concentration range of the proposed method is assessed. To conclude, the Pb isotope ratios measured by HP 4500 ICP-MS in a lead reference material and a group of selected sulfides are compared with those obtained by both sector field ICP-MS and TIMS.

8.2 Instrumentation

Figure 8.1 shows the quadrupole ICP-MS instrument used in this study, a Hewlett Packard (HP) model 4500 *plus* (Yokogawa Analytical System, Tokyo, Japan) with HP ChemStation software. A standard Babington nebuliser and Peltier-cooled glass Scott double pass spray chamber were employed. Prior to performing the Pb isotope ratio measurement, the instrument was tuned daily for sensitivity, oxide, doubly charged ion, background, resolution and axis with a 'testing solution' containing 10 ng g^{-1} of ^{7}Li, ^{89}Y, ^{140}Ce and ^{205}Tl. Typical instrumental settings are outlined in **Table 8.1**. In order to obtain accurate Pb isotope ratios, the sensitivity for 10 ng g^{-1} ^{205}Tl

'testing solution' should be more than 2 x 10^5 cps. Further details regarding this instrument have been reported elsewhere (Minnich et al. 1997; Minnich and Houk 1998; Bayón et al 1998).

Table 8.1. Typical instrumental settings

Instrument	**HP 4500 (*plus*) ICP-MS**
RF power	1160 W
RF matching	1.8 V
Nebuliser	Babington
Argon flow rates:	
Carrier	1.17-1.20 l min^{-1}
Auxiliary	1.00 l min^{-1}
Plasma	15.0 l min^{-1}
Sampling depth	7.0-7.6 mm
Peristaltic pump speed	0.1 rps
Spray chamber	Scott double-pass water cooled (2 °C)
Sampler cone	1.0 mm orifice id
Skimmer cone	0.4 mm orifice id
Sensitivity	> 2 x 10^4 counts per ng g^{-1} ^{205}Tl
Torch-H	0.1 mm
Torch-V	0.0 mm
Ion lens settings:	
Extract 1	-143 V
Extract 2	-110 V
Einzel 1,3	-100 V
Einzel 2	5 V
Omega bias	-40 V
Omega (+)	3 V
Omega (-)	-4 V
QP focus	7 V
Ion def	30 V
Plate bias	2 V
Pole bias	2 V
Discriminator	12.0 mV
EM voltage	-1770 V
Last dynode	-293 V
Resolution/Axis settings	
AMU gain	122*
AMU offset	179*
Axis gain	1.0005*
Axis offset	-0.05*

* These are the numerical values provided by the ChemStation – the control software for HP 4500 *plus* ICP-MS.

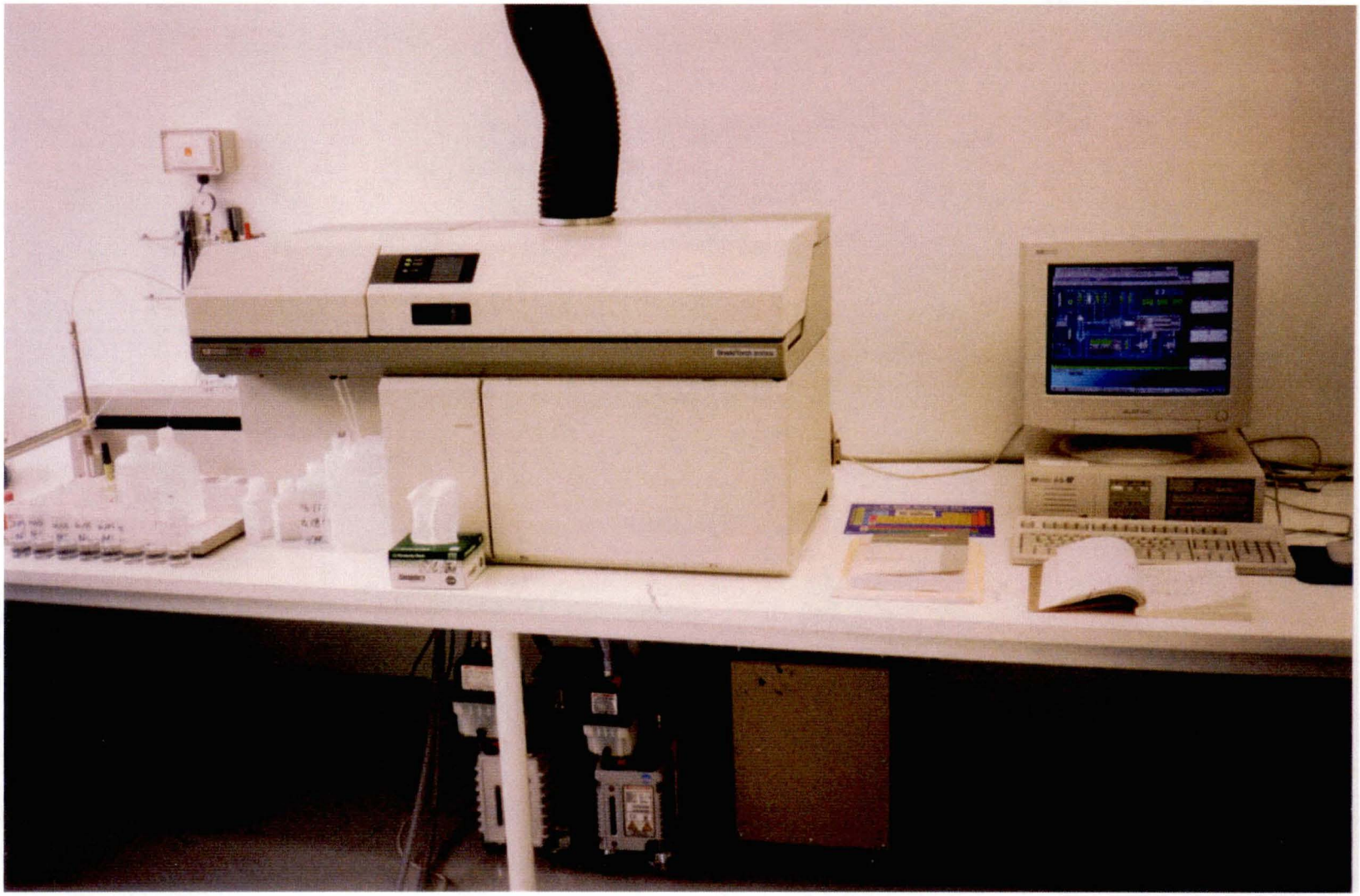

8.3 Optimisation of Instrumental Parameters

8.3.1 Dead Time Correction

In the previous chapter (**7.3.1**) of this project, instrument dead time and its correction were discussed in detail. It was found that the dead time for HR-ICP-MS was in the range of 20 to 50 ns, depending on the detector settings (Townsend et al. 1998). Like HR-ICP-MS, the instrument dead time for quadrupole ICP-MS also depends on detector settings. In the previous studies, it has been reported that most pulse counting systems shows instrument dead time of 10 to 30 ns (Begley and Sharp 1997). In order to minimise the dependence of isotope ratios on concentration and isotopic abundance, it was necessary to measure the instrument dead time before performing any actual lead isotope ratio measurement.

In the present investigation, dead time correction was conducted by measuring lead isotope ratios with 50, 100 and 200 ng g^{-1} multi-element standard solutions (QCD Analysts, USA) at dead time range of 0 to 35 ns. The relationship between dead time and Pb isotope ratios is given in **Table 8.2**. It can be seen that, at first, there was an obvious difference in $^{208}Pb/^{204}Pb$, $^{207}Pb/^{204}Pb$ and $^{206}Pb/^{204}Pb$ ratios measured using 50, 100 and 200 ng g^{-1} lead solutions respectively at dead time = 0 ns. Then increasing dead time, the difference in the isotope ratios diminished, and the measured $^{208}Pb/^{204}Pb$, $^{207}Pb/^{204}Pb$ and $^{206}Pb/^{204}Pb$ ratios for the three different lead solutions became very close at the dead time of 20 ns. With further increase of dead time, differences between the isotope ratios increased again.

Figure 8.2 shows the relationship between $^{208}Pb/^{204}Pb$ ratio and instrument dead time using 50, 100 and 200 ng g^{-1} multi-element standard solutions. It can be seen that the $^{208}Pb/^{204}Pb$ ratio was almost identical for 50, 100 and 200 ng g^{-1} multi-element standard solutions at the dead time of 22.5 ns. Therefore, the dead time was set up at 22.5 ns to minimise the effects of lead concentration and isotope abundances upon lead isotope ratios. However, instrumental dead time should be measured regularly for the accurate measurement of Pb isotope ratios as the instrumental dead time depends on the detector settings.

Table 8.2. Relationship between instrumental dead time and lead isotope ratios using 50, 100 and 200 ng g^{-1} multi-element standard solutions

Dead time	$^{208}Pb/^{204}Pb$			$^{207}Pb/^{204}Pb$			$^{206}Pb/^{204}Pb$		
(ns)	50 ng/g Pb	100 ng/g Pb	200 ng/g Pb	50 ng/g Pb	100 ng/g Pb	200 ng/g Pb	50 ng/g Pb	100 ng/g Pb	200 ng/g Pb
0	38.78	38.14	37.37	15.43	15.39	15.32	19.16	19.00	18.88
5	38.95	38.65	37.94	15.59	15.59	15.53	19.19	19.14	18.94
10	39.14	38.82	38.32	15.70	15.73	15.62	19.19	19.11	18.99
15	39.21	39.09	38.73	15.72	15.74	15.68	19.22	19.22	19.15
20	39.35	39.26	39.23	15.79	15.79	15.77	19.25	19.24	19.26
25	39.46	39.58	39.70	15.77	15.85	15.89	19.26	19.26	19.28
30	39.55	39.75	40.12	15.82	15.88	15.94	19.27	19.32	19.37
35	39.68	40.05	40.56	15.86	15.96	16.00	19.30	19.42	19.50

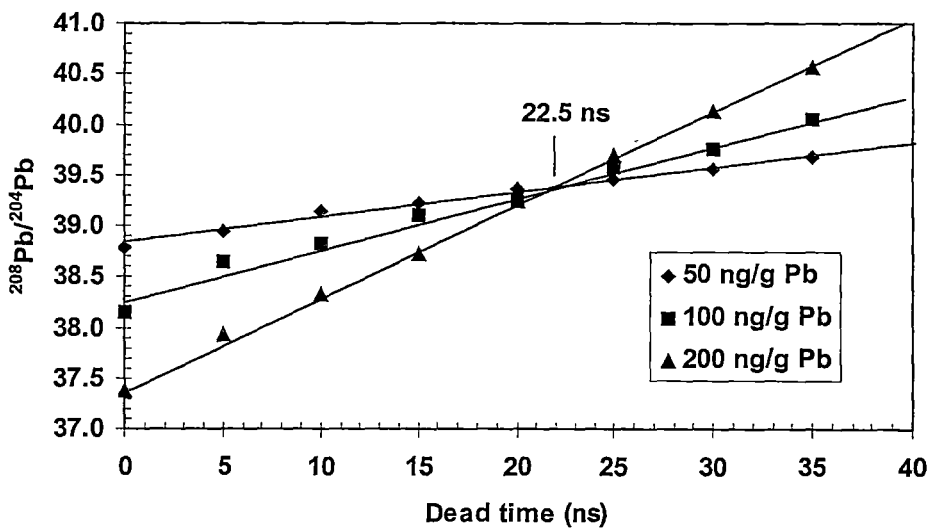

Figure 8.2. Relationship between $^{208}Pb/^{204}Pb$ ratio and instrumental dead time using 50, 100 and 200 ng g^{-1} multi-element solutions

8.3.2 Data Point

In order to determine the optimal instrument operation conditions for the precise measurement of Pb isotope ratios, the HP 4500 ICP-mass spectrometer was run at 1, 3, 6 and 20 data points per mass respectively using 25, 50 and 100 ng g^{-1} NIST SRM 981 solutions. The repetition times were fixed at 10 and the integration time per data point was set at 0.1 second. The instrument signal relative standard deviations (%RSD) for $^{208}Pb/^{204}Pb$, $^{207}Pb/^{204}Pb$, $^{206}Pb/^{204}Pb$, $^{208}Pb/^{206}Pb$ and $^{207}Pb/^{206}Pb$, summarised in **Table 8.3**, improved with the increase of data points per mass for the three lead solutions.

Table 8.3. Instrument signal relative standard deviations (%RSD) of $^{208}Pb/^{204}Pb$, $^{207}Pb/^{204}Pb$, $^{206}Pb/^{204}Pb$, $^{208}Pb/^{206}Pb$ and $^{207}Pb/^{206}Pb$ in 25, 50 and 100 ng g^{-1} Pb solutions at different data points per mass

Data points	Instrument signal relative standard deviation (%RSD)					
per mass	$^{208}Pb/^{204}Pb$	$^{207}Pb/^{204}Pb$	$^{206}Pb/^{204}Pb$	$^{208}Pb/^{206}Pb$	$^{207}Pb/^{206}Pb$	Average
25 ng g^{-1} Pb						
1	5.08	4.81	5.70	1.15	1.43	3.63
3	2.19	1.79	2.00	0.95	1.07	1.60
6	2.46	2.64	2.42	0.54	0.75	1.76
20	1.42	1.54	1.48	0.44	0.47	1.07
50 ng g^{-1} Pb						
1	3.41	3.91	3.51	1.41	1.70	2.79
3	2.44	2.50	2.13	0.81	0.97	1.77
6	2.13	2.34	2.55	0.69	0.74	1.69
20	0.90	0.68	0.83	0.58	0.51	0.70
100 ng g^{-1} Pb						
1	4.13	4.54	4.24	1.28	1.63	3.16
3	2.54	2.26	2.73	0.70	1.14	1.87
6	3.08	2.87	2.80	0.67	0.49	1.98
20	0.86	1.01	0.90	0.51	0.39	0.73

For the experimental conditions, it can be seen that the average signal %RSD of $^{208}Pb/^{204}Pb$, $^{207}Pb/^{204}Pb$, $^{206}Pb/^{204}Pb$, $^{208}Pb/^{206}Pb$ and $^{207}Pb/^{206}Pb$ decreased from 3.63

to 1.07 for 25 ng g^{-1} Pb solution, from 2.79 to 0.70 for 50 ng g^{-1} Pb solution and from 3.16 to 0.73 for 100 ng g^{-1} Pb solution. In other words, the best signal %RSD was observed at 20 data points per mass.

8.3.3 Integration Time

Integration time per data point will also have an effect on instrument signal relative standard deviation. Under the experimental conditions, the number of repetitions was 10 and the data points per mass were set at 20. The instrument signal %RSD was measured using 25 and 50 ng g^{-1} NIST SRM 981 solutions respectively.

Table 8.4. Instrument signal relative standard deviations (%RSD) of $^{208}Pb/^{204}Pb$, $^{207}Pb/^{204}Pb$, $^{206}Pb/^{204}Pb$, $^{208}Pb/^{206}Pb$ and $^{207}Pb/^{206}Pb$ in 25 and 50 ng g^{-1} Pb solutions at different integration time per data point

Integration time (sec)	Instrument signal relative standard deviation (%RSD)					
per data point	$^{208}Pb/^{204}Pb$	$^{207}Pb/^{204}Pb$	$^{206}Pb/^{204}Pb$	$^{208}Pb/^{206}Pb$	$^{207}Pb/^{206}Pb$	Average
25 ng g^{-1} Pb						
0.1	1.42	1.54	1.48	0.44	0.47	1.07
0.2.	1.20	0.72	0.90	0.45	0.41	0.74
0.3	0.63	0.68	0.51	0.36	0.31	0.50
0.4	0.57	0.63	0.56	0.43	0.34	0.51
0.5	0.77	0.99	0.99	0.42	0.28	0.69
0.6	0.64	0.78	0.83	0.38	0.43	0.61
50 ng g^{-1} Pb						
0.1	0.90	0.68	0.83	0.58	0.51	0.70
0.2.	0.82	0.78	0.97	0.47	0.65	0.74
0.3	0.62	0.43	0.46	0.40	0.34	0.45
0.4	0.56	0.76	0.57	0.31	0.48	0.54
0.5	0.68	0.58	0.71	0.61	0.65	0.65
0.6	0.52	0.58	0.69	0.53	0.43	0.55

Table 8.4 shows the instrument signal relative standard deviations (%RSD) of $^{208}Pb/^{204}Pb$, $^{207}Pb/^{204}Pb$, $^{206}Pb/^{204}Pb$, $^{208}Pb/^{206}Pb$ and $^{207}Pb/^{206}Pb$ in 25 and 50 ng g^{-1} Pb solutions at different integration times per data point. From **Table 8.4**, it can be

seen that instrument signal %RSD clearly improved when integration time increased from 0.1 to 0.3 second, but a further increase of the integration time produced no improvement in the instrument signal %RSD.

The outcome indicates that 0.1 and 0.2 seconds of integration is not enough for the detector of the mass spectrometer to give good signal %RSD values. The best average instrument signal %RSDs of $^{208}Pb/^{204}Pb$, $^{207}Pb/^{204}Pb$, $^{206}Pb/^{204}Pb$, $^{208}Pb/^{206}Pb$ and $^{207}Pb/^{206}Pb$ were found at the integration time of 0.3 second for both 25 and 50 ng g^{-1} Pb solutions. Therefore, the integration time per data point should be set at 0.3 second in order to obtain optimal instrument signal %RSD.

8.3.4 Repetition

Finally, the effect of the number of repetitions on the instrument signal %RSD values for $^{208}Pb/^{204}Pb$, $^{207}Pb/^{204}Pb$, $^{206}Pb/^{204}Pb$, $^{208}Pb/^{206}Pb$ and $^{207}Pb/^{206}Pb$ was also investigated using 25 and 50 ng g^{-1} NIST SRM 981 solutions. Based on the previous investigation, the number of data points per mass used was 20 and the integration time per data point was set at 0.3 second. The number of repetitions investigated in this study was in the range of 5 to 25. In other words, the total acquisition time for the measurement of ^{201}Hg, ^{204}Pb, ^{206}Pb, ^{207}Pb and ^{208}Pb isotopes was from 280 to 1398 seconds. **Table 8.5** shows the instrument signal relative standard deviations (%RSD) of $^{208}Pb/^{204}Pb$, $^{207}Pb/^{204}Pb$, $^{206}Pb/^{204}Pb$, $^{208}Pb/^{206}Pb$ and $^{207}Pb/^{206}Pb$ using 25 and 50 ng g^{-1} NIST Pb solutions at different repetitions per mass.

As seen in **Table 8.5**, a repetition number of 10 was high enough for good instrument signal %RSD. Further increasing the number of repetition does not seem to improve the instrument signal %RSD.

From the above discussion, it is clearly seen that optimised operation conditions are crucial to obtain good instrument signal RSD. The optimised instrument operating parameters for the measurement of Pb isotope ratios using HP 4500 ICP mass spectrometer are summarised in **Table 8.6.**

Table 8.5. Instrument signal relative standard deviations (%RSD) of $^{208}Pb/^{204}Pb$, $^{207}Pb/^{204}Pb$, $^{206}Pb/^{204}Pb$, $^{208}Pb/^{206}Pb$ and $^{207}Pb/^{206}Pb$ using 25 and 50 ng g^{-1} Pb solutions at different repetitions per mass

Repetition	Instrument signal relative standard deviation (%RSD)					
per mass	$^{208}Pb/^{204}Pb$	$^{207}Pb/^{204}Pb$	$^{206}Pb/^{204}Pb$	$^{208}Pb/^{206}Pb$	$^{207}Pb/^{206}Pb$	Average
25 ng g^{-1} Pb						
5	0.83	1.10	0.90	0.70	0.61	0.83
10	0.68	0.73	0.82	0.36	0.47	0.61
15	0.61	0.72	0.67	0.43	0.40	0.57
20	0.62	0.67	0.70	0.45	0.60	0.61
25	0.94	0.80	0.93	0.43	0.45	0.71
50 ng g^{-1} Pb						
5	0.59	0.74	0.48	0.59	0.36	0.55
10	0.62	0.43	0.46	0.40	0.34	0.45
15	0.60	0.62	0.58	0.27	0.50	0.51
20	0.53	0.47	0.56	0.30	0.39	0.45
25	0.56	0.51	0.59	0.36	0.43	0.49

Table 8.6. Optimised instrument operating parameters for the measurement of Pb isotope ratios using HP 4500 ICP mass spectrometer

Isotopes considered	^{201}Hg, ^{204}Pb, ^{206}Pb, ^{207}Pb and ^{208}Pb
Data points per mass	20
Integration time per data point	0.3 s
Number of repetition per mass	10
Detector mode	Pules counting
Detector dead time	22.5 ns
Rinse time	2 min (with 5% HNO_3)
Uptake & stabilising time	3 min
Acquisition time	~ 10 min
Total time per sample	~ 15 min

8.4 Precision

In order to assess the capability of the proposed quadrupole ICP-MS technique, both short- and long-term precisions (%RSD) for the lead isotope ratio measurement were investigated. Three lead standards were used in this work:

1. BH2 – A galena from Broken Hill, New South Wales, Australia.
2. NIST SRM 981 – Common lead isotope standard from the National Institute of Standard and Technology, USA.
3. Multi-element standard solution – Standard solution from QCD Analysts, USA.

Sample digestion method for the preparation of BH2 and NIST SRM 981 was described in Section **7.2.2**.

8.4.1 Short Term Precision

Each Pb standard solution was diluted to 50, 100 and 200 ng g^{-1} respectively. Short-term precision was calculated on the basis of 10 consecutive measurements without any mass bias correction. Lead isotope ratios were measured under the optimised operation conditions (**Table 8.6**). **Tables 8.7 – 8.9** show the Pb isotope ratio precision (%RSD) using the three different lead standards. Theoretical precision (%RSD) calculated from Poisson counting statistics represents the uncertainty associated with measurement for a single integration (Stürup et al. 1997; Begley and Sharp 1997).

It is known that the precision of isotopic ratio measurement by ICP-MS is limited not only by Poisson counting statistics but also by other sources of error, such as noise from sample introduction system (mainly from the peristaltic pump), plasma flicker, change of the environment temperature, and so on. In general, precisions are found to be 2 to 3 times greater than these calculated from the counting statistics (Stürup et al. 1997; Begley and Sharp 1997; Townsend et al. 1998). This is in general agreement with the short-term precisions obtained in the present investigation. From **Tables 8.7 – 8.9**, it can be seen that:

- the precision generally improves with increasing Pb concentration due to the limitation of the instrumental signal intensity for ^{204}Pb at low concentration. Similar precisions are observed for Pb concentrations of 100 and 200 ng g^{-1}, despite better theoretical %RSD values predicted from counting statistics at a Pb concentration of 200 ng g^{-1}. This indicates that precision is limited by both counting statistics and other sources of error (Begley and Sharp 1997; Townsend et al. 1998).

- The short-term precisions for $^{208}Pb/^{204}Pb$, $^{207}Pb/^{204}Pb$, $^{206}Pb/^{204}Pb$, $^{208}Pb/^{206}Pb$ and $^{207}Pb/^{206}Pb$ ratio values were found to be generally better than 0.15% at Pb concentrations of either 100 or 200 ng g^{-1}. In comparison with other quadrupole ICP-MS studies, these values were better than those measured using 100 ng g^{-1} Pb 981 solution in an early investigation by Longerich et al. (1992) and similar to those reported by Begley and Sharp (1997) using a 1000 ng g^{-1} Pb 981 solution. The precisions are actually comparable to those measured by sector field ICP-MS (Townsend et al. 1998 and **Chapter 7** of this thesis).

Table 8.7. Lead isotope ratio precision (short-term) and theoretical precision using BH2 digest. Lead ratios were analysed at Pb concentrations of 50, 100 and 200 ng g^{-1}. Number of analyses for each solution was 10.

	$^{208}Pb/^{204}Pb$	$^{207}Pb/^{204}Pb$	$^{206}Pb/^{204}Pb$	$^{208}Pb/^{206}Pb$	$^{207}Pb/^{206}Pb$
50 ng g^{-1} Pb					
Average ratio	36.068	15.03	16.268	2.2169	0.92385
Standard deviation	0.0916	0.0327	0.0377	0.0036	0.0029
Precision, %RSD	0.254	0.217	0.231	0.163	0.311
Theoretical %RSD	0.101	0.151	0.147	0.101	0.109
100 ng g^{-1} Pb					
Average ratio	34.901	15.452	16.210	2.1531	0.95282
Standard deviation	0.0288	0.0235	0.0200	0.0034	0.0013
Precision, %RSD	0.083	0.152	0.123	0.159	0.141
Theoretical %RSD	0.057	0.085	0.083	0.048	0.061
200 ng g^{-1} Pb					
Average ratio	34.837	15.42	16.205	2.1496	0.95147
Standard deviation	0.0435	0.0194	0.0201	0.0020	0.0007
Precision, %RSD	0.125	0.126	0.124	0.094	0.075
Theoretical %RSD	0.042	0.062	0.061	0.035	0.045

Table 8.8. Lead isotope ratio precision (short-term) and theoretical precision using NIST Pb 981. Lead ratios were analysed at Pb concentrations of 50, 100 and 200 ng g^{-1}. Number of analyses for each solution was 10.

	$^{208}Pb/^{204}Pb$	$^{207}Pb/^{204}Pb$	$^{206}Pb/^{204}Pb$	$^{208}Pb/^{206}Pb$	$^{207}Pb/^{206}Pb$
50 ng g^{-1} Pb					
Average ratio	35.166	15.345	16.828	2.0903	0.91188
Standard deviation	0.0806	0.0268	0.0312	0.0044	0.0019
Precision, %RSD	0.229	0.174	0.185	0.212	0.213
Theoretical %RSD	0.093	0.139	0.134	0.078	0.100
100 ng g^{-1} Pb					
Average ratio	36.394	15.556	16.520	2.2014	0.94165
Standard deviation	0.0680	0.0207	0.0221	0.0033	0.0016
Precision, %RSD	0.187	0.133	0.134	0.149	0.165
Theoretical %RSD	0.053	0.080	0.078	0.045	0.057
200 ng g^{-1} Pb					
Average ratio	37.913	15.667	17.272	2.1924	0.90642
Standard deviation	0.0598	0.0200	0.0282	0.0033	0.0013
Precision, %RSD	0.158	0.128	0.163	0.151	0.143
Theoretical %RSD	0.037	0.051	0.049	0.037	0.045

Table 8.9. Lead isotope ratio precision (short-term) and theoretical precision using multi-element standard solution. Lead ratios were analysed at Pb concentrations of 50, 100 and 200 ng g^{-1}. Number of analyses for each solution was 10.

	$^{208}Pb/^{204}Pb$	$^{207}Pb/^{204}Pb$	$^{206}Pb/^{204}Pb$	$^{208}Pb/^{206}Pb$	$^{207}Pb/^{206}Pb$
50 ng g^{-1} Pb					
Average ratio	39.701	15.456	19.806	2.0043	0.7803
Standard deviation	0.0453	0.0295	0.0255	0.0023	0.0014
Precision, %RSD	0.114	0.191	0.129	0.115	0.175
Theoretical %RSD	0.105	0.166	0.112	0.087	0.114
100 ng g^{-1} Pb					
Average ratio	37.485	15.48	18.809	1.9922	0.82257
Standard deviation	0.0517	0.0275	0.0288	0.0035	0.0010
Precision, %RSD	0.138	0.178	0.153	0.175	0.127
Theoretical %RSD	0.060	0.091	0.083	0.049	0.063
200 ng g^{-1} Pb					
Average ratio	38.001	15.533	18.602	2.0428	0.83487
Standard deviation	0.0486	0.0291	0.0270	0.0029	0.0008
Precision, %RSD	0.128	0.187	0.145	0.142	0.091
Theoretical %RSD	0.041	0.063	0.058	0.034	0.044

8.4.2 Long Term Precision

The long-term precision of the Pb isotope ratio measurement by quadrupole ICP-MS was also investigated. Initially, a 100 ng g^{-1} NIST SRM 981 solution was measured for Pb isotope ratios 55 times in 6 days. From **Figure 8.3**, which shows the relationship between time and Pb isotope ratio precision (%RSD), it is clear that the precisions were in the range of 0.075 to 0.201%, and generally under 0.20% except the %RSD for $^{207}Pb/^{206}Pb$ measured on day 4. The average precisions of $^{208}Pb/^{204}Pb$, $^{207}Pb/^{204}Pb$, $^{206}Pb/^{204}Pb$, $^{208}Pb/^{206}Pb$ and $^{207}Pb/^{206}Pb$ ratios were 0.131, 0.151, 0.152, 0.129 and 0.152% respectively over a period of 6 days. The BH2 digest of 100 ng g^{-1} Pb was analysed 27 times over a period of 6 days. The Pb isotope ratios measured were corrected against a 100 ng g^{-1} NIST Pb 981 standard solution for mass bias or discrimination. The precisions for $^{208}Pb/^{204}Pb$, $^{207}Pb/^{204}Pb$, $^{206}Pb/^{204}Pb$, $^{208}Pb/^{206}Pb$ and $^{207}Pb/^{206}Pb$ ratios are summarised in **Table 8.10**. It was found that the precisions for $^{208}Pb/^{204}Pb$, $^{207}Pb/^{204}Pb$, $^{206}Pb/^{204}Pb$, $^{208}Pb/^{206}Pb$ and $^{207}Pb/^{206}Pb$ ratios were 0.135, 0.143, 0.137, 0.109 and 0.121% respectively. Generally speaking, these results are similar to the average long-term precisions measured using 100 ng g^{-1} Pb 981 solution alone without any correction for mass bias or discrimination. In addition, the long-term precisions are similar to the short-term precisions described in the previous section.

From the above discussion, it is clear that a Pb isotope ratio precision (%RSD) of better than 0.15% is generally achievable using the HP 4500 *plus* ICP-mass spectrometer.

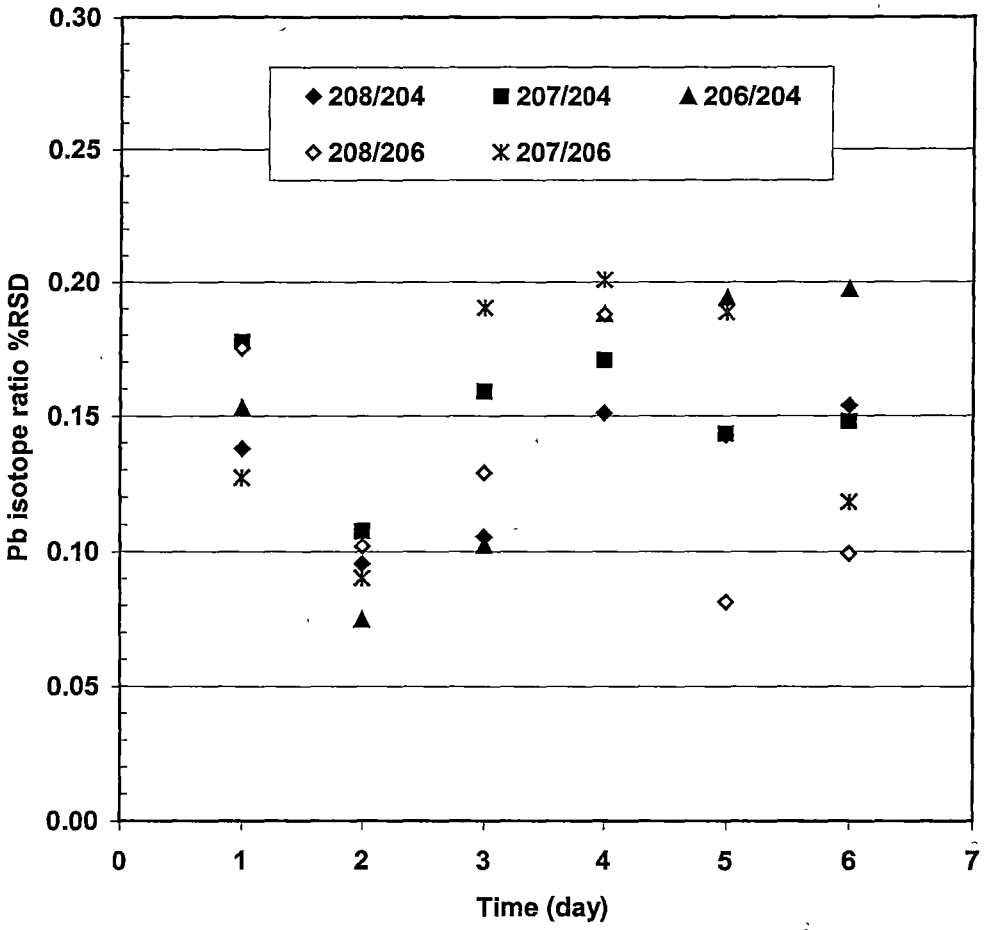

Figure 8.3. Long-term lead isotope ratio precision using 100 ng g^{-1} Pb 981 solution. Number of measurements: Day 1 = 10; Day 2 = 8; Day 3 = 9; Day 4 = 11; Day 5 = 6; Day 6 = 11.

Table 8.10. Long-term lead isotope ratio precision (%RSD) using 100 ng g^{-1} BH2 digest

Result	Long-term lead isotope ratio precision (%RSD)				
	$^{208}Pb/^{204}Pb$	$^{207}Pb/^{204}Pb$	$^{206}Pb/^{204}Pb$	$^{208}Pb/^{206}Pb$	$^{207}Pb/^{206}Pb$
Day 1					
1	35.546	15.395	15.988	2.2298	0.9601
2	35.606	15.405	16.028	2.2281	0.9604
3	35.680	15.401	16.002	2.2270	0.9581
4	35.639	15.366	15.976	2.2304	0.9605
5	35.686	15.366	16.000	2.2313	0.9606
6	35.522	15.336	15.944	2.2277	0.9616
7	35.512	15.390	15.976	2.2293	0.9602
8	35.682	15.401	16.018	2.2287	0.9615
9	35.590	15.380	15.975	2.2273	0.9617
10	35.524	15.335	15.993	2.2213	0.9589
11	35.608	15.356	15.969	2.2293	0.9615
12	35.569	15.365	15.973	2.2308	0.9619
13	35.630	15.361	15.965	2.2327	0.9620
Day 2					
1	35.625	15.362	15.983	2.2307	0.9611
2	35.636	15.377	15.979	2.2300	0.9621
Day 3					
1	35.608	15.382	16.018	2.2272	0.9613
2	35.650	15.396	16.006	2.2277	0.9619
3	35.617	15.392	16.007	2.2281	0.9600
Day 4					
1	35.638	15.366	16.019	2.2275	0.9596
2	35.636	15.402	15.976	2.2285	0.9598
3	35.634	15.382	16.020	2.2267	0.9608
Day 5					
1	35.619	15.397	16.002	2.2267	0.9619
2	35.608	15.402	16.022	2.2253	0.9605
3	35.599	15.362	15.966	2.2301	0.9597
Day 6					
1	35.569	15.342	15.982	2.2261	0.9601
2	35.618	15.357	15.975	2.2269	0.9613
3	35.534	15.342	15.971	2.2235	0.9578
Average	35.607	15.375	15.990	2.2281	0.9606
STD	0.0481	0.0220	0.0218	0.0024	0.0012
%RSD	0.135	0.143	0.137	0.109	0.121

8.5 Dynamic Range of the Method

In this section the suitability of quadrupole ICP-MS analysis for the measurement of Pb isotope ratios is further assessed by investigating the dynamic (appropriate working concentration) range for the technique.

At low Pb concentrations, accurate measurement of Pb isotope ratios is limited by the instrument signal intensity (counting statistics) of ^{204}Pb (1.4% atomic abundance), whereas at high Pb concentrations, the measurement of Pb isotope ratios is limited by high signal intensity of ^{208}Pb (~52% atomic abundance) due to the detector mode jumps from the pulse counting to analogue to avoid detector saturation. In the previous investigation using sector field ICP-MS analysis (Townsend et al. 1998 and **Chapter 7**), it was found that the working Pb concentration range in which accurate Pb isotope ratios could be obtained was from 10 to 50 ng g^{-1}.

In order to study the relationship between Pb isotope ratios and Pb concentrations, $^{208}Pb/^{204}Pb$, $^{207}Pb/^{204}Pb$ and $^{206}Pb/^{204}Pb$ ratios were measured over two consecutive days at Pb concentrations (using NIST Pb 981) of 5, 10, 20, 50, 60, 80, 100, 150, 200, 250 and 300 ng g^{-1} respectively. The relationship between the Pb isotope ratios and Pb concentrations are shown in **Figures 8.4** to **8.6**.

It was found that:

1. at Pb concentration below 50 ng g^{-1}, the measured Pb isotope ratios with ^{204}Pb as the basis were found to be limited by the instrument signal intensity of ^{204}Pb (counting statistics), resulting in less accurate Pb isotope ratio values (a concentration of 50 ng g^{-1} corresponded to approximately 1.3 x 10^4 counts s^{-1} of ^{204}Pb).

2. less accurate results for Pb isotope ratios with ^{208}Pb as the basis were also found when Pb concentrations were above 200 ng g^{-1} in testing solutions; it was observed that 200 ng g^{-1} Pb corresponded to approximately 1.4 x 10^6 counts s^{-1} under normal operating conditions and detector settings.

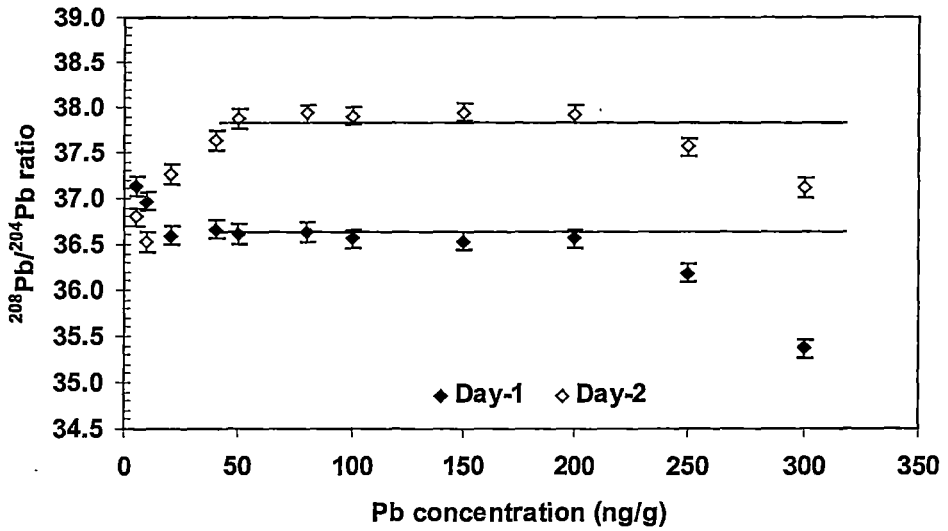

Figure 8.4. Relationship between $^{208}Pb/^{204}Pb$ ratio and lead concentrations. The error bars represent 0.1 unit of $^{208}Pb/^{204}Pb$ ratio. Note that the values shown have not been corrected for any mass bias or discrimination.

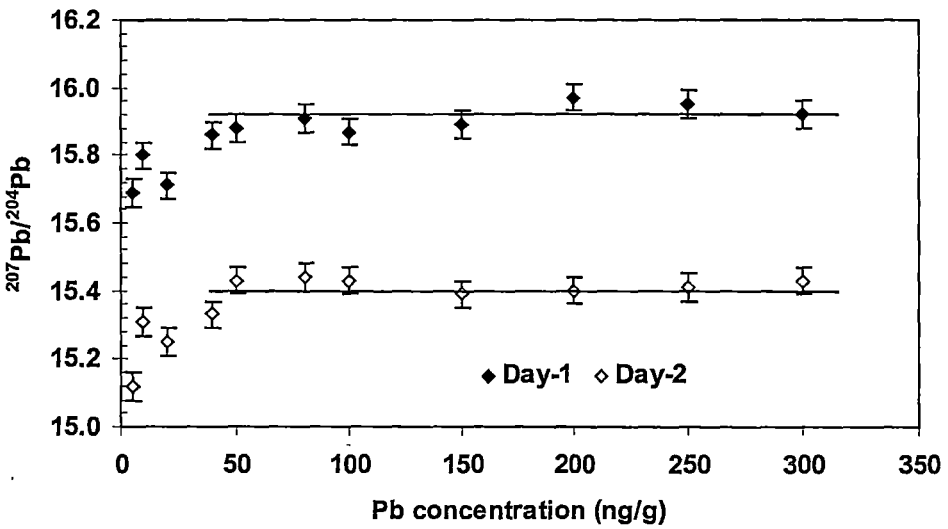

Figure 8.5. Relationship between $^{207}Pb/^{204}Pb$ ratio and lead concentrations. The error bars represent 0.04 unit of $^{207}Pb/^{204}Pb$ ratio. Note that the values shown have not been corrected for any mass bias or discrimination.

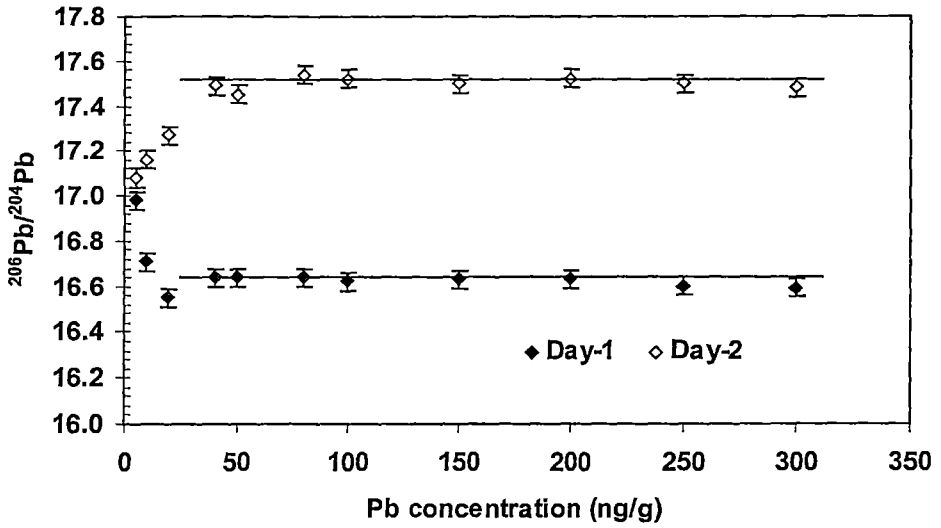

Figure 8.6. Relationship between $^{206}Pb/^{204}Pb$ ratio and lead concentrations. The error bars represent 0.04 unit of $^{206}Pb/^{204}Pb$ ratio. Note that the values shown have not been corrected for any mass bias or discrimination.

From the above discussion, it is clear that all Pb isotope ratios measured by the proposed quadrupole ICP-MS technique should be made at lead concentration range of 50 to 200 ng g^{-1} in order to keep the instrument detector working only at the same detector mode (pulse counting).

8.6 Concentric Nebuliser

All the previously described measurements were obtained using a Babington nebuliser. This type of nebuliser was initially designed by Babington (1973), but the original design was modified by constraining the liquid in a V-groove and introducing carrier gas from a small hole at the bottom of the groove (Suddendorf and Boyer 1978). Although the V-groove nebuliser has a great tolerance to high dissolved solids in solution, it is not an optimum geometry for aerosol generation (Sharp 1988). As an alternative, concentric nebulisers are widely used as ICP-MS aerosol generators (Williams 1992). Concentric nebulisers can be used both with and without a peristaltic pump in order to achieve the best precision.

In previous studies (Begley and Sharp 1997; Shuttleworth et al. 1997; Townsend et al. 1998; **Chapter 7** of this thesis), concentric nebulisers were employed to obtain good precision for the Pb isotope ratio analysis. In the development of the quadrupole technique discussed here, a concentric nebuliser was also used to determine if any improvement on the precision for the Pb isotope ratio measurement could be achieved.

Table 8.11 gives the lead isotope ratio precisions for ten consecutive measurements of a 100 ng g^{-1} NIST SRM 981 solution. The isotopic ratio precisions were determined using both peristaltic pump and free aspiration. In comparison with precisions obtained with a Babington nebuliser, it can be seen that there is slight improvement on those obtained using a concentric nebuliser. Nevertheless, there was little difference between peristaltic pump and free aspiration for the solution introduction. The average Pb isotope ratio precisions obtained using a peristaltic pump were 0.113 and 0.120% on two separate days, whereas those measured under free aspiration were 0.133 and 0.114% respectively. The precisions shown in **Table 8.11** are also found to be comparable to those obtained using high resolution ICP-MS by Townsend et al. (1998).

The relationship between the lead isotope ratios and the precision measured using a concentric nebuliser over a period of two days is also presented in **Figure 8.7**, which shows that the precisions were generally better than 0.15% under the experimental conditions. Therefore, in order to achieve the best precisions for Pb isotope measurement by ICP-MS, it is recommended that a concentric nebuliser should be used.

Table 8.11. Lead isotope precision (%RSD) with concentric nebuliser using 100 ng g^{-1} NIST SRM 981 solution

	$^{208}Pb/^{204}Pb$	$^{207}Pb/^{204}Pb$	$^{206}Pb/^{204}Pb$	$^{208}Pb/^{206}Pb$	$^{207}Pb/^{206}Pb$	Average
With peristaltic pump						
Day 1						
Ratio (n=10)	34.74	15 24	16.64	2.0868	0.9155	
STD	0.0416	0.0236	0.0233	0.0020	0.0005	
%RSD	0.120	0.155	0.140	0.095	0.057	0.113
Day 2						
Ratio (n=10)	35.81	15.37	16.42	2.1800	0.9360	
STD	0.0534	0.0178	0.0160	0.0025	0.0011	
%RSD	0.149	0.116	0.097	0.116	0.121	0.120
Free aspiration						
Day 1						
Ratio (n=10)	35.82	15.36	16.46	2.1761	0.9331	
STD	0.0514	0.0235	0.0237	0.0018	0.0013	
%RSD	0.143	0.153	0.144	0.082	0.141	0.133
Day 2						
Ratio (n=10)	35.86	15.37	16.40	2.1871	0.9374	
STD	0.0521	0.0145	0.0138	0.0033	0.0009	
%RSD	0 145	0.094	0.084	0.153	0.092	0.114

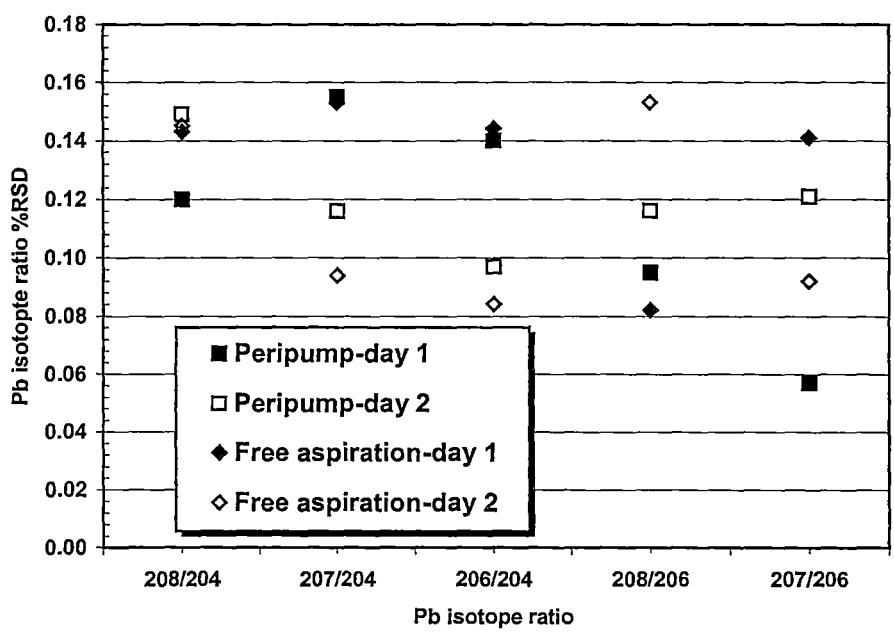

Figure 8.7. Lead isotope ratio precision with concentric nebuliser over a period of two days. Number of measurements was 10 for each day.

8.7 Accuracy

To investigate the accuracy of the Pb isotope ratio measurement using the proposed quadrupole ICP-MS technique, NIST SRM Pb 982 (an equal-atom lead isotopic standard), and 11 galena and galena-bearing samples from several localities in Australia were measured for Pb isotope ratios. The experimental conditions, such as the reagents, standards and sample preparation technique, were the same as those described as in **Chapter 7**.

The measurement of lead isotope ratios for the selected samples was conducted at a lead concentration range of 50 to 200 ng g^{-1}. Lead concentrations of both correction standards and testing samples were carefully matched (controlled at same or very close concentration levels) in order to further minimise the effect of instrument dead time on the measurement of lead isotope ratios. In the present investigation, all mass bias or discrimination was corrected against NIST SRM 981.

The analytical sequence of the measurement for lead isotope ratios was arranged in the same way as that used for the sector field ICP-MS analysis. Each testing sample was bracketed by two correction standards. Further details regarding the analytical sequence for the measurement of lead isotope ratios can be found in **Chapter 7** of this thesis.

As shown in **Table 8.12** and **Figures 8.8 – 8.12**, there was good agreement in lead isotopic compositions analysed by quadrupole ICP-MS, sector field ICP-MS and TIMS techniques. The number of measurements for BH2 was 27; and for NIST SRM 982, EB-72086 and H15 it was 6; the rest of the selected samples were run in triplicate. The relative deviations in the lead isotope ratios between quadrupole ICP-MS and TIMS techniques were found to be comparable to those obtained by sector field ICP-MS (Townsend et al. 1998 and **Chapter 7** of this thesis) and were generally better than ±0.2%, irrespective of the isotope ratios considered. Apart from NIST SRM 982 (an equal-atom lead standard), the absolute deviations of $^{208}Pb/^{204}Pb$, $^{207}Pb/^{204}Pb$, $^{206}Pb/^{204}Pb$, $^{208}Pb/^{206}Pb$ and $^{207}Pb/^{206}Pb$ ratio values between the two methods were in the range of 0.003 – 0.08, 0.001 – 0.043, 0.004 – 0.055, 0.005 – 0.0058 and 0.002 – 0.0023 (in terms of ratio units) respectively. This indicates that

Table 8.12. A comparison of lead isotope ratios in NIST Pb RSM 982 and 11 geological samples from different localities in Australia by quadrupole-ICP-MS, HR-ICP-MS and TIMS

Ratio	Sample I.D.	n	This work Q-ICP-MS	HR-ICP-MS	TIMS	Deviation	Rel Dev (%)
$^{208}Pb/^{204}Pb$							
	SRM 982	6	36.731	36.785	36.7443	-0.013	-0.04
	Z-5199	3	38.201	38.222	38.121	0.080	0.21
	Z-5221	3	38.435	38.402	38.417	0.018	0.05
	Z-5232	3	38.250	38.240	38.241	0.009	0.02
	Z-5237	3	38.533	38.474	38.472	0.061	0.16
	Z-5277	3	38.259	38.288	38.296	-0.037	-0.10
	BH2	27	35.607	35.530	35.599	0.008	0.02
	EB-1007	3	37.952	37.868	37.91	0.042	0.11
	EB-72086	6	37.890	37.887	37.91	-0.020	-0.05
	EB-72087	3	37.914	37.900	37.876	0.038	0.10
	EB-72096	3	38.038	38.083	38.041	-0.003	-0.01
	H-15	6	38.114	38.241	38.178	-0.064	-0.17
$^{207}Pb/^{204}Pb$							
	SRM 982	6	17.134	17.146	17.1595	-0.025	-0.15
	Z-5199	3	15.626	15.603	15.607	0.019	0.12
	Z-5221	3	15.601	15.651	15.622	-0.021	-0.13
	Z-5232	3	15.620	15.648	15.633	-0.013	-0.08
	Z-5237	3	15.644	15.644	15.625	0.019	0.12
	Z-5277	3	15.625	15.620	15.624	0.001	0.01
	BH2	27	15.375	15.384	15.37	0.005	0.03
	EB-1007	3	15.611	15.551	15.58	0.031	0.20
	EB-72086	6	15.572	15.583	15.58	-0.008	-0.05
	EB-72087	3	15.573	15.587	15.57	0.003	0.02
	EB-72096	3	15.589	15.628	15.605	-0.016	-0.10
	H-15	6	15.569	15.634	15.612	-0.043	-0.28
$^{206}Pb/^{204}Pb$							
	SRM 982	6	36.641	36.694	36.7385	-0.097	-0.26
	Z-5199	3	18.336	18.315	18.281	0.055	0.30
	Z-5221	3	18.495	18.492	18.531	-0.036	-0.19
	Z-5232	3	18.341	18.331	18.368	-0.027	-0.15
	Z-5237	3	18.568	18.550	18.561	0.007	0.04

Table 8.12. (Continued).

Ratio	Sample I.D.	n	This work Q-ICP-MS	HR-ICP-MS	TIMS	Deviation	Rel Dev (%)
$^{206}Pb/^{204}Pb$	Z-5277	3	18.374	18.423	18.428	-0.054	-0.29
	BH2	27	15.990	16.004	15.994	-0.004	-0.03
	EB-1007	3	18.110	18.092	18.119	-0.009	-0.05
	EB-72086	6	18.039	18.063	18.075	-0.036	-0.20
	EB-72087	3	18.074	18.095	18.098	-0.024	-0.13
	EB-72096	3	18.187	18.198	18.191	-0.004	-0.02
	H-15	6	18.326	18.383	18.361	-0.035	-0.19
$^{208}Pb/^{206}Pb$							
	SRM 982	6	1.0030	1.0048	1.00016	0.0028	0.28
	Z-5199	3	2.0844	2.0868	2.08528	-0.0009	-0.04
	Z-5221	3	2.0781	2.0753	2.073121	0.0050	0.24
	Z-5232	3	2.0855	2.0894	2.081936	0.0036	0.17
	Z-5237	3	2.0748	2.0753	2.072733	0.0021	0.10
	Z-5277	3	2.0820	2.0841	2.078142	0.0039	0.19
	BH2	27	2.2281	2.2208	2.2258	0.0023	0.10
	EB-1007	3	2.0966	2.0877	2.092279	0.0043	0.21
	EB-72086	6	2.1005	2.0929	2.097372	0.0031	0.15
	EB-72087	3	2.0986	2.0946	2.092828	0.0058	0.28
	EB-72096	3	2.0917	2.0953	2.091199	0.0005	0.02
	H-15	6	2.0825	2.0781	2.079299	-0.0032	-0.19
$^{207}Pb/^{206}Pb$							
	SRM 982	6	0.4678	0.4683	0.467071	0.0007	0.15
	Z-5199	3	0.8523	0.8519	0.853728	-0.0014	-0.16
	Z-5221	3	0.8435	0.8459	0.84302	0.0005	0.06
	Z-5232	3	0.8518	0.8550	0.8511	0.0007	0.08
	Z-5237	3	0.8422	0.8439	0.841819	0.0004	0.05
	Z-5277	3	0.8501	0.8502	0.84784	0.0023	0.27
	BH2	27	0.9606	0.9613	0.961	-0.0004	-0.04
	EB-1007	3	0.8615	0.8609	0.859871	0.0016	0.19
	EB-72086	6	0.8630	0.8627	0.861964	0.0010	0.12
	EB-72087	3	0.8622	0.8613	0.860316	0.0019	0.22
	EB-72096	3	0.8575	0.8588	0.857842	-0.0003	-0.03
	H-15	6	0.8505	0.8502	0.85028	0.0002	0.02

n = number of measurements.

Sector field ICP-MS results were obtained by the Finnigan Element ICP-MS at the Central Science Laboratory, University of Tasmania.

TIMS's values were measured at CSIRO, North Ryde of New South Wales.

Deviation is the difference between the Pb isotope ratios measured by quadrupole ICP-MS and TIMS.

Rel Dev is the relative deviation of the Pb isotope ratios measured by quadrupole ICP-MS and TIMS techniques, negative values indicate the measured value from this work are lower than that obtained from TIMS.

TIMS's values were measured at the CSIRO laboratory in New South Wales and provided by Dr Peter McGoldrick (CODES, University of Tasmania). The isotopic compositions for SRM Pb 982 were provided by National Institute of Standards and Technology (NIST), USA.

Z-5199, 5221, 5232, 5237 and 5277 are galenas from Zeehan mineral field vein deposits and are located in Oceana, Argent#2, Swansea, Montana, and North Tasmania Mine ore deposits in Tasmania respectively. These samples were provided by Dr Paul Kitto (formerly Centre for Ore Deposit Research, SRC, University of Tasmania).

BH2 is a galena from Broken Hill in New South Wales provided by Dr Peter McGoldrick (Centre for Ore Deposit Research, SRC, University of Tasmania)

EB-1007, 72086, 72087, and 72096 are massive sulfides (sphalerite galena) from Elliott Bay deposit in Tasmania provided by Dr J. Bruce Gemmell (Centre for Ore Deposit Research, SRC, University of Tasmania)

H-15 is a pyrite sphalerite galena from Hellyer deposit in Tasmania provided by Dr J. Bruce Gemmell (Centre for Ore Deposit Research, SRC, University of Tasmania).

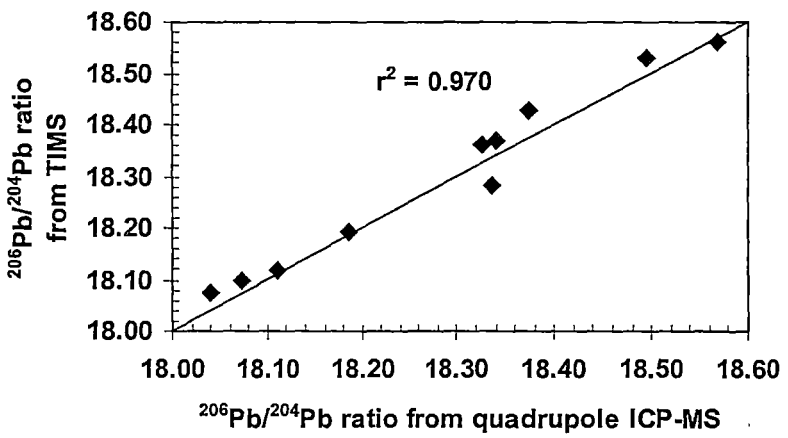

Figure 8.8. Correlation of $^{206}Pb/^{204}Pb$ ratios between the quadrupole-ICP-MS and conventional TIMS techniques. Samples used for the figure are Z-5199, 5221, 5232, 5237 and 5277 galenas from Zeehan mineral field vein deposits (located in Oceana, Argent#2, Swansea, Montana, and North Tasmania Mine ore deposits in Tasmania respectively), EB-1007, 72086, 72087, and 72096 massive sulfides (sphalerite galena) from Elliott Bay deposit in Tasmania, and H-15 pyrite sphalerite galena from Hellyer deposit in Tasmania.

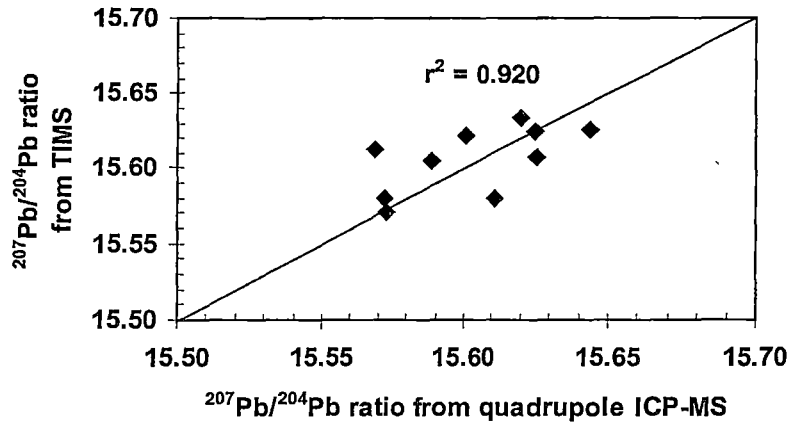

Figure 8.9. Correlation of $^{207}Pb/^{204}Pb$ ratios between the quadrupole-ICP-MS and conventional TIMS techniques. Samples used for the figure are Z-5199, 5221, 5232, 5237 and 5277 galenas from Zeehan mineral field vein deposits (located in Oceana, Argent#2, Swansea, Montana, and North Tasmania Mine ore deposits in Tasmania respectively), EB-1007, 72086, 72087, and 72096 massive sulfides (sphalerite galena) from Elliott Bay deposit in Tasmania, and H-15 pyrite sphalerite galena from Hellyer deposit in Tasmania.

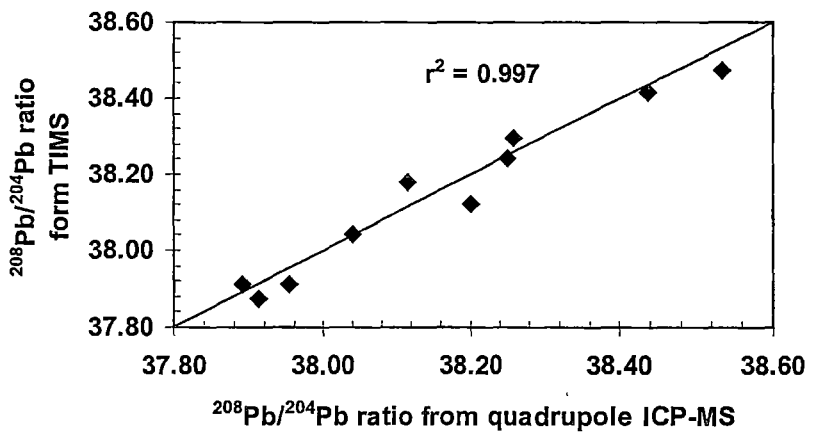

Figure 8.10. Correlation of $^{208}Pb/^{204}Pb$ ratios between the quadrupole-ICP-MS and conventional TIMS techniques. Samples used for the figure are Z-5199, 5221, 5232, 5237 and 5277 galenas from Zeehan mineral field vein deposits (located in Oceana, Argent#2, Swansea, Montana, and North Tasmania Mine ore deposits in Tasmania respectively), EB-1007, 72086, 72087, and 72096 massive sulfides (sphalerite galena) from Elliott Bay deposit in Tasmania, and H-15 pyrite sphalerite galena from Hellyer deposit in Tasmania.

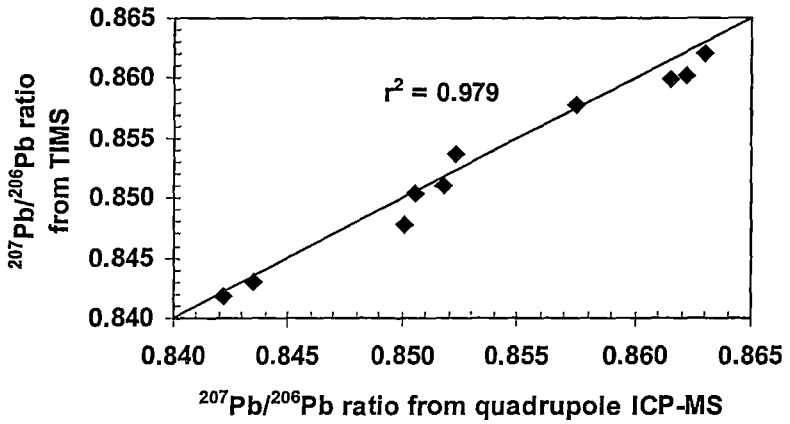

Figure 8.11. Correlation of $^{207}Pb/^{206}Pb$ ratios between the quadrupole-ICP-MS and conventional TIMS techniques. Samples used for the figure are Z-5199, 5221, 5232, 5237 and 5277 galenas from Zeehan mineral field vein deposits (located in Oceana, Argent#2, Swansea, Montana, and North Tasmania Mine ore deposits in Tasmania respectively), EB-1007, 72086, 72087, and 72096 massive sulfides (sphalerite galena) from Elliott Bay deposit in Tasmania, and H-15 pyrite sphalerite galena from Hellyer deposit in Tasmania.

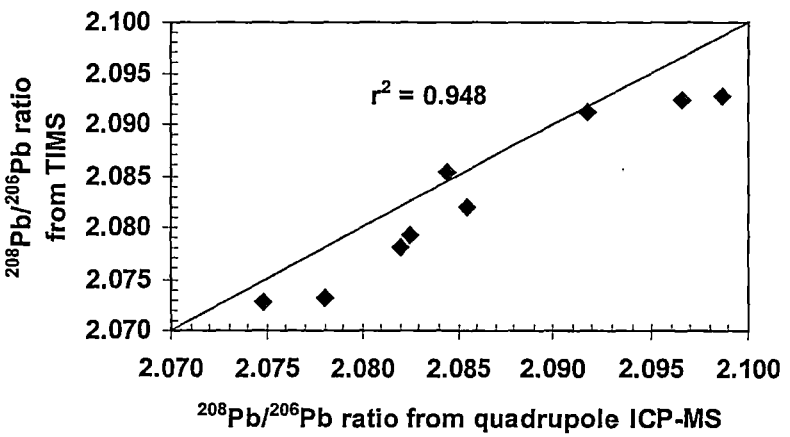

Figure 8.12. Correlation of $^{208}Pb/^{206}Pb$ ratios between the quadrupole-ICP-MS and conventional TIMS techniques. Samples used for the figure are Z-5199, 5221, 5232, 5237 and 5277 galenas from Zeehan mineral field vein deposits (located in Oceana, Argent#2, Swansea, Montana, and North Tasmania Mine ore deposits in Tasmania respectively), EB-1007, 72086, 72087, and 72096 massive sulfides (sphalerite galena) from Elliott Bay deposit in Tasmania, and H-15 pyrite sphalerite galena from Hellyer deposit in Tasmania.

Pb isotope ratios can be accurately and precisely measured by the quadrupole instrument. The quadrupole ICP-MS data, like sector field ICP-MS data, are good enough to clearly separate the Cambrian volcanogenic massive sulfides from post-Cambrian mineralisation in western Tasmania (Gulson 1986).

8.8 Summary

From the previous discussion, it is clear that the quadrupole ICP-MS technique can be used for accurate and precise measurement of Pb isotope ratios. The main conclusions that can be drawn are as follows:

- Based on 90 analyses of 3 different samples (NIST SRM 981, BH2 and a lead standard solution at Pb concentrations of 50, 100 and 200 ng g^{-1} respectively, the short-term precision (%RSD) values for $^{208}Pb/^{204}Pb$, $^{207}Pb/^{204}Pb$, $^{206}Pb/^{204}Pb$, $^{208}Pb/^{206}Pb$ and $^{207}Pb/^{206}Pb$ ratios were generally better than 0.20% (values as 1σ), whereas the long-term precisions (%RSD) measured using 50 ng g^{-1} BH2 digest and 100 ng g^{-1} NIST SRM 981 over a period of 6 days were better than 0.15% (1σ). Furthermore, the precision can be further improved using a concentric nebuliser (generally better that 0.12% for short-term precision).

- The Pb isotope ratio results measured by quadrupole ICP-MS compare favourably with those obtained by both conventional TIMS and sector field ICP-MS. Based on 6 analyses of NIST SRM 982 and 63 determinations of 11 selected geological samples (galenas and galena-bearing ores) from different localities in Australia, the relative deviations between the quadrupole and TIMS data were generally found to be generally less than ±0.2% for $^{208}Pb/^{204}Pb$, $^{207}Pb/^{204}Pb$, $^{206}Pb/^{204}Pb$, $^{208}Pb/^{206}Pb$ and $^{207}Pb/^{206}Pb$ ratios.

- Comparing the cost of quadrupole and sector field instruments, the introduction of the quadrupole ICP-MS technique for lead isotope ratio measurement will obviously result in a further reduction in the cost of analysis.

Chapter 9

LEAD ISOTOPIC COMPOSTION OF THE LADY LORETTA SEDIMENT-HOSTED Zn-Pb-Ag DEPOSIT, NORTHERN AUSTRALIA

9.1 Introduction

In this chapter, the solution quadrupole ICP-MS method developed in **Chapter 8** is used to examine the lead isotopic compositions in a group of selected lead-bearing ore samples from the Lady Loretta deposit, northwest Queensland, Australia. The lead isotope data obtained in this work are compared with previous data obtained using TIMS, and implications for metal sources for the Lady Loretta deposit are discussed.

9.2 The Lady Loretta Deposit

The Lady Loretta deposit (8.3 Mt at 18.4% Zn, 8.5% Pb and 125g/t Ag) is situated in northwest Queensland at 19°46'S and 139°03'E (**Figure 9.1**). It occurs at the southern end of the Lawn Hill platform within Middle Proterozoic rocks that have been metamorphosed to lower greenschist facies (Gulson 1986). Lady Loretta deposit is hosted by metasediments of the Lady Loretta Formation, which comprise dolomitic and sideritic siltstone and sandstone, chert and pyritic carbonaceous shale. Massive sulfide mineralisation (the Sulfide Unit) can be divided into a pyritic sequence up to 60 metres thick, overlain by a sphalerite/galena/pyrite-rich sequence varying from <1 metre to 40 metres in thickness. Additional geological information can be obtained from Loudon et al. (1975), Carr (1984), Hancock and Purvis (1990), and Large and McGoldrick (1998).

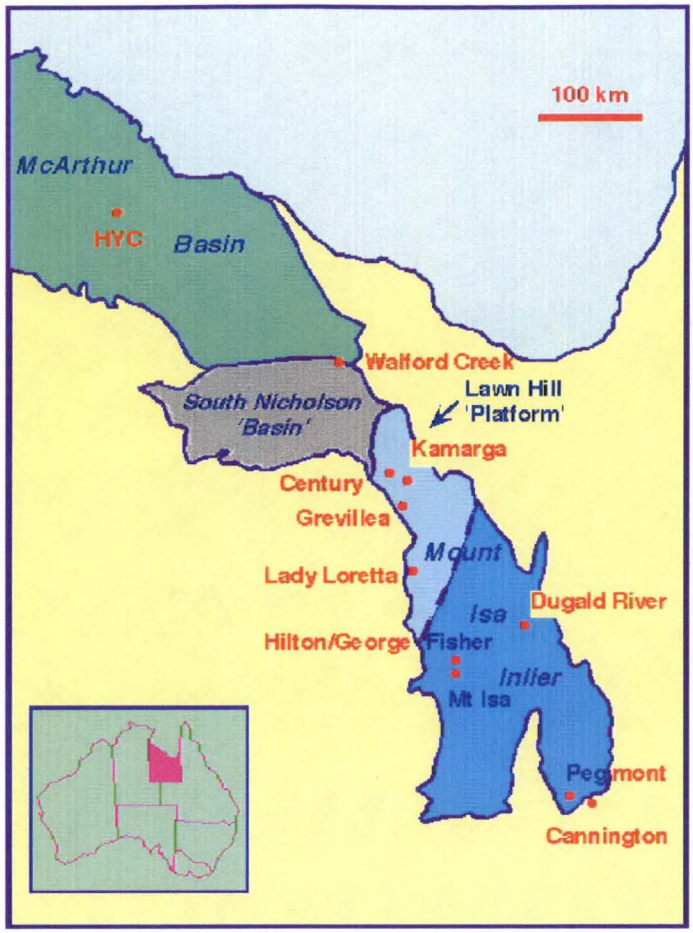

Figure 9.1. Major geological elements and the location of important Zn-Pb deposits of the northern Australian Proterozoic Zinc Belt (Large and McGoldrick 1998)

9.3 Background of Lead Isotope Investigation

In previous studies, lead isotope models related the change in lead isotopic compositions through time to one particular or several reservoirs. Common practice is for lead isotope models to be graphically represented as growth curves, which are lines drawn through points on a group of isochrons of different ages but with common initial U/Pb ratios in the parent material (e.g. Faure 1977). The Holmes-Houtermans Model can be used to interpret the total lead isotope variation of a single reservoir with time, if the following assumptions are satisfied.

- The earth was fluid and homogeneous at the very beginning.
- Uranium, thorium and lead were evenly distributed at that time.
- The lead isotope ratios of this primeval lead were identical everywhere.
- The earth subsequently became solid, and small regional differences arose in the U/Pb ratio.

- The U/Pb ratio changed only as a result of radioactive decay of ^{238}U to ^{206}Pb and ^{235}U to ^{207}Pb.
- Finally, formation of Pb-rich minerals effectively separates Pb from its parent U and Th and so the isotopic composition of Pb-rich minerals remains constant since the time of separation.

However, in some more complex reservoirs, such as the earth's crust or mantle, the calculation of "time" depends on estimations of several variables for each of two or more stages. In general, these variables include (a) U/Pb and Th/U ratios, (b) primeval lead isotopic compositions, and (c) initial ages.

In order to generalise the modelling of the earth's crust using lead isotopic compositions, Stacey and Kramers (1975) developed a two-stage model to minimise the difference between model "age" and accepted ages of massive sulfide deposits by dividing the lead growth curve into two sequential stages each with a different assumed U/Pb and Th/U of the reservoirs. Cumming and Richards (1975) also developed a generalised lead model that constantly changes the U/Pb and Th/U ratios through time to estimate the geological ages of massive sulfide deposits. Although the Stacey & Kramers and Cumming & Richards Models are found to be useful in determining the approximate age difference between sulfide deposits in similar geological terrains, they have never been considered precise in determining absolute ages. For instance, the two models yield a difference in age for the Broken Hill deposit of 75 Ma (Carr and Sun 1996).

In order to minimise the difference between accepted geological ages (U-Pb ages) and model ages, efforts have been made to improve lead isotope model ages. Sun et al. (1994, 1996) used a modified Cumming and Richards (1975) method to estimate several mineralisation ages in Australia, Canada and USA. This modified method is based on:

- treating geological terrains separately, and
- applying controls form independent age evidence within each terrain.

Table 9.1. Comparison of geological ages (U-Pb zircon ages) and Terrain Specific Control Model ages

Deposit	U-Pb zircon ages (Ma)	Terrain Specific Control Model ages (Ma)
Flin Flon (Canada)	1886	1880
Wisconsin (USA)	1860	1875-1820
Koongie Park (Australia)	1840	1820
Cullen Batholith (Australia)	1825	1830
Broken Hill (Australia)	1690	1675
Mount Isa (Australia)	1652	1653
HYC (Australia)	1640	1640
Century (Australia)	1595	1575

This approach is also called the Terrain Specific Control Lead Isotope Model (Carr and Sun 1996). When this model is applied using 1640 Ma HYC Zn-Pb deposit as a control (**Table 9.1**, Sun et al (1996), there is a good agreement between the lead model ages and geological ages for the Broken Hill Pb-Zn deposit and for some Early Proterozoic volcanogenic massive sulfide (VMS) deposits from northern Wisconsin (USA), and the Flin Flon belt (Canada), Koongie Park and Cullen Batholith (Northern Territory).

In contrast, previous work from the Lady Loretta deposit demonstrated a considerable variation in $^{206}Pb/^{204}Pb$ data among the Pb-Zn ore samples (Gulson 1985; Vaàsjoki and Gulson 1985). Sun et al. (1994) suggested that this variation might be a result of either incomplete homogenisation of Pb derived from sources with different initial U/Pb ratio values or protracted period of mineralisation. In order to further investigate this variation, the quadrupole ICP-MS technique described in **Chapter 8** of this thesis is applied to a new set of carefully selected samples from the Lady Loretta deposit.

9.4 Lead Isotope Ratios of Selected Samples

9.4.1 Sample Selection and Preparation

Work by Aheimer (1994) and McGoldrick et al. (1998) has distinguished a variety of textural ore types at Lady Loretta. These include laminated fine grained base metal sulfide; recrystallised base metal sulfide; barite-sphalerite ore and disseminated galena in stromatolite growth bands. For the present study, several of these ore types were carefully sampled from polished slabs using a fine drill. All samples were obtained from diamond drill core from the Small Syncline at Lady Loretta (McGoldrick and Large 1998). Several of the slabs used in this study are illustrated on **Figure 9.2.**

Approximately 5 to 30 mg of each sample was digested at about 130 °C on a hotplate using HNO_3-HCl-HF (1+3+2) acid mixture in Savillex Teflon beaker. After diluting to 100 ml in 2% HNO_3, lead concentration in each solution was analysed prior to lead isotope ratio measurement. Using NIST SRM 981 as mass bias correction standard (see **Chapters 7** and **8**), lead isotope ratios were analysed by HP 4500 (*plus*) ICP-MS with lead concentration adjusted to ~100 ng g^{-1}.

2 cm

recrystallised galena in folded base metal sulfides

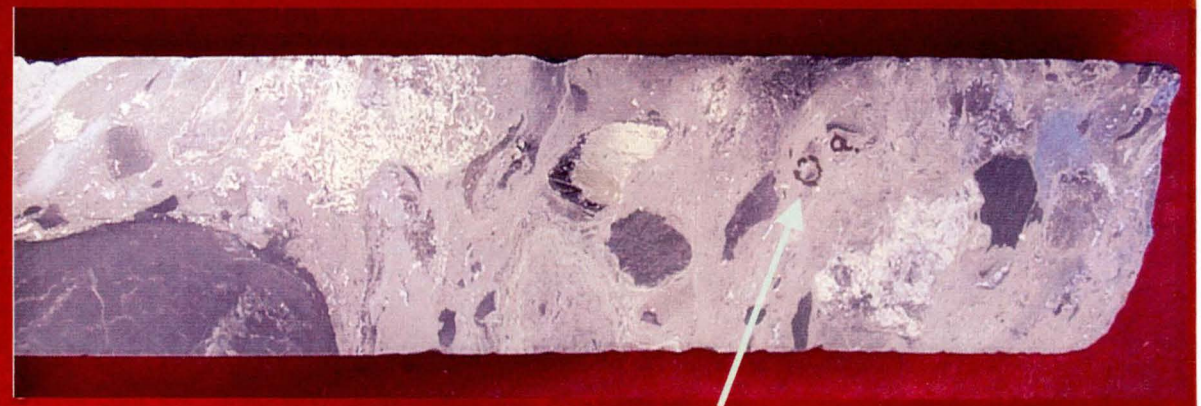

fine grained base metal sulfide fragment in sulfide breccia

fine grained laminated base metal sulfides

recrystallised base metal sulfide in deformed barite-sphalerite ore

9.4.2 Lead Isotopic Compositions

The measured Pb isotopic compositions and concentrations of thirteen different types of ore samples are listed in **Table 9.2.**

Table 9.2. Lead isotopic compositions for the Lady Loretta deposit

Sample no.	Description	$^{206}Pb/^{204}Pb$	$^{206}Pb/^{204}Pb$	$^{206}Pb/^{204}Pb$	$^{207}Pb/^{206}Pb$	$^{208}Pb/^{206}Pb$	Pb ppm
242ED72 76.2m (Z17b)	Recrys/remob ga	16.24	15.48	35.97	2.2272	0.9603	464898
245EI01 25.8m (110803)	Ba/sp ore	16.23	15 50	35.99	2.2165	0.9543	48466
224WD27-33.4(a)	Sp rich ore frag	16.20	15 47	35.92	2.2158	0.9541	13538
224WD27-33.4(b)	Lam ore frag	16.17	15.46	35.87	2.2190	0.9563	50795
224WD27-35.3	Ga sph	16.16	15 44	35.84	2.2174	0.9556	226667
224WD27-35 3 hinge	Ga sph	16.17	15.45	35 87	2.2181	0.9557	484000
224WD27-35 3 limb	Ga sph	16.19	15 47	35 92	2.2191	0.9562	283875
224WD27-35.3 label	Recrys band	16.19	15.47	35.91	2.2179	0.9557	814500
227WD30-41.7	Lam/folded ore, Ga from extrusion vein	16.25	15 47	35.98	2.2134	0.9521	258300
233WD70-111.8(a)	Lam sp/ga	16 29	15.49	36.00	2 2104	0.9510	230444
233WD70-111.8(b)	Lam sp/ga	16 29	15.50	36.04	2.2129	0.9516	105432
234ED30-64 25	Ba/sp ore	16.21	15.47	35.92	2.2154	0.9540	18252
242ED27-52.5	Strom band	16.18	15.46	35.88	2 2182	0.9558	3900
Average		**16.21**	**15.47**	**35.93**	**2.2160**	**0.9540**	

Abbreviations: Recrys = recrystallised; Remob = remobilised; Ga = galena; Sp = sphalerite; Frag = fragment; Sph = spheroid; Ba = barite; Strom = stromatolite

In previous studies, it has been found that lead isotopic compositions for the four largest deposits (i.e., Mount Isa, Hilton, HYC and Dugald River) in the Mount Isa-McArthur River region show homogeneous lead isotopic compositions (Gulson 1985; Vaasjoki and Gulson 1985). For instance, the variations (as mean ± one standard deviation) in $^{206}Pb/^{204}Pb$ ratio for Mount Isa, Hilton, HYC and Dugald River deposits were found to be 16.112 ± 0.013, 16.120 ± 0.013, 16.149 ± 0.009 and

deposits were found to be 16.112 ± 0.013, 16.120 ± 0.013, 16.149 ± 0.009 and 16.055 ± 0.004, respectively. However, in contrast to the four largest ore deposits in this area, there is a considerable variation in the lead isotopic compositions for the Lady Loretta deposit, for instance, the published variations of $^{206}Pb/^{204}Pb$ ratios range from 16.16 to16.29 (Gulson 1985).

The Pb isotope ratios measured by quadrupole ICP-MS in this study (**Figure 8.3** & **Table 8.3**) overlap the range of values determined using thermal ionisation mass spectrometry by Gulson (1985).

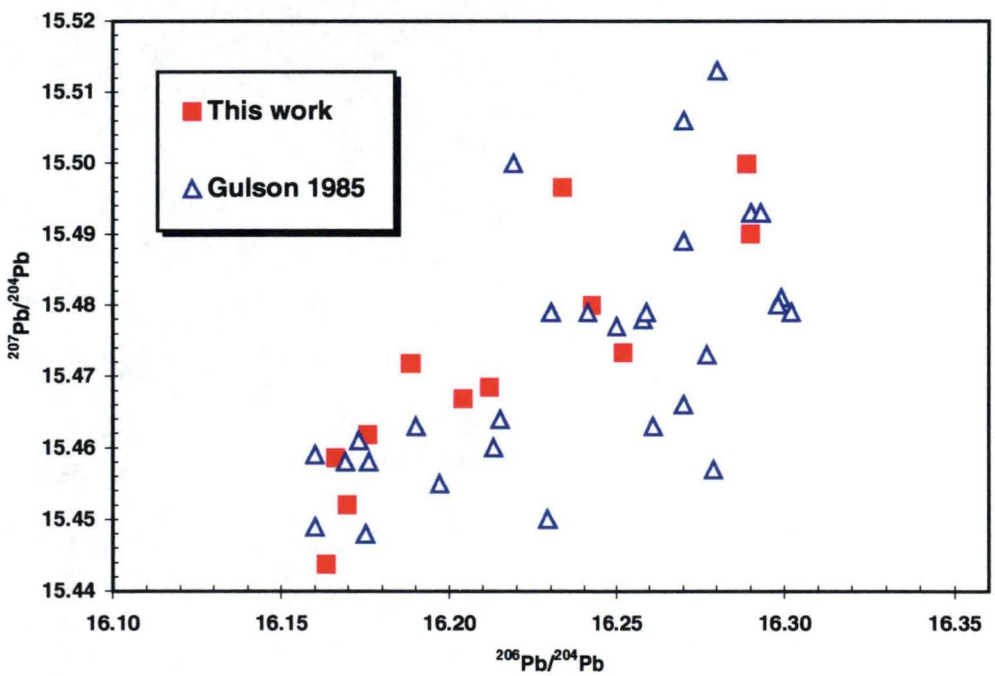

Figure 9.3. Variation of lead isotopic compositions for Lady Loretta deposit. DDH = diamond drill hole.

Table 9.3. Comparison of lead isotopic compositions with previous work

Source	Sample source	Number of sample measured	$^{206}Pb/^{204}Pb$	$^{206}Pb/^{204}Pb$	$^{206}Pb/^{204}Pb$
Gulson 1985	DDH	29	16.169-16.302	15.449-15.513	35.827-36.05
This work	DDH	13	16.16-16.29	15.44-15.50	35.88-36.04

DDH = diamond drill hole

As can be seen in **Figure 9.4**, there is considerably scattering of $^{206}Pb/^{204}Pb$ ratios regardless of textures. There is a difference of 0.13 between the laminated sphalerite/galena sample from drill hole 224WD27 and the two laminated sphalerite/galena samples from the drill hole 233WD70. The $^{206}Pb/^{204}Pb$ and $^{207}Pb/^{204}Pb$ ratios for the laminated sphalerite/galena and recrystallised galena samples from drill hole 224WD27 show a model age similar to the HYC deposit, whereas the lead isotope ratios for the two laminated sphalerite/galena samples from the drill hole 233WD70 give a model age similar to that of the Century deposit. The lead isotope ratios for the rest of samples show a model age of about 1600 Ma (**Figure 9.5**).

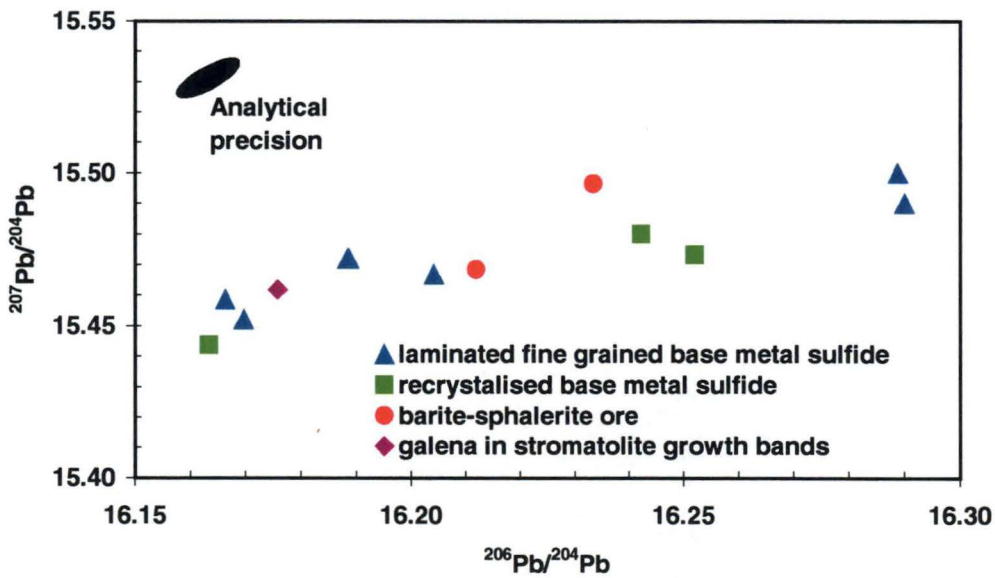

Figure 9.4 $^{206}Pb/^{204}Pb$ and $^{207}Pb/^{204}Pb$ ratio plot of four different group samples from the Lady Loretta deposit. The analytical error shows two standard deviations using HP 4500 ICP-MS.

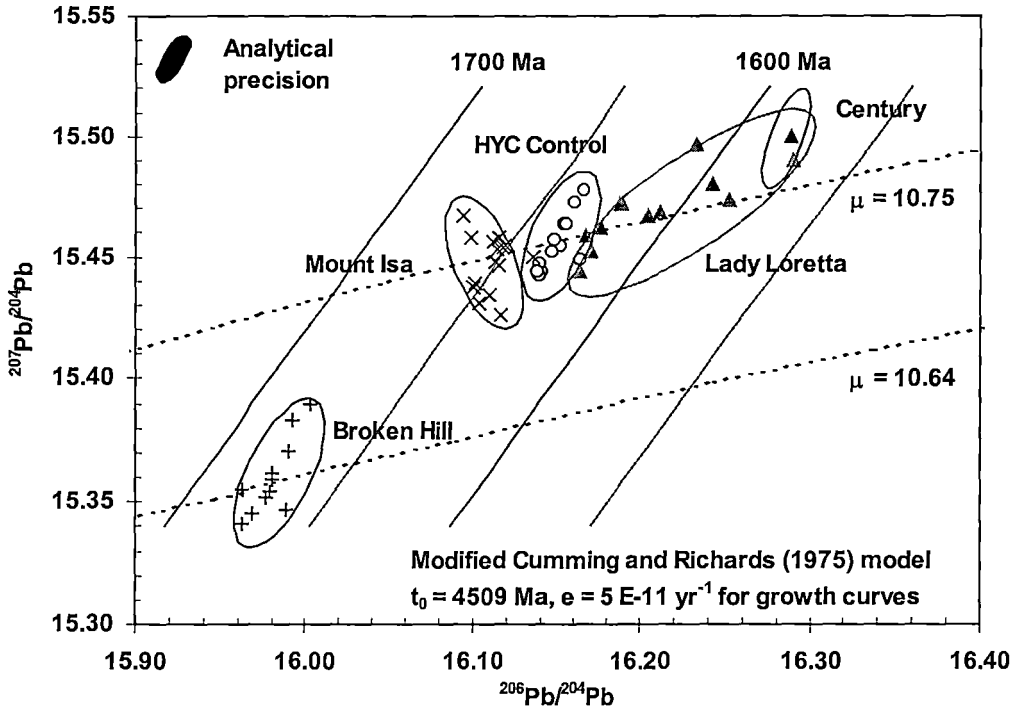

Figure 9.5. Lead isotope composition plots for some sediment-hosted base-metal deposits in the Mount Isa Inlier (modified from Cumming and Richards, 1975). HYC deposit was used as the control with a geological age of 1640 Ma. The analytical precision is shown as 2 σ.

9.5 Summary and Discussion

The Pb isotope ratio results of the selected different types of ore samples from the Lady Loretta deposit are in good agreement with previous work using TIMS (Gulson 1985). This further demonstrates that solution ICP-MS technique can be used to analyse lead isotopic compositions accurately and precisely in geological samples.

The new data reported here confirm the wide spread in Pb isotope ratios reported from Lady Loretta by earlier workers (Gulson 1985; Vaasjoki and Gulson 1985). The spread in $^{206}Pb/^{204}Pb$ ratios is the greatest of any of the northern Australian Proterozoic stratiform Zn deposits, and suggests that either, the lead in the deposit was sourced from rocks with diverse initial U/Pb ratios, or that the orebody formed

from a homogenous Pb source but took up to 50 million years to form (e.g. **Figure 9.6**).

The latter explanation would imply a replacement process for formation of much the Pb-Zn sulfides now seen in the deposit, and for different parts of the orebody to form at different times between about 1650 Ma (deposition of the host sequence) and 1600 Ma (? Beginning of the Isan Orogeny). However, textural evidence presented elsewhere (Carr 1981; Aheimer 1994; McGoldrick et al. 1996) suggests a syn-sedimentation, or early diagenetic timing for most of the Pb-Zn sulfides, so an extended duration mineralising event probably cannot be invoked to explain the range in Pb isotopic values.

An alternative explanation, favoured here, is that lead in the Lady Loretta deposit has multiple sources that were being tapped simultaneously during formation of the deposit, but without mixing or homogenisation of the Pb during fluid flow. This contrast with a modelled scenario for the giant HYC deposit (Garven and Bull 1999 & **Figure 9.6**), whereby convective fluid flow effectively homogenises Pb from several different sources before this fluid is expelled up faults to the site of the ore deposition. At Lady Loretta, fluid flow in the source rocks may have been effectively compartmentalised (**Figure 9.7**) and the homogenisation inferred for the larger deposits could not occurred. Hydrologic and Pb isotope modelling to test this scenario will be the subject of later work.

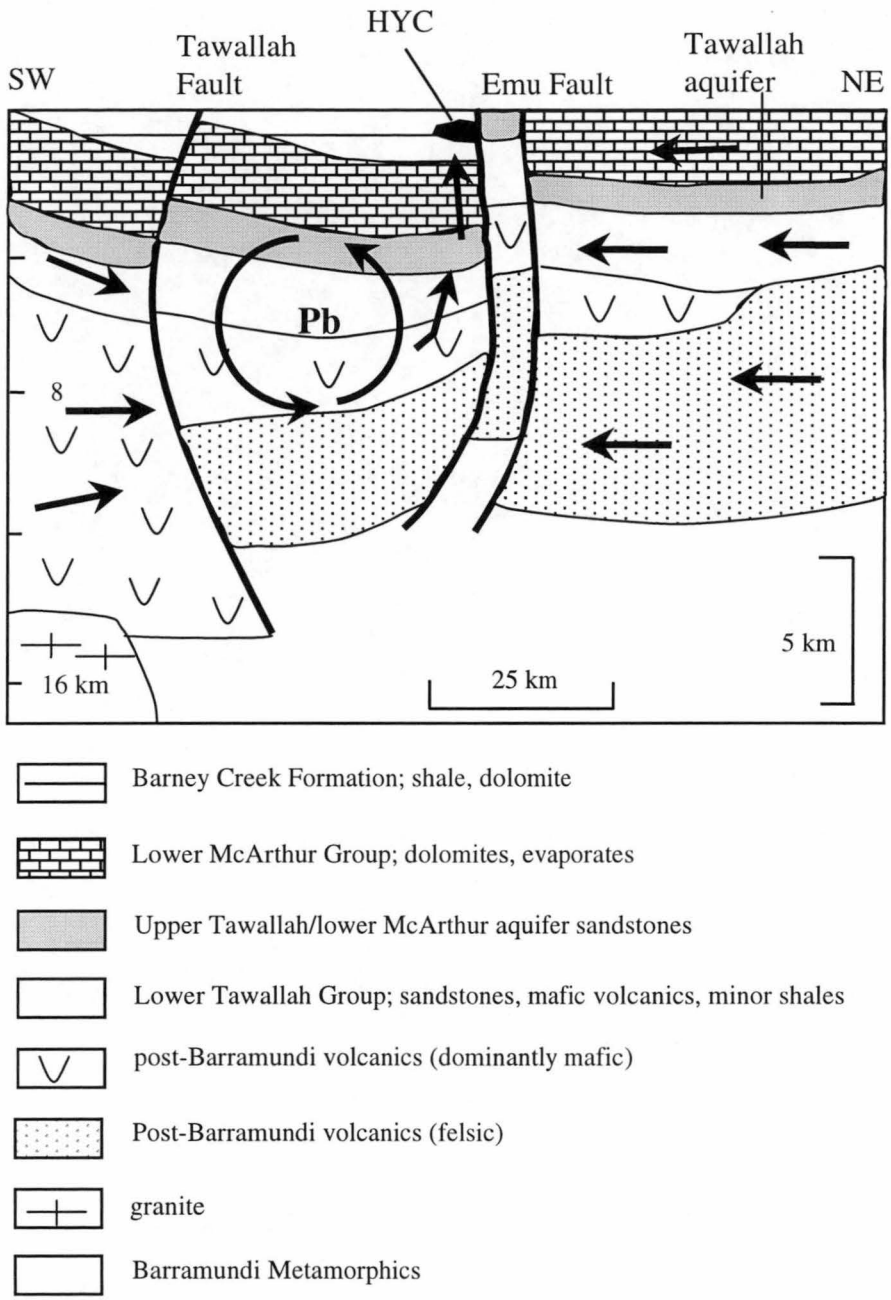

Figure 9.6. Conceptual model of hydrothermal flow for HYC deposit (from Large et al. 1998; Garven and Bull 1999)

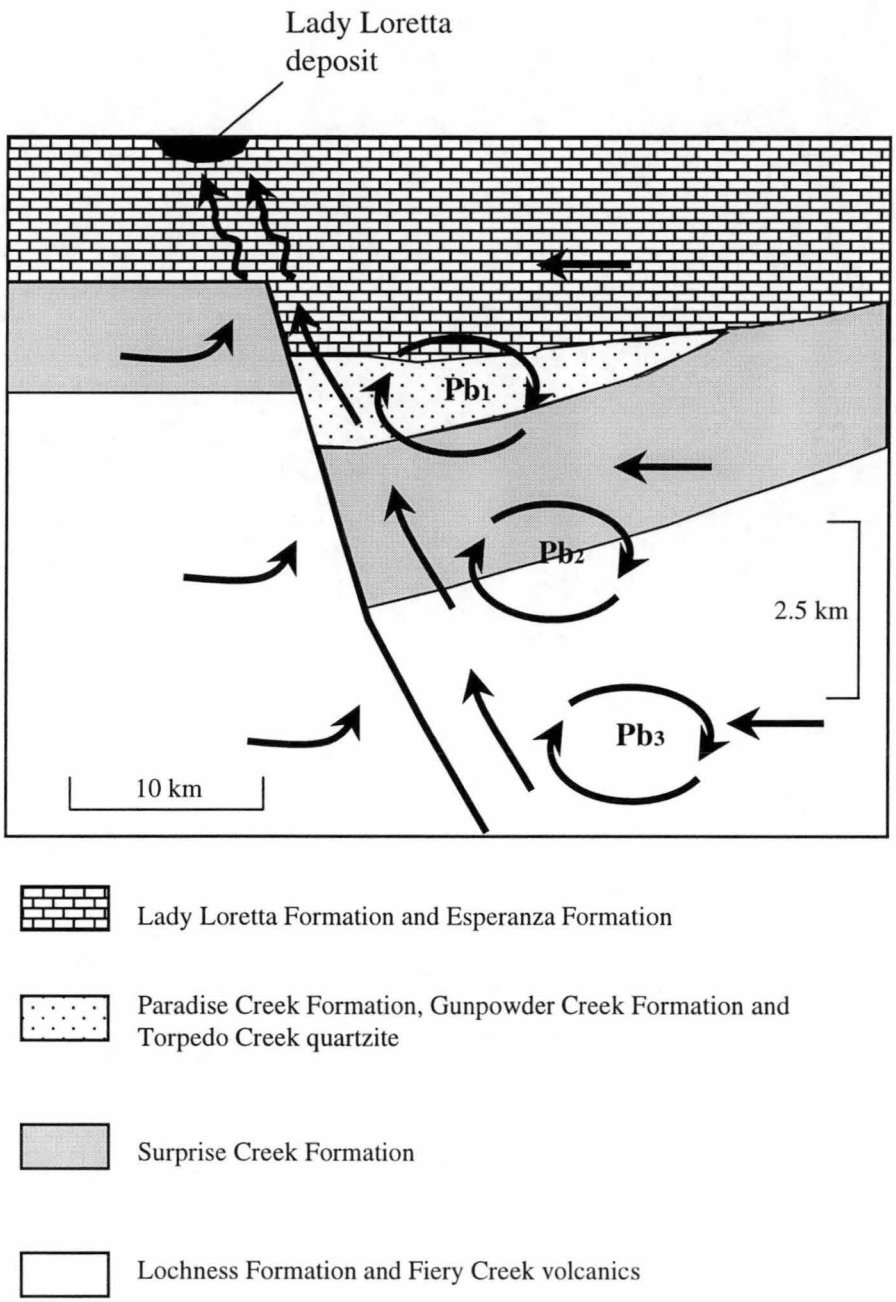

Figure 9.7. Conceptual model of hydrothermal flow showing discrete Pb sources for Lady Loretta deposit (inferred structural setting is from Bull 1998)

Chapter 10
SUMMARY AND CONCLUDING REMARKS

The investigation carried out in this project have established that ICP-MS is a powerful analytical technique capable of measuring trace elements at different levels and lead isotope ratios in geological materials when used in conjunction with appropriate decomposition methods.

Although optimal geoanalytical techniques for a variety of elements and rock types have been developed, there remain a number of questions and problems. They could be addressed in future studies. Some of these are noted below.

The systematic investigation of the performance characteristics of a HR-ICP-MS instrument enable us to better understand this relatively new analytical technique. It has been confirmed that, when operating at low resolution mode (R = 300), the Finnigan MAT Element HR-ICP-MS is a more sensitive technique than some other modern instrumental techniques, such as quadrupole ICP-MS (such as Fisons VG PlasmaQuad PQ2 + STE, HP 4500 instruments, and other models of quadrupole instruments described by Montaser 1998), ICP-AES, INAA and ion exchange-XRF techniques. This technique provides excellent detection limits, which for most trace elements studied are well under ng g^{-1} level, and for some trace elements (such as Sb, Cs, Tb, Er, Tm, Yb, Lu, Hf, Ta, Th, U etc.) can achieve pg g^{-1} level in solution. It has been shown that a single internal standard (such as In) is sufficient to compensate instrumental drift, which makes the HR-ICP-MS a relatively straightforward technique. Some spectral interferences (such as $^{29}Si^{16}O$ and $^{28}Si^{16}O^{1}H$ on ^{45}Sc) can be eliminated using higher resolution mode.

For future studies, it could be an interesting direction to couple this HR-ICP-MS instrument with a laser ablation system to develop some analytical techniques for direct measurement of trace elements in minerals and glasses. Most reference materials used in this study were not mineralized, hence, the solution-based ICP-MS

should be extended to sulfide-rich samples such as Pb-, Zn-, Cu-rich ores in order to better understand the matrix effects of some specific mineralized rocks.

Several digestion methods described and tested in this study can guarantee complete decompositions of different types of geological samples such as basalt, granite and magnetite-rich ironstone. These methods include Savillex Teflon beaker and PicoTrace high pressure acid digestions, lithium tetraborate fusion and sodium peroxide sinter. Without using specialized techniques, such as pre-concentration and ion exchange, several ultramafic rock standards containing very low abundance trace elements have been successfully analyzed using a conjunction of the $HF/HClO_4$ high pressure digestion technique developed here and HR-ICP-MS methods. For future work, it would be useful to investigate multi-stage digestion methods on geological materials using Savillex Teflon beaker and microwave oven. Testing digestion methods for sulfides, amphibolites and individual minerals (such as chromite, zircon, rutile and ilmenite) could be investigated as future projects. In order to better understand dissolution processes, it would be helpful to analyze digestion residues using XRF and electron microprobe.

An alternative approach, worthy of further investigation, is the direct analysis by LA-ICP-MS of $Li_2B_4O_7$ fusion glasses of silicate rocks.

This study has proved that DTPA and HFSE can form stable complexes HFSE in aqueous solutions, which can effectively prevent the hydrolysis of HFSE and hence allow the accurate determination of these elements, particularly at moderate to high levels in geological materials. Rock standards containing high abundances of Nb and Ta, such as MA-N and YG-1, have been successfully analyzed using the complexing method. As an extension of the present study and further assessment of the reliability of this complex method developed, it would be helpful to compare the HFSE data on different types of geological samples by ICP-MS with those measured using XRF.

There was excellent agreement among the trace element data obtained for basaltic glasses by laser ablation (solid sampling), high resolution (solution sampling) and quadrupole (solution sampling) ICP-MS. This further demonstrates that reliable trace element concentrations can be obtained by the refined ICP-MS methods described

and tested in this study. Further studies of the geochemical behaviors of the rarely analyzed (in magmatic studies) elements Mo, Sb, Sn, as well as Cu, Pb and Zn during mantle melting and basalt genesis are certainly warranted, especially comparing basalts from different tectonic environments.

This study has successfully developed analytical methods for the accurate and precise measurement of Pb isotope ratios in galena-bearing geological materials using both a HR-ICP-MS and a quadrupole ICP-MS. The reliability of these techniques has been assessed by a series of analyses of standard reference (NIST Pb SRM 981) and 11 galena-bearing geological samples. The discrepancies of Pb isotope ratios between solution ICP-MS and TIMS are generally better than 0.20%. Because the ICP-MS techniques are simple and low-cost techniques compared to TIMS, they have the potential for broad application to geological problems in the future.

As a test of the solution-based ICP-MS Pb isotope technique, sulfides collected from Lady Loretta have been analyzed. The data confirm trends previously described by Gulson (1985) and Vaasjoki and Gulson (1985) from TIMS data. The variable Pb in the deposit is inferred to reflect a poorly-mixed ore fluid deriving Pb from several different sources.

In practice, the ICP-MS technique is limited to rocks with more than 5 $\mu g\ g^{-1}$ Pb. The utility of preconcentration techniques such as ion-exchange in conjunction with either high resolution or quadrupole ICP-MS technique could be used to measure Pb isotope ratios at lower levels (>5 $\mu g\ g^{-1}$ in solid). Likewise, *in situ* Pb isotope ratio analysis on rocks using laser ablation ICP-MS should be an area of further study.

REFERENCES

Aheimer, M. A., 1994. Geology and geochemistry of the Lady Loretta SSH base metal deposit, northwest Queensland. BSc (Hons) thesis, CODES, University of Tasmania. 130 pp.

Arias, D., Corretgé, C. O., Villa, L., Cuesta, A. and Gallastegui, G., 1996. Lead and sulfur isotope compositions of the Ibias gold vein system (NW Spain), genetic implications. *Economic Geology*, **91,** 1292-1297.

Arribas, A., Jr. and Tosdal, R. M., 1994. Isotopic composition of Pb in ore deposits of the Betic Cordillera, Spain, origin and relationship to other European deposits. *Economic Geology*, **89,** 1074-1093.

Babington, R. S., 1973. It's superspray. *Popular Science*, **May,** 102-104.

Bankston, D. C., Humphris, S. E. and Thompson, G., 1979. Major and minor oxide and trace element determination in silicate rocks by direct current plasma optical emission echelle spectrometry. *Analytical Chemistry*, **51,** 1218-1225.

Bayón, M. M., Alonso, J. I. G. and Medel, A. S., 1998. Enhanced semiquantitative multi-analysis of trace elements in environmental samples using inductively coupled plasma mass spectrometry. *Journal of Analytical Atomic Spectrometry,* **13,** 277-282.

Becker, J. S. and Dietze, H.-J., 1997. Double-focusing sector field inductively coupled plasma mass spectrometry for highly sensitive multi-element and isotopic analysis. *Journal of Analytical Atomic Spectrometry,* **12,** 881-889.

Begley, I. S., and Sharp, B. L., 1997. Characterisation and correction of instrumental bias in inductively quadrupole mass spectrometry for accurate measurement of lead isotope ratios. *Journal of Analytical Atomic Spectrometry*, **12,** 395-402.

Bennett, H. and Oliver, G. J., 1976. Development of fluxes for the analysis of ceramic materials by X-ray fluorescence spectrometry. *Analyst,* **101,** 803-807.

Bernas, B., 1968. A new method for decomposition and comprehensive analysis of silicates by atomic absorption spectrometry. *Analytical Chemistry.* **42,** 1682-1686.

Bock, R., 1979. A Handbook of Decomposition Methods on Analytical Chemistry. International Textbook Company, London, 444 pp.

Borman, S. A., 1988. Microwave dissolution. *Analytical Chemistry,* **60,** 715A-716A.

Boynton, W. V., 1984. Geochemistry of the rare earth elements: meteorite studies. In: Henderson P. (editor), Rare earth geochemistry. Elsevier, 203-213.

Brenner, I. B., Watson, A. E., Russell, G. M. and Goncalves, M., 1980. A new approach to the determination of the major and minor constituents in silicate and phosphate rocks. *Chemical Geology,* **28,** 321-330.

Buchman, S. J. and Dale, L. S., 1986. Inductively coupled plasma-atomic emission spectrometric determination of rare earth elements in geological materials. *Spectrochemica Acta,* **41B,** 237-242.

Buckley, D. E. and Cranston, R. E., 1971. Atomic absorption analysis of 18 elements from a single decomposition of aluminosilicate. *Chemical Geology,* **7,** 273-284.

Burman, J., Ponter, C. and Bostrom, K., 1978. Metaborate digestion procedure for inductively coupled plasma-optical emission spectrometry. *Analytical Chemistry,* **50,** 273-284.

Cannon, R. S., Jr., Piece, A. P., Antweiler, J. C. and Buck, K. J., 1961. The data of lead isotope geology related to problems of ore genesis. *Economic Geology,* **56,** 1-38.

Cantagrel, F. and Pin, C., 1994. Major, minor and rare-earth element determinations in 25 rock standards by ICP-atomic emission spectrometry. *Geostandards Newsletter,* **18,** 123-138.

Carr, G. R., 1981. The mineralogy, petrology and geochemistry of the zinc-lead-silver ores and host sedimentary rocks at Lady Loretta, northwest Queensland. PhD thesis, The University of Wollongong.

Carr, G. R., 1984. Primary geochemical and mineralogical dispersion in the vicinity of the lady Loretta Zn-Pb-Ag deposit, northwest Queensland. *Journal of Geochemical Exploration,* **22,** 217-238.

Carr, G. R. and Sun, S.-s., 1996. Lead isotope models applied to Broken Hill style terrains – syngenetic vs epigenetic metallogenesis. Proceedings of a workshop on " New Development in Broken Hill Type Deposits", CODES, University of Tasmania, 77-87.

Chao, T. T. and Sanzolone, R. F., 1992. Decomposition techniques. *Journal of Geochemical Exploration,* **44,** 65-106.

Cheng, K. L., Ueno, K. and Imamura, T., 1982. CRC Handbook of Organic Analytical Reagents. CRC Press, Inc., Florida, USA, 534 pp.

Childe, F., 1996. U-Pb geochronology and Nd and Pb isotope characteristics of the Au-Ag-rich Eskay Creek volcanogenic massive sulfide deposit, British Colombia. *Economic Geology,* **91,** 1209-1224.

Church, S. E., 1981. Multi-element analysis of fifty-four geochemical reference samples using inductively coupled plasma-atomic emission spectrometry. *Geostandards Newsletter,* **5,** 133-160.

Cotton, F. A. and Wilkinson, G., 1980. Advanced Inorganic Chemistry. John Wiley & Sons, New York, USA, 1396 pp.

Cremer, M. and Schlocker, J., 1976. Lithium metaborate decomposition of rocks, minerals and ores. *American Mineralogist,* **61,** 318-321.

Cumming, G. L. and Richards, J. R., 1975. Ore lead isotope ratios in continuously changing earth. *Economic Geology,* **28,** 155-171.

Czamanske, G. K. and Moore, J. B., 1977. Composition and phase chemistry of sulfide globules in basalt from the Mid-Atlantic ridge rift valley near 37°N lat., *Geological Society of America Bulletin,* **88,** 587-599.

Date, A. R. and Cheung, Y. Y., 1987. Studies in the determination of lead isotope ratios by inductively coupled plasma mass spectrometry. *Analyst,* **112,** 1531-1540.

Date, A. R. and Gray, A. L., 1983a. Development progress in plasma source mass spectrometry. *Analyst,* **108,** 159-165.

Date, A. R. and Gray, A. L., 1983b. Progress in plasma source mass spectrometry. *Spectrochimica Acta,* **38B,** 29-37.

Doe, B. R. and Stacey, J., 1974. The application of lead isotopes to the problem of ore genesis and ore prospect evaluation, a review. *Economic Geology,* **69,** 757-767.

Dulski, P., 1992. Determination of minor and trace elements in four Canadian iron formation standard samples FeR-1, FeR-2, FeR-3 and FeR-4 by INAA and ICP-MS. *Geostandards Newsletter,* **16,** 325-332.

Dulski, P., 1994. Interferences of oxide, hydroxide and chloride analyte species in the determination of rare earth elements in geological samples by inductively coupled plasma-mass spectrometry. *Fresenius Journal of Analytical Chemistry,* **350,** 194-203.

Eggins, S. M., Rudnick, R. L. and McDonough, W. F., 1998. The composition of peridotites and their minerals, a laser-ablation ICP-MS study. *Earth and Planetary Science Letters,* **154,** 53-71.

Eggins, S. M., Woodhead, J. D., Kinsley, L. P. J., Mortimer, G. E., Sylvester, P., McCulloch, M. T. Hergt, J. M. and Handler, M. R., 1997. A simple method for the precise determination of ≥ 40 trace elements in geological samples by ICPMS using enriched isotope internal standardisation. *Chemical Geology,* **134,** 311-326.

Faure, G., 1977. Principles of Isotope Geology. John Wiley & Sons, New York, 464 pp.

Feldman, C., 1983. Behaviour of trace refractory minerals in lithium metaborate-acid dissolution procedure. *Analytical Chemistry,* **55,** 2451-2453.

Flanagan, F. J., 1967. U.S. geological silicate rock standards. *Geochimica et Cosmochimica Acta,* **31,** 289-308.

Foley, N. K. and Ayuso, R. A., 1994. Lead isotope compositions as guides to early gold mineralisation, the North Amethyst vein system, Creede district, Colorado. *Economic Geology,* **89,** 1842-1859.

Garbe-Schönberg, C.-D., 1993. Simultaneous determination of thirty-seven trace elements in twenty-eight international rock standards by ICP-MS. *Geostandards Newsletter,* **17,** 81-97.

Garven, G. and Bull, S. W., 1999. Fluid Flow Modelling of the HYC Ore System, McArthur Basin, Australia. In, Stanley, C. J. (Editor), Mineral Deposits, Processes to Processing (Vol 2), A.A.Balkema/Rotterdam/Brookfield/1999, 849-852.

Gladney, E. S., Jones, E. A. and Nickell, E. J., 1992. 1988 compilation of elemental concentration data for USGS AGV-1, GSP-1 and G-2. *Geostandards Newsletter,* **16,** 111-300.

Govindaraju, K., 1994. 1994 compilation of working values and sample description for 383 geostandards. *Geostandards Newsletter,* **18,** 1-158.

Govindaraju, K., Potts, P. J., Webb, P. C. and Watson, J. S., 1994. 1994 report on Whin Sill dolerite WS-E from England and Pitscurrie microgabbro PM-S from Scotland, assessment by one hundred and four international laboratories. *Geostandards Newsletter,* **18,** 211-300.

Gray, A. L., 1975. Mass spectrometric analysis of solutions using an atmospheric pressure ion source. *Analyst,* **100,** 289-299.

Gray, A. L. and Date, A. R., 1983. Inductively coupled plasma source mass spectrometry using continuum flow ion extraction. *Analyst,* **108,** 1033-1050.

Gray, A. L., 1989. The Origins, Realization and Performmance of ICP-MS Systems. In: Date, A. R. and Gray, A. L. (Editors) *Applications of Inductively Coupled Plasma Mass Spectrometry*. Blackie and Son Ltd., London, 1-42.

Grégoire, D. C., Ansdell, K. M., Goltz, D. M. and Chakrabarti, C. L., 1995. Trace analysis of single zircons for rare-earth elements, U and Th by electrothermal vaporisation-inductively coupled plasma-mass spectrometry (ETV-ICP-MS). *Chemical Geology,* **124,** 91-99.

Gregory, G. R. E. C. and Jeffrey, P. G., 1967. Salicylidenamino-2-thiophenol - a new reagent for the photometric determination of tin, application to the analysis of ores, rocks and minerals. *Analyst,* **92,** 293-299.

Gulson, B.L., 1985. Shale-hosted lead zinc deposits in northern Australia, lead isotope variations. *Economic Geology,* **80,** 2001-2012.

Gulson, B. L., 1986. Lead Isotopes in Mineral Exploration. Elsevier Science Publishers B. V., The Netherlands, 245 pp.

Gulson, B. L. and Mizon, K. J., 1979. Lead isotopes as a tool for gossan assessment in base metal exploration. *Journal of Geochemical Exploration,* **11,** 299-320.

Hall, G. E. M. and Pelchat, J.-C.,1990. Analysis of standard reference materials for Zr, Nb, Hf and Ta by ICP-MS after lithium metaborate fusion and cupferron separation. *Geostandards Newsletter,* **14,** 197-206.

Hall, G. E. M., Pelchat, J.-C. and Loop, J., 1990. Determination of zirconium, niobium, hafnium and tantalum at low levels in geological materials by inductively coupled plasma mass spectrometry. *Journal of Analytical Atomic Spectrometry,* **5,** 339-349.

Hancock, M. C. and Purvis, A. H., 1990. Lady Loretta silver-zinc deposit. In: Fughes, F. E. (editor) *Geology of the Mineral Deposit of Australia and Papua New Guinea.* Australian Institute of Mining and Metallurgy Monograph, **14,** 943-948.

Harding, R. R., 1983. Zr-rich pyroxenes and glauconite minerals in the Tertiary alkali granite of Ailsa Craig. *Scottish Journal of Geology,* **19,** 219-227.

Hee, S. S. Q. and Boyle, J. R., 1988. Simultaneous multielement analysis of some environmental and biological samples by inductively coupled plasma atomic emission spectrometry. *Analytical Chemistry,* **60,** 1033-1042.

Heslop, R. B. and Jones, K., 1976. Inorganic Chemistry. Elsevier Scientific Publishing Company, Amsterdam, 830 pp.

Hollocher, K. and Ruiz, J., 1995. Major and trace element determinations on NIST glass standard reference materials 611, 612, 614 and 1834 by inductively coupled plasma-mass spectrometry. *Geostandards Newsletter,* **19,** 27-34.

Holmes, A., 1913. The Age of the Earth. Harper, New York, 194 pp.

Horlick, G., Tan, S. H., Vaughan, M. A. and Shao, Y., 1987. Inductively Coupled Plasma-Mass Spectrometry. In: Montaser, A. and Golightly, D. W. (Editors) *Inductively Coupled Plasma in Analytical Atomic Spectrometry.* VCH Publishers, Inc., USA, 361-398.

Hou, Q. L., Hughes, T. C., Haukka, M. and Hannaker, P., 1985. Determination of the rare-earth elements in geological materials by thin-film X-ray fluorescence and inductively coupled plasma atomic-emission spectrometry. *Talanta,* **32,** 495-499.

Houk, R. S., Fassel, V. A., Flesch, G. D., Svec, H. J., Gray, A. L. and Taylor, C. E., 1980. Inductively coupled argon plasma spectrometric determination of trace elements. *Analytical Chemistry,* **52,** 2283-2289.

Houk, R. S., Montaser, A. and Fassel V. A., 1983. Mass spectra and ionization temperatures in an argon-Nitrogen inductively coupled plasma, *Applied Spectroscopy,* **37,** 425-428.

Howie, R. A. and Walsh, J. N., 1981. Riebeckitic arfvedsonite and aenigmatite from Ailsa Craig microgranite. *Scottish Journal of Geology,* 17, 123-128.

Ingamells, C. O., 1964. Rapid chemical analysis of silicate rocks. *Talanta,* **11,** 665-666.

Ionov, D. A., Savoyant, L. and Dupuy, C., 1992. Application of the ICP-MS technique to trace element analysis of peridotites and minerals. *Geostandards Newsletter,* **16,** 311-315.

Jackson, S. E., Fryer, B. J., Gosse, W., Healey, D. C., Longerich, H. P. and Strong, D. F., 1990. Determination of the precious metals in geological materials by inductively coupled plasma-mass spectrometry (ICP-MS) with nickel sulphide fire-assay and tellurium copreciptation. *Chemical Geology,* **83,** 119-132.

Jakubowski, N., Moens, L. and Vanhaeche, F., 1998. Sector field mass spectrometers in ICP-MS. *Spectrochimica Acta,* **Part B 53**, 1739-1763.

Jarvis, I. and Jarvis, K. E., 1992. Plasma spectrometry in the earth sciences, techniques, applications and future trends. *Chemical Geology,* **95,** 1-33.

Jarvis, K. E., 1988. Inductively coupled plasma mass spectrometry, A new technique for the rapid or ultra-trace level determination of the rare earth elements in geological materials. *Chemical Geology,* **68,** 31-39.

Jarvis, K. E., Gray, A. L. and Houk, R. S., 1992. Handbook of Inductively Coupled Plasma Mass Spectrometry. Blackie Academic & Professional, London, 380pp.

Jenner, G. A., Longerich, H. P., Jackson, S. E. and Fryer, B. J., 1990. ICP-MS — A powerful tool for high-precision trace-element analysis in earth sciences: Evidence from analysis of selected U.S.G.S. reference samples. *Chemical Geology,* **83,** 133-148.

Jochum, K. P., Rehkämper, M. and Seufert, H. M., 1994. Trace element analysis of basalt BIR-1 by ID-SSMS, HPLC and LIMS. *Geostandards Newsletter,* **18,** 43-51.

Johnson, W. M. and Maxwell, J. A., 1981. Rock and Mineral Analysis. Wiley, New York, 489 pp.

Kamenetsky, V., Everard, J. L., Crawford, A. J., Varne, R. Eggins, S. M. and Lanyon, R., 2000. Enriched end-member of primitive MORB melts: petrology and geochemistry of glasses from Macquarie Island (SW Pacific). *Journal of Petrology,* **41,** 411-430.

Kamenetsky, V. S., Gemmell, J. B., Binns, R. A., Crawford, A. J., Mernagh, T. P., Maas, R. and Steele, D., 2000. Parental basaltic melts and fluids in eastern Manus backarc basin: Implications for felsic magmatism and associated hydrothermal mineralisation. *Earth Planetary Science Letters,* (in press).

Karstensen, K. H. and Lund, W., 1989. Multi-element analysis of a city waste incineration ash reference samples by inductively coupled plasma atomic emission spectrometry. *Journal of Analytical Atomic Spectrometry,* **4,** 357-359.

Kemp, A. J. and Brown, C. J., 1990. Microwave digestion of carbonate rock samples for chemical analysis. *Analyst,* **115,** 1197-1199.

Ketterer, M. E., 1992. Assessment of overall accuracy of lead isotope ratios determined by inductively coupled plasma mass spectrometry using batch quality control and the Youden two-sample method. *Journal of Analytical Atomic Spectrometry,* **7,** 1125-1129.

Kingston, H. M. and Jassie, L. B., 1988. Introduction to Microwave Sample Preparation. American Chemical Society, Washington, D. C., 263 pp.

Kinzler, R. J. and Grove, T. L., 1992. Primary magmas of mid-ocean ridge basalts 2. Applications. *Journal of Geophysical Research,* **97,** 6907-6926.

Koeva, M., Mareva, S. and Jordanov, N., 1975. Photometric determination of tin in ores, rocks and alloys with pyrocatechol violet after extraction with N-benzol-N-phenylhydroxylamine. *Analytica Chemica Acta,* **75,** 464-467.

Lamothe, P. J., Fries, T. L. and Consul, J. J., 1986. Evaluation of a microwave oven system for the dissolution of geologic samples. *Analytical Chemistry,* **58,** 1881-1886.

Langmuir, C. H., Klein, E. M. and Plank, T., 1992. Petrological systematics of mid-ocean ridge basalts, constraints on melt generation beneath ocean ridges. In: Phipps Morgan, J. *et al.* (editors) *Mantle Flow and Melt Generation at Mid-Ocean Ridges.* **71.** Washington, D.C., American Geophysical Union, 183-280.

Langmyhr, F. J. and Paus, P. E., 1968. The analysis of inorganic siliceous materials by atomic absorption spectrophotometry and the hydrofluoric acid decomposition technique. Part I, The analysis of silicate rocks. *Analytica Chemica Acta,* **43,** 397-408.

Lanyon, R., Varne, R. and Crawford, A. J., 1993. Tasmanian Tertiary basalts, the Balleny plume, and opening of the Tasman Sea (southwest Pacific Ocean), *Geology* **21,** 555-558.

Lanyon, R., 1994. Mantle reservoirs and mafic magmatism associated with the break-up of Gondwana-the Balleny Plume and the Australian-Antarctic discordance. U-pb zircon dating of a Proterozoic mafic dyke swarm in the Vestfold Hills, East Antarctic. PhD thesis. University of Tasmania.

Large, R. R. and McGoldrick, P. J., 1998. Lithogeochemical halos and geochemical vectors to stratiform sediment hosted Zn-Pb-Ag deposits, 1. Lady Loretta Deposit, Queensland. *Journal of Geochemical Exploration,* **63,** 37-56.

Lechler, P. J., Roy, W. R. and Leininger, R. K., 1980. Major and trace element analysis of 12 reference soils by inductively coupled plasma-atomic emission spectrometry. *Soil Society,* **43,** 238-241.

Le Guen, M., Lescuyer, J. L. and Marcoux, E., 1992. Lead-isotope evidence for a Hercynian origin of the Salsigne gold deposit (southern Massif Central France). *Mineralium Deosita,* **27,** 129-136.

Liang, Q., Jing, H. and Gregoire, D. C., 2000. Determination of trace elements in granites by inductively coupled plasma mass spectrometry. *Talanta,* **51,** 507-513.

Lichte, F. E., Meier, A. L. and Crock, J. G., 1987. Determination of the rare-earth in geological materials by inductively coupled plasma mass spectrometry. *Analytical Chemistry,* **59,** 1150-1157.

Loudon, A. G., Lee, M. K., Dowling, J. F. and Bourn, R., 1975. Lady Loretta silver-lead-zinc deposit. In: Knight, C. L. (editor) *Economic Geology of Australia and Papua New Guinea.* Australasian Institute of Mining and Metallurgy. 377-382.

Longerich, H. P., Wilton, D. H. C. and Fryer, B. J., 1992. Isotopic and elemental analysis of uraninite concentrates using inductively coupled plasma mass spectrometry. *Journal of Geochemical Exploration,* **43,** 111-125.

Longerich, H. P., 1993. Oxychlorine ions in inductively coupled plasma mass spectrometry, effect of chlorine speciation as Cl^- and $ClO4^-$. *Journal of Analytical Atomic Spectrometry,* **8,** 439-444.

Longerich, H. P., Jackson, S. E. and Gunther, D., 1996. Laser ablation inductively coupled plasma mass spectrometric transient signal data acquisition and analyte concentration calculation. *Journal of Analytical Atomic Spectrometry,* **11**, 899-904.

Makishima, A. and Nakamura, E., 1997. Suppression of matrix effects in ICP-MS by high power operation of ICP, Application to precise determination of Rb, Sr, Y, Cs, Ba, REE, Pb, Th and U at ng g^{-1} levels in milligram silicate samples. *Geostandards Newsletter,* **21,** 307-319.

Marcoux, E. and Möelo, Y., 1991. Lead isotope geochemistry and paragenetic study of inheritance in metallogenesis, examples from base metal sulfide deposits in France. *Economic Geology,* **86,** 106-120.

Martell, A. E. and Smith, R. M., 1974. Critical Stability Constants - Volume 1, Amino Acids. Plenum Press, New York, 469 pp.

Martell, A. E. and Smith, R. M., 1977. Critical Stability Constants - Volume 3, Other Organic Ligands. Plenum Press, New York, 495 pp.

Martell, A. E. and Smith, R. M., 1982. Critical Stability Constants - Volume 5, First Supplement. Plenum Press, New York, 604 pp.

Martell, A. E. and Smith, R. M., 1989. Critical Stability Constants - Volume 6, Second Supplement. Plenum Press, New York, 643 pp.

Mathes, S. A., 1988. Guide-lines for developing microwave dissolution methods for geological and metallurgical samples. In: Kingston, H. M. and Jassie, L.B. (editors) *Introduction to Microwave sample Preparation.* American Chemical Society, Washington, D. C., pp33-51.

Matusiewicz, H. and Sturgeon, R. E., 1989. Present status of microwave sample dissolution and decomposition for element analysis. *Progress in Analytical Spectroscopy,* **12,** 21-39.

McGinnis, C. E., Jain, J. C. and Neal, C. R., 1997. Characterisation of memory effects and development of an effective wash protocol for the measurement of petrogenetically critical trace elements in geological samples by ICP-MS. *Geostandards Newsletter,* **21,** 289-305.

McGoldrick, P., Dunster, D. and Aheimer, M., 1996. New observations from the Lady Loretta Zn-Pb-Ag deposit towards a genic model, MIC'96, the McArthur, Mt Isa, Conclurry minerals province; new developments in metallogenic research; extended conference abstracts, 81-84.

McGoldrick, P., Dunster, D. and Aheimer, M., 1998. New sedimentological, geochemical and textural observations from Lady Loretta deposit: implications for ore genesis. Proceedings of a symposium on "Basins, fluids and Zn-Pb ores" CODES, University of Tasmania, 49-57.

McGoldrick, P. and Large, R., 1998. Halo model for the lady Loretta deposit. In, Sediment-Hosted Base Metal Deposit-Project Outcomes Report, Centre for Ore Deposit Research, University of Tasmania. 71-88.

McLaren, J. W., Berman, S. S., Boyke, Y. J. and Russell, D. S., 1981. Simultaneous determination of major, minor, and trace elements in marine sediments by inductively coupled plasma atomic emission spectrometry. *Analytical Chemistry,* **51,** 1802-1806.

McLaren, J. W., Beauchemin, D. and Berman, S. S., 1987. Determination of trace metals in marine sediments by inductively coupled plasma mass spectrometry. *Journal of Analytical Atomic Spectrometry,* **2,** 277-281.

McQuaker, N. R., Brown, D. F. and Kluckner, P. D., 1979. Digestion of environmental materials for analysis of inductively coupled plasma-atomic emission spectrometry. *Analytical Chemistry,* **51,** 1082-1084.

Minnich, M. G. and Houk, R. S., 1998. Comparison of cryogenic and membrane desolvation for attenuation of oxide, hydride and hydroxide ions and ions containing chlorine in inductively coupled plasma mass spectrometry. *Journal of Analytical Atomic Spectrometry,* **13,** 167-174.

Minnich, M. G. and Houk, R. S., Woodin, M. A. and Christiani, D. C., 1997. Method to screen urine samples for vanadium by inductively coupled plasma mass spectrometry with cryogenic desolvation. *Journal of Analytical Atomic Spectrometry,* **12,** 1345-1350.

Moens, L., Verrept, P., Dams, R., Greb, U., Jung, G. and Laser, B., 1994. New high-resolution inductively coupled plasma spectrometry technology applied for the determination of V, Fe, Cu, Zn and Ag in human serum. *Journal of Analytical Atomic Spectrometry,* **9,** 1075-1078.

Moens, L., Vanhaecke, F., Riondato, J. and Dams, R., 1995. Some figures of merit of a new double focusing inductively coupled plasma mass spectrometer. *Journal of Analytical Atomic Spectrometry,* **10,** 569-574.

Montaser, A., 1998. Inductively Coupled Plasma Mass Spectrometry. Wiley-VCH Inc., New York, 964 pp.

Moselhy, M. M., Boomer, D. W., Bishop, J. N.; Diosady, P. l. and Howlett, A. D., 1978. Multielemental analysis of environmental materials by inductively argon plasma excitation and direct-reading spectrometry. *Canadian Journal of Spectroscopy,* **33,** 186-195.

Münker, C., 1998. Nb/Ta fractionation in a Cambrian arc/back arc system, New Zealand, source constraints and application of refined ICPMS techniques. *Chemical Geology,* **144,** 23-45.

Niu, Y. and Batiza, R., 1997. Trace element evidence from seamounts for recycled oceanic crust in the Eastern Pacific mantle. *Earth and Planetary Science Letters,* **148,** 471-484.

Niu, Y., Collerson K. D., Batiza R., Wendt J. I. and Regelous M., 1999. Origin of enriched-type mid-ocean ridge basalt at ridges far from mantle plumes, The East Pacific Rise at 11°20'N. *Journal of Geophysical Research,* **104,** 7067-7087.

Niu, Y., Waggoner, D. G., Sinton, J. M. and Mahoney, J. J., 1996. Mantle source heterogeneity and melting processes beneath seafloor spreading centres: The East Pacific Rise, 18°-19°S. *Journal of Geophysical Research,* **101,** 27711-27733.

Nölter, T., Maisenbacher, P. and Puchelt, H., 1990. Microwave and digestion of geological and biological standard reference materials for trace element analysis by inductively coupled plasma-mass spectrometry. *Spectroscopy,* **5,** 49-53.

Norman, M. D., Leeman, W. P., Blanchard, D. P., Fitton, J. G. and James, D., 1989. Comparison of major and trace element analyses by ICP, XRF, INAA and ID methods. *Geostandards Newsletter,* **13,** 283-290.

Norman, M., 1997. Drift characteristics of the PE6000 ICPMS for solution analysis of geological samples. The 4th Australian Symposium on Applied ICP-Mass Spectrometry, May 1997, Sydney, Australia.

Norman, M. D., Griffin, W. L., Pearson, N. J., Gracia, M. O. and O'Reilly, S. Y., 1998. Quantitative analysis of trace element abundances in glasses and minerals, a comparison of laser ablation inductively coupled plasma mass spectrometry, solution inductively coupled plasma mass spectrometry, proton microprobe and electron microprobe data. *Journal of Analytical Atomic Spectrometry,* **13,** 477-482.

Olivares, J. A. and Houk, R. S., 1985. Ion sampling for inductively coupled plasma mass spectrometry. *Analytical Chemistry,* **57,** 2674-2679.

Peach, C. L., Mathez, E. A. and Keays, R. R., 1990. Sulfide melt-silicate melt distribution coefficients for noble metals and other chalcophile elements as deduced from MORB: Implications for partial melting. *Geochimica et Cosmochimica Acta,* **54,** 3379-3389.

Perrin, D. D., 1964. Organic Complexing Reagents, Structure, Behaviour, and Application to Inorganic Analysis. Ineterscience Publishers, John Wiley & Sons, Inc., USA, 365 pp.

Pin, C. and Joannon, S., 1997. Low-level analysis of lanthanides in eleven silicate rock reference materials by ICP-MS after group separation using cation-exchange chromotography. *Geostandards Newsletter,* **21,** 43-50.

Poitrasson, F., Pin, C., Telouk, P. and Imbert, J.-L., 1993. Assessment of a simple method for the determination of Nb and Ta at the sub-μg/g level in silicate rocks by ICP-MS. *Geostandards Newsletter,* **17,** 209-215.

Potts, P. J., 1987. A Handbook of Silicate Rock Analysis. Blackie & Son Limited, London, 622 pp.

Potts, P. J. and Holbrook, J. R., 1987. Ailsa Craig - the history of a reference material. *Geostandards Newsletter,* **11,** 257-260.

Price Russ III, G., 1989. Isotope Ratio Measurements Using ICP-MS. In: Date, A. R. and Gray, A. L. (Editors) Applications of Inductively Coupled Plasma Mass Spectrometry. Blackie and Son Ltd., London, 90-110.

Rafter, T. A., 1950. Sodium decomposition of minerals in platinum vessels. *Analyst,* **75,** 485-492.

Rankama, K., 1963. Progress in Isotope Geology. Interscience Publishers, London, 705 pp.

Rantala, R. T. T. and Loring, D. H., 1989. Teflon bomb decomposition of silicate materials in a microwave oven. *Analytica Chemica Acta,* **220,** 263-267.

Rautiainen, L., Hagel-Brunnström, M.-L., Heiskanen, L. and kallio, E., 1996. Production oriented method for the determination of rare earth and other trace elements in rocks by ICP-MS. *Fresenius Journal of Analytical Chemistry,* **355,** 393-396.

Riddle, C., Vander-Voet, A. and Doherty, W., 1988. Rock analysis using inductively coupled plasma mass spectrometry, A review. *Geostandards Newsletter,* **12,** 203-234.

Robinson, P., Higgins, N. C. and Jenner, G. A., 1986. Determination of rare-earth elements, yttrium and scandium in rocks by an ion exchange-X-ray fluorescence technique. *Chemical Geology,* **55,** 121-137.

Robinson, P., Townsend, A. T., Yu, Z. and Münker, C., 1999. Determination of scandium, yttrium and rare earth elements in rocks by high resolution inductively coupled plasma mass spectrometry. *Geostandards Newsletter: The Journal of Geostandards and Geoanalysis,* **23,** 31-46.

Rodgers, K. A., 1972. The decomposition and analysis of chrome spinel. A survey of some published techniques. *Mineralogical Magazine,* **38,** 882-889.

Rollinson, H. R., 1993. Using Geochemical Data, Evaluation, Presentation, Interpretation. Longman Scientific & Technical, England, 352 pp.

Sen Gupta, J. G. and Bertrand, N. B., 1995. Direct ICP-MS determination of trace and ultratrace elements in geological materials after decomposition in a microwave oven, Part II. Quantitation of Ba, Cs, Ga, Hf, In, Mo, Nb, Pb, Rb, Sn, Sr, Ta and Tl. *Talanta*, **42,** 1947-1957.

Sharp, B. L., 1988. Pneumatic nebulisers and spray chambers for inductively coupled plasma spectrometry, A review, part 1. Nebulisers. *Journal of Analytical Atomic Spectrometry,* **3,** 613-652.

Shuttleworth, S., Morris, J., Crombie, K., Ridings, R. and Arvidson, R., 1997. Using Pb isotope measurements by ICP-MS to monitor point source Pb pollution in Southeast Missouri. 3rd International Conference on the Analysis of Geological and Environmental Materials, Colorado, USA, June, 1997, p 100.

Smith, R. G., Brooker, E. J., Douglas, D. J., Quan, E. S. K. and Rosenblatt, G., 1984. The trying of Au and base-metal occurrence by plasma/mass spectrometry, initial results. *Journal of Geochemical Exploration,* **21,** 385-393.

Stacey, J. S. and Kramers, J. D., 1975. Approximation of terrestrial lead isotope evolution by a two-stage model. *Economic Geology,* **26,** 207-221.

Stürup, S., Hansen, M. and MØlgaard, C., 1997. Measurements of ^{44}Ca , ^{43}Ca and ^{42}Ca , ^{43}Ca isotopic ratios in urine using high resolution inductively coupled plasma mass spectrometry. *Journal of Analytical Atomic Spectrometry,* **12,** 919-923.

Suddendorf, R. F. and Boyer, K. W., 1978. Nebuliser for analysis of high salt content samples with inductively-coupled plasma emission spectrometry. *Analytical Chemistry*, **50,** 1769-1771.

Sun, S.-s. and McDonough, W. F., 1989. Chemical and Isotopic Systematics of Oceanic Basalts, Implications for Mantle Composition and Processes. In: Saunders, A. D. and Norry, M. J. (Editors) *Magmatism in the Ocean Basins.* Geological Society Special Publication No 42, Blackwell Scientific Publications, Oxford, 313-345.

Sun, S.–s., Page, R. and Carr, G. R., 1994. Lead-isotope-based stratigraphic correlations and ages of Proterozoic sediment-hosted Pb-Zn deposits in the Mount Isa Inlier. *Australia Geological Survey Organisation Research Newsletter,* **20,** 1-2.

Sun, S.–s., Carr, G. R. and Page, R., 1996. A continued effort to improve Pb isotope model ages. *Australia Geological Survey Organisation Research Newsletter,* **24,** 19-20.

Tan, S. H. and Horlick, G., 1986. Background spectral features in inductively coupled plasma/mass spectrometry. *Applied Spectroscopy,* **40,** 445-460.

Teall, J. J. H., 1892. On a micro-granite containing riebeckite from Ailsa Craig. *Mineralogical Magazine,* **9,** 219-221.

Thompson, M. and Potts, P. J., Kane, J. S. and Chappell, B. W., 1999. GeoPT3. International proficiency test for analytical geochemistry laboratories – report on round 3. *Geostandards Newsletter, The Journal of Geostandards and Geoanalysis,* **23,** 87-121.

Totland, M., Jarvis, I. and Jarvis, K. E., 1992. An assessment of dissolution techniques for the analysis of geological samples by plasma spectrometry. *Chemical Geology,* **95,** 35-62.

Totland, M., Jarvis, I. and Jarvis, K. E., 1995. Microwave digestion and alkali fusion procedures for the determination of the platinum-group elements and gold in geological materials by ICP-MS. *Chemical Geology,* **124,** 21-36.

Townsend, A. T., Yu, Z., McGoldrick P. and Hutton, J. A. 1998. Precise lead isotope ratios in Australian galena samples by high resolution inductively coupled plasma mass spectrometry. *Journal of Analytical Atomic Spectrometry,* **13,** 809-813.

Uchida, H., Uchida, T. and Iida, C., 1980. Determination of major and trace elements in silicate rocks by inductively coupled plasma emission spectrometry. *Analytica Chemica Acta,* **116,** 433-437.

Vaasjoki, M. and Gulson, B. L., 1985. Evaluation of drilling priorities using lead isotope ratios at the Lady Loretta lead-zinc-silver deposit, Australia. *Journal of Geochemical Exploration,* **24,** 305-316.

Vandecasteele, C. and Block, C. B., 1995. Modern Method for Trace Element Determination. John Wiley & Sons. Inc., New York, 330 pp.

Vanhaecke, F., Moens, L. and Dams, R., 1996. Precise measurement of isotope ratios with a double-focusing magnetic sector ICP mass spectrometer. *Analytical Chemistry,* **68,** 567-569.

Vanhaecke, F., Moens, L. and Dams, R., 1997. Applicability of high-resolution ICP-mass spectrometry for isotope ratio measurements. *Analytical Chemistry,* **69,** 268-273.

Vaughan, M. A. and Houlick, G., 1986. Oxide, hydroxide, and doubly charged analyte species in inductively coupled plasma/mass spectrometry. *Applied Spectroscopy,* **40,** 434-445.

Wallace, P. and Carmichael, I. S. E., 1992. Sulfur in basaltic magmas. *Geochimica et Cosmochimica Acta,* **56,** 1863-1874, 1992.

Walsh, J. N. and Howie, R. A., 1980. An evaluation of the performance of an inductively coupled plasma source spectrometer for the determination of the major and trace constituents of silicate rocks and minerals. *Mineralogical Magazine,* **43,** 967-974.

Wang, M. S., 1961. Rapid sample fusion with lithium tetraborate for emission spectroscopy. *Spectroscopy,* **16,** 141-142.

Williams, J. G., 1992. Instrument Options. In, Jarvis, K. E., Gray, A. L. and Houk, R. S. (Editors), Handbook of Inductively Coupled Plasma Mass Spectrometry. Blackie Academic & Professional, London. 58-80.

Xie, X., Yan, M., Li, L. and Shen, H., 1985. Useable values for Chinese standard reference samples of stream sediments, soils, and rocks, GSD 9 - 12, GSS 1 - 8 and GSR 1 - 6. *Geostandards Newsletter,* **9,** 277-280.

Xie, X., Yan, M., Wang, C., Li, L. and Shen, H., 1989. Geochemical standard reference samples GSD 9-12, GSS 1-8 and GSR 1-6. *Geostandards Newsletter,* **13,** 83-179.

Xie, Q., Jain, J., Sun, M., Kerrich, R. and Fan, J., 1994. ICP-MS analysis of basalt BIR-1 for trace elements. *Geostandards Newsletter,* **18,** 53-63.

Xie, Q. and Kerrich, R., 1995. Application of isotope dilution for precise measurement of Zr and Hf in low-abundance and international reference materials by inductively coupled plasma mass spectrometry, implications for Zr (Hf)/REE fractionations in komatites. *Chemical Geology,* **123,** 17-27.

Yoshida, S., Muramatsu, Y., Tagami, T. and Uchida, S., 1996. Determination of major and trace elements in Japanese rock reference samples by ICP-MS. *International Journal of Analytical Chemistry,* **63,** 195-206.

Yu, Z., Robinson, P., Townsend, A. T., Münker, C. and Crawford, A. J., 2000. Determination of high field strength elements, Rb, Sr, Mo, Sb, Cs, Tl and Bi at ng g^{-1} levels in geological reference materials by magnetic sector ICP-MS after HF/$HClO_4$ high pressure digestion. *Geostandards Newsletter: The Journal of Geostandards and Geoanalysis.* **24,** 39-50.

Appendix

PULICATIONS

Contents

Townsend, A. T., Yu, Z., McGoldrick, P. and Hutton, J. A., 1998. Precise lead isotope ratios in Australian galena samples by high resolution inductively coupled plasma mass spectrometry. *Journal of Analytical Atomic Spectrometry*, **13,** 809-813.

Robinson, P., Townsend, A. T., Yu, Z. and Münker, C., 1999. Determination of scandium, yttrium and rare earth elements in rocks by high resolution inductively coupled plasma mass spectrometry. *Geostandards Newsletter: The Journal of Geostandards and Geoanalysis*, **23,** 31-46.

Vachirapatama, N., Doble, P., Yu, Z. and Haddad, P. R., 1999. Determination of niobium (v) and tantalum (v) as 2-(5-bromo-2-pyridylazo)-5-diethylaminophenol (Br-PADAP)-citrate ternary complexes in geological materials using ion-interaction reversed-phase high-performance liquid chromatography. *Chromatographia*, **50,** 601-606.

Yu, Z., Norman, M. and McGoldrick, P., 2000. Precise measurement of lead isotope ratios in sulfides by quadrupole ICPMS. Abstracts and Proceedings, Beyond 2000 New Frontiers in Isotope Geoscience (Lorne, Australia) 197-200.

Yu, Z., Robinson, P., Townsend, A. T., Münker, C. and Crawford, A. J., 2000. Determination of high field strength elements, Rb, Sr, Mo, Sb, Cs, Tl and Bi at ng g^{-1} levels in geological reference materials by magnetic sector ICP-MS after HF/$HClO_4$ high pressure digestion. *Geostandards Newsletter: The Journal of Geostandards and Geoanalysis*. **24,** 39-50.

INTER-LABORATORY NOTE

JAAS Journal of Analytical Atomic Spectrometry

Precise lead isotope ratios in Australian galena samples by high resolution inductively coupled plasma mass spectrometry

Ashley T. Townsend*[a], Zongshou Yu[b], Peter McGoldrick[b] and James A. Hutton[a]

[a]*Central Science Laboratory, University of Tasmania, GPO Box 252-74, Hobart, Tasmania, 7001, Australia*
[b]*Centre for Ore Deposits and Exploration Studies, University of Tasmania, GPO Box 252-79, Hobart, Tasmania, 7001, Australia*

High resolution inductively coupled plasma mass spectrometry (HR-ICP-MS) was used to measure Pb isotope ratios in standard solutions and Pb mineral digests. The RSD values obtained for $^{208}Pb/^{204}Pb$, $^{207}Pb/^{204}Pb$, $^{206}Pb/^{204}Pb$, $^{208}Pb/^{206}Pb$ and $^{207}Pb/^{206}Pb$ were 0.13, 0.11, 0.11, 0.046 and 0.048%, respectively (values as 1σ). These values were obtained from 30 analyses of three different standard sample types (multi-element standard, NIST SRM 981 and a Broken Hill galena digest). Based on 39 analyses of 11 galena samples from different locations around Australia, the difference between HR-ICP-MS and conventional TIMS values for $^{208}Pb/^{204}Pb$, $^{207}Pb/^{204}Pb$, $^{206}Pb/^{204}Pb$, $^{208}Pb/^{206}Pb$ and $^{207}Pb/^{206}Pb$ ratios was generally better than ±0.2%. This paper outlines a very simple and rapid analytical method for the measurement of Pb isotope ratios, and is one of the first studies to use HR-ICP-MS to measure Pb isotope ratios in galena and galena-bearing ores.

Keywords: Lead isotope ratios; high resolution inductively coupled plasma mass spectrometry; galena; ores

The study of the isotopic composition of Pb in rocks and minerals began over 80 years ago and was initially used as a geochronological tool.[1] Subsequent work showed that for many types of geological materials, Pb isotope geochronology was complicated by the presence of 'common' Pb (*i.e.*, non-radiogenic Pb).[2] Hence today, Pb isotope geochronology uses minerals that formed with very little Pb.[3] However, a second important practical application of Pb isotopes is in studying and exploring for mineral deposits.[4] The Pb isotope composition of rocks and Pb-bearing minerals can be used to trace the sources of metal in ores and to help discriminate barren from mineralised ore systems.

At present, thermal ionisation mass spectrometry (TIMS) is the technique of choice for all types of geological Pb isotope measurements. However, the relatively high cost of TIMS instrumentation and the (necessary) extensive chemical pre-treatment of the sample prior to analysis have imposed serious limitations on the routine use of TIMS techniques in geochemical exploration applications.

Quadrupole based ICP-MS instruments have been used in many studies to measure Pb isotope ratios.[5–8] However, owing to the design and manner in which quadrupole mass analysers operate, the technique has been found to be limited in both precision and accuracy. The precision of isotope ratios measured on quadrupole ICP-MS instruments is typically 0.1% RSD, whereas for ratios involving a low abundance isotope such as ^{204}Pb, a precision of 0.2–1% RSD is usually obtained.[8]

Recently, Begley and Sharp[8] undertook an elegant study of Pb isotope ratios using a quadrupole ICP-MS instrument. After careful consideration of all possible causes of instrumental bias, the precision obtained from the analysis of NIST Standard Reference Material (SRM) 981 Natural Lead ranged from 0.04 to 0.12%, depending on the ratio considered. The accuracy and precision reported may be the best obtained from a quadrupole instrument. However, the methodology and detail required to obtain such results could not be called routine.

High resolution ICP-MS (HR-ICP-MS) is a relatively new technique employing a magnetic sector mass analyser. To date it has been applied in a variety of areas such as environmental and biological analysis and the monitoring of radionuclides (see the review by Becker and Dietze[9]). Only a limited number of studies have been reported on measuring isotope ratios.[10–14] With regard to Pb isotope ratios, Vanhaecke *et al.*[10] obtained a precision of 0.04% ($n=10$) for the $^{206}Pb/^{207}Pb$ ratio in a standard lead solution. Little has been reported about the Pb isotope ratio analysis of geological matrices.[14] It should also be noted, however, that double focusing multiple collector ICP-MS instruments have been used recently to measure highly accurate isotope ratios (including Pb), and may see increased use in future work.[15,16]

In this paper, a fast and reliable method for the precise measurement of Pb isotope ratios in geological samples by HR-ICP-MS is reported. The technique was applied to the measurement of the Pb isotope composition of galena and galena-bearing ores from Broken Hill and Western Tasmania, previously measured by TIMS.

EXPERIMENTAL

Reagents

High purity HCl was prepared by doubly quartz distilling analytical-reagent grade acid (Merck, Darmstadt, Germany), and high purity HF was prepared from analytical-reagent grade acid (Merck) that had been further purified *via* a Teflon distillation system. High purity HNO_3 (Mallinckrodt, St. Louis, MO, USA) was used as received for sample digestion and solution acidification. Ultra-pure de-ionised water (≥18 MΩ) was prepared *via* a glass distillation unit followed by further purification with a Modulad water purification system (Continental Water System, Melbourne, Australia).

Standards and sample preparation

Instrument tuning and general Pb solutions were prepared by dilution from a Perkin-Elmer (Norwalk, CT, USA) 10 μg g^{-1} multi-element solution containing Pb (Cat. No. N930-0233).

A stock standard solution of NIST SRM 981 Natural Lead was prepared by dissolving 0.05 g of Pb in 5 ml of dilute HNO_3 (1+4) with heating in a Savillex screw-topped Teflon

beaker.[17] After cooling to room temperature, 1 ml of concentrated HNO_3 was added before dilution to 100 ml total volume (in polycarbonate). The stock standard solution was diluted to working concentrations (generally 10–50 ng g^{-1}) before analysis. This reference solution was used as the external calibration standard in this study.

Galena sample solutions were prepared as follows. Samples were dried at 105 °C overnight and 0.1 g portions were added to Savillex screw-topped Teflon beakers. A 5 ml volume of HF-HNO_3–HCl (2+1+3) acid mixture was added to each sample[18] with overnight heating on a hot-plate at 130 °C. The resulting solution was twice evaporated to incipient dryness, with the addition of 1 ml of HNO_3 after each drying stage. All solutions were stored in sealed polycarbonate containers. Galena solutions were diluted to a Pb concentration between 40 and 50 ng g^{-1} for HR-ICP-MS analysis.

Instrumentation

Pb isotope ratios were measured on an Element HR-ICP-MS instrument (Finnigan MAT, Bremen, Germany). This instrument, utilising a magnetic sector mass analyser of reversed Nier–Johnson geometry, has pre-defined resolution settings ($m/\Delta m$ at 10% valley definition) of 300 (low), 3000 (medium) and 7500 (high). A resolution of 300 was used in this work, providing flat-topped peaks and maximum instrument sensitivity (typically greater than 10^6 counts s^{-1} for 10 ng g^{-1} ^{115}In or 7×10^5 counts s^{-1} for 10 ng g^{-1} ^{208}Pb). Instrument and method settings are outlined in Tables 1 and 2. A standard Meinhard nebuliser and Scott double pass water cooled spray chamber were employed. Isotopes of interest were analysed using electric scanning with the magnet held at fixed mass. The secondary electron multiplier detector (with discrete dynodes) was operated in the counting mode. Instrument tuning and optimisation were performed daily using a 10 ng g^{-1} multi-element solution containing Pb. Further details concerning this instrument have been reported elsewhere.[19–21]

All isotope ratio values were adjusted for instrument dead time.[22] Each Pb isotope ratio was considered in dead time determinations. The dead time was measured regularly throughout the study using three Pb solutions of different concentrations, namely 10, 25 and 50 ng g^{-1} Pb. Dead time values in the range 20–50 ns were typically found, depending on the detector settings. Analyses were also blank corrected.

Table 1 Typical instrumental configuration and settings

Instrument	Finnigan MAT Element
Resolution ($m/\Delta m$)	300 (low)
Rf power	1250 W
Nebuliser	Meinhard concentric
Coolant argon flow rate	~12.5 l min^{-1}*
Auxiliary argon flow rate	~1.1 l min^{-1}*
Nebuliser argon flow rate	~1.1 l min^{-1}*
Spray chamber	Scott (double pass) type cooled to 3.5–5 °C
Sampler cone	Nickel, 1.1 mm aperture id
Skimmer cone	Nickel, 0.8 mm aperture id
Instrument tuning	Performed using a 10 ng g^{-1} multi-element solution
Ion transmission	Typically 10^6 counts s^{-1} per 10 ng g^{-1} ^{115}In or 7×10^5 counts s^{-1} for 10 ng g^{-1} ^{208}Pb
Scan type	Fixed magnet with electric scan over small mass range
Ion sampling depth	Adjusted daily*
Ion lens settings	Adjusted daily†

* Adjusted in order to obtain maximum signal intensity. † Adjusted in order to obtain maximum signal intensity and optimum resolution.

Table 2 Method parameters for Pb isotope ratio measurements

Isotopes considered	^{201}Hg or ^{202}Hg, ^{204}Pb, ^{206}Pb, ^{207}Pb and ^{208}Pb
Scan type	Magnet fixed at ^{201}Hg. Electric scans over other mass ranges
Mass scanning window	3%
Magnet settle time	0.1 s
Dwell time per measurement	0.001 s
Scan duration per sweep	5×0.025 s
Number of sweeps	2000
Measurement time per replicate	250 s
Detector mode	Counting
Integration type	Average
Sample uptake and equilibration time	2 min
Rinse time between each sample	3–5 min (with 5% HNO_3)
Total time per sample	~15 min
Measured dead time	In the range 20–50 ns, depending on detector settings

RESULTS AND DISCUSSION

Mass discrimination correction

Isotope ratio values obtained using ICP-MS may deviate from the 'true' value as a function of the difference in mass between the two isotopes measured. This effect is defined as mass bias and its value may be either positive or negative.[23] The bias or discrimination can only be determined experimentally and will vary with the configuration of the individual ICP-MS system.[22] In this study, instrument mass discrimination was corrected by the use of a NIST SRM 981 external standard. Unknown samples to be measured were typically analysed between alternate standard reference solutions. The use of this correction method allows any measured differences in a Pb standard sample to correct the ratios found in unknown Pb solutions (*i.e.*, Pb standards correcting for Pb unknowns). Also, similar isotope abundances are typically measured for both standards and unknowns. However, on the negative side, there is a time delay between each standard and sample in which changes in plasma conditions can occur. The other option of using a Tl internal standard for mass discrimination correction was not investigated in this study. This method involves measuring another isotope (Tl) which may behave in a different fashion to Pb whilst also increasing the analysis time for each scan (time which could be spent accumulating Pb data). The internal correction approach has an advantage, however, of continuously monitoring the mass discrimination for each individual sample. Both methods have been used in previous Pb isotope studies[6–8,11] and were outlined in detail by Begley and Sharp.[8]

General analytical and methodology considerations

Method parameters were systematically varied and tested in order to obtain the most accurate and precise Pb isotope ratios. The first variable considered was the number of scans for each sample. The ideal situation would be to acquire as many scans as possible in the shortest time interval, hence approaching the behaviour of a multiple collector system. The number of sweeps across the Pb isotopes was varied between 500 (total analysis time 62.5 s) and 3000 (375 s), with 2000 scans (250 s) proving optimum considering Pb signal stabilities. All scanning protocols were at a rate of 8 sweeps s^{-1}, keeping the dwell time for each mass segment constant. Vanhaecke *et al.*[10] used 1200 scans in 2 min to measure $^{206}Pb/^{207}Pb$ isotope ratios in a standard Pb solution.

Vanhaecke *et al.*[11] also found that when considering both Pb or Cu isotope ratios at resolution 3000 using HR-ICP-MS,

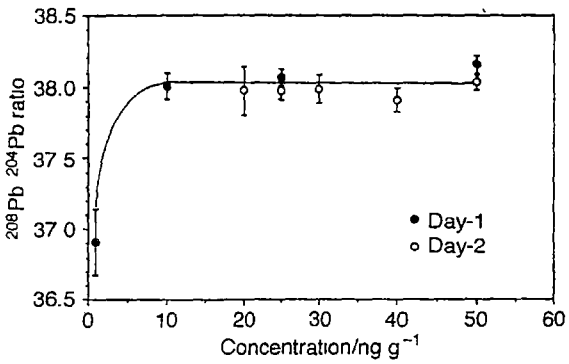

Fig. 1 Measured $^{208}Pb/^{204}Pb$ ratios *versus* Pb concentration in standard solutions. Ratios were measured over two consecutive days. Note that the values shown have not been corrected for any mass discrimination.

the precision was improved when the mass scanning window was reduced from 20 to 10% (the percentage window value is based on the expected mass width of a peak in the respective resolution). It was suggested that when smaller mass windows were used, only the centre of each peak was scanned, minimising the influence of any mass calibration instabilities. Although more crucial at resolution 3000 away from the flat-topped peaks of resolution 300, a similar systematic study was undertaken in this work, considering Pb ratios at low resolution. Mass windows between 1 and 10% were considered, and it was found that a mass scanning window of 3% gave isotope signals with minimum variation over the total number of scans.

The working Pb concentration range for which accurate Pb isotope ratios could be obtained was also investigated. At Pb concentrations below 10 ng g^{-1}, ratios with ^{204}Pb as the basis were found to be limited by counting statistics, resulting in less accurate results (a concentration of 10 ng g^{-1} corresponded to approximately 15 000 counts s^{-1} of ^{204}Pb). This is shown more clearly in Fig. 1 for the $^{208}Pb/^{204}Pb$ ratio measured in Pb standard solutions of various concentrations analysed over two consecutive days. Similar results were found for the other Pb ratios considered. This has not been noted as a problem in other HR-ICP-MS studies as the ratios investigated have typically involved ^{206}Pb, ^{207}Pb and ^{208}Pb isotopes only.[10,14] At the other extreme, Pb concentrations above 50 ng g^{-1} were not considered as the signal from ^{208}Pb required measurement in the analogue detector mode to avoid detector saturation (under normal operating conditions and detector settings, 50 ng g^{-1} of ^{208}Pb corresponded to 3×10^6–3.5×10^6 counts s^{-1}). Rather than limit the accuracy of the ratio determinations it was decided to make all measurements in the same detector mode (counting). Hence ratios were only determined in the Pb concentration range 10–50 ng g^{-1}. Work is continuing to increase the concentration range for which accurate Pb ratios can be obtained.

All ratio measurements were dead time corrected. Even with this adjustment, it was found that the accuracy of each measurement could be further improved when the Pb concentration in the NIST SRM 981 external calibration standard and the unknown sample were closely matched. As such the concentration of Pb in each sample was often adjusted prior to ratio determinations.

Along with the four Pb isotopes of interest, ^{202}Hg and ^{201}Hg were also measured as ^{204}Pb (1.4% abundant) has an isobaric interference from ^{204}Hg (6.85% abundant) in resolution 300. For geological samples that were previously ground in tungsten crushing mills, ^{201}Hg was used to correct ^{204}Pb, as ^{202}Hg suffers interference by $^{186}W^{16}O$.[7] For other samples ^{202}Hg was used. It was expected that during sample digestion any volatile Hg would be driven off during the multiple drying stages, while the Hg:Pb ratio in rocks and sulfides is generally low (1:10–100).[24] No samples analysed in this study were found to have appreciable levels of Hg or W. However, it was important to include these isotopes in method development work for future samples when more appreciable Hg or W concentrations may be encountered.

Precision

Lead isotope ratio precision data for 10 consecutive measurements of three different standard solutions are given in Table 3. Precisions obtained for ratios involving the low abundance ^{204}Pb isotope were 0.10–0.13% for $^{208}Pb/^{204}Pb$, 0.10–0.11% for $^{207}Pb/^{204}Pb$ and 0.10–0.11% for $^{206}Pb/^{204}Pb$ (values as 1σ). Improved precisions were found for those ratios involving the more abundant isotopes, namely 0.041–0.046% for $^{208}Pb/^{206}Pb$ and 0.044–0.048% for $^{207}Pb/^{206}Pb$. No difference in measurement precision was apparent between standard Pb solutions and more 'complex' galena digest samples. Theoretical precisions based on Poisson counting statistics were also calculated and are shown in Table 3 (based on ^{208}Pb signals of the order of 1×10^6–3×10^6 counts s^{-1}). In agreement with other workers,[13] external precisions approximately 2–3 times greater than that predicted from counting statistics alone were found, suggesting noise contributions from other sources such as the sample introduction system and plasma flicker. The precisions obtained for ratios referenced to ^{206}Pb are similar to that found by Vanhaecke *et al.*[10] using a similar HR-ICP-MS instrument to measure the $^{206}Pb/^{207}Pb$ ratio of a standard Pb solution. The external precisions given in Table 3 are also similar to the best obtained using a quadrupole ICP-MS by Begley and Sharp.[8]

Table 3 Pb isotope ratio precision and accuracy data for a standard multi-element solution, NIST SRM 981 and a Broken Hill galena digest. Samples were analysed at a Pb concentration of 45 ng g^{-1}

	$^{208}Pb/^{204}Pb$	$^{207}Pb/^{204}Pb$	$^{206}Pb/^{204}Pb$	$^{208}Pb/^{206}Pb$	$^{207}Pb/^{206}Pb$
Multi-element standard solution—					
Precision for 10 measurements, RSD (%)	0.11	0.11	0.10	0.041	0.047
Theoretical RSD (%)*	0.054	0.055	0.055	0.015	0.016
NIST SRM 981 Natural Lead—					
Precision for 10 measurements, RSD (%)	0.10	0.11	0.11	0.046	0.048
Theoretical RSD (%)*	0.049	0.050	0.050	0.014	0.015
Broken Hill galena—					
Measured ratio	35.520	15.353	15.985	2.222	0.961
Reference value†	35.599	15.370	15.994	2.226	0.961
ICP-MS bias from TIMS value (%)	−0.22	−0.11	−0.06	−0.18	0
Precision for 10 measurements, RSD (%)	0.13	0.10	0.11	0.043	0.044
Theoretical RSD (%)*	0.052	0.053	0.053	0.015	0.016

* From Poisson counting statistics. † From TIMS analysis.

Table 4 Measured Pb isotope ratios in selected Australian galena samples. Ratios from HR-ICP-MS and TIMS are compared

Sample code	Deposit location	n*	208/204		Δ† (%)	207/204		Δ† (%)	206/204		Δ† (%)	208/206		Δ† (%)	207/206		Δ† (%)
			ICP-MS	TIMS		ICP-MS	TIMS		ICP-MS	TIMS		ICP-MS	TIMS		ICP-MS	TIMS	
Z5199	Oceana	2	38.222	38.121	+0.26	15.603	15.607	−0.03	18.315	18.281	+0.19	2.0868	2.0853	+0.07	0.8519	0.8537	−0.21
Z5221	Argent 2	3	38 402	38.417	−0.04	15.651	15.622	+0.19	18.492	18.531	−0 21	2.0753	2.0731	+0.11	0.8458	0.8430	+0.33
Z5232	Swansea	3	38.240	38.241	−0.003	15.648	15.633	+0.10	18.331	18.368	−0.20	2.0894	2 0819	+0.36	0.8550	0.8511	+0.46
Z5237	Montana	3	38.474	38.472	+0.005	15 644	15.625	+0.12	18.550	18.561	−0.06	2.0753	2.0727	+0.13	0.8439	0.8418	+0.24
Z5277	N Tas. Mine	3	38.288	38.296	−0.02	15 620	15.624	−0 03	18.423	18.428	−0 03	2 0841	2.0781	+0 29	0.8502	0.8478	+0 28
H15	Hellyer	2	38.241	38.178	+0.17	15.634	15.612	+0.14	18.380	18.361	+0.10	2.0781	2.0793	−0 06	0 8502	0.8503	−0.01
EB1007	Elliot Bay	2	37.868	37.91	−0.11	15.551	15.58	−0.19	18.092	18.119	−0.15	2.0877	2.0923	−0 22	0 8609	0.8599	+0.12
EB72086	Elliot Bay	2	37.887	37.91	−0.06	15.583	15.58	+0.02	18.063	18.075	−0.07	2.0929	2.0974	−0.21	0.8627	0.8620	+0.08
EB72087	Elliot Bay	2	37 900	37.876	+0.06	15.587	15.57	+0.11	18.095	18.098	−0 02	2.0946	2.0928	+0.09	0.8613	0 8603	+0.12
EB72096	Elliot Bay	2	38.083	38.041	+0.11	15.628	15 605	+0.15	18.198	18 191	+0.04	2.0953	2 0912	+0.20	0.8588	0.8578	+0.12
BH2	Broken Hill	15	35.530	35.599	−0.19	15.384	15.37	+0.09	16.004	15.994	+0.06	2.2208	2.2258	−0.23	0.9613	0.9610	+0 03

* n=Number of analyses performed on each sample (average values shown). † Δ=Difference between ICP-MS and TIMS values.

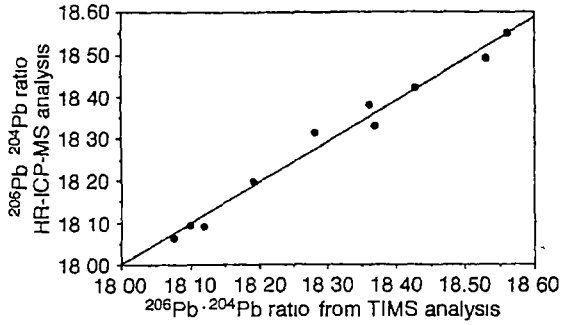

Fig. 2 Comparison between average $^{206}Pb/^{204}Pb$ ratio values obtained *via* HR-ICP-MS and TIMS techniques (for purposes of scale the Broken Hill galena sample has been omitted)

Comparison with TIMS values and accuracy of the analytical method

In order to study the accuracy of the present method, the Pb isotope ratios of 11 galena and galena-rich ore samples were measured by TIMS at CSIRO North Ryde and by HR-ICP-MS at the University of Tasmania. Samples were typically analysed 2–3 times by HR-ICP-MS, with the Pb concentration of the NIST SRM 981 external calibration standard and the unknown Pb sample being closely matched. Comparative data are given in Table 4. There is very good agreement between the two techniques and this is highlighted in Fig. 2, showing HR-ICP-MS values for the $^{206}Pb/^{204}Pb$ ratio plotted against TIMS data ($^{206}Pb/^{204}Pb_{HR\text{-}ICP\text{-}MS} = 0.98 \times {}^{206}Pb/^{204}Pb_{TIMS} + 0.45$, $r^2 = 0.983$ for $n = 10$). The ratio precision from HR-ICP-MS was about 0.05% and that from TIMS was about 0.02–0.05%.[15] A similar figure was presented in work by Date and Cheung[6] using an early model quadrupole ICP-MS. The difference in Pb ratio values between the two analytical techniques was generally less than ±0.2%, and was in the range 0.001–0.1 for $^{208}Pb/^{204}Pb$, 0.004–0.03 for $^{207}Pb/^{204}Pb$, 0.003–0.04 for $^{206}Pb/^{204}Pb$, 0.001–0.008 for $^{208}Pb/^{206}Pb$ and 0.0001–0.004 for $^{207}Pb/^{206}Pb$.

Geological implications

Lead isotopes are powerful tools in exploration for mineral deposits and the investigation of problems of ore genesis.[4] However, unlike multi-element geochemical analyses, they are not commonly used when exploring for new deposits owing to the expense of TIMS analysis. From an earlier study,[4] the Cambrian volcanogenic massive sulfide (VMS) and post-Cambrian (Post C) mineralisation in Western Tasmania can be clearly separated when the Pb isotope ratio precision is less than ±0.1 for $^{208}Pb/^{204}Pb$ and ±0.05 for $^{207}Pb/^{204}Pb$ and $^{206}Pb/^{204}Pb$ (in terms of absolute ratio units). Our work has shown that Pb isotope ratios can be measured relatively quickly by HR-ICP-MS to a precision approaching that obtained by TIMS on the same mixed acid digestion solutions normally used in commercial geochemical analyses. This results in a reduction in cost when compared with TIMS measurements, and opens up the possibility of the routine use of Pb isotopes in geochemical exploration surveys for new mineral deposits.

CONCLUSION

This work has clearly shown that under routine operating conditions, precise and accurate Pb isotope ratios can be measured in Pb mineral concentrates using HR-ICP-MS. Based on the analysis of a series of standard reference solutions, this comparatively fast analytical method provided Pb ratios with precisions of 0.13% RSD or better for ratios to ^{204}Pb. For ratios to ^{206}Pb, the precisions obtained were of the order of 0.045%. TIMS and HR-ICP-MS were found to be in agreement to an accuracy of ±0.2%, irrespective of the ratio considered. This level of accuracy is adequate for many geochemical applications. The relative ease and speed with which these values were obtained suggest that HR-ICP-MS may see increased use for geochemical Pb isotope ratio measurements.

The authors acknowledge the facilities and support provided by the Central Science Laboratory and Centre for Ore Deposits and Exploration Studies (CODES), University of Tasmania. Ross Large, Paul Kitto, Bruce Gemmel and David Steele are thanked for their support, samples and related information.

REFERENCES

1 Holmes, A., *The Age of the Earth*, Harper, New York, 1913, p. 194.
2 Faure, G, *Principles of Isotope Geology*, Wiley, New York, 1977, p. 464.
3 Schaltegger, U., Schneider, J. L., Maurin, J. C., and Corfu, F., *Earth Planet. Sci. Lett.*, 1996, **144**, 403.
4 Gulson, B. L., *Lead Isotopes in Mineral Exploration*, Elsevier, Amsterdam, 1986, p. 245.
5 Smith, R. G., Brooker, E. J., Douglas, D. J., Quan, E. S K, and Rosenblatt, G., *J. Geochem. Explor.*, 1984, **21**, 385.
6 Date, A. R., and Cheung, Y. Y., *Analyst*, 1987, **112**, 1531.
7 Longerich, H. P., Wilton, D. H. C., and Fryer, B. J., *J Geochem. Explor.*, 1992, **43**, 111.
8 Begley, I. S., and Sharp, B. L., *J. Anal. At. Spectrom*, 1997, **12**, 395.
9 Becker, J. S., and Dietze, H -J., *J. Anal. At. Spectrom.*, 1997, **12**, 881.
10 Vanhaecke, F., Moens, L., and Dams, R., *Anal. Chem.*, 1996, **68**, 567.
11 Vanhaecke, F., Moens, L., Dams, R., Papadakis, I., and Taylor, P., *Anal. Chem.*, 1997, **69**, 268.
12 Cornec, F. L., and Correge, T., *J. Anal. At. Spectrom.*, 1997, **12**, 969.
13 Sturup, S., Hansen, M., and Mølgaard, C., *J. Anal. At. Spectrom.*, 1997, **12**, 919
14 Shuttleworth, S., Morris, J., Crombie, K., Ridings, R., and Arvidson, R., in *Proceedings of the 3rd International Conference on the Analysis of Geological and Environmental Materials, Colorado, USA, June 1997*, p. 100.
15 Walder, A. J, Platzner, I., and Freedman, P. A., *J. Anal. At. Spectrom*, 1993, **8**, 19.
16 Walder, A. J., and Furuta, N., *Anal. Sci.*, 1993, **9**, 675.
17 Potts, P. J., *A Handbook of Silicate Rock Analysis*, Blackie, Glasgow, 1987, p. 622.
18 Chao, T. T, and Sanzolone, R. F., *J. Geochem. Explor.*, 1992, **44**, 65.
19 Feldmann, I., Tittes, W., Jakubowski, N., Stuewer, D., and Giessmann, U., *J. Anal. At. Spectrom.*, 1994, **9**, 1007.
20 Moens, L., Verrept, P., Dams, R., Greb, U., Jung, G., and Laser, B., *J. Anal. At. Spectrom.*, 1994, **9**, 1075.
21 Moens, L., Vanhaecke, F., Riondato, J., and Dams, R., *J. Anal. At. Spectrom.*, 1995, **10**, 569.
22 Price Russ, G., in *Applications of Inductively Coupled Plasma Mass Spectrometry*, ed. Date, A. R., and Gray, A. L., Blackie, Glasgow, 1989, pp. 90–110.
23 Jarvis, K. E., Gray, A. L., and Houk, R. S., *Handbook of Inductively Coupled Plasma Mass Spectrometry*, Blackie, Glasgow, 1992, p 380.
24 Sewell, D M., and Wheatley, C J. V., *J. Geochem. Explor*, 1994, **50**, 351.

Paper 8/01397G
Received February 18, 1998
Accepted May 7, 1998

Vol. 23 - N°1 06 99 p. 31-46

GEOSTANDARDS NEWSLETTER
The Journal of Geostandards and Geoanalysis

Determination of Scandium, Yttrium and Rare Earth Elements in Rocks by High Resolution Inductively Coupled Plasma-Mass Spectrometry

Philip **Robinson** (1), Ashley T. **Townsend** (2), Zongshou **Yu** (3) and Carsten **Münker** (1, 3)

(1) School of Earth Sciences, University of Tasmania, Hobart, Tasmania, 7001, Australia. e-mail: Phil.Robinson@utas.edu.au
(2) Central Science Laboratory, University of Tasmania, Hobart, Tasmania, 7001, Australia
(3) Centre for Ore Deposit Research, University of Tasmania, Hobart, Tasmania, 7001, Australia

The high sensitivity, minimal oxide formation and single internal standard capability of high resolution inductively coupled plasma-mass spectrometry (HR-ICP-MS) is demonstrated in the direct determination of Sc, Y and REE in the international reference materials: basalts (BCR-1, BHVO-1, BIR-1, DNC-1), andesite (AGV-1) and ultramafics (UB-N, PCC-1 and DTS-1). Time consuming ion exchange separation or preconcentration were found to be unnecessary. Smooth chondrite normalized plots of the REE in PCC-1 and DTS-1 were obtained in the range 0.8-50 ng g^{-1} (0.01-0.1x chondrite). Method precision was found to be digestion dependent with an average external repeatability of 2-4% for the basalts, AGV-1 and UB-N, and 10% for PCC-1 and DTS-1. The mass peak due to ^{45}Sc was completely resolved from $^{29}Si^{16}O$ and $^{28}Si^{16}O^{1}H$ spectral interferences using medium resolution, which casts doubt on the accuracy of Sc determinations using quadrupole ICP-MS. Literature values for Y in rock reference materials were found to be approximately 9% high after HR-ICP-MS and XRF analysis.

Keywords: Rare earth elements, scandium, yttrium, high resolution inductively coupled plasma-mass spectrometry, silicate rocks, method developments.

La grande sensibilité, la formation minimale d'oxydes et la capacité de normalisation avec un seul standard interne de l'ICP-MS à haute résolution sont démontrées par l'analyse directe de Sc, Y et des Terres Rares dans les matériaux de référence suivants: basaltes (BCR-1, BHVO-1, BIR-1 et DNC-1), andésite (AGV-1) et ultrabasites (UB-N, PCC-1 et DTS-1). Il n'est plus nécessaire d'effectuer de longues préconcentrations ou séparations sur colonne échangeuse d'ion. Des spectres de Terres Rares lissés et normalisés aux chondrites sont obtenus pour PCC-1 et DTS-1, pour des concentrations comprises entre 0.8 et 50 ng g^{-1} (de 0.01 à 0.1 fois les chondrites). La précision de la méthode s'est révélée être dépendante de la phase d'attaque et mise en solution, avec une reproductibilité externe moyenne comprise entre 2 et 4% pour les basaltes, AGV-1 et UB-N et 10% pour PCC-1 et DTS-1. Le pic de la masse 45 du Sc a été complètement séparé des interférences spectrales dues à $^{29}Si^{16}O$ et $^{28}Si^{16}O^{1}H$ en utilisant une résolution moyenne, ce qui laisse planer un doute sur l'exactitude des déterminations de Sc faites par ICP-MS à quadrupôle. Les données de la littérature pour Y dans les matériaux de référence se sont révelées être 9% plus hautes après analyse par HR-ICP-MS et XRF.

Mots-clés : Terres Rares, scandium, yttrium, ICP-MS haute résolution, roches silicatées, développements de méthodes.

For many years instrumental neutron activation analysis (INAA) and isotope dilution mass spectrometry (ID-MS) were the two principal reference techniques used to determine the rare earth elements (REE) in geological samples (Balaram 1996). Ion exchange methods using X-ray fluorescence spectrometry (XRF, e.g. Robinson *et al.* 1986) and inductively coupled plasma-atomic emission spectrometry (ICP-AES, e.g. Jarvis and Jarvis 1988) have also been used. However, a recent survey (Potts 1997) has shown a decline in the use of INAA and ICP-AES from the early-mid 1980's, with a dramatic increase in published data by

Received 06 Aug 98 — Accepted 05 Nov 98

inductively coupled plasma-mass spectrometry (ICP-MS). ICP-MS is now an established technique for the determination of trace elements in geological materials (Jarvis 1988, Jenner *et al.* 1990, Eggins *et al.* 1997), offering a true multi-element capability, fast analysis time, low detection limits, a large linear dynamic range and the capacity to measure isotope ratios. INAA requires the availability of a nuclear reactor and offers only a limited number of the REE, while ICP-AES and XRF are less sensitive, and along with ID-MS, require a lengthy ion exchange separation. ICP-MS also offers the option of using laser ablation (e.g Sylvester and McCandless 1997).

The use of HR-ICP-MS was first reported in 1989 (Bradshaw *et al.* 1989, Morita *et al.* 1989). Compared with traditional ICP-MS instruments which use a quadrupole mass filter, HR-ICP-MS instruments employ a magnetic sector mass analyser, offering the possibility to separate analytes of interest from spectral interferences (resolutions to 10,000 are in use, as reported by Becker and Dietze 1997). This is particularly important for those elements at masses lower than 80 amu, where polyatomic interferences are commonly encountered (e.g. ^{45}Sc and $^{29}Si^{16}O$, ^{51}V and $^{35}Cl^{16}O$, ^{56}Fe and $^{40}Ar^{16}O$ etc). HR-ICP-MS instruments have also been found to offer other advantages over quadrupole spectrometers, namely increased sensitivity (i.e. higher ion transmission) and lower background signals (Moens *et al* 1995). These advantages may be beneficial for the analysis of REE in geological matrices.

It was the aim of this study to demonstrate the capability of HR-ICP-MS for the determination of scandium (atomic mass 45), yttrium (90) and the REE [La (139) to Lu (175)] in rock matrices. The higher resolution available using HR-ICP-MS was applied to the analysis of Sc (resolution 3000), while Y and the REE were analysed using low resolution mode (resolution 300). To date, nearly all published work analysing geological materials has been by quadrupole instrumentation

Also included is a study of the yttrium content in rock reference materials. Many ICP-MS workers (e.g. Jenner *et al.* 1990, Jarvis 1990, Totland *et al.* 1992, Garbe-Schonberg 1993, Shinotsuka *et al.* 1996, Münker 1997 and Norman *et al* 1998) have found low yttrium concentrations by solution ICP-MS compared with published values New synthetic calibration standards were prepared for XRF analysis and a comparison of results is reported.

Experimental

Reagents and labware

De-ionised water, purified with a Modulab Pure One system (≥16.7 Mohm cm^{-1} resistivity), was used for rinsing and solution preparation Analytical grade acids (Univar HCl, HF and BDH Analar HNO_3) were purified by double distillation in sub-boiling stills of silica or poly(tetrafluorethylene) (PTFE). The $HClO_4$ was Merck Aristar grade.

Acid digestions were performed in Savillex 7 ml screw top PTFE vials and PicoTrace PTFE pressure vessels. Before use, polycarbonate sample containers were soaked in 20% (v/v) HCl for one to three days followed by a similar period in 10% (v/v) HNO_3 before a final rinse with ultra-pure water. All PTFE containers were heated overnight in each of the acids at 60-80 °C before rinsing.

HF-HNO_3 decomposition method

This procedure was used for the basalt samples and andesite AGV-1 where results showed good agreement with HF-$HClO_4$ decomposition. Although insoluble fluorides are a well known problem with REE determinations, basalts generally give good results with a long (48 hour) HF-HNO_3 digestion (e.g. Jenner *et al.* 1990). Even though this method has been found to be successful for AGV-1, HF-HNO_3 and also HF-$HClO_4$ decomposition are generally inappropriate for felsic samples since these often contain accessory zircon which is relatively insoluble. Lithium borate fusion or sodium peroxide sinter are good decomposition methods for these samples. Powdered sample (100 mg) was weighed into a Savillex vial and moistened with ultrapure water. HF (2 ml) and HNO_3 (0.5 ml) were added to the sample, the vial sealed and placed on a hotplate for 48 hours at 130 °C At least twice during the first 24 hours, the container was removed from the hotplate, cooled and placed in an ultrasonic bath for two minutes. After 48 hours the vials were opened and evaporated to incipient dryness Nitric acid (1 ml) was added and further evaporated to incipient dryness. The residue was dissolved in 2 ml HNO_3 followed by 10-20 ml water, transferred to a polycarbonate container and diluted to 100 ml (1000x dilution of sample) Indium internal standard was also added to give a final concentration of 10 ng ml^{-1} At least two reagent blank solutions were prepared with each batch of samples.

Table 1.
Typical instrument settings

ICP-MS		
Instrument:	*ELEMENT* (Finnigan MAT)	
Resolutions (m/Δm):	Low = 300, Medium = 3000 and High = 7500	
Rf power:	1250 W	
Gas flows:	Plasma gas:	12.5 l min^{-1}
	Auxiliary:	0.95-1.1 l min^{-1}
	Sample gas:	0.95-1.1 l min^{-1} (optimized daily)
Torch:	Fassel type	
Nebuliser:	Meinhard	
Spray chamber:	Scott-type (double pass), cooled to 3.5-5 °C	
Cones:	Ni sampler (1.1 mm orifice i.d.) and skimmer (0.8 mm orifice i.d.)	
Sample uptake:	Pumping via a Spetec peristaltic pump	
Instrument tuning:	Performed daily using a 10 ng ml^{-1} multi-element solution	
Ion transmission:	~ 100,000 - 150,000 counts s^{-1} per ng ml^{-1} In	
Scan type:	Magnetic jump with electric scan over small mass range	
Number of sample scans:	40	
Ion sampling depth:	Adjusted to obtain maximum signal intensity	
Ion lens settings:	Adjusted to obtain maximum signal intensity and optimum resolution	
XRF (Y Kα analysis)		
Instrument:	Philips PW1480 X-Ray Spectrometer	
X-Ray tube:	3 kW max. Sc Mo anode, operated at 90 kV, 30 mA	
Crystal:	LiF 200	
Background angles:	+0.60 deg., -0.30 deg.	
Collimator:	Primary -fine (0.3 mm) with auxiliary (0.14 mm)	
Detector type:	Scintillation counter	
Total counting time:	200 seconds	
Detection limit:	0.7 μg g^{-1} in a quartz matrix (3σ confidence)	
Counting precision:	10.0 ± 0.2 μg g^{-1}, 50.0 ± 0.2 μg g^{-1} in quartz	

HF-$HClO_4$ decomposition method

This procedure was used for ultramafic and basaltic samples (Heinrichs and Herrman 1990, Münker 1998). $HClO_4$ is more efficient at removing Mg rich fluorides, although decomposition of spinels can still be difficult. HF (3 ml) and $HClO_4$ (3 ml) were added to 100 mg sample in a PicoTrace PTFE vessel. After closing the vessel and stepwise heating for three hours, the sample was digested for fifteen hours under pressure at 180 °C. After evaporation, the sample was dissolved in 2 ml HNO_3 and 1 ml HCl followed by a few ml water and diluted to 100 ml total volume. Indium was also added as internal standard.

Instrumentation

Measurements were carried out using an *ELEMENT* HR-ICP-MS (Finnigan MAT, Bremen, Germany). This instrument has predefined resolution settings (m/Δm at 10% valley definition) of 300 (low), 3000 (medium) and 7500 (high). The signal intensity drops by a factor of eight to twelve when changing from resolution 300 to 3000 (Moens *et al.* 1995). Instrument settings employed in this study are outlined in Table 1. A standard Meinhard nebuliser and Scott double pass water cooled spray chamber were employed in this work. Isotopes of interest (Table 2) were analysed using electric scanning, with the magnet held at fixed mass. The secondary electron multiplier detector was operated in counting mode. Instrument tuning and optimisation were performed daily using a 10 ng ml^{-1} multi-element solution containing the elements of interest. Further details concerning the *ELEMENT* have been reported in the literature (Feldmann *et al.* 1994, Moens *et al.* 1995).

Table 2.
Isotopes, abundances and some potential interferences

Element	m/z	% abundance	Possible interferences	References
*Sc	45	100	SiO, SiOH, ArLi, COOH	C,D,E,G,J
*Y	89	100		B,C,E,G,J
Ba	135	6.59	SnO, BaH	A,B,E,F,H
*Ba	137	11.23	SbO, SnO, BaH	C,E,F,G,J
Ba	138	71.7	Ce, La, BaH	D
*La	139	99.91	SbO, BaH	A,B,C,D,E,F,G,H,J,K
*Ce	140	88.48	TeO, SnO	A,B,C,D,E,F,G,H,J,K
*Pr	141	100	TeO	A,B,C,D,E,F,G,H,J,K
Nd	143	12.18		K
Nd	145	8.3		C,E,F,K
*Nd	146	17.19	BaO, TeO	A,B,D,E,F,G,H,J,K
*Sm	147	15	BaO, BaOH	B,C,D,E,F,H,K
Sm	149	13.8	BaO, BaOH, CsO	F,H,J,K
Sm	152	26.7	BaO, CeO, Gd	A,G
*Eu	151	47.8	**BaO**, BaOH, CsO	A,C,D,E,F,G,H,I,J,K
Eu	153	52.2	**BaO**, BaOH	B,E,F,G,K
Gd	155	14.8	LaO, BaO, BaOH	K
Gd	156	20.47	LaO, BaO, BaOH, CeO, Dy	K
*Gd	157	15.65	**CeOH, PrO**, BaF, BaOH, ArSn	A,B,C,D,E,H,I,K
Gd	158	24.84	NdO, CeO, Dy, ArSn, BaOH	G
Gd	160	21.86	CeO, CeOH, PrOH, NdO, NdOH, SmO, Dy, ArSn	F,J
*Tb	159	100	**NdO**, NdOH, CeO, CeOH, PrO, PrOH, ArSn	A,B,C,D,E,F,G,H,I,J,K
Dy	161	18.9	NdO, NdOH, SmO, SmOH	F,J,K
Dy	162	25.5	**NdO**, SmO, ArSn, Er	K
*Dy	163	24.9	**NdO**, NdOH, **SmO**, SmOH	A,B,C,D,E,F,H,I,K
*Ho	165	100	NdO, NdOH, **SmO**, SmOH, BaCl	A,B,C,D,E,F,G,H,I,J,K
Er	166	33.6	NdO, NdOH, SmO, SmOH	B,E,F,G,K
*Er	167	22 95	NdO, NdOH, SmO, SmOH, **EuO**, BaCl	C,D,F,H,I,J,K
Er	168	26.8	SmO, Yb, CsCl, GdO	A
*Tm	169	100	**EuO**, NdOH, SmO, SmOH, EuOH, GdO, GdOH, BaCl	A,B,C,D,E,F,G,H,I,J,K
Yb	171	14.3	SmO, SmOH, EuO, EuOH, GdO, GdOH, BaCl	F,K
*Yb	172	21.9	SmO, SmOH, EuOH, **GdO**, GdOH, **DyO**, BaCl	B,E,F,K
Yb	173	16.12	**GdO**, Hf, BaCl	C,I,J,K
Yb	174	31.8	**GdO**, Hf, BaCl, ArBa	A,D,G,H
*Lu	175	97.41	GdO, GdOH, **TbO**, DyO, DyOH, BaCl, ArBa	A,B,C,D,E,F,G,H,I,J,K

* Isotopes used in this study Significant interferences are highlighted

(A) Lichte *et al.* (1987), (B) Jarvis (1988), (C) Jenner *et al.* (1990), (D) Ionov *et al.* (1992), (E) Garbe-Schönberg (1993), (F) Dulski (1994), (G) Hollocher *et al.* (1995), (H) Barrat *et al.* (1996), (I) Shinotsuka *et al.* (1996), (J) Eggins *et al.* (1997), (K) Pin and Joannon (1997).

General calibration

Aqueous standard solutions covering the concentration range 0-50 ng ml^{-1} were used for external calibration and were prepared from 10 and 100 µg ml^{-1} multi-element solutions (Perkin Elmer Atomic Spectroscopy and QCD Analysts-Environmental Science solutions). Two further single element yttrium solutions (1000 µg ml^{-1}) were prepared from both Spex high purity (99.999%) and BDH (99.9%) Y_2O_3, ignited at 900 °C and dissolved in HNO_3 before final dilution. All standard solutions were acidified with 2% (v/v) HNO_3 and prepared before each analytical sequence using de-ionised water, twice purified in a quartz sub-boiling still Typically, six standard solutions were used for each element, providing calibration lines having correlation coefficients in excess of 0.995. A drift monitor solution of 10 ng ml^{-1} followed by a blank were analysed every five to eight samples during each analysis sequence. Uptake time for each sample solution was typically three minutes, followed by an analysis time of two minutes, with a final rinse with 5% (v/v) HNO_3 for three minutes.

Internal standards

Unless otherwise stated, In was used as an internal standard and was added to each sample at a concentration of 10 ng ml^{-1} prior to ICP-MS analysis. Indium solutions were prepared from a 1000 µg ml^{-1}

single element solution (High Purity Standards). Thulium (Spex High Purity Tm_2O_3), Lu (High Purity Standards solution), Re (BDH 99.9%), Bi (Spex High Purity) and enriched ^{84}Sr (83.17% ^{84}Sr, University of Adelaide) were also tested as internal standards.

X-Ray fluorescence spectrometry

Yttrium was also determined by XRF using a Philips PW1480 X-ray spectrometer. Instrument settings are listed in Table 1. Pressed powder pellets with a diameter of 32 mm were prepared at 3.5 tonnes cm^{-2} using 6 g of sample powder, polyvinyl alcohol (PVA) as a binder, and a backing of boric acid. Two sets of calibration standards were prepared in duplicate from Spex high purity Y_2O_3, ignited at 900 °C, and Cominex pure quartz. Set A (2000 $\mu g\ g^{-1}$ Y) was prepared by mixing Y_2O_3 with 20 g quartz for two minutes in a Rocklabs ring mill using a chrome steel head. Pressed powder pellets were prepared. A quartz blank passed through the same procedure yielded < 1 $\mu g\ g^{-1}$ Y. Set B, consisting of 0, 50, 100 and 200 $\mu g\ g^{-1}$ Y, was prepared using a method similar to Potts *et al.* (1990). Aliquots of 1 mg ml^{-1} Y solution were thoroughly mixed with 6 g of finely ground quartz in an agate pestle and mortar to give a slurry, dried at 105 °C, mixed again and made into pressed powder pellets with PVA as a binder.

Corrections for mass absorption from the major elements were calculated using Philips X40 software with De Jongh's calibration model and Philips alpha coefficients. The Rb $K\beta_{1,3}$ doublet, overlapping with Y $K\alpha$, is a major interference and must be corrected for carefully. This was achieved using a 1000 $\mu g\ g^{-1}$ Rb/SiO_2 mixture prepared from Spex high purity chemicals. Other interferences such as Pb $L\gamma$ and weak Th lines must be corrected for when Pb and Th levels are very high. This was unnecessary for the reference materials analysed in this study.

Calibration and analysis of low abundance samples

For the mafic and ultramafic samples of very low REE abundances analysed here (PCC-1, DTS-1, UB-N and BIR-1), precautions were taken in order to avoid memory effects. Before each analytical sequence, instrument cones, torch, spray chamber and nebuliser were cleaned and PVC pump tubing replaced. Memory effects for Sc, Y and the REE have been reported to be minimal when compared with high field strength elements (HFSE), in particular Ta and Nb (e.g. McGinnis *et al.* 1997, Münker 1998). Nevertheless, rinsing time and uptake time were extended here to 3.5 min and 4 min, respectively. A rinsing solution similar to the sample solutions was used (e.g. 2% v/v HNO_3 in the case of the HF/HNO_3 digestions). This minimises potential element exchange between the walls of the injection system and the sample solution which might be triggered by a change in acidity from sample to rinsing solution. Low abundance samples were analysed in order of increasing REE content to avoid memory from previous samples. Likewise, calibration solutions of lower concentration (0-1 ng ml^{-1}) were analysed at the beginning of each analytical session. Following the initial calibration standards, a 1 ng ml^{-1} drift monitor, standard blank and two sample blanks were analysed before the first rock sample. Calibration solutions of higher abundance (necessary for high Y and Sc) were analysed after the low abundance rock samples. Each low abundance digestion was performed sometimes in duplicate, mostly in triplicate. This procedure allows monitoring of possible memory effects because in the case of memory, the measured concentrations should decrease within the three repetitions of one sample. All low abundance values reported here are means of replicates which are identical within internal error. Although the above procedure and precautions were regularly applied, memory effects were rarely found for the REE in this study.

Results and discussion

Interferences, isotopes and choice of resolution

It has been well documented that the oxides (and to a lesser extent hydroxides) of Ba and the light rare earth elements (LREE) can cause interference problems with the heavier REE (e.g. Dulski 1994). Possible oxide, hydroxide and isobaric interferences reported in the literature are detailed in Table 2. However, with modern instruments and with careful optimisation of instrument conditions, these interferences can often be minimised. Specific oxide formation rates found in this work were ~ 0.2% for BaO^+/Ba^+ and ~ 0.4% for PrO^+/Pr^+, while hydroxide levels were measured as ~ 0.05% for $BaOH^+/Ba^+$ and ~ 0.03% for $CeOH^+/Ce^+$. Barium, Pr and Ce interfere to a small extent in the determination of Eu and Gd. Oxide formation for the majority of the REE was 0.15-0.25%, which is generally much lower than that reported from quadrupole based ICP-MS instruments (Dulski

Table 3.
Summary of oxide formation for selected 100 ng ml^{-1} REE and 1000 ng ml^{-1} Ba solutions

	Apparent REE concentration (ng ml^{-1}) when the following individual solutions were aspirated									
	Ba 1000 ng ml^{-1}	La 100 ng ml^{-1}	Ce 100 ng ml^{-1}	Pr 100 ng ml^{-1}	Nd 100 ng ml^{-1}	Sm 100 ng ml^{-1}	Eu 100 ng ml^{-1}	Gd 100 ng ml^{-1}	Tb 100 ng ml^{-1}	Dy 100 ng ml^{-1}
^{139}La	0.024	-	-	-	-	-	-	-	-	-
^{140}Ce	0.003	-	-	-	-	-	-	-	-	-
^{141}Pr	-	-	0.004	-	-	-	-	-	-	-
^{146}Nd	0.003	-	0.005	0.003	-	-	-	-	-	-
^{147}Sm	-	-	-	-	0.008	-	-	-	-	-
^{151}Eu	**0.130**	-	-	-	-	-	-	-	-	-
^{157}Gd	0.004	0.022	**0.160**	**3.060**	0.040	-	-	-	-	-
^{159}Tb	-	-	0.003	-	**0.072**	-	-	-	-	-
^{163}Dy	-	-	-	-	**0.057**	**0.114**	-	-	-	-
^{165}Ho	-	-	-	-	-	0.030	-	-	-	-
^{167}Er	-	-	-	-	0.005	0.004	**0.124**	-	-	-
^{169}Tm	-	-	-	-	-	0.003	0.034	-	-	-
^{172}Yb	-	-	-	-	-	-	-	**0.279**	-	**0.065**
^{175}Lu	-	-	-	-	-	-	-	0.005	**0.336**	0.028

Major interferences are highlighted.

1994, Yoshida *et al.* 1996, Pin and Joannon 1997, Makishima and Nakamura 1997, Eggins *et al.* 1997). This could be a function of plasma conditions, sampling depth and the nebulisation system characteristic of the Finnigan instrument.

Some REE isotopes could be separated from oxide and hydroxide interferences using the highest resolution available with our ICP-MS instrument (nominally m/Δm = 7500). For example, ^{157}Gd could be separated from ^{141}Pr^{16}O using 7500 (resolution of ~ 7300 required), while ^{151}Eu and ^{159}Tb require resolutions of 7800 and 7700, respectively, for complete separation from ^{135}Ba^{16}O and ^{143}Nd^{16}O. There is, however, a marked drop in sensitivity when using higher resolution, which for example, would render Gd undetectable using resolution 7500 in most rock types. As low REE concentrations were expected in the rock samples, and few interferences could be overcome using higher resolution, low resolution mode offering maximum sensitivity was employed for the analysis of REE, with subsequent oxide correction.

Table 3 shows the apparent REE concentrations resulting from oxide interferences from individual 100 ng ml^{-1} REE solutions and 1000 ng ml^{-1} Ba prepared from Spex pure reagents (expressed as ng ml^{-1}) The values shown were obtained using resolution 300, with In as the internal standard (10 ng ml^{-1}), under routine operating conditions. Most interferences were found to be minor, with corrections usually only being necessary for BaO on Eu, PrO and CeOH on Gd, and occasionally NdO on Tb. Daily variations of up to 10-15% in the correction factors necessitate their measurement with each calibration. Isotopes determined in this study were chosen based on (a) the oxide formation levels measured on our instrument (Table 3) and (b) the isotopes used in other studies (Table 2).

Medium resolution (m/Δm=3000) was found to be essential for Sc analysis, as higher than expected results were found using low resolution mode. Examples of the mass spectra for Sc in BHVO-1, digested using HF/HNO_3 and measured using resolutions of 300 and 3000, are shown in Figures 1 and 2. The narrower mass range and reduced intensity in resolution 3000 are clearly shown in Figure 2. The presence of polyatomic interferences ^{29}Si^{16}O and ^{28}Si^{16}O^{1}H are also noted. Scandium is unresolved from these interferences in low resolution mode of HR-ICP-MS (Figure 1), and similarly, using quadrupole ICP-MS instruments. Little evidence could be found for $^{13}C^{16}O_2$ and $^{12}C^{16}O_2{}^{1}H$ using resolution 3000, although these potential interferences have previously been reported in the determination of ^{45}Sc in rock samples (Longerich *et al.* 1990, Garbe-Schönberg 1993, Eggins *et al.* 1997). The effect of these interferences on the quantification of Sc is demonstrated by the following examples: Sc in BHVO-1, measured using resolution 300 was found to be 35.4 μg g^{-1}, while that measured using resolution 3000 was 31.9 μg g^{-1}; Tafahi: resolution 300: 51.1 μg g^{-1} and resolution 3000: 45.2 μg g^{-1}, TASBAS (in house standard): resolution 300: 19.0 μg g^{-1} and resolution 3000: 14.1 μg g^{-1} We have found that after dissolution of sample using both the HF/HNO_3 attack and Na_2O_2 sinter (Robinson *et al.* 1986), trace

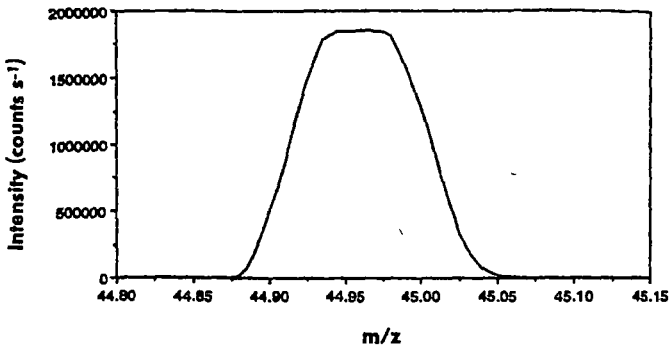

Figure 1. Mass spectrum of ^{45}Sc in BHVO-1 using low resolution (300).

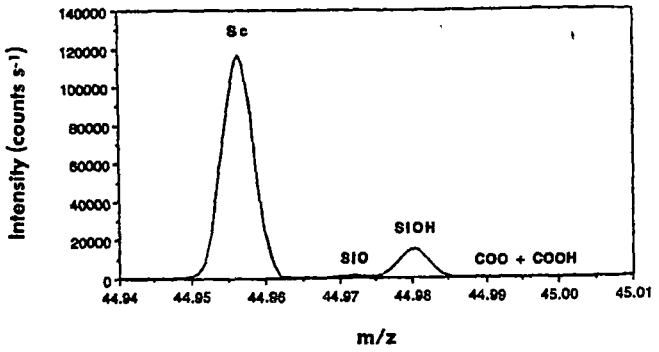

Figure 2. Mass spectrum of ^{45}Sc in BHVO-1 using medium resolution (3000) showing separation of Sc from nearby interferences $^{29}Si^{16}O$, $^{28}Si^{16}O^{1}H$, $^{13}C^{16}O_2$ and $^{12}C^{16}O_2{}^{1}H$.

silica still remains when none might be expected, in the first case owing to volatilisation of SiF_4 and in the second, washing away of sodium silicates. In contrast, no silica peak was observed after $HF/HClO_4$ digestion of BIR-1 and DNC-1. This may be due to the extra volume of acids used in the $HF/HClO_4$ digestion procedure, along with the higher efficiency of $HClO_4$ in removing fluorides (Bock 1979).

Matrix effects

Matrix effects were examined by analysing an in house basalt standard TASBAS, at dilutions of 1000x, 2000x and 5000x. No discernible difference was observed between each dilution. High resolution ICP-MS should be no different from quadrupole ICP-MS in this regard, as dilution dependent matrix problems are typically associated with the plasma source.

Internal standard

It is common practice in ICP-MS analysis to use an internal standard to compensate for matrix effects and instrumental drift (Evans and Giglio 1993). An internal standard element of similar mass and ionisation energy to the analyte is often chosen, with more than

Table 4.
Analysis of BHVO-1 using different internal standards (μg g^{-1})

	^{84}Sr	^{115}In	^{169}Tm	^{175}Lu	^{185}Re	^{209}Bi	Reference (A)	Reference (B)
^{45}Sc	32.1	31.4	-	-	31.9	-	31.8	31.8
^{89}Y	25.2	24.0	24.5	24.8	24.5	-	27.6	28
^{137}Ba	-	133.0	133.0	138.8	135.0	-	139	133
^{139}La	-	15.5	15.5	16.0	15.9	-	15.8	15.5
^{140}Ce	-	37.4	37.5	37.7	38.5	-	39	38
^{141}Pr	-	5.48	5.48	5.68	5.69	-	5.7	5.45
^{146}Nd	-	24.1	23.5	25.3	24 4	-	25.2	24.7
^{147}Sm	-	6.01	5.93	6.47	6.11	-	6.2	6.17
^{151}Eu	-	2.09	2.08	2.22	2.14	-	2.06	2.06
^{157}Gd	-	6.22	6.40	6.56	6.48	-	6.4	6.22
^{159}Tb	-	0.92	0.95	0.96	0.97	-	0.96	0.95
^{163}Dy	-	5.15	5 14	5.53	5.24	-	5.2	5.25
^{165}Ho	-	0.99	1.01	1.03	1.03	-	0.99	1
^{167}Er	-	2.50	2.48	2.69	2.53	-	2.4	2.56
^{169}Tm	-	0.33	-	0.35	0.34	-	0.33	0.33
^{172}Yb	-	1.95	1.91	2.12	1.96	-	2.02	1.98
^{175}Lu	-	0.26	0.27	-	0.28	-	0.291	0.278
^{208}Pb	-	2.12	2.09	2.37	2.09	2.06	2.6	2.1
^{232}Th	-	1.25	1.28	1.30	1.32	1.17	1 08	1.26
^{238}U	-	0.44	0.42	0.44	0.46	0.44	0.42	0.42

Mean of five HF/HNO_3 digestions.

(A) Govindaraju (1994), (B) Eggins *et al.* (1997) "preferred values".

one typically being used for each elemental suite. For example, internal standard combinations have included Ru and Re (Dulski 1994), Rh, In and Re (Munker 1998); In and Bi (Ionov *et al.* 1992); In and Re (Pin and Joannon 1997), Rh and Bi (Balaram *et al.* 1996); Be, In and Re (Garbe-Schonberg 1993); Rh and/or In (Yoshida *et al.* 1996). These studies are typically characterized by two to three internal standards of high and low mass, respectively. Recently, Eggins *et al.* (1997) found one internal standard unsatisfactory for geochemical analysis using a quadrupole ICP-MS instrument, and so developed a method using four enriched and five natural isotopes which gave very precise results (1-2% RSD).

Preliminary results from our HR-ICP-MS indicated that only one internal standard, indium, may suffice for the analysis of rock solutions of 1000x dilution. To confirm this, a series of five basaltic (BHVO-1) solutions were prepared by HF/HNO_3 dissolution and spiked with 10 ng ml^{-1} enriched ^{84}Sr, natural ^{115}In, ^{169}Tm, ^{175}Lu, ^{185}Re and ^{209}Bi to determine the most suitable choice of internal standard(s). Corrections were made for the Sr, Tm and Lu already in the reference material. Scandium, Y, Ba, REE, Pb, Th, and U were measured and results are shown in Table 4.

Compared with ^{115}In, there is little difference in the results when using ^{84}Sr as an internal standard for the analysis of the lighter mass elements ^{45}Sc and ^{89}Y. Likewise, using both ^{115}In and ^{209}Bi as internal standards showed similar results for the heavier masses ^{208}Pb, ^{232}Th and ^{238}U The middle masses showed no improvement using ^{169}Tm, ^{175}Lu or ^{185}Re as internal standards instead of ^{115}In alone. Based on these results, indium was used as a single internal standard for isotopes from ^{45}Sc to ^{238}U. A similar outcome was found by Townsend *et al.* (1998) when analysing urine samples with the same HR-ICP-MS instrument. In that work, little difference was found for the analysis of Cu, Zn, Cd and Pb when using Sc, In and Bi as an internal standard combination over ^{115}In alone.

Detection limits

Although instrument sensitivity is a major factor in achieving good detection limits, a high background caused by memory effects and sample contamination can also have a large influence. Table 5 lists the detection limits measured while aspirating three solutions: (a) ultra pure water (doubly distilled in a sub-boiling quartz still), (b) a 2% v/v HNO_3 solution, and (c) an ordinary sample blank solution ($HF/HClO_4$ digestion followed by final dilution with 2% HNO_3). Detection limits shown were defined as three times the standard deviation of (at least) ten consecutive blank measurements (3σ) Results were obtained under routine operating conditions with no special instrument

Table 5.
ICP-MS detection limits

		*This Study		Ionov *et al.* 1992	Pin and Joannon 1997	Makishima and Nakamura 1997	
Element	*pure water pg ml^{-1} in solution	*2% v/v HNO_3 pg ml^{-1} in solution	*sample blank $HF/HClO_4$ digestion (2% v/v HNO_3 final soln.) pg ml^{-1} in solution (ng g^{-1} in rock, 1000 x dilution)	sample blank pg ml^{-1} in solution (ng g^{-1} in rock, 1000 x dilution)	micro-conc. nebuliser pg ml^{-1} in solution (ng g^{-1} in rock, 1000 x dilution)	flow injection 0.5 mol l^{-1} HNO_3 pg ml^{-1} in solution	low dilution (113x) (ng g^{-1} in rock)
Sc	17.9	13.9	13.3	10	-	-	-
Y	0.38	0.80	2.54	-	-	34	4
La	0.15	0.35	1.74	1.5	1.6	7	0.8
Ce	0 33	0.88	1.37	1.5	6.8	8	0.9
Pr	0 09	0.16	0.34	1	1.4	4	0.5
Nd	1.06	1.21	1.31	2	0 6	20	2
Sm	0.50	1.27	1.28	1.5	0.7	15	2
Eu	0.35	0.37	0.55	0 4	0 4	4	0.4
Gd	0.97	3.02	1.44	1	0.5	26	3
Tb	0 09	0 11	0.21	0.2	0 6	4	0.4
Dy	0.16	0.78	0.58	1	0 4	21	2
Ho	0.04	0 39	0.22	0.25	0 4	3	0 4
Er	0.10	0 28	0.44	0 6	0.5	23	3
Tm	0.05	0.41	0.19	0.2	0.5	3	0.3
Yb	0 12	0.37	0.71	0.4	0.5	6	0.6
Lu	0.05	0 63	0.22	0.2	0.5	4	0.4

* Reported detection limits are three times the standard deviation of 10-15 blank measurements.

Table 6.
Trace element concentrations (μg g^{-1}), precision (%RSD) and published values for rock reference materials

Element	n=2 This work μg g^{-1}	na=4 RSD %	Ref. (A) μg g^{-1}
AGV-1			
Sc	12.4	0.8	12.2
Y	18.7	0.2	20
La	39.2	2.1	38
Ce	72.1	3.6	67
Pr	8.79	2.5	7.6
Nd	32.5	2.2	33
Sm	6.02	3.8	5.9
Eu	1.68	4.2	1.64
Gd	4.94	3.3	5
Tb	0.69	3.8	0.7
Dy	3.5	1.9	3.6
Ho	0.69	2.5	0.67
Er	1.81	4.3	1.7
Tm	0.26	4.7	0.34
Yb	1.68	0.9	1.72
Lu	0.251	4	0.27
Average RSD (%), all elements		**2.8**	

Element	n=2 This work μg g^{-1}	na=4 RSD %	Ref. (A) μg g^{-1}
BCR-1			
Sc	32.3	1.7	32.6
Y	33.6	0.6	38
La	25.2	2	24.9
Ce	53	6.3	53.7
Pr	6.87	3.9	6.8
Nd	27.9	4.2	28.8
Sm	6.57	7.1	6.59
Eu	1.96	2.1	1.95
Gd	6.62	3.3	6.68
Tb	1.05	5.1	1.05
Dy	6.05	2.3	6.34
Ho	1.26	0.9	1.26
Er	3.52	1.8	3.63
Tm	0.52	3	0.56
Yb	3.29	3.2	3.38
Lu	0.5	2.9	0.51
Average RSD (%), all elements		**3.2**	

Element	n=2 This work μg g^{-1}	na=4 RSD %	n=19 This work (19 digestions over 18 months) μg g^{-1}	na=1 RSD %	Ref. (A) μg g^{-1}
BHVO-1					
Sc	31.9	1.8	31	3.5	31.8
Y	24.9	1.9	24	4.2	27.6
La	16	1	15.5	3.6	15.8
Ce	39	3	38	3.2	39
Pr	5.65	1.7	5.5	3.7	5.7
Nd	25.1	2.2	25	4.6	25.2
Sm	6.26	2.2	6.23	4.9	6.2
Eu	2.12	2	2.14	3.4	2.06
Gd	6.26	3.1	6.35	6.6	6 4
Tb	0.97	3.8	0.94	5.2	0.96
Dy	5.34	2.6	5.28	5.3	5.2
Ho	1.02	4	1.01	6 4	0.99
Er	2.59	2.4	2.57	6.4	2.4
Tm	0.34	3.2	0.34	5.4	0.33
Yb	1.99	3.5	2	5.7	2.02
Lu	0.28	3.7	0.28	6.8	0.291
Average RSD (%), all elements		**2.6**		**4.9**	

Element	n=7 This work μg g^{-1}	na=1 RSD %	Ref. (A) μg g^{-1}	n=6 Ref. (C) μg g^{-1}	n=3 Ref. (E) μg g^{-1}
DNC-1					
Sc	30.5	2.7	31	31.1	-
Y	15.9	1.5	18	18.03	-
La	3.66	3.2	3.8	3.68	3.91
Ce	8.04	3.4	10.6	8.17	8.46
Pr	1.11	1.4	1.3	1.113	1.11
Nd	4.89	2.2	4.9	4.95	4.8
Sm	1.47	2.3	1.38	1 44	1.3
Eu	0.61	2.7	0.59	0.592	0.515
Gd	2.04	1.9	2	2.02	1.79
Tb	0.39	1.8	0.41	0.39	0.33
Dy	2.76	2.3	2.7	2.71	2.35
Ho	0 64	1.7	0.62	0.638	0.537
Er	2	2.7	2	1.945	1.63
Tm	0.294	1.9	[0.33]	-	0.271
Yb	2.01	3	2.01	1.915	1.8
Lu	0.308	2.3	0.32	0.292	0.3
Average RSD (%), all elements		**2.3**		**0.9**	1

Element	n=13 This work μg g^{-1}	na=1 RSD %	Ref. (A) μg g^{-1}	Ref. (B) μg g^{-1}
BIR-1				
Sc	42	3.1	44	-
Y	14.1	1.8	16	15.5
La	0.63	5.5	0.62	0 61
Ce	1.89	5.3	1.95	1.95
Pr	0.38	4.6	0.38	0.38
Nd	2 31	3.8	2.5	2.34
Sm	1.07	2.6	1.1	1.1
Eu	0.52	3.4	0.54	0.52
Gd	1.77	2.5	1.85	1.84
Tb	0.35	3.5	0.36	0.36
Dy	2.43	2.8	2.5	2.51
Ho	0.55	3.5	0.57	0.56
Er	1.64	3.1	1.7	1.66
Tm	0.24	4.7	0.26	0.25
Yb	1.61	2.7	1.65	1.63
Lu	0.24	3.9	0.26	0.25
Average RSD (%), all elements		**3.6**		

Element	n=10 na=1 This work μg g^{-1}	Resolution 300 RSD %	n=10 na=1 This work μg g-1	Resolution 3000 RSD %	n=12 Ref. (C) μg g^{-1}
Tafahi					
Sc	Si interference	-	45.24	2.1	45.5
Y	7.76	1.7	8.24	2.1	9.11
La	0.93	1.6	0.95	4.8	0.938
Ce	2.22	2	2.168	3.8	2.22
Pr	0.368	1.6	0.331	3.9	0.361
Nd	1.91	1.5	1.887	3.4	1.93
Sm	0.72	1.5	0.711	6.7	0.722
Eu	0.309	2.2	0.288	6.4	0.305
Gd	1.04	2.1	1.046	5.9	1.069
Tb	0.188	1.4	0.192	6.4	0.207
Dy	1.35	1.5	1.394	5.3	1.384
Ho	0.32	1.3	0.311	6	0.322
Er	0.951	0.9	0.965	5.5	0.98
Tm	0.147	2	0.141	4.5	-
Yb	0.987	0.9	1.029	4.5	0.992
Lu	0.156	1.7	0.147	4	0.153
Average RSD (%), all elements		**1.6**		**4.7**	**1.5**

Table 6 (continued).
Trace element concentrations (μg g^{-1}), precision (%RSD) and published values for rock reference materials

Element	n=8 This work μg g^{-1}	na=2-3 RSD %	Ref. (A) μg g^{-1}	n=12 Ref. (C) μg g^{-1}	n=7 Ref. (D) μg g^{-1}	n=4 Ref. (F) μg g^{-1}
PCC-1						
Sc	8	4 7	8.4	9	7	-
Y	0 079	3 4	[0.1]	0 087	-	0.079
La	0.046	10.7	0.052	0.029	0 039	0 034
Ce	0 0528	1 8	0 1	0 053	0.057	0 061
Pr	0 0076	9	0 013	0 0068	0 0085	0.0091
Nd	0.026	2 5	0.042	0 025	0 03	0.035
Sm	0 007	19.5	0.0066	0.005	0 008	0.0095
Eu	0 0009	22.7	0 0018	0.0011	0.0018	0.0024
Gd	0.0059	16.9	[0.014]	0.0061	0.008	0 013
Tb	0.0011	16 7	0.0015	0.0012	0.0015	0.0014
Dy	0 011	13.9	0 01	0 0087	[0.013]	0 016
Ho	0.003	7.6	0.0025	0 0027	0.0038	0.0034
Er	0 0117	8.3	[0.012]	0.0113	0.0123	0.016
Tm	0 0028	7 4	0.0027	-	0.0025	0.0032
Yb	0.0227	4.6	0.024	0.0213	0 0215	0.028
Lu	0 0047	4 9	0 0057	0 0046	0 0049	0.0054
Average RSD (%), all elements		**9.7**		**17.4**	**10.8**	**13.2**

Element	n=6 This work μg g^{-1}	na=2 RSD %	Ref. (A) μg g^{-1}	n=10 Ref. (D) μg g^{-1}	n=3 Ref. (E) μg g^{-1}
UB-N					
Sc	11.4	1.6	13	14	-
Y	2.45	3.3	2 5	-	-
La	0 323	1 3	0.35	0.33	0 319
Ce	0.76	2.3	0 8	0.8	0.77
Pr	0.12	2.7	0.12	0 123	0 113
Nd	0.6	2	0 6	0 61	0 594
Sm	0.226	2.8	0.2	0.216	0.204
Eu	0 084	1.1	0 08	0.081	0 0726
Gd	0 326	2.7	0.3	0.32	0 294
Tb	0 061	2	0.06	0 06	0.054
Dy	0 433	1.3	0.38	0.42	0.377
Ho	0.099	0.6	0 09	0.097	0.0843
Er	0 308	0 6	0.28	0.282	0.251
Tm	0 046	1.9	0.045	0 0434	0 0415
Yb	0.315	2.6	0 28	0.283	0.272
Lu	0 049	2 5	0.045	0.046	0 0453
Average RSD (%), all elements		**2**		**2.8**	**14.9**

Element	n=7 This work μg g^{-1}	na=2-3 RSD %	Ref. (A) μg g^{-1}	n=2 Ref. (C) μg g^{-1}	n=3 Ref. (D) μg g^{-1}	n=4 Ref. (F) μg g^{-1}
DTS-1						
Sc	3 16	2.2	3.5	5.3	3.5	-
	0.037	8 4	0 04	0.038	-	0.042
La	0.041	6.7	0.029	0.0246	0 025	0.023
Ce	0.05	3.4	0.072	0.1	0 05	0 052
Pr	0.0068	5	0.0063	0.0063	0 0074	0.0066
Nd	0 022	5.2	0.029	0.0234	0 027	0.025
Sm	0.0063	16.5	0 0046	0 0031	[0.007]	0.009
Eu	0 0008	12.4	0 0012	0.0013	0 0013	0 0019
Gd	0 0042	11.7	[0.0038]	0.0044	0 0063	0.0081
Tb	0 0007	18.1	0.0008	0.0007	0.001	0.0012
Dy	0.006	25.1	[0.003]	0 0038	0.0085	0 0082
Ho	0 0017	12 6	0 0013	0.0014	0 0016	0 0024
Er	0 0055	78	[0.004]	0.005	0 0074	0.0061
Tm	0 001	14 2	0.0014	-	0 0013	0 0017
Yb	0 0097	3 5	0.01	0.009	0 01	0.011
Lu	0 0021	5	0 0024	0.0019	0 0022	0 0029
Average RSD (%), all elements		**9.9**				**13**

formation values are shown in brackets. n number of digestions.
number of ICP-MS analyses performed on each digestion.

A) Govindaraju (1994), (B) Jochum *et al.* (1994), (C) Eggins *et al.* 1997), (D) Ionov *et al.* (1992), (E) Pin and Joannon (1997), Makishima and Nakamura (1997).

preparation or maintenance, other than cleaning of cones, torch and spray chamber

Comparing detection limits with other laboratories can be a difficult exercise, since full details of the conditions and solutions used are not always given. Table 5 lists results from three studies using quadrupole instruments, each of which focused on the analysis of low level (ng g^{-1}) samples. Ionov *et al.* 1992 reported exceptionally low detection limits considering the sample blank was used for these measurements. "Special measures" were taken to reduce memory effects, blanks were prepared in a clean room environment, while the ICP-MS instrument was solely dedicated to peridotite analysis. Pin and Joannon (1997) gained increased sensitivity by using ion exchange separation as a sample pretreatment. The blank used to determine detection limits was not specified Makishima and Nakamura (1997) used flow injection analysis, increased plasma power and low sample dilution (113x) to achieve good detection limits (which were measured in an "ideal solution" of 0 5 mol l^{-1} HNO_3)

In this study, the detection limits found under standard conditions with a mixed acid sample blank are comparable to those reported from other laboratories who have specialised in low level determinations. However, with an extra clean blank (pure water only) the detection limits were improved by a factor of (approximately) ten We regard the detection limits obtained from the mixed acid blank as more realistic since they reflect those during the routine analytical procedure. Except for Sm, Eu, Gd and Tb in the reference materials PCC-1 and DTS-1, detection limits obtained here from the mixed acid blanks always lie more than a factor of ten below the abundance in the rock solution

Precision and accuracy

Results for a range of international rock reference materials are compared with published values in Table 6. Initial work using AGV-1, BCR-1 and BHVO-1 produced results derived by averaging measurements from two decompositions, with each determination being the average of four ICP-MS measurements taken separately over several weeks Further work over an eighteen month period resulted in separate digestions and analyses for BHVO-1 (19x), BIR-1 (13x), Tafahi [20x, a basalt with low REE (Eggins *et al* 1997)], DNC-1 (7x), UB-N (6x), PCC-1 (8x) and DTS-1 (7x).

Average precision on the duplicate digestions of AGV-1, BCR-1 and BHVO-1 (eight analyses for each reference material) was 2.6%-3.2%, whereas that for BHVO-1 was 4.9% from nineteen digestions, and 3.6% from thirteen digestions for BIR-1. The poorer average precision in the latter results reflects a variety of factors over time, including different digestion methods by various workers and varied instrument conditions (e.g. plasma stability, cone conditions, inclusion of medium and low resolution results). Excellent average precision of 1.6% was obtained for Tafahi in low resolution (300) when ten samples were digested and analysed simultaneously. A second set of ten digestions were analysed independently using medium (3000) resolution. While the final concentration values were similar for both cases, the average precision using resolution 3000 was only 4.7% because of the lower signal intensities associated with this resolution mode (Moens *et al.* 1995) Ultramafics with very low element concentrations gave 2.0% average precision for UB-N, 9.7% for PCC-1 and 9.9% for DTS-1, which compares well with results from other workers (2.8%-17.4%) where special analytical conditions or modifications were often employed. (e.g. Ionov *et al.* 1992, Eggins *et al.* 1997, Makishima and Nakamura 1997).

Internal (instrumental) precisions of 1-2% were obtained using HR-ICP-MS Much higher external repeatabilities, however, were found when multiple sample digestions were considered (Table 6). While dissolution is relatively straightforward for mafic rocks as in this study, samples with refractory minerals such as zircon, sphene, spinel and garnet can be extremely difficult. Often the HREE, Th, U and Zr-Hf reside in such minerals. Preparation techniques such as a sodium peroxide sinter (Robinson *et al.* 1986) or a lithium borate fusion can be employed (e.g. Jarvis 1992, Chao and Sanzolone 1992) However, problems found with the fusion method include contamination from fusion reagents and possible loss of volatile elements such as Pb, Tl and Sb (Totland *et al.* 1992). As a result, acid digestion research work is preferred in our laboratory using a pressure digestion system such as PicoTrace.

Accuracy can be judged by comparing results found in this work with those from other studies, and plotting chondrite normalized data (Figures 3-7). With few exceptions, our results are in agreement with those found for the well characterized reference materials AGV-1, BCR-1, BHVO-1, BIR-1 and DNC-1. Exceptions are Y for all reference materials, as well as Ce, Pr and Tm in AGV-1 and DNC-1. Our Y values are approximately 9% lower than published values, and are discussed further in the next section Cerium is approximately 8% higher in AGV-1 and 24% lower in DNC-1 compared with Govindaraju's 1994 compilation. Pr is 16% higher in AGV-1 and 15% lower in DNC-1, Tm is 24% lower in AGV-1 and 11% lower in DNC-1. Our chondrite normalized data plot smoothly for AGV-1 and DNC-1, suggesting published results may be in error. Results for low level reference materials Tafahi, UB-N, PCC-1 and DTS-1 are in general agreement with other workers, although PCC-1 and DTS-1 are so low that there is little reliable data published. Chondrite normalized REE patterns for DTS-1 and PCC-1 (Figures 6 and 7) show good agreement with those from available literature references The consistent V-shape observed by the different laboratories suggests that ICP-MS can be a reliable method at

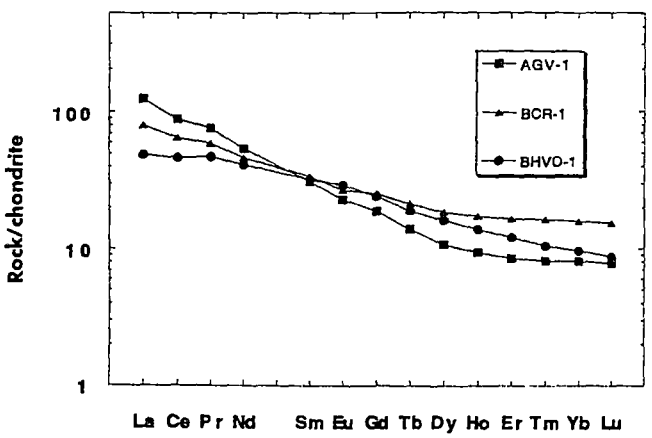

Figure 3. Chondrite normalized plots for AGV-1, BCR-1 and BHVO-1.

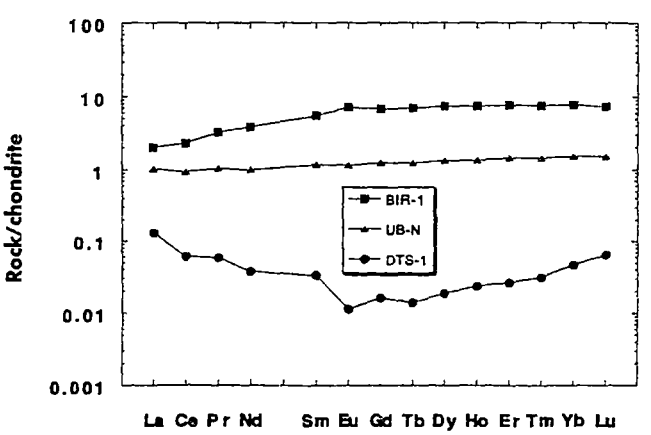

Figure 4. Chondrite normalized plots for BIR-1, UB-N and DTS-1.

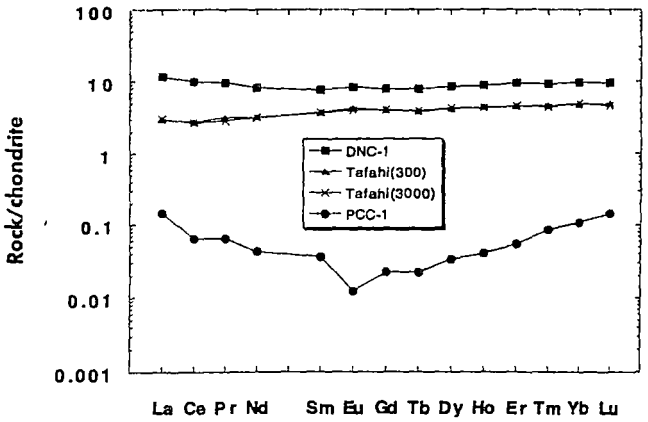

Figure 5. Chondrite normalized plots for DNC-1, Tafahi (resolution 300 and 3000) and PCC-1.

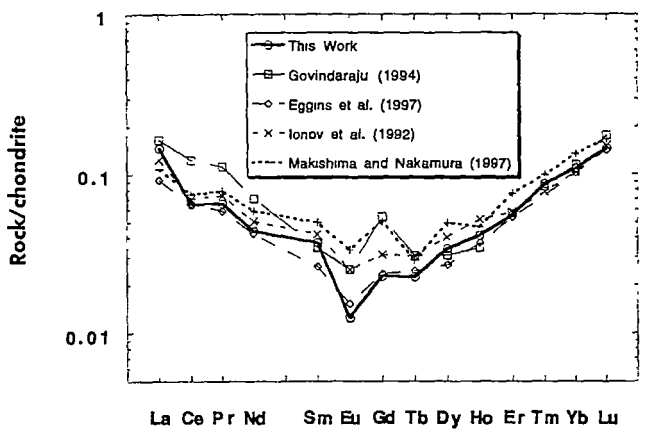

Figure 6. Chondrite normalized plot for PCC-1. Comparison with other laboratories.

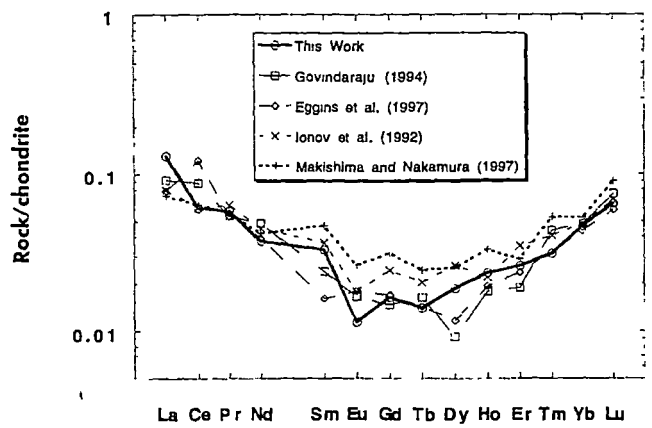

Figure 7. Chondrite normalized plot for DTS-1. Comparison with other laboratories.

such low abundance. This steep, linear, positive HREE-MREE gradient and upward-inflected LREE pattern seems to be characteristic of peridotite from subduction environments (Parkinson and Pearce 1998)

There has been some concern noted in the literature on the possible interference of La and Pr by $CaClO_4$, formed during $HF/HClO_4$ digestions (Longerich 1993) This interference was not apparent in this work, as demonstrated by the fact that similar La and Pr values were obtained for BIR-1 when prepared by both $HF/HClO_4$ and HF/HNO_3 (Cl-free) digestion. Occasionally, however, spurious high results were obtained for La in BIR-1 (e.g. 0.6-0.8 $\mu g\ g^{-1}$ compared with an expected value of ~ 0.62 $\mu g\ g^{-1}$) found from both acid mixtures. As all sample blanks were consistently low, this was attributed to accidental contamination in the BIR-1 sample, possibly from the use of La as a heavy element absorber in XRF flux in our laboratory. Lanthanum values (though not Pr) for PCC-1 (0.046 $\mu g\ g^{-1}$) and DTS-1 (0.041 $\mu g\ g^{-1}$) were found to be slightly higher than some published results (e.g. Ionov *et al.* 1992 and Makishima and Nakamura 1997, who reported La values of 0.023-0.039 $\mu g\ g^{-1}$) also using $HF/HClO_4$ digestion. Lanthanum in these reference materials is well above our detection limit (25x) and gave good precision (~ 7-10%) in multiple digestions over three months, which suggests there is no contamination in these samples. Another ultramafic rock, UB-N (0.32 $\mu g\ g^{-1}$ La), and Tafahi basalt (0.94 $\mu g\ g^{-1}$ La) were in good agreement with published values.

Yttrium in rock reference materials

Work in our laboratory consistently found low yttrium results in rock reference materials in comparison with published values Poor dissolution was initially suspected as the cause of this discrepancy. However, good agreement was found for many other elements (such as Zr, Hf, Th, U and the HREE) that often reside in minerals which are the main hosts to Y. Low yttrium values have been noted in other studies (e.g. Totland *et al.* 1992, Shinotsuka *et al.* 1996). From the analysis of approximately one hundred samples (basalts through to rhyolites) for yttrium by both ICP-MS and XRF, Münker (1997) found ICP-MS results to be consistently 10-15% lower than XRF results. It is relevant to note that rock reference materials were used for the XRF calibration

Yttrium in a range of rock samples was measured by XRF using pure chemical reagents as calibration

Table 7.
Yttrium concentration (μg g^{-1}) in rock reference materials by HR-ICP-MS and XRF

	HR-ICP-MS	XRF (a)	XRF (b)	mean XRF	Published values		ICPMS/ published	XRF/ published
BCR-1	33.6	33 9	33	33.5	38		0.884	0.88
BHVO-1	24.5	24.9	24.3	24.6	27.6		0.888	0.891
AGV-1	18.7	17.9	17.6	17.8	20		0.935	0.888
DNC-1	15.9	16.6	16.3	16.5	18		0.883	0.914
BIR-1	14.1	14.4	14.2	14.3	15.5		0.912	0.923
Tafahi	8	7.9	8	8	9.11		0.878	0.873
UB-N	2 4	2.4	2.6	2.5	2.5		0.96	1
PCC-1	0.077	< 1	< 1	< 1	0.087		0.885	
DTS-1	0 036	< 1	< 1	< 1	0.04		0.900	
						mean =	0.903	0.91
						RSD =	0.022	0.031

XRF (a) 2000 μg g^{-1} Y calibration standards (mixed powders, Y_2O_3 with pure quartz).
XRF (b) 0, 50, 100, 200 μg g^{-1} Y calibration standards (mixed Y solution with pure quartz).

standards. Results are reported in Table 7 and are compared with ICP-MS values calibrated using standard solutions from four manufacturers (solutions from Perkin Elmer, QCD, Spex and BDH Y_2O_3 were all similar). The XRF results listed in this table were derived using two sets of synthetic Y standards prepared via different methods. Both XRF and ICP-MS values were found to be in agreement and were (on average) 9% lower than published results, suggesting that the literature values may be in error. There are a number of possible reasons for this. Yttrium is a mono-isotopic element and cannot be determined by isotope dilution mass spectrometry. INAA is also inappropriate as there is no emission of γ rays from ^{90}Y, which is the only nuclide produced by (n,γ) reaction on Y (e.g. Shinotsuka *et al.* 1996). Thus, the majority of reported values for yttrium have been obtained using XRF where rock reference materials of uncertain value are often used for calibration. Yttrium determinations are not straightforward by XRF as there is a large Rb correction involved. Yttrium also contributes a spectral interference to the Compton line if a Mo X-ray tube is used, affecting absorption corrections, particularly on high Y samples such as is likely to be found in calibration standards. The use of Compton scattering (where the Compton peak on the 2000 μg g^{-1} calibration standards was inadequately corrected for Y overlap) gave results on the rock reference materials 3% lower than literature values, instead of 9% using alpha coefficients.

In summary, the reason for many recommended Y values in rock reference materials being high may be poor quality XRF data. The danger of using a rock reference material for calibration e.g. BHVO-1 (Eggins *et al.* 1997) is illustrated here, as although such results agree with recommended values, they are not necessarily correct.

The possibility of Y results being 9% high in the literature has significant geological implications. Yittrium shows a geochemical behaviour similar to that of Ho, a heavy rare earth element (HREE). This is manifested by virtually constant Y/Ho ratios in mafic rocks and chondrites (Jochum *et al.* 1986). Yttrium is, therefore, used to understand petrogenetic processes in igneous rocks. Recent work (Bau 1996) showed that the Y/Ho ratio can be substantially changed in felsic magmatic and hydrothermal systems. Yttrium in conjunction with Ho might, therefore, be used for monitoring hydrothermal alteration processes It may be prudent to reassess the Y content in chondrites by ICP-MS and improved XRF methods using synthetic Y calibration standards for both

Advantages of HR-ICP-MS

High resolution magnetic sector ICP-MS offers a number of advantages over quadrupole-based instruments. High ion transmission combined with a low background signal provides superior detection limits.

HR-ICP-MS sensitivity is typically 100,000 - 150,000 counts s^{-1} per ng ml^{-1} In. Four quadrupole ICP-MS groups (Pin and Joannon 1997, Shinotsuka *et al.* 1996, Eggins *et al* 1997, Niu and Batiza 1997) quote sensitivities ranging from 8,000 to 35,000 counts s^{-1} per ng ml^{-1} In It should be noted, however, that sensitivity for modern HR-ICP-MS and quadrupole systems has increased substantially since this paper was initially prepared With HR-ICP-MS, reagent blanks are often the limiting factor with regard to low level analysis. Although excellent detection limits have often been obtained by quadrupole ICP-MS (Ionov *et al* 1992, Eggins *et al.* 1997), such values are more easily obtained by HR-ICP-MS Without a clean room or specific dedication of the instrument to continued low level work, the increased sensitivity of HR-ICP-MS enabled abundances of REE in the ultramafic rocks PCC-1 and DTS-1, which have REE contents in the range of 0.8-50 ng g^{-1} (0 01-0.1x chondrite), to be accurately and precisely quantified. No sample preconcentration was necessary, reducing the risk of contamination and analyte loss, while saving preparation time and associated costs.

Low oxide formation was also found when using this HR-ICP-MS instrument. Oxide corrections were generally only required for Pr and Ce on Gd, and Ba on Eu. When observed, oxide and hydroxide interferences could often not be separated from the analytes of interest with the higher resolutions available using HR-ICP-MS. Medium resolution ($m/\Delta m$ = 3000), however, was found to be necessary for the accurate quantification of Sc. Using this resolution, $^{29}Si^{16}O$ and $^{28}Si^{16}O1H$ interferences could be identified as the major causes for imprecise Sc results using quadrupole instruments. These Si-based interferences were completely resolved from ^{45}Sc when using high resolution. Depending on the dissolution procedure, Sc determinations using conventional ICP-MS with pure element calibration solutions may be expected to give too high Sc results in rock samples, while the use of rock reference materials for calibration may give, apparently, more accurate results.

The successful use of synthetic (pure element) calibration solutions and a single internal standard (indium) was demonstrated using HR-ICP-MS, provided rock samples were dissolved and diluted by at least a factor of 1000 Indium (^{115}In) was found to be a satisfactory internal standard in comparison with a mix of ^{84}Sr, ^{169}Tm, ^{175}Lu, ^{185}Re and ^{209}Bi for the analysis of ^{45}Sc through to ^{238}U, providing a true simplified procedure without the need to resort to more complicated internal standard combinations (e.g Eggins *et al.* 1997).

Although this study only reports Sc, Y and REE data, typically thirty two elements are often determined by HR-ICP-MS during each analysis in our laboratory. It is planned to report findings on other elements in due course

Acknowledgements

The following are thanked for their various contributions to this study· Joe Stolz for early advice and preparation of a number of rock reference material solutions, John Foden (University of Adelaide) for providing ^{84}Sr solution and Steve Eggins (Australian National University, Canberra) for the donation of Tafahi basalt powder. The facilities of the Central Science Laboratory, University of Tasmania, are gratefully acknowledged. This project was supported by Australian Research Council grants and industry research funding to the School of Earth Sciences and Centre for Ore Deposit and Exploration Studies, University of Tasmania.

References

Balaram V. (1996)
Recent trends in the instrumental analysis of rare earth elements in geological and industrial materials Trends in Analytical Chemistry, 15, 475-485

Balaram V., Ramesh S.L. and Anjaiah K.V. (1996)
New trace element and REE data in thirteen GSF reference samples by ICP-MS Geostandards Newsletter, 20, 71-78

Barrat J.A., Keller F., Amossé J., Taylor R.N., Nesbitt R.W. and Hirata T. (1996)
Determination of rare earth elements in sixteen silicate reference samples by ICP-MS after Tm addition and ion exchange separation Geostandards Newsletter, 20, 133-139.

Bau M. (1996)
Controls on the fractionation of isovalent trace elements in magmatic and aqueous systems Evidence from Y/Ho, Zr/Hf, and lanthanide tetrad effect Contributions to Mineralogy and Petrology, 123, 323-333

Becker J.S. and Dietze H.-J. (1997)
Double focusing sector field inductively coupled plasma-mass spectrometry for highly sensitive multi-element and isotopic analysis. Journal of Analytical Atomic Spectrometry, 12, 881-889.

Bock R. (1979)
A handbook of decomposition methods in analytical chemistry Blackie (Glasgow and London), 60-61

Bradshaw N., Hall E.F.H. and Sanderson N.E. (1989)
Inductively coupled plasma as an ion source for high-resolution mass spectrometry. Journal of Analytical Atomic Spectrometry, 4, 801-803.

references

Chao T.T. and Sanzolone R.F. (1992)
Decomposition techniques Journal of Geochemical Exploration, 44, 65-106

Dulski P. (1994)
Interferences of oxide, hydroxide and chloride analyte species in the determination of rare earth elements in geological samples by inductively coupled plasma-mass spectrometry Fresenius' Journal of Analytical Chemistry, 350, 194-203.

Eggins S.M., Woodhead J.D., Kinsley L.P.J., Mortimer G.E., Sylvester P., McCulloch M.T., Hergt J.M. and Handler M.R. (1997)
A simple method for the precise determination of ≥ 40 trace elements in geological samples by ICP-MS using enriched isotope internal standardisation Chemical Geology, 134, 311-326.

Evans H.E. and Giglio J.J. (1993)
Interferences in inductively coupled plasma-mass spectrometry. A review Journal of Analytical Atomic Spectrometry, 8, 1-18.

Feldmann I., Tittes W., Jakubowski N., Stuewer D. and Giessmann U. (1994)
Performance characteristics of inductively coupled plasma-mass spectrometry with high mass resolution Journal of Analytical Atomic Spectrometry, 9, 1007-1014.

Garbe-Schönberg C.-D. (1993)
Simultaneous determination of thirty seven trace elements in twenty eight international rock standards by ICP-MS Geostandards Newsletter, 17, 81-97

Govindaraju K. (1994)
1994 Compilation of working values and sample description for 383 geostandards Geostandards Newsletter, 18 (Special Issue), 158pp.

Heinrichs H. and Herrman A.G. (1990)
Praktikum der analytischen Geochemie Springer Verlag, Berlin, 669pp

Hollocher K., Fakhry A. and Ruiz J. (1995)
Trace element determinations for USGS basalt BHVO-1 and NIST standard reference materials 278, 688 and 694 by inductively coupled plasma-mass spectrometry. Geostandards Newsletter, 19, 35-40

Ionov D.A., Savoyant L. and Dupuy C. (1992)
Application of the ICP-MS technique to trace element analysis of peridotites and their minerals Geostandards Newsletter, 16, 311-315

Jarvis I. (1992)
Sample preparation for ICP-MS In: Jarvis K.E., Gray A.L. and Houk R.S. (eds.), Handbook of inductively coupled plasma-mass spectrometry. Blackie, (Glasgow) 172-224

Jarvis K.E. and Jarvis I. (1988)
Determination of the rare earth elements and yttrium in thirty seven international silicate reference materials by inductively coupled plasma-atomic emission spectrometry Geostandards Newsletter, 12, 1-12.

Jarvis K.E. (1988)
Inductively coupled plasma-mass spectrometry: a new technique for the rapid or ultra-trace level determination of the rare earth elements in geological materials Chemical Geology, 68, 31-39

Jarvis K.E. (1990)
A critical evaluation of two sample preparation techniques for low-level determination of some geologically incompatible elements by inductively coupled plasma-mass spectrometry Chemical Geology, 83, 89-103.

Jenner G.A., Longerich H.P., Jackson S.E. and Fryer B.J. (1990)
ICP-MS - A powerful tool for high-precision trace element analysis in Earth sciences Evidence from analysis of selected USGS reference samples. Chemical Geology, 83, 133-148

Jochum K.P., Rehkämper M. and Seufert H.M. (1994)
Trace element analysis of basalt BIR-1 by ID-SSMS, HPLC and LIMS. Geostandards Newsletter, 18, 43-51.

Jochum K.P., Seufert H.M., Spettel B. and Palme H. (1986)
The solar-system abundances of Nb, Ta and Y, and the relative abundances of refractory lithophile elements in differentiated planetary bodies. Geochimica et Cosmochimica Acta, 50, 1173-1183

Lichte F.E., Meier A.L. and Crock J.G. (1987)
Determination of the rare earth elements in geological materials by inductively coupled plasma-mass spectrometry. Analytical Chemistry, 59, 1150-1157.

Longerich H.P. (1993)
Oxychlorine ions in inductively coupled plasma-mass spectrometry Effect of Cl speciation as Cl^- and ClO_4^-. Journal of Analytical Atomic Spectrometry, 8, 439-444

Longerich H.P., Jenner G.A., Fryer B.J. and Jackson S.E. (1990)
Inductively coupled plasma-mass spectrometric analysis of geological samples. A critical evaluation based on case studies Chemical Geology, 83, 105-118

Makishima A. and Nakamura E. (1997)
Suppression of matrix effects in ICP-MS by high power operation of ICP Application to precise determination of Rb, Sr, Y, Cs, Ba, REE, Pb, Th and U at ng g^{-1} levels in milligram silicate samples Geostandards Newsletter: The Journal of Geostandards and Geoanalysis, 21, 307-319

McGinnis C.E., Jain J.C. and Neal C.R. (1997)
Characterisation of memory effects and development of an effective wash protocol for the measurement of petrogenetically critical trace elements in geological samples by ICPMS Geostandards Newsletter: The Journal of Geostandards and Geoanalysis, 21, 289-305

Moens L., Vanhaecke F., Riondato J. and Dams R. (1995)
Some figures-of-merit of a new double focusing inductively coupled plasma-mass spectrometer Journal of Analytical Atomic Spectrometry, 10, 569-574

references

Morita M., Ito H., Uehiro T. and Otsuka K. (1989)
High resolution mass spectrometry with inductively coupled argon plasma ionisation source Analytical Sciences, 5, 609-610

Münker C. (1997)
Geochemical and isotopic systematics of the Cambrian Devil River Volcanics in the Takaka Terrane, New Zealand PhD thesis, University of Göttingen, Germany

Münker C. (1998)
Nb/Ta fractionation in a Cambrian arc/back arc system, New Zealand. Source constraints and application of refined ICP-MS techniques. Chemical Geology, 144, 23-45.

Niu Y. and Batiza R. (1997)
Trace element evidence from seamounts for recycled ocean crust in the Eastern Pacific mantle Earth and Planetary Science Letters, 148, 471-483

Norman M.D., Griffin W.L., Pearson N.J., Garcia M.O. and O'Reilly S.Y. (1998)
Quantitative analysis of trace element abundances in glasses and minerals A comparison of laser ablation inductively coupled plasma-mass spectrometry, solution inductively coupled plasma-mass spectrometry, proton microprobe and electron microprobe data Journal of Analytical Atomic Spectrometry, 13, 477-482

Parkinson I.J. and Pearce J.A. (1998)
Peridotites from the Izu-Bonin-Mariana forearc (ODP Leg 125): Evidence for mantle melting and melt-mantle interaction in a supra-subduction zone setting Journal of Petrology, 39, 1577-1688.

Pin C. and Joannon S. (1997)
Low level analysis of lanthanides in eleven silicate rock reference samples by ICP-MS after group separation using cation-exchange chromatography. Geostandards Newsletter: The Journal of Geostandards and Geoanalysis, 21, 43-49.

Potts P.J. (1997)
Geoanalysis. Past, Present and Future. The Analyst, 122, 1179-1186

Potts P.J., Webb P.C. and Watson J.S. (1990)
Zirconium determination by ED-XRF. A critical evaluation of silicate reference materials as calibration standards. Geostandards Newsletter, 14, 127-136

Robinson P., Higgins N.C. and Jenner G.A. (1986)
Determination of rare earth elements, yttrium and scandium in rocks by an ion exchange-X-ray fluorescence technique Chemical Geology, 55, 121-137.

Shinotsuka K., Hidaka H., Ebihara M. and Nakahara H. (1996)
ICP-MS analysis of geological standard rocks for yttrium, lanthanoids, thorium and uranium Analytical Sciences, 12, 917-922.

Sylvester P.J. and McCandless T.E. (1997)
Guest editors in special issue on LA-ICP-MS. Geostandards Newsletter: The Journal of Geostandards and Geoanalysis, 21, 173-305

Totland M., Jarvis I. and Jarvis K.E. (1992)
An assessment of dissolution techniques for the analysis of geological samples by plasma spectrometry Chemical Geology, 95, 35-62

Townsend A.T., Miller K.A., McLean S. and Aldous S. (1998)
The determination of copper, zinc, cadmium and lead in urine by high resolution ICP-MS. Journal of Analytical Atomic Spectrometry, 13, 1213-1219.

Yoshida S., Muramatsu Y., Tagami K. and Uchida S. (1996)
Determination of major and trace elements in Japanese rock reference samples by ICP-MS International Journal of Environmental Analytical Chemistry, 63, 195-206.

Determination of Niobium(V) and Tantalum(V) as 2-(5-bromo-2-pyridylazo)-5-diethylaminophenol (Br-PADAP)-Citrate Ternary Complexes in Geological Materials using Ion-Interaction Reversed-Phase High-Performance Liquid Chromatography

N. Vachirapatama[1] / P. Doble[1] / Z. S. Yu[2] / P. R. Haddad[1]*

[1]Separation Science Group, School of Chemistry, University of Tasmania, GPO Box 252-75, Hobart, TAS 7001, Australia
[2]School of Earth Sciences, University of Tasmania, GPO Box 252-79, Hobart, TAS 7001, Australia

Key Words

Column liquid chromatography
Niobium and Tantalum complexes
Geological samples

Summary

A method for the simultaneous separation and determination of Nb(V) and Ta(V) as ternary complexes with 2-(5-bromo-2-pyridylazo)-5-diethylaminophenol (Br-PADAP) and citrate using ion-interaction reversed-phase high performance liquid chromatography on a C 18 column has been developed. The mobile phase compositions and pre-column complex formation conditions were optimised. Under the optimum conditions, the Nb(V) and Ta(V) complexes were eluted within 4 min with a mobile phase of methanol-water (50 % v/v) containing 12 mM tetrabutylammonium bromide and 12 mM citrate buffer at pH 7, with absorbance detection at 600 nm. The resulting % relative standard deviation of retention times, peak area and peak height for Nb(V) and Ta(V) complexes were 0.007, 0.000, 0.67. 2.69, 0.44 and 2.17, respectively. The detection limits (signal to noise ratio = 3) for Nb(V) and Ta(V) were 0.03 ppb and 0.41 ppb, respectively The method was applied to the analysis of geological samples (granite, basalt and andesite) and the results for Nb(V) obtained by the HPLC method using standard addition calibration agreed well with ICP-MS analysis and with certified values for all materials. For Ta(V), good agreement with certified values was obtained for granite samples using standard addition, but interferences were observed for basalt and andesite which prohibited the determination of Ta(V) in these samples.

Introduction

The Nb:Ta ratio in rock samples is a significant indicator of geochemical processes which have occurred in the crust-mantle system [1]. The background levels of Nb and Ta in various rocks are dependent on major rock types and most rocks contain Nb at low ppm levels and Ta at sub-ppm levels. Few analytical methods can be used for the analysis of Nb and Ta at such low levels in solid rock samples (or generally lower than ppb levels for 1/1000 dilution of digested rock solutions), but ICP-AES [2–3] and ICP-MS [4–8] have been applied successfully. The major disadvantage of these methods is the high cost of instrumentation.

Reversed-phase high-performance liquid chromatography (RP-HPLC) is a simple and low cost analysis technique, which has found widespread application in the determination of metal ions by separation of complexes formed between the metal ions and suitable ligands. Ta(V) and Nb(V) can form ternary complexes with a metallochromic reagent, such as 4-(2-pyridylazo) resorcinol (PAR) or 2-(5-bromo-2-pyridylazo)-5-diethylaminophenol (BrPADAP), and an auxiliary ligand such as tartrate [9–10], and these ternary complexes have formed the basis of some RP-IPLC methods for these metals. PAR-tartrate [9] and PADAP-H_2O_2 [10] have been used for pre-column ternary complex formation and subsequent RP-HPLC separation of Nb(V) and Ta(V) complexes by RP-HPLC. The reported method using PAR and tartarte [9] gave poor detection limits and a broad peak for Ta(V), whilst incomplete separation of the Nb(V) and Ta(V) ternary complexes occurred using PADAP and H_2O_2 [10].

Recently, we have presented a method for the separation of ternary complexes of Nb(V) and Ta(V) with PAR and citrate [11] (formed pre-column). This method provided good separation of standard solutions of the Nb(V) and Ta(V) ternary complexes, with detection limits of 0.4 ppb and 1.4 ppb for Nb(V) and Ta(V), respectively. However, whilst these detection limits were satisfactory for the determination of Nb(V) in digested rock samples, they were insufficiently low for the method to be used for the determination of Ta(V). Therefore there is a requirement for a more sensitive method (with sub-ppb detection limits) if the determination of Nb(V) and Ta(V) in rock samples is to be accomplished by RP-HPLC.

0009-5893/99/11 601-06 $ 03 00/0

The aims of the present research were to develop an RP-HPLC method for the separation and trace determination of Nb(V) and Ta(V) by using pre-column ternary complex formation with Br-PADAP and citrate and to apply this method to geological samples. It was anticipated that Br-PADAP would provide better sensitivity than previous methods [9–11], and exhibit different separation selectivity for the matrix components of the geological samples.

Experimental

Instrumentation

The chromatographic system consisted of a Waters (Milford, MA, USA) Model 600E pump, a Rheodyne (Cotati, CA, USA) model 7125 stainless steel injector (100 μL loop), a SPD-6AU UV-VIS spectrophotometric detector (Shimadzu, Tokyo, Japan) operated at 600 nm, and a Maxima 820 Chromatography Data Station (Waters). A NovaPak C 18 reversed-phase column (3.9 mm. I.D × 150 mm., particle size 4 μm, Waters) was used as the analytical column, and was fitted with a C 18 (10 μm particle size) guard column housed in a Guard-Pak pre-column module (Waters). The flow-rate of the mobile phase was maintained at 1.0 mL min^{-1} and the column temperature was kept at 30 °C. Detection was accomplished by absorbance measurements at 600 nm.

Screw-top Savillex® Teflon beakers (Savillex, Minnesota, USA) were used for digestion of rock samples Spectrophotometric studies were carried out using a Cary 5E UV-VIS-NIR spectrophotometer (Varian, Mulgrave, VIC, Australia).

Reagents and Solutions

Atomic absorption standard solutions of Nb(V) (1.005 mg mL^{-1}) and Ta(V) (0.990 mg mL^{-1}) were obtained from Aldrich (Milwaukee, WI, USA.) and a standard mixture of Nb(V) and Ta(V) containing 0.100 mg mL^{-1} of each was obtained from QCD Analysts (NJ, USA). Br-PADAP was obtained at more than 95 % purity from Fluka Chemie (AG, Buchs, Switzerland) and solutions of the dye were prepared freshly in ethanol before use. AR grade citric acid (BDH, Poole, England) solutions were also prepared freshly in water before use, and AR grade tetrabutylammonium bromide (TBABr, Sigma, St. Louis, USA) and AR grade ammonium hydroxide (Ajax Chemicals, Sydney, Australia) were used. Reagents used in the preparation of the geological samples were as follows: 99.99+% purity hydrofluoric acid (Aldrich), AR grade hydrochloric acid (BDH), AR grade nitric acid (BDH). Concentrated HF and HNO_3 were doubly distilled before use.

The following reference geological rock materials were used. GSR-1 (granite) was obtained from the institute of Rock and Mineral Analysis (Beijing, PRC). ACE (granite) was provided by the Geostandards (B.P.20, 54501 Vandoeuvre Cedex, France). AGV-1 (andesite) and BHVO-1 (basalt) were obtained from the National Institute of Standards and Technology (NIST, Gaithersburg, MD, USA). TASBAS (an in-house basalt standard) was obtained from School of Earth Science (University of Tasmania, Hobart, Australia). A further basaltic sample, G1485, was supplied by T. Crawford (from Macquarie Island, Antarctic, Australia).

Mobile phases were prepared by dissolving TBABr, and citric acid in water, adding the required volume to the desired amount of methanol, adjusting the pH with ammonium hydroxide and then diluting with water in order to adjust the final methanol concentration to the desired level. The optimal mobile phase composition was methanol-water (50 % v/v) pH 7 containing 12 mM of each TBABr and citric acid. Throughout this study all water used was distilled and then deionised using a Milli-Q system (Millipore, Bedford, MA, USA.), after which it was filtered through a 0.45 μm membrane filter (type HA, Millipore, Bedford, MA, USA.) before use. HPLC grade methanol was obtained from BDH (Poole, England).

Procedures

Sample Preparation

Duplicate 0.1000 g powdered rock samples were prepared in screw-top® Savillex Teflon beakers using a previously described procedure [8]. A few drops of water were added to wet the powdered rock. After carefully adding 2 mL of conc. HF and 0.5 mL of conc. HNO_3 into the container, the lids were screwed on. The samples were digested on a hotplate for 48 h, at about 130 °C. During the first 24 h of heating, the beakers were placed in an ultrasonic bath for about 2 min in order to disaggregate granular material and render it more susceptible to acid attack. This was performed a minimum of two times. The beakers were then removed from the hotplate and allowed to cool. The lids were opened carefully and the sample solutions were evaporated to incipient dryness at low temperature. Once inciplent dryness was reached, 1 mL conc. HNO_3 was added and the samples were evaporated again to incipient dryness. 2 mL of conc. HNO_3 followed by 1 mL of conc. HCl and 5 mL water were then added to the solid residues. The lids of the beakers were closed and each was warmed up to about 60 °C on a hotplate and kept for about 1 h until solutions were clear. Each solution was then transferred to a plastic container, made up to 20 mL with water, and divided into two portions. The first portion was used for HPLC experiments. This analysis was performed as quickly as possible in order to prevent loss of Nb(V) and Ta(V) loss from the solution due to hydrolysis reactions and precipitation. The second portion was prepared for ICP-MS measurements by taking 4 mL of original solution and diluting to 20 mL using 2 mM diethylenetriaminepentaacetic acid (DTPA). The solutions prepared for ICP-MS were analysed within 24 h to limit the

0009-5893/99/11 601-06 $ 03.00/0

risk of insufficient stabilisation of Nb(V) and Ta(V) and prevent adsorption on the wall of the container.

Pre-column Complex Formation

The following techniques were used for pre-column formation of the ternary complex for standard solutions and for samples:

In the case of standard solutions, citric acid (2.50 mL, 100 mM) was added into a 25 mL plastic container and then a standard solution of Nb(V) and Ta(V) was added, followed by a 0.75 mL of freshly prepared Br-PADAP solution (5×10^{-3} M). A 3.25 mL aliquot of ethanol was then added and the solution adjusted to pH 6.2 with dilute ammonia. At this stage the volume was approximately 15 mL. The solution was then transferred to a 25 mL plastic volumetric flask and made up to the mark with water. The pH at final solution was 6.0. After 60 min. to allow complete colour formation, the standard solution was filtered through a 0.45 μm filter before injection of a 100 μL aliquot of the solution onto the HPLC column. The concentration of the metal ions was determined by measuring peak areas.

In the case of a geological sample, the digested sample (2.00 mL) was added to 2.50 mL of citric acid solution (100 mM) in a plastic container. 2.00 mL, 2.50 mL or 3.50 mL aliquots of freshly prepared Br-PADAP solution (5×10^{-3} M) were added into granite rock solutions, andesite solutions and basalt solutions, respectively, leading to final concentrations of 0.4 mM PADAP for granite, 0.5 mM PADAP for andesite, and 0.7 mM PADAP for basalt. 2.00 mL, 1.50 mL and 0.50 mL aliquots of ethanol were added into the granite, andesite and basalt solutions, respectively. Each solution was then adjusted to pH 6.2 with dilute ammonia. At this stage the volume of each solution was approximately 15 mL. The solutions were then transferred to a 25 mL plastic volumetric flask and made up to the mark with water. The pH of the final solutions was 6.0. After 60 min to allow complete colour formation, the sample solution was filtered through a 0.45 μm filter. 100 μL of each of the solutions was injected onto the HPLC column. The analyte concentrations were determined using standard addition.

ICP-MS

Analyses were performed using a Finnigan Element High Resolution ICP-MS (Bremen, Germany) Nb and Ta were analysed at masses 93 and 181, respectively, and were calibrated using freshly prepared standard solutions. Instrument detection limits for Nb and Ta were approx. 10 ppt and 3 ppt, respectively. Indium was used as an internal standard for both elements. All results were corrected for drift by analysing standard solutions throughout each analytical sequence. Instrument sensitivity was typically 100.000 counts per second per ppb of ^{115}In (i. e. 100 MHz/ppm). Analyses of the real samples were performed on the same solutions, which were used for the HPLC analysis.

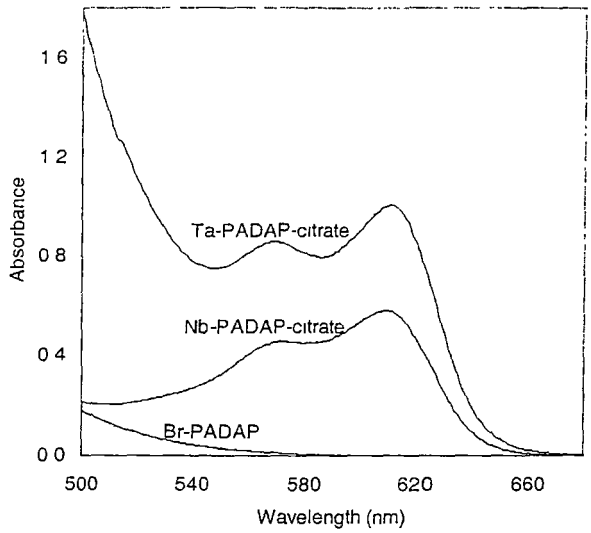

Figure 1

Absorption spectra of Br-PADAP-citrate, Nb-PADAP-citrate (1 ppm) and Ta-PADAP-citrate (4 ppm) at pH 6. Conditions: [Br-PADAP] = 0.2 mM, [citrate] = 10 mM.

Results and Discussion

Formation of the Ternary Complexes and their Absorption Spectra

Br-PADAP is well known to form coloured complexes with many metal ions, including Nb(V) and Ta(V) [12]. In this work, blue ternary complexes of Nb(V) and Ta(V) were formed with Br-PADAP in a citric acid medium throughout the pH range of 5.2-6.5. Absorption spectra of Nb(V) and Ta(V) complexes measured at various pH values were similar (except that different absorptivities were observed) with both complexes showing strong absorbance at pH 6. The wavelength of maximum absorbance was 610 nm for both Nb(V) and Ta(V) complexes but a detection wavelength of 600 nm was used for HPLC because the detector exhibited less noise at this wavelength. Figure 1 shows a comparison of spectra of the Nb(V) and Ta(V) complexes at the optimal pH of 6; the corresponding molar absorptivities (in 4 % ethanol at final solution) were 5.8×10^4 L mol^{-1} cm^{-1} and 4.1×10^4 L mol^{-1} cm^{-1} for Nb(V) and Ta (V) complexes, respectively.

Optimisation of the Complex Formation

The optimum conditions for pre-column complex formation of Nb(V) and Ta(V) with Br-PADAP and citric acid were investigated in order to obtain the highest sensitivity and reproducibility. The addition of ethanol to the standard and sample solutions was found to be necessary to keep the Br-PADAP reagent in solution for a sufficiently long period to enable full colour development to occur. The optimum concentration of ethanol was between 16 and 20 % v/v. Less than 16 % v/v of ethanol resulted in precipitation of Br-PADAP within 30 min, whereas greater than 20 % v/v of ethanol re-

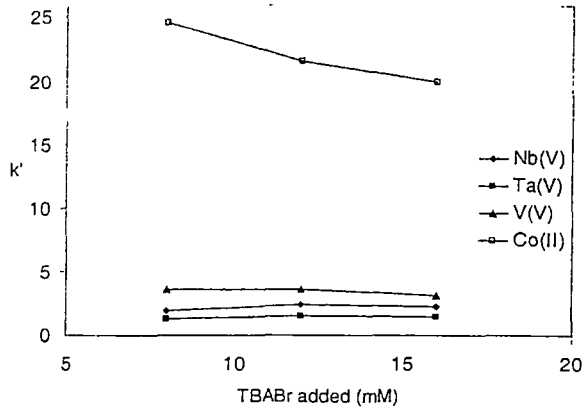

Figure 2

Effect of TBABr concentration on k' of Nb-PADAP-citrate, Ta-PADAP-citrate, V-PADAP and Co-PADAP Mobile phase was methanol-water 50 % v/v containing 12 mM citrate buffer and various concentration of TBABr at pH 7; separator column 150 × 3 9 mm I.D., 4 μm, NovaPak, C 18; flow rate 1 mL min^{-1}; temperature 30 °C, detection by absorbance at 600 nm

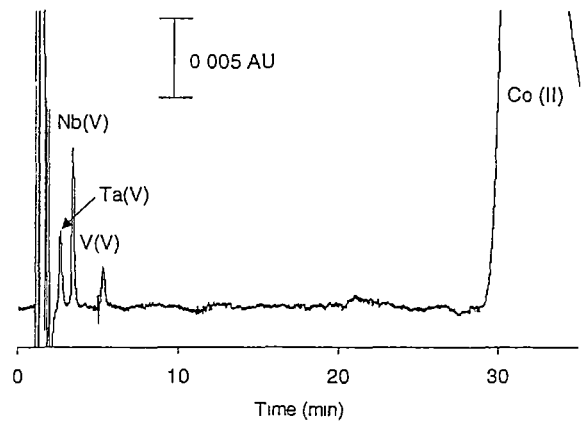

Figure 3

Chromatogram of Nb-PADAP-citrate (2 ppb), Ta-PADAP-citrate (10 ppb), V(V)-PADAP (40 ppb), Co(II)-PADAP (160 ppb). Mobile phase was methanol-water 50 % v/v containing 12 mM TBABr and 12 mM citrate buffer at pH 7; separator column 150 × 3.9 mm I.D., 4 μm, NovaPak, C 18, flow rate 1 mL min^{-1}; temperature 30 °C, injection volume 100 μL, detection by absorbance at 600 nm.

duced the absorptivity of the complex and caused the Nb(V) and Ta(V) peaks to overlap in the final separation.

Absorption spectra studies indicated that both Ta(V) and Nb(V) complexes exhibited strong absorptivities at pH 6, so this pH was chosen for preparation of both the standard and sample solutions. The optimum concentration of Br-PADAP was investigated over the range of 0.025-0.20 mM for a standard mixture of Nb(V) (20 ppb) and Ta(V) (80 ppb) in 10 mM citric acid. The highest absorptivities for both Nb (V) and Ta(V) were obtained with a final concentration of Br-PADAP of 0. 15 mM. Since other metal ions present in the rock samples were capable of forming complexes with Br-PADAP, the optimum concentration of Br-PADAP was determined for each of the different types of rock samples. Comparison of both peak height and peak area of Nb(V) and Ta(V) complexes at different concentrations of BrPADAP showed that 0 40 mM, 0.50 mM and 0.70 mM Br-PADAP gave the best performance for granite, andesite and basalt samples, respectively. The optimum concentration of citrate was also investigated over the range of 6–18 mM. 10 mM citrate offered the best results for Nb(V) and Ta(V) complexes in both standard and rock sample solutions. However, 60 min was required for full colour development, and both complexes were stable for approximately 45 min. Therefore, metal-PADAP-citrate complexes were prepared externally prior to injection onto the C 18 column.

Separation Parameters

The Nb(V) and Ta(V) complexes were eluted from the C 18 column at the void volume when a mobile phase containing only a citrate buffer in a methanol-water mixture was used. The lack of appreciable hydrophobic interaction of the analytes suggested that the ternary complexes were quite polar or carried a charge. For charged species, retention on C 18 stationary phases can be increased by addition of amphiphilic ions of opposite charge to the mobile phase. The addition of cationic tetrabutylammonium ion (TBA^+) into the mobile phase caused an increase in retention time of both complexes, which indicated that the complexes were anionic.

A very strong effect of methanol in the mobile phase on retention of both complexes was observed over the range 46–52 % v/v methanol. Resolution of the complexes was best at less than 50 % v/v methanol. Increasing the concentration of methanol above 50 % resulted in unacceptable resolution of the complexes. However, peak height increased markedly at higher methanol concentrations. After consideration of these two factors, the optimum concentration of methanol was selected as 50 %.

Other components of the mobile phase were optimised as follows. First, the citrate concentration in the mobile phase also exerted a strong effect on retention of Nb(V) and Ta(V) complexes over the range 6–18 mM. The retention times of both complexes decreased at higher citrate concentration, resulting in poor resolution of the peaks. However, the peak area and peak height of the Ta(V) complex increased strongly at higher citrate concentration, whilst the peak area and height of Nb(V) was unaffected. Therefore, the optimum citrate concentration was selected at 12 mM. Second, the eluent pH had a significant effect on peak area of the Ta(V) complex over the range 6–7.5, whilst the effect was smaller for the Nb(V) complex. Increasing the pH from 6 to 7 increased the peak area for both complexes. Beyond pH 7 the peak areas of both complexes decreased. Therefore, the optimum for both Nb(V) and Ta(V) complexes was pH 7. Finally, the concentration of tetrabutylammonium ions in the mobile phase exerted a minor influence on the retention of Nb(V) and Ta(V), as well as on the

retention of other selected matrix metal ions (Figure 2). The TBA^+ concentration over the range 8–16 mM was investigated. 12 mM TBA^+ provided a good separation of both analytes and the matrix metal ions. The separation of a standard mixture of several metal ions is illustrated in Figure 3 and shows a separation of Ta(V) and Nb(V) in 4 min and elution of all the matrix metal ions within about 45 min.

Analytical Performance Parameters

The effect of potential interference metal ions was investigated. No interference was observed for Cd^{2+}, Zn^{2+}, Ni^{2+}, Cr^{3+}, Mn^{2-}, Cu^{2+}, Fe^{3+} and Ti^{4+}. Further, all reagents added during the sample preparation and complex formation were investigated as blank solutions and the subsequent chromatograms showed no baseline disturbances over the entire retention time range after 2.2 min.

The detection limits (determined at signal to noise ratio = 3) were 0.03 ppb and 0.41 ppb for Nb(V) and Ta(V), respectively, in the injected sample solution. Since each of the geological samples was diluted by a factor of 1000 the above values corresponded to detection limits in the geological samples of 0.03 ppm and 0.41 ppm for Nb(V) and Ta(V), respectively. A separation of Nb(V) and Ta(V) at levels close to the detection limits is shown in Figure 4. Five replicate injections of standard solution (20 ppb Nb(V) and 80 ppb Ta(V) were carried out and the resulting %RSD (relative standard deviation) for retention time, peak area and peak height of Nb(V) were 0.007, 0.67 and 0.44 respectively and for Ta(V) were 0.000, 2.69 and 2.17 respectively. External standard calibration curves exhibited good linearity ($r^2 = 0.994$ and $r^2 = 0.999$ for Nb(V) and Ta(V), respectively) and the standard addition calibration curves also showed good linearity ($r^2 = 0.993$ to $r^2 = 0.999$ for both Nb(V) and Ta(V).

Determination of Nb(V) and Ta(V) in Rock Samples

Stabilisation of the sample solution after dissolution was necessary to prevent loss of Nb(V) and Ta(V). This was achieved by dilution of the digest in a mixture of 10% HNO_3 and 5% HCl. The samples were then analysed by HPLC without delay to prevent errors arising from possible hydrolysis and precipitation of Nb(V) and Ta(V). In order to discriminate between errors associated with insufficient stabilisation of Nb(V) and Ta(V) and errors arising from the HPLC procedure, all rock solutions were analysed simultaneously by both HPLC and ICP-MS.

A range of representative reference rock samples (GSR-1, ACE, AGV-1, BHVO-1 and TASBAS) and a basaltic rock of unknown composition (G1485) were chosen for analysis. (see Table I). HPLC analysis of all the representative rock samples showed that simultaneous determination of Nb(V) and Ta(V) was possible for the granite samples, but the andesite and basalt samples exhibited an interfering peak at the retention time of Ta(V). Chromatograms obtained without and with a standard addition of Nb(V) and Ta(V) are given in Figure 5 for GSR-1 (granite) and show that clear peaks were observed for Nb(V) and Ta(V) in GSR-1. On the

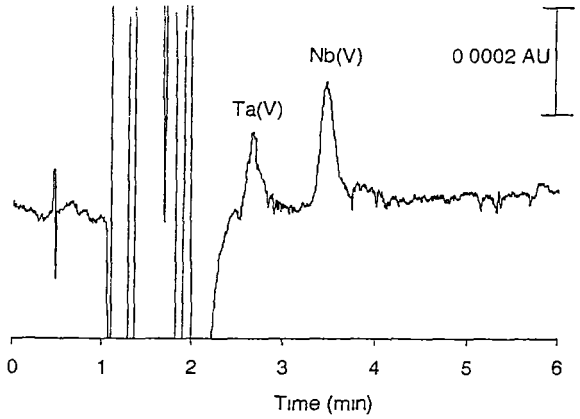

Figure 4
Chromatogram of Nb-PADAP-citrate (0.25 ppb) and Ta-PADAP-citrate (2 ppb) containing [PADAP] = 0.15 mM, [citrate] = 10 mM Chromatographic conditions as for Figure 3

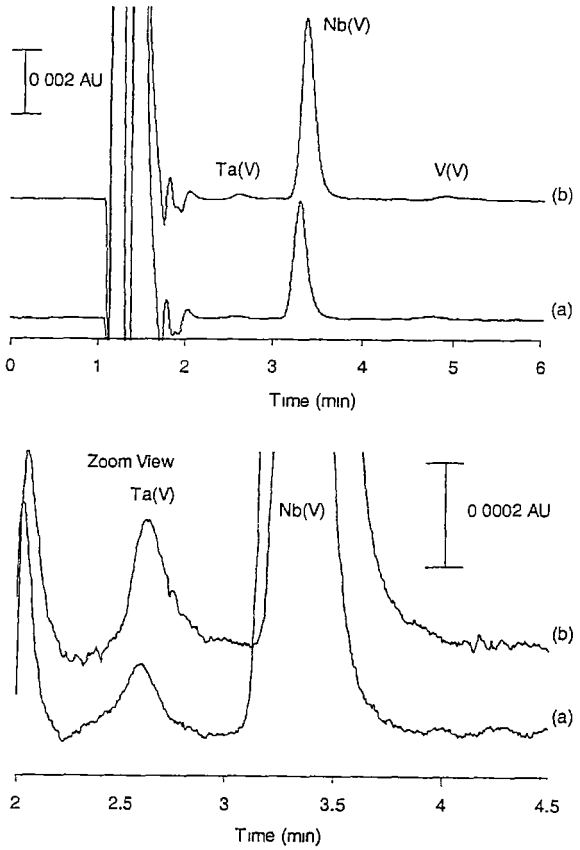

Figure 5
Chromatogram of (a) reference granite rock GSR-1 and (b) reference rock GSR-1 spiked with 10 ppb Nb(V) and 4 ppb Ta(V). Top: complete view. Bottom: zoom view. The samples contained [PADAP] = 0 4 mM; [citrate] = 10 mM Chromatographic conditions as for Figure 3.

Table I. Comparison of the results for Nb and Ta obtained by RP-HPLC, ICP-MS and the certified values. All values are expressed as ppm in the original sample (or ppb in the digested sample).

Rocks	Metal	Certified value [13]	ICP-MS	HPLC (Standard addition)
GSR-1 (granite)	Nb	40	41.2	38.5
	Ta	7.2	7.6	8.1
ACE (granite)	Nb	110	113	97.7
	Ta	6.4	7	7.3
BHVO-1 (basalt)	Nb	19	18.9	16.5
AGV-1 (andesite)	Nb	15	14.3	15.7
G1485 (unknown)	Nb	157 (XRF)*	168	158.4
TASBAS (basalt)	Nb	55 (XRF)* 62 (ICP-MS)**	57.5	62.9

* Value provided by P. Robinson, School of Earth Sciences, University of Tasmania

* Value provided by S. M. Eggins, Research School of Earth Sciences, Australian National University

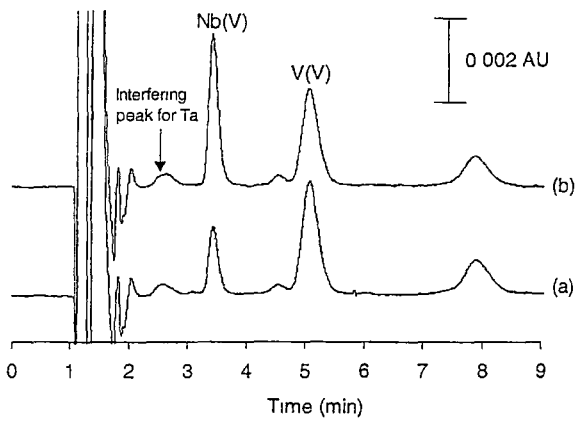

Figure 6

Chromatogram of (a) reference andesite rock AGV-1 and (b) reference rock AGV-1 spiked with 6 ppb Nb(V) and 2 ppb Ta(V). The samples contained [PADAP] = 0.5 mM; [citrate] = 10 mM. Chromatographic conditions as for Figure 3.

other hand, Figure 6 shows that for AGV (andesite) a clear peak was observed for Nb(V) but a large interfering peak was observed at the retention time of Ta(V), rendering quantitation of Ta (V) impossible. The cobalt peak was not detected in any of the rock samples.

Both external standard and standard addition methods were used to quantify the amount of Nb(V) and Ta(V) in rock samples. Only the standard addition method was found to provide satisfactory agreement with both the certified values and the ICP-MS results, with the external standard method generally returning low results. A possible reason was reproducible adsorption of the Nb(V) and Ta(V) complexes on solid residues from the sample treatment, leading to a lower response for each of the analytes. Nevertheless, the standard addition method overcame this limitation and Table I showed the values obtained using this method.

Conclusions

Retention and separation of anionic metal-PADAP-citrate ternary complexes of Nb(V) and Ta(V) has been achieved on a C 18 column using tetrabutylammonium as an ion-interaction reagent in the mobile phase. The separation selectivity was governed mainly by the concentrations of methanol and citrate in the mobile phase. The detection sensitivity depended on the conditions used for the pre-column complex formation, such as pH, concentration of Br-PADAP and citrate and reaction time, and was also affected by the concentration of methanol and citrate in mobile phase, and the mobile phase pH. Based on a comparison with ICP-MS and certified values in reference rock materials, accurate results were obtained for the determination of both Nb(V) and Ta(V) in granite and the determination of Nb(V) in basalt and andesite, using standard addition calibration methods. Determination of Ta(V) in basalt and andesite rock samples requires the use of more selective metallochromic ligand than PADAP.

Acknowledgements

The authors thank Dr. Brett Paull and Dr. Miroslav Macka for valuable suggestions and discussions, Dr Ashley Townsend, for the ICP-MS determinations, and Mr. Philip Robinson and Dr. Tony Crawford for supply of all rock samples. Financial support from the Dionex Corporation is gratefully acknowledged.

References

[1] *T H. Green,* Chemical Geology **120,** 347 (1995).
[2] *P RoyChowdhury, N. K Roy, A K. Das,* At Spectrosc. **16,** 104 (1995)
[3] *K. Satyanarayana, M. A Nayeem,* At Spectrosc. **14,** 180 (1993).
[4] *G. E. M. Hall, J. C. Pelchat and J Loop, J* Anal At Spectrom. **5,** 339 (1990).
[5] *G. A Jenner, H. P Longerich, S E Jackson, B. J. Fryer,* Chemical Geology **83,** 133 (1990).
[6] *F. Poitrasson, C. Pin, P Telouk, J. L Imbert,* Geostandard Newsletter **17,** 209 (1993).
[7] *J. G Sen Gupta, N B Bertrand,* Talanta **42,** 1947 (1995).
[8] *S M Eggins, J. D. Woodhead, L. P. J. Kinsley, G. E. Mortimer, P. Sylvester, M T. McCulloch, J M. Hergt, M R. Handler,* Chemical Geology **134,** 311 (1997)
[9] *S. J. Tsai, Y S. Lee,* Analyst **116** 615 (1991)
[10] *S. Oszwaldowski,* Analyst **120** 1751 (1995).
[11] N. Vachirapatama, M. Macka, B. Paull, C Munker, P. R. Haddad, J. Chromatogr. A in press.
[12] *K. Ueno, T Imamura, K L. Cheng,* Handbook of Organic Analytical Reagents, 2 nd. ed., CRC Press, Boca Raton, 1992, p. 238.
[13] *K. Govindaraju,* Geostandards Newsletter, **18** 1 (1994).

Received: Jun 15, 1999
Accepted. Jul 14, 1999

PRECISE MEASUREMENT OF LEAD ISOTOPE RATIOS IN SULFIDES BY QUADRUPOLE ICPMS

Z. Yu, M. Norman and P. McGoldrick

Centre for Ore Deposit Research (CODES), University of Tasmania, GPO Box 252-79, Hobart Tasmania 7001, Australia

A Hewlett-Packard 4500 quadrupole ICP-MS has been used to measure lead isotope ratios in galena or galena-bearing samples, mainly from localities in Tasmania. A concentric nebuliser with or without peristaltic pump was used to obtain an average precision (RSD) for $^{208}Pb/^{204}Pb$, $^{207}Pb/^{204}Pb$, $^{206}Pb/^{204}Pb$, $^{208}Pb/^{206}Pb$ and $^{207}Pb/^{206}Pb$ of approximately 0.12%, which is comparable to results produced previously using a field sector ICPMS (Townsend *et al.* 1997) We demonstrate good agreement between the lead isotope ratio results measured by quadrupole ICPMS and conventional thermal ionisation mass spectrometry (TIMS) based on a calibration to standard materials run with the unknowns. While not as precise as TIMS data, Pb isotope ratios determined by quadrupole ICPMS provide a useful and cost effective tool for geochemical exploration for sulfide ore deposits.

Introduction

The study of lead isotopic compositions in rocks and minerals is a well established tool for geochronology and for tracing the sources of magmas and sulfide ore deposits. Lead isotopes can provide information related to both age and genesis of sulfide deposits, and their application to understanding the tectonic evolution and relations to metallogeny has the potential to enhance our understanding of the origin of ore formation and the ability of exploration geologists to find new deposits. High precision measurement of Pb isotope ratios for research is accomplished using thermal ionisation mass spectrometry (TIMS), but the relatively high cost of instrumentation and laboratory infrastructure has limited the widespread application of Pb isotopes as a routine tool for geological exploration.

Quadrupole mass spectrometers using a plasma ionisation source (ICPMS) offer potential advantages for the determination of Pb isotope ratios, including rapid analysis times at relatively modest cost. The capability of quadrupole ICPMS instrumentation to measure lead isotopic ratios for direct application to geological problems was demonstrated initially by Smith *et al.* (1984), followed by Date and Cheung (1987) and Longerich *et al.* (1992). In general, older generations of quadrupole ICP-mass spectrometers were designed specifically for the rapid scanning of relatively large mass ranges and sensitivities were relatively low. Therefore, the measurement of lead isotope ratios with ^{204}Pb as the basis was limited by counting statistics, resulting in relatively poor precision and less accurate results. We have developed a reliable method to accurately determine lead isotope ratios using the new generation of ICPMS instrumentation, and we have applied this technique to measure $^{208}Pb/^{204}Pb$, $^{207}Pb/^{204}Pb$, $^{206}Pb/^{204}Pb$, $^{208}Pb/^{206}Pb$ and $^{207}Pb/^{206}Pb$ ratios in geological samples.

Experimental

The analyses were conducted using a Hewlett-Packard 4500 Plus quadrupole ICPMS equipped with a concentric nebuliser and a Peltier-cooled, glass Scott double pass spray chamber. Prior to performing the Pb isotope ratio measurement, the ICPMS was tuned for sensitivity, oxide production, doubly charged ion production, background intensity, and resolution with a 'tune solution' containing 10 ng g^{-1} of ^{7}Li, ^{89}Y, ^{140}Ce and ^{205}Tl. In order to obtain accurate Pb isotope ratios, the sensitivity for 10 ng g^{-1} ^{205}Tl 'tune solution' was adjusted to be greater than 2 x 10^5 counts per second (cps). For the Pb isotope ratio measurements, intensities on masses 204, 206, 207, and 208 were measured using 10 msec dwell times per mass and 1000 sweeps of the mass range in isotope ratio data collection mode

Detector dead time corrections was applied by measuring lead isotope ratios with 50, 100 and 200 ng g^{-1} Pb (QCD Analysts, USA), over a dead time range of 0 to 35 ns. In order to measure precisely the instrument dead time, as a common practice, Figure 1 show the relationship between $^{208}Pb/^{204}Pb$ ratio

and instrument dead time measured using 50, 100 and 200 ng g^{-1} Pb. It can be seen that for this example, the $^{208}Pb/^{204}Pb$ ratio was almost identical for 50, 100 and 200 ng g^{-1} lead solutions at the dead time of 22.5 ns, and the same ratios for $^{207}Pb/^{204}Pb$ and $^{206}Pb/^{204}Pb$ were also found. Therefore, the dead time was set at 22.5 ns to minimise the affects of lead concentration and isotope abundances upon lead isotope ratios. Dead time factors are determined prior to each session of Pb isotope ratio measurements as the instrument dead time varies depending on the detector settings.

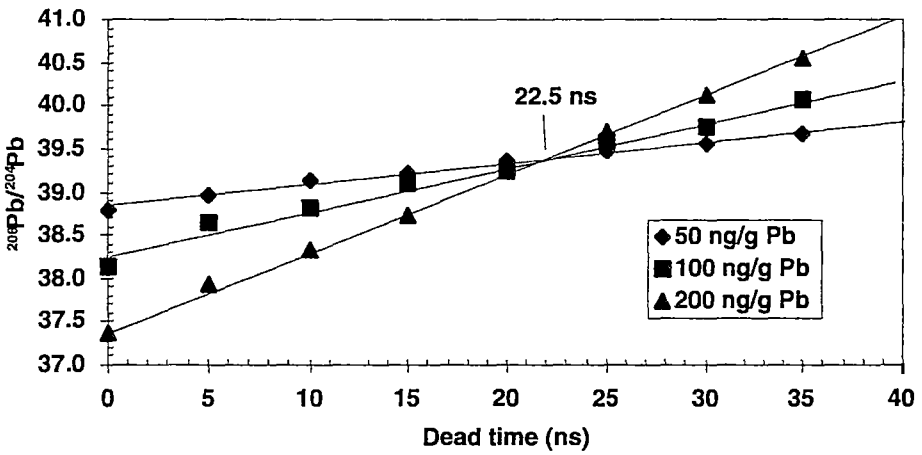

Figure 1 Relationship between $^{208}Pb/^{204}Pb$ ratio and instrument dead time using 50, 100 and 200 ng g^{-1} lead solutions

To prepare calibration standards, 0.01 - 0.05 g of the lead isotope standards SRM 981 and SRM 982 were dissolved by 25 ml 25% (v/v) HNO_3 (Potts, 1987) in a Savillex screw-top Teflon beaker on a hotplate for one hour at 130°C. After cooling to room temperature, 1 ml ultra-pure HNO_3 was added and the solution was diluted to 100 ml with ultra-pure water. The solution was further diluted to a working concentration of 100 ppb before ICPMS analysis.

Samples of galena-bearing sulfide ore were dissolved in Savillex screw-top Teflon beakers using HF-HNO_3-HCl (2:1:3) mixture on a hot plate at 130°C overnight, followed by evaporating to dryness twice with the addition of 1 ml HNO_3 between the evaporations. The concentration of the final solution was 0.01 g in 100 ml in 2% HNO_3.

Results

Table 1 shows the lead isotope ratio results for ten consecutive measurements of a 100 ng g^{-1} NIST SRM 981 solution. No significant difference in precision between samples introduced using a peristaltic pump and free aspiration was observed for these measurements. The average Pb isotope ratio precisions obtained using peristaltic pump were 0.113 and 0.120% on two separate days, while those measured under free aspiration were 0.133 and 0.114% respectively. In general, the external precisions shown in Table 1 are also found to be similar to those previously obtained using a Finnigan Element high resolution ICP-MS (Townsend *et al.* 1998).

The accuracy of the method is demonstrated by the good agreement obtained by the quadrupole ICP-MS, high-resolution ICPMS and TIMS techniques on ore samples. The relative deviations in the Pb isotope ratios between quadrupole ICPMS and TIMS measurements were comparable to those obtained using the Element HR-ICPMS (Townsend *et al.* 1998) and was generally better than ±0.2%, irrespective of the isotope ratios considered. Apart from NIST SRM 982 (an equal-atom lead standard), the absolute deviations of $^{208}Pb/^{204}Pb$, $^{207}Pb/^{204}Pb$, $^{206}Pb/^{204}Pb$, $^{208}Pb/^{206}Pb$ and $^{207}Pb/^{206}Pb$ ratios for 11 selected geological samples between the quadrupole ICP-MS and TIMS methods were in the range of 0.003 - 0.08, 0 001 - 0.043, 0.004 - 0.055, 0.005 - 0 0058 and 0 002 - 0.0023 (in ratio units) respective-

ly. In terms of applications to ore deposit application, these results allow us to clearly separate the Cambrian volcanogenic massive sulfide (VMS) and post-Cambrian (Post C) mineralisation in western Tasmania (Gulson 1986).

Figure 2 shows the correlation of $^{208}Pb/^{204}Pb$ ratios measured by quadrupole ICPMS and data obtained by conventional TIMS techniques for the ore samples measured for this study. These results are typical of those we have obtained in our ongoing studies of lead isotope ratios in ore materials, lending confidence that lead isotope ratios in geological samples can be measured to sufficient accuracy and precision by quadrupole ICPMS that these data can be applied as a useful tool for assessing the age and origin of certain types of ore deposits.

	$^{208}Pb/^{204}Pb$	$^{207}Pb/^{204}Pb$	$^{206}Pb/^{204}Pb$	$^{208}Pb/^{206}Pb$	$^{207}Pb/^{206}Pb$	Average
With peristaltic pump						
Day 1						
Ratio (n=10)	34.74	15.24	16.64	2.0868	0.9155	
STDEV	0.0416	0.0236	0.0233	0.0020	0.0005	
%RSD	0.120	0.155	0.140	0.095	0.057	0.113
Day 2						
Ratio (n=10)	35.81	15.37	16.42	2.1800	0.9360	
STDEV	0.0534	0.0178	0.0160	0.0025	0.0011	
%RSD	0.149	0.116	0.097	0.116	0.121	0.120
Free aspiration						
Day 1						
Ratio (n=10)	35.82	15.36	16.46	2.1761	0.9331	
STDEV	0.0514	0.0235	0.0237	0.0018	0.0013	
%RSD	0.143	0.153	0.144	0.082	0.141	0.133
Day 2						
Ratio (n=10)	35.86	15.37	16.40	2.1871	0.9374	
STDEV	0.0521	0.0145	0.0138	0.0033	0.0009	
%RSD	0.145	0.094	0.084	0.153	0.092	0.114

Table 1. Lead isotope precision (%RSD) with concentric nebuliser using 100 ng g^{-1} NIST SRM 981 solution over two consecutive days.

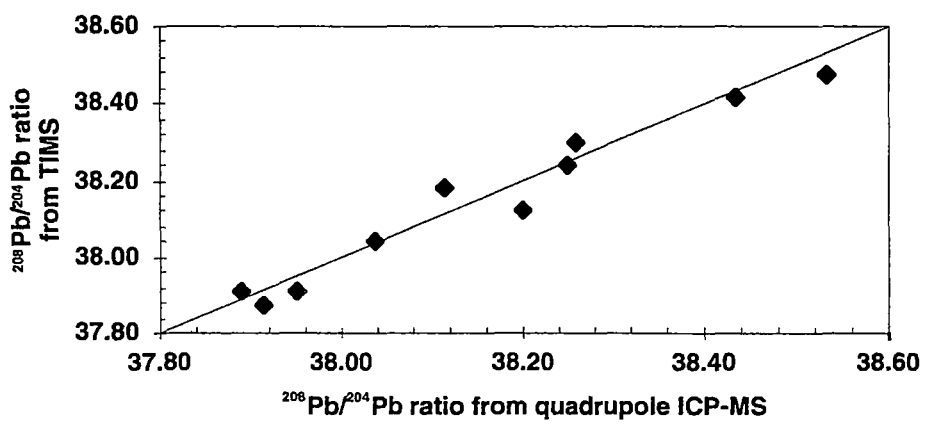

Figure 2 Correlation of $^{208}Pb/^{204}Pb$ ratios between the quadrupole-ICP-MS and conventional TIMS techniques. Samples used for the figure are Z-5199, 5221, 5232, 5237 and 5277 galenas from Zeehan mineral field vein deposits (located in Oceana, Argent#2, Swansea, Montana, and North Tasmania Mine ore deposits in Tasmania respectively), EB-1007, 72086, 72087, and 72096 massive sulfides (sphalerite galena) from Elliott Bay deposit in Tasmania, and H-15 pyrite sphalerite galena from Hellyer deposit in Tasmania.

Conclusion

We conclude that the new generation ICPMS instrumentation can measure Pb isotope ratios in sulfide minerals with an accuracy and precision sufficient to warrant routine application of the method to studies of ore genesis and geochemical exploration for sulfide deposits. The method offers cost and productivity advantages compared to other techniques, and further opens the possibility of the employment of lead isotopes as a routine tool for mineral exploration and investigation of the origin of certain types of sulfide mineralisation.

Gulson, B L, 1986 Lead Isotopes in Mineral Exploration Elsevier Science Publishers B V, The Netherlands, 245 pp

Longerich, H P, Wilton, D H C. and Fryer, B J, 1992 Isotopic and elemental analysis of uraninite concentrates using inductively coupled plasma mass spectrometry Journal of Geochemical Exploration, 43· 111-125

Potts, P J, 1987. A Handbook of Silicate Rock Analysis Blackie and Son Limited, London, 622 pp.

Townsend, A T, Yu, Z, McGoldrick P and Hutton, J. A. 1998 Precise lead isotope ratios in Australian galena samples by high resolution inductively coupled plasma mass spectrometry Journal of Analytical Atomic Spectrometry, 13 809-813.

Vol. 24 – N°1 06 00 p. 39-50

GEOSTANDARDS NEWSLETTER
The Journal of Geostandards and Geoanalysis

Determination of High Field Strength Elements, Rb, Sr, Mo, Sb, Cs, Tl and Bi at ng g^{-1} Levels in Geological Reference Materials by Magnetic Sector ICP-MS after HF/$HClO_4$ High Pressure Digestion

Zongshou **Yu** (1), Philip **Robinson** (2), Ashley T. **Townsend** (3), Carsten **Münker** (1, 2)* and Anthony J. **Crawford** (1)

(1) Centre for Ore Deposit Research, (2) School of Earth Sciences and (3) Central Science Laboratory, University of Tasmania, GPO Box 252-79, Hobart, 7001, Australia e-mail: Phil.Robinson@utas.edu.au
*Present address Zentrallabor fur Geochronologie, Institut fur Mineralogie, Corrensstrasse 24, 48149 Munster, Germany

Six low abundance rock reference materials (basalt BIR-1, dunite DTS-1, dolerite DNC-1, peridotite PCC-1, serpentine UB-N and basalt TAFAHI) have been analysed for high field strength elements (Zr, Nb, Hf, Ta, Th and U), Rb, Sr, Mo, Sb, Cs, Tl and Bi at ng g^{-1} levels (in rock) by magnetic sector inductively coupled plasma-mass spectrometry after HF/$HClO_4$ high pressure decomposition. The adopted method uses only indium as an internal standard. Detection limits were found to be in the range of 0.08 to 16.2 pg ml^{-1} in solution (equivalent to 0.08 to 16.2 ng g^{-1} in rock). Our data for high field strength elements, Rb, Sr, Mo, Sb, Cs, Tl and Bi for the six selected low abundance geological reference materials show general agreement with previously published data. Our Ta values in DTS-1 and PCC-1 (1.3 and 0.5 ng g^{-1}) are lower than in previously published studies, providing smooth primitive mantle distribution patterns. Lower values were also found for Tl in BIR-1, DTS-1 and PCC-1 (2, < 0.4 and 0.8 ng g^{-1}). Compared with quadrupole ICP-MS studies, the proposed magnetic sector ICP-MS method can generally provide better detection limits, so that the measurement of high field strength elements, Rb, Sr, Mo, Sb, Cs, Tl and Bi at ng g^{-1} levels can be achieved without pre-concentration, ion exchange separation or other specialised techniques.

Keywords: magnetic sector ICP-MS, geological reference materials, ng g^{-1} levels, high pressure digestion, memory effects, internal standards.

Les concentrations de six matériaux géologiques de référence à faibles teneurs en certains éléments en traces (basalte BIR-1, dunite DTS-1, dolérite DNC-1, péridotite PCC-1, serpentine UB-N et basalte TAFAHI) ont été mesurées pour les éléments à haut champ de force (Zr, Nb, Hf, Ta, Th et U) et pour Rb, Sr, Mo, Sb, Cs, Tl et Bi par ICP-MS à secteur magnétique après une décomposition sous pression avec HF/$HClO_4$. La méthode adoptée n'utilise que l'indium comme standard interne. Les limites de détection trouvées sont de l'ordre de 0.08 à 16.2 pg ml^{-1} dans les solutions (soit 0.08 à 16.2 ng g^{-1} dans la roche). Nos données pour les élements à haut champ de force et pour Rb, Sr, Mo, Sb, Cs, Tl et Bi dans les six roches selectionnées sont en bon accord avec les données déjà publiées. Nos valeurs de Ta dans DTS-1 et PCC-1 (1.3 et 0.5 ng g^{-1}) sont plus basses que celles précédemment publiées, donnant des spectres de concentrations du manteau primitif lissés. Des valeurs plus basses ont été trouvées aussi pour Tl dans BIR-1, DTS-1 et PCC-1 (2, < 0.4 et 0.8 ng g^{-1}). La méthode proposée, avec ICP-MS à secteur magnétique, fournit généralement des limites de détection meilleures que celles obtenues avec un ICP-MS à quadrupôle, ce qui permet de doser les éléments à haut champ de force ainsi que Rb, Sr, Mo, Sb, Cs, Tl et Bi, sans le recours à une pré-concentration, une séparation sur résine échangeuse d'ions ou à toute autre technique spécialisée.

Mots-clés . ICP-MS à secteur magnétique, matériel géologique de référence, ng g^{-1}, attaque sous pression, effets de mémoire, standard interne.

Received 09 Jun 99 — Accepted 28 Sep 99

GEOSTANDARDS NEWSLETTER
The Journal of Geostandards and Geoanalysis

Inductively coupled plasma-mass spectrometry (ICP-MS) has rapidly become a powerful tool for the analysis of trace elements in geological samples since its arrival in the mid-1970's (Gray 1975). To date, quadrupole ICP-MS has been widely used to determine trace and rare earth elements (REE) in various geological materials (e.g. Jarvis 1988, Jenner *et al.* 1990, Garbe-Schonberg 1993, Xie *et al.* 1994, Eggins *et al.* 1997), and has been found to provide reliable analytical results at relatively low concentration levels. However many lithophile trace elements occur at very low levels (~ ng g^{-1}) in some rocks, particularly ultramafic rocks, and the limited instrumental sensitivity associated with quadrupole ICP-MS means that their quantitative measurement often becomes problematical and complicated. For instance, Makishima and Nakamura (1997) used flow injection ICP-MS to measure Rb, Sr, Y, Cs, Ba, REE, Pb, Th and U at ng g^{-1} levels in silicate samples.

The determination of high field strength elements (HFSE) in solution is particularly difficult. High field strength elements are often contained in refractory minerals that are resistant to acid attack and have a tendency to polymerise or hydrolyse when taken into solution. Memory effect is one of the most important problems associated with the accurate measurement of HFSE. As reported by McGinnis *et al.* (1997), the HFSE generally exhibit a "sticky" nature in which they may adhere to the surfaces of the sample introduction system, from which they can be remobilized by trace amounts of hydrofluoric acid (HF) present in the rock solution. When analysing low levels, sample dissolution often needs to be carried out in strict "clean-room" laboratory conditions (Ionov *et al.* 1992).

Magnetic sector ICP-MS is a highly sensitive analytical technique, employing a double focusing mass analyser. This relatively new technique has been applied to many fields such as food, semi-conductor, soil and environmental sample analysis (see review by Jakubowski *et al.* 1998). However, little has been reported concerning the measurement of trace elements at low levels in geological materials. Recently in our laboratories, magnetic sector ICP-MS has been used for the analysis of the REE in geological reference materials (Robinson *et al.* 1999), including some low abundance reference materials (BIR-1, DTS-1, PCC-1 etc).

In this study, we have investigated (1) the feasibility of magnetic sector ICP-MS for the measurement of HFSE, Rb, Sr, Mo, Sb, Cs, Tl and Bi at ng g^{-1} levels; (2) techniques to minimise memory effects associated with the HFSE; (3) the possibility of using a single internal standard to measure accurately the concentration of the trace elements of interest. Finally, we have applied the magnetic sector ICP-MS method to the measurement of HFSE, Rb, Sr, Mo, Sb, Cs, Tl and Bi at ng g^{-1} levels in six selected low abundance rock reference materials, in which solutions were analysed immediately following sample decomposition without using clean laboratory conditions or other specialised techniques, such as pre-concentration or ion-exchange separation. Indium (^{115}In) alone was used as an internal standard to compensate for instrumental drift and matrix effects during the measurement of trace elements at low levels.

Experimental

Reagents

Hydrofluoric acid (50% m/m Analar, AR grade), HCl (33% m/m BDH, AR grade) and HNO_3 (70% m/m BDH, AR grade) were all used for sample decomposition in this study. HCl and HNO_3 were further doubly distilled in a sub-boiling quartz distillation system before use. HF was doubly distilled in a sub-boiling Teflon distillation system and ultra-pure perchloric acid ($HClO_4$; 70% m/m ARISTAR®, BDH Chemicals) was also used. Ultra-pure water (≥16.7 MΩ) used in the study was first distilled with a glass distillation system and then further purified with a MODULAB Water Purification System (Continental Water System Corporation, Melbourne, Australia).

External calibration standards (0.25, 0.50, 1.00 ng g^{-1}) were prepared by gravimetric serial dilution from 100 µg ml^{-1} multi-element standards (QCD Analyst, USA). The standard solutions were prepared at the beginning of each run with doubly distilled water, HNO_3 (2% v/v) and HCl (1% v/v).

Indium and lutetium standard solutions (1000 ± 3 µg ml^{-1} in 2% v/v HNO_3, High-Purity Standards (South Carolina, USA)) were diluted to working concentration in 2% v/v HNO_3 before use as internal standards for magnetic sector ICP-MS analysis. An ^{84}Sr isotope solution (83.2% ^{84}Sr, provided by the University of Adelaide) and Bi (high purity standard from Spex Chemical & Sample Preparation, USA) were additionally used as internal standards for comparison purposes.

Sample decomposition

The acid pressure digestion system used in the study was a PicoTrace® TC-805 Pressure Digestion System (Bovenden, Germany) Sixteen to thirty two samples could be digested per run Our sample decomposition procedure was as follows:

Powdered sample (100 mg) was weighed into 30 ml PTFE digestion containers and wetted with a few drops of ultra-pure water. Hydrofluoric acid (3 ml) was slowly added and the sample container was shaken a few times to disaggregate the sample. Then, 3 ml $HClO_4$ was added and the PTFE container was shaken a few times again to mix up the (HF + $HClO_4$ + sample) mixture thoroughly. After sealing, the closed PTFE containers were left in the digestion block at 180 °C for ~ 16 hours. The sample solution was then evaporated to dryness at 180 °C for about 12 hours with the evaporation block on. Acid fumes were removed by a water vacuum pump and adsorbed in a strong alkaline solution. Next, another 1.00 ml aliquot of $HClO_4$ was added and the sample was evaporated to dryness again. Nitric acid (2 ml), HCl (1 ml) and ultra-pure water (10 ml) were added to the PTFE containers and the residue was taken up by warming the solution at about 60 °C in the digestion block for approximately one hour After the solution became clear, it was transferred into a clean 100 ml polycarbonate bottle An indium spike (0 1 ml of 10 µg ml^{-1}) was added and the sample solution was diluted to 100 g with ultra-pure water prior to magnetic sector ICP-MS analysis

All rock samples were digested at least in duplicate and preferably in triplicate in the case of samples such as peridotites that contain very low levels of trace elements. Two procedural (reagent) blanks were prepared as part of each sixteen sample digestion run.

In addition, in order to minimise any possible contamination during sample digestion and ICP-MS analysis, PTFE digestion vessels were washed with laboratory detergent, rinsed and soaked in 20% v/v HCl followed by 10% v/v HNO_3 solutions each at ~ 80 °C for at least 24 hours. The vessels were then rinsed with ultra-pure water before adding 2 ml HF and heating at 180 °C under pressure for ~ 20 hours. This additional cleaning step using HF was found to be particularly necessary to remove traces of HFSE that would otherwise contribute to the memory effect. Finally, the digestion vessels were rinsed with ultra-pure water prior to sample digestion. Plastic containers, pipette tips and test tubes used in the experimental work were soaked in 20% v/v HCl followed by 10% v/v HNO_3 solutions at room temperature for at least 24 hours each, and finally rinsed with ultra-pure water before use

Geological reference materials

Five well-known rock reference materials of low incompatible trace element abundances were used in this study (see Govindaraju 1994) BIR-1 (basalt), DNC-1 (dolerite), DTS-1 (dunite), PCC-1 (peridotite) and UB-N (serpentine) Another rock sample also analysed was a basalt (TAFAHI), with low concentrations of Nb, Mo, Sb, Cs, Hf, Ta, Bi, Th and U, provided by the Research School of Earth Sciences, Australian National University (Eggins *et al* 1997).

Instrumentation

A magnetic sector ICP-mass spectrometer (Finnigan MAT "ELEMENT", Bremen, Germany) was used in this study. The instrument was equipped with a compact double-focusing magnetic sector mass spectrometer of reversed Nier-Johnson geometry, with an available mass range of 5 to 260 amu Pre-defined resolution settings of 300, 3000 and 7500 M/ΔM allowed the operating resolution to be adjusted, depending mainly on the analytical matrices and the isotopes of interest. Typical instrumental settings used during this study are summarized in Table 1. Further details regarding this instrument have been reported elsewhere (Moens *et al.* 1994, Townsend *et al* 1998, Robinson *et al.* 1999).

In this study, HFSE, Rb, Sr, Mo, Sb, Cs Tl and Bi were determined in low resolution mode Take-up and wash times used in this study were 240 and 200 seconds (with a take-up rate of ~ 0 75 ml min^{-1}) in order to minimise the memory effects of the "sticky" HFSE The rinse solution used in this study was 5% v/v HNO_3 and 0.05% v/v HF. In addition, clean sampler and skimmer cones, ICP torch, spray chamber, nebuliser and sample introduction tubes (including the auto-sampler tubing) were found to be essential for the analysis of elements at very low levels. Ideally a special set of these items dedicated to low level work would be very advantageous. Prior to sample analysis, the instrument was purged for at least 24 hours with 5% v/v HNO_3 and 0 05% v/v HF rinse solution.

Table 1.
Typical instrumental settings for the determination of trace elements at ng g^{-1} levels in rocks (pg ml^{-1} in solution)

Instrument	Finnigan MAT ELEMENT
Resolution	300 M/ΔM ("low" resolution)
RF power	~ 1250 W
Nebuliser	Meinhard
Coolant argon flow rate	12-13 l min^{-1}
Auxiliary argon flow rate	0.95-1 l min^{-1}
Nebuliser argon flow rate	0.95-1.2 l min^{-1}
Spray chamber	Scott (double pass) type cooled at 3.5-5 °C
Sample uptake	0 75 ml min^{-1}
Sample cone	Nickel, 1.1 mm aperture i d
Skimmer cone	Nickel, 0.8 mm aperture i d.
Instrument tuning	Performed using a 10 ng ml^{-1} multi-element solution without tantalum
Ion transmission	› 1,200,000 cps per 10 ng ml^{-1} indium
Scan type	Magnetic jump with electric scan over small mass range
Ion sampling depth	Adjusted daily in order to obtain maximum signal intensity
Ion lens settings	Adjusted daily in order to obtain maximum signal intensity and optimum resolution

Sample analysis

Sample solutions were analysed by magnetic sector ICP-MS within 24 hours after dissolution All solutions (including calibration standards, procedural blanks and sample solutions) were prepared in 2% v/v HNO_3 and 1% v/v HCl with ultra-pure water. An instrumental drift monitor solution (of 1 ng ml^{-1}) was analysed after every five to ten sample solutions. Procedural blanks were analysed every two hours to monitor variations in blank levels. A 10 ng ml^{-1} standard solution was also analysed at the end of an analytical sequence to check the concentration of elements present at elevated levels. A typical sequence consisted of standard blank (a blank solution prepared at the same time as the calibration standards), calibration standards (0.25, 0.50 and 1.00 ng ml^{-1}), drift monitor, rinse solution (using the standard blank), five to ten samples, drift monitor, rinse (using the standard blank), . , drift monitor and 10 ng ml^{-1} standard solution. Procedural blanks were measured after rinse solutions to minimise any memory effects. Each sample solution was analysed in either duplicate or triplicate to monitor memory effects of HFSE, particularly Ta. Results for which the measured abundance dropped between repetitions of the same solution could then be discarded since a contribution of memory to the signal was obvious. Instrumental drift was corrected against the concentration variations between successive measurements of the instrumental drift monitors.

Detection limits

Detection limits are influenced by instrumental sensitivity, memory effects, spectral interferences and contamination from analytical reagents. In this study, the detection limits (Table 2) were calculated as the concentration equivalent to three times the standard deviation of the procedural blank solution (3 ml HF and 3 ml $HClO_4$ taken from the digestion process, followed by dilution to 100 g with ultra-pure water in 2% v/v HNO_3 and 1% v/v HCl) intensities on the basis of an average for fifteen data acquisition runs. Detection limits for HFSE, Rb, Sr, Mo, Sb, Cs, Tl and Bi measured by magnetic sector ICP-MS range between 0.08 and 16.2 pg ml^{-1} in solution (equivalent to 0 08 to 16 2 ng g^{-1} in solid samples). Detection limits for Nb, Cs, Hf, Ta, Bi, Th and U were all better than 1 pg ml^{-1}, and for Rb, Sr, Zr, Mo and Sb, were 16.2, 3.9, 1.8, 2.5 and 1.9 pg ml^{-1}, respectively, in solution. In general, the detection limits measured in this work are two to ten times better than those previously obtained using quadrupole ICP-MS instruments under either "clean-room" laboratory conditions, or with flow injection (Ionov *et al* 1992, Makishima and Nakamura 1997). The higher detection limit found for Rb was possibly due to interference of oxychlorine species, such as $^{37}Cl^{16}O_3$ (Longerich 1993). Under the proposed digestion conditions, trace amounts of perchlorate remained in the final solution, as perchloric acid was used to drive off HF in the sample residue.

For comparison, the ultra-pure water detection limits for this instrument are also shown in Table 2. Using ultra-pure water, the detection limits were calculated in a similar way as used for the calculation of the above procedural detection limits. Comparing the pure water detection limits with the procedural detection limits, an improvement can be clearly seen for

Table 2.
Magnetic sector ICP-MS detection limits and comparison with those reported by previous workers

Element	Isotope measured	Pure-water detection limits pg ml^{-1}	Method detection limits pg ml^{-1}	Detection limit* pg ml^{-1}	Detection limits** pg ml^{-1}
Rb	85	1.6	16.2	2	8
Sr	88	1.7	3.9	6	15
Zr	90	0.38	1.8	7	-
Nb	93	0 23	0 95	1	-
Mo	95	0.67	2 5	-	-
Sb	121	0.75	1.9	-	-
Cs	133	0.41	0 49	-	0 7
Hf	178	0.12	0 36	1	-
Ta	181	0.09	0 12	0.2	-
Tl	205	0.37	0 37	-	-
Bi	209	0.14	0.38	-	-
Th	232	0.02	0 17	0.3	5
U	238	0.01	0.08	0.3	1

* Reported by Ionov *et al.* (1992). ** Reported by Makishima and Nakamura (1997). - no value available.

HFSE, Rb, Sr, Mo, Sb, Cs, Tl and Bi, suggesting that the proposed magnetic sector ICP-MS technique is so sensitive that trace elements at levels of < 1 ng g^{-1} in solid samples can be analysed if ultra-pure reagents such as $HClO_4$, HF, HCl and HNO_3 were available

Results and discussion

Memory effects

Memory effects can be induced by (1) contaminated Teflon vessels at the decomposition stage and (2) by the sample introduction system during ICP-MS analysis. These effects can be minimised by thorough cleaning of the Teflon decomposition vessels (using HF) and monitored by measurement of procedural blanks as described under "Sample Decomposition" and "Sample Analysis". However, it should also be noted that the reagents used in sample digestion can markedly affect the end result particularly if there are F^- left in solution.

In order to investigate this, four replicates (100 mg) of the international basaltic rock reference material BIR-1 were digested with HF/HNO_3 in Savillex Teflon beakers. The digestion method was similar to that used by Robinson *et al.* (1999). However, at the evaporation stage, two of the samples were evaporated to dryness twice with the addition of 1 ml $HClO_4$, whereas the other two samples were evaporated to dryness twice with the addition of 1 ml HNO_3. Finally, all of the residues were taken up with 2 ml HNO_3 and 1 ml HCl, and diluted to 100 g. Indium (10 ng ml^{-1}) was spiked into each solution as an internal standard before magnetic sector ICP-MS analysis

For measurement of these samples, a comprehensive wash protocol similar to that reported by McGinnis *et al.* (1997) was used to minimise memory effects associated with HFSE. Before and after the analysis of sample solutions, the sample introduction system was flushed with 10% v/v HNO_3 + 0.05% v/v HF solution for 120 seconds, followed by a 120 seconds flush of 10% v/v HNO_3 only, and a final 120 seconds flush of 5% v/v HNO_3.

Initially, the four BIR-1 solutions were analysed by magnetic sector ICP-MS with an unclean sample introduction system (i.e nebuliser, spray chamber, sampler and skimmer cones were not cleaned and Teflon tubes were not replaced with a new set). Then, we cleaned the sample introduction system by soaking the nebuliser and spray chamber in concentrated HNO_3 overnight, polishing the sampler and skimmer cones with special grinding paste and replacing the Teflon tubes with a new set. The four BIR-1 solutions were analysed again with the clean sample introduction system.

Table 3 shows HFSE memory effects associated with the analysis of BIR-1 It can be seen that, even using this complicated wash protocol, results for the BIR-1 solutions with HNO_3 evaporation showed clear memory effects for Nb, Hf, Ta, Th and U using the unclean sample introduction system, and for Nb and Ta using the clean sample introduction system. No obvious memory effect for Zr was observed due to the high concentration for Zr in BIR-1. Low and consistent Ta results were obtained with $HClO_4$ evaporation and a clean sample introduction system, whereas high and

Table 3.
Example HFSE memory effects associated with the determination of BIR-1 rock reference material

Element	Unclean SIS		Clean SIS	
	$HClO_4$ evaporation n = 2	HNO_3 evaporation n = 2	$HClO_4$ evaporation n = 2	HNO_3 evaporation n = 2
Zr	15.4	15.2	14.9	15.0
Nb	0.40	0.68	0.51	0.66
Hf	0.72	0.82	0.62	0.63
Ta	0.026	0 490	0.021	0 254
Th	0.030	0.045	0.032	0 036
U	0.0094	0 0129	0 0104	0.0104

Analyses reported in $\mu g\ g^{-1}$. SIS sample introduction system n number of measurements.

erratic Ta occurred with HNO_3 evaporation. Tantalum from calibration standards and samples hydrolyses easily and is, therefore, likely to precipitate in the tubing. A subsequent change in the F^- concentration might complex the tantalum oxide again and cause the observed high and erratic values. The different memory effects between $HClO_4$ and HNO_3 evaporations are clearly due to the different boiling points of these acids. That is, $HClO_4$ with a relatively high boiling point of 203 °C can virtually drive off all of the HF (boiling point 112 °C) in solution during the repeat evaporations, whereas the boiling point of HNO_3 (120 °C) is only slightly higher than that of HF, and cannot completely drive off all HF in solution. The trace amounts of F^- left in sample solutions can subsequently remobilize any "sticky" HFSE in the ICP sample introduction system, and cause the observed memory effects (McGinnis *et al* 1997). Although the memory effects of the "sticky" HFSE after HNO_3 evaporation, as shown in Table 3, can be largely minimised for Hf, Th and U using a clean sample introduction system, the memory effects of Nb and Ta cannot be neglected due to the presence of trace amounts of F^- in sample solutions.

In summary, we found that a clean sample introduction system and $HClO_4$ evaporation are essential to achieve low Nb and Ta analyses with our instrument. Digestion involving HF/HNO_3 resulted in trace F^- remaining in solution that leached residual Nb and Ta from the instrument. This residual Nb and Ta could neither be removed by extensive cleaning nor by using the McGinnis *et al.* (1997) wash protocol. It is believed that the latter may be an option on a new instrument when few rock samples have been analysed or if the instrument is dedicated to very low level Nb and Ta samples for long periods (e.g. Ionov *et al.* 1992, Eggins *et al.* 1997). However, the risk of remobilizing residual Nb and Ta in the sample injection system is great. Another option (Jenner *et al* 1990) is to keep Nb and Ta standard solutions out of the ICP-MS entirely and use a surrogate calibration.

A disadvantage, however, of not having a trace of F^- in the final solution is the danger that Nb and Ta will drop out of solution as a result of hydrolysis. A final sample solution of 2% v/v HNO_3 + 1% v/v HCl (Munker 1998) instead of the more commonly used HNO_3 solution, along with analysing all samples in duplicate or triplicate, helps with this problem for rocks with typical Nb-Ta abundances. Organic complexing agents also provide the possibility of keeping the Nb and Ta in solution and work is progressing on this development in our laboratories

Blank subtraction

Blank subtraction is generally not crucial for the analysis of medium and high abundance elements since the blank contribution to these samples is often within the analytical error. However, when low abundance samples are measured, blank subtraction becomes very important since the blank contribution to the measured signal is much higher. Any incorrect blank subtraction will result in a significant error in analytical results.

In order to demonstrate the importance of blank subtraction for the measurement of low abundance samples, the behaviour of two procedural blanks was observed through a 12 hour analytical run. Trace elements in these procedural blanks were measured seven times at approximately 2 hour intervals. The measured concentrations of Sr, Zr, Mo and Bi in the two procedural blanks were found to be relatively stable throughout this lengthy sample sequence, and the blank level variations (1*s* on the basis of seven measurements) were 0.0558 ± 0 0094, 0.0148 ± 0 0029, 0 0229 ± 0 0045 and 0 0088 ± 0.0015 ng ml^{-1}

in solution respectively. In contrast, blank level variations for Rb, Nb, Sb, Cs, Hf, Ta, Tl, Th and U in both of the procedural blanks were clearly observed. The blank level variations (1*s* on the basis of seven measurements) of Rb, Nb, Sb, Cs, Hf, Ta, Tl, Th and U for one of the procedural blanks were found to be 0 0477 ± 0.0195, 0.0075 ± 0.0033, 0.0120 ± 0.0048, 0.0027 ± 0.0014, 0 0022 ± 0.0024, 0 0016 ± 0 0008, 0.0011 ± 0 0004, 0 0018 ± 0 0017 and 0 0004 ± 0.0002 ng ml^{-1} respectively Since these data were obtained, the absolute blank levels for these trace elements have been considerably improved in our laboratories Hence, considering the concentrations of trace elements in some of the selected low abundance rocks such as DTS-1 and PCC-1, special attention needs to be paid to the blank subtraction, particularly for Nb and Ta. In general, it is recommended that blank levels used for trace element analysis should be carefully monitored throughout any low level analytical sequence and blank subtraction should be performed using the procedural blank value measured adjacent to the sample. In case of possible contamination, two procedural blanks prepared per batch of samples are essential.

Despite low procedural blanks and an apparently clean instrument, spuriously high levels of the HFSE can still result from matrix effects caused by the rock solutions themselves. A typical whole rock sample solution often seems to be more effective at leaching the HFSE, particularly Ta, from the instrument. Therefore, it is advisable to check that the instrument is truly clean, by aspirating extremely low level rock solutions prepared from reference materials, such as PCC-1 and DTS-1 or an artificial rock matrix made from Specpure oxides analysed in triplicate before a sample sequence, to see if there is any memory or tailing effects.

Interferences

In this study, final sample solutions were prepared in 2% v/v HNO_3 and 1% v/v HCl to stabilise the HFSE in solution (Munker 1998). Most background species such as ^{35}ClH, $^{35}Cl^{14}N$, $^{35}Cl^{16}O$, $^{35}Cl^{16}O^{16}O$ and $^{26}Ar^{35}Cl$ caused by the presence of hydrochloric acid do not interfere with the high mass trace elements (> 84 amu) (Vandecasteele and Block 1995). Under the proposed digestion conditions, trace amounts of perchlorate remained in the sample solutions, because $HClO_4$ was used to drive off HF from the digestion residue Results for ^{85}Rb were found to be improved by subtracting the $^{37}Cl^{16}O_3^+$ interference (Longerich 1993) as measured for a procedural blank. Possible interferences reported by Jenner *et al.* (1990), Vandecasteele and Block (1995) and Eggins *et al.* (1997) for some HFSE are caused by doubly charged REE and their oxides. For instance, $^{170}Er^{2+}$ and $^{170}Yb^{2+}$ interfere with ^{85}Rb, while $^{176}Lu^{2+}$ and $^{176}Yb^{2+}$ interfere with ^{88}Sr. However, as reported by Vandecasteele and Block (1995), the ratio of M^{2+} to M^+ is generally below 0 01% for the doubly charged ions under investigation, and the concentrations of the REE in the six selected geological reference materials used in this study are very low. Hence, the interference of doubly charged ions was not considered in this study Although the interferences of $^{162}Dy^{16}O$ on ^{178}Hf and $^{165}Ho^{16}O$ on ^{181}Ta have been reported (e.g. Jenner *et al.* 1990, Eggins *et al* 1997), these interferences were not significant here due to the low REE concentrations in the six selected geological samples (Govindaraju 1994, Robinson *et al* 1999), and no corrections were made. The oxide formation rate measured in this study was found to be low due to the specific design features of the magnetic sector ICP-MS instrument. As reported in a separate investigation (Robinson *et al.* 1999) the formation rates of BaO^+/Ba^+ and PrO^+/Pr^+ were about 0 2% and 0.4% respectively, which is generally lower than those produced using early model quadrupole ICP-MS instruments (e.g. Dulski 1994, Eggins *et al.* 1997, Norman *et al.* 1998).

Choice of internal standard

In order to monitor and correct for any fluctuation in instrumental signal and matrix effects, many users of ICP-MS instruments (e.g. Garbe-Schonberg 1993, Hollocher and Ruiz 1995, Eggins *et al.* 1997, Norman *et al.* 1998) have used several internal standards for data correction. Garbe-Schonberg (1993) used ^{9}Be, ^{115}In and ^{187}Re as internal standards to determine thirty seven elements in rock reference materials. NIST glass reference materials SRM 611, 612, 614 and 1834 were analysed using five internal standards (^{9}Be, ^{71}Ga, ^{115}In, ^{187}Re and ^{209}Bi) by Hollocher and Ruiz (1995) In another investigation, Eggins *et al* (1997) used nine internal standards (^{6}Li, ^{84}Sr, ^{103}Rh, ^{115}In, ^{147}Sm, ^{169}Tm, ^{187}Re, ^{209}Bi and ^{235}U) to measure more than forty trace elements in geological samples. In routine ICP-MS analysis, however, it can be troublesome to select and prepare a suitable set of internal standards that do not suffer from severe spectral interferences. In practical work, an element which occurs naturally in the sample, and which has been determined prior to ICP-MS analysis, may be

Table 4.
A comparison of measured concentrations (μg g^{-1}) for TAFAHI between a single and four internal standards

Element	Measured*		Eggins *et al.* 1997
	One internal std n = 10	Four internal stds n = 10	
Rb	1.72 ± 0.05	1.75 ± 0.05	1.75
Zr	11.3 ± 0.27	11.5 ± 0.28	12.07
Nb	0 55 ± 0.02	0.56 ± 0.02	0 46
Mo	0.52 ± 0.02	0 52 ± 0.02	0 44
Sb	0 024 ± 0.001	0 024 ± 0.001	0.024
Cs	0.067 ± 0.003	0.067 ± 0.003	0.066
Hf	0 39 ± 0.02	0.42 ± 0 02	0.40
Ta	0 025 ± 0.003	0.027 ± 0.004	0.022
Tl	0.018 ± 0.004	0 024 ± 0.006	0.0142
Th	0.11 ± 0.006	0.12 ± 0.006	0.12
U	0.074 ± 0.004	0.079 ± 0 004	0.073

n number of analyses. * ± 2 standard deviations.

chosen. In this case, the concentration will probably vary from sample to sample and this must be taken into account during the final data manipulation stage

In this study, we investigated the use of a single internal standard (^{115}In) instead of several internal standards for the measurement of HFSE, Rb, Mo, Sb, Cs and Tl by magnetic sector ICP-MS. The reference sample TAFAHI was digested using the $HF/HClO_4$ high pressure technique and analysed for HFSE, Rb, Mo, Sb, Cs and Tl using either a single (^{115}In) or four (^{84}Sr, ^{115}In, ^{175}Lu and ^{209}Bi) internal standards. The average results of ten independent digestions are summarized in Table 4. In the investigation of the four internal standards, each selected isotope was used to monitor a particular mass range (e g. ^{84}Sr was used to correct ^{85}Rb through to ^{95}Mo, ^{115}In to correct ^{121}Sb to ^{133}Cs, ^{175}Lu to correct ^{178}Hf and ^{181}Ta, and ^{209}Bi to correct ^{205}Tl, ^{232}Th and ^{238}U) A correction was made for Sr already present in the TAFAHI sample (Eggins *et al* 1997). No corrections were necessary for Lu and Bi due to the low concentrations of these elements in this sample (0.153 and 0.003 ng ml^{-1} in solution, respectively).

As seen in Table 4, general agreement was found between the concentration of trace elements measured using a single and four internal standards respectively The average relative variation was found to be not larger than 4% for Rb, Zr, Nb, Mo, Hf, Ta, Th and U (Sb and Cs were measured using ^{115}In as internal standard in both the single and four internal standards procedures). Figure 1 further demonstrates the good correlation of the trace elemental concentrations measured using single and four internal standards. Therefore, it can be concluded that a single internal standard (^{115}In) is sufficient for the accurate measurement of the trace and ultra trace elements in geological materials by magnetic sector ICP-MS. Robinson *et al.* (1999) noted a similar outcome for the REE, Y and Sc in rocks, as did Townsend *et al.* (1998) when measuring Cu, Zn, Cd and Pb in urine specimens by the same instrument. No significant difference was found when they compared the analytical results of Cu, Zn, Cd and Pb obtained using three internal standards (^{45}Sc, ^{115}In and ^{209}Bi) with a single internal standard (^{115}In).

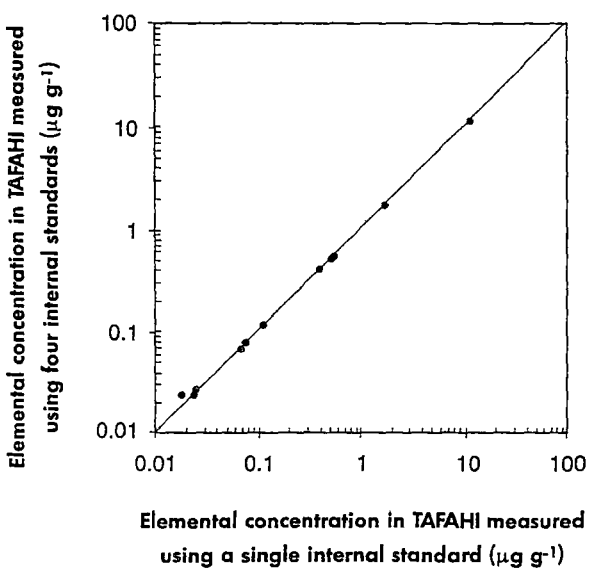

Figure 1. Correlation between single (^{115}In) and four (^{84}Sr, ^{115}In, ^{175}Lu and ^{209}Bi) internal standards for the basaltic rock reference material TAFAHI.

Table 5.
Measured results (μg g^{-1}), precision (% RSD) and reference values (μg g^{-1}) for six geological reference materials

Element	BIR-1						DNC-1				UB-N				
	Measured n = 7	% RSD	(A)	(B)	(C)	(D)	Measured n = 5	% RSD	(C)	(D)	Measured n = 5	% RSD	(E)	(F)	(C)
Rb	0.210	2.5	0.24	0 172	0.25	0.195	3.74	2 0	(4.5)	3 6	3 69	3 0	3 5	3.27	4
Sr	109	3.5	110	112	108	106.4	140	0.8	145	141.4	749	2.8	78	7.09	9
Zr	14.9	2.6	15.4	15 7	15.5	14.47	35.2	1.5	41	36.4	4.24	3 6	3 3	3 6	4
Nb	0 51	6 4	0 50	0 738	0.6	0.558	1.60	2 0	3	1.564	0 068	4.7	0.080	‹ 0 1	0.05
Mo	0.055	16 3	-	-	(0.5)	0.037	0 151	3.5	(0 7)	0.121	0.35	2 7	-	0.4	0.55
Sb	0.47	77	-	-	0 58	0 50	0.92	6.1	0 96	0.870	0.28	177	-	-	0 3
Cs	0.0051	9.6	0 004	0.007	0.005	0.0053	0.21	2.0	(0.34)	0.213	11 2	1 5	-	10.7	10
Hf	0 53	1.9	0.51	0 639	0.6	0.562	0.98	2.1	1.01	0.955	0.148	2.2	0 122	0.15	0.1
Ta	0.031	12.5	0 03	0 213	0.04	0.041	0.091	4.9	0.098	0 089	0.012	27	0.015	-	0 02
Tl	0 002	53 5	-	-	(0 01)	0 004	0.022	8.3	(0.026)	-	0.041	4.7	-	-	0.06
Bi	0 004	33.7	-	-	(0.02)	-	0.0082	10 2	(0 02)	-	0.12	32	-	0 11	0 1
Th	0 0301	1 8	0.031	0.06	0.03	0.0302	0.234	3 1	(0.2)	0.240	0.073	5 7	0.063	0.06	0 07
U	0 0096	6.8	0.0097	0.011	0.01	0.0100	0.052	3.8	(0.1)	0 0549	0.061	3 0	0.060	0 06	0.07

Element	DTS-1						PCC-1						TAFAHI		
	Measured n = 5	% RSD	(E)	(C)	(D)	(G)	Measured n = 9	% RSD	(E)	(C)	(D)	(G)	Measured n = 7	% RSD	(D)
Rb	0.090	13.1	0.095	0.058	0.078	0.084	0.067	13.2	0 068	0 066	0.058	0 083	1 85	3 1	1 75
Sr	0 28	13.3	0.30	0 32	0.31	0.32	0.32	11.6	0.38	0.4	0.33	0.37	140.7	0.7	138 9
Zr	0.17	11.3	0.11	(4)	0.253	-	0.145	5.0	0.13	10	0.191	-	11.7	2 2	12.07
Nb	0 032	6.9	0 042	(2.2)	0.012	-	0 024	12.5	0.042	(1)	0.011	-	0 50	6 2	0 456
Mo	0 054	11.2	-	(0.14)	-	-	0 035	17.7	-	(2)	0 032	-	0.44	4.4	0 44
Sb	0.43	8.6	-	0.5	-	-	1 39	8.7	-	1.28	1.36	-	0 024	3.7	0.024
Cs	0 0061	13.0	-	0 0058	0.0073	0.0069	0 006	27.3	-	0.0055	0.0045	0.0052	0 066	2 1	0.066
Hf	0.0056	17.7	0 0046	0.015	0.0069	-	0 0038	11 1	0.0055	(0.04)	0.0054	-	0.38	6.1	0.395
Ta	0.0013	21.9	0.0021	0.039	0 002	-	0.0005	59	0.003	(0.02)	0.002	-	0 021	13 6	0 0219
Tl	‹ 0 0004	-	-	(0 002)	-	-	0 0008	55	-	(0.002)	-	-	0 009	12.0	0 0142
Bi	0 006	25.0	-	0.006	-	-	0 0046	16.8	-	0 008	-	-	0 003	379	-
Th	0 011	13.0	0.0083	0.01	0.0098	0.011	0.011	13.7	0 0095	0.013	0.0115	0.012	0.114	3.3	0.12
U	0.0038	25 0	0 0038	0 0036	0.0018	0.0030	0.0042	9.6	0 0042	0 0045	0.0039	0 0051	0 070	3 4	0.0728

n number of digestions. - no value available. () Information values. Data underlined are recommended values.

(A) Jochum *et al.* (1994), (B) Xie *et al.* (1994), (C) Govindaraju (1994), (D) Eggins *et al.* (1997), (E) Ionov *et al.* (1992), (F) Garbe-Schönberg (1993), (G) Makishima and Nakamura (1997).

GEOSTANDARDS NEWSLETTER
The Journal of Geostandards and Geoanalysis

Results for rock reference materials

Table 5 shows the measured results, precisions and reference values of the six selected geological reference materials. The precisions (% RSD, 1 *s*) were calculated on the basis of nine independent digestions for PCC-1, seven independent digestions for BIR-1 and TAFAHI, and five independent digestions for DNC-1, UB-N and DTS-1 (spread over a period of three to six months) The precisions were found to vary considerably from element to element, generally in accordance with elemental abundance For instance, the RSD values for Rb, Sr, Zr, Nb, Th and U in BIR-1, DNC-1, UB-N and TAFAHI were generally less than 7%, whereas the RSD values for these elements in DTS-1 and PCC-1 were generally more than 10% due to the decrease in elemental concentrations The precisions for Ta in the six selected samples varied from 4.9% to 59% as tantalum concentrations ranged from 91 down to 0.5 ng g^{-1} in the rock samples The RSD values for Tl were found to be 54%, 55% and 12% for BIR-1, PCC-1 and TAFAHI, respectively, due to the low thallium concentration, whereas the RSD values were 8 3% and 4.7% for DNC-1 and UB-N at the higher thallium concentrations. The RSDs quoted in this study represent a good approximation to the true external reproducibility, compared to an internal (within run) repeatability which is generally much better. However, it should be pointed out that RSD values are also affected by other factors such as instrumental sensitivity and stability, heterogeneous distributions of trace elements in solid samples, blank levels and sample digestion efficiency.

The measured results of HFSE, Rb, Sr, Mo, Sb, Cs, Tl and Bi in the six selected geological reference materials by magnetic sector ICP-MS are in general agreement with previous published values (Ionov *et al* 1992, Garbe-Schönberg 1993, Govindaraju 1994, Jochum *et al* 1994, Xie *et al* 1994, Eggins *et al.* 1997, Makishima and Nakamura 1997, Munker 1998). Our data for Ta were found to be 12, 1.3 and 0.5 ng g^{-1} for UB-N, DTS-1 and PCC-1 respectively, which are lower than previously published values. The measured results for Tl in DTS-1 and PCC-1 were found to be < 0.4 and 0.8 ng g^{-1}, respectively. These values are lower than the information values (2 ng g^{-1} for both rock standards) compiled by Govindaraju (1994). The results for Bi were found to be 4, 8 2, 6, 4.6 and 3 ng g^{-1} in BIR-1, DNC-1, DTS-1 PCC-1 and TAFAHI, respectively

As an additional assessment of the quality of the analytical data measured in this study, Figure 2 shows

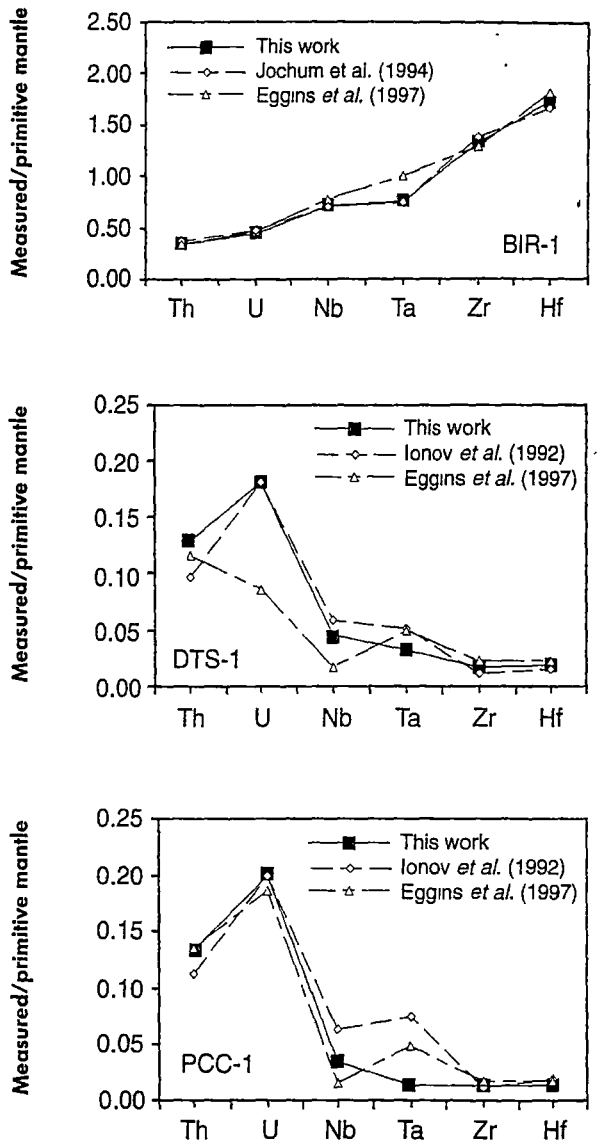

Figure 2. Comparison of primitive mantle-normalized patterns for BIR-1 DTS-1 and PCC-1 (values for primitive mantle after Sun and McDonough 1989).

the comparison of primitive mantle-normalized distributions of HFSE for BIR-1, DTS-1 and PCC-1. Our new data for these three geological reference materials, when plotted normalized to the primitive mantle concentrations recommended by Sun and McDonough (1989), agree well with published results (Ionov *et al.* 1992, Jochum *et al.* 1994, Eggins *et al.* 1997). It can also be seen that there are smooth primitive mantle-normalized distribution patterns from Nb to Hf for DTS-1 and PCC-1, suggesting that the proposed magnetic sector ICP-MS technique produces accurate low abundance analytical data for the petrogenetic interpretation of these elements in geological materials.

Conclusions

Our work has demonstrated that HFSE, Rb, Sr, Mo, Sb, Cs, Tl and Bi at ng g^{-1} levels in geological reference materials can be determined by magnetic sector ICP-MS in conjunction with $HF/HClO_4$ high pressure decomposition. The detection limits obtained by the proposed magnetic sector ICP-MS method were found to be generally superior to those reported using quadrupole ICP-MS. The analytical procedure is simplified, as only indium (^{115}In) is used as an internal standard to compensate for instrumental drift and matrix effects, in contrast to other methods which use three to nine internal standards Regarding the mobilisation of HFSE by trace amounts of HF in solution, we suggest that any HF used for sample dissolution should be driven off completely by $HClO_4$, as this is crucial for the reliable measurement of HFSE at very low abundance, including ultramafic samples. Hydrofluoric acid removal must be consistent and this is not the case with an HF/HNO_3 digestion Even small amounts of F^- left in solution can change the memory behaviour dramatically and in an unreproducible way The analytical accuracy of the magnetic sector ICP-MS method reported in this study is comparable with or better than that found when using quadrupole ICP-MS instruments, especially when elements at ng g^{-1} levels in rock samples are analysed. The high ion transmission of the magnetic sector instrument allows the analysis of HFSE at very low levels, which enables us to report these new data for dunite and peridotite geological materials.

Acknowledgements

Ross R. Large and Peter McGoldrick at the Centre for Ore Deposit Research of the University of Tasmania are thanked for the financial support and encouragement for this work The facilities of the Central Science Laboratory, the University of Tasmania, are acknowledged. The authors are also grateful to S.M. Eggins at Research school of Earth Sciences of Australian National University for offering the basalt standard-TAFAHI. John Foden at the University of Adelaide is also thanked for donating the ^{84}Sr isotope solution

References

Dulski P. (1994)
Interferences of oxide, hydroxide and chloride analyte species in the determination of rare earth elements in geological samples by inductively coupled plasma-mass spectrometry Fresenius' Journal of Analytical Chemistry, 350, 194-203

Eggins S.M., Woodhead J.D., Kinsley L.P.J., Mortimer G.E., Sylvester P., McCulloch M.T., Hergt, J.M. and Handler M.R. (1997)
A simple method for the precise determination of ≥40 trace elements in geological samples by ICP-MS using enriched isotope internal standardisation Chemical Geology, 134, 311-326

Garbe-Schönberg C.-D. (1993)
Simultaneous determination of thirty-seven trace elements in twenty-eight international rock standards by ICP-MS Geostandards Newsletter, 17, 81-97

Govindaraju K. (1994)
1994 compilation of working values and sample description for 383 geostandards Geostandards Newsletter, 18 (Special Issue), 158pp.

Gray A.L. (1975)
Mass spectrometric analysis of solutions using an atmospheric pressure ion source. Analyst, 100, 289-299.

Hollocher K. and Ruiz J. (1995)
Major and trace element determinations on NIST glass standard reference materials 611, 612, 614 and 1834 by inductively coupled plasma-mass spectrometry. Geostandards Newsletter, 19, 27-34.

Ionov D.A., Savoyant L. and Dupuy C. (1992)
Application of the ICP-MS technique to trace element analysis of peridotites and minerals. Geostandards Newsletter, 16, 311-315

Jakubowski N., Moens L. and Vanhaeche F. (1998)
Sector field mass spectrometers in ICP-MS Spectrochimica Acta Part B, 53, 1739-1763.

Jarvis K.E. (1988)
Inductively coupled plasma-mass spectrometry. A new technique for the rapid or ultra-trace level determination of the rare earth elements in geological materials Chemical Geology, 68, 31-39.

Jarvis I. (1992)
Sample preparation for ICP-MS In: Jarvis, K.E., Gray, A.L. and Houk, R.S. (eds), Handbook of inductively coupled plasma mass spectrometry. Blackie (London), 172-224

Jenner G.A., Longerich H.P., Jackson S.E. and Fryer B.J. (1990)
ICP-MS - A powerful tool for high-precision trace-element analysis in Earth sciences Evidence from analysis of selected U.S.G.S reference samples. Chemical Geology, 83, 133-148

Jochum K.P., Rehkämper M. and Seufert H.M. (1994)
Trace element analysis of basalt BIR-1 by ID-SSMS, HPLC and LIMS Geostandards Newsletter, 18, 43-51

Longerich H.P. (1993)
Oxychlorine ions in inductively coupled plasma-mass spectrometry Effect of chlorine speciation as Cl^- and ClO_4^- Journal of Analytical Atomic Spectrometry, 8, 439-444

references

McGinnis C.E., Jain J.C. and Neal C.R. (1997)
Characterisation of memory effects and development of an effective wash protocol for the measurement of petrogenetically critical trace elements in geological samples by ICP-MS Geostandards Newsletter: The Journal of Geostandards and Geoanalysis, 21, 289-305

Makishima A. and Nakamura E. (1997)
Suppression of matrix effects in ICP-MS by high power operation of ICP Application to precise determination of Rb, Sr, Y, Cs, Ba, REE, Pb, Th and U at ng g^{-1} levels in milligram silicate samples Geostandards Newsletter: The Journal of Geostandards and Geoanalysis, 21, 307-319.

Moens L, Verrept P., Dams R., Greb U., Jung G. and Laser B. (1994)
New high-resolution inductively coupled plasma-mass spectrometry technology applied for the determination of V, Fe, Cu, Zn and Ag in human serum Journal of Analytical Atomic Spectrometry, 9, 1075-1078

Münker C. (1998)
Nb/Ta fractionation in a Cambrian arc/back arc system, New Zealand. Source constraints and application of refined ICP-MS techniques Chemical Geology, 144, 23-45.

Norman M.D., Griffin W.L., Pearson N.J., Gracia M.O. and O'Reilly S.Y. (1998)
Quantitative analysis of trace element abundances in glasses and minerals: A comparison of laser ablation inductively coupled plasma-mass spectrometry, solution inductively coupled plasma-mass spectrometry, proton microprobe and electron microprobe data Journal of Analytical Atomic Spectrometry, 13, 477-482.

Robinson P., Townsend A.T., Yu Z. and Münker C. (1999)
Determination of scandium, yttrium and rare earth elements in rocks by high resolution inductively coupled plasma-mass spectrometry. Geostandards Newsletter: The Journal of Geostandards and Geoanalysis, 23, 31-46

Sun S.-S. and McDonough W.F. (1989)
Chemical and isotopic systematics of oceanic basalts Implications for mantle composition and processes. In: Saunders, A.D. and Norry, M.J. (eds), Magmatism in the ocean basins. Geological Society of London Special Publication, 42, 313-345

Townsend A.T., Miller K.R., McLean S. and Aldous S. (1998)
The determination of copper, zinc, cadmium and lead in urine by high resolution ICP-MS. Journal of Analytical Atomic Spectrometry, 13, 1213-1219

Vandecasteele C. and Block C.B. (1995)
Modern methods for trace element determination John Wiley (New York), 330pp.

Xie Q., Jain J., Sun M., Kerrich R. and Fan J. (1994)
ICP-MS analysis of basalt BIR-1 for trace elements Geostandards Newsletter, 18, 53-63.